
# The REST/NRSF Pathway as a Central Mechanism in CNS Dysfunction

Thesis submitted in accordance with the requirements of the University of Liverpool for the degree of Doctor in Philosophy by

**Alix Warburton**

April 2015

# Disclaimer

The data in this thesis is a result of my own work. The material collected for this thesis has not been presented, nor is currently being presented, either wholly or in part for any other degree or other qualification. All of the research, unless otherwise stated, was performed in the Department of Physiology and Department of Pharmacology, Institute of Translational Medicine, University of Liverpool. All other parties involved in the research presented here, and the nature of their contribution, are listed in the Acknowledgements section of this thesis.

# Acknowledgements

First and foremost, I would like to express my upmost gratitude to my primary and secondary supervisors Professor John Quinn (a.k.a Prof. Quinny) and Dr Jill Bubb for all of their support, guidance, wisdom (thank you Jill) and encouragement throughout my PhD; I could not have wished for a better pair. I am also extremely grateful to the BBSRC for funding my PhD project.

I would also like to extend my thanks to Dr Graeme Sills for providing samples and assistance with my work on the SANAD epilepsy project, Dr Fabio Miyajima for offering his knowledge and knowhow on many occasions, Dr Gerome Breen for being a bioinformatics wizard and providing support on several projects, Dr Minyan Wang's lab for their help and hospitality during my 3 month visit to Xi'an Jiaotong-Liverpool University, Dr Roshan Koron for assisting with the breast cancer study, Dr Chris Murgatroyd for his invaluable advice on ChIP and Professor Dan Rujescu's lab for providing clinical samples and support with statistical analyses on the schizophrenia project.

A massive thank you to Abigail Savage (Savbot), Kate Haddley (Katie Bear), Paul Myers (Curly), Veridiana Miyajima (Master of the Sushi), Maurizio Manca, Olympia Gianfrancesco, Kejhal Khursheed and all other members of White Block, past and present, for making my time in the lab an absolute ball and for keeping me sane on the science-fail days and celebrating the success days. To the Pub Friday peeps (you know who you are), thank you for drinking wine/beer/lemonade with me and for being beautiful and fabulous individuals.

To my Mum, Poppy (Dad) and beautiful sisters Donna and Gina, thank you for being the most amazing family EVER and for supporting me throughout my studies and for making me smile every single day ☺ - I love you all to bits! And a huge thanks to all my other family and friends for being such a fabulous bunch. I would also like to say a special thank you to Big Dave and Tina-Bean for welcoming me into the Peeney residence and for supporting me during my thesis write-up; it means a lot to me. Last but not least, thank you to David Peeney for being the best; encouraging me, keeping me well fed and watered, putting-up with my write-up tantrums, saving me from spiders and giving me lots of cuddles.

# Contents

# Publications

- Warburton A., Breen G., Rujescu D., Bubb V.J., and Quinn J.P. Characterization of a REST-Regulated Internal Promoter in the Schizophrenia Genome-Wide Associated Gene MIR137. *Schizophrenia Bulletin*. 2014. doi:10.1093/schbul/sbu117. http://schizophreniabulletin.oxfordjournals.org/cgi/content/full/sbu117?ijkey=ClpJeb8FHJnc2DR&keytype=ref

- Warburton A., Savage A.L., Myers P., Peeney D., Bubb V.J., and Quinn J.P. Molecular Signatures of Mood Stabilisers Highlight the Role of the Transcription Factor REST/NRSF. Journal of Affective Disorders. 2014. doi: 10.1016/j.jad.2014.09.024. http://www.sciencedirect.com/science/article/pii/S0165032714005783

- Quinn J.P., Warburton A., Myers P., Savage A.L., and Bubb V.J. Polymorphic variation as a driver of differential neuropeptide gene expression. Neuropeptides. 2013 Dec; 47(6):395-400. doi: 10.1016/j.npep.2013.10.003. Epub 2013 Oct 23.

- Warburton A., Miyajima F., Shazadi K., Taylor J., Baker G.A., Quinn J.P., and Sills G.J. (2015). NRSF/REST and BDNF Single Nucleotide Polymorphisms as Biomarkers for Cognitive Dysfunction in Adults with New-onset Epilepsy. *Epilepsy & Behavior* (In review).

# Abbreviations

| | |
|---|---|
| A | Adenine |
| Aβ | β-amyloid |
| AC | Anterior cingulate cortex |
| ACC | Adenylate cyclise |
| AD | Alzheimer's disease |
| AED | Anti-epileptic drug |
| AGO | Argonaute |
| ALS | Amyotrophic lateral sclerosis |
| Am | Amygdala |
| AMIPB | Adult memory and information processing battery |
| AMP | Adenosine monophosphate |
| AMPA | Alpha-amino-3-hydroxy-5-methyl-4-isoxazole propionate |
| ANS | Autonomic nervous system |
| AP-1 | Activator protein-1 |
| AS | Anti-sense |
| ATP | Adenosine-5'-triphosphate |
| AVLT | Auditory Verbal Learning Task |
| AVP | Arginine vasopressin |
| BDNF | Brain-derived neurotrophic factor |
| BG | Basal ganglia |
| BLAT | BLAST-like alignment tool |
| BLAST | Basic Local Alignment Search Tool |
| Bp | Base pairs |
| BRCA1/2 | Breast cancer, early onset 1/2 |
| BRG1 | Brahma-related gene-1 |
| BS | Binding site |
| β | Beta coefficient |
| C | Cytosine or cortex |
| C- | Carboxy- |
| CACNA1C | Calcium Channel, Voltage-Dependent, L Type, Alpha 1C Subunit |
| cAMP | cyclic AMP |
| Cb | Cerebellum |
| CCR4 | Chemokine (C-C motif) receptor 4 |
| cDNA | Complementary deoxyribonucleic acid |
| CD16 | Fc receptor III |
| CEPH | Centre de'Etude du Polymorphism Humain |
| CGI | CpG island |
| ChIP | Chromatin immunoprecipitation |
| ChIP-seq | ChIP-sequencing |
| CI | Confidence interval |
| CNS | Central nervous system |
| CoREST | Cofactor for REST |
| CpG | CG dinucleotides |
| CREB | cAMP response element-binding protein |
| CR1 | Chicken repeat 1 |
| CSD | Cortical spreading depression |

| | |
|---|---|
| CSMD1 | CUB and Sushi multiple domains 1 |
| c-Src | V-Src Avian Sarcoma (Schmidt-Ruppin A-2) Viral Oncogene |
| ctBP | Carboxyl-terminal binding protein |
| CTCF | CCCTC binding-protein |
| CT-RD | C-terminal repressor domain |
| CVST | Computerised Visual Search Task |
| C5a | Complement component 5a |
| C9ORF72 | Chromosome 9 open reading frame 72 |
| C10orf26 | Chromosome 10 open reading frame 26 |
| DAT | Dopamine transporter |
| DBR1 | Debranching RNA Lariats 1 enzyme |
| d.f. | Degrees of freedom |
| DGCR8 | DiGeorge syndrome critical region 8 |
| dlPFC | Dorsolateral PFC |
| DMEM | Dulbecco's modified eagle's medium |
| DMSO | Dimethylsulphoxide |
| DNA | Deoxyribonucleic acid |
| dNTP | Deoxynucleotide triphosphate |
| DRD3 | Dopamine D3 |
| ECR | Evolutionary conserved region |
| EDTA | Ethylenediamine tetraacetic acid |
| EGFR | Epidermal growth factor receptor |
| EGTA | Ethylene glycol tetraacetic acid, |
| EM | Expectation-Maximisation |
| ENCODE | Encyclopaedia of DNA Elements |
| eQTL | Expression quantitative trait loci |
| ErbB | v-erb-b2 erythroblastic leukemia viral oncogene |
| ERK | Extracellular signal-regulated kinase |
| ERVL | Endogenous retroviral element |
| ESC | Embryonic stem cells |
| ESR1 | Estrogen receptor 1 |
| EZH2 | Enhancer of zeste homolog 2 |
| FC | Frontal cortex |
| FOS | FBJ murine osteosarcoma viral oncogene homolog |
| FMRP | Fragile-X mental retardation protein |
| FXS | Fragile-X sydrome |
| G | Guanine |
| GABA | Gamma-aminobutyric acid |
| GAD1 | Glutamate decarboxylase 1 (brain, 67kDa) |
| Genevar | Gene Expression Variation |
| GxE | Gene-environment interaction |
| GnRH | Gonadotropin-releasing hormone |
| GPR | Global Pattern Recognition |
| GRIA2 | Glutamate receptor, ionotropic, AMPA 2 |
| GRIN1 | Glutamate receptor, ionotropic, NMDA 1 |
| GSK3β | Glycogen synthase kinase-3β |
| GST | Glutathione-S-transferase protein |
| GWAS | Genome wide association study |
| x g | Times gravity |
| H | Hippocampus |
| HD | Huntington’s disease |

| | |
|---|---|
| HDAC | Histone deacetylase complex |
| HeLa | Henrietta Lacks clonal cell line |
| HEPES | 4-(2-hydroxyethyl)-1-piperazineethanesulfonic acid |
| hg | Human genome |
| HGF | Hepatocyte growth factor |
| htSNP | Haplotype-tagging SNP |
| Htt | Huntingtin |
| HWE | Hardy-Weinberg Equilibrium |
| H2A/B | Histone H2 subunit A/B |
| H3 | Histone H3 |
| H4 | Histone H4 |
| H3K4me2 | Dimethylation of lysine 4 in histone H3 |
| H3K9me1 | Monomethylation of lysine 9 in histone H3 |
| H3K9me3 | Trimethylation of lysine 9 in histone H3 |
| H3K27me3 | Trimethylation of lysine 27 in histone H3 |
| IL-1 | Interleukin-1 |
| Imir137 | Internal MIR137 promoter |
| JAr | Human placental choriocarcinoma cells |
| JUN | Jun oncogene |
| Kb | Kilobase |
| KEGG | Kyoto Encyclopaedia of Genes and Genomes |
| LB | Luria-bertani broth |
| LD | LD Linkage disequilibrium |
| LINE | Long interspersed nuclear elements |
| LOD | Logarithm of odds |
| LSD1 | Lysine-specific demethylase 1 |
| LTR | Long terminal repeat |
| MAF | Minor allele frequency |
| MALDI-TOF | Matrix Assisted Laser Desorption/Ionization-Time of Flight |
| MB | Midbrain |
| MBD | Methyl binding domain |
| MCF-7 | Human-derived breast adenocarcinoma cells |
| MDD | Major depressive disorder |
| MeCP2 | Methyl-CpG-binding protein 2 |
| MeDIP | Methylated DNA Immunoprecipitation |
| MIF | Macrophage migration inhibitory factor |
| MIR | microRNA gene/ mammalian-wide interspersed repeats |
| miR | mature microRNA |
| miRISC | miRNA-induced silencing complex |
| miRNA | microRNA |
| MIR137HG | MIR137 host gene |
| ML | Maximum likelihood |
| mPFC | Medial PFC |
| mRNA | Messenger ribonucleic acid |
| mSin3A | Mammalian homologue of yeast Sin3A |
| $m^7G$ | 7-methylguanosine 5' cap |
| μ | Mu- |
| N- | Amino- |
| NAc | Nucleus accumbens |
| NaCl | Sodium chloride |
| NCBI | National Center for Biotechnology Information |

| | |
|---|---|
| ncRNA | Non-coding RNA |
| NK | Natural killer |
| NKG2D | Natural-killer group 2, member D |
| NMDA | N-methyl-D-aspartate |
| NOT | Negative regulator of transcription |
| NRG1 | Neuregulin 1 |
| NRSE | Neuron restrictive silencing element |
| NRSF | Neuron restrictive silencing factor |
| NS | Non-synonymous |
| NSC | Neural stem cell |
| nt | Nucleotide |
| NT-RD | N-terminal repressor domain |
| NTRK3 | Neurotrophic tyrosine kinase receptor type 3 |
| OFC | Orbitofrontal cortex |
| ORF | Open reading frame |
| PAFAH1B3 | Platelet-activating factor acetylhydrolase, isoform Ib, gamma subunit 29kDa |
| PBS | Phosphate buffer saline |
| PCR | Polymerase chain reaction |
| PcG | Polycomb-group |
| PD | Parkinson's disease |
| PER3 | Period circadian clock 3 |
| PFC | Prefrontal cortex |
| PIC | Protease inhibitor cocktail |
| PI3K | Phosphoinositide 3-kinase |
| PKA | Protein kinase A |
| PKC | Protein kinase C |
| PLB | Passive lysis buffer |
| PLC | Phospholipase C |
| PLN | Prefrontal-limbic network |
| Pol II | Polymerase II |
| PR | Progesterone receptor |
| pre-miR | precursor-microRNA |
| pri-miR | primary-microRNA |
| PWM | Position weight matrices |
| qPCR | Quantitative PCR |
| $r^2$ | Squared correlation coefficient |
| RAR-alpha | Retinoic acid receptor *alpha* |
| RE1 | Repressor element-1 |
| RELN | Reelin |
| REML | Restricted Maximum Likelihood |
| REST | Repressor element-1 silencing transcription factor |
| RGS4 | Regulator of G-protein signaling 4 |
| RILP | REST-interacting LIM domain protein |
| RISC | RNA-induced silencing complex |
| RPM | Revolutions per minute |
| RNA | Ribonucleic acid |
| RS | Rett syndrome |
| RT-PCR | Reverse transcriptase PCR |
| SANAD | Standard and New Antiepileptic Drug |
| SCG10 | Superior cervical ganglion 10 |
| SCLC | Small cell lung cancer |

| | |
|---|---|
| SCN2A | Sodium channel type II-alpha |
| SCZ | Schizophrenia |
| SDS | Sodium dodecyl sulphate |
| SH-SY5Y | Human-derived neuroblastoma cells |
| SINE | Short interspersed nuclear element |
| siRNA | Small-interfering RNA |
| SLC6A4 | Serotonin transporter |
| SLC | Solute carrier gene family |
| SMARCA4 | SWI/SNF related, matrix associated, actin-dependent regulator of chromatin, subfamily A, member 4 |
| SNAP25 | Synaptosomal-associated protein, 25 kDa |
| SNP | Single nucleotide polymorphism |
| sNRSF | Short-form neuron restrictive silencing factor |
| SP3 | Sp3 transcription factor |
| STIN2 | Second intron of the serotonin transporter |
| SVA | SINE-VNTR-Alu element |
| SV40 | Simian virus 40 |
| SWI/SNF | Switch/sucrose Non-fermentable |
| TAC1 | Tachykinin 1 |
| TAC3 | Tachykinin 3 |
| TBE | Tris/Borate/EDTA |
| TBP | TATA-box-binding protein |
| TCF4 | Transcription factor 4 |
| TE | Tris-EDTA/ transposable element |
| TFBS | Transcription factor binding sites |
| TGF-β | Transforming growth factor beta |
| TRANSFAC | Transcription factor database |
| TRBP | TAR (trans-activating response element) RNA binding protein |
| TrkB | Tropomyosin-related kinase-B |
| TSS | Transcriptional start site |
| UCSC | University of California, Santa Cruz |
| UTR | Untranslated region |
| vmPFC | Ventromedial PFC |
| VRT | Visual Reaction Time |
| VS | Ventral striatum |
| VTA | Ventral tegmental area |
| Wt | Wild type |
| YB-1 | Y box binding protein 1 |
| YY1 | Yin Yang 1 |
| ZNF804A | Zinc finger protein 804A |
| 5'aza-DC | 5-Aza-2′-deoxycytidine |
| 5-HTT | 5-hydroxy- tryptamine (serotonin) |
| 5-HTTLPR | Serotonin-transporter-linked polymorphic region |

# List of Figures

# List of Tables

# Abstract

Deciphering the complex molecular circuitry of the brain is crucial for understanding how processes such as higher cognitive function and behaviour are disrupted in neurological disease. Thus it is imperative to explore further the regulatory mechanisms centred on key transcription factors that orchestrate such processes including REST/NRSF (restrictive element-1 silencing transcription factor/neuron restrictive silencing factor); NRSF targets over 2,000 human genes and plays a central and dynamic role in a myriad of CNS processes. To address the function of NRSF, I employed several research disciplines including bioinformatics, gene association studies for complex polygenic diseases and model systems for understanding the structure and function of several NRSF directed pathways in the CNS. My data demonstrated that disruption of the normal balance of NRSF within the cell may be a fundamental mechanism across a range of common neuropathologies. These included 1) *schizophrenia*, where NRSF was shown to be capable of directing allele-specific and stimulus-driven expression of MIR137 through identification of a novel promoter in this key schizophrenia genome wide associated gene; 2) *cognitive dysfunction*, polymorphisms within NRSF and its gene target BDNF influenced memory performance in patients with newly diagnosed epilepsy; 3) *mood disorders*, NRSF-signalling was identified as a significant pathway regulating cellular processes relevant to mood modification by pharmaceutical challenge and 4) NRSF-mediated regulation of microRNA-137 (miR-137) expression was demonstrated *in vivo* using a model of cortical spreading

depression, consistent with its involvement in associated neuropathologies including epilepsy and ischemia. The analysis was expanded to a common non-neurological disease, breast cancer, where the previous work of others was extended to demonstrate a link between NRSF and miR-137 through the novel promoter identified in this study. Collectively these findings emphasise NRSF as a major contributor to cell pathogenesis, in part by modulation of miR-137, not only in a neuronal context but also in other systems.

# Chapter 1

## General Introduction

## 1.1 Overview

A transcriptional regulator that has been extensively studied for its role in modulating neuron-specific gene expression is repressor element-1 silencing transcription factor (REST) (Chong et al., 1995), also termed neuron restrictive silencing factor (NRSF) (Schoenherr and Anderson, 1995). NRSF signalling has been implicated in a number of neurological disorders including age-related cognitive dysfunction, epilepsy, schizophrenia and Huntington's disease; however the exact role of NRSF in these pathological conditions and the associated regulatory mechanisms involved remain uncertain. To better understand the dynamic role of NRSF in disease processing, the purpose of this thesis was to dissect the pathways centred on NRSF regulation of key target genes important for CNS function, including BDNF (brain-derived neurotrophic factor) and microRNA-137 (miR-137). BDNF is a well characterised neurotrophin essential for neurodevelopment, synaptic plasticity and adult neurogenesis whose dysregulation has been associated with several CNS disorders including epilepsy, schizophrenia and cognitive decline both in disease and in normal ageing; the latter of which has previously been addressed in our group through genetic association (Miyajima et al., 2008b). miR-137 is also essential for neuronal development and function (Crowley et al., 2015), and is an important post-transcriptional regulator of genes implicated in several cancers and more recently schizophrenia through genome wide association studies (GWAS) (The Schizophrenia Psychiatric GWAS Consortium, 2011, Ripke et al., 2013). The main focus of this study was to 1) investigate the role of NRSF and its alternative isoform sNRSF, whose expression has been identified as a marker of disease states in both tumourgenesis and epilepsy (Coulson et al.,

2000, Spencer et al., 2006, Wagoner et al., 2010), in modulating gene expression under normal physiological conditions and in response to cellular challenge (*in vitro* drug exposure) as a model of neurological dysfunction and 2) address genetic variation within the NRSF signalling pathway as clinical correlates for neurological disease and/or modulators of transcription that could underpin a disease-associated pathway.

In *Chapter 3*, genotype analysis of single nucleotide polymorphisms (SNPs) within the NRSF and BDNF genes in patients with newly-diagnosed epilepsy was explored to determine genetic influences on cognitive dysfunction; a common co-morbidity in people with epilepsy. Both NRSF and BDNF have been implicated in rodent models of epilepsy (Palm et al., 1998, Calderone et al., 2003, Spencer et al., 2006, Hu et al., 2011b, Quinn et al., 2002, Roopra et al., 2001, Garriga-Canut et al., 2006, Liu et al., 2012b, Ballarín et al., 1991, Nibuya et al., 1995) and human studies of cognitive function (Voineskos et al., 2011, Honea et al., 2013, Miyajima et al., 2008a), including work by our group that showed an additive interaction between these two genes in determining cognitive performance in the elderly (Miyajima et al., 2008b), suggesting a potential role for these factors in epilepsy-associated cognitive impairments. A cross-sectional and longitudinal study design was employed to assess genetic effects on cognitive performance measured using a psychological battery test at both baseline, when individuals were initially recruited into the study and were naïve to anti-epileptic drug (AED) treatment; a factor reported to effect cognition (Taylor et al., 2010), and at 12-month reassessment following admission onto a treatment regime with AEDs. Several non-coding SNPs within

NRSF and BDNF were identified as being significantly associated with memory performance suggesting a regulatory role.

The regulatory potential of NRSF over the human BDNF gene locus was also addressed in *Chapter 3*. The BDNF gene is extremely complex, giving rise to more than 34 different mRNA transcripts through alternative splicing that are expressed in a tissue-specific and stimulus-inducible manner within the CNS and periphery (Aid et al., 2007, Pruunsild et al., 2007, Baj and Tongiorgi, 2009). Expression of BDNF from its distinct promoters is induced by a variety of stimuli including electrical, chemical, hormonal, steroidal and inflammatory (Koibuchi et al., 1999, Toran-Allerand, 1996, Reichardt, 2006). Although many transcriptional pathways have been identified as being important for regulation of BDNF expression, the exact regulatory mechanisms are yet to be fully elucidated. NRSF has been shown to modulate distinct BDNF promoters in the rodent brain and in cell line models (Palm et al., 1998, Timmusk et al., 1999, Tabuchi et al., 2002b, Tabuchi et al., 1999, Abuhatzira et al., 2007); however, to my knowledge, NRSF-mediated regulation of human BDNF promoter utilisation has not been previously addressed. We therefore interrogated NRSF-mediated regulation of the BDNF gene locus in human-derived SH-SY5Y neuroblastoma cells using chromatin immunoprecipitation (ChIP) and correlated this with BDNF mRNA expression under basal conditions and following cocaine treatment; a known modulator of NRSF and BDNF expression in rodent models of cocaine-induced plasticity (Chandrasekar and Dreyer, 2009, Sadri-Vakili et al., 2010, Le Foll et al., 2005, Liu et al., 2006, Graham et al., 2007, Kumar et al., 2005).

Following on from this, NRSF regulation of the MIR137 gene was addressed. MIR137 is a novel target identified as being the most significantly correlated locus associated with schizophrenia from GWAS (The Schizophrenia Psychiatric GWAS Consortium, 2011, Ripke et al., 2013). The intronic location of the associated MIR137 SNPs suggests one mechanism in which transcriptional or post-transcriptional regulation of miR-137 expression could underlie schizophrenia. The genomic architecture surrounding miR-137, such as active histone marks, RNA polymerase II (Pol II) binding and an overlapping CpG island, identified from *in silico* analysis suggested the presence of an internal promoter in the region. Bioinformatic analysis of the locus using the UCSC Genome Browser (accessed January 2012; http://genome.ucsc.edu/) identified NRSF as the only other transcription factor in addition to RNA Pol II required for miRNA transcription binding over this putative internal promoter (see **Figure 4.1**). A variable number tandem repeat (VNTR) domain adjacent to the precursor sequence of miR-137 was also located within this potential regulatory domain which contained a conserved NRSF binding site identified using the TRANSFAC (transcription factor) database; a resource containing data on transcription factors, their computationally-predicted and experimentally-validated binding sites and regulated target genes (Matys, 2003). We hypothesised that NRSF and the MIR137 VNTR may act individually or in combination to modulate the expression and function of miR-137 in schizophrenia and further that genotypic variation at the VNTR might be associated with schizophrenia by modulation of gene expression levels. We validated and addressed the function of this novel promoter using an *in vitro*

model system and genotyped the MIR137 VNTR in a schizophrenia cohort and compared it to that of a matched control group.

To further investigate the regulatory mechanisms and pathways that might coordinate the cell response to a specific drug, in *Chapter 5* we addressed the affects of mood modifying drugs, which are commonly used therapeutically or recreationally, on the transcriptome, in a tissue culture model, using qPCR arrays of mood disorder genes. Enrichment analysis of transcriptional networks relating to this gene set using pathway analysis tools identified NRSF as an important regulatory mechanism, highlighting a role for this transcriptional pathway, synergistically or separately, in the modulation of specific neuronal gene networks in response to mood modifying drugs.

In the final chapter we attempted to extend our NRSF-MIR137 network, which we hypothesise to be one regulatory mechanism that may be modified in disease processes relevant to neurological dysfunction, to both animal models and disease mechanisms outside of the CNS. Specifically we explored the NRSF-MIR137 pathway using a rodent model of cortical spreading depression (CSD) to assess both the evolutionary conservation of this neuronal network and, based on the assumption that it is conserved, make comparisons on the modulation of this pathway across different species in response to CNS insults. A human cell line model of breast cancer was also addressed as this cancer type has been identified from the literature to involve these two regulatory factors (Wagoner et al., 2010, Zhao et al., 2012) and was also identified as a significant disease ontology pathway from analysis of transcriptional networks centred on NRSF signalling (see *Chapter 5*).

## 1.2 Understanding CNS disorders

Disorders of the CNS are conditions which affect either the brain or spinal cord resulting in neurological or psychiatric illness. There are more than 1,000 disorders of the CNS ranging from functional disorders, such as epilepsy and migraine; degenerative disorders, such as Alzheimer's and Parkinson's disease and psychiatric disorders, such as mood disorders and schizophrenia. These neurological conditions are extremely debilitating and are a major cause of morbidity and mortality in both males and females worldwide, with an estimated 1/3 of the adult population suffering from a mental disorder (Kessler et al., 2009). CNS pathologies account for approximately 13% of the global disease burden in high income countries, resulting in more hospitalisations and loss in productivity than any other disease group (Collins et al., 2011). Despite such high prevalence existing treatments for a large number of neurological conditions remain inadequate, in part owing to the complex and heterogeneous nature of this disease group. Understanding the regulatory mechanisms underlying neuropathologies will allow for better classification and diagnosis of such conditions, drug target identification through direct biochemical methods, genetic interactions or computational inference and development of more appropriate pharmaceutical and/or therapeutic interventions.

Many common diseases and traits are multifactorial in nature and are influenced by both genetic and environmental factors, including chemical, physiological, sociocultural and psychological. In terms of mental health, extensive interaction between an individual's genetic makeup and their genetic response to environmental stimuli will influence not only their immediate behaviour but could also leave an epigenetic mark of the event that might

manifest in later years as a psychiatric phenotype. Genetic response in this context refers to the influence of genetic variation on the transcriptional machinery in driving differential gene expression following exposure to an environmental pathogen. The clinical presentations of neuropathologies vary immensely between individuals; supporting such a notion of gene-environment interaction (GxE). The multifactorial and polygenic nature of neuropathologies poses a tremendous challenge in teasing out the underlying processes involved. However, recurring themes in the genetic vulnerability, high heritability rates and neuropsychological dysfunction in common cognitive domains associated with different neurological conditions, such as bipolar disorder and schizophrenia, suggests that common regulatory networks that are both essential and ubiquitous to neural functioning may be important in defining such diseases (Lipton and Rosenberg, 1994, Fuller Torrey, 1999, Fatemi et al., 2000, Fatemi et al., 2001a, Fatemi et al., 2001b, Torrey et al., 2005, Ahmed et al., 2011, Morris et al., 2012, Cross-Disorder Group of the Psychiatric Genomics, 2013a, Network and Pathway Analysis Subgroup of the Psychiatric Genomics Consortium, 2015). With this in mind we sought to address the regulatory mechanisms centred on NRSF, a factor originally defined as a 'master regulator' of neuronal gene expression and whose dysregulation is implicated in multiple disorders of the CNS in order to define potentially important transcriptional networks underlying or modulating common neurological pathologies.

## 1.3 Regions of the brain important in mental health

Our conscious awareness of self and emotional state of mind in response to our environment reflects the elaborate neuronal circuitry of the cerebral cortex. Appropriate responses to environmental stimuli involve integration and processing of sensory input through dynamic interaction of the cortex with the thalamus, cerebellum and subcortical regions, such as the limbic system and basal ganglia. Interaction between prefrontal neocortical regions, which are implicated in moderating higher-order cognitive functions such as mood, conscious perception of emotional experiences and social behaviour, along with the amygdala and hippocampus forms the prefrontal-limbic network (PLN). The central nucleus of the amygdala is believed to be the principle excitatory hub in response to emotional stimuli (Sotres-Bayon et al., 2004). It receives input from the lateral nucleus of the amygdala, either directly or via intra-amygdala circuitries, and sends out projections to various cortical and subcortical regions. The principle inhibitory pathways of this circuitry are the medial prefrontal cortex (mPFC) (Rosenkranz et al., 2003, Phelps et al., 2004, Izquierdo et al., 2005, Urry et al., 2006, Johnstone et al., 2007) and the hippocampal formation (Corcoran and Maren, 2001, Sotres-Bayon et al., 2004); regions important in the regulation and fine-tuning of attention, cognitive control and emotional responses (Bush et al., 2000). The encoding and storage of emotional memories is dependent, in part, upon the amygdala, hippocampus and their reciprocal interactions. The hippocampal formation is the primary system for declarative memory (Squire and Zola-Morgan, 1991). Following emotional arousal, it can generate episodic representations of the event which can influence the role of the amygdala in the perception and processing of such stimuli (Richardson et

al., 2004). Some of the major anatomical structures of the brain important in mental health are shown in **Figure 1.1** and their functions summarised in **Table 1.1**.

Signal transduction following stimulus-induced activation of neuronal networks relies on extensive cross-talk between a vast number of regulatory mechanisms, including cellular depolarisation, neurotransmitter systems and neurotrophic signalling pathways, which modulate downstream signalling cascades leading to transcriptional responses. Disruption of these connections is apparent in several neuropsychiatric disorders including major depressive disorders (Johnstone et al., 2007, Bennett, 2011), bipolar disorder (Green et al., 2007, Chen et al., 2011a, Morris et al., 2012) and schizophrenia (Morris et al., 2012, Radulescu and Mujica-Parodi, 2009, Sigmundsson et al., 2001, Williams et al., 2004) and may in part reflect genetic perturbations. This is suggested from analysis of structural variations of white matter in the cerebral hemispheres of control subjects, schizophrenia patients and their relatives which have been shown to vary in accordance with relatedness to a patient (Phillips et al., 2011). Neuroimaging studies of schizophrenia provide considerable evidence of diffuse structural defects in several brain regions, primarily the association cortex of the frontal, temporal and limbic regions (Zipursky et al., 1992, Harvey et al., 1993, Sigmundsson et al., 2001, Dickey et al., 2007); subcortical regions such as the basal ganglia (Lim et al., 1996, Perez-Costas et al., 2010) and the axonal trajectories between them (Andreasen et al., 1994, Andreasen, 1999, Sigmundsson et al., 2001, Radulescu and Mujica-Parodi, 2009, Morris et al., 2012). This may be reflective of the heterogeneous nature of the syndromes making up this condition and suggests that underlying dysfunction of several

key neural processing systems central to emotional responses (Williams et al., 2004), neuroendocrine function (Ritsner et al., 2004, Goldman et al., 2011) and behavioural and autonomic control (Dawson et al., 1994, Mujica-Parodi et al., 2005) may be important in disease aetiology. Dissecting the transcriptional mechanisms mediating disease-associated phenotypic presentations to environmental cues and addressing the potential regulatory impact of genetic variants embedded within these processing systems will allow for better understanding of the underlying pathways involved in schizophrenia. Throughout this thesis we explore the regulatory potential of common genetic variants within non-coding regions of the genome through several mediums including *in silico* predictions of regulatory function, genetic association and reporter gene assays, in order to investigate the effects of genetic variation on transcriptional responses which may underpin a pathway modulating neurological disease or pathological traits.

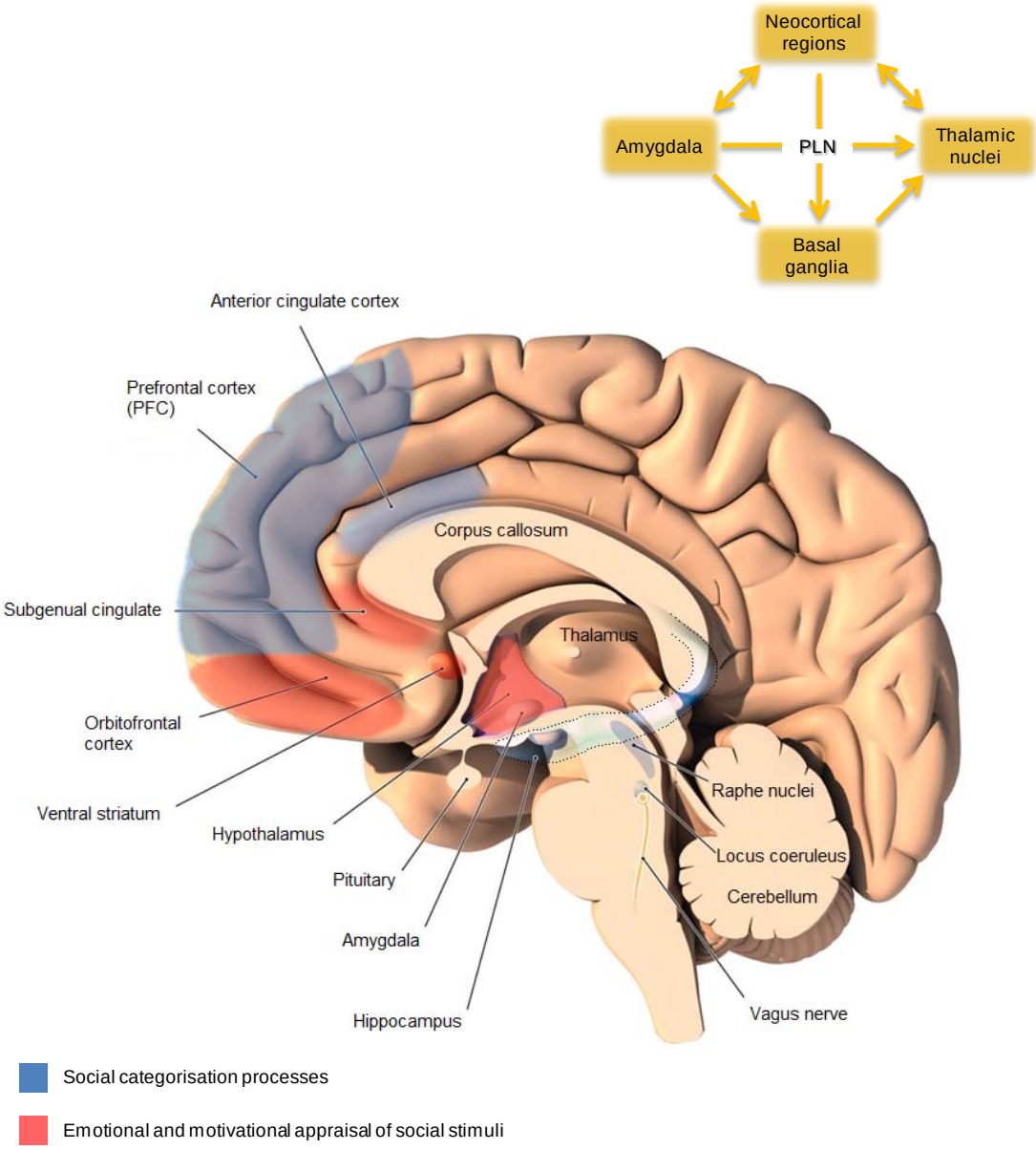


**Figure 1.1. Areas of the brain important in mental health.** Interaction between prefrontal neocortical regions (ACC, PFC, OFC, vmPFC) with the amygdala, thalamic nuclei and hippocampus forms the prefrontal-limbic network (PLN). Dynamic modulation of the PLN through interaction with the hypothalamic, basal ganglia and brainstem effector systems is important for eliciting appropriate behavioural, peripheral autonomic, endocrine and somatomotor responses to emotional stimuli. Highlighted regions represent key areas involved in social functioning, a factor which is closely related to mental health as demonstrated by frequent social deficits of neuropsychiatric patients and increased rates of psychiatric conditions in people exposed to social environmental adversity. Figure adapted from aan het Rot et al. (2009). *ACC, anterior cingulate cortex; OFC, orbitofrontal cortex; PFC; prefrontal cortex; vmPFC, ventromedial prefrontal cortex.*

**Table 1.1.** Areas of the brain important in mental health

| Region | Function | Examples of dysfunction in neurological disease |
|---|---|---|
| **BASAL GANGLIA:**<br>▪ Corpus striatum<br>▪ Substantia nigra<br>▪ Subthalamic nucleus<br>▪ Ventral tegmental area | Involved in movement, emotions and integration of sensory information. Connections to the limbic system via the corpus striatum and VTA play a key role in motivation. The reward circuit, which includes the NAc of the VS, OFC, ACC, amygdala and dopaminergic projections from the midbrain (VTA), is also embedded within this system and is a key driving force for associated behaviours e.g. anticipation and value. | HD; degeneration of striatal neurons<br>PD; loss of dopaminergic neurons in the substantia nigra<br>SCZ; positive symptoms linked to excess dopamine transmission in the striatum (nigrostriatal pathway) |
| **LIMBIC SYSTEM:** | | |
| ▪ **Neocortex** (ACC, OFC and vmPFC) | Mediates conscious perception of emotional experiences/feelings such as fear, anger, pleasure and satisfaction through interactions with subcortical centres, in particular the amygdala. Plays a central role in encoding goal-directed behaviours, emotional decision making, social categorisation, motivation and reward. | SCZ; Structural abnormalities in frontal, temporal and limbic regions and interconnecting white matter tracts reported in patients with prominent negative symptoms. Linked to reduced dopamine transmission along the mesocortical, mesolimbic and tuberoinfundibular pathways. Disturbances in cortico-cortical glutamatergic pathways (between cortex and thalamus) linked to psychosis, cognitive deficits and emotional processing. |
| ▪ **Amygdala** | Essential for sensing and evaluating the affective significance of incoming stimuli and activating the appropriate responses for its three principal functional roles:<br>1. Behaviour for preservation of self (fight or flight response)<br>2. Learning through association and co-ordination of diverse sensory inputs to generate new behavioural and autonomic responses (e.g. classical conditioned emotional responses)<br>3. Emotional processing; Connections with hypothalamic and brainstem effector systems mediate peripheral autonomic, endocrine and somatomotor responses to stimuli which evoke an emotional response. | |
| ▪ **Hippocampal formation** (hippocampus proper, dentate gyrus and subiculum) | Pre-commissural fibres connect with the neocortex, pre-optic nuclei and VS. Post-commissural fibres connect to the anterior nucleus of the thalamus and hypothalamic nuclei, including the mammillary bodies. Inputs from the cingulate, temporal, orbital, and olfactory cortices and amygdala communicated to the hippocampus. Also receives monoaminergic input from the brainstem nuclei: | AD; neurofibrillary tangles and neuritic plaques appear initially in pyramidal cells of the entorhinal cortex and spread to the temporal pole and PFC. |

| | | |
|---|---|---|
| | raphe nuclei (serotonin), the locus coeruleus (noradrenaline) and the VTA (dopamine). Important for declarative memory, spatial navigation, control of attention and emotions and controlling corticosteroid production. | |
| ▪ **Hypothalamus** | Mediates ANS (visceral) responses that accompany the expression of emotions in response to projections from the limbic system. | MDD; structural brain changes in patients with major depressive disorder have been attributed to abnormal function of the hypothalamic–pituitary–adrenal axis. |
| ▪ **Thalamus:** Anterior nuclear group of the Thalamus | The 'limbic nuclei' of the thalamus, mainly the anterior nuclear group receive input from the amygdala and hypothalamus and in turn project to the limbic lobe cortex, in particular the cingulate gyrus. These nuclei are thought to be involved in visceral emotions, the visceral aspects of behaviour and learning and memory. | |

*Note:* ACC, anterior cingulate cortex; AD, Alzheimer's disease; ANS, autonomic nervous system; HD, Huntington's disease; MDD, major depressive disorder; NAc, nucleus accumbens; OFC, orbitofrontal cortex; PD, Parkinson's disease; PFC; prefrontal cortex; SCZ, schizophrenia; vmPFC, ventromedial prefrontal cortex; VS, ventral striatum; VTA; ventral tegmental area.

## 1.4 The effects of mood modifying drugs on the brain

Neuronal plasticity in the brain is necessary for learning and memory and allows us to respond to environmental changes. Extended periods of stress can result in alterations in excitatory circuitries associated with affective disorders such as anxiety and depression which can be alleviated by pharmaceutical intervention. Drugs which affect mood can therefore be used to investigate the neural circuitries important in regulating mental health through identifying changes in gene expression associated with a particular drug pathway and therefore implicated in treatment responses or off-target/adverse effects. Tissue culture models allow for transcriptome profiling of cellular responses to drug challenge, offering both a human-derived and cell-specific system for defining drug pathways, modes of action and neuronal plasticity within the brain. Mood modifying drugs may have a single mode of action or exert their effects through multiple mechanisms in a concentration dependent manner. Principle mechanisms of drug action include modulation of intracellular signalling pathways and neurotransmission; targeting voltage-gated ion channels, 7-transmembrane G-protein coupled receptors or neurotransmitter metabolic enzymes, which ultimately lead to the modulation of transcription factors controlling the expression of genes encoding growth factors, neurotrophic factors, ion channels and other proteins involved in neuronal function. *In vitro* assessment of the transcriptional responses of key mood disorder genes following exposure to the mood stabilisers lithium and sodium valproate and the psychostimulants amphetamine and cocaine are investigated in *Chapter 5* of this thesis as a means of assessing pathways implicated in neuronal and behavioural plasticity.

### 1.4.1 Mood stabilisers

Mood stabilisers are drugs that are used in the clinical treatment of manic-depressive disorders. Lithium and sodium valproate are two widely used mood stabilising drugs; lithium is a simple monovalent cation used as the first choice drug for the treatment of bipolar disorder, whereas valproate is a simple branched-chain fatty acid (2-propylpentanoic acid) used in the treatment of epilepsy and acute mania. Both drugs are used in augmentation therapy for depression and in preventative treatment of manic-depression (Fountoulakis et al., 2005), and share overlapping mechanisms of action involving the integration of second-messenger systems and neurotransmitter pathways which are thought to be central to their stabilising and neuroprotective effects. The exact mechanism of action remains unclear for both lithium and valproate; however their modulation of protein kinase signalling cascades and downstream effects on the expression of transcriptional regulators and genes important in synaptic plasticity and neurogenesis are well documented.

One of the earlier theories on lithium's therapeutic mode of action relate to its inhibitory affect over the phosphoinositide pathway termed the 'inositol depletion hypothesis' (Berridge et al., 1989), which postulates that lithium exerts its therapeutic effect through cell-specific depletion of *myo*-inositol leading to subsequent alterations in the activity of downstream inositol phosphates, protein kinase C (PKC) signalling and modulation of signal transduction cascades important in neural plasticity. Dysregulation of PKC distribution and activation, and abnormal receptor-G protein coupling have been implicated in the pathophysiology of bipolar disorder, with lithium treatment alleviating such impairments (Lenox, 1987, Manji and Lenox, 1994,

Manji et al., 1993, Friedman et al., Lenox and Wang, 2003, Hahn et al., 2005). Other molecular targets inhibited by the action of lithium include glycogen synthase kinase-3β (GSK3β) and adenylate cyclise (AC). Lithium-induced inhibition of GSK3β, an essential component of the canonical Wnt/β-catonin signalling pathway, has been shown to stabilise β-catonin which mediates Wnt-dependent transcriptional activation of genes involved in neurogenesis and neuroprotection against several cellular stressors including glutamate excitotoxicity and β-amyloid toxicity (Forde and Dale, 2007, Chuang et al., 2002, Chuang et al., 2011, Wan et al., 2014, Marchetti et al., 2013). The effect of lithium on the AC second-messenger system results in stabilisation of cyclic AMP (cAMP) through modulation of different AC subtypes dependent upon the state of neural activation (Dousa and Hechter, 1970, Newman and Belmaker, 1987, Mann et al., 2008, Mann et al., 2009). The bimodal affect of lithium on cellular levels of cAMP have been proposed as one mechanism through which this mood stabiliser can be used in the treatment of both mania and depression (Jope, 1999). It has been proposed that the inhibitory effect of lithium on several cellular transduction pathways is the result of $Li^{+}/Mg^{2+}$ competition for sites on biomolecules involved in second-messenger systems due to their similar physicochemical properties (Mork and Geisler, 1987, Ramasamy and de Freitas, 1989, Mota de Freitas et al., 1994, Amari et al., 1999). In addition, lithium has also been shown to inhibit voltage-dependent sodium channels independent of the effects of GSK3β (Yanagita et al., 2007). NRSF is a regulator of voltage-gated sodium channel transcription and signalling and has been shown to be modulated in response to lithium treatment in mouse neural stem cells (Mori et al., 1992, Chong et al., 1995, Ishii et al., 2008, Nadeau and Lester,

2002), suggesting lithium-induced modulation of neuronal gene expression along the NRSF-signalling pathway.

Lithium has also been shown to modulate neurotransmission, in part through mechanisms involving second-messenger signalling, reducing excitatory dopaminergic and glutamatergic pathways (Dunigan and Shamoo, 1995, Fonseca et al., 2009) and increasing serotonergic and GABAergic pathways (Scheuch et al., 2010, Malhi et al., 2013). In addition, lithium induces the up-regulation and secretion of cortical BDNF and activation of its receptor TrkB (tropomyosin-related kinase-B) (Hashimoto et al., 2002), which correlated with inhibition of GSK3β and is thought to be perquisite for lithium's neuroprotective effects (Chuang et al., 2011). Binding of BDNF to its receptor activates the ERK (extracellular signal-regulated kinase), PI3K (phosphoinositide 3-kinase) and PLC (phospholipase C) signalling pathways, mediating a range of cellular processes important for neuronal survival, differentiation, synaptic transmission and long-term potentiation (Blum and Konnerth, 2005). Independent studies have also shown lithium-induced activation of the ERK-signalling pathway and downstream modulation of transcriptional regulators important in neuronal function such as AP-1 (activator protein-1), CREB (cAMP response element-binding protein) and NRSF (Ozaki and Chuang, 2002, Einat et al., 2003, Ishii et al., 2008) which are important modulators of the BDNF-signalling pathway. Other NRSF target genes, including TAC1 which encodes for substance P, have also been shown to be modulated in response to lithium (Haddley et al., 2011).

Sodium valproate is a histone deacetylase (HDAC) inhibitor used as a broad spectrum drug in the treatment of a wide range of seizure types and

epilepsy syndromes (Kwan et al., 2001). The exact mechanisms of action for the anticonvulsant properties of valproate are yet to be fully elucidated and are attributed to its inhibition of voltage-gated sodium channels and increased activation of GABAergic neurotransmission (Johannessen, 2000). In its role as a mood stabiliser, valproate has been shown to have several overlapping mechanisms of action with lithium, including depletion of inositol, activation of ERK-signalling, reduced PKC activation, increased expression of BDNF and modulation of transcription factors AP-1 and CREB (Rouaux et al., 2007, Chen et al., 1999, Hahn et al., 2005, Einat et al., 2003, Fukumoto et al., 2001, Shaltiel et al., 2004). Valproate has also been shown to activate Wnt-dependent gene expression however, distinct from the action of lithium, this involves inhibition of HDACs as opposed to GSK3β (Phiel et al., 2001). Several studies have also demonstrated valproate-induced inhibition of GSK3β, however this may reflect its role in modulating epigenetic parameters (Rosenberg, 2007).

### 1.4.2 Psychostimulants

Psychostimulants such as cocaine and amphetamine have been used to mimic human psychosis in animal models of schizophrenia (Pihlgren and Boutros, 2007). This is largely based on the pharmacological actions of these drugs on the dopaminergic pathway resulting in extracellular increases in dopamine within mesostriatal and mesolimbic areas of the brain (Giros et al., 1996), a mechanism comparable to the 'dopamine hypothesis' of schizophrenia which postulates that the underlying disease aetiology reflects perturbations in the prefrontal cortex resulting in exaggerated dopamine release in subcortical regions (Howes and Kapur, 2009). Mesocortical and mesolimbic dopaminergic

projections from the ventral tegmental area (VTA) of the midbrain innervate several structures within the limbic lobe (such as the amygdala and nucleus accumbens) and mPFC which are areas implicated in cognition, reward and locomotion (Oades and Halliday, 1987). High doses of these drugs can result in transient stimulus-induced psychotic episodes which reflect the positive symptoms of schizophrenia, including delusions, hallucinations and paranoia, in individuals free of neuropsychiatric diathesis and also provoke or exasperate such symptoms in schizophrenic individuals at much lower drug thresholds than in non-schizophrenics (Lieberman et al., 1990, Serper et al., 1999). In addition, acute and chronic cocaine abuse has also been associated with negative symptoms of schizophrenia such as social withdrawal and also affective symptoms such as anxiety and depression both in schizophrenic and non-schizophrenic individuals (Serper et al., 1999) which may reflect its modulation of several neurotransmitter pathways including the monoamines (dopamine, noradrenaline and serotonin) and glutamatergic synaptic transmission (Serper et al., 1999, Fernandez-Castillo et al., 2012). Cocaine is a lipophilic alkaloid that mainly exerts its psychomotor effects through blockade of the dopamine transporter (DAT) (Ritz et al., 1987, Horn, 1990), a protein which functions to modulate the spatiotemporal activity of dopamine through rapid reuptake of this neurotransmitter into the pre-synaptic terminals of dopaminergic neurons for recycling or degradation by monoamine oxidase (Meiser et al., 2013). In contrast to cocaine, amphetamine results in increased extracellular dopamine levels through stimulating its release from pre-synaptic nerve terminals as opposed to inhibiting its reuptake. Amphetamine belongs to the class of drugs called the β-phenylethylamines and shares a similar chemical

structure to that of noradrenaline and dopamine. Consistent with this, amphetamine has been shown to non-selectively release monoamines from rat brain tissues slices and synaptomosomes (Heal et al., 2013).

Recent evidence suggests that the medium- to long-term changes in neuroplasticity in response to psychostimulants, a mechanism implicated in models of addiction, reflects alterations in glutamatergic neurotransmission within the VTA to the amygdala, PFC and nucleus accumbens (Kalivas, 2004). In support of this, a study in rat midbrain slices showed that acute cocaine resulted in a delayed increased N-methyl-D-aspartate (NMDA) glutamate receptor activation in the VTA via a $D_5$ receptor-dependent pathway involving cAMP/PKA (protein kinase A) signalling (Schilstrom et al., 2006). Acute cocaine and amphetamine administration in mice also results in reduced phosphorylation of GSK3β in the ventral striatum and cerebral cortex, resulting in its increased activation which is dependent upon both dopaminergic and glutamatergic receptor signalling in terms of cocaine (Miller et al., 2014, Mines and Jope, 2012). This is in contrast to the role of the mood stabilisers lithium and valproate that inhibited GSK3β activity. The overlapping pathways targeted by these mood modifying drugs suggests that common neuronal networks may be involved in the stabilisation of mood and that modulation of these may be important mechanisms in the development of adverse behaviours to drugs of abuse such as addiction. Throughout this thesis we use cocaine as our cellular challenge of choice as it is a robust model for studying stimulus-induced activation of pathways linked to mood, psychosis, cognition and cellular stress (Vasiliou et al., 2012, Pihlgren and Boutros, 2007, Spronk et al., 2013). It is also well documented that several NRSF target genes including BDNF (Le Foll et al.,

2005, Liu et al., 2006), which is addressed in *Chapter 3*, are modulated by cocaine and that miRNA-mediated pathways (see *Chapter 4* for modulation of miR-137 in response to cocaine) may be important regulators of such cocaine-induced plasticity genes (Chandrasekar and Dreyer, 2009). Furthermore, NRSF has been implicated in both dopaminergic and glutamatergic signalling pathways through its targeting of dopamine-beta-hydroxylase and several glutamate receptor subunits (Roopra et al., 2001), suggesting a key role for this transcription factor in processes relevant to mood as discussed in *Chapter 5*.

## 1.5 Polymorphic variation as a biomarker for CNS disease

Recent advances in GWAS and next generation sequencing technologies have provided great insight into the genetic underpinnings of complex diseases, with many common (low risk), rare (moderate to high risk) and *de novo* disease-susceptibility variants being identified and replicated across several neuropsychiatric disorders. The focus has been largely based on the influence of SNPs involving substitution of one nucleotide base for another within the DNA sequence. Such studies utilise genotyping platforms to measure in the range of 1 million common SNPs to identify risk loci that have significantly different genotype frequencies between individuals with a particular disease or pathological trait compared to the general population. Linkage disequilibrium (LD) analysis shows that associated SNPs can represent a large genetic region conferring risk due to the fact that SNPs in close proximity within the genome are inherited as a block. It is therefore a difficult challenge to identify which markers within a region of strong LD are biologically important for disease processing. Meta-analyses of GWAS have shown that approximately 88% of

trait/disease-associated SNPs are located within intronic or intergenic regions of the genome (Hindorff et al., 2009), with the majority of genome-wide risk loci identified from LD analysis also being non-coding (MacKenzie et al., 2013).

Considerable efforts have been made to overlap GWAS data with *cis*- and *trans*-regulatory domains identified through the ENCODE (Encyclopaedia of DNA Elements) project, a resource which details functional elements within the genome including protein-coding and non-coding transcripts, DNase I–hypersensitive sites, active histone marks and transcription factor binding sites (TFBS) (The ENCODE Project Consortium, 2011). A recent study which mapped chromatin marks in nine different cell lines showed a two-fold enrichment of GWAS SNPs within predicted enhancer regions (Ernst et al., 2011), suggesting that the biological significance of these polymorphisms reflects their impact on regulatory mechanisms. **Figure 1.2** summarises the potential functional effects of polymorphisms dependent upon their location within the genome. Despite their success, GWAS only account for a small portion of the heritability behind complex disorders (Manolio et al., 2009). This may reflect several factors including the contribution of SNPs not captured on commercial SNP-arrays, other common sources of genetic variation such as DNA tandem repeats and copy number variations, epistasis (gene-gene interactions), epigenetics and GxE interactions; all of which have been implicated in disease susceptibility and are thought to contribute towards the so called 'missing heritability' (Hannan, 2010, Breen et al., 2008, Kaminsky et al., 2009, Wei et al., 2011, Gray-McGuire et al., 2000, Stefansson et al., 2009). DNA tandem repeats are frequent within the human genome accounting for an estimated 3% of the genomic sequence which is more than the sum of protein-coding sequence (~1%) (International Human

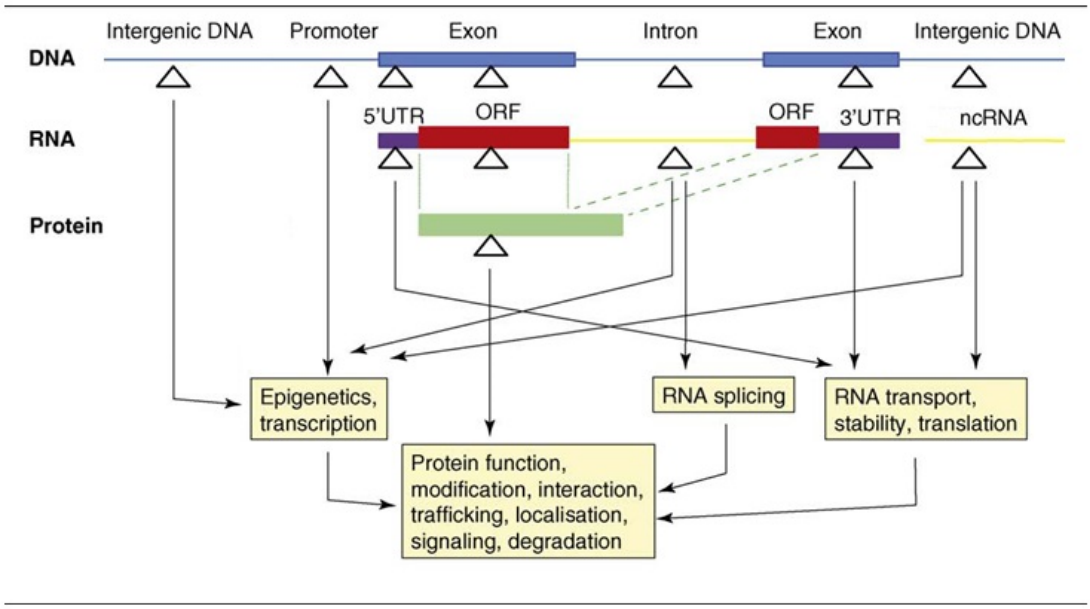


**Figure 1.2. Locations of polymorphisms in the genome and their potential effects.** Polymorphisms (e.g. single nucleotide polymorphisms, tandem repeat polymorphisms) are indicated by triangles and can be located in exons, introns or intergenic regions. They have the potential to modulate the levels of gene expression (e.g. through altering the composition of binding sites for transcription factors or epigenetic regulators), particularly when located in cis-trans regulatory elements such as those found within promoter regions (cis) or acting from a distance within intergenic regions (trans). When located within coding sequences, polymorphisms can alter the structure and function of RNAs and proteins (e.g. codon repeats translated into amino acid runs as seen in trinucleotide repeat expansion disorders such as Huntington's disease). Thus, a wide range of molecular processes can be disrupted at the DNA, RNA and protein levels due to the effects of genetic variations. Abbreviations: *ncRNA, non-coding RNA; ORF, open reading frame; UTR, untranslated region*. Figure adapted from Hannan (2010).

Genome Sequencing Consortium, 2001). They include the microsatellites which have short motif lengths between 1-6 bp and minisatellites of longer motif lengths. Both microsatellites and minisatellites are frequently polymorphic in nature and are often termed VNTRs, however strictly speaking VNTRs represent only the minisatellites. Microsatellites and minisatellites are respectively thought to arise through DNA-replication slippage (transient dissociation of the replicating DNA strands followed by misalignment re-association) and unequal-crossing-over or gene conversion events (non-reciprocal exchange of genetic material among chromosomes) (King et al., 1997). VNTRs have been shown to exhibit several functional properties, including transcriptional regulation (Haddley et al., 2008), alternative splicing (Lian and Garner, 2005), recombination (Harding et al., 1992) and disease processing (Bowater and Wells, 2001). The latter is best exemplified through the trinucleotide repeat expansion disorders, such as Huntington's disease, in which the associated repeats show somatic and germline instability (Orr and Zoghbi, 2007). Genetic variation within the coding sequence of a gene which alters the primary sequence of a protein has allowed tremendous insight into the underlying mechanisms associated with predisposition, progression and severity of diseases. As with the case of Huntington's disease, expansion of a translated CAG repeat containing more than 35 copies encodes for the mutant huntingtin (Htt) protein, with repeat length of the expanded allele inversely correlating with age of onset in a dominant fashion (Lee et al., 2012). VNTRs with non-coding sequences have also been identified as being mechanistically involved in disease processing, such as the Amyotrophic lateral sclerosis (ALS)

associated CCCCGG repeat expansion in the C9ORF72 gene (DeJesus-Hernandez et al., 2011).

Variable repeats are enriched within functional regions of the genome, such as gene promoters and enhancers (Breen et al., 2008), and have been shown to contribute towards phenotypic traits such as behaviour. The well-characterised human 5-HTTLPR (serotonin-transporter-linked polymorphic region) and STIN2 (second intron of the serotonin transporter) VNTRs within the 5-HTT gene locus are prime examples of copy number variants respectively found within promoter and enhancer sequences, identified as both clinical correlates for behavioural disorders and as allele-specific and stimulus-inducible modulators of reporter gene expression (Haddley et al., 2008, Klenova et al., 2004, Roberts et al., 2007, Ali et al., 2010, Collier et al., 1996). The regulatory potential of such repetitive domains is not surprising considering their capacity for encoding numerous recognition sites within their sequence motifs which may bind factors that interact with DNA such as transcription factors, polymerase, splicing factors and microRNAs (miRNAs). *In silico* analysis predicts that VNTRs are more represented than SNPs for overlapping conserved TFBS and, on average, VNTRs encode for approximately two TFBS with many encoding for more (Breen et al., 2008). Therefore with increasing repeat length VNTRs may bind multiple copies of a transcription factor or influence the likelihood of keeping them bound to the DNA, supporting a role in the modulation of gene expression. Again, this can be demonstrated from our own studies on the 5-HTT VNTRs which display allele-specific and stimulus inducible binding of transcriptional regulators including CTCF (CCCTC-binding factor), MeCP2 (methyl-CpG–binding protein 2), YB-1 (Y box binding protein 1)

and HDACs *in vitro* (Vasiliou et al., 2012, Roberts et al., 2007, Ali et al., 2010, Klenova et al., 2004). Further, the highly polymorphic nature (suggestive of high mutation rates) and regulatory capacity of these two VNTRs supports the hypothesis that repeat variation is an evolutionary mechanism that allows for rapid adaptation of phenotypic traits in response to environmental changes through tandem repeat mutations (King et al., 1997, Fondon et al., 2008). In *Chapter 4*, a VNTR within the genome-wide associated schizophrenia candidate gene MIR137 is investigated as a clinical correlate for schizophrenia, as has been done previously with the 5-HTT variants. Both genetic association and functional analysis of allele-specific differences in transcriptional regulation over the region are explored to address potential GxE mechanisms operating at this repetitive domain which may uncover important disease pathways involved in neurological dysfunction.

## 1.6 Gene-environment interactions in the CNS

In addition to the role of genetic variation in predicting disease risk, epidemiological studies have also identified a number of important environmental pathogens (e.g. early life trauma, lifestyle, urban upbringing) and it is widely accepted that interplay between genes and environment is an important determinant in disease aetiology and may explain the 'missing heritability' of common disorders; that is the failure—so far—to uncover specific polymorphic variants that account for the substantial genetic influences on particular traits/disease phenotypes identified from twin and family studies. The synergistic effect of genotype and environmental exposure in the modulation of physical and psychological health is referred to as gene-

environment interactions or GxE (Moffitt et al., 2005). The transcriptional machinery, which forms the genetic side of the GxE equation, has evolved to mediate the cellular responses to environmental challenge through induction, repression or modulation of neuronal gene expression. Superimposed on this, genetic polymorphisms within neuronal pathways can influence the GxE component through allele-specific differential regulation of gene expression and therefore have the potential to modify several processes implicated in behaviour. Polymorphisms can thus act as predisposing factors in the aetiology of neuropsychiatric disease by sensitising individuals to certain environmental stressors (Quinn et al., 2013, Hill et al., 2013). Environmental factors not only influence immediate transcriptional responses but can also potentiate medium to long-term affects through modulation of epigenetic parameters. Epigenetics refers to changes in gene expression or cellular phenotypes brought about by chemical modifications to the DNA and its associated histone proteins, independent of changes to the composition of the underlying nucleotide sequence. Such 'accessorising' of the genome is important in developmental processes such as the establishment of cellular identity and the hardwiring of neuronal circuitries within the brain. Epigenetic mechanisms are also important in the mature nervous system and are thought to play essential roles in modulating neuronal plasticity and lasting states of neuronal gene expression (Borrelli et al., 2008).

## 1.7 Epigenetics: Bridging the GxE response in neurological disease

It is widely accepted that any approach to understanding the mechanisms of transcriptional regulation in eukaryotic cells has to take into account that nuclear DNA is condensed and packaged into nucleosomes, the repeating structural units of chromatin, by wrapping around a histone octomer core composed of the four canonical histone proteins H2A, H2B, H3 and H4 (Luger et al., 1997). When a gene goes from an inactive to an actively transcribing state, chromatin remodelling is required to allow binding of the basal transcriptional machinery and other regulatory factors to the underlying naked DNA sequence, which is often inaccessible due to the presence of nucleosomes. During transcription, several chromatin remodelling mechanisms permit access to the underlying nucleasomal DNA including: unwrapping or lifting of the DNA from the surface of the histone octamer, partial or entire nucleosome ejection and translational repositioning (sliding) of the histone octamer along the DNA (Saha et al., 2006). In addition to nucleosome remodelling, histones acquire distinct epigenetic signatures, including acetylation of lysine side chains, methylation of lysines and/or arginines and phosphorylation of serines, which provide a molecular platform for readers of the histone code which mediate appropriate transcriptional responses. Simplistically, depending on the nature of its associated epigenetic marks, chromatin will adopt an open or closed conformation, mediated through the action of the transcriptional machinery, resulting in gene activation or repression respectively. Chromatin remodelling and histone modifications are

not mutually exclusive of each other, as it has been demonstrated that the latter serves as a coded mark to elicit the former during transcriptional activation (Riffo-Campos et al., 2015).

Epigenetic mechanisms, including DNA methylation, histone modifications and ncRNA-mediated processing, have been identified as dynamic modulators of neuronal gene expression and function. They link environmental experiences to genetic effects through modulation of cellular gene expression profiles (**Figure 1.3**). Cross-talk between multiple epigenetic parameters is important in the regulation of neuronal development and adult neurogenesis (Jobe et al., 2012, Szulwach et al., 2010), both of which have been implicated in the pathogenicity of neuropsychiatric disorders (Jun et al., 2012). NRSF is an important player in this dynamic regulatory network in part due to its interaction with miRNAs (see *section 1.8.5*) (Wu and Xie, 2006, Packer et al., 2008, Conaco et al., 2006, Johnson et al., 2008) and chromatin remodelling complexes (see *section 1.8.2*) (Ballas et al., 2005) which together orchestrate gene regulation through altering chromatin structure. Disruptions in epigenetic regulatory networks have been implicated in the aetiology of many common diseases including cancer and disorders of the CNS (Urdinguio et al., 2009, Kubota et al., 2012). Rett syndrome, an X-linked neurodevelopmental condition associated with mutations in the gene encoding MeCP2, is one such disorder characterised by epigenetic dysregulation (Zachariah and Rastegar, 2012). Several common neuropsychiatric conditions have also been attributed to neurodevelopmental causes and may also be linked to aberrant epigenetic signalling induced by genetic mutation and/or environmental pathogens. In support of this, studies of both maternal stressors during pregnancy in human

subjects and maternal separation in rodents suggest that epigenetic signatures established during early life experiences can influence infant and adult behaviours (Weaver et al., 2004, Murgatroyd and Spengler, 2011, Hill et al., 2013), which may manifest as a neuropsychiatric condition in response to particular environmental stressors.

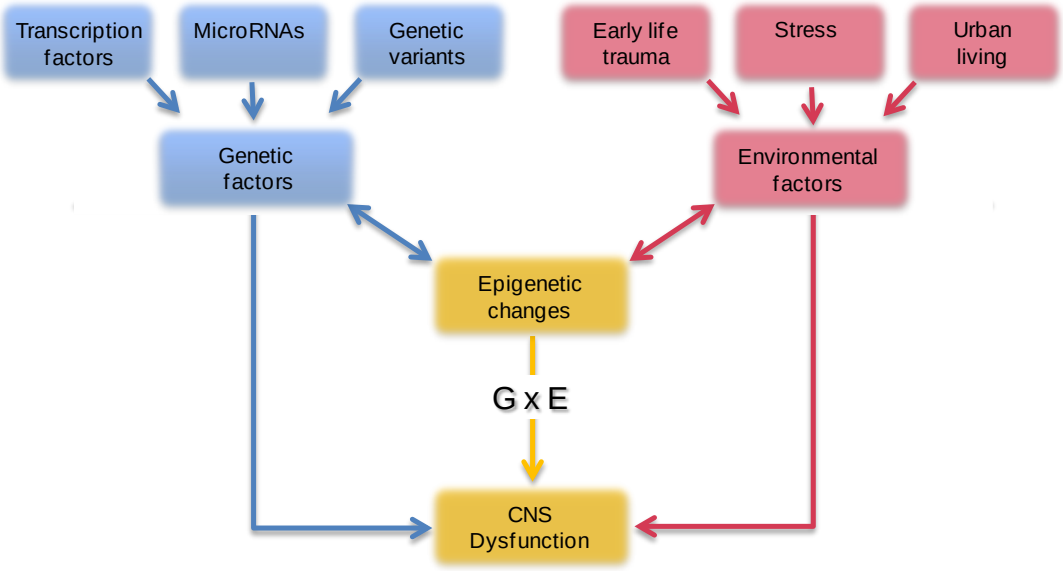


**Figure 1.3. Gene-environment interactions (GxE) in neurological disease.** Genetic and environmental factors, or interplay between the two, can predispose an individual to neurological impairments through altering cellular gene expression profiles. Genetic variants embedded within neuronal pathways have the potential to regulate the transcription of genes implicated in behavioural processes which may lead to sensitisation of an individual to certain environmental stressors. Epigenetic mechanisms, such as histone modifications and DNA methylation, can bridge the GxE response through laying down a molecular signature of an environmental experience which can underpin behavioural, neuroendocrine and stress responses throughout later life. This in turn will be exacerbated by intrinsic (age, sex) and/or extrinsic (drugs, stress, lifestyle) factors which may manifest as a neurological condition.

## 1.8 The NRSF signalling pathway

NRSF is a key transcriptional regulator involved in modulating several neuronal processes important for CNS integrity. It predominantly functions as a silencer of neuronal gene expression in differentiated non-neuronal cells through binding of a conserved motif termed the RE1 (repressor element-1) or NRSE (neuron restrictive silencing element) (Chong et al., 1995, Schoenherr and Anderson, 1995) located within the regulatory regions of its target genes (see *section 1.8.1*); however increasing evidence also supports a role for NRSF in neuronal gene activation within the CNS. The regulatory capacity of NRSF has extended from the initial definition of 'master regulator' of neuronal gene expression to include many biological processes including neurodevelopment, adult neurogenesis and neuronal plasticity (Kuwabara et al., 2004, Ballas et al., 2005, Gao et al., 2011). It has also been implicated in many disease processes from disorders of the CNS to cancer were it has been proposed to act as both a tumour suppressor and oncogene dependent upon cellular context and isoform usage (Negrini et al., 2013, Coulson et al., 2000, Wagoner et al., 2010), as discussed in *Chapter 6*. Maintaining the balance between different NRSF isoforms within the cell may be paramount to its role in disease processing, as suggested from our work on small cell lung cancer (SCLC) and epilepsy, see *section 1.8.4* (Spencer et al., 2006, Gillies et al., 2009, Coulson et al., 1999, Coulson et al., 2000).

### 1.8.1 The NRSE

The canonical NRSE is a highly conserved 21 bp sequence motif which has been shown from *in silico* analysis and ChIP-seq studies in Jurkat human T cells and human embryonic stem cells (ESCs) to overlap with more than 2,000 known genes within the human genome (Bruce et al., 2004, Johnson et al., 2007, Satoh et al., 2013), many of which are enriched in processes relevant for neuronal function, **Figure 1.4**. It was initially discovered by two independent groups in the genes encoding voltage-dependent sodium channel type II-alpha (SCN2A) and superior cervical ganglion 10 (SCG10) were it was defined as an element capable of mediating transcriptional repression in non-neuronal cells (Chong et al., 1995, Schoenherr and Anderson, 1995, Mori et al., 1992). Approximately 15% of human NRSEs are located within gene promoters, defined in this instant as regions within 5 Kb upstream of the transcriptional start site (TSS), however the majority are found within intergenic regions (40%) (Jothi et al., 2008), **Figure 1.5**, suggesting they may function as trans-regulatory elements. Unlike many other TFBS, NRSEs are non-symmetrical and can be subdivided into two half-sites by a non-conserved central region at residues 10-11, **Figure 1.5**. These half-sites have been shown to bind NRSF however they are non-functional in terms of their individual repressive capabilities (Jothi et al., 2008, Johnson et al., 2007), suggesting the necessary role of co-binding factors in NRSF-mediated gene repression (Timmusk et al., 1999, Zuccato et al., 2003), which are discussed in *section 1.8.2*.

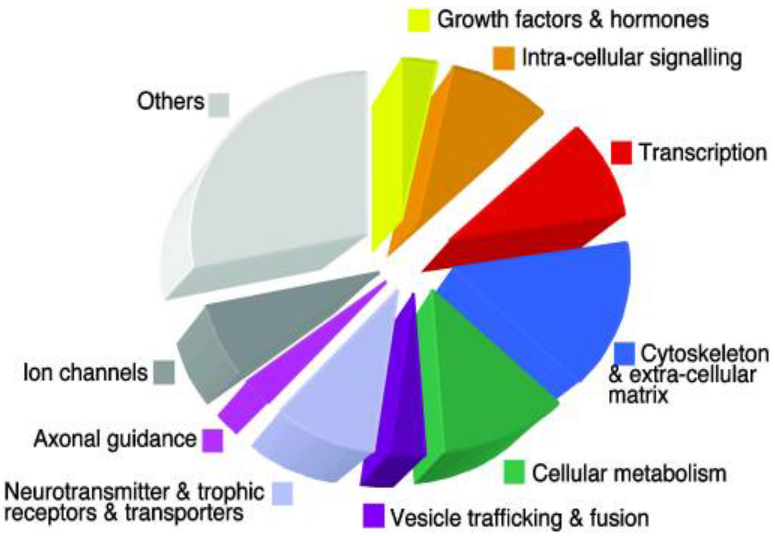


**Figure 1.4. Functional assignment of putative NRSEs within the human genome.** Many NRSE-containing genes identified from *in silico* and ChIP-seq analyses encode for proteins involved in neuronal processes including neurotransmission (e.g. M4 muscarinic, DRD3 and GABA type β3 receptors; GABA transporter 4), neurotrophic factor pathways (e.g. BDNF and NTRK3), vesicle trafficking and fusion (e.g. SNAP25; synaptotagmins IV, V and VII; syntaxin 8 and Rab3), ion channel signalling (e.g. sodium, potassium and calcium subunits) and axonal guidance (e.g. SCG10, netrin-2 and roundabout). Overlap of NRSF target genes identified from ChIP-seq studies in human T-lymphocytes (Johnson et al., 2007) and embryonic stem cells (Satoh et al., 2013) identified corticotropin releasing hormone signalling, glutamate receptor signalling, calcium signalling, synaptic long-term depression and circadian rhythm signalling as the top 5 most significant pathways, all of which are important for neuronal function. There are also many genes that encode proteins that do not have obvious neuron-specific functions, such as those involved in cellular metabolism, or that specify proteins that are expressed in both neuronal and non-neuronal tissues (e.g. nitric oxide synthase involved in the regulation of cardiovascular tone). Figure taken from *Bruce et al.* (2004). *Abbreviations: BDNF, brain derived neurotrophic factor; DRD3, dopamine D3; GABA, gamma-aminobutyric acid; NRSE, neuron restrictive silencing element; NTRK3, neurotrophic tyrosine kinase receptor type 3; SNAP25, synaptosomal-associated protein, 25 kDa*.

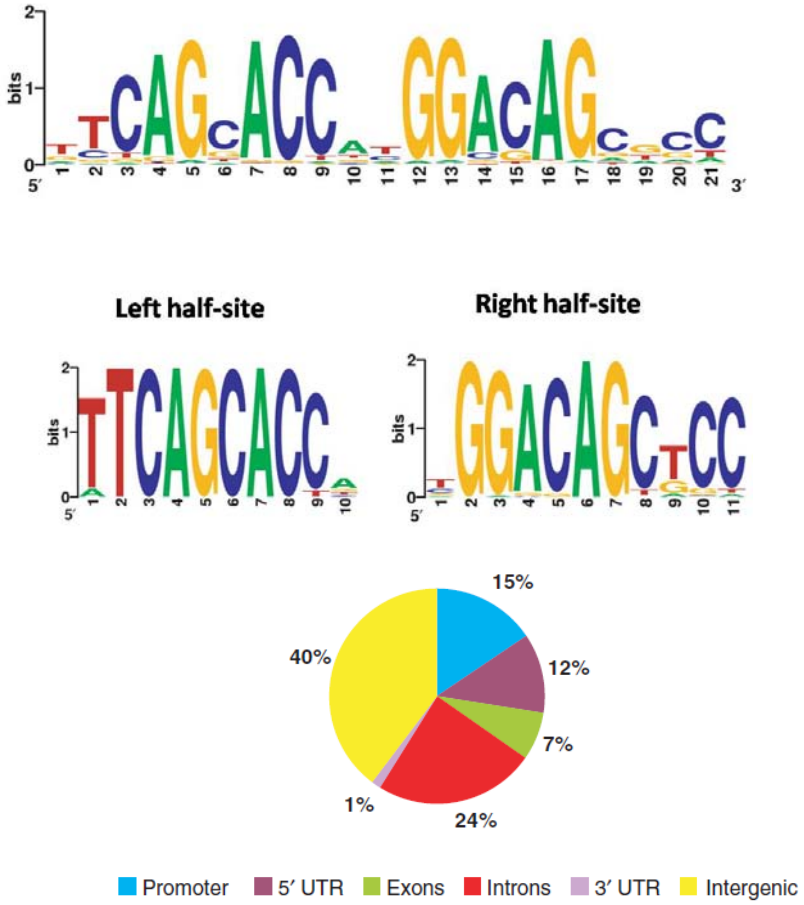


**Figure 1.5. The NRSE consensus sequence and genomic distribution.** *Top*, the canonical 21 bp NRSF binding site found within NRSF target genes (Wu and Xie, 2006). Residues 7-9 (ACC) and 12-17 (GGACAG) are thought to be essential for DNA binding, with residues 1-6 (TTCAGC) functioning in binding stability. *Bottom*, Division of the NRSE into two functional half sequences, termed the left-half and right-half sites. NRSF occupancy at either of these two sites is thought to result in weaker binding affinity compared to binding at the canonical sequence. *B*, Distribution of NRSF binding sites across the human RefSeq reference genome according to Jothi et al. (2008). Promoters were defined as the region 5 Kb upstream of the transcriptional start site.

Other non-canonical NRSEs have been described from computational predictions based on position weight matrices (PWMs); probabilistic representations of signals in DNA or protein sequences which can be used to model approximate patterns of DNA-protein or protein-protein interactions, and ChIP-seq assays which vary in their central residues by 3-9 bp insertions (Zheng et al., 2009). Interestingly, these motifs have been shown to not only bind NRSF but can also mediate transcriptional regulation (Otto et al., 2007, Johnson et al., 2006, Patel et al., 2007) suggesting that such bipartite NRSEs could facilitate differences in gene expression and may present hotspots for phenotypic evolution (Wray et al., 2003). In support of this, polymorphisms within NRSEs have been shown to encode DNA binding affinity hierarchies, resulting in differential modulation of genes important in lineage-specific and developmental processes (Bruce et al., 2009). This coincides with earlier studies whereby point mutations in NRSEs located proximal to (within 2 Kb) the transcription start site of key genes involved in neuronal function, including the SCN2A, SCG10, nicotinic acetylcholine receptor β2-subunit and BDNF, resulted in up-regulation of reporter gene expression *in vitro* and/or *in vivo* (Kraner et al., 1992, Mori et al., 1992, Bessis et al., 1997, Tabuchi et al., 1999). Consistent with these findings, Quinn et al. (2002) identified NRSE-like motifs within close proximity of the major TSS of the neuropeptide genes AVP (arginine vasopressin), TAC1 (tachykinin 1) and more recently TAC3 (tachykinin 3) that could support differential gene expression *in vitro*, which was speculated to reflect both the location and variation in the 3'sequences of these motifs relative to the classical NRSEs found within the SCN2A and SCG10 genes (Coulson et al., 1999, Quinn et al., 2002, Gillies et al., 2009). A potential

role for the truncated isoform sNRSF was also proposed at these regulatory domains, which is discussed further in *section 1.8.4.1*. These data collectively suggest that the primary sequence of the NRSE dictates the function of these regulatory domains within a particular cell type, supporting a role for NRSF in processes other than transcriptional repression. This would be consistent with expression of NRSF within the brain and in differentiated neuronal cells which goes against its originally proposed function as a silencer of neuronal gene expression in non-neuronal cells (Chong et al., 1995, Mori et al., 1992, Schoenherr and Anderson, 1995).

### 1.8.2 Regulation of target genes by NRSF

NRSF is a member of the Krüppel-type zinc finger family which binds to its target motifs through its eight zinc-finger DNA binding domain, whereas repressor activity, as dogma suggests, is mediated through recruitment of co-repressor complexes to either its amino (N)-terminal or carboxy (C)-terminal repressor domains (Naruse et al., 1999, Tapia-Ramirez et al., 1997). A schematic of the structural organisation of full-length NRSF and the truncated isoform sNRSF is shown in **Figure 1.6**. The N-terminal of NRSF interacts with the transcriptional co-repressor mSin3A (mammalian homologue of yeast Sin3A) (Huang et al., 1999, Naruse et al., 1999, Grimes, 2000) which mediates active gene repression through its recruitment of HDAC1/2 (Ballas and Mandel, 2005), whereas the C-terminal potentiates long-term gene silencing through its interaction with CoREST (cofactor for REST/NRSF) (Andres et al., 1999, Lunyak et al., 2002), **Figure 1.6**. CoREST activates the recruitment of other chromatin-modifying partners involved in gene repression, such as HDAC1/2, the histone

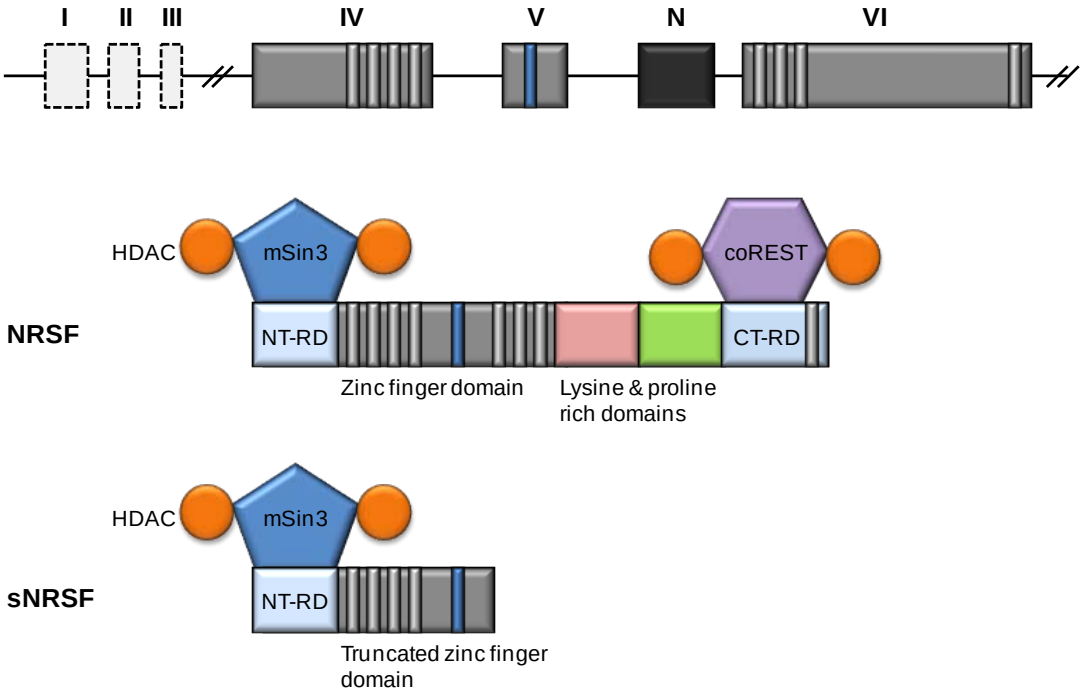


**Figure 1.6. Structural organisation of NRSF and sNRSF.** Schematic representation of the NRSF gene structure and the full-length NRSF and truncated sNRSF transcripts. *Top*, The human NRSF gene has three alternative 5' exons (I-III) which gives rise to different protein isoforms. Exons are represented as boxes and introns as the interconnecting lines. Vertical bars within exons denote the nine zinc finger motifs which are associated with DNA binding (grey bars) and nuclear targeting (blue bar). Alternative exon N is present in the sNRSF splice variant and introduces a premature stop codon, giving rise to the truncated protein variant. *Middle*, The full-length NRSF protein comprises an amino-terminal repressor domain (NT-RD), a DNA binding domain composed of eight zinc fingers, a lysine and proline-rich domain and a carboxy-terminal repressor domain (CT-RD) containing the ninth zinc finger motif. The mSin3 and coREST co-repressor proteins interact with the NT-RD and CT-RD of NRSF, respectively, initiating the recruitment of cofactors involved in chromatin remodelling such as histone deacetylases (HDACs), enabling NRSF to orchestrate a set of epigenetic signatures that alter gene expression profiles in the medium- to long-term. The mSin3-HDAC complex is associated with transient neuronal-gene repressive states, whereas the coREST-HDAC complex has been implicated in long-term neuronal-gene silencing. *Bottom*, sNRSF lacks four of the nine zinc fingers and the CT-RD.

H3K4 demethylase LSD1 (lysine-specific demethylase 1), the methyltransferase G9a, MeCP2 and the SWI/SNF ATP-dependent nucleosome-remodelling factor BRG1/SMARCA4 and MeCP2 (Lee et al., 2005, Lunyak et al., 2002, Roopra et al., 2004, Battaglioli et al., 2002, Ooi et al., 2006). **Figure 1.7** illustrates some of the major chromatin-modifying partners shown to assemble within the NRSF-signalling complex upon binding of its target DNA sequence, facilitating chromatin condensation and NRSF-mediated gene repression (Ooi and Wood, 2007).

The co-repressor complexes that bind at NRSF target DNA varies between cell-types and promoter sequences meaning that NRSF can mediate both transient repression and long-term gene silencing. In gene repression, certain co-repressors such as CoREST and MeCP2 can remain bound following NRSF dissociation to maintain low levels of neuronal gene expression in certain cell types. The extent to which neuronal genes are de-repressed following dissociation of NRSF and its co-repressors during neuronal differentiation can be used to categorise NRSF target genes. Class I genes are those which are maximally expressed by default upon loss of NRSF binding during neuronal differentiation of ESCs/neural progenitors into cortical neurons implying that NRSF occupancy of their promoter sequences is adequate for their repression (Ballas et al., 2005). Class II genes, such as BDNF, are those that are expressed at lower levels than Class I genes due to the presence of CoREST and MECP2 at methyl CpG sites following dissociation of the NRSF/co-repressor complex from the NRSE site. Upon neuronal activation, MeCP2, mSin3 and HDAC leave the regulatory sequence of some Class II neuronal genes allowing for increased expression levels (Ballas et al., 2005, Ballas and Mandel, 2005). This dynamic

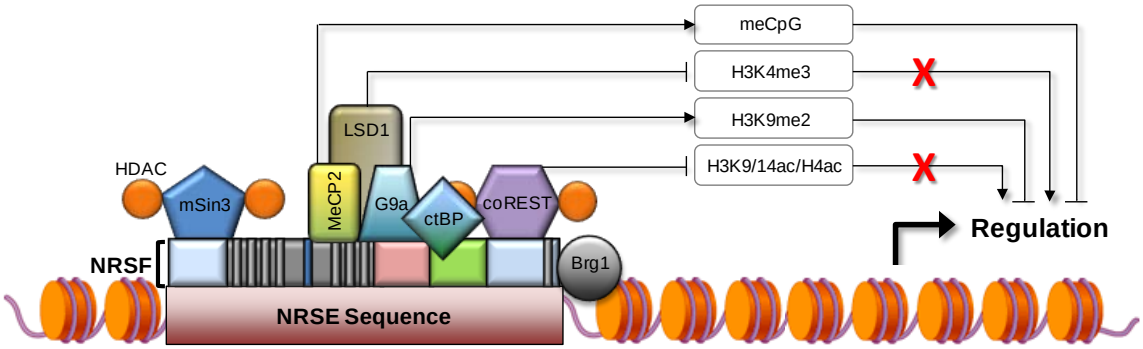


**Figure 1.7. Chromatin remodelling mediated by the NRSF-signalling complex upon interaction with its target DNA**. Following nucleosome repositioning (mechanism uncertain), a process which involves BRG1 (component of the of the SWI/SNF ATP-dependent chromatin-remodelling complex), NRSF binds to its target genes through the NRSE (neuron restrictive silencing element). Recruitment of co-repressor proteins allows for interaction with multiple chromatin remodelling partners including histone deacetylases (HDACs), G9a (histone methyltransferase), ctBP (carboxyl-terminal binding protein; NADH-binding factor) and MeCP2 (methyl-CpG binding protein), enabling NRSF to orchestrate a set of epigenetic signatures which alter the chromatin structure to a condensed heterochromatin state resulting in gene repression. Such repressive epigenetic modifications include: decreased levels of histone acetylation and increased deacetylation, increased methylations at residues known to promote gene repression or silencing (H3K9me2/3 and H3K27me3) and decreased methylations at residues usually involved in gene activation (H3K4me3 and H3K9me1). Depending on cellular context co-activators may be recruited by NRSF, mediating open chromatin structure and gene activation.

regulatory mechanism allows for the orderly expression of neuronal genes during development and permits the fine tuning of neuronal gene expression in response to the cellular environment. It may also be an important mechanism for neural plasticity in mature neurons in response to specific stimuli. Long-term silencing of NRSF target genes is also dependent, in part, upon the NRSF/CoREST/MeCP2 co-repressor complex. Tissue-specific and promoter-dependent associations of this silencing complex at distinct target sequences has been shown to orchestrate methyl CpG-dependent inactive chromatin states across extended chromosomal intervals, including neighbouring genes that do not contain a NRSF binding site, suggesting that this complex may be involved in nucleation and spreading of silenced chromatin states in its role in gene silencing (Lunyak et al., 2002).

In addition to modulating chromatin structure, the NRSF complex can also regulate the rate of transcription. It does this through targeting the basal transcription machinery including the TATA-box-binding protein (TBP), inhibiting the formation of the transcription pre-initiation complex, and RNA polymerase II through the recruitment of small C-terminal domain phosphatases which inhibit polymerase activity of neuronal genes (Murai et al., 2004, Yeo et al., 2005). The role of NRSF and its co-repressors in modulating transcription inhibition is thought to be important in regulating genes in which the NRSE is located far from the corresponding transcription start sites, however the relative contributions of chromatin modification over interaction with the transcriptional machinery in regulating gene expression is not known (Ooi and Wood, 2007).

The role of NRSF as a transcriptional repressor in non-neuronal cells is well documented; however its expression within several mature neuronal cell types suggests that it may have alternative functions other than transcriptional repression within the CNS. It has been proposed that NRSF may also act as a transcriptional enhancer and translational activator dependent upon cellular context, genomic location, isoform usage and associated cofactor binding assemblies at its target sequences (Bessis et al., 1997, Seth and Majzoub, 2001, Kallunki et al., 1998, Yoo et al., 2001, Kim et al., 2008, Spencer et al., 2006, Coulson et al., 1999, Coulson et al., 2000, Gillies et al., 2009). Bessis et al. (1997) showed that in neuronal cells NRSEs can direct transcriptional activation of reporter gene constructs when positioned within 50 bp upstream or 50-250 bp downstream of a synthetic promoter. This effect was not observed in non-neuronal cells or following exogenous expression of NRSF in neuronal cells suggesting that NRSF will act as a transcriptional repressor, regardless of promoter context, when expressed at high levels (Bessis et al., 1997). The role of NRSF as a transcriptional enhancer is supported by previous work in our group relating to NRSF-mediated regulation of neuropeptide gene expression within rat hippocampal neurons and human neuroblastoma cells as discussed in *section 1.8.4*. In addition, it has been demonstrated that NRSF plays a dual role in the activation and repression of the glucocorticoid response *in vitro*; full-length NRSF or its C-terminal domain repressed the hormonal response induced by cortisol treatment across different cell types (chick retinal cells, monkey fibroblast-like cells and human cervical cancer cells), whilst the N-terminal domain enhanced it markedly (Abramovitz et al., 2008). Over-expression of REST4, which is analogous to the truncated human variant sNRSF

and therefore lacks the C-terminal domain, in mouse neuroblastoma cells devoid of detectable levels of the full-length protein similarly enhanced this activity suggesting that the truncated variant may be involved in activation rather than antagonising the activity of full-length NRSF (Abramovitz et al., 2008). This was also demonstrated *in vivo* whereby elevated levels of REST4 in the mPFC of neonatal mice and adult rats correlated with the up-regulation of several NRSE-containing genes including those encoding for miR-9-3, miR-132 and miR-212 (Uchida et al., 2010). Full-length NRSF has also been shown to promote transcriptional activation of neuronal gene targets in differentiating adult hippocampal stem cells through binding of a double stranded ncRNA containing a NRSE site which mediates co-repressor dismissal and recruitment of co-activators (Kuwabara et al., 2004, Ballas and Mandel, 2005). Collectively these data suggest that NRSF is more complex than its initial role in regulating neuronal gene expression in non-neuronal tissues and may serve a dual function as both a repressor and activator of neuronal circuitries not only at the transcriptional level but also post-transcriptionally as suggested from studies on its modulation of the μ-opioid receptor (Kim et al., 2008). It may therefore serve as a mechanism in fine-tuning the expression of key genes implicated in essential biological processes relevant to development, normal physiology and disease.

### 1.8.3 Regulation of NRSF expression

NRSF is highly expressed in embryonic stem cells and is down-regulated upon terminal differentiation of neuronal progenitor cells into neurons. In line with this lineage specific patterning, NRSF has been shown to be necessary for appropriate development as aberrant expression in the developing embryo results in ectopic expression of neuronal genes in non-neuronal tissues and early embryonic lethality (Chen et al., 1998). In mature tissues, NRSF is highly expressed in non-neuronal cells but is also found at much lower levels in specific neuronal tissue types suggesting that its expression is largely dependent upon the cellular and physiological environment. Furthermore, NRSF expression can be up-regulated in different regions of the adult brain, including the cortex, hippocampus and basal nuclei, in response to neuronal activation as demonstrating by treatment with cocaine and the glutamate analogue kainic acid (Chandrasekar and Dreyer, 2009, Palm et al., 1998, Spencer et al., 2006). Low levels of NRSF in mature neurons are maintained through its cytoplasmic sequestering in part through interaction with the Huntingtin (Htt) protein (Zuccato et al., 2003). Despite the extensive number of studies to elucidate the regulatory function of NRSF, relatively few have addressed the modulation of its own expression. Different isoforms encoded from the NRSF gene have been described which arise through alternative splicing of the first three non-coding exons (Palm et al., 1998). Three promoters have also been identified from the region which show high sequence conservation, however none of these appear to support cell– or species-specific expression based on reporter gene analysis in a number of cell lines and tissue types, and from expression profiling of the alternative 5' exons which have been

found to be expressed across a range of different cells tested to date (Koenigsberger et al., 2000). It is therefore possible that the levels of endogenous NRSF are not fully governed by transcription *per se* but are perhaps modulated in a cell-specific manner at the post-transcriptional level through differential splicing, mRNA stability or epigenetic modifications.

Several transcription factors have been identified as potential modulators of NRSF expression. For example, based on *in silico* predictions, CREB and Sp1 have been suggested to regulate NRSF expression due to the presence of binding sites for these factors within the flanking sequences of the 5' exons of the NRSF gene. These have been experimentally validated as positive regulators of NRSF expression in human small cell lung cancer (SCLC) and embryonic kidney cell lines for CREB (Kreisler et al., 2010), and in rodent neuroblastoma/glioma cells for Sp1 (Ravache et al., 2010), through knock-down, over-expression and/or reporter gene assays. NRSF is also a direct target of Oct4 and Nanog, with knock-down of these two transcription factors resulting in reduced NRSF transcription in mouse ESCs (Loh et al., 2006). Regulation along the Wnt-signalling pathway has also been shown to modulate NRSF expression patterns during development, with over-expression of Wnt or β-catenin enhancing NRSF expression in chick embryos (Nishihara et al., 2003). In addition, several epigenetic mechanisms have been identified in the down-regulation or repression of this transcription factor including CpG methylation, MeCP2 binding and miRNA mediated processes (Kreisler et al., 2010, Abuhatzira et al., 2007, Mortazavi et al., 2006). Much remains to be explored in terms of the mechanisms governing NRSF mRNA and protein expression and likely reflects dynamic interaction between transcriptional regulation,

epigenetic processing and regulatory feedback networks suggested from bidirectional interactions between NRSF and the brain-expressed miRNAs (see *section 1.8.5*) (Wu and Xie, 2006) and the presence of a NRSE motif within its own genomic sequence; indicative of autoregulation (Johnson et al., 2007).

### 1.8.4 The NRSF pathway in disease

The majority of our understanding about the role of NRSF in normal adult tissues has come from studies of disease states in which NRSF function is modified. Dysregulation of NRSF and its target genes has been associated with a catalogue of disease processes ranging from CNS pathologies to tumourigenesis in multiple cancer types. Our group has previously performed extensive analysis of cell-specific transcriptional regulation of the neuropeptide genes AVP, TAC1 and TAC3 by NRSF. As previously mentioned, all of these neuropeptide genes contain NRSEs within their proximal promoter regions and have been shown to be differentially regulated by NRSF *in vitro* in both a cell-specific and stimulus-dependent manner (Coulson et al., 1999, Quinn et al., 2002, Spencer et al., 2006, Gillies et al., 2009). The action of the NRSF-signalling complex at these gene promoters has, in part, been implicated in disease models which are discussed in *section 1.8.4.1*, suggesting that normal levels of NRSF, and thus its target genes within the cell, may be important for disease processing. NRSF is also a modulator of multiple epigenetic parameters as illustrated in **Figure 1.7**. Association with multiple chromatin-modifying partners could lead to medium- to long-term changes in gene expression such that target genes for NRSF implicated in neuronal activation are no longer able to respond appropriately to the normal physiological cues required for CNS

function. This is demonstrated in a rodent model of hippocampal neurodegeneration associated with ischemia, whereby binding of NRSF and CoREST at a subset of transcriptionally active genes, including the clinically relevant GRIA2 (glutamate receptor, ionotropic, AMPA 2) and GRIN1 (glutamate receptor, ionotropic, NMDA 1) genes encoding glutamate receptor subunits, in response to an ischemic insult resulted in NRSF-mediated epigenetic remodelling and aberrant gene silencing in these cells (Noh et al., 2012). In addition to the complex role of NRSF in modulating cell-specific neuronal gene expression under physiological and pathological states, this regulatory network is complicated by the putative antagonistic properties of the disease-associated variant sNRSF whose function is little understood and not well investigated due to its low cellular expression (approximately 1% of total NRSF) in comparison to the full-length protein (Palm et al., 1998).

#### 1.8.4.1 sNRSF

NRSF has several different isoforms generated through alternative splicing of the 5' exon. The most well studied of these is sNRSF (short NRSF) which arises through coding of an alternative exon, termed exon N, producing a premature stop codon which results in a truncated protein lacking the C-terminal repressor domain (Palm et al., 1998). sNRSF (analogous to rodent REST4), which is specifically expressed in neurons or certain cancers (Palm et al., 1998, Coulson et al., 2000, Wagoner et al., 2010), has been shown to display dominant-negative effects over full-length NRSF (Shimojo et al., 1999, Coulson et al., 2000). This was first documented in SCLC were it was shown to antagonise the action of the full-length protein causing de-repression of the

neuropeptide gene AVP, which is speculated to be an early marker in defining the neuroendocrine phenotype of this aggressive tumour type (Coulson et al., 2000). More recently, a similar mechanism has been reported in breast cancer whereby ''REST-Less'' tumours, an aggressive subset of breast cancers that lack functional REST/NRSF, often express a truncated NRSF isoform (Wagoner et al., 2010). Loss of NRSF in breast cancer has previously been correlated with inappropriate expression of TAC1 (Reddy et al., 2009). Patients with the 'REST–less' breast cancer subtype were identified as being significantly more at risk of earlier disease recurrence than those with fully functional NRSF, in this case irrespective of the usual risk factors; oestrogen receptor or HER2 status.

Alternatively, it has been suggested that NRSF may function as a transcriptional enhancer as exemplified by previous work from our group on the tachykinin genes TAC1 and TAC3 (Spencer et al., 2006, Gillies et al., 2009). Using *in vitro* and *in vivo* models of epilepsy, both NRSF and REST4 were shown to be significantly up-regulated in rat hippocampal neurons following kainic acid treatment which correlated with up-regulation of mRNA expression for the proconvulsant gene TAC1. This increase was most dramatic for REST4. Analysis of TAC1 promoter activity using reporter gene constructs and mRNA expression following over-expression of NRSF in dissociated rat hippocampal neurons supported increased TAC1 transcription for the truncated variant but not full-length NRSF which in contrast supported up-regulation of the anticonvulsant gene galanin (Spencer et al., 2006). This suggests that during seizure full-length NRSF may function in neuroprotection whereas the truncated isoform modulates neuropathological processes. A similar mechanism was observed for another proconvulsant gene TAC3 in human neuroblastoma cells. Consistent

with a model in which NRSF modulation of tachykinin gene expression is a mechanism operating during epilepsy, increases in both endogenous gene expression and the activity of the TAC3 promoter by the full-length and truncated NRSF variants were diminished by the action of anticonvulsant drug treatment (Gillies et al., 2009). The role of sNRSF in target gene activation and its inferred association with disease processes may in part result from its absence of the C-terminal repressor domain (see **Figure 1.6**) (Abramovitz et al., 2008), meaning that distinct interactions mediated by CoREST cannot be initiated. This in turn may result in aberrant gene expression profiles associated with modulation of NRSF levels under several pathological states. However, the mechanistic role of sNRSF remains controversial. Differential expression of NRSF and its target genes, such as the neuropeptides, in models ranging from cancer to epilepsy suggests a commonality of mechanisms in cellular responses to cellular stress and damage and may reflect an overlapping mechanism between CNS physiology, pathology and cancer; particularly those with an endocrine phenotype such as SCLC.

### 1.8.5 NRSF and the brain-expressed miRNAs

The overlapping role of NRSF and miRNAs in negatively regulating neuronal gene expression, and their associations with neurological disorders, suggests a common pathway in the development of CNS dysfunction. Comparative sequence analysis has shown that NRSF and its co-repressors CoREST and MeCP2 may both target or be targeted by numerous brain-expressed miRNAs (Wu and Xie, 2006), see **Figure 1.8** and **Table 1.2**. This has been experimentally validated for some of these putative interactions. For

example, NRSF has been shown to play a role in determining neuronal identity through negatively regulating the transcriptional expression of neuron-specific miR-124 through binding to its promoter sequence in neuronal progenitors and non-neuronal cells (Conaco et al., 2006). In addition, the NRSF-regulated bi-functional miRNA miR-9/miR-9* has also been shown to negatively regulate NRSF and CoREST expression, respectively, using an *in vitro* reporter gene system and pre-miRNA over-expression assays (Packer et al., 2008). In relation to neurological disease pathways, in a recent mouse cell line model of Huntington's disease, NRSF knock-down was shown to up-regulate the expression of several miRNAs including miR-137 which was validated as a direct target of NRSF through ChIP (Soldati et al., 2013). The human MIR137 gene has also been validated as a NRSF target (Warburton et al., 2014), as discussed in *Chapter 4* of this thesis. Furthermore, miR-137 expression, amongst others (Urdinguio et al., 2010), has been shown to be epigenetically regulated by a core member of the NRSF-complex, MeCP2, in a mouse model of Rett syndrome (Szulwach et al., 2010), suggesting an important role for this regulatory network in mediating aberrant neuronal gene expression associated with CNS disorders. A role for the truncated variant REST4 in modulating brain-related miRNA expression has also been demonstrated. In a rodent model of early-life stress, increases in REST4 mRNA and protein levels in the mPFC of postnatal rats subjected to maternal separation were observed relative to control rats which correlated with significant up-regulation of miR-9-3, miR-132 and miR-212 (Uchida et al., 2010); all of which contain NRSEs within 5 Kb of their major TSS, **Table 1.2**, which is in fitting with previous studies showing that NRSEs located proximal to the TSS of target genes may function in gene

activation (Spencer et al., 2006, Gillies et al., 2009, Quinn et al., 2002). The changes in REST4 and target miRNA expression in maternally separated rats were associated with depressive-like behaviours in adult rats when exposed to stressful environments, highlighting an important role for NRSF-signalling in the development of stress-vulnerability (Uchida et al., 2010). Collectively these findings support the existence of extensive regulatory networks involving the NRSF-signalling pathway and the brain-related miRNAs in modulating the transcriptional landscape and maintaining neuronal identity, possibly through double-negative feedback mechanisms suggested from reciprocal interactions between these regulatory factors. Factors such as genetic variation and the environment have the potential to modify this regulatory circuit which may result in differential gene expression that could manifest as a disease trait. Such an interaction is explored in *Chapter 4* using the schizophrenia genome-wide associated hit MIR137 as a candidate miRNA potentially involved in NRSF-signalling as a mechanism underlying schizophrenia and other disease pathways, as discussed in *Chapter 6*.

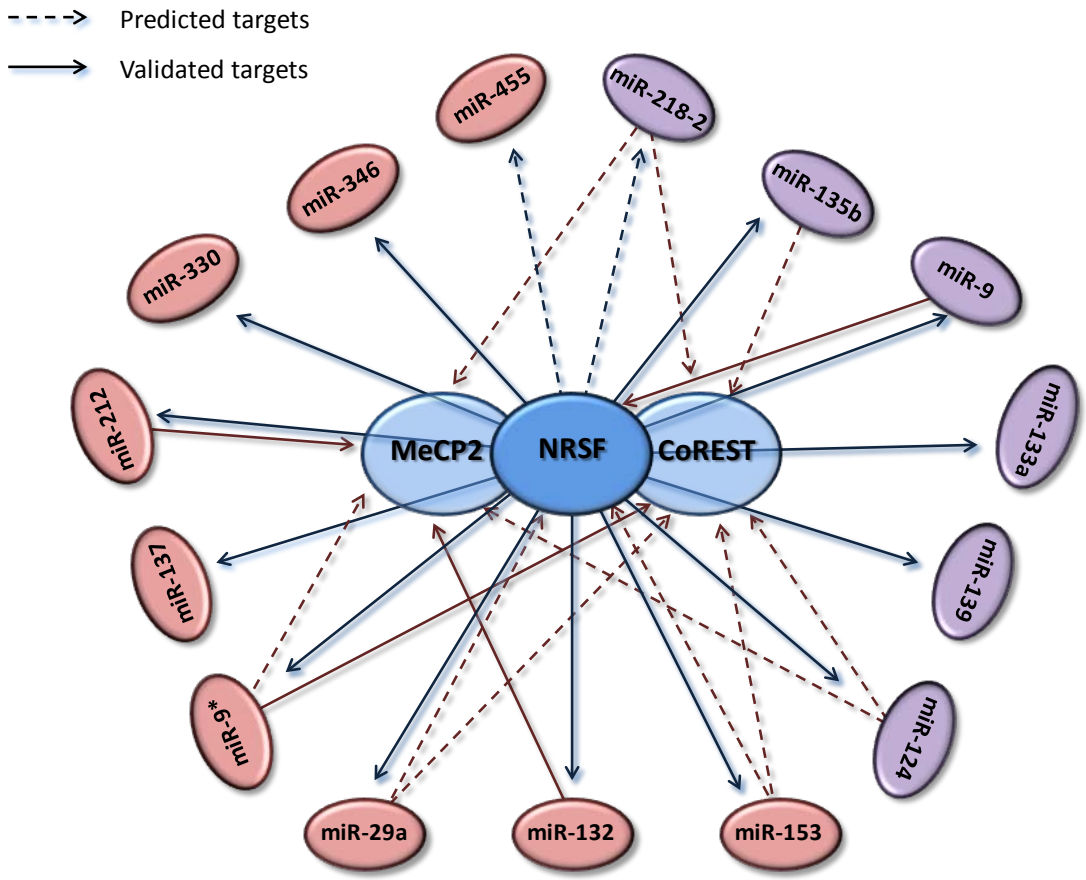


**Figure 1.8. NRSF-miRNA signalling pathway.** Schematic showing interactions between the NRSF-signalling complex and the brain enriched miRNAs. Blue ovals represent members of the NRSF-signalling complex, pink and purple ovals represent miRNAs; pink symbolise miRNAs implicated in schizophrenia from genome-wide association studies or expression analysis in post-mortem brains, see Beveridge and Cairns (2012). Blue and pink arrows represent predicted (dashed lines) or validated (block lines) targets of the NRSF-complex and the miRNAs, respectively.

**Table 1.2.** Brain-enriched microRNAs that are validated targets of NRSF

| miRNA | Host gene | NRSE Consensus Sequence<br>T AG A CG G<br>TTCAGCACCNNGGACAGCGCC | Distance of NRSE from pre-miRNA (Kb) | Reference | Comments |
|---|---|---|---|---|---|
| miR-9<br>miR-9*/miR-9-3 | C1orf61<br>LINC00925 | TCCAGCACCACGGACAGCTCC<br>CTCAGCACCATGGCCAGGGCC | 0.5 upstream<br>3.0 upstream | Mortazavi et al., 2006; Johnson et al., 2008; Uchida, 2010; Soldati et al., 2013 | Validated through ChIP in striatal cells derived from mutant HTT knock-in mice, mouse NSC line and human Jurkat T-lymphocyte cells (miR-9 only). REST4 target in rat mPFC. |
| miR-29a<br>miR-29b | LOC646329 | TTCAGCACCATGGTCAGAGCC | 11.1 downstream<br>11.8 downstream | Mortazavi et al., 2006; Johnson et al., 2008; Soldati et al., 2013 | Validated through ChIP in striatal cells derived from mutant HTT knock-in mice (miR-29b only), mouse NSC line and human Jurkat T-lymphocyte cells. |
| miR-124-1<br>miR-124-2<br>miR-124-3 | LINC00599<br>MIR124-2HG<br>*Intergenic* | TTCAGTACCGAAGACAGCGCC<br>ATCAAGACCATGGACAGCGAA<br>TTCAACACCATGGACAGCGGA | 21.7 upstream<br>3.7 upstream<br>2.4 upstream | Mortazavi et al., 2006; Johnson et al., 2008; Soldati et al., 2013 | Validated through ChIP in striatal cells derived from mutant HTT knock-in mice, mouse NSC line and human Jurkat T-lymphocyte cells (miR-124-1 only). |
| miR-132/212 | *Intergenic* | ATCAGCACCGCGGACAGCGGC | 272 bp upstream | Johnson et al., 2008; Soldati et al., 2013 | Validated through ChIP in striatal cells derived from mutant HTT knock-in mice and mouse NSC line. REST4 target in rat mPFC. |
| miR-135b | BLACAT1 | TTCAGCACCTAGGACAGGGCC | 10.7 upstream | Johnson et al., 2008; Soldati et al., 2013 | Validated through ChIP in striatal cells derived from mutant HTT knock-in mice and mouse NSC line. |
| miR-137 | MIR137HG | GTCAGAGGACCAAGCTGCCGC<br>TTGAGTGCCATGGCGGCCAGA | Overlapping<br>0.4 upstream | Soldati et al., 2013; Warburton et al., 2014 *Chapters 4 & 6* | Validated through ChIP in human SH-SY5Y neuroblastoma and MCF-7 breast cancer cells, rat cortex and striatal cells derived from mutant HTT knock-in mice. Epigenetically regulated by NRSF co-repressor MeCP2. |
| miR-139 | PDE2A | TTCAGCACCCTGGAGAGAGGC | 61.8 upstream, 2.5 upstream of PDE2A host gene | Mortazavi et al. 2006; Johnson et al., 2008 | Validated through ChIP in mouse NSC line and human Jurkat T-lymphocyte cells. |
| miR-153 | PTPRN | TTCAGCACCGCGGACAGCGCC | 14.1 upstream | Mortazavi et al.2006; Soldati et al., 2013 | Validated through ChIP in striatal cells derived from mutant HTT knock-in mice and human Jurkat T-lymphocyte cells. |

*Note:* Neuron restrictive silencing element (NRSE) sequences taken from Wu and Xie (2006) and Warburton et al. (2014) (for miR-137). *ChIP, chromatin immunoprecipitation; HTT, Huntingtin; NSC, neural stem cell.*

## 1.9 MicroRNAs in the CNS

The discovery of miRNAs over two decades ago revolutionised our understanding of the role of small RNAs in the regulation of gene expression. They are a large family of single-stranded ncRNAs of approximately 18-25 nucleotides (nt) in size that can be highly conserved throughout evolution, present in both plants and animals (Zhang et al., 2006, Bartel, 2004). Many miRNAs share sequence homology across different species suggesting an important role in essential biological processes. The significance of these regulatory RNAs in almost every aspect of cellular functioning is rapidly being recognised. It is estimated that 1-5% of the human genome encodes for miRNAs and that at least 30% of protein-coding genes are under their regulatory control (Krol et al., 2010). Furthermore, individual miRNAs can regulate hundreds of target mRNAs in tandem (Lim et al., 2005) making them an intriguing area of study in normal physiological and disease processes.

### 1.9.1 MicroRNA Biogenesis

Based on their genomic location, miRNAs can be classified as being intergenic or intragenic (**Figure 1.9**). Intergenic miRNAs are located within currently undefined regions of the genome and are transcribed from their own unique promoters (Corcoran et al., 2009). In contrast, intragenic miRNAs are encoded as part of their respective host gene and are thought to share the same transcriptional machinery (Lee et al., 2004). In support of this, evidence has shown that intragenic miRNAs are expressed in parallel with their host transcripts and, as such, studies have successfully utilised primary (pri)-miRNA expression profiling in the identification of miRNA target mRNAs through

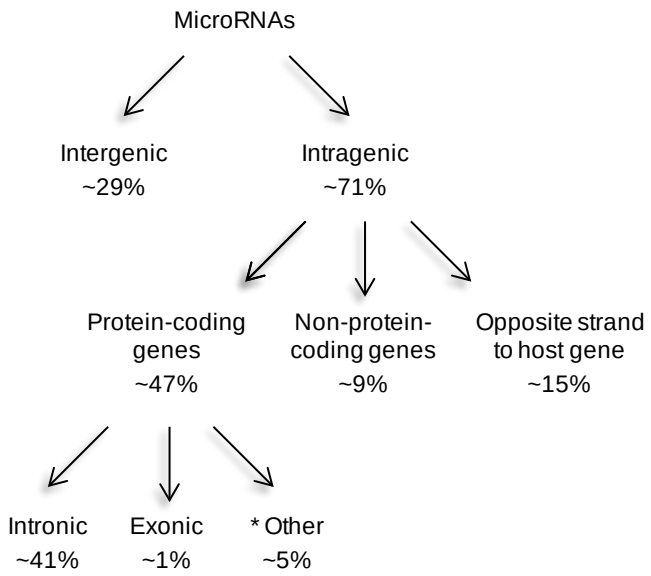


**Figure 1.9. Genomic location of human miRNAs.** **Other* refers to miRNA genes within untranslated regions or 'mixed' miRNA genes that can be assigned to either intronic or exonic miRNA groups depending on the alternative splicing patterns (Godnic et al., 2013).

inverse correlation of expression levels (Rodriguez et al., 2004, Baskerville and Bartel, 2005, Ronchetti et al., 2008, Gennarino et al., 2009). For the canonical pathway, subsequent steps in miRNA biogenesis are conserved between the miRNAs regardless of their genomic location. The miRNA biogenesis pathway is represented in **Figure 1.10**. During miRNA synthesis, a long pri-miRNA transcript (typically more than 1 Kb in length) is transcribed by RNA Pol II, forming an imperfectly base-paired, double stranded hairpin structure that has a 5' cap and 3' poly-A tail, typical of mRNA (Lee et al., 2004). Following transcription, the stem-loop structure of pri-miRNAs is recognised by the microprocessor complex composed of the RNase III endonuclease Drosha and its associated protein DGCR8 (DiGeorge syndrome critical region 8). This complex cleaves the pri-miRNA forming a small (70-100 nt) hairpin structure

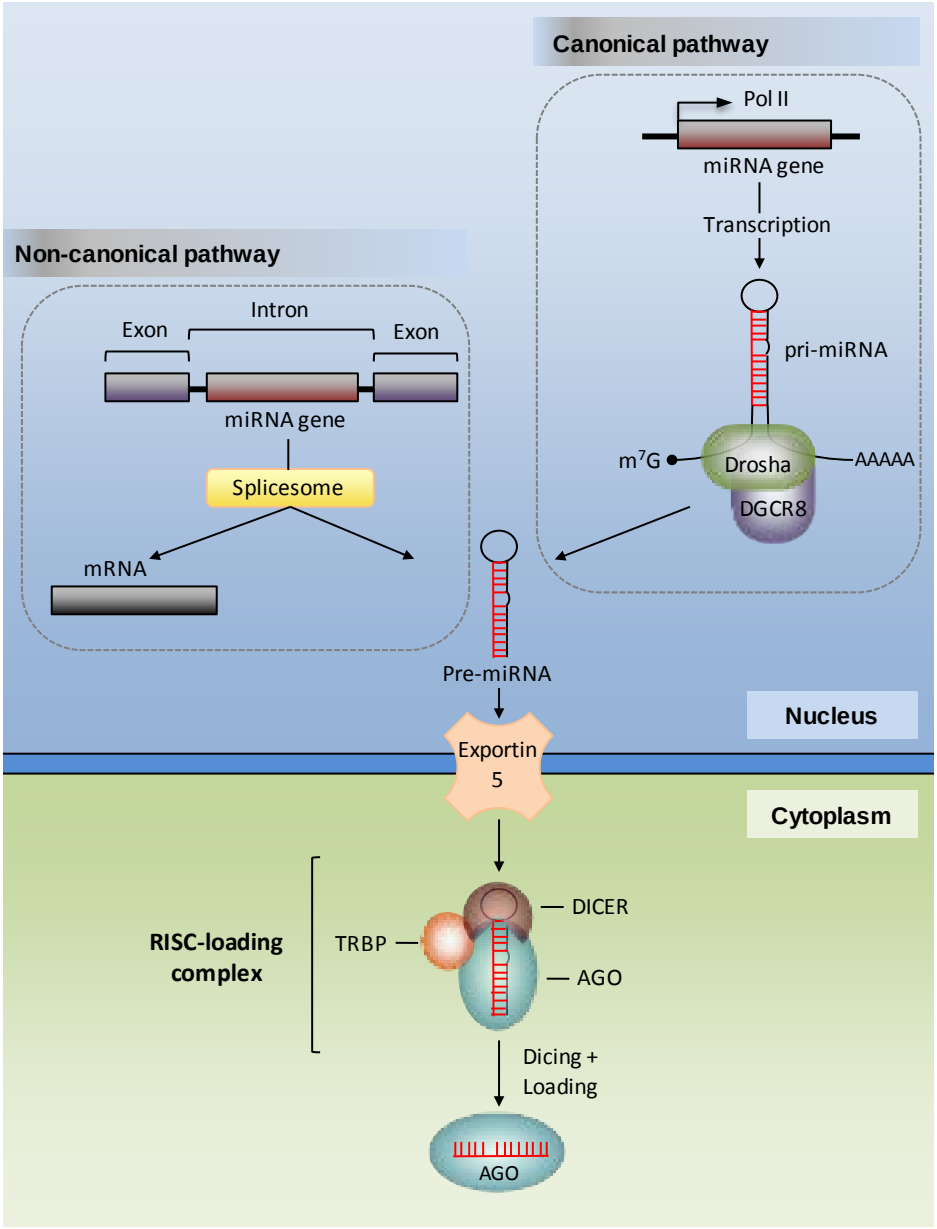


**Figure 1.10. The miRNA biogenesis pathway.** Canonical miRNA genes are transcribed as primary (pri)-miRNAs (typically more than 1 Kb in length) by RNA Pol II and cleaved by the Microprocessor complex composed of the RNase III enzyme Drosha and the double-stranded RNA binding protein, DGCR8, forming a precursor (pre)-miRNA. Intronic miRNAs require an additional splicing event to generate the pre-miRNA; some of which are processed independent of the Microprocessor complex (non-canonical pathway). Pre-miRNAs are exported to the cytoplasm by Exportin-5 and incorporated into the RISC-loading complex for further cleavage into a ~22 nt mature miRNA (miR) duplex by the RNAse III enzyme Dicer. One strand of the miR duplex is preferentially loaded into the RISC complex with along with members of the AGO family of proteins producing a functional complex for targeting mRNA (see **Figure 1.12**). Abbreviations: *AGO, Argonaute; DGCR8, DiGeorge syndrome critical region 8; m$^7$G, 7-methylguanosine 5' cap; RISC, RNA-induced silencing complex; TRBP, TAR (trans-activating response element) RNA binding protein.*

termed the precursor (pre)-miRNA. For intronic miRNAs, an additional splicing step takes place following co-transcription of the miRNA gene with its host transcript. For unknown reasons, this splicing event occurs more slowly in miRNA-containing introns than it does in adjacent introns and is thought to involve a splicing commitment complex which tethers the intron whilst Drosha cleaves the miRNA hairpin, forming the pre-miRNA (Kim et al., 2009). Some intronic miRNAs do not require the microprocessor complex and are instead processed by a non-canonical pathway. These miRNAs are termed mirtrons and represent pre-miRNAs that are defined by the entire length of the intron from which they are processed. They contain a splice site necessary for their excision from the primary transcript and are linearised by DBR1 (debranching RNA Lariats 1 enzyme) generating the pre-miRNA (Havens et al., 2012). Pre-miRNAs are exported from the nucleus to the cytoplasm by the Ran-dependent nuclear transport receptor exportin-5 for further processing. Once in the cytoplasm, the pre-miRNA is incorporated into the RISC (RNA-induced silencing complex)-loading complex and further cleaved by the cytoplasmic RNase III Dicer forming a mature miRNA duplex of approximately 22 nt. The low internal stability of these duplexes, generally at the 5'-anti-sense terminus, causes them to unwind allowing incorporation of the thermodynamically unstable strand into the RISC complex and rapid degradation of the alternative strand (Khvorova et al., 2003).

### 1.9.2 Mode of action of mature miRNAs in gene regulation

Mature miRNAs predominantly function as negative regulators of target mRNAs, and thus inhibitors of protein synthesis, through RNA-interference based mechanisms. The miRNA-induced silencing complex (miRISC) binds to

the 3'-untranslated region (UTR) of target mRNAs through imperfect complementary base-pairing involving positions 2-8 of the 5'-proximal sequence of the guide miRNA, termed the 'seed' sequence (Bartel, 2009). This imperfect hybridisation results from miRNA-mRNA duplexes containing mismatches and bulges in the central region corresponding to positions 10-12 of the miRNA sequence (**Figure 1.11**), preventing mRNA cleavage by endonuclease activity which is typical of the closely related small-interfering RNAs (siRNAs) (Hutvagner and Zamore, 2002).

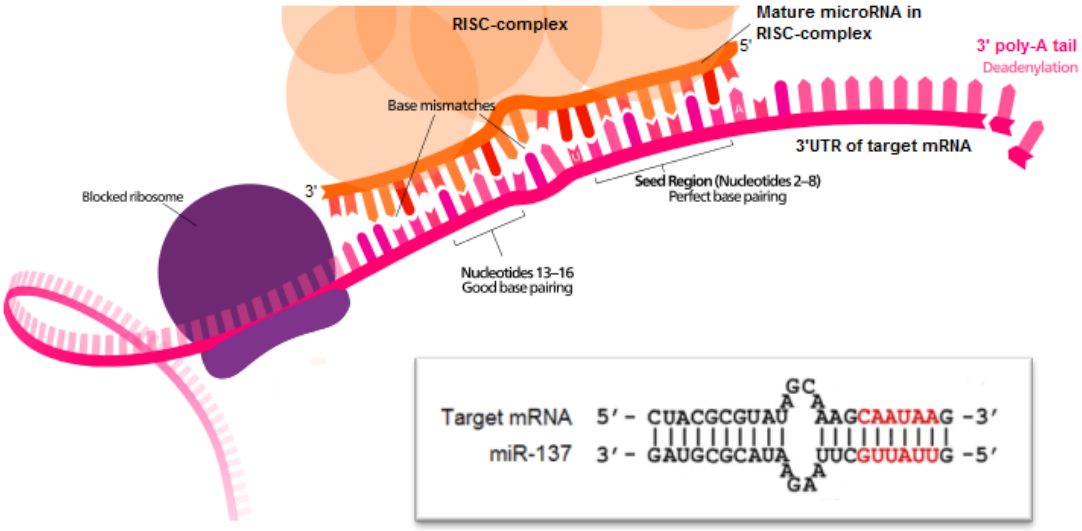


**Figure 1.11. Binding of the miRNA-induced silencing complex (miRISC) to target mRNA.** The miRISC-complex binds to the 3'-untranslated region (UTR) of target mRNAs through imperfect complementary base-pairing involving the 'seed' sequence (typically position 2-8) of the guide miRNA; highlighted in red in the mature miRNA sequence for miR-137. Binding of the miRISC-complex represses mRNA translation or promotes deadenylation and degradation or storage (see **Figure 1.12**). Mismatches in the central region corresponding to positions 10-12 of the miRNA sequence forms bulges that prevent endonuclease mRNA cleavage and permit targeting of hundreds of mRNAs through imperfect hybridisation. Figure adapted from http://upload.wikimedia.org/wikipedia/commons/a/a7/MiRNA.svg.

As a consequence each individual miRNA can potentially target hundreds of target mRNAs. Furthermore, target mRNA 3'UTRs can present several miRNA binding sites and it has been shown *in vitro* that multiple copies of the same miRNA or different miRNAs can act in a concerted manner to inhibit mRNA translation (Doench and Sharp, 2004). This effect was dependent upon the cellular concentration of both mRNA and miRNA suggesting that miRNAs regulate the fine-tuning of protein synthesis in a context-dependent manner. Upon binding of target mRNAs, the miRISC complex mainly exerts its repressive function through translational repression and/or facilitating mRNA deadenylation and subsequent storage or degradation within processing bodies (P-bodies), **Figure 1.12**. The degree of sequence identity appears to determine which miRNA-mediated post-transcriptional regulatory mechanism is employed as it has been shown that perfect complementary base-pairing results in Argonaute (Ago)-2-mediated mRNA cleavage and degradation (Hutvagner and Zamore, 2002, Hammond et al., 2001). Although the majority of predicted and experimentally characterised miRNA seed sequences are located within mRNA 3' UTRs, they have also been identified within coding regions and 5'UTRs. Interestingly, targeting of mRNA 5' UTRs has been associated with translational activation (Orom et al., 2008, Fehr et al., 2012). The miRNAs may also function in transcriptional regulation. It has recently been demonstrated that miRNAs function in transcriptional repression and activation through targeting of gene promoters (Turner and Morris, 2010). The mechanisms involved remain unclear however miRNA-mediated repression was shown to involve the recruitment of Ago-1, Polycomb-group (PcG) component enhancer

of zeste homolog 2 (EZH2) and histone methylation (H3K27me3) at the targeted promoters (Gonzalez et al., 2008).

### 1.9.3 Expression and function of miRNAs in the brain

Approximately 70% of mammalian miRNAs can be experimentally detected in the brain or in primary neuronal cultures (Cao et al., 2006), however only a small set have been shown to be brain-specific or enriched (Landgraf et al., 2007). Some of the current miRNAs identified as playing important roles in neurodevelopment and function, and validated targets of NRSF (see **Table 1.2**), are summarised in **Table 1.3**. Studies addressing the expression profiles of brain-related miRNAs have shown them to display regional, cell-specific and sub-cellular compartmentalisation (Bak et al., 2008, Landgraf et al., 2007, Olsen et al., 2009, Boudreau et al., 2014, Krichevsky et al., 2003, Cougot et al., 2008). Several miRNAs have been shown to be enriched or depleted in dendrites, axons and synaptoneurosomal preparations (Pichardo-Casas et al., 2012). In addition, components of the miRISC complex such as Ago2 and Dicer have been isolated from pre- and post-synaptic terminals (Murashov et al., 2007, Hengst et al., 2006, Lugli et al., 2008) suggestive of localised miRNA synthesis for rapid reposes to neuronal-activation. The mechanisms underlying localisation of miRNAs within specific neuronal compartments remain unknown and may involve associations with RNA-binding proteins that shuttle or anchor miRNAs to particular sub-cellular compartments. Support for this comes from interactions between brain-enriched miRNAs such as miR-132 with FMRP (fragile-X mental retardation protein), an important RNA-binding protein that interacts with components of the RISC, in modulating dendritic spine

morphology through regulation of localised protein translation (Edbauer et al., 2010). These findings demonstrate the dynamic tempo-spatial expression of miRNAs in the developing and adult brain, indicating a central role in modulating neuronal gene expression in response to developmental and environmental cues. Given the complex nature of their biogenesis and their extensive regulatory potentials, it is unsurprising that dysregulation of several brain expressed miRNAs and their target mRNAs have been implicated in the aetiology of neurological disorders (see **Table 1.3**). Exploration of a regulatory network involving NRSF and the brain-enriched miRNAs is addressed in this thesis using MIR137 as a novel NRSF target gene (*Chapter 4*) and through *in silico* predictions of NRSF modulation of miRNA networks using a selection criteria based on our functional analysis of MIR137 (*Chapter 5*).

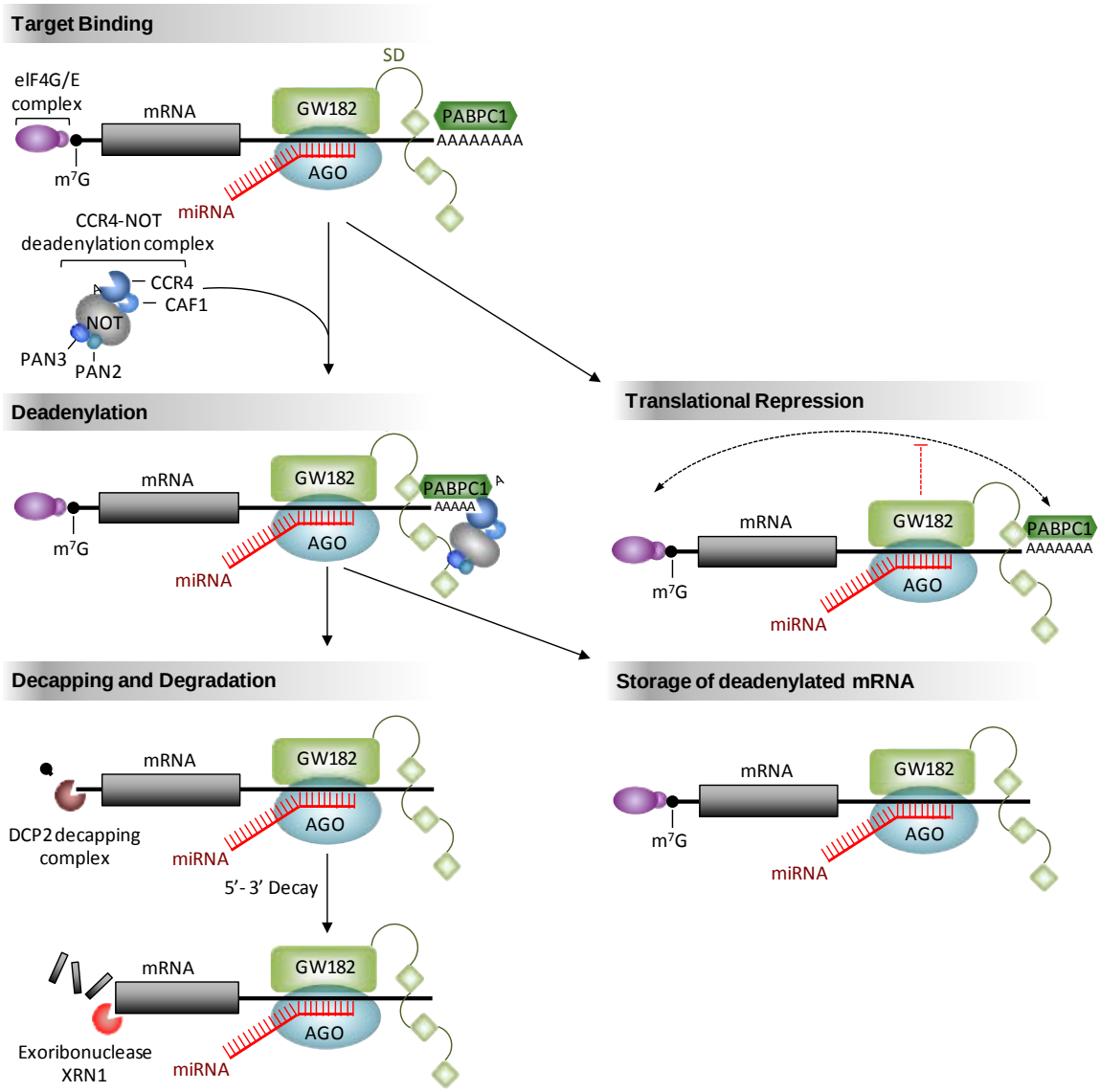


**Figure 1.12. Mechanisms involved in microRNA-mediated gene regulation.** Mature miRNAs are incorporated into the miRNA-induced silencing complex (miRISC) containing an AGO RNA-interference family member (1-4 in humans). The miRNA guides RISC to the 3'UTR of target mRNAs for RNA-interference based gene regulation which is thought to occur through several different mechanisms. Destabilisation of mRNA targets and subsequent translational inhibition and mRNA degradation is the main repressive mechanism (Guo et al., 2010). This process is not fully understood but is thought to involve GW182 (glycine-tryptophan protein of 182 kDa) recruitment which binds Ago providing a direct docking-platform for interaction with associated protein complexes. One such interaction involves the poly-A-binding protein 1 (PABPC1) which binds the poly-A tail of mRNAs and serves to recruit several proteins important in translational regulation and mRNA decay. The N-terminal of PABPC1 interacts with the mRNA 5' cap structure via the eukaryotic initiation factor 4G (eIF4G) inducing the closed-loop conformation which is thought to stimulate translation and protect the mRNA termini from degradation. GW182 is thought to compete with eIF4G for PABPC1 binding sites, inhibiting formation of the closed-loop and thus preventing translation (Tritschler et al., 2010). PABPC1 also interacts with the CCR4-NOT deadenylation complex, which causes poly-A tail deadenylation and subsequent mRNA storage or decay (Fabian et al., 2011). *Abbreviation: AGO, Argonaute; CCR4, chemokine (C-C motif) receptor 4; NOT, negative regulator of transcription.*

**Table 1.3.** Brain enriched miRNAs important for neurodevelopment and disease

| MicroRNA | Target genes | Expression and function | Disease associations |
|---|---|---|---|
| miR-9 | Foxg1, Gsh2, NRSF, TLX | Highly expressed during cortico-genesis with reduced cortical levels in postnatal and adult brain. Highly expressed in FC, H, MB and Cb. Over-expressed in primary brain tumours (astrocytoma, oligodendroglioma, glioblastoma multiforme). Represses glial cell differentiation, inhibits proliferation and stimulates migration and neuronal differentiation of ES cells *in vitro*. | ↓ AD and HD |
| miR-9* | CoREST | Highly expressed in NSCs and during mammalian corticogenesis with reduced cortical levels in postnatal and adult brain. Over-expressed in primary brain tumours (astrocytoma, oligodendroglioma, glioblastoma multiforme). Induces neuronal differentiation. | ↓ HD, SCZ |
| miR-29a/b | BACE1 | Undetectable in embryonic tissues. Highly expressed in adult cortex, striatum and astrocytes. | ↓ AD, SCZ |
| miR-124 | Cdc42, CDK6, CREB1, PTBP1, Rac1, SCP1, SOX9 | Highly expressed in the FC, H, MB and Cb. Expressed in neuronal cells and microglia but not astrocytes. Expression levels increase throughout neurodevelopment; plays a key role in the differentiation of NPCs to mature neurons. Stimulates neuronal differentiation and represses glial differentiation of ES cells *in vitro* in concert with miR-9. Involved in synaptic plasticity, adult neurogenesis, memory formation, neuronal survival under ischemic conditions and alleviating neuronal cell death. | ↓ FXS, AD, HD |
| miR-132 | BDNF, GluR1, kalirin7, MeCP2, NR2A/B, p250GAP (brain-enriched NMDA receptor-interacting RhoGAP), Rac1 | Highly expressed in the H, FC and Cb. Involved in neuro-development and maturation. Enriched at synapses and dendrites, plays a key role in activity-dependent dentritic development, morphology and plasticity, neurite outgrowth and synaptic plasticity. | ↑ RS, SCZ; ↓FXS and HD |

| | | | |
|---|---|---|---|
| miR-135b | DISC1, FOXO1, NDR2 TGF-β | Highly expressed in Cb and mediodorsal nucleus of thalamus. Regulates neuronal differentiation in hESC, regulation of immune system and renin-angiotensin-aldosterone system, inhibits differentiation of osteoprogenitor cells, regulates Wnt-signalling pathway. | *In vitro* allele-specific regulation of DISC1 by seed sequence SNP rs11122396; in LD with rs3737597 previously associated with SCZ and MD. Dysregulated in mouse cell line model of HD. |
| miR-137 | CACNA1C, CSMD1, C10orf26, EZH2, LSD1, TCF4, ZNF804A | Highly expressed in the Am and H. Also expressed in the ACC, dlPFC, NAc, OFC and BG. Regulates neurodevelopment, neuronal maturation, adult neurogenesis, NSC differentiation and inhibits dendritic spine outgrowth. | ↓ AD, SCZ; SCZ GWAS |
| miR-153 | APLP2, APP, SNAP-25 | Highly expressed in the developing brain. Implicated in pre-synaptic vesicle release, protein secretion and motor neuron patterning and outgrowth. | ↑ SCZ; ↓ AD |

*Note:* Disease associations are based on studies in human samples unless stated otherwise and are reported or reviewed in Maes et al. (2009), Chang et al. (2009), Olde Loohuis et al. (2012), Beveridge and Cairns (2012), Yin et al. (2014), Rossi et al. (2014) and Long et al. (2012). Abbreviations: *ACC, anterior cingulate cortex; AD, Alzheimer's disease; Am, amygdala; BG, basal ganglia; C, cortex; Cb, cerebellum; dlPFC, dorsolateral prefrontal cortex; FC, frontal cortex; FXS, Fragile-X sydrome; GWAS, genome-wide association study; hESC, human embryonic stem cell; H, hippocampus; HD, Huntington's disease; MB, midbrain; MD, major depression; NAc, nucleus accumbens; NCS, neural stem cell; OFC, orbitofrontal cortex; RS, Rett syndrome*.

## 1.10 Project aims

- Address the functional significance of genetic polymorphisms within the NRSF-signalling pathway in transcriptional regulation of candidate genes implicated in CNS dysfunction and/or as biomarkers for clinical predisposition to disease
- Explore the NRSF-MIR137 pathway as a potential common mechanism across multiple disease states

# Chapter 2

## Materials and Methods

## 2.1 Materials

### 2.1.1 Commonly used Buffers and Reagents

*5X TBE Buffer:* 108 g Tris Base (Sigma), 55 g Boric acid (Sigma), 5.84 g EDTA (Sigma) made up to 2L using d.$H_2O$.

*LB Agar:* 40 g/L in d.$H_2O$ (Fluka Analytical). LB agar was autoclaved the same day and stored at room temperature.

*LB Broth:* 25 g/L in d.$H_2O$ (Fluka Analytical). LB broth was autoclaved the same day and stored at room temperature.

### 2.1.2 Chromatin Immunoprecipitation (ChIP) buffers

*Tris-EDTA (TE) buffer:* 10 mM Tris and 0.1 mM EDTA (pH 8.0) made up to the final volume with sterile d.$H_2O$. Adjust pH to between 7.5 and 8.0.

*Cell lysis buffer:* 10 mM Hepes (pH 7.9), 1.5 mM $MgCl_2$, 10 mM KCl and 0.5% NP-40 made up to the final volume with sterile d.$H_2O$. Supplement with 10 µl/ml of 100X PIC (protease inhibitor cocktail, Sigma) immediately before use and store on ice.

*Nuclear lysis buffer:* 50 mM Tris-HCl (Tris adjusted to pH 8.1 with HCl), 1% SDS and 10 mM EDTA made up to the final volume with sterile d.$H_2O$. Supplement with 10 µl/ml 100X PIC immediately before use and store on ice.

*Sonication buffer:* 50 mM Hepes (pH 7.5), 140 mM NaCl, 1 mM EDTA, 1 mM EGTA, 1% Triton X-100, 0.1% sodium deoxycholate and 0.1% SDS made up to the final volume with sterile d.$H_2O$. Supplement with 10 µl/ml 100X PIC immediately before use and store on ice.

*ChIP dilution buffer:* 16.7 mM Tris–HCl, 167 mM NaCl, 1.1% Triton X-100, 0.01% SDS and 1.2 mM EDTA made up to the final volume with sterile d.$H_2O$. Supplement with 10 µl/ml 100X PIC immediately before use and store on ice.

*Low-salt wash buffer:* 20 mM Tris–HCl, 150 mM NaCl, 0.1% SDS, 1% Triton X-100 and 2 mM EDTA made up to the final volume with sterile d.$H_2O$.

*High-salt wash buffer:* 20 mM Tris–HCl, 500 mM NaCl, 0.1% SDS, 1% Triton X-100 and 2 mM EDTA made up to the final volume with sterile d.$H_2O$.

*LiCl wash buffer:* 10 mM Tris–HCl, 250 mM LiCl from a 10M stock, 1% Igepal, 1% sodium deoxycholate and 1 mM EDTA made up to the final volume with sterile d.$H_2O$.

*Elution buffer:* 50 mM Tris–HCl, 1 mM EDTA, 1% SDS and 50 mM $NaHCO_3$ made up to the final volume with sterile d.$H_2O$.

### 2.1.3 Drug Treatment Solutions

*Amphetamine* (Sigma): dissolved in sterile filtered d.$H_2O$ to make a 1 mM stock which was diluted in complete SH-SY5Y tissue culture media to a final concentration of 10 µM (Jones and Kauer, 1999, Shyu et al., 2004).

*Cocaine hydrochloride* (Sigma): dissolved in sterile filtered d.$H_2O$ to make a 1 mM stock which was diluted in complete SH-SY5Y tissue culture media to a final concentration of 1 µM or 10 µM (Vasiliou et al., 2012).

*Lithium chloride* (Sigma): dissolved in sterile filtered d.$H_2O$ to make a 1 M stock which was diluted in complete SH-SY5Y tissue culture media to a final concentration of 1 mM (Hing et al., 2012, Roberts et al., 2007).

*Nicotine hydrogen tartrate salt* (Sigma): dissolved in complete SH-SY5Y tissue culture media to a final concentration of 1mM (Dunckley and Lukas, 2003, Cui et al., 2012).

*Valproic acid sodium salt* (Sigma): dissolved in sterile filtered $dH_2O$ to make a 1 M stock which was diluted in complete SH-SY5Y tissue culture media to a final concentration of 5 mM (Pan et al., 2005, Zhang et al., 2003, Phiel et al., 2001).

*5-Aza-2′-deoxycytidine* (5'aza-DC, Sigma): dissolved in DMSO to make a 10 mM stock which was diluted in complete MCF-7 tissue culture media to a final concentration of 1 μM and 10 μM.

### 2.1.4 Human DNA Samples

#### 2.1.4.1 Breast cancer cohort

Genomic DNA was obtained for a BRCA1/2 positive, BRCA wild-type and matched female control cohort from the National Genetics References Laboratory, St Mary's Hospital, Manchester.

#### 2.1.4.2 Epilepsy SANAD cohort

##### *2.1.4.2.1 Subjects*

Genomic DNA from 84 patients recruited into the SANAD (Standard and New Antiepileptic Drug) trials (Marson et al., 2007a, Marson et al., 2007b) that were included in a subgroup analysis of cognitive function (Taylor and Baker, 2010, Taylor et al., 2010) were kindly provided by our collaborator Dr. Graeme Sills, University of Liverpool. A comprehensive description of the patient population is provided elsewhere (Taylor and Baker, 2010, Taylor et al., 2010,

Marson et al., 2007a, Marson et al., 2007b). All subjects were of self-reported Caucasian ancestry and were neurologically normal, MRI negative and had not previously been treated with any antiepileptic drug (AED). DNA collection was approved by the North-West Multicentre Research Ethics Committee in August 2002 (ref: MREC 02/8/45) and all patients provided written informed consent to the use of their DNA and relevant clinical information in this analysis.

#### *2.1.4.2.2 Cognitive assessment data*

Patients recruited into the SANAD trial were assessed for cognitive function at baseline and during follow-up studies using a neuropsychological test battery designed to assess multiple cognitive domains, including memory, psychomotor speed, information processing, mental flexibility and mood. The test battery methods are described in detail elsewhere (Taylor et al., 2010). Only those aspects of the battery that had previously been shown to differ significantly between epilepsy patients and healthy controls were employed in the genetic association analysis (*Chapter 3*). Cognitive tests used for cross-sectional and longitudinal analyses are listed in **Table 3.1**. All 84 subjects contributed to a cross-sectional analysis of genetic influences on baseline cognitive function. The 70 patients who also had a 12-month neuropsychological assessment were additionally included in a longitudinal analysis, investigating the influence of genetic variants on the change in cognitive function from baseline (see *section 2.2.10.4*).

#### 2.1.4.3 HapMap CEU cohort

Genomic DNA from 89 Utah residents with Northern and Western European ancestry from the commercially available *CEPH* (Centre de'Etude du Polymorphism Humain) trio collection of the HapMap Project were kindly provided by our collaborator Dr. Gerome Breen, Institute of Psychiatry, King's College London. A description of the study cohort is available at (https://catalog. coriell.org/).

#### 2.1.4.4 Schizophrenia cohort

Genomic DNA samples from 823 patients with schizophrenia (mean age 37.66 years, range 18-71) and 762 healthy controls (mean age 46.27, range 19-72) were kindly provided by our collaborator Prof. Dan Rujescu, Department of Psychiatry, University of Halle-Wittenberg. Subjects were all of German or central European descent and provided written informed consent. Schizophrenic patients were selected based on diagnosis under the Diagnostic and Statistical Manual of Mental Disorders (DSM-IV) and International Classification of Disease-10 (ICD-10). Detailed medical and psychiatric histories were collected for each patient, including the Structured Clinical Interview for DSM-IV (SCID), to evaluate lifetime Axis I and II diagnoses. Unrelated healthy controls were selected at random from the general population of Munich, Germany. To exclude any healthy volunteers with neuropsychiatric disorders, both the subjects and their first-degree relatives completed an initial screening process followed by detailed medical and psychiatric history assessment using a semi-structured interview. Participants that did not meet the exclusion criteria were invited to a comprehensive interview including the SCID I and SCID II to

validate the absence of any lifetime psychotic disorder. All participants provided written informed consent following a detailed and extensive description of the study, which was approved by the local ethics committee of Ludwig Maximilians University, Munich, Germany and carried out in accordance to the ethical standards outlined in the Declarations of Helsinki.

### 2.1.5 Human cell lines

#### 2.1.5.1 SH-SY5Y

Human-derived neuroblastoma cell-line obtained from the *American Type Culture Collection* (*ATCC).*

#### 2.1.5.2 MCF-7

Human-derived breast adenocarcinoma cell line kindly provided by Prof. Rudland and Prof. Palmieri, The Royal Liverpool University Hospital.

### 2.1.6 Cell culture media

#### 2.1.6.1 Complete media for SH-SY5Y cells

Earle's modified Eagle's medium (Sigma) and HAM's F12 (Sigma) at a ratio of 1:1, supplemented with 10% foetal bovine serum (Sigma), 1% 200 mM L-glutamine, 1% 100 mM sodium pyruvate and 100 U/ml penicillin/ 100 ug/ml streptomycin.

#### 2.1.6.2 Low serum media for SH-SY5Y cells

Has the same composition as complete SH-SY5Y media (*section 2.1.6.1*) but with 2% foetal bovine serum (Sigma).

#### 2.1.6.3 Complete media for MCF-7 cells

Dulbecco's Modified Eagles medium with 4500 mg glucose/L (Sigma), supplemented with 10% foetal bovine serum (Sigma), 100 U/ml penicillin and 100 µg/ml streptomycin.

#### 2.1.6.4 Freezing media

90% foetal bovine serum (Sigma), 10% DMSO (Sigma).

### 2.1.7 Rat DNA Samples

Left and right cortex, hippocampi and amygdala from adult male Sprague Dawley rats (Slaccas Laboratory Animal co., LTD, Shanghai) were generously provided by our collaborator Dr. Minyan Wang, Xi'an Jiaotong-Liverpool University (*XJTLU*). The average weight of the rats was 327 g [range 295 – 360 g]. Tissues were stored at -80°C prior to processing for RNA and DNA extractions (*section 2.2.5.2*). The treatment groups were untreated (n=3), sham control (n=3) and CSD (cortical spreading depression) (n=3). Methods used by our collaborators for eliciting CSD are outlined in *Appendix 1*.

### 2.1.8 PCR primers

**Table 2.1.** PCR primers used for gene expression profiling, genotyping and ChIP

| Gene | Forward (5'- 3') | Reverse (5'- 3') | Species | Application | Product size (bp) | Position | Annealing temp |
|---|---|---|---|---|---|---|---|
| ACTB | AGGCTGTGCTATCCCTGTACGC | ATGGGCACAGTGTGGGTGAC | Human | RT-PCR | 85 | - | 60 |
| | CTGTCCACCTTCCAGCAGAT | CGCAGCTCAGTAACAGTCCG | Rat | RT-PCR | 105 | - | 60 |
| AK311400 | ACTCTCTTCGGTGACGGGTA | TCCACTCTGGGTCATCCTTC | Human | RT-PCR | 274, 451 | - | 63 |
| AK311400 | ACTCTCTTCGGTGACGGGTA | ACTCTTGCTAGGTCCGCTTG | Rat | RT-PCR | 232, 409 | | |
| BDNF I | ATCGATGCCAGTTGCTTTGT | AGCCTTCATGCAACCAAAGT | Human | RT-PCR | 307 | - | 60 |
| BDNF IIb | GTTGGCTTCCTAGCGGTGTA | ATTCACGCTCTCCAGAGTCC | Human | RT-PCR | 211 | - | 60 |
| BDNF IIc | | | | | 294 | | |
| BDNF III | TTAGAGGGTTCCCGCTTTCT | TTCGAAAGTGTCAGCCAATG | Human | RT-PCR | 301 | - | 60 |
| BDNF IV | TTTGCTGCAGAACAGAAGGA | CACCTTGTCCTCGGATGTTT | Human | RT-PCR | 284 | - | 60 |
| BDNF Va | GTGCGATTTCATTGTGTGCT | TTTCTGGTCCTCATCCAACA | Human | RT-PCR | 298 | - | 60 |
| BDNF Vb | | | | | 308 | | |
| BDNF V-VIII | | | | | 591 | | |
| BDNF V-VIII-VIIIh | | | | | 708 | | |
| BDNF VIa | GGGGGCTTTAATGAGACACC | ATTCACGCTCTCCAGAGTCC | Human | RT-PCR | 291 | - | 60 |
| BDNF VIb | | | | | 309 | | |
| BDNF VIb-IXbd | | | | | 416 | | |
| BDNF VII | AAGTCCGAAGCCAATGTAGC | ATTCACGCTCTCCAGAGTCC | Human | RT-PCR | 403 | - | 60 |
| BDNF IXabcd | TTTTGTGTTTCTCGTGACAGC | CCGAACTTTCTGGTCCTCAT | Human | RT-PCR | 616 | - | 60 |
| BDNF IXabd | | | | | 382 | | |
| CACNA1C | TCGAGTCCAGTGAGAAACTC | GGTGACCTCGATGAACTTG | Human/Rat | RT-PCR | 248 | - | 60 |
| Calca_CGRP | AACCTTGGAAAGCAGCCCAGGCATG | GTGGGCACAAAGTTGTCCTTCACCA | Rat | RT-PCR | 246 | - | 63 |
| Calca_CT | CCCTTTCCTGGTTGTCAGCATCTT | AGCATGCAGGTACTCAGATTCCCA | Rat | RT-PCR | 258 | - | 63 |

| | | | | | | | |
|---|---|---|---|---|---|---|---|
| c-fos | AGATACGCTCCAAGCGGAGA | CGGTGGGCTGCCAAAATAAA | Rat | RT-PCR | 117 | - | 60 |
| c-jun | AGCCAAGAACTCGGACCTTC | TCGGTGTAGTGGTGATGTGC | Rat | RT-PCR | 116 | - | 60 |
| GAD1 | TCTCCTGGGGGAGCCATATC | TGAAGAGGACCAGTTTGGGC | Rat | RT-PCR | 112 | - | 60 |
| MIR137HG | CAGAGGAAAGCACTGGGAGA | CACCCAAGAATACCCGTCAC | Human/Rat | RT-PCR | 291 | - | 63 |
| MIR137-MIR2682 | GTGACGGGTATTCTTGGGTG | AGACTCATCCCAAAGGCAGA | Rat | RT-PCR | 187 | - | 60 |
| NRSF | TATGCGTACTCATTCAGGTGAG | TTTGAAGTTGCTTCTATCTGCTGT | Human | RT-PCR | 166, 216 | - | 60 |
| | AGCGAATACCACTGGCGGAAACA | AATTAAGAGGTTTAGGCCCGTTG | Rat | RT-PCR | 313 | - | 60 |
| RELN | CGTCCTAGTAAGCACTCGCA | TATCGCCTAAGCGACCTTCG | Rat | RT-PCR | 102 | - | 60 |
| REST4 | AGCGAATACCACTGGCGGAAACA | TCACCCAACTAGATCACACT | Rat | RT-PCR | 235 | - | 63 |
| sNRSF | GGATACCATTTGGTAATATTTAC | TGAACCTGTCTTGCATGGCG | Human | RT-PCR | 124 | - | 57 |
| TCF4 | CAAAGCCGAATTGAAGATCG | AAGAGAATGGCTGCCTCTCA | Human/Rat | RT-PCR | 255/253 | - | 60 |
| MIR137 VNTR | CACCCAAGAATACCCGTCAC | TGGGAGAGCACCAGGTAAAC | Human | ChIP/ | 399 ±15 | -263 to +136 | 60 |
| MIR137 VNTR | CACCCAAGAATACCCGTCAC | TGGGTGATCACCAGGTACAC | Rat | Genotyping | 395 | - | 60 |
| pBDNF I | CCCATTAGAGCAAACGCAGT | CGCTgTTTACGTGACCGACT | Human | ChIP | 354 | -412 to -58 | 60 |
| pBDNF II | GAGATTTTTAAGCCTTTTCCTC | CTTGCCAAGAGTCTATTCC | Human | ChIP | 323 | +22 to +345 | 60 |
| pBDNF IV | GGGCTGGAAGTGAAAACATC | ATTGCATGGCGGAGGTAATA | Human | ChIP | 334 | -193 to +141 | 60 |
| pBDNF VI | ATCGAAGCTCAACCGAAGAG | GTCACATCGTGGTTCCGATT | Human | ChIP | 301 | -16 to +284 | 60 |
| pBDNF IX | ATGGCCATTGCATGTATGTG | CTCTTCCTGTTTGCCAGAGG | Human | ChIP | 283 | -432 to -149 | 60 |
| pMIR137HG | TCAGAGAGAGGTGCTGTGAA | CGCCTGCCACTATACACAAA | Human/Rat | ChIP | 323/324 | -325 to -3 | 60 |
| MIR137HG_CpG | CTAAGTGGGCCTGAGCTTTG | CGGAGCTGCTTAAGACCTGA | Human | MeDIP | 314 | +4,140 to +4,453 | 60 |
| MIR137HG_NRSF BSI | ACCTACCCAATGTTCCACCA | CGACAGCTTAAGGAGGCTTG | Human | ChIP | 213 | +1,116 to +1,328 | 60 |

*Note:* PCR primers for RT-PCR cross exon-intron boundaries for each target gene. *Position* for ChIP primers is relative to the first base of the first exon, labelled +1, of the corresponding gene.

### 2.1.9 DNA constructs and commercial vectors

**Table 2.2.** Reporter gene and expression constructs generated for use in *in vitro* luciferase and over-expression assays

| Name | Vector | Orientation | RE sites of insertion | DNA insert and source | Primers for amplification (5' – 3') | Application |
|---|---|---|---|---|---|---|
| Imir137(4/12)F | pGL3B | Forward | XhoI, MluI | Internal MIR137 (Imir137) promoter VNTR, 4- and 12-copy alleles cloned from ALS cohort, plate 1, samples G7 and A7, respectively. | F: ATACCTCGAGACCCAAGAATACCCGTCA<br>R: ATACACGCGTTGGGAGAGCACCAGGTAAA | Luciferase |
| Imir137(4/12)R | pGL3B | Reverse | XhoI, MluI | | F: ATACACGCGTACCCAAGAATACCCGTCA<br>R: ATACCTCGAGAGCAGCAAGAGTTCTGGT | Luciferase |
| Imir137(4)+C | pGL3B | Forward | XhoI, MluI | Imir137 promoter VNTR including rs2660304 SNP. Cloned from HapMap DNA, sample ID NA12057. | F: ATACCTCGAGACCCAAGAATACCCGTCA<br>R: ATACACGCGTTCATACCACCTAGAGTGGAC | Luciferase |
| Imir137(4)+A | pGL3B | Forward | XhoI, MluI | Imir137 promoter VNTR including rs2660304 SNP. Cloned from HapMap DNA, sample ID NA06993. | F: ATACCTCGAGACCCAAGAATACCCGTCA<br>R: ATACACGCGTTCATACCACCTAGAGTGGAC | Luciferase |
| VNTRmir137(4/12)F | pGL3P | Forward | XhoI, MluI | MIR137 VNTR alone, 4- and 12-copy alleles cloned from ALS cohort, plate 1, samples G7 and A7, respectively. | F: ATACCTCGAGACCCAAGAATACCCGTCA<br>R: ATACACGCGTAGCAGCAAGAGTTCTGGT | Luciferase |
| VNTRmir137(4/12)R | pGL3P | Reverse | XhoI, MluI | | F: ATACACGCGTACCCAAGAATACCCGTCA<br>R: ATACCTCGAGAGCAGCAAGAGTTCTGGT | Luciferase |
| RE-EX1 | pcDNA6 | Forward | - | Construct kindly provided by *Prof. G. Mandel,* School of Medicine, OHSU. | - | mRNA over-expression |
| sNRSF | pcDNA3.1 | Forward | HindIII, BamHI | cDNA amplified from human SH-SY5Y neuroblastoma cell line. | F: CTAAAAGCTTGTTATGGCCACCCAGGTA<br>R: CTAAGGATCCTCACACTCTAGTAAATATTACC | mRNA over-expression |

*Note:* Underlined sequences indicate restriction (RE) sites for direct cloning into the specified vector. *Highlighted text in the sNRSF primer set represents the Kozak consensus sequence* ([G/A]NNATGG) which *is required for efficient initiation of translation and the translational stop codon.*

### 2.1.10 ChIP grade antibodies

**Table 2.3.** Antibodies used for ChIP in human SH-SY5Y and MCF-7 cell lines and rat brain tissue

| Antibody | Host Species | Species Reactivity | Immunogen | Company and Catalogue Number | Amount per ChIP |
|---|---|---|---|---|---|
| Anti-EZH2 | Mouse (Monoclonal) | Human, Mouse, Rat | Recombinant protein corresponding to amino acids 353-451 of human EZH2. | Active Motif, 39875 | 3.0 µg |
| Anti-H3 | Rabbit (Polyclonal) | Human, mouse, rat | Synthetic peptide corresponding to the carboxy-terminal of human Histone H3. | Abcam, 1791 | 2.5 µg |
| Anti-H3K9me3 | Rabbit (Polyclonal) | Human, mouse, rat | Synthetic peptide derived from within residues 1-100 of Human H3, trimethylated at lysine 9. | Abcam, 8898 | 3.5 µg |
| Anti-H3K4me2 | Rabbit (Monoclonal) | Human, mouse, rat | Synthetic peptide corresponding to residues surrounding Lys4 of human Histone H3. | Abcam, 32356 | 3.0 µg |
| Anti-MeCP2 | - | Human | Kind gift from Dr Cardoso, Darmstadt. | - | 3.0 µg |
| Anti-RNA Pol II CTD phospho Ser5 | Rat (Monoclonal) | Human | Synthetic peptide containing the RNA pol II C-terminal domain (CTD) sequence phosphorylated at serine 5. | Active Motif, 61085 | 5.0 µg |
| Anti-REST | Rabbit (Polyclonal) | Human, mouse, rat | GST fusion protein corresponding to residues 801-1097 of full-length human REST/NRSF. | Upstate, Millipore, 07-579 | 3.0 µg |
| Anti-NRSF (H-290-X) | Rabbit (Polyclonal) | Human, mouse, rat | Epitope corresponding to amino acids 1-290 of the human REST/NRSF amino-terminal. Identifies all known isoforms of the NRSF protein. | Santa Cruz Biotechnology, sc-25398-X | 5.0 µg |
| Normal rabbit IgG | Rabbit (Polyclonal) | - | Unconjugated antibody not directed against any known antigen. Used as a non-specific IgG control in ChIP assays. | NEB, 2729 check | 5.0 µg |

*Note: Amount per ChIP* refers to the concentration of antibody used per ChIP assay with 5 µg of sheared chromatin.

### 2.1.11 StellARray™ Mood disorder genes

**Table 2.4.** Gene name and description for the Human Mood Disorder 96-well qPCR StellARray™

| Gene Name | Entrez Gene | Description |
|---|---|---|
| ACE | 1636 | Angiotensin I converting enzyme (peptidyl-dipeptidase A) 1 |
| ADCYAP1 | 116 | Adenylate cyclase activating polypeptide 1 (pituitary) |
| ADRBK2 | 157 | Adrenergic, beta, receptor kinase 2 |
| ARNTL | 406 | Aryl hydrocarbon receptor nuclear translocator-like |
| ATP2A2 | 488 | ATPase, Ca++ transporting, cardiac muscle, slow twitch 2 |
| BCR | 613 | Breakpoint cluster region |
| BDNF | 627 | Brain-derived neurotrophic factor |
| CASP8 | 841 | Caspase 8, apoptosis-related cysteine peptidase |
| CCND2 | 894 | Cyclin D2 |
| CHRNA7 | 1139 | Cholinergic receptor, nicotinic, alpha 7 |
| CIT | 11113 | Citron rho-interacting serine/threonine kinase |
| CLOCK | 9575 | Clock circadian regulator |
| COMT | 1312 | Catechol-O-methyltransferase |
| CREB1 | 1385 | CAMP responsive element binding protein 1 |
| CRH | 1392 | Corticotropin releasing hormone |
| CRHBP | 1393 | Corticotropin releasing hormone binding protein |
| DAO | 1610 | D-amino-acid oxidase |
| DISC1 | 27185 | Disrupted in schizophrenia 1 |
| DLX1 | 1745 | Distal-less homeobox 1 |
| DRD1 | 1812 | Dopamine receptor D1 |
| DRD3 | 1814 | Dopamine receptor D3 |
| DRD4 | 1815 | Dopamine receptor D4 |
| DTNBP1 | 84062 | Dystrobrevin binding protein 1 |
| ERBB3 | 2065 | V-erb-b2 erythroblastic leukemia viral oncogene homolog 3 |
| FAT1 | 2195 | FAT atypical cadherin 1 |
| FKBP5 | 2289 | FK506 binding protein 5 |
| FOS | 2353 | FBJ murine osteosarcoma viral oncogene homolog |
| GABRA5 | 2558 | Gamma-aminobutyric acid (GABA) A receptor, alpha 5 |
| GAD1 | 2571 | Glutamate decarboxylase 1 (brain, 67kDa) |
| GCH1 | 2643 | GTP cyclohydrolase 1 |
| GPR50 | 9248 | G protein-coupled receptor 50 |
| GRIK3 | 2899 | Glutamate receptor, ionotropic, kainate 3 |
| GRIK4 | 2900 | Glutamate receptor, ionotropic, kainate 4 |
| GRIN2B | 2904 | Glutamate receptor, ionotropic, N-methyl D-aspartate 2B |
| GRM3 | 2913 | Glutamate receptor, metabotropic 3 |
| GRM4 | 2914 | Glutamate receptor, metabotropic 4 |
| GSK3B | 2932 | Glycogen synthase kinase 3 beta |
| Hs18s | - | Human 18S ribosomal RNA |
| HS Genomic | - | Human genomic DNA control |
| HSP90B1 | 7184 | Heat shock protein 90kDa beta (Grp94), member 1 |
| HSPA5 | 3309 | Heat shock 70kDa protein 5 (glucose-regulated protein, 78kDa) |
| HTR1B | 3351 | 5-hydroxytryptamine (serotonin) receptor 1B |
| HTR2A | 3356 | 5-hydroxytryptamine (serotonin) receptor 2A |
| IL1RN | 3557 | Interleukin 1 receptor antagonist |
| IMPA1 | 3612 | Inositol(myo)-1(or 4)-monophosphatase 1 |
| IMPA2 | 3613 | Inositol(myo)-1(or 4)-monophosphatase 2 |
| INPP1 | 3628 | Inositol polyphosphate-1-phosphatase |

| | | |
|---|---|---|
| ISYNA1 | 51477 | Myo-inositol 1-phosphate synthase A1 |
| JUN | 3725 | Jun oncogene |
| KCNN3 | 3782 | Potassium intermediate/small conductance calcium-activated channel, subfamily N, member 3 |
| MAG | 27307 | Malignancy-associated gene |
| MAL | 4118 | Mal, T-cell differentiation protein |
| MAOA | 4128 | Monoamine oxidase A |
| MLC1 | 23209 | Megalencephalic leukoencephalopathy with subcortical cysts 1 |
| MOBP | 4336 | Myelin-associated oligodendrocyte basic protein |
| MOG | 4340 | Myelin oligodendrocyte glycoprotein |
| MTHFR | 4524 | 5,10-methylenetetrahydrofolate reductase (NADPH) |
| NAPG | 8774 | N-ethylmaleimide-sensitive factor attachment protein, gamma |
| NCAM1 | 4684 | Neural cell adhesion molecule 1 |
| ND4 | 4538 | Mitochondrially encoded NADH dehydrogenase 4 |
| NDUFV1 | 4723 | NADH dehydrogenase (ubiquinone) flavoprotein 1, 51kDa |
| NDUFV2 | 4729 | NADH dehydrogenase (ubiquinone) flavoprotein 2, 24kDa |
| NOS1AP | 9722 | Nitric oxide synthase 1 (neuronal) adaptor protein |
| NR1D1 | 9572 | Nuclear receptor subfamily 1, group D, member 1 |
| NR3C1 | 2908 | Nuclear receptor subfamily 3, group C, member 1 (glucocorticoid receptor) |
| NRG1 | 3084 | Neuregulin 1 |
| NTRK2 | 4915 | Neurotrophic tyrosine kinase, receptor, type 2 |
| OLIG2 | 10215 | Oligodendrocyte lineage transcription factor 2 |
| P2RX7 | 5027 | Purinergic receptor P2X, ligand-gated ion channel, 7 |
| PAFAH1B1 | 5048 | Platelet-activating factor acetylhydrolase, isoform Ib, alpha subunit 45kDa |
| PAFAH1B3 | 5050 | Platelet-activating factor acetylhydrolase, isoform Ib, gamma subunit 29kDa |
| PCNT | 5116 | Pericentrin |
| PDLIM5 | 10611 | PDZ and LIM domain 5 |
| PER3 | 8863 | Period circadian clock 3 |
| PIP4K2A | 5305 | Phosphatidylinositol-5-phosphate 4-kinase, type II, alpha |
| PLA2G1B | 5319 | Phospholipase A2, group IB (pancreas) |
| PLA2G4A | 5321 | Phospholipase A2, group IVA (cytosolic, calcium-dependent) |
| PLCG1 | 5335 | Phospholipase C, gamma 1 |
| PLP1 | 5354 | Proteolipid protein 1 |
| POLG | 5428 | Polymerase (DNA directed), gamma |
| PTGS2 | 5743 | Prostaglandin-endoperoxide synthase 2 (prostaglandin G/H synthase and cyclooxygenase) |
| RELN | 5649 | Reelin |
| RFX4 | 5992 | Regulatory factor X, 4 (influences HLA class II expression) |
| RGS4 | 5999 | Regulator of G-protein signaling 4 |
| SLC12A6 | 9990 | Solute carrier family 12 (potassium/chloride transporters), member 6 |
| SLC6A2 | 6530 | Solute carrier family 6 (neurotransmitter transporter, noradrenalin), member 2 |
| SLC6A3 | 6531 | Solute carrier family 6 (neurotransmitter transporter, dopamine), member 3 |
| SLC6A4 | 6532 | Solute carrier family 6 (neurotransmitter transporter, serotonin), member 4 |
| SULT1A1 | 6817 | Sulfotransferase family, cytosolic, 1A, phenol-preferring, member 1 |
| SYNGR1 | 9145 | Synaptogyrin 1 |
| TAAR6 | 319100 | Trace amine associated receptor 6 |
| TF | 7018 | Transferrin |
| TIMELESS | 8914 | Timeless circadian clock |
| TPH1 | 7166 | Tryptophan hydroxylase 1 (tryptophan 5-monooxygenase) |
| TPH2 | 121278 | Tryptophan hydroxylase 2 |
| XBP1 | 7494 | X-box binding protein 1 |

## 2.2 Methods

### 2.2.1 Designing PCR primers

Polymerase chain reaction (PCR) primers were designed using the online primer designer software Primer3 (http://biotools.umassmed.edu/bioapps/primer3_www.cgi) which generates a list of suitable PCR primers for amplification of the sequence of interest based on appropriate melting temperatures, GC% content and potential dimerisation and hairpin formation. In general, primers were designed to be 18-25 nucleotides in length, have a melting temperature of 50-65°C and a GC-content between 40-60%. Primer specificity was determined using the *In-Silico PCR* and *Pick Primers* tools available from the UCSC Genome Browser (http://genome.ucsc.edu/index.html) and National Center for Biotechnology Information (NCBI) (http://www.ncbi.nlm.nih.gov/tools/primer-blast/). Primers were purchased from Eurofins MWG Operon and are listed in **Table 2.1**.

### 2.2.2 General Cloning Methods

2.2.2.1 PCR primer design for direct cloning into commercial vectors

Primers were designed as outlined in *section 2.2.1* with a minimum length of 15 bp. Appropriate restriction sites (present in the multiple cloning site of the chosen vector but absent in the target sequence) were added to the 5' end of the forward and reverse primers so that they are incorporated at the ends of the target DNA sequence following PCR amplification. To ensure efficient DNA cleavage by the restriction enzymes, a random sequence of 6 bp was also included 5´ of the restriction sites. Primers used for direct cloning are listed in **Table 2.2** and PCR methods outlined below in *section 2.2.2.2*.

#### 2.2.2.2 PCR using a proof-reading polymerase

Phusion High-Fidelity DNA Polymerase (NEB) was used in PCR for the amplification of DNA targets. The Phusion DNA Polymerase master mix is outlined below:

| **Component** | **Volume (n=1)** | **Final Concentration** |
|---|---|---|
| 5X Phusion HF buffer | 4 µl | 1X |
| PCR nucleotide mix (10 mM of each dNTP) | 1 µl | 200 µM |
| Forward primer (10 µM) | 1 µl | 0.5 µM |
| Reverse primer (10 µM) | 1 µl | 0.5 µM |
| Phusion DNA polymerase (2 U/µl) | 0.2 µl | 0.4 U |
| Nuclease free water | X µl | - |
| DNA template | X µl | - |
| Final volume | 20 µl | - |

PCR reactions were performed in a QB-96 (Quanta Biotech) or peqSTAR 2X (peqlab) thermocycler. The amount of DNA template used varied between primer sets depending on the abundance of the target for amplification. Thermal cycling conditions were as follows: initial denature at 98˚C for 30 seconds, followed by 25 cycles of denature, annealing and extension at 98˚C for 10 seconds, X˚C for 30 seconds and 72˚C for 30 seconds, respectively, with a final extension cycle at 72˚C for 10 minutes. The annealing temperature of each primer set was optimised using a gradient PCR and are listed in **Table 2.1** along with primer sequences and expected product sizes. PCR products were analysed by agarose gel electrophoresis, see *section 2.2.2.3*.

#### 2.2.2.3 Analysis of DNA using agarose gel electrophoresis

DNA fragments from PCR reactions or restriction digests were analysed by gel electrophoresis on 1-2.0% agarose gels supplemented with GelRed (1:10,000 dilution) (Cambridge Bioscience) or 0.5 µl per 10 ml of ethidium bromide (Sigma 10 mg/ml) and measured against a 100 bp or 1 Kb DNA ladder (Promega). The voltage (standard is 5 V/cm) and time for which the gel was run was dependant on the percentage of the gel and fragment size. The DNA was visualised using a UV transillumintor (BioDoc-it Imaging System).

#### 2.2.2.4 Recovery of DNA from agarose-gels

Following separation through gel-electrophoresis, DNA fragments of the expected size were extracted from the agarose gel and column-purified using the QIAquick Gel Extraction Kit (QIAGEN), following manufacturer's instruction. The purified DNA was eluted in 30 µl Elution Buffer.

#### 2.2.2.5 Restriction digest and DNA purification

Restriction enzyme digests were used either to create specific nucleic acid overhangs for ligation or as a diagnosis tool for determining the presence and/or orientation of inserts. Restriction enzymes were purchased from Promega and digests performed using the following reaction components:

| | |
|---|---|
| Nuclease free water | X µl |
| 10X Buffer | 2 µl |
| Acetylated BSA (10 µg/µl) | 0.2 µl |
| DNA (1 µg) | X µl |
| Restriction Enzyme (10 U/µl) | 0.5 µl |
| Final volume | 20 µl |

Recommended buffers for optimum enzyme activity were used, digestions were incubated at the appropriate temperature for the enzyme activity for 1-4 hours and fragments run on agarose gels to visualise their size (*section 2.2.2.3*).

### 2.2.2.6 Ligation

Purified DNA fragments were ligated into the appropriate vectors at an insert : vector molar ratio of 3:1 using the following ligation calculation:

$$\frac{\text{ng vector} \times \text{insert size kb}}{\text{vector size kb}} \times \text{molar ratio of } \frac{\text{insert}}{\text{vector}} = \text{ng insert}$$

For the ligation reaction, 1 µl (100 ng) of vector and the appropriate volume of insert were added to 1 µl Ligase 10X Buffer (Promega) and 1 µl T4 DNA Ligase (1-3 U/µl) (Promega) and made up to a final volume of 10 µl with nuclease free water. The reaction was incubated at room temperature for 4 hours or at 16°C overnight.

### 2.2.2.7 Transformation of chemically competent E. Coli cells

Following ligation, the resulting plasmids were transformed into chemically competent *E. Coli* Sub-cloning Efficiency™ DH5-α cells (Invitrogen), following manufacturer's instruction. Briefly, 5 µl of the ligation reaction or 10 ng plasmid DNA was added to 50 µl of competent DH5-α cells and incubated on ice for 30 minutes. The cells were then subjected to 'heat-shock' for 20 seconds at 42°C in a water bath followed by 2 minutes incubation on ice. Next, 950 µl of pre-warmed LB broth was added to the cells and the culture incubated with constant shaking (225 rpm) at 37°C for 1 hour. Following this, 200 µl of the

culture was spread evenly onto LB agar plates supplemented with 100 µg/ml ampicillin and incubated overnight at 37°C.

#### 2.2.2.8 Isolation of plasmid DNA from bacterial cultures

##### *2.2.2.8.1 Mini-preparation of plasmid DNA*

In order to test plasmid DNA for inserts following molecular cloning, a small scale preparation of DNA (up to 20 µg) was undertaken. Individual colonies grown on LB agar plates (*section 2.2.2.7*) were transferred to 5 ml LB broth supplemented with 100 µg/ml ampicillin and cultured overnight at 37°C on a shaker at 225 rpm. DNA was isolated from the resulting bacterial culture using the QIAprep Spin Miniprep Kit (QIAGEN), according to manufacturer's guidelines. Purified plasmid DNA was eluted in 50 µl nuclease-free water into fresh 1.5 ml microcentrifuge tubes and subject to restriction enzyme digestion to check for the correct size and orientation of the insert (*section 2.2.2.5*).

##### *2.2.2.8.2 Maxi-preparation of plasmid DNA*

A Plasmid Maxi Kit (Qiagen) was used to purify high yields of plasmid DNA from transformed bacteria of greater purity than that generated from mini-preparations for use in downstream applications such as *in vitro* reporter gene assays. A 200 µl aliquot of the 5 ml starter culture from *section 2.2.2.8.1* or starter culture grown from a small scraping of a glycerol stock (*section 2.2.2.10*) was grown overnight at 37°C with shaking (225 rpm) in 100 ml of LB broth supplemented with the appropriate antibiotic to generate a sufficient quantity of bacteria for extraction of the plasmid DNA. DNA purification was carried out according to manufacturer's instruction for high-copy plasmids. The resulting

DNA pellet was resuspended in 200-500 µl of EB buffer and quantified using a Nanodrop 8000 and then stored at -80°C for long-term storage or at -20°C for working stocks.

#### 2.2.2.9 Sequencing

Plasmid DNA with cloned inserts and PCR products were sequenced externally by Dundee DNA Sequencing and Service or Source Bioscience Life Sciences. The samples and primers were supplied as required by the companies.

#### 2.2.2.10 Glycerol stocks

Glycerol stocks of transformed bacteria were made for long term storage. 1.4 ml of the overnight culture was transferred to a microcentrifuge tube and pelleted by centrifugation at 8,000 rpm for 3 minutes at room temperature. The supernatant was removed and the pellet resuspended in 0.5 ml of sterile 15% glycerol (v/v in LB broth) and transferred into a cryovial. This was then immediately frozen at -80°C.

#### 2.2.2.11 Generation of MIR137 reporter gene constructs

##### *2.2.2.11.1 pGL3-Basic (pGL3B) constructs*

MIR137 Internal promoter fragments containing either the 4-copy or 12-copy variant of the MIR137 variable number tandem repeat (VNTR) were amplified from human DNA (ALS cohort, plate 1, wells G7 and A7, respectively) and ligated into the pGL3B vector, which lacks a minimal promoter sequence, at the MluI and XhoI restriction sites. Specifically we included nucleotides -361/ -481 to +38 numbered from the first base of the precursor miRNA sequence as

+1. The difference in 5' end of these fragments reflected the two distinct VNTRs and were termed Imir137(4) and Imir137(12), respectively.

The Imir137(4) fragment containing alternative alleles of the SNP rs2660304 that is present within the second exon of the non-protein coding gene MIR137HG (AK094607) and in linkage disequilibrium with the schizophrenia associated GWAS SNP rs1625579 was amplified using primers listed in **Table 2.2** and human DNA samples from the HapMap CEU cohort (Imir137(4)+C, sample ID NA12057 and Imir137(4)+A, sample ID NA06993) using methods described above for the Imir137 reporter gene constructs.

#### *2.2.2.11.2 pGL3-Promoter (PGl3P) constructs*

The MIR137 VNTR alone was also cloned into reporter gene constructs, either −86 or −206 to +38 bp (reflecting the 4- and 12-copy repeats) into the pGL3-Promoter (pGL3P) vector upstream of the minimal SV40 promoter in forward and reverse orientations. These were termed VNTRmir137(4)F or R and VNTRmir137(12)F or R, respectively, to indicate both copy number and orientation of fragment. Details of primers and restriction sites are listed in **Table 2.2**.

### 2.2.2.12 Generation of sNRSF gene expression construct

The truncated human NRSF variant, sNRSF, was amplified from human SH-SY5Y cDNA and directly cloned into the pcDNA3.1 expression vector (Invitrogen) using the primers and restriction sites listed in **Table 2.2**. For correct initiation of sNRSF translation within the expression construct, the forwards primer was designed to generate an insert conferring a Kozak

consensus sequence ([G/A]NNATGG) containing an ATG initiation codon and the reverse primer designed to include the sNRSF stop codon.

### 2.2.3 Cell Culture

#### 2.2.3.1 Culturing of SH-SY5Y and MCF-7 cells

Human SH-SY5Y neuroblastoma and human MCF-7 breast adenocarcinoma cells were maintained in culture media outlined in *section 2.1.6* at 37°C, 5% $CO_2$, in T175 tissue culture flasks until 70-80% confluent. To passage cells, media was removed and the cells washed down with 1X sterile PBS (Sigma) pre-warmed at 37°C. Following removal of the PBS, 5 ml of pre-warmed 1X trypsin (Sigma) was washed over the cells and then removed, and the cells incubated at 37°C for approximately 3 minutes or until the cells began to detached from the bottom of the flask. To neutralise the trypsin, cells were washed down in 10 ml of pre-warmed complete tissue culture media and mixed into a single cell suspension through pipetting. Between 1-2 ml (approximately 1-2.4 million cells depending on cell type) of the cell suspension was then transferred into a new T175 flask with 40 ml of the appropriate media for that cell line. Cell lines were tested for mycoplasm infection every six months using MycoAlert Mycoplasma Detection kit (Lonza).

#### 2.2.3.2 Cell counts with a haemocytometer

To determine the number of cells per ml of media cell counts were performed using a haemocytometer. Cells were passaged as described in *section 2.2.3.1* up to the cells being washed down with 10 ml of media. Prior to the coverslip being placed onto the counting surface of the haemocytometer both

parts were washed with 70% ethanol. On the centre of the counting surface of the haemocytometer there are 25 squares (5x5) bounded by three parallel lines each containing 25 smaller squares (5x5). To perform the cell count, 20 µl of the cell suspension was introduced under the coverslip and the counting surface visualised under a light microscope on the 10X objective. The number of cells within the 25 larger squares bounded by three parallel lines were counted including cells touching the top or left hand borders of the 25 squares and excluding those in contact with the bottom or right hand border. This area corresponds to 0.1 $mm^3$ therefore the number of cells was multiplied by $1x10^4$ (10,000) to give the number of cells in 1 $cm^3$ which is the equivalent of 1 ml. This gave the number of cells per ml of media used for calculating the density at which the cells were seeded.

#### 2.2.3.3 Freezing cells for storage in liquid nitrogen

For long term storage, cell lines were frozen in freezing media (*section 2.1.6.4*) in liquid nitrogen. The cells were grown in T175 flasks until 70-80% confluent and then passaged as described in *section 2.2.3.1* but the cells were washed from the surface of the flask using 10 ml of freezing media and the cell suspension split across cryovials with 1.8 ml in each. The cryovials were immediately placed into a Mr Frosty with isopropanol at $-80^0C$ for 24 hours and then transferred to liquid nitrogen.

#### 2.2.3.4 Drug treatments

Drug treatments were performed using concentrations previously optimised in our lab or reported in the literature to be effective in cell culture. These are detailed in *section 2.1.3*. Cells were serum-starved 24 hours prior to drug treatments to promote cell-cycle synchronisation (Zetterberg and Skold, 1969, Kramer et al., 2010). This involved culturing the cells in low serum media outlined in *section 2.1.6.2*. Drugs were diluted in appropriate volumes of complete cell culture media and added to the cells for the specified time. For 72 hour treatment of MCF-7 cells with the 5'aza-DC DNA demethylation agent, fresh media alone or media containing the drug or drug vehicle (DMSO) was added to the cells 24 and 48 hours following the initial treatment. For each drug treatment, n=4. Basal (untreated) and drug vehicle control cells were also included. For mRNA expression profiling (*section 2.2.5*), RNA extractions were performed immediately after the drug treatment. For luciferase and over-expression assays, drug treatments were performed 4 hours post-transfection (*section 2.2.3.5*).

#### 2.2.3.5 Delivery of plasmid DNA to cultured cells

##### *2.2.3.5.1 Single transfection assays*

For NRSF over-expression assays, SH-SY5Y cells were seeded into 6-well plates at approximately 400,000 cells per well and transfected with either 4 μg of RE-EX1 or pcDNA3.1_sNRSF using the TurboFect (Thermo Scientific) transfection reagent following the manufacturer's guidelines. pcDNA3.1 alone was used as a negative control. Cells were incubated for 48 hours before being processed for RNA extraction (*section 2.2.5.1*).

*2.2.3.5.2 Co-transfection assays*

For luciferase assays, SH-SY5Y cells were seeded in 24-well plates at approximately 100,000 cells per well and transfected with 1 µg plasmid DNA and 10 ng pMLuc2 (Novagen) (internal control for transfection efficiency) using TurboFect (Thermo Scientific). Addition of 1 µg RE-EX1 or pcDNA3.1_sNRSF was also included for assessment of NRSF over-expression on reporter gene activity; pcDNA3.1 alone was used as a negative control. Transfected cells were processed 48 hours post-transfection using the Dual-Luciferase Reporter Assay System (Promega).

### 2.2.4 Luciferase Reporter Gene Assays

2.2.4.1 Cellular lysis

At 48 hours post-transfection, tissue culture media was removed from the cells and the cells washed with 1X PBS. For cellular lysis, 100 µl of 1X passive lysis buffer (PLB) was added to each well of the 24-well plate and the plate incubated at room temperature on a rocking platform for 15 minutes. 20 µl of the cell lysate was then transferred to an opaque 96-well plate for analysis.

2.2.4.2 Measurement of reporter gene activity

The appropriate amount of luciferase assay reagent II (LARII) and Stop and Glo reagent was prepared for the number of measurements required and allowed to reach room temperature. The opaque 96-well plate containing the cell lysate was placed into a Glomax 96 Microplate Luminometer (Promega) which had been setup under default settings for dual-luciferase reporter gene assays for experiments using two-injectors. The injectors were first flushed

with distilled water, 70% ethanol, distilled water and air to thoroughly clean them and then primed with the luciferase reagents (LARII in injector 1 and Stop and Glo in injector 2) before the Promega dual luciferase program is run, which measures the bioluminescence from the reaction catalysed by the firefly and *renilla* luciferase enzymes. The LARII is added first to measure the bioluminescence produced by the reaction catalysed by the firefly luciferase protein and then the Stop and Glo quenches this reaction and is used to measure the bioluminescence from the reaction catalysed by the *renilla* luciferase protein.

#### 2.2.4.3 Statistical analysis

Using the measurements recorded for the activity of the two co-transfected reporter gene constructs, the activity of the constructs across the different wells can be accurately compared as the internal control reduces experimental variability caused by differences in transfection efficiencies. Fold changes in firefly luciferase activity (normalised to *renilla* luciferase activity) supported by the reporter gene constructs over the pGL3 controls were calculated and significance determined using one-tailed *t*-tests. Significance was scored as follows */# $P<0.05$, **/## $P<0.01$, ***/### $P<0.001$. For each transfection, a minimum of n= 4 was used.

### 2.2.5 mRNA expression analysis

#### 2.2.5.1 *In vitro* RNA extraction

Total RNA was extracted using TRIzol reagent (Invitrogen) following manufacturer's instruction. Briefly, SH-SY5Y and MCF-7 cells were plated out into 6-well plates at approximately 400,000 cells per well and incubated for 24 hours. The media from each well was removed and 1 ml of TRIzol was added per 10 $cm^2$ and pipetted up and down to lyse the cells. The cell lysate/TRIzol mix was added to a nuclease-free microcentrifuge tube and incubated for 5 minutes at room temperature. To each sample 0.2 ml of chloroform (per 1ml of TRIzol reagent) was added, shaken vigorously by hand for 15 seconds and then incubated at room temperature for 2-3 minutes. Samples were then centrifuged at 12,000 x g for 15 minutes at 4$^{o}$C for phase separation into three layers: a colourless aqueous upper layer containing the RNA, a middle interphase layer and a lower red organic layer containing the DNA and protein. The upper colourless layer (approximately 500 µl) was carefully removed and transferred into a new microcentrifuge tube and 0.5 ml of 100% molecular grade isopropanol (per 1ml of TRIzol reagent) added to each sample and incubated for 10 minutes at room temperature. Samples were then centrifuged at 12,000 x g for 10 minutes at 4$^{o}$C and the resulting supernatant removed leaving behind the RNA pellet.

To purify the RNA, 1 ml of 75% ethanol (per 1 ml of TRIzol reagent used in the initial step) was added and the sample vortexed and centrifuged at 7,500 x g for 5 minutes at 4$^{o}$C. The supernatant was removed and the pellet air dried for 5 to 10 minutes before being resuspended in 20 µl of nuclease free water and incubated on a heat block at 55$^{o}$C for 10-15 minutes. The RNA samples

were kept on ice for quantification (*section 2.2.5.3*) and first strand cDNA synthesis steps (*section 2.2.5.4*) or stored at -80°C for later use.

### 2.2.5.2 *In vivo* co-extraction of RNA and DNA

Rat brain tissue samples described in *section 2.1.7* (25–100 mg) were homogenised for approximately 10-20 seconds in 1 ml of TRI Reagent (Sigma) using a TissueRuptor (QIAGEN) and the upper aqueous phase processed for RNA isolation following manufacturer's instruction. RNA pellets were resuspended in 20 µl nuclease free water and stored at -80°C or kept on ice ready for quantification (*section 2.2.5.3*) and first strand cDNA synthesis steps (*section 2.2.5.4*). DNA was isolated from the lower organic phase (samples were kept at 4°C until ready for processing) following a protocol described elsewhere (Kotorashvili et al., 2012). Briefly, DNA was precipitated by addition of 1.2 ml of 100% ethanol and 20 µl of sodium acetate (NaAc), incubated at room temperature for 3 minutes and then centrifuged at 16,000 rpm for 30 minutes at 4°C. The resulting DNA pellet was washed with 100% ethanol and then air-dried at 50°C before being resuspended in 180 µl AL buffer from the DNeasy Blood & Tissue Kit (QIAGEN) and subjected to proteinase K digestion and subsequent steps of the DNA extraction according to manufacturer's protocol. Resulting DNA pellets were resuspended in 50 µl nuclease free water and stored at -20°C.

#### 2.2.5.3 Measurement of RNA concentration by spectrometry

RNA was quantified using a Nanodrop 8000. The Nanodrop was set to the RNA setting and calibrated with nuclease free water (the solvent the RNA was diluted in). A 1.5 µl aliquot of the RNA sample was loaded onto the pedestal and the absorbance measured. The amount of UV light absorbed at 260 nm by nucleic acids is dependent on their concentration. The Nanodrop measures the optical density (OD) of the RNA and then calculates its concentration (an $OD_{260nm}$ of 1 equals an RNA concentration of 40 µg/ml). The Nanodrop was also used to assess the quality of the RNA through measuring the 260/280 and 260/230 ratios; expected values for high quality RNA are approximately 2.0 and 2.0-2.2, respectively. The RNA was then stored at -80°C.

#### 2.2.5.4 First strand cDNA synthesis

cDNA was synthesised from total RNA, extracted using methods outlined in *sections 2.2.5.1* and *2.2.5.2*, using the GoScript Reverse Transcription System (Promega) following the recommended manufacturer's protocol. For each sample in the experiment the same amount of RNA was used in the reverse transcriptase reaction, combined in a PCR tube with the following components:

| | |
|---|---|
| RNA (up to 5 µg) | X µl |
| Random Primers (0.5 µg/reaction) | 1 µl |
| Nuclease free water | X µl |
| Final volume | 5 µl |

The mixture was denatured at 70°C for 5 minutes and then cooled on ice. The following reverse transcription mix was added to the RNA, random primers and nuclease free water and made up to a final reaction volume of 20 µl:

| Component | Volume (n=1) | Final Concentration |
|---|---|---|
| Nuclease free water (to a final volume of 15 µl) | Xµl | - |
| GoScript 5X reaction buffer | 4 µl | 1X |
| $MgCl_2$ (25 mM) | 4 µl | 5 mM |
| PCR nucleotide mix (10 mM of each dNTP) | 1 µl | 0.5 mM |
| Recombinant RNasin Rinonuclease inhibitor (40 U/µl) | 0.5 µl | 1 U/µl |
| GoScript Reverse Transcriptase | 1 µl | - |

The reaction mixtures were incubated at 25°C for 5 minutes to allow primer annealing and then incubated at 42°C for 60 minutes for the extension step. The reverse transcriptase was inactivated by heating the reaction to 70°C for 15 minutes. The cDNA was diluted appropriately (if 2 µg RNA was converted a 1:20 dilution was made) using nuclease free water and stored at -20°C.

### 2.2.5.5 Semi-quantitative PCR analysis of mRNA expression

For analysis of gene expression, cDNA generated as previously described was amplified using GoTaq DNA polymerase (Promega) following manufacturer's guidelines. The GoTaq Flexi DNA Polymerase master mix is:

| Component | Volume (n=1) | Final Concentration |
|---|---|---|
| 5X Green GoTaq Flexi buffer | 5 µl | 1X |
| $MgCl_2$ (25 mM) | 4 µl | 4 mM |
| PCR nucleotide mix (10 mM of each dNTP) | 1 µl | 0.4 mM |
| Forward primer (20 µM) | 0.25 µl | 0.2 µM |
| Reverse primer (20 µM) | 0.25 µl | 0.2 µM |
| GoTaq DNA polymerase (5u/µl) | 0.25 µl | 0.05 U/µl |
| Nuclease free water | X µl | - |
| cDNA template (1:10 dilution) | 1 µl | - |
| Final volume | 25 µl | - |

The PCR was performed in a thermocycler: QB-96 (Quanta Biotech) or peqSTAR 2X (peqlab). The annealing temperature of each primer set was optimised using a gradient PCR and are detailed in **Table 2.1**. The amount of cDNA template used varied between primer sets depending on the abundance of the target for amplification. In general, 1 µl of a 1:20 dilution of cDNA generated from 2 µg of RNA was used for target genes and a 1:200 dilution of cDNA used for reference genes. Standard thermal cycling conditions were as follows: incubation at 95˚C for 5 minutes, followed by 25 or 35 cycles (for reference and target genes, respectively) of 95˚C for 30 seconds, 57-65˚C for 30 seconds and 72˚C for 30 seconds, with a final cycle at 72˚C for 10 minutes. Samples were kept at 4˚C prior to gel electrophoresis (*section 2.2.2.3*) or at -20˚C for long-term storage.

#### 2.2.5.6 Quantitative PCR (qPCR)

Total RNA and cDNA was harvested as previously described and qPCR performed using GoTaq qPCR Master Mix (Promega) according to the manufacturer's amplification protocol. 10 µl reactions were used consisting of 5 µl 2X master mix, 0.1 µl forward and reverse primers (20 µM), 2 µl cDNA and 0.1 µl CXR 100X reference dye, made up to the total reaction volume with nuclease free water. Analysis was performed on a ViiA™ 7 Real-Time PCR System (Applied Biosystems). All primers used were shown to have an amplification efficiency of between 80-110% (primer sequences are shown in **Table 2.1**). Relative expression ratio was determined using the Pfaffl method (Pfaffl, 2001), explained below:

**Target gene:**
*Untreated sample:*
If A = average Ct of the target gene in untreated sample(s)

*Treated sample:*
If B = average Ct of the target gene in treated sample(s)
$E_1$ = Target efficiency

**Reference ("Housekeeping") gene:**
*Untreated sample:*
If F = average Ct of the reference gene in untreated sample(s)
*Treated sample:*
If G = average Ct of the reference gene in treated sample(s)
$E_2$ = Target efficiency

Then, the fold difference in target gene between the untreated and treated sample(s) is:

$$\text{Relative ratio} = E_1^{(A-B)}/E_2^{(F-G)}; \text{ where } E = 10^{(-1/\text{slope})}$$

2.2.5.7 Lonza StellARray™ Gene Expression system

qPCR analysis was performed on an iQ5 real-time PCR system (Bio-Rad) using 1 µl of cDNA per reaction (approximately 50 ng/µl) and GoTaq qPCR Master Mix (Promega) with the addition of Fluorescene Calibration Dye (Bio-Rad) at a final concentration of 10 nM. Changes in gene expression were analysed on the Lonza website (http://array.lonza.com/gpr), using the Global Pattern Recognition™ (GPR) analysis software designed by Bar Harbor Biotechnology (https://www.bhbio.com/BHB/dw/home.html). This algorithm internally normalised the real-time qPCR data set of each gene with respect to all genes within the experiment and generated a list of genes that are ranked on the basis of the difference between the test and control expression levels and the consistency of the data between the biological replicates. This proprietary

software calculated both the fold-change data and the respective *p*-values. The results for the qPCR arrays are displayed as change with respect to the normaliser genes that were selected based on minimal changes in expression (defined on Ct values) across treatment conditions obtained using the GPR analysis software (Akilesh et al., 2003). A list of genes on the mood array is given in **Table 2.4**.

### 2.2.6 Bioinformatic Analysis

#### 2.2.6.1 ECR (Evolutionary Conserved Regions) Browser

Conservation of transcription factor consensus binding sequences were addressed based on the TRANSFAC 4.0 database (Matys, 2003) available through the rVista 2.0 tool on the ECR Browser (http://ecrbrowser.dcode.org/) using the following parameters: minimum matrix conservation (similarity between the consensus binding site for a transcription factor and a potential binding site in the query sequence), 70%; minimum number of homologous sites (the minimum number of sites of which a matrix is built), 4; factor class level (the classification of transcription factors in the TRASNFAC database is hierarchical and include 6 levels, from family of transcription factors to splice variants), 4; and similarity of the sequence to the matrix, 1.

#### 2.2.6.2 Genevar (Gene Expression Variation) suite

Analysis and visualisation of eQTL (expression quantitative trait loci) association patterns within the NRSF and BDNF genes was performed using the Java-based application platform Genevar, version 3.3.0, accessible at (http://www.sanger.ac.uk/resources/software/genevar). eQTL data from the

HapMap study based on lymphoblastoid cell lines from CEU individuals was used to address SNP-gene associations (Stranger et al., 2012). Analysis parameters were set to default (Spearman's rank correlation coefficient, rho) with 10,000 permutations in order to construct a distribution of the test statistic, under the null hypothesis of no SNP–probe associations. This involves randomly re-assigning expression intensities to the individuals' genotypes and re-computing the correlation coefficient and statistical significance for the shuffled dataset, which is repeated 10,000 times (Yang et al., 2010).

#### 2.2.6.3 HapMap Genome Browser and Haploview

SNP genotype data for genomic regions of interest corresponding to individuals from the CEPH trios of European descent were downloaded from the HapMap Genome Browser, release #28 (August 2010, NCBI build 36, dbSNP b126), which can be accessed at http://hapmap.ncbi.nlm.nih.gov/. Genotype data was uploaded into Haploview 4.1 (www.broad.mit.edu/mpg/haploview/), freely available software for measuring linkage disequilibrium (LD), defining haplotype blocks and identifying haplotype tagging SNPs (htSNPs) (Barrett et al., 2005). Under the standard *Linkage* format, htSNPs were identified using the *pairwise-tagging* function ($r^2$ threshold, 0.8). SNPs were filtered to include only those with a minor allele frequency (MAF) of greater than 5% within a Caucasian population.

LD analysis was performed using the D-prime (D') statistic, which is derived from the earliest measures of disequilibrium, termed D**.** D quantifies disequilibrium as the difference between the observed frequency of a two-locus haplotype (combination of alleles at adjacent loci on a single chromosome) and

the frequency it would be expected to show if the alleles were segregating at random. Adopting the standard notation for two adjacent loci — *A* and *B*, with two alleles (Aa and Bb) at each locus — the observed frequency of the haplotype that consists of alleles *A* and *B* is represented by *PAB*. Assuming the independent assortment of alleles at the two loci, the expected haplotype frequency is calculated as the product of the allele frequency (*P*) of each of the two alleles, or *PA* × *PB*. Therefore, one of the simplest measures of disequilibrium is: $D = PAB - PA \times PB$, which states the linear relationship between a given pair of markers, were a D' value of 1 represents complete LD. The squared correlation coefficient ($r^2$), used for htSNP analysis and therefore also a measure of LD, is determined by dividing D' by the product of the four allele frequencies. When $r^2 = 1$, this indicates that two markers have equal allele frequencies and are therefore in complete LD (D' = 1).

#### 2.2.6.4 HaploReg

To determine the potential regulatory effects of non-coding SNPs within the genome, we uploaded SNPs of interest into the online package HaploReg, version 2, accessible at http://www.broadinstitute.org/mammals/haploreg/haploreg.php. This tool allows for annotation of the functional effects of non-coding SNPs on evolutionary conservation, chromatin states and regulatory elements. The latter is assessed through allele-specific alterations to position weight matrices (PWMs) of known transcription factors using ENCODE (Encyclopaedia of DNA elements) data, determined by logarithm of odds (LOD) calculations (Ward and Kellis, 2012).

#### 2.2.6.5 NCBI

Sequence alignments between human and rat genomes were performed using the basic local alignment search tool of nucleotide databases (BLASTN) (Altschul et al., 1997), available at NCBI (http://blast.ncbi.nlm.nih.gov/Blast.cgi). BLAST finds regions of local similarity between sequences through making comparisons of nucleotide or protein sequences to sequence databases, calculating the statistical significance of matches. BLAST can be used to infer functional and evolutionary relationships between sequences as well as help to identify members of gene families.

#### 2.2.6.6 Pathway analysis tools

##### *2.2.6.6.1 MetaCore™*

Gene expression data generated from GPR analysis (see *section 2.2.5.7*) was uploaded into the online biological pathway analysis software MetaCore™, version 6.15 build 62452. Functional enrichment of the experimental dataset was performed using: 1) the Pathway Map analysis tool to identify significantly associated pathways based on p-value and GPR fold-change and 2) Build Network for Your Experimental Data feature using the Transcription Factor Targets Modelling algorithm with default settings under Analyse Networks (Transcription Factors) to generate sub-networks based on the presence of transcription factors and/or receptor targets within the original input file. Genes/proteins uploaded from experimental datasets and from which pathways were built upon were termed 'seed nodes'.

*2.2.6.6.2 DIANA-miRPath*

Predicted NRSF target miRNAs were uploaded into the freely available DIANA-miRPath pathway analysis web-server that utilises experimentally validated miRNA interactions derived from DIANA-TarBase v6.0. Using a complex meta-analysis algorithm, the software performs enrichment analysis of miRNA gene targets with the Kyoto Encyclopaedia of Genes and Genomes (KEGG) pathway database; a resource of pathway maps based on metabolism, cellular processes, genetic processing, environmental interactions and human diseases, generating KEGG pathway hits with a p-value of <0.05 (Vlachos et al., 2012). Diana-miRPath can be accessed from: http://diana.imis.athena-innovation.gr/ DianaTools/index.php?r=mirpath/index.

2.2.6.7 Sequence Manipulation Suite

The CpG Islands sequence analysis function available at the Sequence Manipulation Suite (http://www.bioinformatics.org/sms2/cpg_islands.html) reports potential CpG islands using the method described by Gardiner-Garden and Frommer (1987). The calculation is performed using a 200 bp window moving across the sequence at 1 bp intervals. CpG islands are defined as sequence ranges were the observed/expected value is greater than 0.6 and the GC content is greater than 50%. The expected number of CpG dimers in a window is calculated as the number of 'C's multiplied by the number of 'G's divided by the window length.

#### 2.2.6.8 UCSC Genome Browser and Galaxy

Bioinformatic analysis of human and rat genomes were performed using the UCSC Genome Browser, assembly hg19 and rn5, respectively (http://genome.ucsc.edu/). For intersection of NRSF binding sites taken from ENCODE transcription factor ChIP-seq data (March 2012 release) with flanking sequences of precursor-microRNAs (pre-miRNAs), data was uploaded through the Table Browser function on UCSC into the web-based platform Galaxy (https://usegalaxy.org/). NRSF binding sites were overlapped with the 10 Kb upstream flanking sequences of pre-miRNAs using the *intersect* tool under the *Operate on Genomic Intervals* function, which allows for intersection of the intervals of two datasets. Data was downloaded as a spreadsheet for analysis.

### 2.2.7 Genotyping

#### 2.2.7.1 SNP analysis

Markers mapping the NRSF and BDNF genes and their respective flanking sequences (10 Kb upstream and downstream) were selected based on implications from the literature (see **Table 3.2** and **3.3**) and/or maximum genetic coverage through the selection of htSNPs (see *section 2.2.6.3*). A total of 38 SNPs were selected for genotyping; 14 in NRSF and 24 in BDNF. Multiplex primer assays were designed using Sequenom Assay Design software (https://mysequenom.com/default.aspx). SNPs were divided across two 20-plex assays. Oligonucleotides were purchased from Metabion (Martinsried, Germany). PCR assays were carried out on a Veriti thermal cycler (Applied Biosciences) in a 384-well microtitre plate using 20 ng of genomic DNA from the SANAD cohort (see *section 2.1.4.2.1*) and with a final reaction volume of 4 µl.

As a measure of quality control, six replication samples and six blank controls were used. Genotyping was performed on a MALDI-TOF (Matrix Assisted Laser Desorption/Ionization-Time of Flight)-based Sequenom iPLEX MassARRAY® platform (Sequenom Inc., San Diego, CA, USA), according to the manufacturer's instructions.

#### 2.2.7.2 VNTR analysis

The MIR137 VNTR was genotyped on an ABIPRISM 3130XL Genetic Analyser (Applied Biosystems) capillary electrophoresis platform. DNA amplification was performed using 5 ng genomic DNA following the protocol described in *section 2.2.5.5* and the human MIR137 VNTR primer set detailed in **Table 2.1**. The reverse primer was synthesised with the addition of a 5'-terminal 6-carboxyfluorescein (FAM) (Eurofins MWG Operon). For analysis on the 3130XL platform, 2 µl of PCR product was subjected to capillary electrophoresis against an internal size standard (GeneScan 500 ROX) (Applied Biosystems) following the manufacturers' protocol. The appropriate run module was selected for a 36 cm array length and the POP-7 Polymer (Applied Biosystems), with an injection time of 2,400 seconds.

Fragment analysis was performed using the GeneMapper Software version 4.0 (Applied Biosystems) and validated using gel electrophoresis. For gel electrophoresis, PCR products were separated on a 2% agarose gel as described in *section 2.2.2.3*. Expected fragment sizes ranged between 399-518 bp, ±15 bp. Duplicate samples were tested and negative controls were included on each 96-well plate. Genotyping was performed blind to age and gender. Statistical analysis for genotype data is detailed in *section 2.2.10.1*.

### 2.2.8 Chromatin Immunoprecipitation (ChIP)

#### 2.2.8.1 *In vitro* ChIP

Cells were grown to 80% confluence in T175 flasks and treated for 1 hour under one of the following conditions: basal (untreated), 1 or 10 μM cocaine or vehicle alone (see *section 2.2.3.4*). Samples were processed following methods described by Murgatroyd et al. (Murgatroyd et al., 2012). ChIP buffers are listed in *section 2.1.2*. Immunoprecipitation was performed using ChIP grade antibodies detailed in **Table 2.3**. PCR analysis of the immunoprecipitated chromatin samples was performed using primers targeting predicted NRSF binding sites (BS) across the BDNF (*Chapter 3*) and MIR137 gene loci (*Chapter 4*). Primer sequences are detailed in *section 2.1.8*, **Table 2.1**.

#### 2.2.8.2 *In vivo* ChIP

Tissue punches were taken from the left and right hemispheres of rat cortex, hippocampus and amygdala of male Sprague Dawley rats (n=3 for each treatment condition, see *section 2.1.7*) using a 1 mm tissue punch. Samples were processed as described in Murgatroyd et al. (2012), with the following adjustments: 1) homogenisation was performed in 500 μl 1X PBS, the samples gently vortexed and further homogenised using a pipette, 2) fixation was performed with 13.5 μl 37% formaldehyde and the samples incubated for 10 minutes at room temperature with shaking (1,000 rpm) and quenched with 51.35 μl 1.25M glycine and incubated at room temperature for 5 minutes with shaking at 800 rpm, 3) 3X washes with ice-cold 500 μl 1X PBS supplemented with 1X PIC (Sigma, P8340, 100X in DMSO) were performed, 4) 500 μl cellular lysis buffer and nuclear lysis buffer (composition outlined in *section 2.1.2*) was

used for cellular lysis and nuclear extraction, 5) samples were sonicated in nuclear lysis buffer using a BioRuptor Plus (Diagenode) on high power settings for 13 cycles of 30 seconds on/30 seconds off with mixing of the samples using a pipette and centrifugation performed after 7 cycles and 6) sonicated samples were pelleted by centrifugation at 10,000 x g for 10 minutes at 4°C to release the DNA and proteins, 7) to determine the concentration of each sample 25 µl aliquots were taken and made up to 50 µl using nuclease free water and supplemented with 3 µl 5M NaCl and 1 µl RNAse1 (10 U/(Promega) and incubated at 37°C for 30 minutes with shaking (800 rpm) and then 1 µl proteinase K (20 mg/ml) was added and the samples incubated at 65°C with shaking (800 rpm) for 2 hours before the samples were column purified using the Wizard® SV Gel and PCR Clean-Up System (Promega) following manufacturer's instruction and eluted in 20 µl nuclease free water and the concentration determined using a Nanodrop 8000 and 8) recovered DNA was subjected to gel electrophoresis on a 1% agarose gel to check fragment sizes (*section 2.2.2.3*).

For each immunoprecipitation (IP), 5 µg of the sheared chromatin was made up to 250 µl using ChIP Dilution Buffer, supplemented with 10 µl/ml 100X PIC and incubated overnight at 4°C on a rotating wheel with antibodies raised against histone H3, NRSF (C- and N-terminal antibodies were used), MeCP2 and EZH2. Details of the concentration of antibody used per IP are outlined in **Table 2.3**. The protein–DNA complexes were added to 40 µl Dynabeads™ (Thermo Scientific), which were first pre-cleared by washing twice with 1 ml ChIP dilution buffer supplemented with PIC; the second wash step was left for 2 hours, and then incubated on a rotating wheel for 1 hour at 4°C. The magnetic

Dynabead™/protein–DNA complexes were captured by placing the tubes in a magnetic rack for 1 minute to separate the beads from the solution and the supernatant discarded. DNA bound magnetic beads were subjected to 5 minute wash steps (performed in a 4°C cold room) with rotation to remove non-specific DNA and proteins associated with the Dynabeads™. Firstly, the beads were washed with 1 ml of low-salt wash buffer, followed by high-salt wash buffer, LiCl wash buffer and finally TE buffer. The immune complex was eluted by adding 50 µl of elution buffer containing 50 µg/ ml proteinase K to the magnetic bead/protein–DNA complexes and the supernatant transferred to a new microcentrifuge tube and mixed at 65°C for 2 h to release the protein-bound DNA and reverse the cross-linking. The samples were then incubate at 95°C for 10 min to denture the proteins and inactivate the proteinase K and the DNA recovered from the sample through spin column purification using the Wizard® SV Gel and PCR Clean-Up System (Promega) in a volume of 20 µl. The DNA was quantified using a Nanodrop 8000 and analysed by PCR (*section 2.2.5.5*).

### 2.2.9 Methylated DNA Immunoprecipitation (MeDIP)

Methylated double stranded DNA was isolated from genomic DNA samples using the CpG Methyl Quest DNA Isolation Kit (Merck Millipore), following manufacturer's instruction. Briefly, 300 ng (recommended concentration) of sonicated genomic DNA was incubated for 1 hour at room temperature on a rotating wheel with 5 µl of pre-cleared CpG MethylQuest glutathione paramagnetic beads, which are pre-coupled to a GST (glutathione-S-transferase protein)-MBD (methyl binding domain) fusion protein that specifically binds methylated double stranded DNA. Methylated sequences

bound to the CpG Methyl Quest fusion-protein/bead complex were subjected to wash steps and the supernatant containing the non-methylated DNA was kept for comparison. The methylated DNA was eluted from the beads by heating the samples at 80°C for 10 minutes with mixing in 100 µl TE buffer. The sample was separated from the beads by placing the tubes in a magnetic rack and transferred to a new microcentrifuge tube and the beads discarded. Samples were subjected to PCR analysis (*section 2.2.5.5*) and then stored at -20°C.

### 2.2.10 Statistical Analysis

#### 2.2.10.1 *Clump* analysis

Significance-testing of allele frequency and genotype data for the MIR137 VNTR between cases and controls of the schizophrenia cohort (*Materials section 2.1.4.4*) and BRCA wild type (Wt) individuals, BRCA1 positive individuals, BRCA2 positive individuals, BRCA1 and 2 positive individuals combined and healthy controls of the breast cancer cohort (*Materials section 2.1.4.1*) was performed using *Clump 24* analysis software which can be accessed from http://www.davecurtis.net/dcurtis/software.html. The *Clump* program assesses the significance of the departure of observed values from the expected values using a Monte Carlo-based approach. It does this by performing repeated simulations (10,000) to generate contingency tables (2 x N) that have the same marginal totals as the one under consideration and counting the number of times that a chi-squared value associated with the real table is achieved by the randomly simulated data. The *Clump* software also generates a novel chi-squared value (T4) by 'clumping' columns together into a new two-by-two table in a way which is designed to maximise the chi-squared value and directly tests

the hypothesis that several alleles are more common among the cases than among the controls (Sham and Curtis, 1995). The *Clump* program generates four test statistics using Monte Carlo methods to evaluate the significance of chi-squared values by assessing how many times the observed value produced is exceeded by chance from the randomly generated simulated datasets. The four tables are as follows:

**T1:** The raw 2-by-N table supplied by the user

**T2:** The original table with columns containing small numbers 'clumped' together

**T3:** The most significant of all 2-by-2 tables obtained by comparing each (non-rare) column of the original table against the total of all the other columns

**T4:** A 2-by-2 table obtained by 'clumping' the columns of the original table to maximise the chi-squared value

#### 2.2.10.2 Composite genotype analysis

Composite genotype analysis between NRSF rs2227902 and BDNF rs6265 was performed using SPSS 2.1. Markers were grouped by the number of risk alleles and scored as follows: group 1 represented 0-1 risk alleles, group 2 represented 2 risk alleles in individuals that were either heterozygous for each SNP or homozygous for rs2227902 (G) and group 3 represented 3-4 risk alleles. Groupings for the presence or absence of the minor alleles for each SNP were also performed as previously described (Miyajima et al., 2008b). Linear regression analysis was performed to determine associations between composite-genotypes with cognitive test scores for the SANAD dataset (see *section 2.1.4.2*) over time (i.e. the difference between each individual's cross-

sectional and longitudinal test scores). Age, sex and epilepsy type were controlled for by covarying their effects. Scatter plots illustrating these associations were generated using GraphPad Prism, version 5.03. Significant differences between genotypes for individual SNPs with cognitive test scores were determined using the Mann-Whitney test. $P<0.05$ were regarded significant.

#### 2.2.10.3 Hardy-Weinberg Equilibrium (HWE)

As a measure of quality control in our SNP association study, we tested our genotype data for departure from HWE as this can be used as an indicator of genotyping errors and population stratification. For analysis of HWE, we used the *Hardy-Weinberg equilibrium calculator* (http://www.oege.org/software/hwe-mr-calc.shtml) which implements the Pearson chi-square ($X^2$) test statistic to assess goodness-of-fit of the observed genotype frequency against the expected under HWE (Rodriguez et al., 2009).

#### 2.2.10.4 Regression analysis

Associations between cognitive test scores and genotype frequency data for the SANAD cohort (see *section 2.1.4.2*) were analysed using regression analysis and Expectation-Maximisation (EM), which was kindly performed by Dr. Fabio Miyajima, University of Liverpool, using Stata v.9.2. EM was used to compute maximum likelihood (ML) estimates of parameters for the longitudinal model based on probability distribution (Dempster et al., 1977). Briefly, ML estimations are based on a mixed model accounting for both the fixed- and random-effects of the variance components in longitudinal models. Mixed-

effects represent the regression coefficient (the slope that represents the rate of change in the dependent variable as a function of change in the independent variables) of the average individual in the study population (fixed-effects) and individual-specific random deviations from the overall slope (random-effects).

In the mixed-effect ML model, the likelihood function for a given parameter is maximized with respect to the fixed-effects, finding the most likely value for the parameter based on the dataset collected. However, the degrees of freedom (d.f.) lost by estimating the fixed-effects are not taken into account using this model as it assumes that the fixed-effects are known without error, which leads to biased estimates of the variance components (Visscher et al., 2004). To overcome this, the longitudinal analysis was based on mixed-effects linear regression using Restricted Maximum Likelihood (REML) which maximises the estimated likelihood of the variance components affecting the observed measurement, invariant to the fixed-effects (Patterson and Thompson, 1971). In contrast to ML estimates, REML accounts for the d.f. lost by estimating the fixed-effects making it a less biased estimation of the error variance. REML was applied to correct for biases that may have arisen due to selection (Henderson, 1986, Searle, 1989).

To correct for multiple testing, the data was permutated 1,000 times. Permutation testing was performed with respect to the number of markers at the gene level. Cognitive data was normally distributed and age, sex, epilepsy type, number of previous seizures at baseline (continuous variable, cross-sectional analysis) and freedom from seizure since baseline (categorical variable, longitudinal analysis) were accounted for by covarying their effects. P-values lower than 5% were regarded as significant. See *Appendix 4* for scripts.

# Chapter 3

## The NRSF-BDNF Pathway Underlies Multiple CNS Disorders

**Part I:** *The NRSF-BDNF pathway in genetic predisposition to cognitive decline in epilepsy*

**Part II:** *Complex promoter usage and transcriptional regulation of the human BDNF gene in response to cocaine*

# Part I: *The NRSF-BDNF pathway in genetic predisposition to cognitive decline in epilepsy*

## 3.1 Introduction

People with epilepsy often experience cognitive impairments but the exact cause remains unclear and may be reflective of the underlying aetiology of the disorder, the neurobiological consequences of seizures, the adverse effects of antiepileptic drug (AED) treatment and psychosocial dysfunction (Motamedi and Meador, 2003, Tellez-Zenteno et al., 2007, Taylor and Baker, 2010, Taylor et al., 2010, Berg, 2011). AEDs have been considered the principal culprits, with memory, attention, psychomotor speed and information processing being the cognitive domains most commonly reported to be affected following drug treatment (Park and Kwon, 2008). However, recent work suggesting that some people with epilepsy are cognitively compromised from the time of initial diagnosis would advocate the involvement of more intrinsic biological processes, including epileptogenesis (Taylor et al., 2010, Hermann et al., 2006). Genetics may also play an important contributory role as suggested from genetic association studies which have identified 'risk genes' for cognitive dysfunction in normal ageing and neurological disease. Polymorphisms in the NRSF and BDNF genes have previously been associated with age-related and disease-associated cognitive decline such as in Alzheimer's disease (Miyajima et al., 2008a, Honea et al., 2013, Voineskos et al., 2011, Lu et al., 2014). Moreover, an additive interaction between genetic variants within these two genes correlates with general intelligence scores in the normal ageing population (Miyajima et al., 2008b), suggesting that the NRSF-BDNF pathway may be an

important mechanism in cognitive dysfunction; a common co-morbidity in several neurological disorders.

NRSF and its downstream target BDNF, a neuron-specific growth factor involved in neurogenesis, cell survival and synaptic plasticity (Huang and Reichardt, 2001, Scharfman et al., 2005, Pencea et al., 2001, McAllister et al., 1999, Ghosh et al., 1994), have been shown to be differentially regulated in rodent models of epilepsy (Palm et al., 1998, Calderone et al., 2003, Spencer et al., 2006, Hu et al., 2011b, Roopra et al., 2001, Garriga-Canut et al., 2006, Liu et al., 2012b, Ballarín et al., 1991, Nibuya et al., 1995, McClelland et al., 2011, McClelland et al., 2014). The involvement of these two genes in both cognition and epilepsy supports a role for the NRSF-BDNF pathway in epilepsy-associated cognitive dysfunction. Consistent with this pathway being modulated by drug action, several AEDs modify NRSF and BDNF signalling in neuronal cells (Gillies et al., 2011, Gillies et al., 2009, Shi et al., 2010).

In this chapter, the genetic effects of single nucleotide polymorphisms (SNPs) spanning the NRSF and BDNF genes on the cognitive profile of individuals with newly-diagnosed epilepsy were explored using DNA samples and cognitive data drawn from the subgroup analysis of the SANAD (Standard and New Anti-epileptic drugs) trial available through collaborators within the *Department of Molecular and Clinical Pharmacology, University of Liverpool* (Taylor and Baker, 2010, Taylor et al., 2010). Both a cross-sectional and longitudinal model was employed to determine genetic association at both baseline, when subjects were first recruited into the study and were drug naïve, and at 12-month reassessment, to address change in cognitive function over the first year of treatment following diagnosis.

## 3.2 Aims

- Determine whether there is a genetic influence of common variants within the NRSF and BDNF genes on the cognitive profile of adults with new-onset epilepsy
- Investigate the longitudinal effects of genetic variation on the progression of cognitive dysfunction associated with epilepsy
- Address the potential functional significance of NRSF and BDNF SNPs identified as genetic correlates of memory performance by overlapping them with expression quantitative trait loci and regulatory elements using the online databases Genevar and HaploReg

## 3.3 Results

### 3.3.1 Demographic and clinical characteristics of the study cohort

Descriptive analysis of the patient cohort was carried out using SPSS 22.0. A summary of the study population is provided in **Table 3.1**. The mean age of subjects at baseline was 40 years, with a range of 15 to 71 years. There were marginally more females (55%) and the majority of subjects were considered to have focal epilepsy (82%). The mean number of days from baseline assessment to the 12-month follow-up assessment was 388 days, ranging from 350 to 566 days. The number of individuals that were seizure free at the 12-month assessment was 19. Cognitive tests used for the cross-sectional and longitudinal analyses are listed in **Table 3.2**. The test battery methods are described in detail elsewhere (Taylor et al., 2010). Only those aspects of the battery that had previously been shown to differ significantly between epilepsy patients and healthy controls were employed in the genetic association analysis.

**Table 3.1.** Demographic and clinical profile of the study cohort at baseline and 12-month assessment

| **Variable** | | **Baseline** (n=82) | **12 months** (n=70) |
|---|---|---|---|
| *Sex* | Males (n) | 37; 45% | 31; 44% |
| | Females (n) | 45; 55% | 39; 56% |
| *Age* | Mean [range] | 40 [15 - 71] | 42 [16 - 70] |
| *Years of education* | Mean [range] | 12.9 [11 - 19] | - |
| *Epilepsy type* | Generalised (n) | 15; 18% | 13; 19% |
| | Focal (n) | 67; 82% | 57; 81% |
| *No. of previous seizures at baseline* | Mean [range] | 112 [2 – 3,300] | - |
| *Remission status at follow-up* | Seizure-free (n) | - | 19; 27% |

**Table 3.2.** Selected cognitive tests employed in this analysis

| Analysis | Domain | Test | Measured variable |
|---|---|---|---|
| *Cross-sectional* | Memory | Figure recognition (serial task) | Number of figures correctly identified in the serial task |
| | | Rey Auditory Verbal Learning Task, AVLT (immediate and delayed) | Sum of words recalled over the 5 trials and the number of words recalled following a 30 minute delay |
| | | Story Recall (immediate) | Number of story units recalled immediately and following a 10 minute delay |
| | Psychomotor speed | Finger tapping (dominant hand) | Average number of taps for the dominant hand across five trials |
| | | Adult Memory and Information Processing (average speed) | Average number of digits crossed-out over two trials |
| *Longitudinal* | Memory | Rey Auditory Verbal Learning Task, AVLT (immediate and delayed) | Sum of words recalled over the 5 trials and the number of words recalled following a 30 minute delay |
| | Psychomotor speed | Visual Reaction Time, VRT (non-dominant hand) | Average reaction time (min/sec) for the dominant and non-dominant hand |
| | Information processing | Computerised Visual Search Task, CVST | Average speed of response (seconds) |

*Note:* Cognitive tests selected based on aspects of the battery previously shown to significantly differ between epilepsy patients and healthy controls (Taylor et al., 2010).

### 3.3.2 Association of NRSF and BDNF SNPs with memory related tasks

A total of 36 SNPs were successfully genotyped across the two genes; these are listed in **Table 3.3**. All were in Hardy-Weinberg equilibrium (HWE) and had a minor allele frequency (MAF) of >0.05. Two of the SNPs (NRSF rs11736869 and BDNF rs11030119) from the original panel were excluded as they had a call rate of less than 95%, the accepted cut-off for genotype-based studies (Edenberg and Liu, 2009). Two patient samples were excluded from the

**Table 3.3.** Minor allele frequencies and Hardy-Weinberg equilibrium of NRSF and BDNF SNPs

| Gene | Marker | Chromosomal position | Base pair change | Genotype distribution | HWE *P*-value | MAF |
|---|---|---|---|---|---|---|
| NRSF | rs3806746 | 57773330 | A>G | 25/40/6 | 0.07 | 0.37 |
| | rs4109037 | 57775609 | A>T | 65/17/0 | 0.30 | 0.10 |
| | rs3755901 | 57775996 | A>T | 64/17/1 | 0.91 | 0.12 |
| | rs3000 | 57777945 | C>T | 27/36/9 | 0.57 | 0.38 |
| | rs1713985 | 57786450 | A>C | 68/14/0 | 0.40 | 0.09 |
| | rs13125082 | 57787000 | T>G | 38/27/6 | 0.70 | 0.28 |
| | rs6847086 | 57791864 | G>A | 25/36/9 | 0.48 | 0.39 |
| | rs1277306 | 57792078 | T>C | 35/40/7 | 0.34 | 0.33 |
| | **rs1105434** | 57793751 | G>A | 29/33/9 | 0.93 | 0.36 |
| | **rs2227902** | 57797100 | G>T | 57/15/0 | 0.32 | 0.10 |
| | **rs3796529** | 57797414 | G>A | 49/26/2 | 0.50 | 0.20 |
| | rs2227901 | 57798189 | G>A | 54/26/2 | 0.58 | 0.18 |
| | rs781667 | 57798469 | T>C | 40/38/4 | 0.18 | 0.28 |
| BDNF | rs1491851 | 27752763 | C>T | 33/27/12 | 0.13 | 0.35 |
| | rs2049048 | 27750586 | C>T | 47/18/4 | 0.22 | 0.19 |
| | **rs1491850** | 27749725 | T>C | 24/44/14 | 0.42 | 0.44 |
| | rs11030123 | 27748285 | G>A | 65/14/2 | 0.24 | 0.11 |
| | **rs12273363** | 27744859 | T>C | 45/27/0 | 0.05 | 0.19 |
| | rs11030121 | 27736207 | C>T | 34/28/9 | 0.40 | 0.32 |
| | rs7934165 | 27731983 | A>G | 16/35/14 | 0.53 | 0.49 |
| | **rs2030324** | 27726915 | T>C | 25/37/16 | 0.73 | 0.44 |
| | rs988748 | 27724745 | C>G | 50/28/3 | 0.70 | 0.21 |
| | rs2049046 | 27723775 | A>T | 28/35/18 | 0.27 | 0.44 |
| | rs7127507 | 27714884 | T>C | 34/27/11 | 0.16 | 0.34 |
| | rs7103411 | 27700125 | T>C | 43/27/2 | 0.35 | 0.22 |
| | **rs11030108** | 27695464 | G>A | 38/31/11 | 0.26 | 0.33 |
| | rs2049045 | 27694241 | G>C | 55/25/2 | 0.67 | 0.18 |
| | rs11030104 | 27684517 | A>G | 51/28/3 | 0.72 | 0.21 |
| | rs11030102 | 27681596 | C>G | 43/34/3 | 0.23 | 0.25 |
| | **rs6265** | 27679916 | G>A | 53/27/2 | 0.50 | 0.19 |
| | **rs7124442** | 27677041 | T>C | 38/31/13 | 0.13 | 0.35 |
| | rs4923463 | 27672500 | A>G | 52/27/3 | 0.83 | 0.20 |
| | rs10501087 | 27670108 | T>C | 44/26/2 | 0.42 | 0.21 |
| | rs7927728 | 27667472 | G>A | 60/8/1 | 0.25 | 0.07 |
| | rs11602246 | 27660926 | C>G | 63/9/0 | 0.57 | 0.06 |
| | **rs11030094** | 27659775 | G>A | 28/33/11 | 0.80 | 0.38 |

*Note:* Markers in bold font represent the 10 SNPs selected for further analysis. *Base pair change* represents major>minor allele. *Genotype distribution* represents AA/Aa/aa, where 'A' is the wild type allele and 'a' the variant allele. *HWE, Hardy-Weinberg equilibrium; htSNPs, haplotype-tagging single nucleotide polymorphisms; MAF, minor allele frequency.*

analysis as they failed quality control checks. Ten non-coding or non-synonymous SNPs were selected for inclusion in the genetic association analysis on the basis of maximum genetic coverage through the use of haplotype-tagging SNPs (htSNPs) (see *section 2.2.6.3*) or based on known or proposed functional effects, see **Table 3.4.** These included three SNPs in NRSF (rs1105434, rs2227902, rs3796529) and seven SNPs in BDNF (rs1491850, rs12273363, rs2030324, rs11030108, rs6265, rs7124442, rs11030094). Squared correlation coefficient ($r^2$) estimates were used to determine htSNPs (see *section 2.2.6.3*). This is a measure of LD that directly depends on allele frequencies were an $r^2$ value of 1 indicates that two SNPs have identical allele frequencies and every occurrence of one allele of a SNP perfectly predicts the allele of the second SNP (i.e. the two SNPs are in perfect LD), meaning that only one SNP needs to be genotyped to know the genotype of the other. Pairwise tagging SNP analysis ($r^2$>0.8) of the genotype data revealed that NRSF rs1105434, rs2227902 and rs3796529 were in strong LD with the rs3000 ($r^2$=0.94), rs3755901 ($r^2$=1.0) and rs2227901 ($r^2$=1.0) markers, respectively. For BDNF, the markers rs1491850, rs12273363, rs2030324, rs11030108, rs6265, rs7124442 and rs11030094 represented 13/24 SNPs genotyped for this gene. A schematic representation of the genomic coverage of these htSNPs is shown in **Figure 3.1**.

To determine associations between cognitive test scores and genotype frequency, regression analysis and Expectation-Maximisation (EM) were performed (see *section 2.2.10.4*). Statistical modelling was kindly performed by Dr. Fabio Miyajima, University of Liverpool, using Stata v.9.2. EM is a method for estimating the maximum likelihood (ML) of a parameter based on probability distribution of the independent observations. Briefly, ML estimations are based

**Table 3.4.** Functional SNPs included in the genetic association analysis

| Gene | Marker | SNP type | Function | *Reference* |
|---|---|---|---|---|
| NRSF | rs1105434 | Intronic | Located 30 bp upstream of an alternative exon (exon N) within the NRSF gene which encodes for a truncated protein, sNRSF, associated with epileptogenesis. | (*See section 3.3.4*) |
| | rs2227902 | Exonic, NS (missense) | In LD with a coding VNTR within NRSF. Common haplotype associated with lower scores of *g* in the elderly. Additive interaction between minor haplotype and major allele of BDNF rs6265 (Val66-G) associated with higher scores of *g*. | (Miyajima et al., 2008b) |
| | rs3796529 | Exonic, NS (missense) | Minor allele associated with neuroprotective effects in subjects with amnestic mild cognitive impairment. | (Nho et al., 2015) |
| BDNF | rs1491850 | Promoter (6.1 Kb upstream of transcript NM_170731) | Associated with hippocampal atrophy in AD and anti-depressant treatment response phenotypes in MDD. | (Honea et al., 2013, Kocabas et al., 2011, Gratacos et al., 2008) |
| | rs12273363 | Promoter (1.3 Kb upstream of transcript NM_170731) | Minor allele associated with autism (haplotype analysis), BPD, MDD, reduced BDNF hippocampal density in Stanley Consortium[a] subjects, silencing of BNDF promoter IV reporter gene activity in rat hippocampal and cortical cultures and reducing rat promoter VI response to neuronal activation by KCl depolarisation. | (Gratacos et al., 2008, Dunham et al., 2009, Liu et al., 2008, Hing et al., 2012, Nishimura et al., 2007) |
| | rs2030324 | Internal promoter (3.7 Kb upstream of transcript NM_170733) | Associated with BPD, cognitive abilities in the elderly and visual cognitive processing in multiple sclerosis. | (Miyajima et al., 2008a, Liu et al., 2008, Weinstock-Guttman et al., 2011) |
| | rs11030108 | Intronic | Associated with mild cognitive impairment in AD. | (Honea et al., 2013) |
| | rs6265 | Exonic, NS (missense) | Minor allele (Met66-A)associated with disrupted cellular processing and secretion of BDNF, hippocampal atrophy in AD, non-responsiveness to anti-depressant drugs in MDD, reduced cognitive function in normal ageing and neurological disorders. | (Miyajima et al., 2008a, Mercader et al., 2007, Hall et al., 2003, Lang et al., 2005, Jiang et al., 2005, Hariri et al., 2003, Lin et al., 2014, Cheah et al., 2014, Honea et al., 2013, Egan et al., 2003) |
| | rs7124442 | 3'UTR | Haplotype containing major allele associated with high BDNF plasma levels which correlate with eating disorders. | (Mercader et al., 2007) |
| | rs11030094 | Intronic (BDNF-AS) | Associated with cognitive decline and whole-brain atrophy in AD. | (Honea et al., 2013, Laumet et al., 2010) |

*Note: Function* is with reference to regulatory function and/or disease associations from the literature. [a] Stanley Foundation Neuropathology Consortium consists of subjects with BPD, MDD, schizophrenia and matched controls. Abbreviation: *AD, Alzheimer's disease; AS, anti-sense; BPD, bipolar disorder; g, general intelligence; MDD, major depressive disorder; NS, non-synonymous; VNTR, variable number tandem repeat.*

on a mixed model accounting for both the fixed-effects (an estimated parameter that is associated with the entire study population and is corrected for with repeated measurements; within-subject variability) and random-effects (a parameter describing the variability between individuals) of the variance components in longitudinal models (Dempster et al., 1977). ML estimation is a method that finds the most likely value for the parameter based on the dataset collected, maximising with respect to the fixed-effects. This method assumes that the fixed-effects are known without error, which leads to biased estimates of the variance components (Visscher et al., 2004). We therefore implemented Restricted Maximum Likelihood (REML) regression in our study design which accounts for the degrees of freedom lost by estimating the fixed-effects making it a less biased estimation of the error variance (Patterson and Thompson, 1971). REML does this by maximising the estimated likelihood of the variance components affecting the observed measurement, in this case the cognitive test scores, independent to the fixed-effects. This model was used to correct for repeated measures and within-subject covariance (Henderson, 1986, Searle, 1989, Patterson and Thompson, 1971). Cognitive data was normally distributed and age, sex, epilepsy type, number of previous seizures at baseline (continuous variable, cross-sectional analysis) and freedom from seizure since baseline (categorical variable, longitudinal analysis) were accounted for by covarying their effects. P-values lower than 5% were regarded as significant.

Regression analysis of cross-sectional cognitive test scores with individual SNP genotypes indicated statistically significant associations for the respective NRSF markers rs1105434 (P=0.03) and rs2227902 (P=0.02) with delayed recall, as assessed by the Rey Auditory Verbal Learning Task (AVLT),

**Figure 3.1. Schematic representation of genotyped haplotype-tagging SNPs (htSNPs) spanning the BDNF (*top*) and NRSF (*bottom*) genes.** Highlighted markers represent those selected for genotype analysis; grey indicates htSNPs and/or functional SNPs selected for inclusion in the genetic association and yellow indicates SNPs captured by these selected htSNPs ($r^2$>0.88) from linkage disequilibrium (LD) analysis of the genotype data. The remaining SNPs represent genetic coverage over the entire locus, including 10 Kb flanking sequence, as determined by pairwise-tagging ($r^2$>0.8, indicating that a pair of SNPs are in strong LD and that one allele at one locus tags another allele at separate locus meaning that only one SNP needs to be genotyped) using HapMap CEU genotype data and Haploview 4.1 software (www.broad.mit.edu/mpg/haploview/). *SNPs shown to be significantly associated from genetic analysis. Image generated using UCSC Genome browser (https://genome.ucsc.edu/). [Figure presented on opposite page].

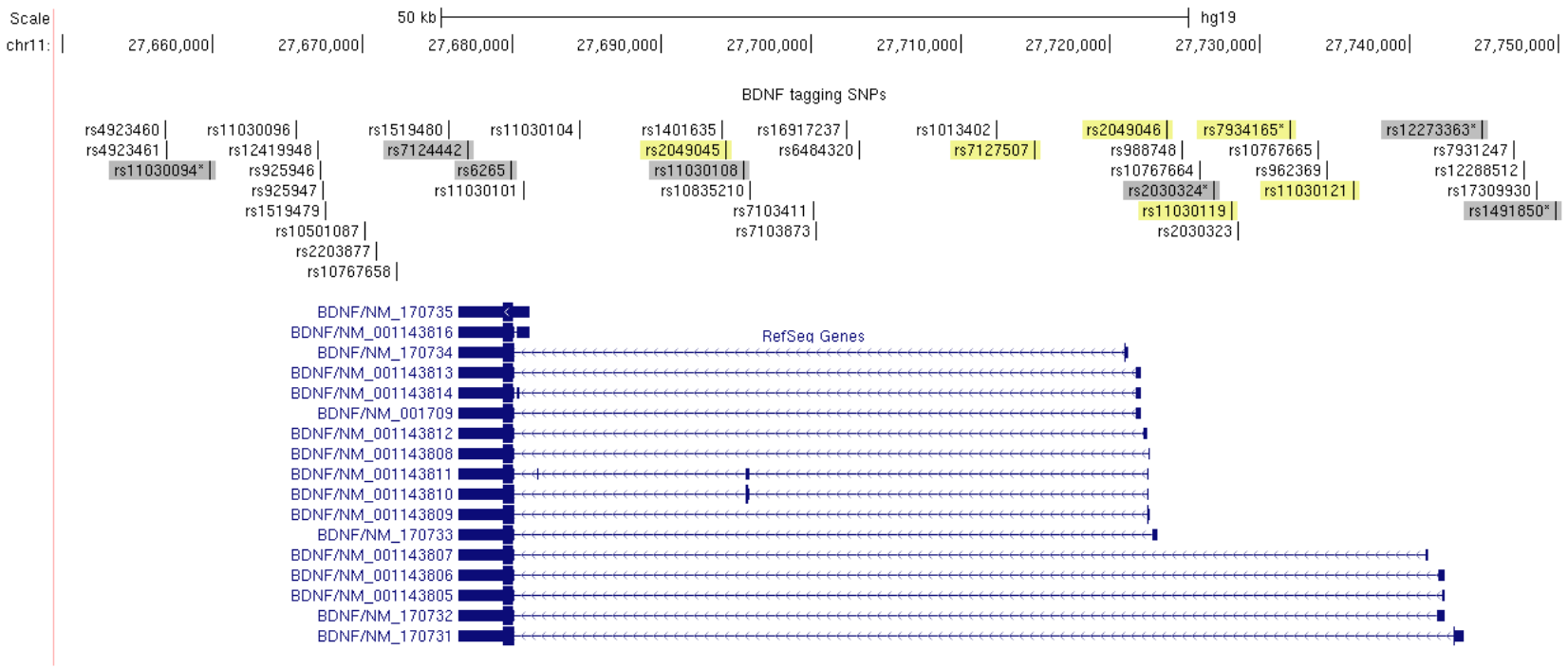
Scale
50 kb
hg19
chr11:
27,660,000
27,670,000
27,680,000
27,690,000
27,700,000
27,710,000
27,720,000
27,730,000
27,740,000
27,750,000
BDNF tagging SNPs
rs4923460
rs4923461
rs11030094*
rs11030096
rs12419948
rs925946
rs925947
rs1519479
rs10501087
rs2203877
rs10767658
rs1519480
rs7124442
rs6265
rs11030101
rs11030104
rs1401635
rs2049045
rs11030108
rs10835210
rs7103411
rs7103873
rs16917237
rs6484320
rs1013402
rs7127507
rs2049046
rs2030324*
rs11030119
rs2030323
rs7934165*
rs988748
rs10767664
rs11030121
rs12273363*
rs10767665
rs962369
rs7931247
rs12288512
rs17309930
rs1491850*
RefSeq Genes
BDNF/NM_170735
BDNF/NM_001143816
BDNF/NM_170734
BDNF/NM_001143813
BDNF/NM_001143814
BDNF/NM_001709
BDNF/NM_001143812
BDNF/NM_001143808
BDNF/NM_001143811
BDNF/NM_001143810
BDNF/NM_001143809
BDNF/NM_170733
BDNF/NM_001143807
BDNF/NM_001143806
BDNF/NM_001143805
BDNF/NM_170732
BDNF/NM_170731

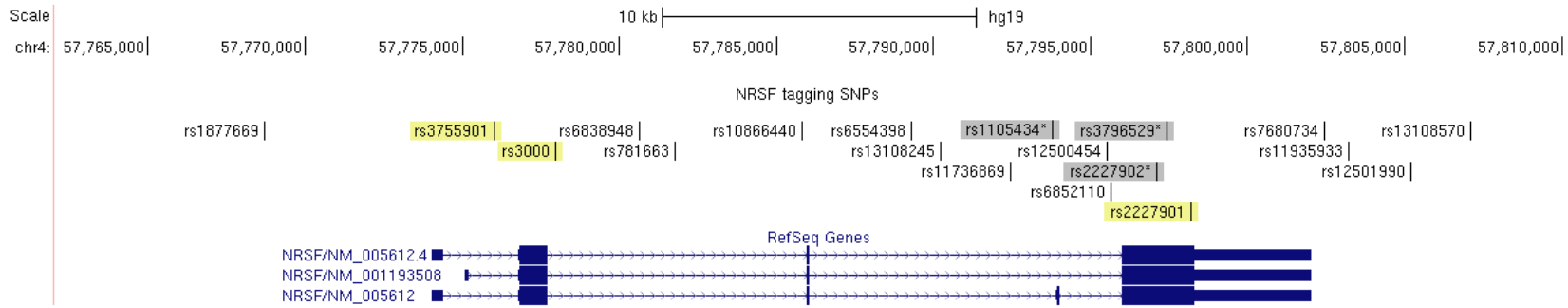
Scale
10 kb
hg19
chr4:
57,765,000
57,770,000
57,775,000
57,780,000
57,785,000
57,790,000
57,795,000
57,800,000
57,805,000
57,810,000
NRSF tagging SNPs
rs1877669
rs3755901
rs3000
rs6838948
rs781663
rs10866440
rs6554398
rs13108245
rs11736869
rs6852110
rs1105434*
rs12500454
rs2227902*
rs2227901
rs3796529*
rs7680734
rs11935933
rs13108570
rs12501990
RefSeq Genes
NRSF/NM_005612.4
NRSF/NM_001193508
NRSF/NM_005612

and serial recall, as assessed by the figure recognition task (**Table 3.5**). Three BDNF markers were also associated with the Rey AVLT in the cross-sectional analysis; rs1491850 (P=0.05, immediate recall), rs11030094 (P=0.02, delayed recall) and rs2030324 (P=0.03, immediate recall and P=0.01, delayed recall) (**Table 3.5**). In the longitudinal analysis, NRSF rs2227902 was again identified as being significantly (P=0.02) associated with memory function as was BDNF rs12273363 (P=0.01) and both in relation to Rey AVLT delayed recall scores. These observations account for the influence of age on cognitive test scores and reflect the interaction between the two variables (age and genotype). The independent effect of these SNPs in predicting memory function showed only BDNF rs12273363 to be significant (P=0.04) (**Table 3.6**). Psychomotor speed was also found to be significantly affected by genotype (NRSF rs3796529, P=0.04) in the longitudinal analysis, assessed through visual reaction time (non-dominant hand), **Table 3.6**. In both the cross-sectional and longitudinal analysis, no significant associations were found between individual SNP genotypes and cognitive test scores measuring information processing (**Table 3.5** and **3.6**).

### 3.3.3 Haplotype structure of the NRSF and BDNF genes

Particular alleles at adjacent loci on a chromosome tend to be inherited together in blocks known as haplotype blocks. For tightly linked loci, this may lead to non-random associations between alleles in the population; a property known as linkage disequilibrium (LD). LD can be used as a tool for mapping ancestral inheritance and also the structure of complex disease loci from genome wide association studies by comparing patterns of LD between

**Table 3.5.** Genetic association analysis of cross-sectional cognitive data using a regression model adjusted for age, sex, epilepsy type and number of previous seizures at baseline

| Gene | SNP | Cognitive test | β | Adjusted P-value [a] | 95% CI | |
|---|---|---|---|---|---|---|
| | | | | | Lower | Upper |
| NRSF | rs1105434 | Finger tapping (dominant hand) | -0.98 | 0.61 | -4.53 | 2.57 |
| | | Story recall (immediate) | 0.64 | 0.22 | -0.43 | 1.71 |
| | | Figure recognition (serial) | 1.31 | 0.07 | -0.22 | 2.83 |
| | | Rey AVLT (immediate) | 1.78 | 0.23 | -1.27 | 4.82 |
| | | Rey AVLT (delayed) | 1.00 | **0.03*** | 0.04 | 2.00 |
| | | AMIPB average speed | -3.57 | 0.06 | -7.37 | 0.24 |
| | rs2227902 | Finger tapping (dominant hand) | -1.78 | 0.52 | -7.63 | 4.06 |
| | | Story recall (immediate) | 0.26 | 0.74 | -1.48 | 2.00 |
| | | Figure recognition (serial) | -2.63 | **0.02*** | -5.06 | -0.19 |
| | | Rey AVLT (immediate) | 1.52 | 0.55 | -3.42 | 6.46 |
| | | Rey AVLT (delayed) | 0.20 | 0.83 | -1.80 | 1.41 |
| | | AMIPB average speed | -0.93 | 0.76 | -7.16 | 5.31 |
| | rs3796529 | Finger tapping (dominant hand) | 1.19 | 0.58 | -2.90 | 5.28 |
| | | Story recall (immediate) | -0.50 | 0.42 | -1.69 | 0.69 |
| | | Figure recognition (serial) | 0.85 | 0.36 | -0.93 | 2.62 |
| | | Rey AVLT (immediate) | -1.20 | 0.49 | -4.73 | 2.34 |
| | | Rey AVLT (delayed) | -0.48 | 0.40 | -1.63 | 0.68 |
| | | AMIPB average speed | 0.73 | 0.78 | -3.86 | 5.32 |
| BDNF | rs1491850 | Finger tapping (dominant hand) | -1.76 | 0.28 | -5.06 | 1.53 |
| | | Story recall (immediate) | 0.44 | 0.37 | -0.51 | 1.38 |
| | | Figure recognition (serial) | 0.71 | 0.28 | -0.66 | 2.08 |
| | | Rey AVLT (immediate) | 2.81 | **0.05*** | 0.11 | 5.51 |
| | | Rey AVLT (delayed) | 0.56 | 0.20 | -0.32 | 1.44 |
| | | AMIPB average speed | -2.78 | 0.12 | -6.30 | 0.73 |
| | rs12273363 | Finger tapping (dominant hand) | -3.96 | 0.12 | -8.69 | -0.76 |
| | | Story recall (immediate) | 0.82 | 0.25 | -0.62 | 2.25 |
| | | Figure recognition (serial) | 0.21 | 0.84 | -1.88 | 2.30 |
| | | Rey AVLT (immediate) | 2.62 | 0.20 | -1.46 | 6.71 |
| | | Rey AVLT (delayed) | 0.55 | 0.42 | -0.78 | 1.88 |
| | | AMIPB average speed | -1.32 | 0.60 | -6.53 | 3.90 |
| | rs2030324 | Finger tapping (dominant hand) | 0.33 | 0.85 | -2.87 | 3.53 |
| | | Story recall (immediate) | -0.50 | 0.29 | -1.42 | 0.43 |
| | | Figure recognition (serial) | -1.08 | 0.09 | -2.35 | 0.19 |
| | | Rey AVLT (immediate) | -2.78 | **0.03*** | -5.43 | -0.13 |
| | | Rey AVLT (delayed) | -1.19 | **0.01*** | -2.01 | -0.36 |
| | | AMIPB average speed | 0.96 | 0.60 | -2.54 | 4.46 |
| | rs11030108 | Finger tapping (dominant hand) | -1.49 | 0.34 | -4.68 | 1.70 |
| | | Story recall (immediate) | 0.59 | 0.19 | -0.30 | 1.47 |
| | | Figure recognition (serial) | 0.61 | 0.34 | -0.69 | 1.90 |
| | | Rey AVLT (immediate) | 2.57 | 0.06 | -0.02 | 5.17 |
| | | Rey AVLT (delayed) | 0.74 | 0.09 | -0.10 | 1.57 |
| | | AMIPB average speed | 1.10 | 0.53 | -2.26 | 4.47 |
| | rs6265 | Finger tapping (dominant hand) | 0.91 | 0.67 | -3.19 | 5.00 |
| | | Story recall (immediate) | -0.31 | 0.61 | -1.49 | 0.88 |
| | | Figure recognition (serial) | 0.32 | 0.71 | -1.37 | 2.01 |
| | | Rey AVLT (immediate) | 0.89 | 0.60 | -2.56 | 4.35 |
| | | Rey AVLT (delayed) | 0.33 | 0.58 | -0.78 | 1.43 |
| | | AMIPB average speed | -1.14 | 0.07 | -8.48 | 0.20 |

| | | | | | |
|---|---|---|---|---|---|
| rs7124442 | Finger tapping (dominant hand) | -1.62 | 0.29 | -4.65 | 1.40 |
| | Story recall (immediate) | 0.44 | 0.33 | -0.43 | 1.30 |
| | Figure recognition (serial) | 0.45 | 0.48 | -0.80 | 1.69 |
| | Rey AVLT (immediate) | 2.34 | 0.06 | -0.13 | 4.81 |
| | Rey AVLT (delayed) | 0.69 | 0.08 | -0.11 | 1.48 |
| | AMIPB average speed | 1.02 | 0.53 | -2.19 | 4.23 |
| rs11030094 | Finger tapping (dominant hand) | 2.57 | 0.16 | -0.87 | 6.00 |
| | Story recall (immediate) | -0.36 | 0.48 | -1.42 | 0.69 |
| | Figure recognition (serial) | -1.30 | 0.07 | -2.79 | 0.20 |
| | Rey AVLT (immediate) | -2.79 | 0.05 | -5.73 | 0.15 |
| | Rey AVLT (delayed) | -1.01 | **0.02*** | -2.02 | -0.13 |
| | AMIPB average speed | 2.62 | 0.15 | -1.21 | 6.47 |

*Note:* [a] Permutation testing for the number of markers at the gene level ≤ 31. * $P \leq 0.05$. Negative β values indicate lower test scores for each copy of the minor allele. Statistical modelling was kindly performed by Dr. Fabio Miyajima, University of Liverpool, using Stata v.9.2. Abbreviations: *AMIPB, Adult Memory and Information Processing Battery; AVLT, Auditory Verbal Learning Task; β, beta coefficient; CI, confidence interval.*

individuals with a particular disorder and healthy matched controls. As cognition is a highly heritable phenotype relevant to both normal and abnormal neurological function, we wanted to ensure that the markers identified from our genetic association were reflective of genetic differences associated with cognitive performance as opposed to differences in ancestry. To address this, we performed LD analysis of our genotype data using *Lewontin's normalized D′* statistic (Lewontin, 1964) and compared it to LD patterns generated using genotype data from the HapMap CEU cohort as a reference group (**Figures 3.2** and **3.3**). Haplotype blocks were defined using 95% confidence intervals proposed by Gabriel et al. (2002). Using this method, markers within the BDNF gene were shown to be inherited as a single haplotype block spanning 76 Kb, with evidence of recombination within the promoter sequence represented by low D' values (**Figure 3.2**). Within the NRSF gene, a single haplotype block spanning 774 bp was defined, composed of the rs3796529 and rs2227901

**Table 3.6.** Genetic association analysis of longitudinal cognitive data using a mixed-effect REML regression model adjusted for age, sex, epilepsy type and remission status at 12 month follow-up (seizure free or not)

| Gene | SNP | Cognitive test | β | *P*-value | Adjusted *P*-value [a] | 95% CI | |
|---|---|---|---|---|---|---|---|
| | | | | | | Lower | Upper |
| NRSF | rs1105434 | VRT (non-dominant hand)† | 0.06 | 0.64 | 0.70 | -0.21 | 0.34 |
| | | CVST† | -0.01 | 0.95 | 0.85 | -0.36 | 0.34 |
| | | Rey AVLT (immediate) | 0.52 | 0.91 | 0.90 | -8.20 | 9.25 |
| | | Rey AVLT (delayed) | 0.12 | 0.94 | 0.74 | -2.74 | 2.98 |
| | rs2227902 | VRT (non-dominant hand)† | -0.07 | 0.68 | 0.96 | -0.43 | 0.28 |
| | | CVST† | 0.04 | 0.84 | 0.89 | -0.42 | 0.52 |
| | | Rey AVLT (immediate) | -6.68 | 0.23 | 0.08 | -17.50 | 4.14 |
| | | Rey AVLT (delayed) | 3.53 | 0.08 | **0.02*** | -7.49 | 0.42 |
| | rs3796529 | VRT (non-dominant hand)† | 0.36 | **0.04*** | 0.08 | 0.02 | 0.71 |
| | | CVST† | -0.25 | 0.29 | 0.29 | -0.71 | 0.21 |
| | | Rey AVLT (immediate) | 2.23 | 0.68 | 0.38 | -8.30 | 12.77 |
| | | Rey AVLT (delayed) | -1.29 | 0.53 | 0.94 | -5.28 | 2.69 |
| BDNF | rs1491850 | VRT (non-dominant hand)† | 0.15 | 0.26 | 0.43 | -0.11 | 0.40 |
| | | CVST† | 0.17 | 0.27 | 0.73 | -0.14 | 0.48 |
| | | Rey AVLT (immediate) | -2.33 | 0.58 | 0.43 | -10.52 | 5.86 |
| | | Rey AVLT (delayed) | -1.81 | 0.19 | 0.08 | -4.55 | 0.92 |
| | rs12273363 | VRT (non-dominant hand)† | 0.09 | 0.59 | 0.69 | -0.23 | 0.41 |
| | | CVST† | 0.25 | 0.24 | 0.45 | -0.16 | 0.65 |
| | | Rey AVLT (immediate) | -8.15 | 0.12 | 0.07 | -18.28 | 1.97 |
| | | Rey AVLT (delayed) | -3.99 | **0.04*** | **0.01*** | -7.74 | -0.25 |
| | rs2030324 | VRT (non-dominant hand)† | 0.08 | 0.52 | 0.31 | -0.17 | 0.34 |
| | | CVST† | -0.13 | 0.39 | 0.36 | -0.45 | 0.18 |
| | | Rey AVLT (immediate) | -3.80 | 0.32 | 0.43 | -11.35 | 3.75 |
| | | Rey AVLT (delayed) | -1.10 | 0.43 | 0.84 | -3.80 | 1.60 |
| | rs11030108 | VRT (non-dominant hand)† | 0.05 | 0.44 | 0.88 | -0.18 | 0.28 |
| | | CVST† | -0.00 | 0.98 | 0.90 | -0.30 | 0.29 |
| | | Rey AVLT (immediate) | -0.73 | 0.83 | 0.51 | -7.35 | 5.89 |
| | | Rey AVLT (delayed) | -0.58 | 0.66 | 0.33 | -3.12 | 1.97 |
| | rs6265 | VRT (non-dominant hand)† | 0.06 | 0.69 | 0.97 | -0.23 | 0.35 |
| | | CVST† | -0.02 | 0.93 | 0.53 | -0.39 | 0.36 |
| | | Rey AVLT (immediate) | 1.03 | 0.84 | 0.64 | -8.77 | 10.82 |
| | | Rey AVLT (delayed) | -0.46 | 0.81 | 0.86 | -4.08 | 3.16 |
| | rs7124442 | VRT (non-dominant hand)† | 0.08 | 0.48 | 0.61 | -0.14 | 0.30 |
| | | CVST† | -0.02 | 0.92 | 0.88 | -0.29 | 0.26 |
| | | Rey AVLT (immediate) | -1.39 | 0.71 | 0.46 | -8.62 | 5.84 |
| | | Rey AVLT (delayed) | -0.37 | 0.78 | 0.48 | -3.01 | 2.26 |
| | rs11030094 | VRT (non-dominant hand)† | 0.21 | 0.13 | 0.05 | -0.06 | 0.48 |
| | | CVST† | -0.09 | 0.61 | 0.69 | -0.45 | 0.27 |
| | | Rey AVLT (immediate) | -6.44 | 0.18 | 0.19 | -15.76 | 2.87 |
| | | Rey AVLT (delayed) | -1.86 | 0.24 | 0.47 | -4.95 | 1.22 |

*Note:* [a] Corrected for significant covariate effects (age). *P<0.05. †Analysis undertaken on log-transformed data. Negative β values indicate lower test scores for each copy of the minor allele. Abbreviations: *AVLT, Auditory Verbal Learning Task; β, beta coefficient; CI, confidence interval; CVST, Computerised Visual Search Task; REML, Restricted Maximum Likelihood; VRT, Visual Reaction Time.*

markers. As illustrated in **Figure 3.3A**, there are a number of recombination hotspots across the NRSF gene, depicted by the white regions on the LD plot (D′<1; logarithm of odds, LOD, <2). However, analysis of the genetic coverage over the locus captured by the htSNPs selected for inclusion in our genetic analysis using genotype data from the HapMap CEU cohort showed an additional haplotype block of strong LD spanning 21 Kb, with evidence of recombination in the region containing a coding variable number tandem repeat (VNTR) within exon 4 of the NRSF gene that is tagged by the rs2227902 SNP (Miyajima et al., 2008b) (**Figure 3.3B**), shown from our genetic association to be significantly correlated with memory performance in patients with newly diagnosed epilepsy (**Table 3.5** and **3.6**). LD patterns across the BDNF and NRSF genes in this modest sample showed no major differences in comparison to those generated using data for the HapMap CEU cohort (**Figure 3.2** and **3.3**), eliminating the possibility of population stratification in our model.

### 3.3.4 Location of associated SNPs suggests a regulatory function

Of the seven SNPs identified as being important for memory processing in adults with newly diagnosed epilepsy, five of these (NRSF rs1105434; and BDNF rs1491850, rs12273363, rs2030324 and rs11030094) were located in non-coding regions of the genome. To explore the potential functionality of these non-coding SNPs we uploaded them into HaploReg V2, an online resource compiling information relating to epigenetic signatures, transcription factor binding sites (TFBS), regulatory motifs and expression quantitative trait loci (eQTLs) relating to an expanded list of markers based on dbSNP-137 (Ward and Kellis, 2012). To minimise the background noise generated through

| BDNF Haplotypes | | | | | | | | | | | | | | | | Frequency | | P-Value |
|---|---|---|---|---|---|---|---|---|---|---|---|---|---|---|---|---|---|---|
| | | | | | | | | | | | | | | | | SANAD | CEU | ($X^2$) |
| A | T | T | G | C | A | G | G | T | T | T | C | C | G | A | C | 0.38 | 0.35 | *0.74* |
| G | T | C | G | G | A | G | A | T | C | A | C | T | A | G | T | 0.24 | 0.27 | |
| G | C | T | A | C | G | C | G | C | T | A | G | T | G | G | C | 0.17 | 0.20 | |
| G | T | C | G | C | A | G | A | T | C | A | C | T | A | G | T | 0.07 | 0.08 | |
| G | T | T | G | C | A | G | G | T | T | T | C | C | G | A | C | 0.07 | 0.05 | |

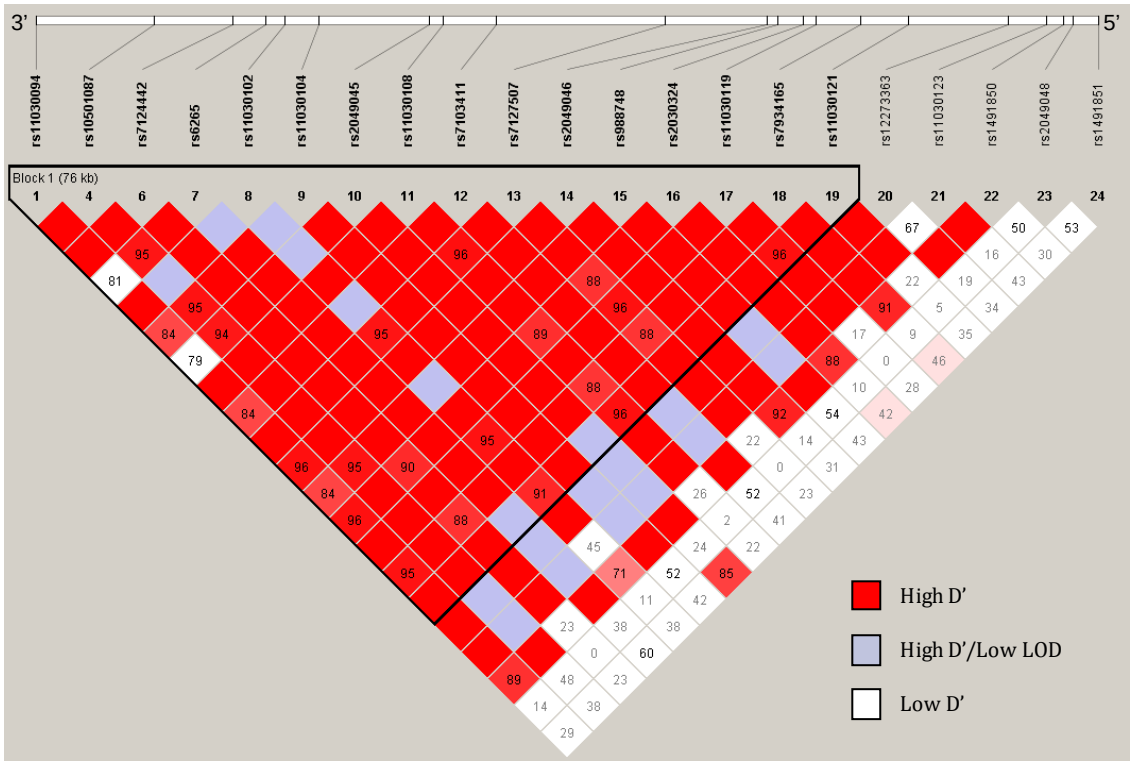


**Figure 3.2. Linkage disequilibrium (LD) and haplotype analysis of BDNF markers in newly-diagnosed epilepsy patients.** Haplotype block structure of the BDNF gene indicating strong LD (red squares) based on D′ estimates calculated from 82 individuals with newly -diagnosed epilepsy. Haplotype blocks, represented by a black triangular border, were determined using 95% confidence intervals proposed by Gabriel et al. (2002) which defined a single block for the BDNF gene. Individual haplotypes making up the BDNF haplotype block are depicted above the LD plot and are compared to haplotype frequencies present in the HapMap CEU cohort. Haplotypes with a minor allele frequency of 0.05 or above were included. Haplotype structure did not significantly differ between the two cohorts (P=0.74, chi-square test; $X^2$). *LOD; log of the likelihood odds ratio, a measure of confidence in the D' value.*

**A**

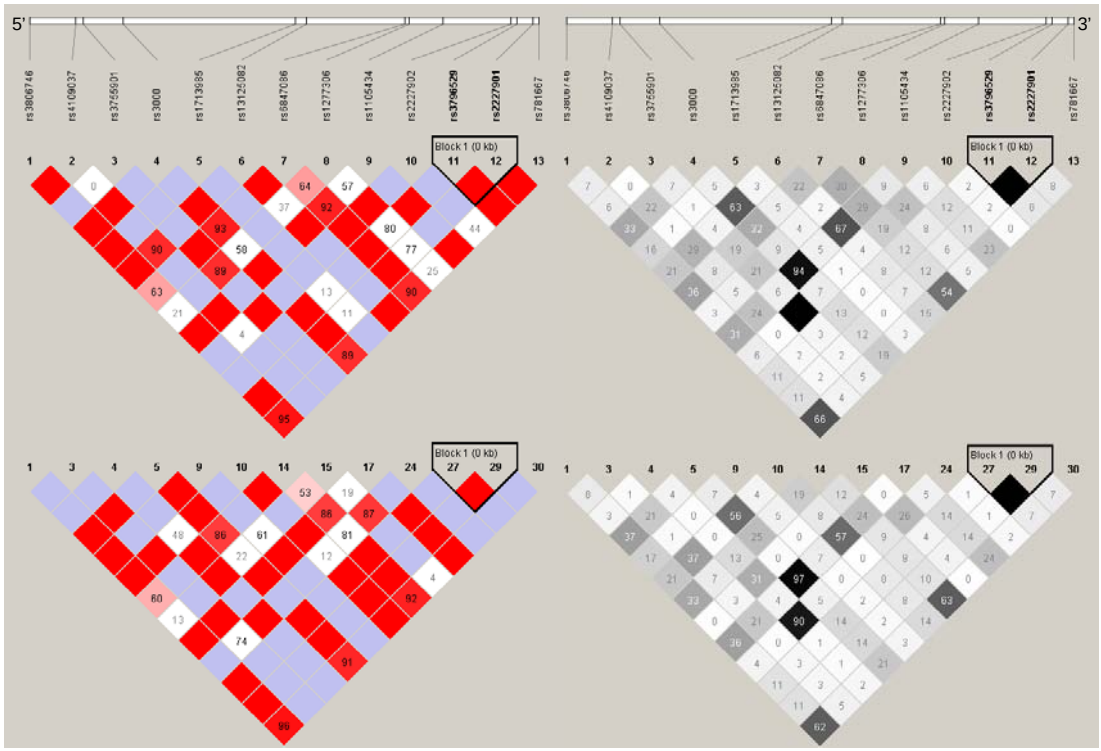


**B**

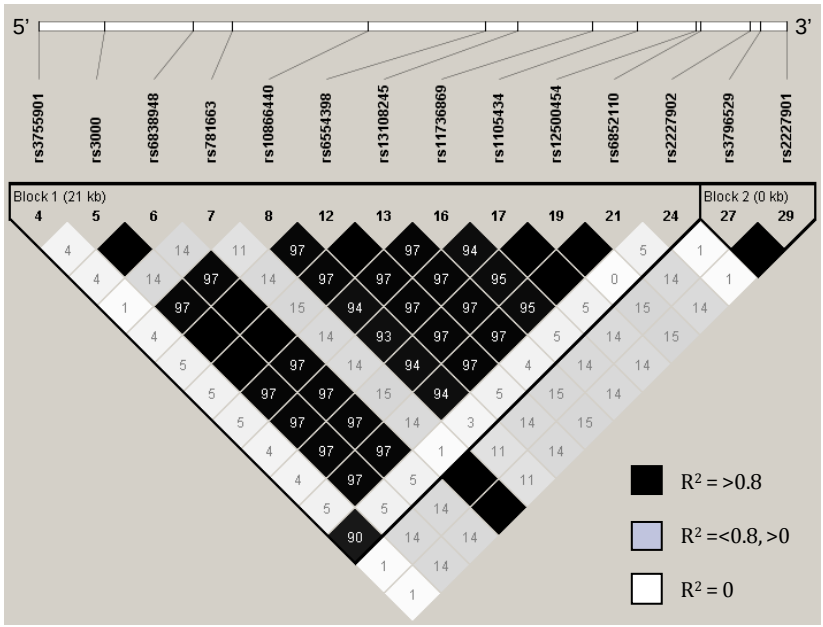


**Figure 3.3. Linkage disequilibrium (LD) and haplotype analysis of NRSF markers in newly-diagnosed epilepsy patients. A**, Haplotype block structure of the NRSF gene in the SANAD cohort (*top*) and the HapMap CEU cohort (*bottom*) indicating low LD and possible recombination sites (white squares) based on D́ (*left*) and $r^2$ (*right*) estimates. Haplotype blocks, represented by a black triangular border, were determined using 95% confidence intervals proposed by Gabriel et al. (2002) which defined a single block for the NRSF gene. A similar pattern of LD was observed between the two study cohorts. **B**, LD analysis in HapMap CEU cohort using alleles captured through haplotype-tagging indicates two haplotype blocks and strong LD over the region.

computational predictions, HaploReg only reports the intersection of SNPs with regulatory motifs which pass the stringent threshold ($P < 4x10^{-8}$) of a position weight matrix (PWM); probabilistic representations of signals in DNA or protein sequences which can be used to model approximate patterns of DNA-protein or protein-protein interactions (Ward and Kellis, 2012). Interestingly, using this web-base tool, allele-specific changes in the PWM scores for the most enriched discovered motif for NRSF was identified for the BDNF rs1491850 promoter SNP (http://www.broadinstitute.org/mammals/haploreg/detailv2.php). In addition, the intronic NRSF rs1105434 SNP which is located 30 bp upstream of an alternative exon within the NRSF gene termed exon N (**Figure 3.1**), which encodes a truncated protein sNRSF, alters the PWM scores for several regulatory motifs including that of the Yin Yang 1 (YY1) transcription factor which has recently been identified as playing a role in intron-mediated enhancement of human ubiquitin C gene expression and modulation of its splicing efficiency (Bianchi et al., 2013). Computational modelling of SNP-associated changes in PWM scores for a discovered TFBS motif, such as NRSF and YY1 in this case, highlight regions of potential perturbation in the regulation of gene expression through altering transcription factor binding and alternative splicing. We also examined the influence of the SNPs identified as being significantly associated with cognitive function on eQTL patterns using data accessed from the Genevar (Gene Expression Variation) suite, see *section 2.2.6.2* (Stranger et al., 2012). BDNF and NRSF gene expression levels for individuals in the HapMap CEU population were correlated with matched SNP genotype data for the same study cohort, **Figure 3.4**. SNP-gene eQTL data was not available for the BDNF rs2030324 marker, therefore data was inferred from

the htSNP ($r^2$=1) rs10767665. The NRSF rs1105434 SNP, identified in our cross-sectional analysis to be significantly associated with delayed recall scores on the Rey AVLT task and to modify the PWM score for the YY1 Transcription factor from our *in silico* analysis, was shown to significantly affect NRSF gene expression levels (**Figure 3.4**, P<0.045; presence of minor allele correlated with higher expression levels). A trend was observed for BDNF rs1491850 and rs12273363 also associated with the Rey AVLT task in our cross-sectional and longitudinal analyses, respectively, with BDNF gene expression levels however these did not reach significance (P=0.57 and 0.55, respectively). No significant correlations between NRSF genotype and BDNF expression levels, or vice versa, were found for any of the markers addressed in this study (data not shown, with the exception of NRSF rs2227902 on BDNF expression, **Figure 3.4H**, see *section 3.3.5*). These findings support a potential role for the NRSF and BDNF cognitive variants, identified from our genetic association analysis to influence memory function in patients with newly-diagnosed epilepsy, in modulating the expression levels of their corresponding genes; both of which have previously been implicated in normal and abnormal cognition (Miyajima et al., 2008a, Honea et al., 2013, Voineskos et al., 2011, Lu et al., 2014).

**Figure 3.4. Effects of NRSF and BDNF cognitive variants on gene expression levels.** Expression quantitative trait (eQTL) plots for BDNF (**A-D**) and NRSF (**E-G**) gene expression levels, for the HapMap CEU population plotted against genotypes of the BDNF rs11030094 (**A**), rs12273363 (**B**), rs2030324 (**C**) and rs1491850 (**D**), and NRSF rs1105434 (**E**), rs2227902 (**F**) and rs3796529 (G) SNPs shown to be significantly associated with cognitive function in patients with newly diagnosed epilepsy. NRSF rs2227902 was also plotted against BDNF expression (**H**); see *section 3.3.5*. Plots represent AA/Aa/aa, where 'A' is the wild type allele and 'a' the variant allele. [a] Data inferred from haplotype-tagging SNP rs10767665 which is in complete linkage disequilibrium (LD) ($r^2$=1) with rs2030324. *P < 0.05. Plots were obtained from the Genevar portal, version 3.3.0. Empirical P-values (*Pemp*) represent permutated data controlling for the number of genetic variants per gene and in LD. [Figure presented on opposite page].

A

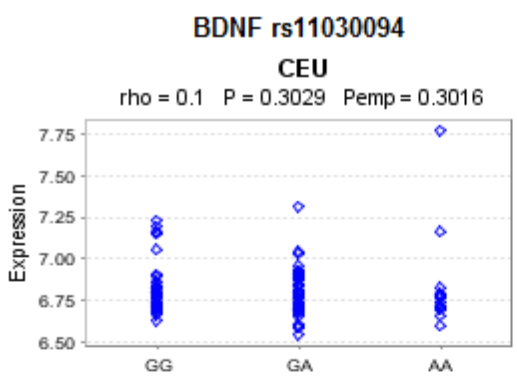
BDNF rs11030094
CEU
rho = 0.1 P = 0.3029 Pemp = 0.3016
Expression
7.75
7.50
7.25
7.00
6.75
6.50
GG
GA
AA

B

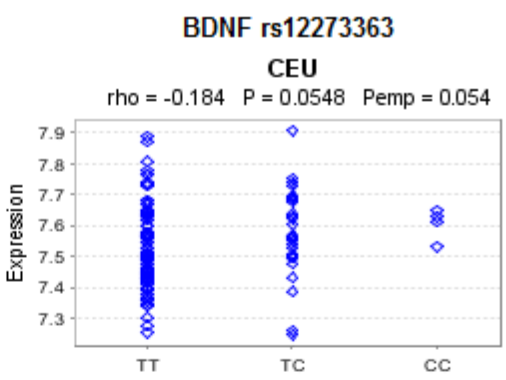
BDNF rs12273363
CEU
rho = -0.184 P = 0.0548 Pemp = 0.054
Expression
7.9
7.8
7.7
7.6
7.5
7.4
7.3
TT
TC
CC

C

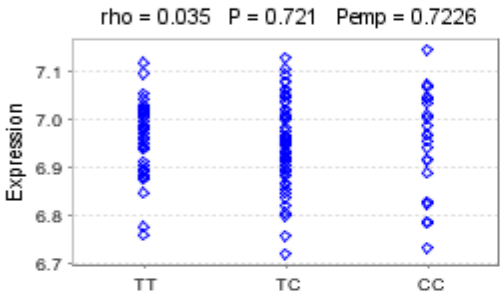
BDNF rs2030324 a
CEU
rho = 0.035 P = 0.721 Pemp = 0.7226
Expression
7.1
7.0
6.9
6.8
6.7
TT
TC
CC

D

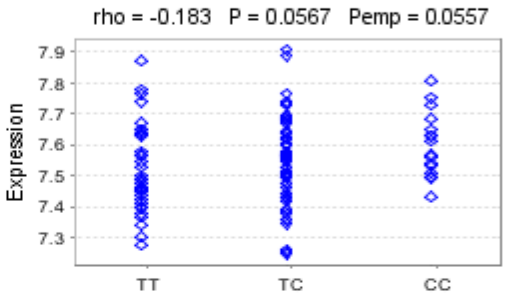
BDNF rs1491850
CEU
rho = -0.183 P = 0.0567 Pemp = 0.0557
Expression
7.9
7.8
7.7
7.6
7.5
7.4
7.3
TT
TC
CC

E

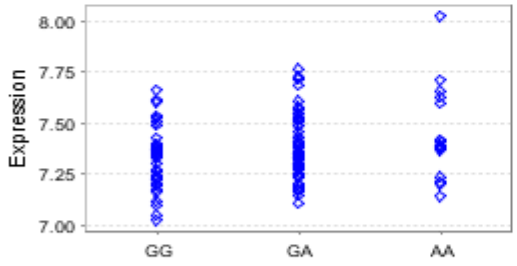
NRSF rs1105434 *
CEU
rho = -0.193 P = 0.0454 Pemp = 0.0457
Expression
8.00
7.75
7.50
7.25
7.00
GG
GA
AA

F

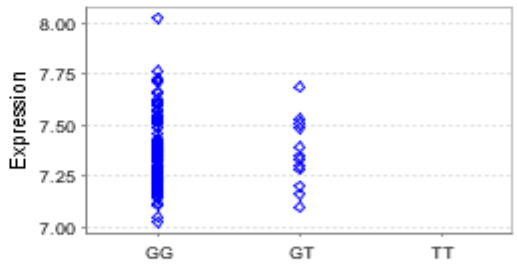
NRSF rs2227902
CEU
rho = -0.095 P = 0.3301 Pemp = 0.3338
Expression
8.00
7.75
7.50
7.25
7.00
GG
GT
TT

G

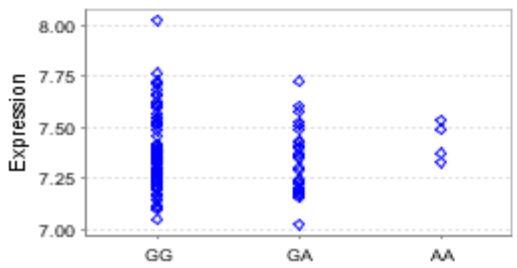
NRSF rs3796529
CEU
rho = -0.061 P = 0.5333 Pemp = 0.5354
Expression
8.00
7.75
7.50
7.25
7.00
GG
GA
AA

H

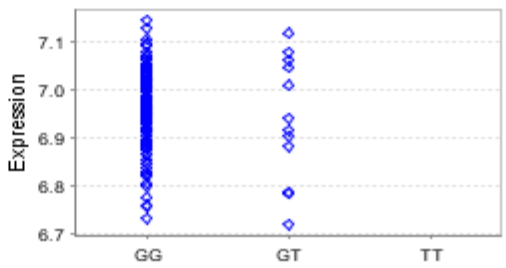
NRSF rs2227902
CEU
rho = -0.034 P = 0.7292 Pemp = 0.7385
Expression
7.1
7.0
6.9
6.8
6.7
GG
GT
TT

### 3.3.5 Association of NRSF-BDNF composite genetic model with Rey AVLT (delayed) scores

We have previously shown that the major allele of NRSF rs2227902 (G) is associated with reduced cognitive performance in the elderly (Miyajima et al., 2008b). To determine its effect on cognition in adults with newly-diagnosed epilepsy, we correlated the number of rs2227902 risk alleles with delayed recall Rey AVLT scores as these were shown to be significantly associated in our longitudinal analysis (P=0.02, **Table 3.6**). **Figure 3.5A** illustrates a similar trend to that observed in the ageing population, with individuals homozygous for the wild type (WT) allele deteriorating to a significantly (P=0.014, unpaired t-test) greater extent than individuals possessing at least one copy of the minor allele in terms of delayed recall in the Rey AVLT. Interaction between the rs2227902 marker and the BDNF rs6265 marker has also been described previously (Miyajima et al., 2008b). This was therefore assessed in our dataset. A composite-genotype model was used in order to determine association between the cross-sectional and longitudinal cognitive test scores with the sum of risk alleles for the rs2227902 and rs6265 markers. The WT allele (G), which tags a 5-copy coding VNTR within exon 4 of the NRSF gene, was considered to be the risk allele for rs2227902, whereas the minor allele (Met66-A) was considered the risk allele for rs6265 (Miyajima et al., 2008b, Miyajima et al., 2008a). Linear regression analysis showed that the change in delayed recall in Rey AVLT in the longitudinal analysis was significantly associated with the number of risk alleles (P value=0.02; **Figure 3.5B**). In the previous report by Miyajima et al. (2008b) this interaction was shown to specifically reflect a haplotype containing the rs2227902 (T) marker, which tags a 4-copy variant of

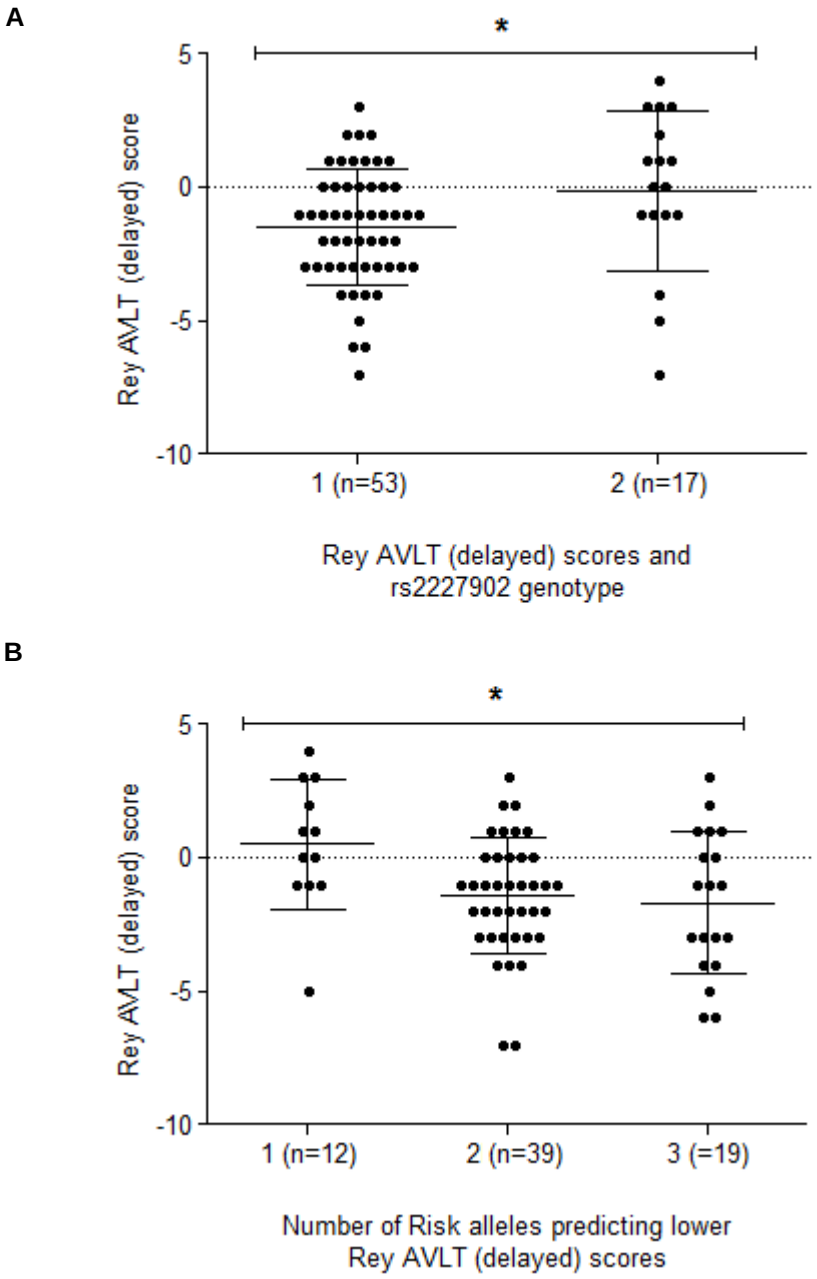


**Figure 3.5. Association of NRSF-BDNF composite-genotype with Rey Auditory Verbal Learning Task (AVLT) delayed recall scores over time. A**, Association of NRSF rs2227902 with Rey AVLT delayed recall scores. A/A represents individuals homozygous for the wild type risk allele rs2227902 (G); A/a represents individuals possessing at least 1 copy of the minor non-risk allele rs2227902 (T). Horizontal lines represent the mean change with standard deviation from baseline to 12 month reassessment scores. A lower score correlates with a greater reduction in memory performance. A significant decrease in test scores was observed between the two groups (Mann-Whitney test, P=0.014). **B**, Risk alleles for NRSF rs2227902 and BDNF rs6265 were grouped and the number of alleles scored as follows: Group 1 represents 0-1 risk alleles, Group 2 represents 2 risk alleles in individuals that were either heterozygous for each SNP or homozygous for rs2227902 (G) and Group 3 represents 3-4 risk alleles. Linear regression analysis showed a significant difference between the groups (P=0.02).

the NRSF VNTR, and BDNF rs6265 (Val66-G). Individuals possessing this haplotype had significantly higher scores of general intelligence than those with one or neither of these variants, or in individuals possessing the NRSF-BDNF risk variants. To test the direction of this interaction in terms of risk or non-risk alleles predicting cognitive performance, linear regression was applied to different allele groupings as shown in **Table 3.7**. Due to the low minor allele frequencies of rs2227902 and rs6265, individuals were grouped by the presence or absence of the minor alleles. Data were controlled for age, sex and epilepsy type by covarying their effects. Consistent with an additive interaction between the rs2227902 and rs6265 'non-risk' alleles in determining higher cognitive performance in the elderly, our composite genotype model showed a positive correlation between the presence of the rs2227902(T)_rs6265(G) genotype and higher Rey AVLT scores in our epilepsy cohort (**Table 3.7**, P=0.01; beta-coefficient 0.31). No such interaction was observed between the other NRSF-BDNF groupings and cognitive test scores which again supports previous findings (Miyajima et al., 2008b).

The additive interaction between NRSF rs2227902 (T) and BDNF rs6265 (G) and its influence on cognitive performance in patients with newly-diagnosed epilepsy (**Table 3.7**) and normal ageing (Miyajima et al., 2008b) may reflect differences in the regulation of BDNF gene expression levels along the NRSF signalling pathway. To try and address this, we correlated eQTL patterns between NRSF rs2227902 and BDNF expression levels using data from the HapMap CEU reference cohort. No significant differences in BDNF expression levels between homozygous WT and heterozygous individuals for the NRSF rs2227902 SNP were observed (no homozygotes for the minor allele were

present in the dataset; **Figure 3.4H**). Similarly, BDNF rs6265 genotype did not affect NRSF expression (data not shown). We were unable to address the additive effect of the rs2227902 and rs6265 markers on BDNF gene expression levels using this dataset due to restrictions on accessing the raw data files.

**Table 3.7.** Association of NRSF-BDNF composite-genotype with Rey Auditory Verbal Learning Task (AVLT) delayed recall scores over time

| NRSF-BDNF Haplotype | N | Frequency | β | P-value [a] |
|---|---|---|---|---|
| rs2227902(G)_rs6265(G) | 35 | 50.0 | -0.12 | 0.31 |
| rs2227902(G)_rs6265(A) | 18 | 25.7 | -0.13 | 0.30 |
| rs2227902(T)_rs6265(G) | 12 | 17.1 | 0.31 | **0.01*** |
| rs2227902(T)_rs6265(A) | 5 | 7.1 | -0.01 | 0.97 |

*Note:* [a] Linear regression model for association between the NRSF marker rs2227902 and the BDNF marker rs6265 with Rey AVLT delayed recall scores over time. Major allele of NRSF, rs2227902 (G), and minor allele of BDNF, rs6265 (A), were considered risk alleles. Negative β scores indicate that the presence of risk alleles (or absence of non-risk alleles) correlates with lower test scores. Positive β scores indicate that the presence of non-risk alleles (or absence of risk alleles) correlates with higher test scores. Abbreviations: *AVLT, Auditory Verbal Learning Task; β, beta coefficient*.

## 3.4 Discussion

Cognitive dysfunction has been reported in people with newly-diagnosed epilepsy. These individuals are naïve to the long-term effects of AED treatment and the cumulative effects of recurrent seizures, factors implicated in disease-associated cognitive impairments (Taylor et al., 2010, Hermann et al., 2006, Park and Kwon, 2008), suggesting the involvement of other intrinsic and/or environmental influences. In this study, we provide preliminary evidence to suggest that variants within the NRSF and BDNF genes influence cognitive function in adults with newly-diagnosed epilepsy at both baseline and over the first year after diagnosis. Genetic effects were specific to memory-related tasks and psychomotor speed (longitudinal analysis). In the cross-sectional analysis we found significant associations for the non-redundant SNPs (based on $r^2$ estimates) NRSF rs1105434 and rs2227902 and BDNF rs1491850, rs2030324 and rs11030094, with NRSF rs2227902 and rs3796529 and BDNF rs12273363 implicated in the longitudinal model. These findings are consistent with previous studies showing association between the NRSF and BDNF genes and cognitive function in a normal ageing population and in neurological disorders. For example, nuclear NRSF levels have been shown to be increased in the normal ageing human brain, where it is thought to play a neuroprotective role against oxidative stress and β-amyloid protein toxicity, but reduced in prefrontal cortex (PFC) and hippocampal neurons in individuals with mild cognitive impairments and Alzheimer's disease (Lu et al., 2014). Similarly, decreased serum levels of BDNF have been correlated with Alzheimer's disease and associated cognitive deficits implicated in this neurodegenerative disorder (Laske et al., 2011). Reduced BDNF expression in the PFC and hippocampus has

also been observed in neuroimaging and post-mortem studies of affective disorders including major depressive disorder and bipolar disorder, which coincided with reduced brain matter, impaired spatial memory and executive function (Hing et al., 2012).

All of the SNPs identified in this study have previously been associated with neurological disease (BDNF SNPs only) or as markers of phenotypic traits associated with CNS dysfunction, see **Table 3.4**. For example, genetic association studies have identified the BDNF SNPs rs1491850 and rs11030094, shown in our cross-sectional analysis to be associated with immediate and delayed recall in the Rey AVLT, respectively, to be correlated with whole brain and/or hippocampal atrophy and cognitive decline in Alzheimer's disease (Honea et al., 2013, Laumet et al., 2010). BDNF rs1491850 has also been implicated in treatment response phenotypes and remission status in major depressive disorder (Kocabas et al., 2011, Gratacos et al., 2008). We also observed an association between Rey AVLT scores and the BDNF SNP rs2030324 which has previously been associated with speed processing in normal ageing (Miyajima et al., 2008a) and visual cognitive processing in multiple sclerosis (Weinstock-Guttman et al., 2011).

Significant associations with delayed recall performance were also apparent in our longitudinal analysis with respect to NRSF rs2227902 and BDNF rs12273363. This may reflect a distinct regulatory pathway in the modulation of verbal memory in late-onset epilepsy. Dysregulation of the BDNF gene is well documented in neurological disorders (Chen et al., 2001, Dwivedi et al., 2003, Thompson Ray et al., 2011, Ray et al., 2014, Dunham et al., 2009). Elaborate modulation of BDNF mRNA expression is mediated by nine functional

promoters, some of which are influenced by *cis*-regulatory elements (Pruunsild et al., 2011, Hing et al., 2012). One such element, BE5.2, which contains the non-coding SNP rs12273363, implicated in memory performance in our longitudinal assessment, has been shown to differentially regulate BDNF promoter IV activity in a stimulus-inducible, allele-specific and tissue-dependent manner (Hing et al., 2012). This correlates with previous findings of allele-specific differences in pro-BDNF density in post-mortem tissue from the Stanley Foundation Neuropathology Consortium brains (for schizophrenia, major depressive disorder, bipolar disorder and matched control subjects) in which the minor allele of rs12273363 was associated with reduced hippocampal expression (Dunham et al., 2009). Association between NRSF rs3796529 and psychomotor speed was also found in our longitudinal study however this did not withstand correcting for covariate effects.

The location of five of the seven associated SNPs from our analysis within promoter or intronic regions of the genome is suggestive of a regulatory role. Several studies have shown enrichment of disease-associated SNPs within tissue-specific enhancers (Bhandare et al., 2010, Ward and Kellis, 2012, Ernst et al., 2011, Gerasimova et al., 2013, Rhie et al., 2013). Polymorphisms within regulatory elements can alter transcription factor binding motifs and thus the expression of a gene in part through modulation of signal transduction responses in both a tissue-specific and stimulus-dependent manner. A recent study demonstrated allele-specific transcription factor binding affinities using a panel of disease-associated SNPs (Butter et al., 2012), providing further insight into the molecular mechanisms by which non-coding SNPs may exert their effect on gene regulation. To address the potential function of the five

associated non-coding SNPs identified in this study, we uploaded these markers into the web-based platform HaploReg V2 which can be used to predict the cell-specific chromatin state, mammalian conservation and effect on regulatory motifs for a particular marker (Ward and Kellis, 2012). The BDNF rs1491850 promoter I SNP was identified as modifying the genome-wide enriched NRSF motif, measured by a change in the PWM score. This is of interest as it may potentiate differences in NRSF binding affinities to BDNF promoter I, a validated NRSF binding site in rodents (Timmusk et al., 1999), resulting in changes in BDNF gene expression. NRSF modulation of BDNF promoter activity is discussed further in *section II* of this chapter. Furthermore, analysis of the influence of these SNPs on NRSF and BDNF gene expression levels were also addressed using eQTL data from Genevar 3.3.0 (Yang et al., 2010). The intronic NRSF rs1105434 SNP was shown to be significantly associated with NRSF expression levels in the HapMap CEU reference cohort, with the minor allele correlating with higher expression levels (**Figure 3.4E**). The intronic location of this SNP 30 bp upstream of NRSF exon N which encodes the truncated sNRSF protein suggests that it may function as a *cis*-acting modulator of alternative splicing (Hull et al., 2007, Fu and Ares, 2014). This is supported by the presence of a sequence motif for the bivalent DNA-RNA binding protein YY1 which has recently been implicated in modulating splicing efficiency and intron-mediated enhancement of gene expression (Bianchi et al., 2013). Different alleles of this marker may therefore alter the binding affinities of sequence-specific binding factors such as YY1 which may be important for controlling context-dependent expression of the NRSF gene, an important mechanism in neuronal plasticity as

suggested from our studies on isoform usage following seizure induction (Spencer et al., 2006).

The BDNF SNP rs6265, which encodes a missense mutation in the only coding exon of the BDNF gene, has been extensively studied in the field of cognition, with many publications supporting its role in the regulation of cognitive function. The first publication investigating such a role reported that the minor rs6265 (Met66-A) allele, defined in this current study as the risk allele, impaired human hippocampal activation and activity-dependent secretion of BDNF and reduced delayed episodic memory (Egan et al., 2003). Our study did not find a direct association between rs6265 and cognitive function in epilepsy patients. However, when this SNP was analysed in combination with NRSF rs2227902 based on the previous finding of an additive interaction between these two polymorphisms in age-related cognitive function (Miyajima et al., 2008b), the number of risk alleles was inversely correlated with memory performance over time (**Figure 3.5B**). Linear regression analysis of the different groupings of these two SNPs based on the presence or absence of the risk or non-risk alleles showed that the genetic association was significant in relation to a haplotype containing the non-risk alleles NRSF rs2227902 (T) and BDNF rs6265 (Val66-G), which correlated with higher Rey AVLT test scores as indicated by the positive beta coefficient value (**Table 3.7,** $P=0.01$; $\beta=0.31$). This is consistent with previous findings in the elderly cohort suggesting that this allelic combination may improve cognitive performance or slow the rate of cognitive decay over individuals possessing the proposed risk variants which may predict risk for more rapid cognitive decline over time, as demonstrated in BDNF rs6265 (Met66-A) carriers relative to rs6265 (Val66-G)

homozygotes in Alzheimer's disease (Lim et al., 2014). In mature CNS neurons, BDNF regulates higher cognitive processes through elaboration and refinement of neuronal circuitries and modulation of synaptic plasticity and hippocampal long-term potentiation (LTP), a process central to memory and learning (Bramham and Messaoudi, 2005, Bramham, 2008). Reduced levels of neuronal and circulating BDNF have been linked to cognitive impairments in several neurological conditions suggesting that dysregulation of this gene may be important in neurological dysfunction. The NRSF rs2227902 (T) non-risk allele is in LD with a 4-copy coding VNTR within the NRSF gene may reduce the binding efficiency of the NRSF protein to its target genes, such as BDNF, altering their expression levels relative to the 5-copy VNTR which is tagged by the proposed risk variant of this SNP (Miyajima et al., 2008b). To address this proposed mechanism, the rs2227902 genotype was correlated with BDNF expression levels based on data from lymphoblastoid cell lines derived from individuals of the HapMap CEU cohort. There was no significant difference in eQTL expression patterns based on the rs2227902 genotype in this reference cohort (**Figure 3.4H**). Nor was there an effect of BDNF rs6265 genotype on NRSF levels (data not shown). This may reflect several factors including cell-specificity (lymphoblast cells may not be an appropriate model for addressing interactions associated with cognition); age-related or disease-associated interactions as suggested from our previous work in the elderly and epilepsy cohorts and the additive nature of this polymorphism with the rs6265 marker which could not be addressed in this dataset.

Support for the NRSF-BDNF pathway as a potential mechanism in cognitive dysfunction associated with neurological disorders comes from

studies on Huntington's disease, were it has been shown that WT but not mutant huntingtin protein regulates BDNF transcription through cytoplasmic sequestering of NRSF (Zuccato et al., 2003). Furthermore, genetic variants of the REST-interacting LIM domain protein (RILP/Prickle-1), an important candidate involved in the nuclear translocation and repressive functioning of NRSF (Shimojo and Hersh, 2006), have been associated with autosomal-recessive progressive myoclonus epilepsy-ataxia syndrome, the symptoms of which include seizures and cognitive decline (Bassuk et al., 2008). Epigenetic parameters may also be important in this regulatory network as suggested by interaction of the NRSF-silencing complex with the histone demethylase SMCX, a gene implicated in X-linked mental retardation and epilepsy (Tzschach et al., 2006), resulting in chromatin remodelling and downstream regulation of NRSF target genes including BDNF. Other chromatin remodelling proteins associated with this silencing complex have been implicated in memory impairment, including histone deacetylase 2 (HDAC2) (Guan et al., 2009, Graff et al., 2012) and methyl CpG binding protein 2 (MeCP2) which is mutated in Rett syndrome resulting in NRSF/CoREST-mediated repression of BDNF expression (Abuhatzira et al., 2007). Further support comes from evidence that glycolytic inhibitor 2-deoxy-D-glucose modulation of the NRSF-ctBP (C-terminal binding protein) complex enhances the repressive chromatin environment surrounding the BDNF gene, consequently blocking epileptogenesis (Hu et al., 2011b, Garriga-Canut et al., 2006). In addition, investigations into functional abnormalities observed in patients with Korsakoff's syndrome, a neurological disorder caused by thiamine deficiency, found a strong correlation between reduced glycolysis and delayed memory performance (Paller et al., 1997). Both

NRSF and BDNF have been linked to impairments of neurogenesis in this disorder (Tateno and Saito, 2008). Collectively these studies support a role for dysregulation of the NRSF-BDNF pathway in cognitive decline associated with neurological disease.

## 3.5 Summary

In summary, the data presented supports a trend towards association of polymorphic variants within the NRSF and BDNF genes and memory-related tasks in patients with a new diagnosis of epilepsy. These associations reached statistical significance in both the cross-sectional and longitudinal assessment suggesting the influence of genetic background on the susceptibility to memory decline in adults with new onset epilepsy. These findings are consistent with previous literature in the field but should be considered with caution, not least because of the small sample size and lack of a matched control group. In addition, potentially confounding variables including the influence of AED exposure or possible practice effects associated with repeat application of cognitive tests could not be accounted for. Although replication in a larger study sample is required, these observations lend weight to the known involvement of NRSF-BDNF markers in the modulation of cognitive performance in normal ageing and also in neurological and psychiatric disorders.

## Part II: *Complex promoter usage and transcriptional regulation of the human BDNF gene in response to cocaine*

## 3.6 Introduction

In the previous section a number of promoter and intronic SNPs were identified within the NRSF and BDNF genes that associated with cognitive performance in memory-related tasks in patients with newly-diagnosed epilepsy. The location of these SNPs within non-coding regions of the genome indicates a regulatory function which may act through altering gene regulatory sequences as suggested from *in silico* analysis of transcription factor biding site (TFBS) perturbations, outlined in *section 3.3.4*, or to modify post-transcriptional mechanisms. Quantification of the levels of circulating BDNF or its expression and/or function within the brain has been investigated as a potential biomarker in a number of neurological conditions including Alzheimer's disease, mild cognitive impairments, schizophrenia and mood disorders (Laske et al., 2011, Thompson Ray et al., 2011, Lim et al., 2014). Although several studies support a role for aberrant BDNF-signalling in these conditions or associated cognitive defects, the mechanisms involved remain unclear. To better understand the regulatory mechanisms operating at the human BDNF gene and potentially involved in disease-associated dysregulation of this neurotrophic factor, the *in vitro* effects of cocaine, a known modulator of BDNF expression in animal and cell line models (Chandrasekar and Dreyer, 2009, Sadri-Vakili et al., 2010, Le Foll et al., 2005, Liu et al., 2006, Graham et al., 2007, Kumar et al., 2005, Lepsch et al., 2009), were addressed in the human neuronal cell line SH-SY5Y. Cocaine was selected for cellular challenge as it provides a robust signal for studying

stimulus-induced activation of neuronal pathways linked to mood, psychosis, cognition and cellular stress in cell lines (Vasiliou et al., 2012, Pihlgren and Boutros, 2007, Spronk et al., 2013), which can be difficult to model *in vitro*.

The human BDNF gene is extremely complex, comprising eleven exons and nine functional promoters which initiate tissue-specific and stimulus-inducible transcription of distinct mRNA transcripts (Pruunsild et al., 2007). At least 34 alternative BDNF mRNA transcripts are encoded from the BDNF gene locus through alternative splicing (Baj and Tongiorgi, 2009, Pruunsild et al., 2007). Differential expression of these BDNF transcripts is initiated through its alternative promoters which have been shown to be regulated by several mechanisms including DNA methylation, histone modifications and transcription factor binding (Huang et al., 2002, Tsankova et al., 2006, Abuhatzira et al., 2007, Lubin et al., 2008, Tabuchi et al., 2002a, Lipsky et al., 2001, Bredy et al., 2007, Martinowich et al., 2003, Pruunsild et al., 2011). Although transcriptional regulation of BDNF is well documented the majority of studies have focussed on the rodent gene, specifically transcripts 1-4 owing to the incomplete annotation of more recently defined alternative transcripts of this gene (Liu et al., 2006, Aid et al., 2007). Transcriptional regulation over the entire BDNF gene locus is yet to be fully elucidated.

Several BDNF promoters have been shown to be under the transcriptional control of NRSF. Specifically, modulation of rodent BDNF promoters I, II and IV by NRSF or its isoforms have previously been documented (Tabuchi et al., 2002b, Tabuchi et al., 1999, Tian et al., 2009, Timmusk et al., 1999, Abuhatzira et al., 2007, Palm et al., 1998, Hara et al., 2009) and promoter I and II of the human gene (Hara et al., 2009); however, to my knowledge, differential NRSF-

mediated regulation of human BDNF promoter utilisation has not been previously addressed. NRSF-mediated regulation of BDNF expression has been associated with both glutamatergic signalling (Timmusk et al., 1999, Tian et al., 2009) and associated disease pathways, including rodent models of epilepsy, Huntington's disease and Rett syndrome (Abuhatzira et al., 2007, Zuccato et al., 2003, Spencer et al., 2006). Furthermore, as discussed in *section I* of this chapter, the NRSF-BDNF pathway may also play a contributory role to cognitive impairments associated with new-onset epilepsy, assessed through genetic association, implicating this regulatory network in several disease pathways. To better understand the role of NRSF modulation of human BDNF transcription using a human model of neurological dysfunction, the *in vitro* effects of cocaine on the binding of NRSF to potential NRSEs within the BNDF gene locus were explored using chromatin immunoprecipitation (ChIP), which was correlated with expression profiling of the alternatively spliced BDNF mRNAs encoded from distinct promoters.

## 3.7 Aims

- Bioinformatic analysis of NRSEs spanning the human BDNF gene and their special relation to the different BDNF proximal promoters
- Characterise BDNF mRNA expression in human SH-SY5Y neuroblastoma cells and investigate differential promoter utilisation in response to cocaine treatment
- Address NRSF binding of the well characterised and/or transcriptionally active BDNF promoters in SH-SY5Y cells by ChIP
- Correlate BDNF expression data with NRSF promoter occupancy and histone modifications

## 3.8 Results

### 3.8.1 BDNF transcripts are modulated in a time-dependent manner in SH-SY5Y cells in response to cocaine

In accordance with the most recently defined nomenclature for BDNF (Pruunsild et al., 2007), **Figure 3.6** provides a schematic representation of the human BDNF gene locus illustrating the mRNA transcripts addressed in this study. PCR primers were designed to cross exon-intron boundaries for each transcript; the forwards primer targeting the 5' exon and the reverse primer targeting the common 3' exon (exon IX). Primer details are listed in **Table 2.1** of the *Methods* section. SH-SY5Y cells were used in this study due to their neuronal phenotype and endogenous expression of BDNF. Transcripts containing exons I, II, IV, V, VI and IX have been previously characterised in SH-SY5Y cells, with exons II, IV and VI identified as being common across studies (Garzon and Fahnestock, 2007, Baj and Tongiorgi, 2009). In line with these reports, moderate to high levels of mRNA transcripts II, IV, VI and IX were observed under basal conditions, **Figure 3.7A-B**. Exons I, III, V, VII and VIII were undetectable under all conditions tested. This coincides with data from the literature for exons III, VII and VIII (Garzon and Fahnestock, 2007, Baj and Tongiorgi, 2009). Discrepancies in the expression of exon I in SH-SY5Y cells has previously been reported and low levels of exon V has also been observed (Baj and Tongiorgi, 2009). Differences in expression patterns may be the result of differing culture conditions used across studies.

Acute cocaine treatment can induce differential BDNF mRNA expression in the rodent brain (Liu et al., 2006, Le Foll et al., 2005). The effects of cocaine on the expression of human BDNF transcripts was therefore addressed using a

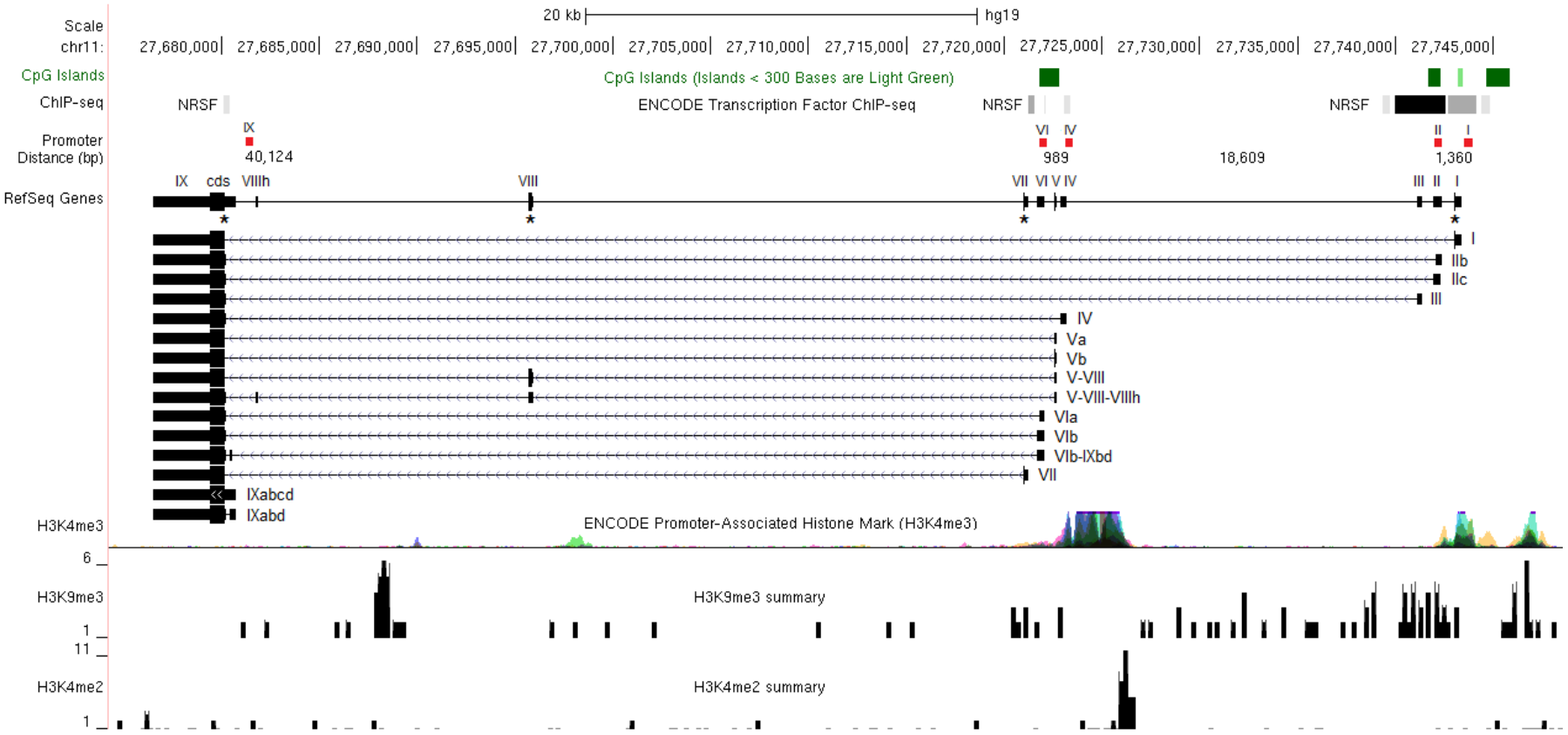


**Figure 3.6. BDNF gene locus.** Schematic representation of human BDNF gene structure and its alternative splice variants according to Pruunsild et al. (2007). Black boxes represent exons; connecting lines introns, with arrow heads representing the direction of transcription. Coding sequence (cds) is marked by thicker black boxes and * mark in-frame ATG codons that could be used as alternative start sites for translation. Green boxes represent CpG islands; red boxes promoter sequences analysed in our ChIP assays with numbers below stating the distance in bp between neighbouring promoter sequences. Grey boxes represent NRSF binding from ENCODE ChIP-seq data; the darkness of the box is proportional to the maximum signal intensity for NRSF binding observed in any of the cell lines tested. H3K4me3 (ENCODE), H3K9me3 and H3K4me2 (Barski et al., 2007) histone methylation signals are displayed as peaks corresponding to signal intensity. Image generated to scale using the UCSC Genome Browser (http://genome.ucsc.edu/index.html).

cell line model as described in *section 2.2.3.*4. Cells were subjected to 24 hour serum-starvation prior to drug treatment to promote cell-synchronisation (Zetterberg and Skold, 1969, Kramer et al., 2010). Therefore drug vehicle control conditions (sterile-filtered d.$H_2O$) also reflect changes in serum concentration. Drug treatments were performed at a final concentration of 10 μM cocaine in accordance with previous studies in the lab (Vasiliou et al., 2012). To obtain signatures relating to the direct mechanisms of drug action, relatively short time-points of 1 and 4 hours for drug treatments were used, with a subset also profiled at 24 hours for comparison. RT-qPCR analysis (see *section 2.2.5.7*) showed BDNF II, which was undetectable under control conditions at 1 hour and under all conditions tested at 4 and 24 hours, to be induced following 1 hour cocaine treatment, **Figure 3.7B**. BDNF IX was also significantly up-regulated in treated cells versus controls following 1 hour exposure to cocaine (fold change, 12.84; SD, 0.70; ***P<0.001), **Figure 3.7C**. Transcripts IV and VI were not significantly affected by cocaine treatment at 1 hour. At 4 hours post-treatment transcripts IV, VI and IX were significantly up-regulated 8.11- (SD, 0.95; **P<0.01), 9.09- (SD, 0.92; *P<0.05) and 3.53-fold (SD, 0.35; *P<0.05), respectively (**Figure 3.7C**). Up-regulation of BDNF IV following 4 hour treatment with cocaine is consistent with *in vivo* expression of this conserved transcript in the rodent brain in response to acute cocaine administration at this time-point (Liu et al., 2006). Conversely, prolonged exposure of SH-SY5Y cells to cocaine resulted in down-regulation of BDNF IV (fold change, 4.57; SD 0.46; ***P<0.001), which supports previous findings in human neuroblastoma cells showing reduced expression of total BDNF mRNA at 24 hours post-treatment (Feng et al., 2006). BDNF VI and IX were unaffected at 24 hours cocaine exposure relative to untreated cells, **Figure 3.7C**.

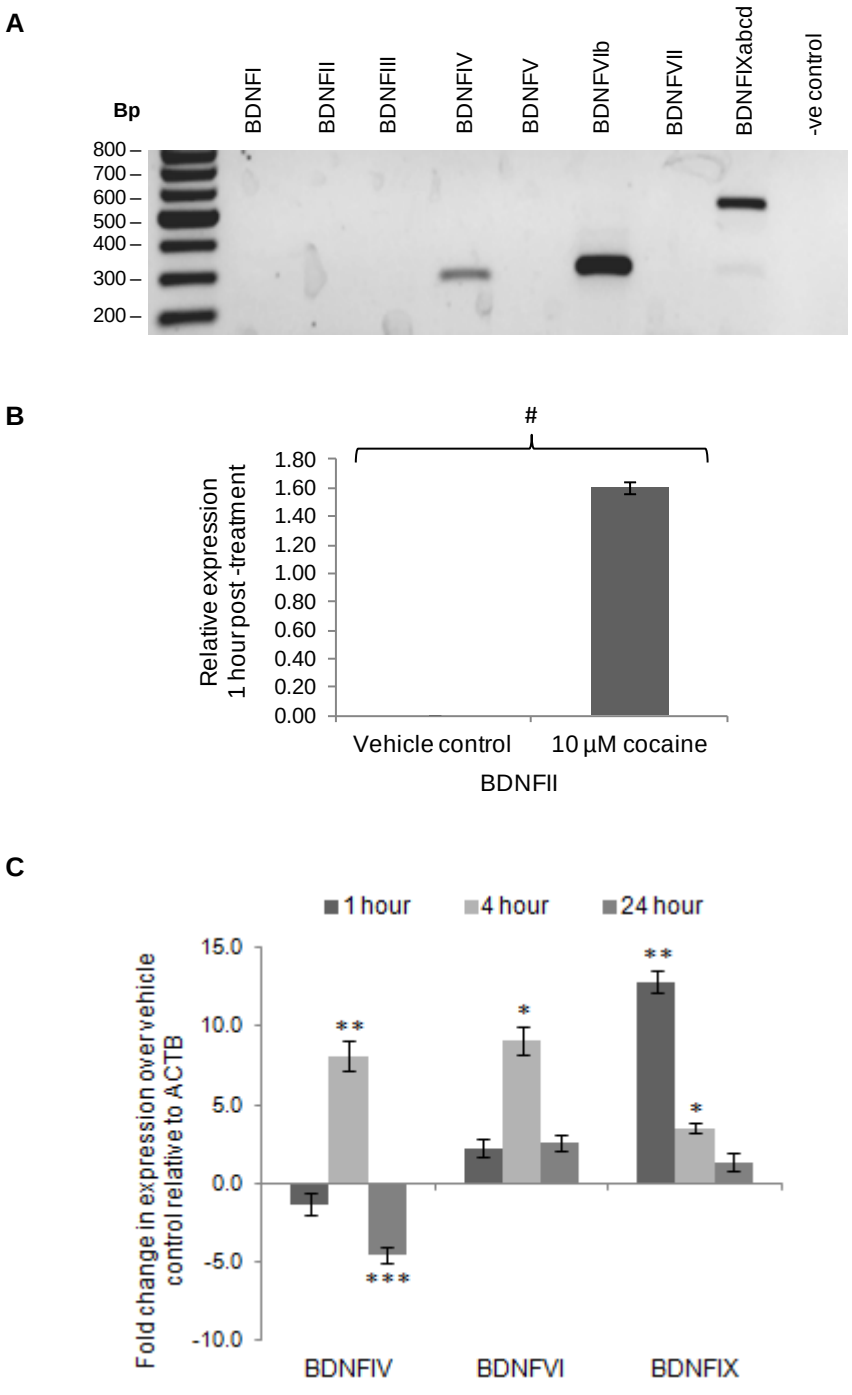


**Figure 3.7. Characterisation of BDNF mRNA expression in human-derived SH-SY5Y neuroblastoma cells following cocaine treatment. A**, PCR analysis of BDNF mRNAs under basal conditions. SH-SY5Y cells express BDNF transcripts II (*see* **B**), IV, VI and IX. **B**, BDNFII was undetectable under vehicle control conditions at 1 hour but was induced by cocaine. Expression is displayed as fold change relative to ACTB. **C**, Expression profiling of BDNF transcripts following treatment with 10 µM cocaine at 1, 4 and 24 hours. Bars represent the average fold change in BDNF expression of treated cells versus control cells analysed using the Delta-Delta Ct method. Each sample was measured in triplicate and normalised to ACTB expression. RT-qPCR data is representative of 3 biological replicates. Error bars represent the SD for relative fold change between experimental replicates. Significant changes in expression between treated and control cells were determined using a two-tailed student *t*-test. * P<0.05, ** P<0.01, *** P<0.001.

### 3.8.2 Cocaine induces co-ordinate and differential regulation of distinct BDNF promoter regions by NRSF

NRSF has previously been shown to regulate rodent BDNF promoter I, II and VI activity-dependent gene transcription (Tabuchi et al., 2002b, Tabuchi et al., 1999, Tian et al., 2009, Timmusk et al., 1999, Abuhatzira et al., 2007, Palm et al., 1998, Hara et al., 2009). To explore NRSF-mediated regulation of the human BDNF gene locus, NRSF occupancy of different BDNF promoters was addressed under control conditions and following drug challenge with cocaine; a known modulator of NRSF (Chandrasekar and Dreyer, 2009) and BDNF expression (Sadri-Vakili et al., 2010, Le Foll et al., 2005, Liu et al., 2006, Graham et al., 2007, Kumar et al., 2005). Potential NRSF binding sites over the human BDNF gene locus were identified using ENCODE ChIP-seq data for transcription factor binding (The ENCODE Project Consortium, 2011) and the rVista portal, a web-based tool for analysing the regulatory potential of evolutionarily conserved regions of non-coding DNA through comparative genomics and transcription factor binding site predictions (Loots and Ovcharenko, 2004). These are represented in **Figure 3.6** and **Table 3.8**. ChIP was carried out in SH-SY5Y cells under control conditions and following 10 μM cocaine treatment at 1, 4 and 24 hours (**Figure 3.8A**) to correlate with gene expression data. The same passage cells were used across all experiments. ChIP was performed using anti-H3, a positive control for immunoprecipitation efficiency across samples; anti-NRSF (H-290-X), raised against the amino-terminal of human NRSF and therefore targets all isoforms; and an IgG control antibody for assessment of non-specific background noise. PCR primers used to address NRSF binding of the different BDNF promoters are detailed in **Table 2.1**. The distance between the promoter

**Table 3.8.** Predicted NRSF regulation of the human BDNF gene

| Transcript | NRSF binding site (NRSE)<br>T AG A CG G<br>TTCAGCACCNNGGACAGCGCC | Position (bp) | Validated NRSF target |
|---|---|---|---|
| BDNF I | T**C**CAG**T**ACCATA**C**AC**GTAAAA**<br>TTCAGAAC**A**CCAGACA**A**C**C**C**T** | -6,111<br>-4,008 | Rat cortical neurons and glial cells, rat brain, human HeLa cervical cancer cell line |
| BDNF IIb | TTCAGCACCTTGGACAG**A**GCC | +103 | Rodent brain, rat cortical neurons and C6 glioma cells, mouse Neuro-2A neuroblastoma cells, human HeLa cervical cancer cell line |
| BDNF III | TTC**TC**CACCGC**CT**CCAGC**C**GC | +363 | - |
| BDNF IV | TTCA**C**CGC**G**GAG**AG**G**GCT**GC**T** | +33 | Whole brain tissue from new born mice |
| BDNF V | T**C**C**T**GCAC**T**ACGGAG**CTT**GC**G** | +69 | - |
| BDNF VIb | **AG**CAGCACCGCG**A**CG**G**G**GA**CC | +243 | - |
| BDNF VII | **G**TCAG**G**ACCCT**C**GACAGC**T**C**T** | -125 | - |
| BDNF IXabcd | ENCODE binding | +850 | - |

*Note:* Gene nomenclature is according to Pruunsild et al. (2007). *Position* is the location of predicted NRSF binding sites (identified using ENCODE ChIP-seq data or the rVista Transfac database) relative to the transcription start site; negative and positive values indicate upstream and downstream positions, respectively. Bold font indicates sequence variation from the canonical NRSE (Wu and Xie, 2006) displayed under the heading *NRSF binding site*. BDNF rs1491850 (A/G) SNP is highlighted grey.

regions tested are outlined in **Figure 3.6**. Sonication of the chromatin samples yielded fragments ranging between 100 - 1,500 bp, see *Appendix 2*. Due to the close proximity of promoters IV and VI, located 989 bp apart, these regions were analysed as a single cluster (termed BDNF promoter IV) as previously described (Baj and Tongiorgi, 2009). MIR137 NRSF binding sites I (chr1:98511689-98512088) and II (chr1:98513921-98514133) located within the MIR137 gene locus were respectively used as a negative and positive control for NRSF binding within SH-SY5Y cells, **Figure 3.8B**. They are located 1,833 bp apart and so act as an internal control for specificity of NRSF enrichment at closely situated binding sites. See *Chapter 4* for further details of NRSF regulation of the MIR137 locus.

Under control conditions at 1 hour treatment, strong signals for NRSF binding were observed at BDNF promoters II, IV and IX. In response to cocaine, binding was lost at promoters II and IV with no effect on promoter IX (**Figure 3.8A**). Typical of NRSF predominantly functioning as a transcriptional repressor, loss of binding at promoter II correlated with induction of BDNF II mRNA expression a 1 hour (**Figure 3.7B**). Furthermore, NRSF occupancy of BDNF promoter II at 4 and 24 hours under control and treatment conditions corresponded with undetectable levels of this transcript by RT-qPCR (data not shown). Loss of binding at promoter IV also correlated with a significant increase in the levels of transcripts IV and VI expressed from this region at the 4 hour time point, whereas increased NRSF signal at 4 hours correlated with significant down-regulation of transcript IV at 24 hours (**Figures 3.7C**), again supporting a role for NRSF in transcriptional repression at this promoter. At 24 hours cocaine treatment, NRSF occupancy of BDNF promoter IV was comparable to control levels suggesting that NRSF modulation of this region (and promoter II) is an

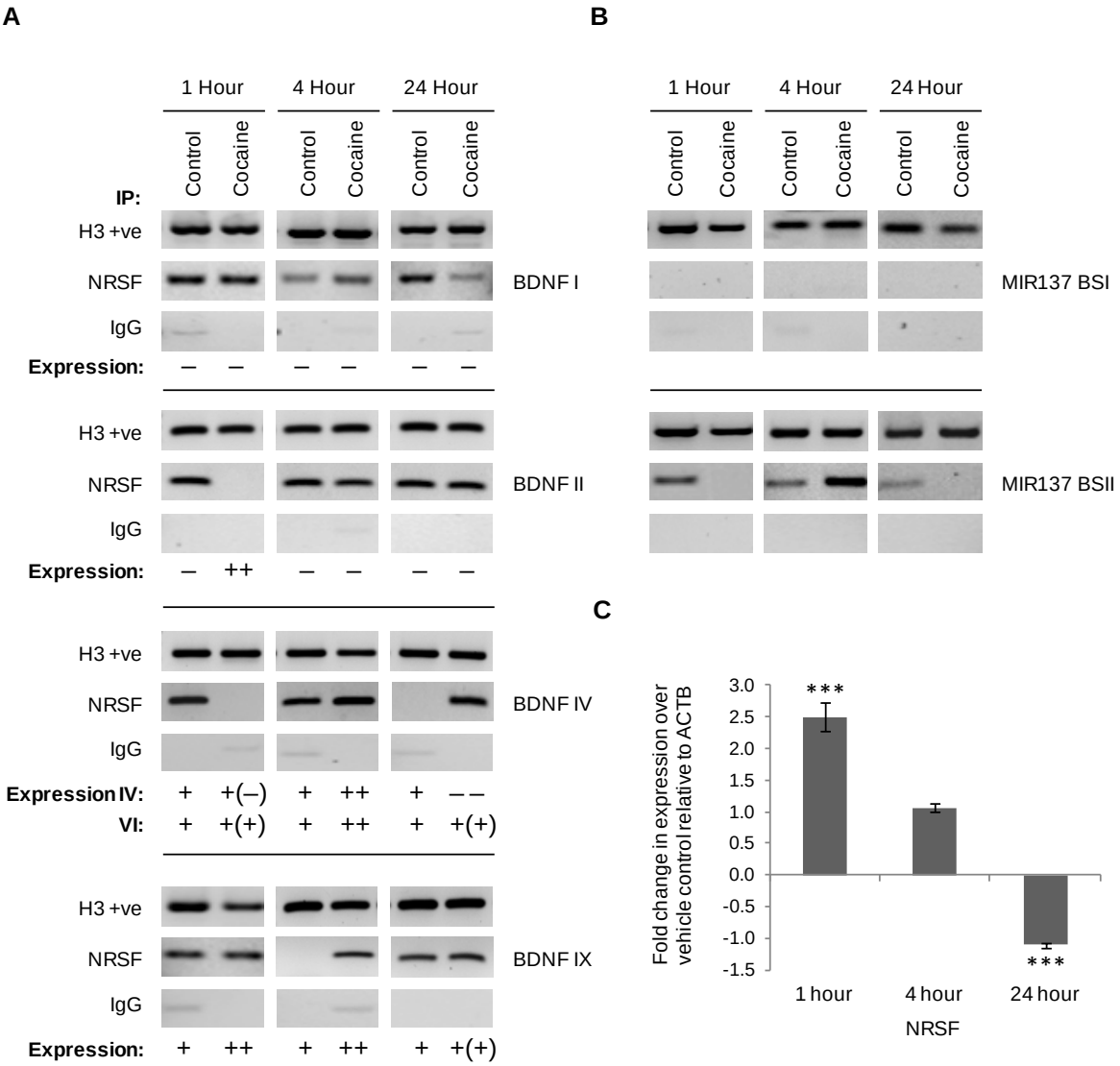


**Figure 3.8. NRSF modulation of BDNF promoters following cocaine treatment in human SH-SY5Y cells. A**, ChIP analysis of NRSF binding to BDNF promoter regions under control conditions and following treatment with 10 μM cocaine for 1, 4 and 24 hours. Histone H3 antibody (H3 +ve) was included as a positive control for the immunoprecipitation (IP) and IgG was included as a control for non-specific background binding. *Expression* is with respect to RT-qPCR data for the corresponding BDNF transcripts (see **Figure 3.7B-C**); - / - - / +(-) / + / +(+) / ++ represents no / reduced (significant) / reduced (non-significant) / basal / increased (non-significant) / increased (significant) expression in treated cells relative to untreated cells. **B**, MIR137 NRSF binding sites (BS) I and II were used as a positive and negative control for NRSF binding. For ChIP assays, n=1. **C**, Expression profiling of NRSF in response to 10 μM cocaine. Bars represent the average fold change in expression of treated cells versus control cells analysed using the Delta-Delta Ct method. Each sample was measured in triplicate and normalised to ACTB expression. RT-qPCR data is representative of 3 biological replicates. Error bars represent the SD for relative fold change between experimental replicates. Significant changes in expression between treated and control cells were determined using a two-tailed student *t*-test. *** P<0.001. Differences in NRSF binding under control conditions likely reflect the effects of serum changes (cells cultured in low serum media 24 hours prior to drug treatments).

early response to cocaine challenge (**Figure 3.8A**). Under all conditions tested, enrichment of NRSF at BDNF promoter I was observed which correlated with undetectable levels of the corresponding transcript originating from this region.

In contrast to promoters I, II and IV, transcript IX was significantly up-regulated in response to cocaine at 1 and 4 hours despite NRSF occupancy of its promoter (**Figure 3.7C**), suggesting that mechanisms other than NRSF are necessary for transcriptional regulation of this transcript in response to cocaine. The NRSF antibody used in this study targets an epitope at the amino-terminal of NRSF and therefore recognises all isoforms of this protein. The presence of NRSF at promoter IX following cocaine treatment might alternatively reflect the action of the truncated variant sNRSF which is thought to exert dominant-negative effects over the full-length protein (Coulson et al., 2000, Shimojo et al., 1999) or function as a transcriptional enhancer (Spencer et al., 2006, Gillies et al., 2009). REST4, the rodent analogue of human sNRSF, has previously been shown to modulate BDNF expression. Tabuchi et al. (2002b) demonstrated that over-expression of REST4 increased the basal transcription of a reporter gene construct containing a duplicated NRSE upstream of BDNF promoter I in rat primary cortical neurons, supporting its proposed role as a transcriptional enhancer. They further showed that co-expression of REST4 with NRSF resulted in a competitive interaction between the two isoforms which supported a dominant-negative effect of the truncated variant over the full-length protein allowing for BDNF promoter I directed gene activation. A similar mechanism may be operating at the human BDNF IX promoter in response to cocaine whereby the repressive effect of NRSF is inhibited by sNRSF, or sNRSF mediates transcriptional activation, resulting in up-regulation of the corresponding

transcript. The potential role of sNRSF can only be speculated in this model as there is no commercial antibody available to specifically target this isoform.

To check whether NRSF binding of the BDNF gene locus correlated with its cellular expression, we quantified NRSF mRNA levels across the different treatment conditions (**Figure 3.8C**). NRSF was up-regulated in response to cocaine at 1 and 4 hours, however this was only significant for the earlier time-point (fold change, 2.51; SD, 0.23; ***P<0.001). Increased NRSF expression coincided with increased binding at BDNF promoter IV at the 4 hour time point and significant down-regulation of transcript IV at 24 hours post-treatment. At 24 hours, NRSF was down-regulated 1.1 fold relative to basal expression (SD, 0.04; ***P<0.001). Expression of sNRSF was also addressed by RT-PCR however no signal was detected under all of the conditions tested (data not shown). The cellular levels of sNRSF are extremely low relative to the full-length protein (approximately 1% of total NRSF) (Palm et al., 1998) and its up-regulation in response to neuronal activation is often transient (Spencer et al., 2006) making it difficult to address the endogenous function of this isoform. Undetectable levels of sNRSF mRNA in this experiment may reflect differences in cell passage number as its expression can be detected under normal culture conditions in the SH-SY5Y cell line (see *Appendix 3*). Nevertheless, the data presented here points to a dual role for NRSF in the modulation of human BDNF gene expression in response to cocaine in both a promoter- and time-dependent manner; acting as a transcriptional repressor of transcripts initiating from BDNF II and IV and a potential activator of BDNF IX which may involve differential isoform usage.

### 3.8.3 BDNF promoters can be grouped into distinct clusters dependent upon their epigenetic status in response to cocaine

Analysis of transcriptional regulation of the human BDNF gene in response to cocaine challenge indicated time-dependent and promoter-specific modulation by NRSF. Distinct promoter clustering of the BDNF gene has previously been reported in SH-SY5Y cells in response to cytotoxic stress (Baj and Tongiorgi, 2009) and likely reflects the molecular architecture surrounding the promoter. To further investigate the transcriptional mechanisms operating at these distinct promoter clusters, we investigated the relationship between histone modification patterns, NRSF binding and BDNF expression in cocaine treated and untreated SH-SY5Y cells. Specifically, we addressed trimethylation of histone 3 lysine 9 (H3K9me3); a repressive histone mark associated with NRSF occupancy of canonical (21 bp consensus sequence) and non-canonical (left and right half sites separated by 0 or 3-9 bp) NRSEs in the human genome (Zheng et al., 2009), and dimethylation of histone 3 lysine 4 (H3K4me2); an active histone mark enriched at, or in close proximity to, the transcription start site (TSS) of active gene promoters (Koch et al., 2007) and that has been shown to be significantly depleted at NRSEs occupied by NRSF relative to unbound NRSEs (Zheng et al., 2009). As predicted, signals for H3K9me3 and absence of H3K4me2, particularly at promoter II in the presence of NRSF occupancy, correlated with transcriptional silencing (promoter II at 1 hour) or repression as determined by gene expression profiling. Moreover, H3K4me2 signals were enriched at the transcriptionally permissive promoter IX across all treatment conditions tested. In addition, contradictory H3K4me2/H3K9me3 signals were observed at all promoters tested and correlated with basal or increased transcription levels

(**Figure 3.9**). The epigenetic profile of promoter IV was more variable which may be the result of contaminating signals from promoters (V-VII) located in close proximity (see **Figure 3.6**). Other histone modifications have been associated with modulation of this promoter region including histone acetylation (Sadri-Vakili et al., 2010, Bredy et al., 2007). DNA methylation may also be important due to the presence of an overlapping CpG island (**Figure 3.6**), which is supported by known regulation of this promoter by the methyl CpG binding protein MeCP2 (Abuhatzira et al., 2007, Sadri-Vakili et al., 2010). Variation in histone methylation patterns across control conditions for all promoters tested likely reflects the effects of serum starvation which has previously been shown to affect H3K9me3 and H3K4me2 signals at other gene promoters which encode for trophic fators, such as insulin-like growth factor 1 (Sanchez et al., 2009).

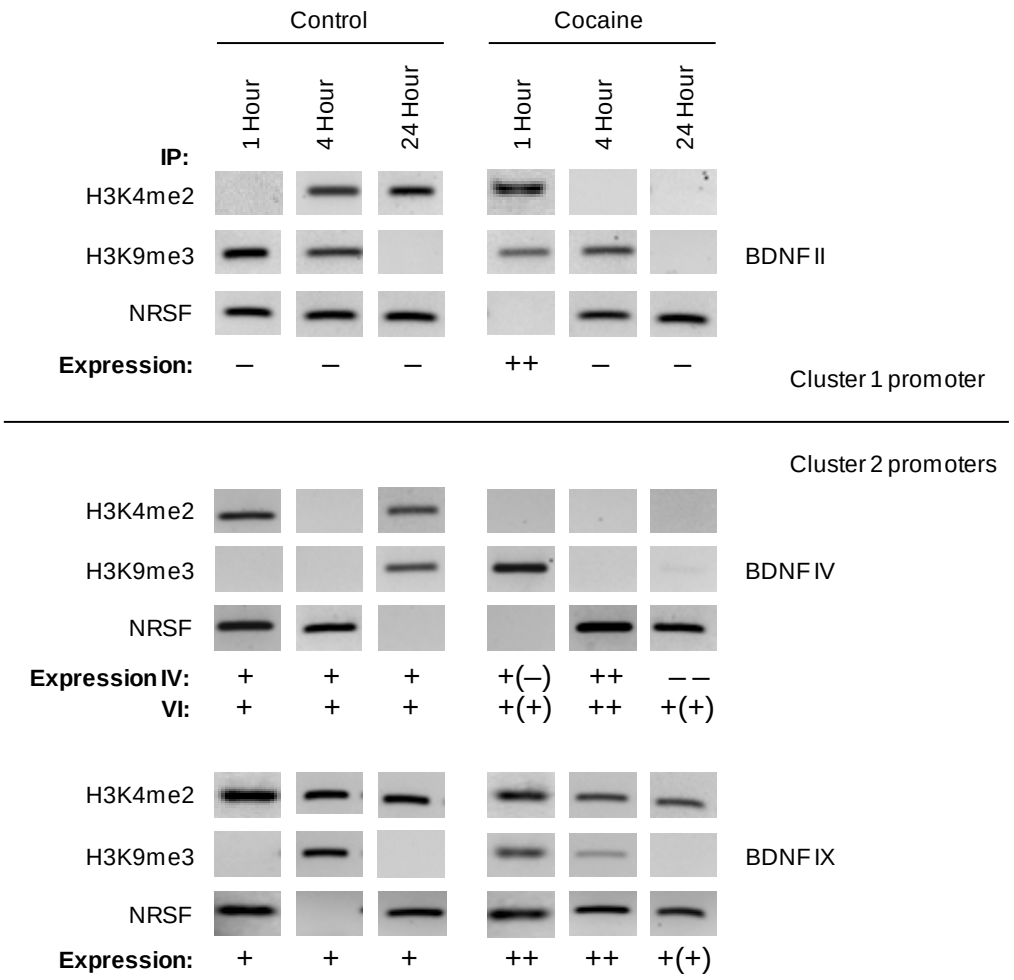


**Figure 3.9. Histone methylation of BDNF promoters in response to cocaine treatment in SH-SY5Y cells.** ChIP analysis of active (dimethylation of histone 3 lysine 4, H3K4me2) and repressive (trimethylation of histone 3 lysine 9, H3K9me3) histone marks at BDNF promoters II (cluster 1 promoter), IV and IX (cluster 2 promoters) under control conditions and following 10 μM cocaine treatment at 1, 4 and 24 hours. Expression is with respect to RT-qPCR data for the corresponding BDNF transcripts (*see* **Figure 3.7B-C**); - / - - / +(-) / + / +(+) / ++ represents no / reduced (significant) / reduced (non-significant) / basal / increased (non-significant) / increased (significant) expression in treated cells relative to untreated cells. Differences in NRSF binding and histone marks under control conditions likely reflect the effects of serum changes (cells cultured in low serum media 24 hours prior to drug treatments).

## 3.9 Discussion

BDNF is an important neurotrophic factor involved in neurogenesis, cell survival and synaptic plasticity (Huang and Reichardt, 2001, Scharfman et al., 2005, Pencea et al., 2001, McAllister et al., 1999, Ghosh et al., 1994). The structure of the BDNF gene is extremely complex, with differential expression from the locus being well documented in response to a variety of stimuli and in disease models. Epigenetic modifications of the BDNF gene are thought to be important in the aetiology of psychiatric disorders, such as schizophrenia and mood disorders. Support for this comes from human studies which have correlated increased BDNF promoter methylation with reduced circulating BDNF levels in patients diagnosed with bipolar disorder (D'Addario et al., 2012), major depression (D'Addario et al., 2013) and schizophrenia (Kordi-Tamandani et al., 2012). Post-mortem studies have also shown an inverse correlation between cortical BDNF expression and promoter DNA methylation in normal ageing (Keleshian et al., 2013) and in Alzheimer's disease (Rao et al., 2012). NRSF is an important mediator of epigenetic parameters through its interaction with a complex of co-repressor proteins resulting in chromatin remodelling at its target sequence. Disruption of this regulatory network has been associated with aberrant BDNF expression in a variety of disease models (Abuhatzira et al., 2007, Zuccato et al., 2003, Spencer et al., 2006). Furthermore, the overlapping role of NRSF and BDNF in several neuropsychiatric conditions suggests that inappropriate regulation of these two candidate genes along a common regulatory network may be important in defining neurological dysfunction.

To investigate this, we explored the effects of cocaine treatment on NRSF-mediated regulation of the BDNF gene locus in human SH-SY5Y cells. Cocaine was used in this study as it has previously been shown to modulate the expression of both of these genes *in vitro*, with a recent study linking NRSF-signalling as an important regulatory mechanism in the fine-tuning of BDNF expression in response to this drug (Chandrasekar and Dreyer, 2009). Cocaine therefore permitted manipulation of the endogenous expression of these genes for *in vitro* analysis of the NRSF-BDNF signalling pathway in response to cellular challenge. Gene expression and ChIP analysis pointed to a role for NRSF as both a transcriptional repressor and activator of the BDNF gene in a promoter-dependent fashion. Moreover, this dual function appeared to be co-ordinated at distinct promoter clusters. Typical of Class I NRSF target genes which are maximally expressed by default upon loss of NRSF binding of their promoters during neuron differentiation (Ballas et al., 2005), enrichment of NRSF at promoters I and II (cluster 1 promoters) correlated with silencing of the corresponding transcripts with expression of BDNF II observed following NRSF dissociation from its promoter. SH-SY5Y cells are immature neuroblasts that maintain stem cell characteristics, which is in fitting with NRSF-mediated repression of neuronal gene expression in neural progenitor cells. The repressive function of NRSF at BDNF promoters I and II is in agreement with previous studies in both human HeLa cervical cancer cells, rat glial cells and exogenous NRSF expression in rat cortical neurons (Palm et al., 1998, Timmusk et al., 1999, Abuhatzira et al., 2007, Hara et al., 2009, Tabuchi et al., 1999). Distinct from BDNF cluster 1 promoters, NRSF occupancy of BDNF promoters IV and IX (cluster 2 promoters) under control conditions correlated with basal

expression of the corresponding mRNAs. Similar to the NRSF 'Class I' promoters, loss of NRSF binding at promoter VI coincided with significant up-regulation of transcripts IV and VI encoded from the region but this was only detected at the 4 hour time point. NRSF may play a role in maintaining the basal levels of these transcripts as their expression was observed under control conditions even in the presence of NRSF promoter occupancy. BDNF has previously been categorised as a Class II NRSF target gene, defined as those that are not maximally expressed upon NRSF dissociation from their promoters due to the presence of the co-repressors CoREST and MECP2 at methyl CpG sites within the regulatory sequence. Increased expression of Class II neuronal genes following dissociation of the NRSF/co-repressor complex from the NRSE site also requires the loss of MeCP2, mSin3 and HDAC (Ballas et al., 2005), a regulatory mechanism which allows for the fine tuning of neuronal gene expression in response to specific stimuli. The role of NRSF at the most distal promoter IX is more complex and representative of the dynamic regulatory mechanisms associated with this epigenetic modulator. NRSF occupancy of promoter IX correlated with basal expression of this transcript under control conditions and significant up-regulation following cocaine challenge, suggesting that transcriptional mechanisms additional to, and distinct from, the well characterised repressive function of NRSF are responsible for the regulation of this promoter.

Several studies have indicated that both sequence variation within NRSEs and the promoter architecture within which they are located may dictate the regulatory function of these domains upon NRSF binding. Tabuchi et al. (1999) demonstrated that introducing two point-mutations into the NRSE located

within promoter I of the rat BDNF gene resulted in the partial de-repression of this promoter in glial cells, whilst Bessis et al. (1997) showed that NRSEs located within 50 bp upstream or 50-250 bp downstream of a synthetic promoter could direct transcriptional activation of reporter gene constructs in rodent neuroblastoma but not fibroblast cells. *In silico* analysis of potential NRSEs located within the human BDNF gene locus through comparative sequence analysis of conserved TFBS identified several NRSEs within close proximity to BDNF IV and VI (**Table 3.8**). Two of these elements were located 33 bp and 243 bp downstream of the TSS of the respective transcripts IV and VI, and displayed greater sequence variation than those proximal to promoters I and II which showed high sequence homology to that of canonical NRSEs, **Table 3.8**. A computational study addressing the potential functional significance of sequence variation within the NRSE through precise mapping of NRSF binding sites using short sequence reads generated from ENCODE ChIP-Seq data, showed that residues 7-21 (in particular 7–9 and 12–17) were important for DNA binding whereas residues 1-6 were identified as being important for binding stability (Jothi et al., 2008). This observation is supported by the action of NRSF at tandem NRSEs within the CACNA1A gene in which those sites with high sequence identity to that of the canonical NRSE (determined by PWM scores), particularly within the first 6 bp, showed higher binding affinities and enrichment for NRSF relative to other functional NRSEs within the gene with lower PWM scores, determined through electrophoretic mobility shift assays and ChIP (Johnson et al., 2006). The biological relevance of tandem NRSE clusters of different sequence composition within NRSF-target genes may reflect their ability to differentially recruit NRSF at varying concentrations of

this transcription factor within the cell, which may dictate the action of NRSF as either a transcriptional repressor or enhancer. This would be consistent with our observation of the differential action of NRSF at the distinct BDNF promoter clusters in response to cocaine, such as repression of BDNF promoters I and II which both share high sequence homology with the classical NRSE originally defined as a repressor element (Chong et al., 1995, Schoenherr and Anderson, 1995, Mori et al., 1992).

Alternative NRSF isoforms may also be important in modulating the activity of the BDNF gene as suggested from their differential roles in regulating neuropeptide gene expression. The truncated variant sNRSF, or REST4 in rodents, which is specifically expressed in neurons or certain cancers (Palm et al., 1998, Coulson et al., 2000, Wagoner et al., 2010), is believed to function as a gene enhancer or exert dominant-negative effects over the full-length protein (Coulson et al., 2000, Spencer et al., 2006, Shimojo et al., 1999, Tabuchi et al., 2002b, Gillies et al., 2009). This was demonstrated in rat cortical neurons were over-expression of REST4 resulted in increased basal activation of a reporter gene construct containing a duplicated NRSE within BDNF promoter I, supporting its role as transcriptional activator (Tabuchi et al., 2002b). However, the same study showed that over-expression of REST4 alone or in combination with full-length NRSF resulted in repression of this promoter region following neural activation with KCl. This effect was weak in relation to the repressive potential of the full-length protein alone suggesting that the truncated variant acts to competitively inhibit the action of NRSF. The ChIP antibody used in this study targets all isoforms of NRSF therefore the action of NRSF at promoter IX could reflect sNRSF however this could not be specifically addressed as there is

no commercial antibody available for specifically targeting the truncated variant. RT-PCR analysis was unable to detect sNRSF which is known to be expressed at extremely low levels within the cell and only transiently up-regulated in response to neuronal activation (Spencer et al., 2006, Palm et al., 1998). Gene expression profiling can only offer a snapshot of the transcriptional response to cellular challenge therefore it is plausible that any potential spikes in sNRSF activity may have been missed under the time course used in this experiment and cannot be ruled out as a potential regulatory mechanism operating at the BDNF gene locus.

Although our data clearly supports a dual role for NRSF in modulating the transcriptional activity of BDNF in response to cocaine challenge, the exact mechanism of action is yet to be elucidated and likely reflects the molecular architecture surrounding the promoter in both a genetic- and context-specific manner. NRSF has been shown to interact with many factors implicated in epigenetic regulation of gene expression through its cofactor CoREST, including the histone H3K4 and H3K9 demethylase LSD1*, the methyltransferase G9a, the* SWI/SNF ATP-dependent nucleosome-remodelling factor BRG1/SMARCA4 and MeCP2 (Lee et al., 2005, Lunyak et al., 2002, Roopra et al., 2004, Battaglioli et al., 2002, Ooi et al., 2006). To investigate potential chromatin remodelling events associated with NRSF-signalling at the different BDNF promoters upon occupancy or dissociation of this transcription factor, we performed ChIP using histone markers of active and inactive chromatin states. As expected, the active H3K4me2 mark was concomitant with transcriptional activation in response to cellular challenge whereas promoters undergoing transcriptional repression were marked by H3K9me3. Previous studies addressing epigenetic regulation

of the BDNF gene following cocaine challenge reported increased histone acetylation of BDNF promoters II and IV which correlated with transcriptional activation (Sadri-Vakili et al., 2010, Bredy et al., 2007, Kumar et al., 2005). We observed up-regulation of BDNF II at 1 hour cocaine treatment which coincided with H3K4me2 signals at the corresponding promoter region but at longer exposure times transcriptional repression was observed which associated with loss of this active chromatin mark. BDNF IV was up-regulated at 4 hours cocaine treatment but reduced at 24 hours. A previous study in neuroblastoma cells reported reduced BDNF expression following 24 hours exposure to cocaine through inhibition of CREB (Feng et al., 2006). NRSF occupancy of target gene promoters can mediate transcriptional repression through antagonising transcriptional activators such as CREB; a known regulator of BDNF promoter I and IV expression (Tabuchi et al., 2002a, Sadri-Vakili et al., 2010, Pruunsild et al., 2011). This is exemplified through its action at the NRSE-containing CART (Cocaine- and amphetamine-regulated transcript) promoter, resulting in transcriptional repression through blockade of CREB signalling (Zhang et al., 2012a). A similar mechanism may be operating in our cell-line model at BDNF promoter I, whereby saturation of NRSF correlated with silencing of this transcript under all conditions tested. Enrichment of the two contradictory histone markers, H3K4me2/H3K9me3, across different conditions at all promoters tested were also observed which correlated with either basal levels of transcription or activation in response to cocaine. This bivalent H3 modification has previously been associated with the TSS of several genes within human ovarian cancer cells and was reported to be a marker of epigenetic plasticity, reflecting transcriptional flexibility for context-specific

phenotypic variation within tumour microenvironments (Bapat et al., 2014). Other bivalent histone modifications such as the well characterised H3K4me2/H3K27me3 mark have been associated with 'transcriptional readiness' of developmental genes in embryonic and tissue-specific stem cells, allowing for activation or repression of genes involved in lineage-specific differentiation (Bernstein et al., 2006). Association of this bivalent modification at the BDNF gene locus in response to cocaine challenge may be reflective of cocaine-induced plasticity over the region which has been linked to the medium- to long-term alterations in behaviour following drug exposure (Kumar et al., 2005).

## 3.10 Summary

In summary, the different BDNF promoters could be characterised by their distinct epigenetic signatures which were shown to be dynamically modulated in response to cocaine. These signatures extended to neighbouring promoters suggesting that clustering of closely related transcripts was in operation in response to cellular challenge. This is in line with previous studies in SH-SY5Y which showed that distal promoters forming clusters 1 (promoters I-III) and 2 (IV-VII) are differentially regulated in response to cytotoxic stress (Baj and Tongiorgi, 2009). The distinct mechanisms of NRSF action at different BNDF promoters could be one mechanism regulating plasticity over the gene locus in response to cocaine challenge, suggesting that the BDNF transcripts function in different cellular roles in response to this drug. Although we did not address the functional significance of differential BDNF transcript levels within the cell, co-ordinate and differential regulation of multiple BDNF promoters in part by

NRSF-signalling may be important in the sub-cellular localisation of distinct mRNAs encoded from the locus which are believed to play distinct roles in neural plasticity and compensatory neuroadaptations to cellular challenge.

# Chapter 4

## Characterisation of a NRSF Regulated Internal Promoter in the Schizophrenia Genome-Wide Associated Gene MIR137

## 4.1 Introduction

The role of genetic variants in the pathophysiology of schizophrenia has been well documented (The International Schizophrenia Consortium, 2008, Walsh et al., 2008, Xu et al., 2008, Stefansson et al., 2008, The International Schizophrenia Consortium, 2009, Sebat et al., 2009, Kirov et al., 2009, Shi et al., 2009, Rujescu et al., 2009, Stefansson et al., 2009, The Schizophrenia Psychiatric GWAS Consortium, 2011, Van Den Bossche et al., 2012, Xu et al., 2013). Genetic variants within miRNA genes or their binding sites within target mRNAs may potentiate aberrations in the fine-tuning of complex regulatory networks causing cellular dysfunction which may manifest as a neuropsychiatric phenotype (Rossi et al., 2014). Genome-wide association studies have identified the MIR137 gene locus to be strongly associated with schizophrenia (The Schizophrenia Psychiatric GWAS Consortium, 2011, Ripke et al., 2013). MIR137 encodes for miR-137 which functions in neurodevelopment, adult neurogenesis (Smrt et al., 2010, Szulwach et al., 2010) and is a validated regulator of GWAS candidate genes for schizophrenia, including CACNA1C, CSMD1, C10orf26, TCF4 and ZNF804A (The Schizophrenia Psychiatric GWAS Consortium, 2011, Kim et al., 2012, Kwon et al., 2013), suggesting that impairments in the regulation and/or function of miR-137 may be a key mechanism in neuropsychiatric disease.

Bioinformatic analysis of the MIR137 locus predicted an internal promoter adjacent to the miR-137 sequence (**Figure 4.1**). This promoter encompassed a VNTR, which has previously been shown to modulate the processing and function of miR-137 in melanoma cell lines (Bemis et al., 2008). Down-regulation of miR-137 has been implicated in a number of cancers as

discussed in *Chapter 6* which explores a potential role for miR-137 dysregulation in breast cancer. Polymorphic domains, found in both coding and non-coding regions of the genome, have been implicated in the pathogenesis of several neurological disorders. It was postulated that there may be transcriptional properties associated with the MIR137 VNTR as repetitive DNA can act as transcriptional regulators in both a tissue-specific and stimulus-inducible manner (Fiskerstrand et al., 1999, MacKenzie and Quinn, 1999, Lovejoy et al., 2003, Klenova et al., 2004, Guindalini et al., 2006, Haddley et al., 2008, Ali et al., 2010, Vasiliou et al., 2012, Paredes et al., 2013). As such, these regulatory domains have been identified as clinical correlates of psychiatric conditions, including schizophrenia (Liu et al., 1999, Prata et al., 2009). The functional significance of these polymorphisms is likely to be reflected through gene-environment interplay (GxE), with VNTR genotype acting mechanistically to influence disease phenotype. This could result in modification of gene-expression in a tissue-specific pattern or in response to a particular environmental challenge, which may be differential dependent on VNTR copy number and/or the presence of single nucleotide polymorphisms (SNPs) within the VNTR sequence (Strazisar et al., 2014); modulation of post-transcriptional processing; or both.

Haplotype analysis of the MIR137 gene locus using genotype data from the HapMap CEU cohort showed that the MIR137 GWAS SNPs for schizophrenia were not in linkage disequilibrium (LD) with the MIR137 VNTR but that the rs1625579 GWAS SNP did tag another SNP (rs2660304) within the proposed internal MIR137 promoter. This SNP has previously been associated with smoking-related cancers (Roy et al., 2014a, Roy et al., 2014b). The global

prevalence of smoking in patients with schizophrenia is two- to four-fold that of the general population (Kumari and Postma, 2005) suggesting there may be a genetic link between increased smoking rates and schizophrenia. A GxE interaction using smoking as an environmental pathogen was therefore addressed in a large schizophrenia and matched control cohort.

ENCODE ChIP-Seq data (Release 2, May 2012) indicated that NRSF was binding at the internal promoter. NRSF has been implicated in several neurological diseases, including schizophrenia through modulation of associated signal transduction pathways (Loe-Mie et al., 2010). NRSF has several isoforms, most notably the truncated isoform sNRSF which has been shown to have distinct functions from the full-length protein and whose expression is often associated with cellular stress or disease progression (Howard et al., 2008, Quinn et al., 2002, Coulson et al., 2000, Palm et al., 1998, Abramovitz et al., 2008, Spencer et al., 2006). The transcriptional mechanisms that may operate at the proposed internal promoter VNTR to regulate cellular levels of miR-137 are addressed in this chapter which could underpin a pathway modulating schizophrenia. It was hypothesised that NRSF and the MIR137 VNTR may act individually or in combination to modulate the expression and function of miR-137 in a cellular model of CNS dysfunction. This hypothesis was tested by 1) addressing allele-specific and stimulus-inducible regulation of the internal MIR137 promoter region, focussing specifically on the transcription factor NRSF and DNA methylation, under control conditions and following cellular challenge and 2) genotyping the MIR137 VNTR for association with schizophrenia in a case-control study cohort.

## 4.2 Aims

- Validate a potential internal promoter VNTR within the MIR137 gene characterised from *in silico* analysis of the locus
- Investigate NRSF regulation over the MIR137 locus predicted from ENCODE data using chromatin immunoprecipitation
- Explore the differential roles of NRSF and its truncated isoform sNRSF in regulating MIR137 expression using over-expression assays
- Explore differential regulation of transcripts originating from the locus in response to drug challenge and correlate with promoter methylation status
- Genotype and linkage disequilibrium analysis of the MIR137 VNTR to determine whether it can be used as a biomarker for predisposition to schizophrenia
- Analysis of GxE interaction using smoking status as an environmental pathogen

## 4.3 Results

### 4.3.1 Bioinformatic analysis of the MIR137 genomic locus

Bioinformatic analysis of the MIR137 gene locus was performed using the UCSC genome browser, hg19 release (Kent et al., 2002, Rosenbloom et al., 2013), as described in *section 2.2.6.8*. MIR137 is located on chromosome 1p22 within the non-protein coding RNA genes MIR137HG (MIR137 host gene)/AK094607 (Bemis et al., 2008) and AK311400 (Suzuki et al., 2011). Within the pri-miRNA-137 sequence there is a 15 bp VNTR, 6 bp upstream of the precursor from which the functional miR-137 is processed (Bemis et al., 2008) (**Figure 4.1A**). Interrogation of ChIP-seq data from ENCODE (The ENCODE Project Consortium, 2011, Rosenbloom et al., 2013) identified both RNA pol II binding, necessary for mRNA transcription, and NRSF binding over the region encompassing the MIR137 VNTR (position, chr1:98511662-98511917). ENCODE data also identified NRSF occupancy within the first intron of MIR137HG (position, chr1:98513800-98514144). The rVista portal, a web-based tool for analysing the regulatory potential of evolutionarily conserved regions of non-coding DNA through comparative genomics and transcription factor binding site predictions (Loots and Ovcharenko, 2004), also supported NRSF binding at the VNTR adjacent to miR-137 (position, chr1:98511764-98511782, Motif ID: V$NRSF_Q4) from the Transfac database (Matys, 2003) and sequence analysis validated the presence of a NRSF binding site (**Figure 4.1B**). Similar to the predicted NRSE located within this identified promoter, our lab has previously shown that NRSF can modulate the expression of neuropeptide genes (AVP, TAC1 and TAC3) and BDNF (as discussed in *Chapter 3*) through binding to NRSE-like motifs located within close proximity to their major

**Figure 4.1. Characterisation of an internal promoter for MIR137. A**, Schematic showing the non-protein coding genes MIR137HG (AK094607), AK311400, and AK309618 as described in the UCSC Genome Browser, Assembly GRCh37/hg19, accessed May 2012. Exons represented as black boxes; introns as connecting lines. The numbers above indicate size in bp, unless stated otherwise. The direction of transcription is indicated by a dashed arrow. MicroRNA (miR)-137 and miR-2682 are denoted by dark grey boxes. A 15-bp variable number tandem repeat (VNTR) immediately upstream of miR-137 is represented as a light grey bar and CpG islands as green boxes. NRSF binding sites identified from ENCODE ChIP-seq data are marked as vertical arrows *i* and *ii. Lower panel,* Transcription factor binding and histone marks over the internal MIR137 promoter from ENCODE V2 data. **B**, Sequence targeted by PCR primers for the internal MIR137 promoter (Imir137). Upper case font indicates exons and lower case font introns. PCR primer sequences are marked by horizontal arrows; the dashed horizontal arrow marks the alternative forward primer targeting the VNTR alone. The first line of sequence not targeted by the PCR primers represents the additional sequence included in the Imir137(4)+A/C constructs containing the rs2660304 SNP. Thick arrows represent the transcription start sites of the AK311400 and AK309618 transcripts, respectively. The VNTR sequence is highlighted grey; the repetitive element is marked with brackets, *n* representing copy-number variation. Sequence variation in the first repeat of the VNTR is highlighted in bold font; known SNPs (dbSNP 142) are highlighted in red font and labelled with their SNP ID. Underlined text indicates miR-137 sequence. Sequence marked with asterisks' represents predicted NRSF binding sites identified using rVista 2.0 (http://rvista.dcode.org/). [Figure presented on opposite page].

**A**

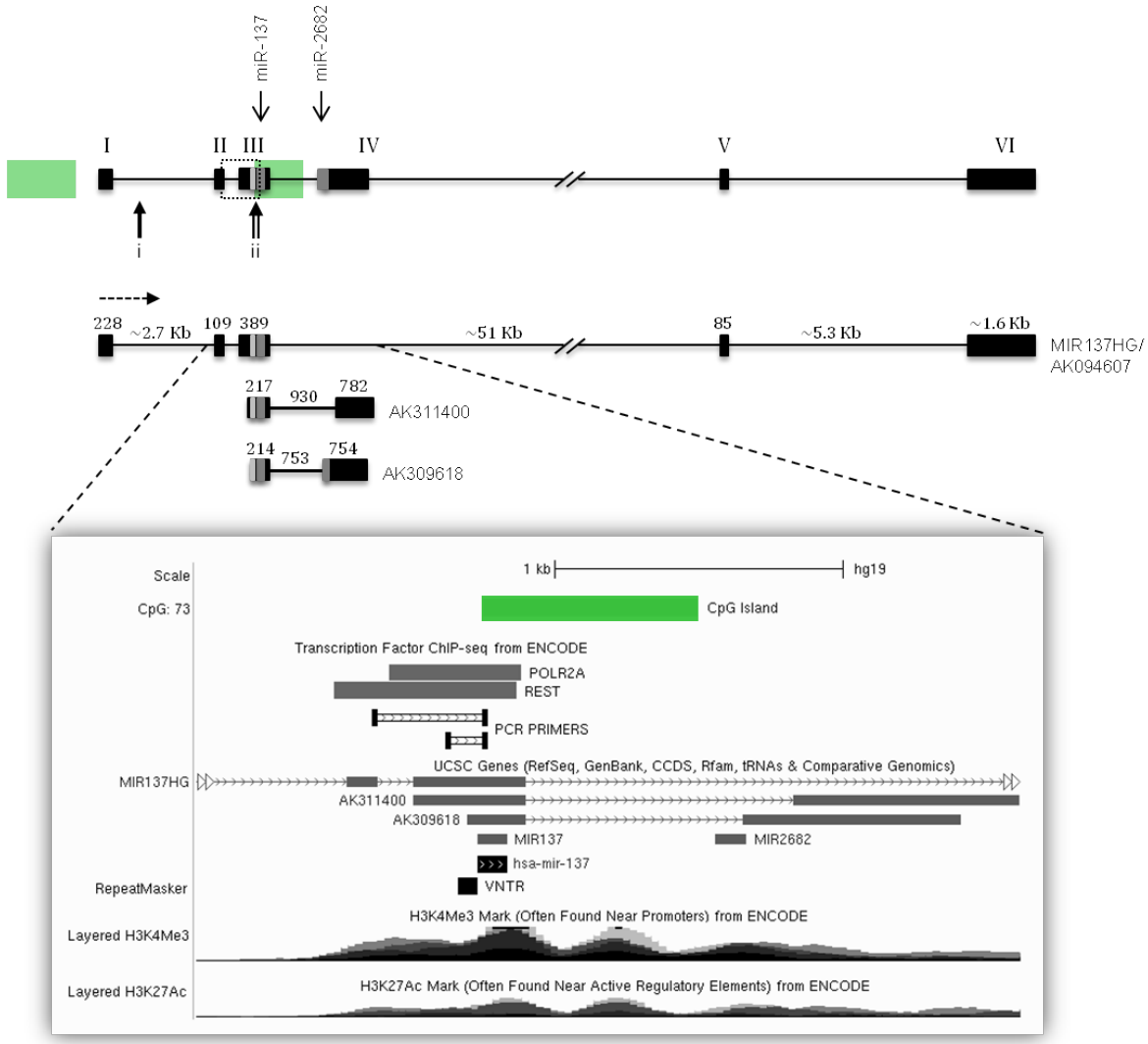


**B**

rs2660304

TCATACCACCTAGAGTGGACTGGCCGAGACCAGACTGGGTACCAAGCAGAGAAGTGCAGAGGAAAGCA

CTGGGAGAGCACCAGgtaaactgaaggttacttgtcactcccacttgtgcccaaaaagccttgccaca

tcttccctcctcactggaaagacagcactcttctgtgttaagtatttgattttgtgatttgtctttca

gAATTGGAAATAGAGCGGCCATTTGGATTTGGGCAGGAAGCAGCCGAGCACAGCTTTGGATCCTTCTT

TAGGGAAATCGAGTTATGGATTTATGGTCCCGGTCAAGCTCAGCCCATCCCCAGGCAGGGGCGGGCTC

AGCGAGCAGCAAGAGTTCTGGTGGCGGCGGCGGCAG[TAGCAGCGGCAGCGG]$_n$CAGCTTGGTCC

TCTGACTCTCTTCGGTGACGGGTATTCTTGGGT

rs552418648 rs188223290 rs75853046 rs185304769

transcriptional start sites (Coulson et al., 1999, Quinn et al., 2002, Spencer et al., 2006, Gillies et al., 2009). The genomic architecture surrounding the MIR137 gene, such as active histone marks and CpG islands identified from UCSC data, suggests there is a promoter in this region which was hypothesised to be important for the regulation of miR-137 expression and the expression of neighbouring transcripts. This is summarised in **Figure 4.1**. This putative internal promoter was termed Imir137.

### 4.3.2 The Imir137 promoter supports reporter gene expression in the SH-SY5Y neuroblastoma cell line

To assess the regulatory function of the putative Imir137 promoter VNTR, both a 4-copy and 12-copy repeat of this polymorphic domain was cloned into the pGL3-Basic (pGL3B) luciferase reporter gene vector which lacks promoter and enhancer sequences (see *section 2.2.2.11*). The constructs included -361/ -481 to +38 bp of the Imir137 promoter using the first base of the pre-miRNA sequence as +1, which incorporated the entire VNTR sequence (**Figure 4.1B**). To determine the direction of promoter activity, this sequence was cloned in both the forward and reverse orientation (**Figure 4.2A**). One previous report demonstrated that the low (3-copy) and high (12-copy) VNTRs differentially affected miR-137 processing *in vitro* (Bemis et al., 2008). The ability of these two variants to modulate transcription was therefore tested. The 4-copy variant was selected over the 3-copy variant in this study as it was the most common allele observed in individuals of European ancestry, determined from genotype analysis of the HapMap CEU cohort and a schizophrenia and matched control cohort. Allele and genotype frequencies for the MIR137 VNTR

in the schizophrenia cohort are detailed in **Table 4.1** and **4.2** of *section 4.3.6*. The difference in the 5' end of these fragments reflected the two distinct VNTRs and were termed Imir137(4) and Imir137(12), respectively. In this *in vitro* system, the ability of Imir137 to act as a promoter was clearly demonstrated, showing a 65.0- or 75.0-fold increase in activation when containing either the 4- or 12-copy repeats, respectively, in the forward orientation (**Figure 4.2B**; ***$p<0.001$ for the average fold difference of luciferase activity supported by both alleles of the MIR137 promoter VNTR over the pGL3B control). Consistent with promoter function in this domain, the reverse orientation had no activity. A small but significant difference was observed when the two alleles were compared with one another suggesting that copy number supports differential regulation (**Figure 4.2B**; ##$p<0.01$ for allelic differences in luciferase activity supported by Imir137).

To determine if any effect was contributed by the VNTR alone, the two variants of this domain including -86 or -206 to +38 bp of the proximal flank sequence (reflecting the 4- and 12-copy repeats) were cloned into the pGL3-Promoter (pGL3P) vector, upstream of the minimal SV40 promoter in forward and reverse orientations (**Figure 4.2A**). These were termed VNTRmir137(4)F or R and VNTRmir137(12)F or R, respectively, to indicate both copy-number and orientation of the fragment. There was very little change in activity directed by the VNTR alone compared with the pGL3P control. Nevertheless, when subjected to Dunnett's one-tailed t-test the 4-copy variant supported a small increase in reporter activity compared with pGL3P (0.2-fold increase) whereas the 12-copy variant repressed activity (~0.2-fold decrease). This resulted in a significant difference in activity when the two VNTRs in the forward orientation

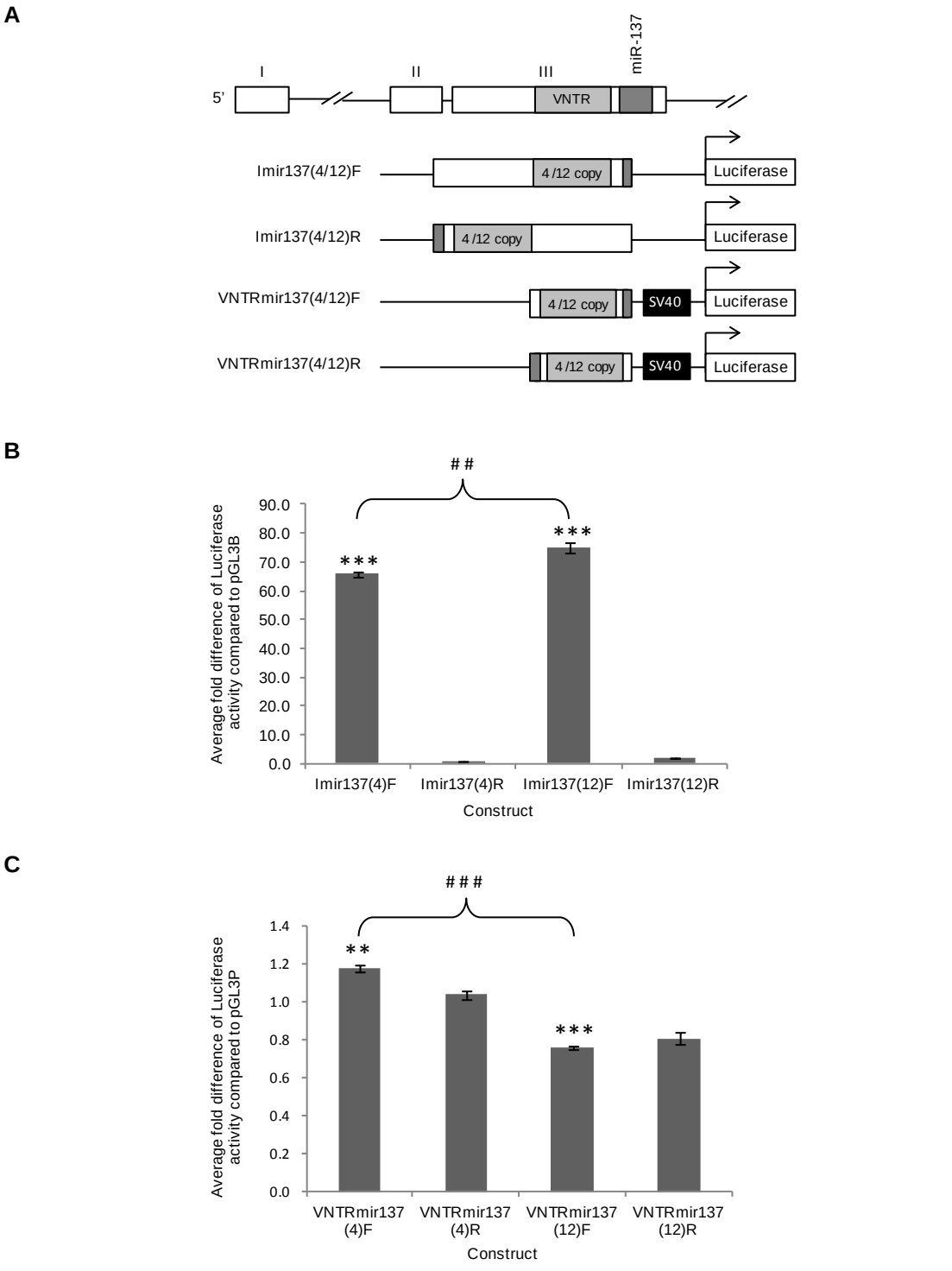


**Figure 4.2. Validation of an internal promoter in the MIR137 gene. A**, Schematic representation of MIR137 constructs aligned to the MIR137 gene showing the 4-copy, Imir137(4), and 12-copy, Imir137(12), variants of the MIR137 VNTR ± the proximal flank region in the pGL3B (Basic) and pGL3P (Promoter) reporter vectors, respectively, in forwards (F) and reverse (R) orientation. **B-C**, Average fold change in luciferase activity supported by the MIR137 constructs over vector controls in SH-SY5Y cells. *N=4.* *Significant changes in luciferase activity over backbone control. #Significant changes in luciferase activity between experimental conditions. */#P<0.05, **/##P<0.01, ***/###P<0.001.

were compared to one another (**Figure 4.2C**; ###p<0.001, allelic differences in luciferase activity supported by the SV40 promoter), however the VNTR does not possess major regulatory properties, such as enhancer or repressor functions, under the conditions and cells tested.

### 4.3.3 NRSF can bind to the Imir137 promoter region and modulate its activity in a stimulus-inducible and allele-dependent manner

Using consensus DNA binding sequence analysis, several potential NRSF binding sites were identified within the MIR137 gene locus. Two of these are predicted from ENCODE data over the locus; one within intron 1 of the MIR137HG gene, which was termed binding site I (BSi), and the other within the Imir137 promoter, termed BSii (**Figure 4.3A-B**). To validate NRSF occupancy of these regions, ChIP assays were performed (see *section 2.2.8.1*) in human SH-SY5Y cells which are homozygous for the 4-copy repeat variant of the MIR137 promoter VNTR. The anti-NRSF (H-290 X) antibody (**Table 2.3**) used in this experiment recognises the amino terminal of NRSF and therefore identifies all known isoforms of this protein. SH-SY5Y cells express both full-length NRSF and the sNRSF isoform. Under control conditions (sterile filtered d.$H_2O$), enrichment for NRSF binding was observed over the Imir137 promoter (BSii) but not at the intronic site of MIR137HG (BSi) (**Figure 4.3C**). It is known that many cocaine-induced plasticity genes, including BDNF as discussed in *Chapter 3*, are regulated by NRSF (Bruce et al., 2004). Cocaine is a psychostimulant that has been used *in vivo* to mimic human psychosis in models of schizophrenia (Pihlgren and Boutros, 2007). It can also be used as a robust signal for modulating NRSF expression *in vitro* as demonstrated in *Chapter 3*. To address

**A**

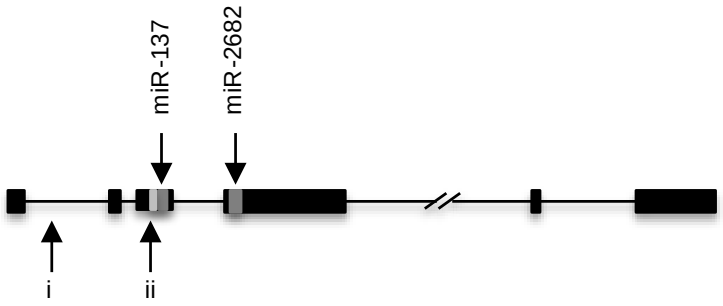


**B**

| | |
|---|---|
| **T CG A CG G** | |
| **TTCAGAACC**NN**GGACAGCGCC** | NRSF consensus sequence |
| G**TCAGAG**GACC**A**AG**C**T**GC**C**GC** | MIR137 VNTR (BS ii) |
| **TT**G**AG**T**GCCA**T**GGCG**GC**CA**G**A | MIR137 +378 bp of VNTR |
| CAG**AGAACC**CT**G**T**A**AGAGACG | MIR137 +395 bp of VNTR |
| **TTCAGAG**AG**A**G**A**AT**C**TCT**G**TG | MIR137 +957 bp of VNTR |
| A**TCAGAA**T**CACAGC**ATAAATA | MIR137 +1,950 bp of VNTR (BS i) |

**C**

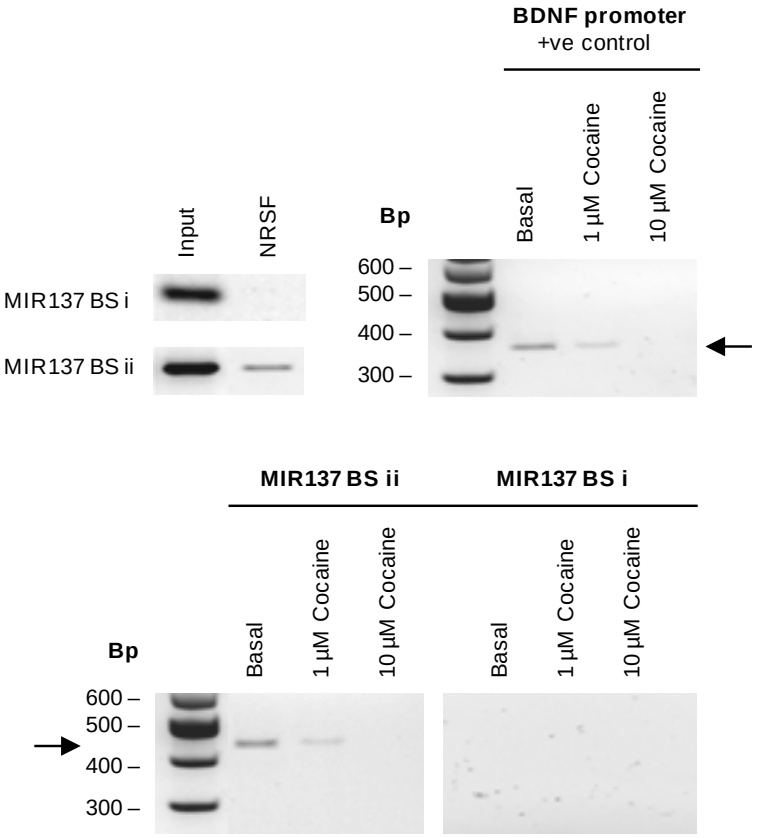

**D**

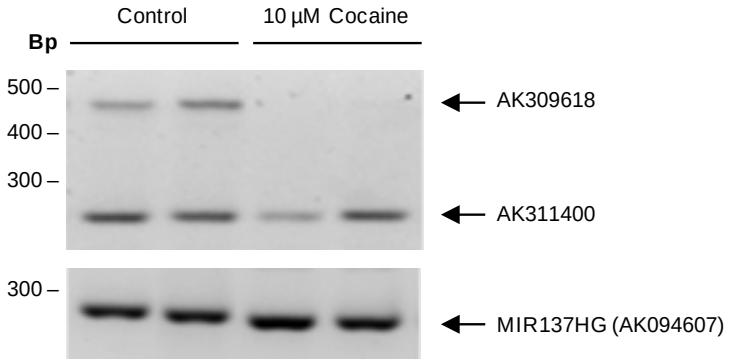


**E**

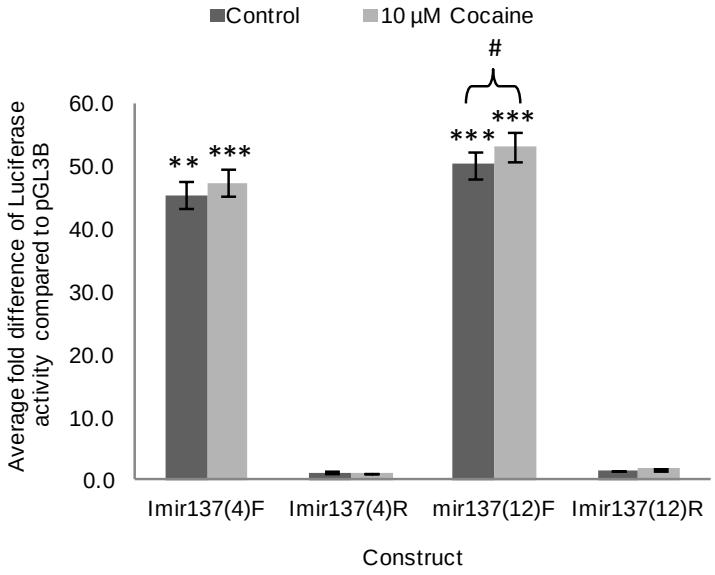


**Figure 4.3. NRSF modulation of the MIR137 internal promoter in SH-SY5Y cells. A**, Predicted NRSF binding sites (BS) across MIR137 identified from *Transcription Factor ChIP-seq from ENCODE,* UCSC Genome Browser (http://genome.ucsc.edu/). **B**, Canonical 21 bp NRSF binding motif found within NRSF target genes and sequence homology with predicted BS within MIR137. **C**, Chromatin immunoprecipitation (ChIP) assays showing NRSF binding at the putative BSii encompassing the internal MIR137 promoter (Imir137) VNTR under control conditions (sterile filtered d.$H_2O$) and after 1 hour treatment with cocaine. **D**, Expression profiling of mRNAs expressed from the MIR137 locus after 1 hour treatment with 10 µM cocaine. *E*, Relative levels of luciferase expression supported by the Imir137(4/12)F/R constructs in response to 1 hour treatment with 10 µM cocaine. *N*=4. *Significant changes in luciferase activity over backbone control levels. #Significant changes in luciferase activity between experimental conditions. */#*P*<0.05, **/##*P*<0.01, ***/###*P*<0.001.

a potential role for NRSF-mediated regulation of the MIR137 locus, SH-SY5Y cells were treated with cocaine and processed for ChIP and RT-PCR. Following 1 hour treatment with 1 μM cocaine, NRSF binding was reduced at the Imir137 promoter (BSii), with loss of binding observed following 10 μM cocaine treatment (**Figure 4.3C**). As a control, it was demonstrated that cocaine reduced NRSF binding at the previously characterised BDNF promoter II NRSE domain (**Figure 4.3C**) (Palm et al., 1998, Timmusk et al., 1999). The loss of binding to BSii was correlated with loss of AK309618 mRNA expression but not MIR137HG and AK311400 expression (**Figure 4.3D**). Cocaine had no affect on the level of reporter gene expression supported by either Imir137(4) or Imir137(12) suggesting that other domains outside of the proximal promoter may be involved in the response of the endogenous gene (**Figure 4.3E**).

### 4.3.4 The MIR137 locus is differentially regulated in response to NRSF over-expression and cocaine treatment

To further investigate the role of NRSF-mediated regulation of the MIR137 locus, the effect of over-expression of full-length NRSF (RE-EX1) and sNRSF on both endogenous MIR137 mRNA expression and the activity of reporter gene constructs containing the internal promoter in SH-SY5Y cells were analysed. Over-expression of RE-EX1 but not sNRSF resulted in down-regulation of both AK311400 and AK309618 mRNAs (**Figure 4.4A**) whose transcripts initiate from the Imir137 promoter region which has been shown to be bound by NRSF in ChIP assays (**Figure 4.3C**). This was not a metabolic or non-specific affect on the cell transcriptome as MIR137HG was not significantly affected (**Figure 4.4A**). Co-transfection of the Imir137 promoter constructs

**Figure 4.4. Differential regulation of the MIR137 locus following NRSF over-expression in SH-SY5Y cells. A**, Expression of AK311400, AK309618 and MIR137HG/AK094607 mRNA following over-expression of full-length human NRSF (RE-EX1) and sNRSF. Expected band sizes for AK311400, AK309618 and MIR137HG were 274 bp, 451 bp and 291 bp, respectively. **B-C**, Average fold change in luciferase activity compared to pGL3B (**B**) and pGL3P (**C**) controls following transfection of MIR137 reporter gene constructs under control conditions (pcDNA3.1 backbone alone) or in combination with RE-EX1 or sNRSF over-expression constructs. N=4. *Significant changes in luciferase activity over backbone control. #Significant changes in luciferase activity between experimental conditions. */#$p<0.05$, **/##$p<0.01$, ***/###$p<0.001$. [Figure presented on opposite page].

A

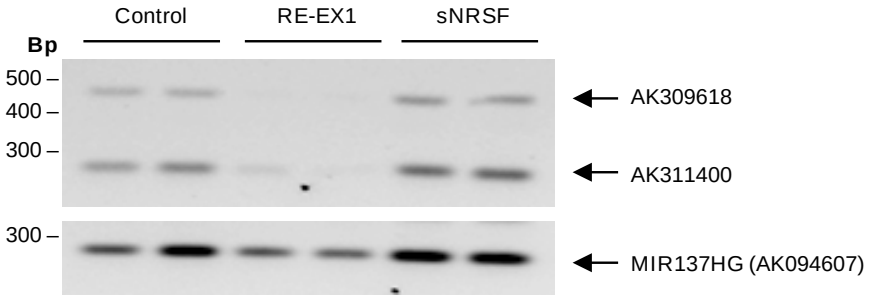
Control
RE-EX1
sNRSF
Bp
500 –
400 –
300 –
AK309618
AK311400
300 –
MIR137HG (AK094607)

B

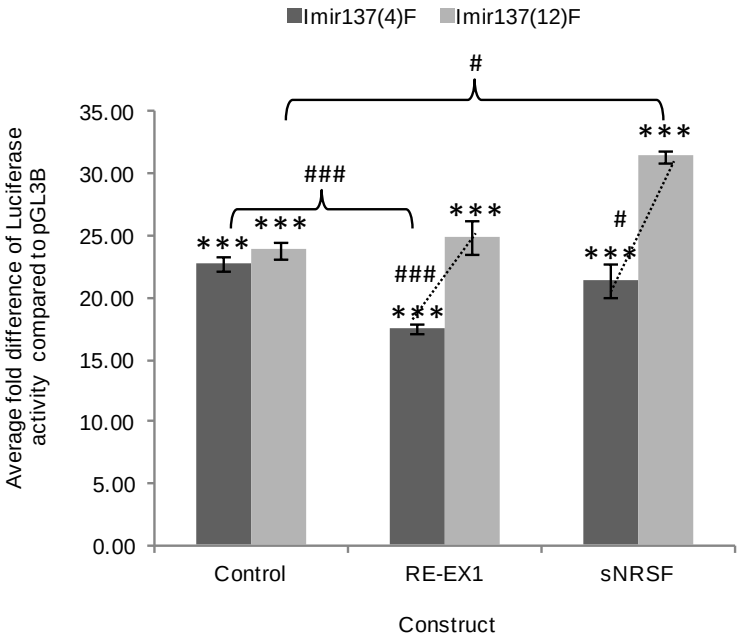
Imir137(4)F
Imir137(12)F
Average fold difference of Luciferase activity compared to pGL3B
35.00
30.00
25.00
20.00
15.00
10.00
5.00
0.00
Control
RE-EX1
sNRSF
Construct

C

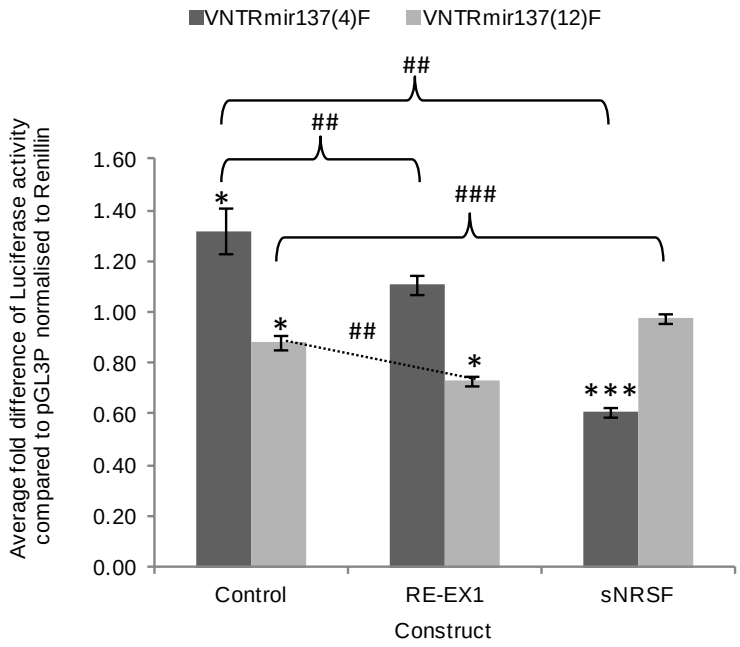
VNTRmir137(4)F
VNTRmir137(12)F
Average fold difference of Luciferase activity compared to pGL3P normalised to Renillin
1.60
1.40
1.20
1.00
0.80
0.60
0.40
0.20
0.00
Control
RE-EX1
sNRSF
Construct

with either RE-EX1 or sNRSF demonstrated a differential response dependent on the genotype of the VNTR. RE-EX1 over-expression demonstrated a 2-fold decrease in reporter gene activity on the Imir137(4) (*p<0.05) whereas the Imir137(12) was not affected (**Figure 4.4B**). SH-SY5Y cells are homozygous for the 4-copy allele of the MIR137 VNTR, therefore down-regulation of reporter gene expression supported by Imir137(4) correlates with down-regulation of the AK311400 and AK309618 mRNAs expressed from the MIR137 locus following over-expression of NRSF (**Figure 4.4A**). Conversely, sNRSF had no affect on Imir137(4) but increased activity supported by Imir137(12). The difference between activity supported by Imir137(4) and Imir137(12) in response to RE-EX1 and the truncated isoform sNRSF was 1.4-fold (###p<0.001) and 1.5-fold (#p<0.05), respectively. The lab has previously shown that NRSF and its alternative isoforms do not always function as transcriptional repressors (Spencer et al., 2006, Gillies et al., 2011, Coulson et al., 1999), especially when the NRSE motif is located within the promoter region of its target genes as exemplified by the neuropeptide genes AVP (Coulson et al., 1999, Quinn et al., 2002), TAC1 (Quinn et al., 2002) and TAC3 (Gillies et al., 2009). When the VNTR domain alone was investigated in conjunction with RE-EX1 over-expression, it was noted that a small and comparable reduction in activity (## p<0.01) was seen for both VNTRmir137(4)F (1.2-fold) and VNTRmir137(12)F (1.4-fold) (**Figure 4.4C**). However the greatest difference observed was in response to sNRSF over-expression, which resulted in major repression of the 4-copy VNTR (2.2-fold). There is a potential NRSF binding site within the MIR137 VNTR sequence domain (**Figure 4.1B**) which supports the

finding of allele-specific differences in reporter gene activity following over-expression of NRSF and sNRSF.

### 4.3.5 Cocaine-induced methylation over the Imir137 promoter

Cocaine exposure has been shown to induce differential gene expression through modification of epigenetic signatures, including promoter DNA methylation (Anier et al., 2010). The presence of two annotated CpG islands within the promoter regions of the MIR137HG (chr1:98519002-98519983) and AK311400/AK309618 (chr1:98510967-98511710) transcripts suggests active regulation of these non-protein coding RNAs in a tissue-specific and stimulus-inducible manner through modification of the CpG residues. To address this, the methylation status of the MIR137HG and Imir137 promoters in SH-SY5Y cells was investigated under normal growth conditions and in response to cocaine using methylated DNA immunoprecipitation (MeDIP), a technique that utilises a GST (glutathione-S-transferase protein)-MBD (methyl binding domain) fusion protein which enriches for methylated double stranded DNA (see *section 2.2.9*). PCR analysis of the immunoprecipitated DNA using primers targeting the CpG island (CGI) upstream of MIR137HG (-3753 to -4734 bp) showed that cocaine had no effect on DNA methylation in this region (**Figure 4.5**). This is consistent with our expression data in which cocaine had no effect on the levels of MIR137HG mRNA (**Figure 4.3D**). Under both control conditions and following 1 hour treatment with 10 μM cocaine, signal was observed in both the methylated and unmethylated samples for the MIR137HG CGI suggesting allele-specific methylation over this region or variation in the methylation patterns across the population of cells. In contrast, MeDIP analysis over the CGI

encompassing the Imir137 promoter VNTR showed allele-specific enrichment in response to cocaine treatment (**Figure 4.5**) inferring that this promoter may be a DNA methylation regulated domain for one of the expressed MIR137 transcripts in SH-SY5Y cells. Loss of AK309618 mRNA in response to cocaine treatment provides support for this (**Figure 4.3D**).

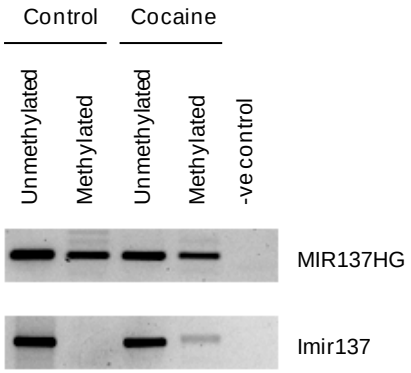


**Figure 4.5. Methylation status of the MIR137 gene promoters in SH-SY5Y cells.** PCR analysis of genomic DNA samples following incubation with a GST-MBD fusion protein which targets methylated double stranded DNA. Signal for the MIR137HG promoter CpG island (CGI) was observed in both the methylated and unmethylated samples under control conditions (sterile filtered d.$H_2O$) and following 1 hour treatment with 10 μM cocaine in SH-SY5Y cells. Methylation over the MIR137 internal promoter VNTR was observed following cocaine exposure. *MBD, methyl binding domain; GST, glutathione-S-transferase protein*.

### 4.3.6 Genotype Variation of the MIR137 VNTR in Schizophrenia

Functional analysis of the MIR137 locus supported differential gene regulation dependent upon both copy number of the VNTR and the cellular environment (cocaine or NRSF levels). We therefore hypothesised that the VNTR copy number may be an important predisposing factor in the development of neurological dysfunction including schizophrenia. This might be especially true in conjunction with an environmental insult to modulate the function of the VNTR. To test this hypothesis, the genotype of this repetitive element was addressed in 823 schizophrenic patients and 762 healthy controls, as described in *section 2.2.7.2*. Twelve alleles of the 15 bp promoter VNTR were identified; the smallest had 3-copies of the repeat, the largest 14-copies, with a plurality of individuals homozygous for the 4-copy variant, **Figure 4.6**. Allele and genotype frequencies are outlined in **Table 4.1** and **Table 4.2**, respectively.

*Clump* analysis (Sham and Curtis, 1995) was performed to determine significant differences between cases and controls with respect to allele frequencies and genotype of the MIR137 VNTR. Using this statistical model, no significant difference was observed under the conventional chi-squared ($X^2$) approach (**Table 4.3**). This is consistent with two recent studies, one in individuals of European ancestry (Molecular Genetics of Schizophrenia cohort) and the other in Japanese patients, which found no association for this VNTR with schizophrenia (Egawa et al., 2013, Duan et al., 2014). Examination of cognitive endophenotypes did not show any associations that withstood correction for multiple testing (see *Appendix 5*, data generated by Dr. Bettina Konte, University of Halle-Wittenberg, Halle, Germany). The lack of statistical correlation may reflect the rare higher copy-number variants being significantly

underrepresented in the population thus giving us little power to address the role of the functionally distinct 12-copy variant found both in this study and previously as a modulator of miR-137 processing in a cell line model (Bemis et al., 2008), as a simple genetic correlate for risk to schizophrenia.

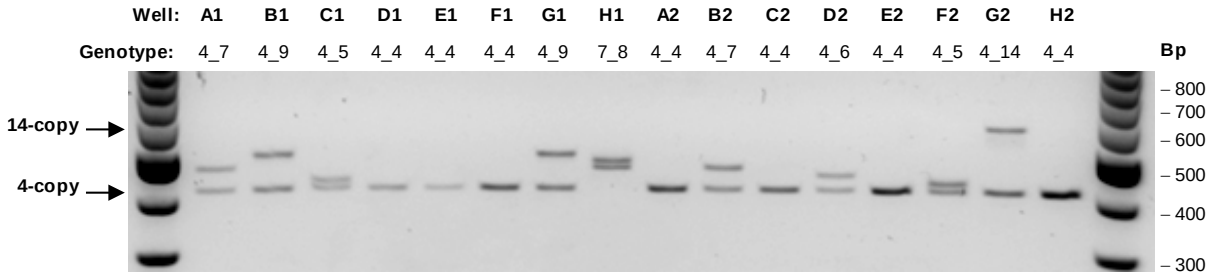


**Figure 4.6. Genotyping the MIR137 VNTR in a schizophrenia cohort.** Genomic DNA samples extracted from human blood of patients with schizophrenia or healthy matched controls were amplified by standard PCR using modified primers (*5*' 6-*FAM,* fluorescein) targeting the MIR137 VNTR. Amplicons were separated on a 2% agarose gel supplemented with ethidium bromide and sized against a DNA ladder, as represented above. Genotype calls were verified using capillary electrophoresis. Numbers represent copy-number of the repeat.

**Table 4.1.** MIR137 VNTR allele frequencies in schizophrenia cohort

| Allele Frequency (%) | 4 | 5 | 6 | 7 | 8 | 9 | 10 | 11 | 12 | 13 | 14 | 12-14 |
|---|---|---|---|---|---|---|---|---|---|---|---|---|
| *Cases* | 68.65 | 11.48 | 5.29 | 3.10 | 2.49 | 2.61 | 2.31 | 2.19 | 1.15 | 0.36 | 0.36 | 1.88 |
| *Controls* | 70.14 | 10.37 | 5.58 | 3.02 | 2.69 | 2.43 | 2.56 | 1.90 | 0.92 | 0.26 | 0.13 | 1.31 |

*Note:* Numbers in the top row represent VNTR copy number. Rare 3-copy alleles were combined with the 4-copy allele count.

**Table 4.2.** Genotype data for MIR137 VNTR in schizophrenic individuals against matched controls

| Genotype | Schizophrenia | | Controls | |
|---|---|---|---|---|
| | Number of Counts | Frequency (%) | Number of Counts | Frequency (%) |
| 3_3 | 0 | 0.00 | 1 | 0.13 |
| 3_4 | 1 | 0.12 | 1 | 0.13 |
| 4_4 | 381 | 46.29 | 377 | 49.48 |
| 4_5 | 138 | 16.77 | 102 | 13.39 |
| 4_6 | 54 | 6.56 | 64 | 8.40 |
| 4_7 | 38 | 4.62 | 31 | 4.07 |
| 4_8 | 24 | 2.92 | 28 | 3.67 |
| 4_9 | 33 | 4.01 | 30 | 3.94 |
| 4_10 | 33 | 4.01 | 25 | 3.28 |
| 4_11 | 26 | 3.16 | 21 | 2.76 |
| 5_5 | 9 | 1.09 | 9 | 1.18 |
| 5_6 | 14 | 1.70 | 7 | 0.92 |
| 5_7 | 2 | 0.24 | 10 | 1.31 |
| 5_8 | 4 | 0.49 | 5 | 0.66 |
| 5_9 | 1 | 0.12 | 3 | 0.39 |
| 5_10 | 3 | 0.36 | 7 | 0.92 |
| 5_11 | 4 | 0.49 | 3 | 0.39 |
| 6_6 | 2 | 0.24 | 2 | 0.26 |
| 6_7 | 4 | 0.49 | 1 | 0.13 |
| 6_8 | 4 | 0.49 | 2 | 0.26 |
| 6_9 | 5 | 0.61 | 1 | 0.13 |
| 6_10 | 0 | 0.00 | 3 | 0.39 |
| 6_11 | 1 | 0.12 | 3 | 0.39 |
| 7_8 | 2 | 0.24 | 1 | 0.13 |
| 7_10 | 1 | 0.12 | 1 | 0.13 |
| 7_11 | 2 | 0.24 | 0 | 0.00 |
| 8_8 | 1 | 0.12 | 2 | 0.26 |
| 8_9 | 3 | 0.36 | 0 | 0.00 |
| 8_11 | 2 | 0.24 | 1 | 0.13 |
| 9_9 | 0 | 0.00 | 1 | 0.13 |
| 9_10 | 0 | 0.00 | 1 | 0.13 |
| 9_11 | 1 | 0.12 | 0 | 0.00 |
| 12_14* | 30 | 3.65 | 19 | 2.49 |
| **Total** | **823** | | **762** | |

*Note:* Numbers represent copy-number of the repeat. *Genotypes containing at least one high-copy allele (12-14 repeats) were grouped together.

**Table 4.3.** Significance-testing of allele and genotype frequency data between schizophrenia cases and healthy controls using *Clump* analysis

| | Allele | Genotype |
|---|---|---|
| **T1** | 0.855 | 0.188 |
| **T2** | 0.943 | **0.021*** |
| **T3** | 0.202 | **0.014*** |
| **T4** | 0.859 | 0.332 |

*Note:* Values represent adjusted P-values for permutation testing of the differences between cases and controls with respect to allele and genotype frequencies. * P<0.05.

### 4.3.7 Haplotype structure of the MIR137 Gene

The functional significance of the previously identified GWAS SNPs for schizophrenia, rs1625579 within the MIR137 gene and rs1198588 less than 40 Kb upstream of MIR137, remains elusive and their presence within non-coding regions of the genome suggests that modulation of gene expression or post-transcriptional processing of miR-137 is a more likely explanation of their functional significance in schizophrenia. LD analysis was therefore performed using the HapMap CEU sample panel, integrating the VNTR genotypes using a down coding procedure whereby each allele is coded as a SNP depending on its dosage (2, 1, 0 becoming 1 1, 1 2, 2 2). The position of each consecutive SNP was +15 bp, which indicates the repeat length of the VNTR, starting from chr1:98,284,369 for the 4-copy variant. This marks the position of the INDEL (insertion or deletion) rs71738863 within the repeat element sequence which was determined to be the VNTR insertion site. Squared correlation coefficient ($r^2$) analysis indicated that the VNTR was not in LD with the GWAS SNPs nor tagged by any other markers within the same haplotype blocks defined using confidence intervals (Gabriel et al., 2002), **Figure 4.7**.

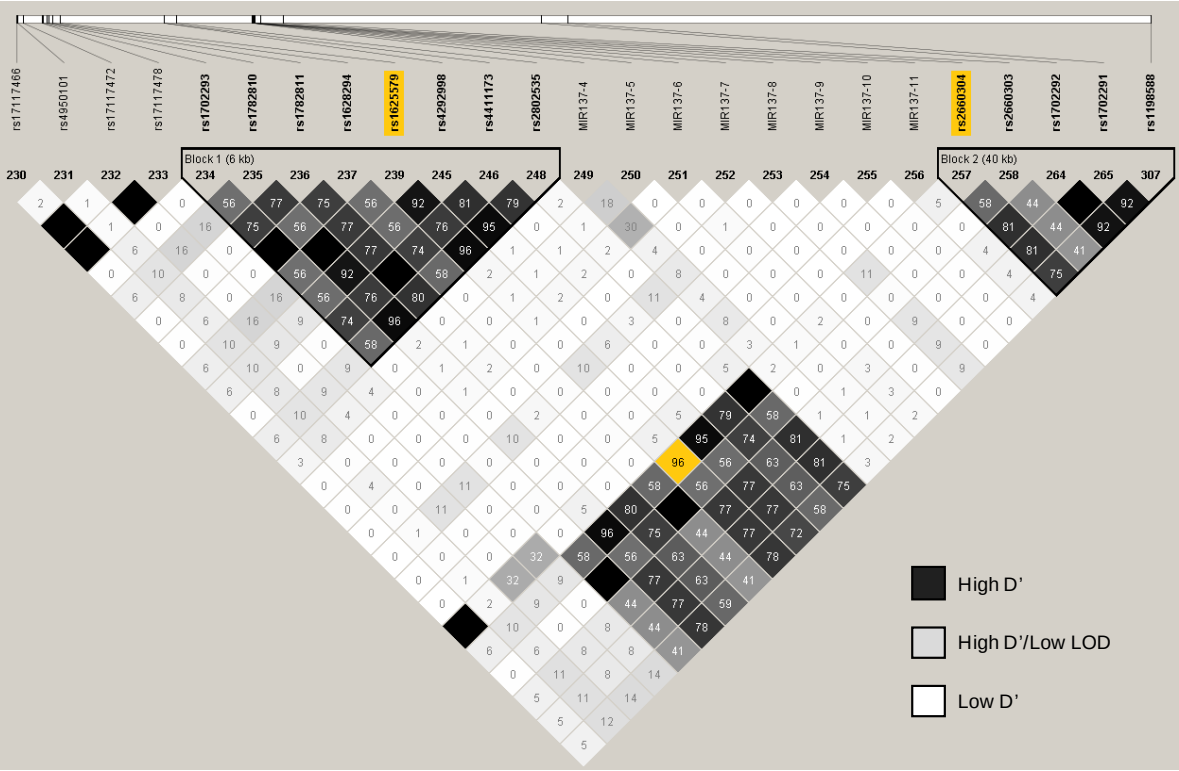


**Figure 4.7. Linkage disequilibrium (LD) analysis of MIR137 gene locus.** Haplotype block structure of the MIR137 gene based on squared correlation coefficient ($r^2$) values calculated from 89 individuals from the CEPH collection of the International HapMap Project using the Linkage Format feature in Haploview 4.2 (Hardy-Weinberg p-value cut-off, 0.001; minimum genotype cut-off, 0.75; maximum number of Mendel errors, 1; minimum minor allele frequency, 0.01). SNPs spanning chromosome 1: 98,075,522-98,711,836 were downloaded from the HapMap Genome Browser, release #28 (http://hapmap.ncbi.nlm.nih.gov/index.html.en). Haplotype blocks, represented by a black triangular border, were determined using 95% confidence intervals proposed by Gabriel et al. which defined two haplotype blocks separated by the MIR137 VNTR which is located within a recombination hot spot represented by white squares. Pair-wise tagging SNP analysis ($r^2$>0.8) revealed that the GWAS SNP rs1625579 and the MIR137 VNTR were not in LD. However, high LD ($r^2$=0.96) was observed between rs1625579 and the internal MIR137 promoter SNP rs2660304, highlight yellow on the LD plot.

### 4.3.8 MIR137 and schizophrenia-smoking associations

Pair-wise tagging SNP analysis using genotype data from the HapMap CEU cohort revealed that the intronic GWAS SNP rs1625579 and a SNP (rs2660304) situated 175 bp and 373 bp upstream of the AK311400 transcript and pre-miR-137, respectively, were in strong LD ($r^2$ = 0.96), **Figure 4.7**. The functional significance of this SNP was addressed using reporter gene constructs containing the common 4-copy variant of the Imir137 promoter VNTR. These constructs were named Imir137(4)+A for the major allele and Imir137(4)+C for the minor allele (MAF; 0.168 in HapMap CEU). Sequencing confirmed that these constructs varied only at the position of rs2660304. **Figure 4.8A** illustrates the position of the rs2660304 SNP in relation to the Imir137 promoter and the rs1625579 GWAS SNP. A significant difference in activity was observed between the two alleles in SH-SY5Y cells (**Figure 4.8B**, ##p<0.01). There was no significant difference in luciferase activity between the Imir137(4) and Imir137(4)+C constructs, the latter of which includes an additional 69 bp of sequence, supporting that the difference in expression directed by the Imir137(4)+A and Imir137(4)+C constructs is a function of the SNP, **Figure 4.8B**. The rs2660304 SNP has previously been studied for its association with tobacco-related squamous cell carcinomas (Roy et al., 2014a, Roy et al., 2014b), with several studies identifying miR-137 dysregulation important in lung cancer (Dacic et al., 2010, Zhu et al., 2013a). The prevalence of smoking in patients with schizophrenia is two- to four-fold the rate seen in the general population and it has been suggested that smoking may be a form of self-medication in schizophrenic individuals due to the normalising effects of nicotine on neuropsychiatric phenotypes (Kumari and Postma, 2005).

**A**

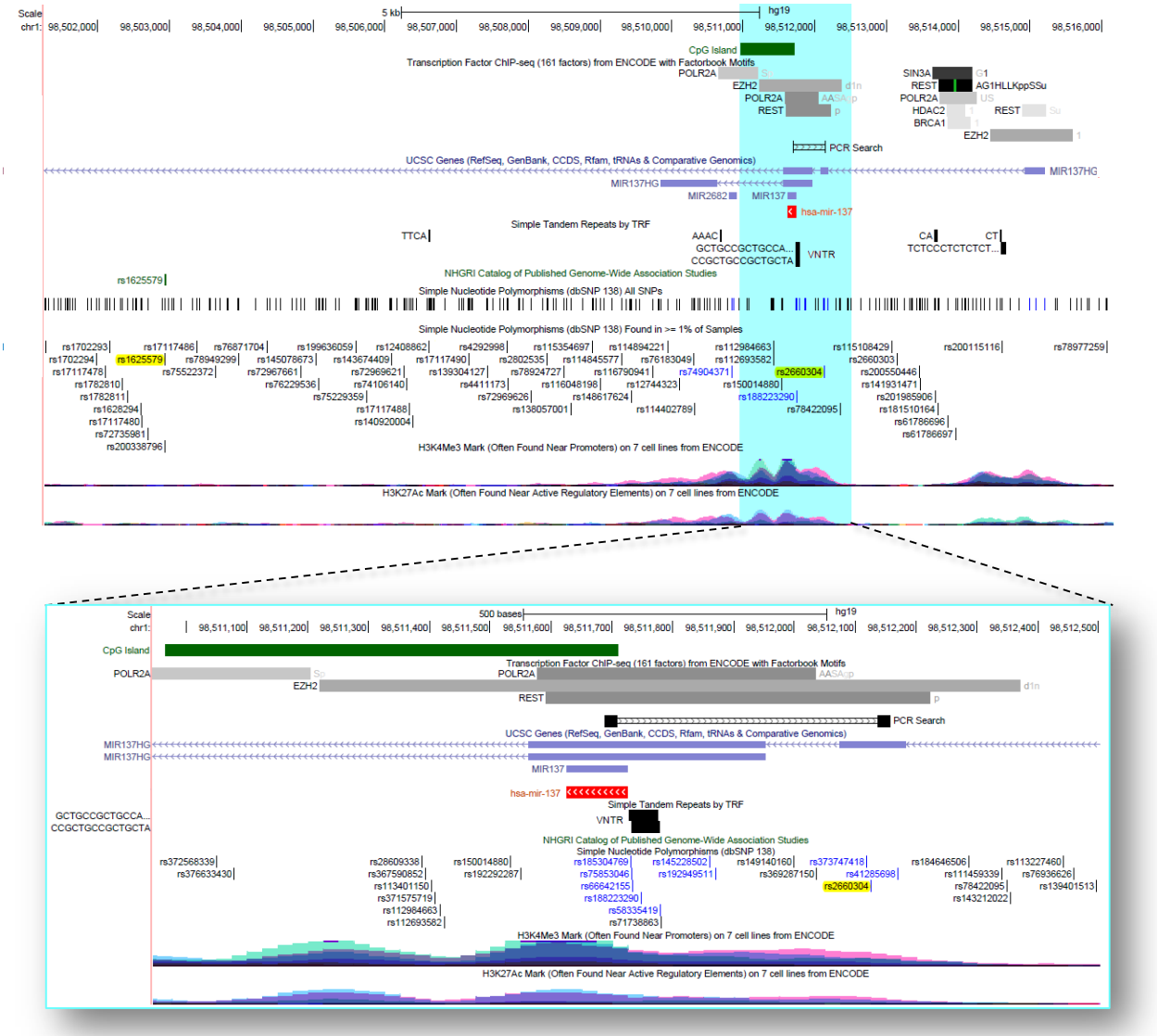
Scale
chr1:
5 kb
hg19
98,502,000
98,503,000
98,504,000
98,505,000
98,506,000
98,507,000
98,508,000
98,509,000
98,510,000
98,511,000
98,512,000
98,513,000
98,514,000
98,515,000
98,516,000
CpG Island
Transcription Factor ChIP-seq (161 factors) from ENCODE with Factorbook Motifs
POLR2A
EZH2
REST
SIN3A
G1
AG1HLLKppSSu
HDAC2
BRCA1
PCR Search
UCSC Genes (RefSeq, GenBank, CCDS, Rfam, tRNAs & Comparative Genomics)
MIR137HG
MIR2682
MIR137
hsa-mir-137
Simple Tandem Repeats by TRF
TTCA
AAAC
GCTGCCGCTGCCA...
CCGCTGCCGCTGCTA
VNTR
CA
CT
TCTCCCTCTCTCT...
NHGRI Catalog of Published Genome-Wide Association Studies
rs1625579
Simple Nucleotide Polymorphisms (dbSNP 138) All SNPs
Simple Nucleotide Polymorphisms (dbSNP 138) Found in >= 1% of Samples
H3K4Me3 Mark (Often Found Near Promoters) on 7 cell lines from ENCODE
H3K27Ac Mark (Often Found Near Active Regulatory Elements) on 7 cell lines from ENCODE
500 bases
98,511,100
98,511,200
98,511,300
98,511,400
98,511,500
98,511,600
98,511,700
98,511,800
98,511,900
98,512,000
98,512,100
98,512,200
98,512,300
98,512,400
98,512,500
rs2660304
rs188223290
rs74904371

**B**

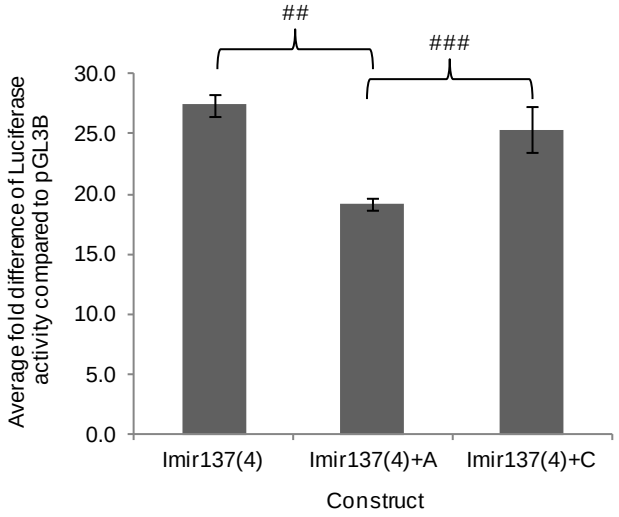
##
###
Average fold difference of Luciferase activity compared to pGL3B
30.0
25.0
20.0
15.0
10.0
5.0
0.0
Imir137(4)
Imir137(4)+A
Imir137(4)+C
Construct

**C**

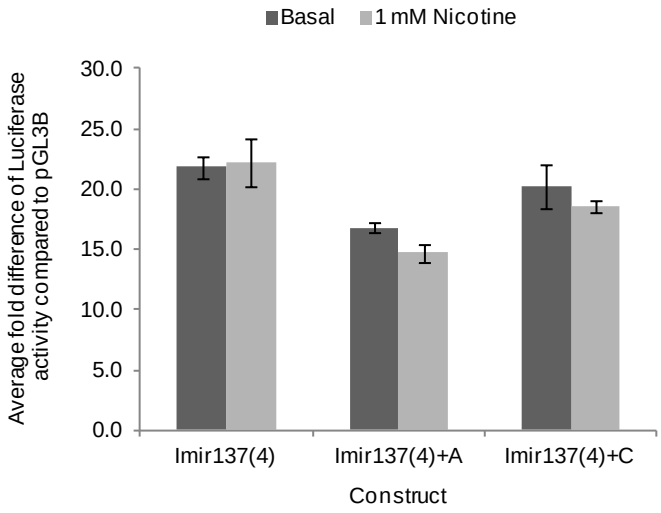


**Figure 4.8. Functional analysis of the MIR137 promoter SNP rs2660304. A**, Schematic showing the location of rs2660304 within the Imir137 promoter and its relation to the GWAS SNP rs1625579; SNPs are highlighted yellow. *Lower panel* represents the region highlighted blue in the *top panel*, showing the region targeted by PCR primers (labelled *PCR search*) for cloning into the pGL3B luciferase vector system. **B-C**, Luciferase activity supported by the Imir137(4), Imir137(4)+A (major allele) and Imir137(4)+C (minor allele) constructs in SH-SY5Y under basal conditions (**B**) or following 1 hour treatment with 1 mM nicotine (**C**). N=4. #Significant changes in luciferase activity between experimental conditions. ##p<0.01, ###p<0.001. Image taken from the UCSC Genome Browser (http://genome.ucsc.edu/index.html), accessed September 2013.

Nicotine has been previously shown to up-regulate the expression of miR-137 *in vitro* (Huang and Li, 2009). The effect of nicotine on the activity of the Imir137 promoter SNPs was therefore addressed. **Figure 4.8C** shows that 1 hour treatment of SH-SY5Y cells with 1 mM nicotine did not significantly regulate the Imir137 promoter SNP constructs. Tissue culture models may not be appropriate for addressing transcriptional changes at the Imir137 promoter in response to nicotine as the cells are only exposed to the drug over short time points which are not representative of chronic exposures associated with long-term smoking.

To investigate an association between smoking rates, measured by cigarettes smoked per day, and rs2660304 genotype (inferred from genotype data obtained for the GWAS SNP rs1625579 which is in strong LD with this SNP, $r^2$ = 0.96), linear regression analysis was performed in a sub-group of the schizophrenia and matched control cohort accounting for age and sex as covariates. Differences in allele and genotype frequencies between the schizophrenia and control groups and smokers and non-smokers were also evaluated using $X^2$ tests. No significant differences were found between rs1625579/rs2660304 genotype and allele distributions between cases and controls (genotype frequency, $X^2$=3.55, df=2, p=0.17; allele frequency, $X^2$=0. 33, df=1, p=0.56) or smokers and non-smokers in the schizophrenia group (genotype frequency, $X^2$=2.19, df=2, p=0.33; allele frequency, $X^2$=0.01, df=1, p=0.93) and matched control group (genotype frequency, $X^2$=0.42, df=2, p=0.81; allele frequency, $X^2$=0.40, df=1, p=0.53), **Table 4.4**. After adjusting for age and sex using a regression model, there were still no significant associations between rs1625579/rs2660304 genotype and smoking rates in both the case and control groups (**Table 4.5**). The MIR137 VNTR alone or in combination with the

rs1625579/rs2660304 SNP did not confer a genetic influence on smoking rates (data not shown). In line with previous studies (Llerena et al., 2003, de Leon and Diaz, 2005), we found significant differences ($P<0.05$) between schizophrenic and non-schizophrenic individuals in terms of smoking status (smoker, non-smoker) and rates (**Table 4.4** and **4.5**, respectively). Sex and age were found to be associated in the schizophrenic and control groups, respectively, with higher smoking rates found in schizophrenic males and correlating with increasing age in the control group, as indicated by negative beta coefficient values (**Table 4.5**). These results do not support a role for the rs1625579/rs2660304 SNP or MIR137 VNTR in predicting smoking status and/or rates in schizophrenic or healthy individuals. However our data is consistent with previous findings of a high prevalence of smoking in schizophrenic individuals, particularly males.

**Table 4.4.** Demographic profiling of schizophrenia cases and healthy controls in relation to MIR137 rs1625579/rs2660304

| | **Cases : controls** | | | | **Cases** | | | | **Controls** | | | |
|---|---|---|---|---|---|---|---|---|---|---|---|---|
| | Cases | | Controls | | Smokers | | Non-smokers | | Smokers | | Non-smokers | |
| Total | 696 | 0.52 | 655 | 0.48 | **512** | **0.74** | 184 | 0.26 | 297 | 0.45 | 358 | 0.55 |
| Male | 440 | 0.63 | 295 | 0.45 | **343** | **0.67** | 97 | 0.53 | 143 | 0.48 | 152 | 0.42 |
| Female | 256 | 0.37 | 360 | 0.55 | 169 | 0.33 | 87 | 0.47 | 154 | 0.52 | 206 | 0.58 |
| Age (mean, range) | 38 | 18-71 | 46 | 19-72 | 37 | 18-67 | 40 | 18-71 | 47 | 19-72 | 45 | 20-72 |
| AA | 468 | 0.67 | 421 | 0.64 | 341 | 0.67 | 127 | 0.69 | 187 | 0.63 | 234 | 0.65 |
| AC | 193 | 0.28 | 209 | 0.32 | 148 | 0.29 | 45 | 0.24 | 98 | 0.33 | 111 | 0.31 |
| CC | 35 | 0.05 | 25 | 0.04 | 23 | 0.04 | 12 | 0.07 | 12 | 0.04 | 13 | 0.04 |
| A[a] | 1129 | 0.81 | 1051 | 0.80 | 830 | 0.81 | 299 | 0.82 | 472 | 0.79 | 579 | 0.81 |
| C[b] | 263 | 0.19 | 259 | 0.20 | 194 | 0.19 | 69 | 0.19 | 122 | 0.21 | 137 | 0.19 |
| Allele | $X^2 = 0.33$ | | P= 0.56 | | $X^2 = 0.01$ | | P= 0.93 | | $X^2 = 0.40$ | | P= 0.53 | |
| Genotype | $X^2 = 3.55$ | | P= 0.17 | | $X^2 = 2.19$ | | P= 0.33 | | $X^2 = 0.42$ | | P= 0.81 | |
| Smoking status | $X^2 = 111.86$ | | **P= 0.00 *** | | | | | | | | | |

*Note:* [a] Major allele, [b] minor allele. Values represent total counts (n) and frequencies within each grouping unless stated otherwise. Bold font indicates high smoking rates. P-values represent permutation testing of the differences between cases and controls and/or smokers and non-smokers with respect to allele and genotype frequencies and smoking status. * $P<0.05$.

**Table 4.5.** Regression analysis of rs1625579/rs2660304 genotype and smoking rates adjusted for age, sex and disease status

| Smoking rate (cpd) | β | Std. Error | t | P-value | 95% CI | |
|---|---|---|---|---|---|---|
| | | | | | Lower | Upper |
| Cases: | | | | | | |
| rs2660304 | -0.03 | 0.08 | -0.36 | 0.72 | -0.20 | 0.13 |
| Age | 0.00 | 0.00 | 0.70 | 0.49 | -0.01 | 0.01 |
| **Sex *** | -0.35 | 0.10 | -3.38 | **0.00 *** | -0.56 | -0.15 |
| (Constant) | 3.08 | 0.30 | 10.36 | 0.00 | 2.50 | 3.67 |
| Controls: | | | | | | |
| rs2660304 | -0.08 | 0.07 | -1.21 | 0.23 | -0.22 | 0.05 |
| **Age *** | 0.01 | 0.00 | 2.57 | **0.01 *** | 0.00 | 0.01 |
| Sex | -0.14 | 0.08 | -1.81 | 0.07 | -0.30 | 0.01 |
| Combined: | | | | | | |
| rs2660304 | -0.05 | 0.05 | -0.97 | 0.33 | -0.16 | 0.05 |
| **Disease status *** | -0.85 | 0.07 | -12.76 | **0.00 *** | -0.98 | -0.72 |
| Age | 0.00 | 0.00 | 1.89 | 0.06 | 0.00 | 0.01 |
| **Sex *** | -0.26 | 0.06 | -4.03 | **0.00 *** | -0.38 | -0.13 |
| (Constant) | 3.80 | 0.20 | 18.95 | 0.00 | 3.41 | 4.19 |

*Note:* Smoking rates were measured as cigarettes smoked per day. Disease status refers to schizophrenic or healthy matched control. Negative β values indicate lower smoking rates for each copy of the minor allele of rs1625579/rs2660304 and in females. Positive β values indicate positive correlation between smoking rates and age. *P<0.05. Abbreviations: *β, beta coefficient; CI, confidence interval; cpd, cigarettes smoked per day*.

## 4.4 Discussion

MIR137 has been identified as a gene that has a significant association with schizophrenia based on GWAS data (The Schizophrenia Psychiatric GWAS Consortium, 2011, Ripke et al., 2013). However the location of the associated SNPs within non-coding sequence suggests that the functional significance could be related to transcriptional or post-transcriptional regulation of the MIR137 gene. As such, any challenge to an individual that affects those pathways regulating miR-137 concentration, even in the absence of a genetic association, could have an impact on parameters associated with schizophrenia. The genomic architecture of the MIR137 gene suggested the presence of a promoter in the region adjacent to the sequence of miR-137 itself and thus internal to the main precursor message. This putative promoter region was termed Imir137. The structure of this promoter was also of interest as it contained a VNTR domain 6 bp upstream of the precursor sequence of miR-137. We confirmed the existence of this promoter by reporter gene analysis and validating the presence of two mRNAs, AK311400 and AK309618, which originate in this area of the gene locus (**Figures 4.2** and **4.3**) (Warburton et al., 2014).

Encode data predicted the presence of an NRSF binding site at the Imir137 promoter which was confirmed by ChIP, **Figure 4.3**. Not all predicted NRSF binding sites in the locus were validated in this experiment as a second NRSF binding site in the promoter of MIR137HG was not occupied in this analysis, **Figure 4.3**. To address if NRSF was in part involved in the differential regulation of mRNAs at the Imir137 promoter, the levels of NRSF were

modulated with an expression construct. This resulted in a decrease in both transcripts (AK311440 and AK309618) originating at the Imir137 promoter with a minimal affect observed on the expression of full-length MIR137HG. This was consistent with the binding observed in ChIP for NRSF at the internal promoter. We next addressed the action of cocaine, a known modulator of NRSF expression in this cell line (see *Chapter 3*), a robust activator of other signalling pathways relevant to mood disorders in tissue culture models (discussed in *Chapter 5*) and a psychostimulant *in vivo* (Pihlgren and Boutros, 2007), to modulate mRNA expression at this locus. Cocaine resulted in the loss of NRSF binding to the Imir137 promoter and correlated with the loss of expression of AK309618; one of the two transcripts originating at the internal promoter. There was no affect on the expression of AK311400, which would originate from a similar position, and the full-length MIR137HG transcript (**Figure 4.3**). Furthermore, analysis of methylation over the MIR137HG and Imir137 promoters identified a differentially methylated region within the gene locus that correlated with differential expression of the AK309618 transcript in response to cocaine treatment. NRSF and its co-repressors regulate the fine-tuning of genes involved in neural plasticity through dynamic regulation of epigenetic mechanisms including DNA methylation (Ballas et al., 2005). NRSF binding of low-methylated target regions has been shown to be sufficient and necessary to maintain a hypomethylated state, with NRSF knock-out resulting in hypermethylation (Stadler et al., 2011). This is consistent with correlations between reduced NRSF binding of target genes and promoter DNA hypermethylation and gene dysregulation in models of neurological dysfunction (Jin et al., 2013). This is in line with our data of reduced NRSF binding and

increased DNA methylation over the Imir137 promoter region, which contains an overlapping CGI (regions associated with low levels of CpG methylation), following treatment with cocaine. Regulation over the Imir137 promoter in response to cocaine may involve the NRSF co-repressor MeCP2 (methyl CpG binding protein 2) which has the ability to selectively recognise methylated DNA and has been shown to remain bound to NRSF target genes even following NRSF dissociation (Ballas et al., 2005). MeCP2 has previously been shown to modulate the activity of both NRSF and miR-137 (Abuhatzira et al., 2007, Szulwach et al., 2010), and another NRSF target miRNA, miR-212 (Uchida et al., 2010), which was shown to be an important mechanisms in the modulation of the NRSF target gene BDNF (see *Chapter 3*) in response to cocaine challenge (Im et al., 2010). We cannot determine in this experiment if NRSF levels modulate the differential expression of transcripts directed by the Imir137 promoter in response to cocaine, but only that cocaine induces a specific set of transcriptional responses acting at the internal promoter, of which NRSF is only one. Nevertheless, the data points to a central role for NRSF in modulating the activity of the Imir137 promoter, potentially through the recruitment of co-binding partners such as MeCP2 which is further discussed in *Chapter 6*.

Modification of epigenetic pathways by NRSF in association with the SWI/SNF chromatin remodelling complex has been implicated in intermediate phenotypes associated with schizophrenia in part through modulation of the GWAS candidate genes TCF4, SMARCA2 and CSF2RA (Loe-Mie et al., 2010). Interestingly, TCF4 has been identified as a target of miR-137 (Kwon et al., 2013), extending this regulatory network to include another major schizophrenia candidate gene. Furthermore, it has been shown that perturbed

regulation of genes functionally relevant to phenotypic traits associated with other neurological disorders may be modulated in part by the NRSF-SWI/SNF complex (Lepagnol-Bestel et al., 2009). We propose that a similar model involving NRSF could operate at the MIR137 locus, in particular at the Imir137 promoter, with NRSF regulating medium- to long-term expression through the activity of its cofactors which could mediate both histone modifications and DNA methylation at this region. Such a mechanism could be modified by any genetic variants embedded at the gene locus thus further modulating miR-137 levels. Such differential regulation of transcripts from the major MIR137 and Imir137 promoters would be expected to not only vary the levels of miR-137 but also the ratio of miR-137 to a second microRNA at this locus, miR-2682 (**Figure 4.1**). The function or significance of miR-2682 has not been addressed in previous communications. miR-2682 is not present in the AK311440 transcript but its primary sequence overlaps by 12 bp with the second exon of AK309618. Similarly, the different transcripts expressed from this region may be post-transcriptionally processed leading to different levels of either microRNA which could result in CNS dysfunction. *In vivo*, the modulation of NRSF levels that modulate the transcripts expressed could be directed by psychological stressors or other trauma; however the action of the drug used in this communication validates the plasticity in expression at this locus.

Regulation by NRSF is complicated by the distinct functions which have been assigned to various isoforms of this gene. The proteins corresponding to these isoforms have not been examined as extensively as the full-length protein. In this study, over-expression of the truncated isoform sNRSF resulted in data that was distinct from the action of full-length NRSF on both the endogenous

MIR137 gene and several of the reporter gene constructs. Mechanistically, the different NRSF isoforms have been suggested to have distinct regulatory functions. Previous data from our group on NRSF-mediated regulation of neuropeptide gene expression supports these differential roles of the NRSF isoforms. For example, in a rodent model of epilepsy, over-expression of NRSF and a construct containing sequence for the human truncated variant in dissociated rat hippocampal neurons supported increased endogenous expression of the proconvulsant TAC1 gene for the truncated variant but not full-length NRSF (Spencer et al., 2006). This correlated with marked up-regulation of reporter gene activity driven by the TAC1 promoter following co-transfection with an expression construct for the truncated variant suggesting its role as a transcriptional enhancer (Spencer et al., 2006). A similar mechanism involving full-length NRSF and sNRSF was also demonstrated in human neuroblastoma cells for another proconvulsant gene TAC3 (Gillies et al., 2009). Furthermore, human sNRSF has been shown to antagonise the action of the full-length protein in small cell lung cancer cells causing de-repression of the neuropeptide gene AVP (Coulson et al., 2000). The data presented in this current study on the action of NRSF or sNRSF on the regulation of the endogenous MIR137 gene or the reporter gene constructs is consistent with this differential action of these distinct NRSF isoforms. However, SH-SY5Y cells endogenously express both isoforms (see *Appendix 3*) therefore over-expression assays reflect manipulation of the ratio of NRSF/sNRSF in the cell. We predict that in schizophrenia, environmental challenges and stress might result in alterations in the ratios of NRSF isoforms that could ultimately result in an altered pattern of gene expression. Significantly, the data from reporter

gene constructs indicated that the genotype of the VNTR could modulate the cellular response to the change in NRSF levels. This would suggest that a GxE factor is driving the modulation of expression over the locus.

The identification of the VNTR was of interest in part because the copy-number of this type of repetitive domain within the promoter of other genes our group has previously analysed, such as MAOA, SLC6A3 or SLC6A4, both correlates with susceptibility to CNS disease and supports differential reporter gene expression (Hill et al., 2013, Guindalini et al., 2006, Haddley et al., 2008, Ali et al., 2010, Vasiliou et al., 2012, Galindo et al., 2011, Roberts et al., 2007). In this study, it was demonstrated that the genotype of the Imir137 promoter VNTR could mediate differential reporter gene expression both under control conditions and in the presence of over-expressed NRSF or sNRSF. To address the potential role of this polymorphism as a biomarker for schizophrenia, the VNTR was genotyped in the HapMap CEU cohort to determine association with previously identified risk variants within the gene locus using LD analysis. This analysis indicated that the VNTR was not in LD with the previously identified MIR137 GWAS SNPs rs1625579 and rs1198588 (**Figure 4.7**). We therefore tested if the VNTR could independently impart a significant genetic risk for schizophrenia using a large schizophrenia and matched control cohort. Although there were a large number of variants of the VNTR in the population tested, 3- to 14-copies, a plurality of individuals, approaching 50%, were homozygous for the 4-copy variant. Furthermore, as the VNTR increased in size, the allele frequency in the population decreased, thus giving us little power to address the role of the functionally distinct 12-copy variant found in this communication, and previously found as a modulator of miR-137 processing in

a cell line model (Bemis et al., 2008), as a simple genetic correlate for risk to schizophrenia.

Interestingly, haplotype analysis over the MIR137 locus showed strong LD ($r^2 = 0.96$) between the schizophrenia-associated SNP rs1625579 with a SNP (rs2660304) within the identified Imir137 promoter (**Figure 4.7** and **4.8A**). Absence of LD between these markers and the MIR137 VNTR which is flanked by the two SNPs is compatible with this repetitive element mutating through recombination as indicated by white regions of low D' on the LD plot shown in **Figure 4.7**. Due to the location of the rs1625579 GWAS SNP within the first intron of the MIR137HG gene, approximately 8.7 Kb upstream of pre-miR-137, we reasoned that the tagged rs2660304 Imir137 promoter SNP located only 373 bp upstream of pre-miR-137 may be a more appropriate marker for schizophrenia through differential modulation of miR-137 expression levels driven by the internal MIR137 promoter. Analysis of the transcriptional potential of this promoter variant using reporter gene constructs containing the common 4-copy variant of the MIR137 VNTR and different alleles of the rs2660304 SNP showed allele-specific regulation in SH-SY5Y cells. The Imir137(4)+A promoter construct containing the major allele of rs2663004 supported reduced activity relative to the Imir137(4)+C minor allele construct. This difference in reporter gene activity was specific to the rs2660304 SNP as expression levels supported by the Imir137(4)+C construct containing the minor allele did not significantly differ from the Imir137(4) construct which contains 69 bp less sequence than the Imir137(4)+A/C promoter constructs (**Figure 4.1B**). Interestingly, the major allele of the rs1625579 GWAS SNP is defined as the risk variant for schizophrenia (The Schizophrenia Psychiatric

GWAS Consortium, 2011), which has previously been associated with reduced miR-137 expression levels in post-mortem brains of homozygous individuals relative to carriers of the minor non-risk allele (Guella et al., 2013). The significant reduction in reporter gene activity supported by the Imir137(4)+A promoter construct containing the major allele of rs2660304 (A) which is in LD with the rs1625579 GWAS SNP for schizophrenia is consistent with this finding and implicates this promoter SNP and the internal MIR137 promoter VNTR as a potential mechanism driving differential miR-137 expression. A role for rs2660304 in the pathophsyiology of schizophrenia is further supported by a recent study that reported a nominal genetic association of this SNP with this neuropsychiatric condition (Duan et al., 2014), which is in line with it being a proxy-SNP for the rs1625579 schizophrenia variant, **Figure 4.7**.

The rs2660304 SNP shown in this communication to differentially modulate the activity of the Imir137 promoter has previously been associated with smoking-related cancers (Roy et al., 2014a, Roy et al., 2014b). The global prevalence of smoking in patients with schizophrenia is two- to four-fold that of the general population, even after correcting for confounding variables such as socio-economic status, alcohol intake, antipsychotic drug regimes or institutionalism (Kumari and Postma, 2005). It has been proposed that schizophrenic individuals smoke as a means of self-medicating due to the reported effects of nicotine on reducing psychiatric symptoms (Glynn and Sussman, 1990, Smith et al., 2002, Zhang et al., 2012b, Strube et al., 2014), reducing the adverse effects of antipsychotic drug treatment (Goff et al., 1992, Anfang and Pope, 1997, Yang et al., 2002) and remediating sensory gating and cognitive deficits associated with neuropsychiatric pathologies (Kumari et al.,

2001, Sacco et al., 2004). Genetic variants within the nicotinic receptors through which nicotine exerts its effects have been implicated in both smoking and schizophrenia (Faraone et al., 2004), and it has also been demonstrated that smoking differentially normalises impaired gene expression associated with schizophrenia relative to levels in healthy controls (Mexal et al., 2005). In addition, the μ-opioid receptor (MOR), which has been associated with the antinociceptive and rewarding effects of nicotine, has been shown to be transcriptionally and post-transcriptionally regulated by NRSF (Kim et al., 2004, Kim et al., 2008). Both nicotine and NRSF have been identified as modulators of miR-137 levels *in vitro* (Huang and Li, 2009, Warburton et al., 2014) and dysregulation of this miRNA and NRSF have been implicated in lung cancer (Dacic et al., 2010, Zhu et al., 2013a, Coulson et al., 1999, Coulson et al., 2000), suggesting that a mechanism involving NRSF-mediated regulation of miR-137 via the internal Imir137 promoter may be important for predicting vulnerability to smoking and/or smoking-associated cancers. We therefore investigated the rs2660304 Imir137 promoter SNP as a mechanism involved in 1) regulating Imir137 promoter function in response to nicotine exposure using the Imir137(4) reporter gene construct variants and 2) influencing smoking status through genetic association in schizophrenic individuals and healthy matched controls using a linear regression model. The latter was performed using genotype data obtained for the rs1625579 SNP from our collaborator Prof. Dan Rujescu which is in strong LD with the rs2660304 marker ($r^2 = 0.96$). No significant affects on reporter gene expression were observed in response to nicotine in our tissue culture model which may reflect cell-specific responses to this treatment and therefore requires further investigation in a more

appropriate cell line such as those derived from lung cancer to address this model in smoking-related cancer or regions of the brain associated with nicotine induce-signalling, such as the nucleus accumbens and prelimbic area implicated in reward pathways; the orbitofrontal cortex associated with compulsive drug taking behaviours and the insular cortex associated with nicotine craving and relapse (Bruijnzeel et al., 2014).

Our regression analysis did not find an individual or additive genetic interaction for the rs1625579/rs2660304 SNP and MIR137 VNTR in predicting risk for schizophrenia or smoking. The rs1625579 GWAS SNP for schizophrenia has been reported to correlate with specific endophenotypes of the condition, with the major allele associating with cognitive deficits relating to working memory and executive function in individuals with negative symptoms; miR-137 expression levels; structural variations in the brain (reduced white matter density, diminished hippocampal volume and enlarged lateral ventricles) and earlier age of onset relative to carriers on the non-risk allele (Cummings et al., 2013, Lett et al., 2013, Green et al., 2012, Guella et al., 2013), which may explain the lack of association from our regression analysis. Similar candidate gene association studies on the influence of genetic variants (e.g. BDNF Val/Met66 polymorphism) in predicting smoking rates in schizophrenia have given conflicting results (Montag et al., 2008, Lang et al., 2007, Novak et al., 2010, Zhang et al., 2014), with analysis of haplotype blocks normalising these inconsistencies (Novak et al., 2010). In this study, we did not address the effects of SNPs (see **Figure 4.1B**) or INDELS within the MIR137 VNTR previously associated with modulating miR-137 expression levels *in vitro* (Strazisar et al., 2014). Such variants within promoter VNTRs may act as clinical correlates of

disease through GxE mechanisms as demonstrated by the rs25531 SNP within the long allele of the 5-HTT-linked polymorphic region (5-HTTLPR), whereby the presence of the minor allele of this variant confers clinical phenotypes normally associated with the short 'risk' allele of 5-HTTLPR through modifying an AP2 transcription factor binding site (Hu et al., 2006, Wray et al., 2009). Through ongoing collaboration with Prof. Dan Rujescu's group, University of Halle-Wittenberg, we are addressing haplotype patterns across the MIR137 and NRSF gene loci, including common SNPs and rare variants such as the higher alleles of the MIR137 promoter VNTR and previously described INDELs (Strazisar et al., 2014), in addition to environmental factors such as smoking rates, to identify potential clinical correlates for schizophrenia predisposition or markers that may distinguish distinct endophenotypes of schizophrenia.

## 4.5 Summary

In summary, the internal Imir137 promoter described in this communication can be regulated in an allele-specific and stimulus-inducible manner in part by the transcription factor NRSF. NRSF could in part modulate epigenetic parameters in response to environmental factors, such as stress, in the medium to long term in addition to the immediate changes observed in our cell line model. This is consistent with a GxE mechanism regulating miR-137, and potentially miR-2682, levels in the cell, with alterations in the concentration of these miRNAs resulting in differential repression of their gene targets in response to environmental cues. This differential expression directed by NRSF could be further affected by VNTR genotype. The resulting levels of

these miRNAs could play a significant role in CNS dysfunction, including schizophrenia. The MIR137 VNTR was not in LD with the previously reported GWAS SNPs within the locus suggesting allele-specific regulation operating at this repetitive domain is distinct from the mechanisms associated with these polymorphisms. However, high LD between the GWAS SNP rs1625579 and a SNP within the Imir137 promoter suggests that these SNPs may flank an associated haplotype that confers risk for schizophrenia, which may include rare high copy number variants of the VNTR such as the 12-copy variant demonstrated in our reporter gene assays to be functionally distinct from the common 4-copy variant. The importance of these variants in disease predisposition may only be apparent at the level of GxE; the cellular response to which can be dynamically shaped by cell-specific or stimulus induced activation of transcriptional and epigenetic regulators such as NRSF shown in this communication to be one such factor operating at this complex disease locus.

# Chapter 5

## NRSF Pathway as an Integrator of Distinct Pathways in Mood Disorders

## 5.1 Introduction

Mental health is in part dependent upon transcriptional responses to cues which can be environmental, chemical, physiological and psychological; this is termed the GxE component. These changes not only affect our health in the short term, but can have medium- to long-term impact via epigenetic modulation of gene expression, altering our response to environmental challenges. Genome wide association studies (GWAS) of neuropsychiatric disorders have identified many common polymorphisms associated with this disease group (Cross-Disorder Group of the Psychiatric Genomics, 2013a), however the biological significance of such variation is not well understood. The vast majority of GWAS-supported variants are located within non-coding regions of the genome (Hindorff et al., 2009), suggesting a regulatory function rather than a protein variant. This is exemplified in *Chapter 4* through the use of reporter gene constructs containing genetic variants within the promoter region of the schizophrenia associated candidate gene MIR137 to address allele-specific expression from the locus. The efforts of genetic consortia have uncovered substantial shared genetic components between several neuropsychiatric conditions, for example schizophrenia and bipolar disorder (Cross-Disorder Group of the Psychiatric Genomics, 2013a, Cross-Disorder Group of the Psychiatric Genomics, 2013b, Lichtenstein et al., 2009, The International Schizophrenia Consortium, 2009), implying common pathological mechanisms across related disorders. Therefore, a systematic approach to uncovering the functional consequence of such genetic perturbation and/or the global effects of environmental stimuli (in line with a GxE component) would greatly benefit the discovery of molecular mechanisms underlying disease

aetiology and, consequently, the application and development of therapeutic intervention.

It is difficult to address the signal cascade in response to specific challenges *in vivo* due to the heterogeneity of cells involved in processing the environmental signals mediating a cellular response. However, *in vitro* cell line models offer a window of opportunity to address in fine detail the signal pathways modulated in response to a specific challenge (Lamb et al., 2006). In this chapter, we analysed the cellular response to distinct mood modifying drugs in the human neuroblastoma cell line SH-SY5Y targeting a commercially available compilation of mood disorder genes to address whether they leave a molecular signature of transcriptional change to the challenge. These changes reflect one window for the spectrum of changes that could occur *in vivo*, but nonetheless outline the potential for a concerted cellular response to drug exposure. The drugs chosen for comparison included two psychostimulant challenges, amphetamine and cocaine, and two mood stabilisers, sodium valproate and lithium. All of these drugs have been shown previously to modulate signal pathways in SH-SY5Y cells at the transcriptional and/or post-transcriptional level (Di Daniel et al., 2005, Pan et al., 2005, Asghari et al., 1998, Lew, 1992, Kantor et al., 2002). Enrichment analysis of transcriptional networks relating to this gene set was performed using pathway analysis software to identify potentially important transcription factors involved in the drug response.

## 5.2 Aims

- Address the *in vitro* affects of mood modifying drugs on the transcriptome using qPCR arrays as a cost effective approach to identifying regulatory networks and pathways that might coordinate the cell response to a specific drug
- Perform enrichment analysis of transcriptional networks relating to this gene set to identify potentially important factors mediating drug-associated regulatory mechanisms
- Explore associated disease pathways to single out molecular mechanisms which may be characteristic of several disease states
- Bioinformatic analysis of the overlap between several transcriptional mechanisms (NRSF binding sites, repetitive DNA and miRNA genes) to identify potential hotspots for GxE mechanisms operating in disease models as demonstrated in *Chapter 4*

## 5.3 Results

### 5.3.1 Gene expression profiling of human SH-SY5Y cells in response to mood-modifying drugs using Global Pattern Recognition analysis

To investigate the effects of mood modifying drugs on the expression of a panel of genes associated with mood disorders (see **Table 2.4** in *Materials section 2.1.11* for a list of genes included on the array), human derived SH-SY5Y neuroblastoma cells were treated for 1 hour under one of the following conditions: basal (untreated), vehicle control (sterile filtered $dH_2O$), 10 μM cocaine, 10 μM amphetamine, 1 mM lithium or 5 mM sodium valproate based on previous in-house optimisation. Differences in gene expression across treatment conditions were measured using the commercially available Human Mood Disorder 96 StellARray™ qPCR arrays (Lonza Group Ltd**)** and analysed using the proprietary Global Pattern Recognition™ (GPR) algorithm (see *section 2.2.5.8*) which compares the change in expression of a gene normalised to the expression of every other gene in the array (Akilesh et al., 2003). This software calculates both the fold-change data and the respective *p*-values with respect to genes that showed minimal changes, generating a list of genes that are ranked on the basis of the difference between the test and control expression levels and the consistency of the data between the biological replicates. Our group and others have recently demonstrated that drugs used in the treatment of mood disorders can differentially affect the expression stability of traditionally used housekeeping genes, impacting upon their usefulness as normalising factors (Sugden et al., 2010, Powell et al., 2013, D'Souza et al., 2013). Unfortunately, these large changes in gene expression may mask small but biologically important changes in gene expression, such as master regulator genes (e.g.,

transcription factors). The data in **Table 5.1** therefore represents a more appropriate display of the genes most changed within the experiment by comparing all genes against themselves. As the array contains validated mood genes we addressed the top 10 genes which significantly changed in response to each drug to define pathways and networks within the larger gene list.

Following 1 hour treatment of SH-SY5Y cells with the mood stabiliser sodium valproate, 8 genes were significantly up- or down-regulated compared to the vehicle control; 2 up-regulated (JUN and PAFAH1B3) and 6 down-regulated (DRD3, GAD1, NRG1, PER3, RELN and RGS4). When compared to the results obtained after treatment with another common mood stabiliser, lithium, similarities in the gene expression profile with respect to the top 10 altered genes was observed; namely down-regulation of GAD1, NRG1, PER3, RELN and RGS4, however, only GAD1 reached statistical significance at this time point for lithium treatment. In addition, FOS was significantly down-regulated in response to lithium. Treatment with the two psychomotor stimulants cocaine and amphetamine demonstrated no statistically significant changes in gene expression following 1 hour treatment. Furthermore the genes with the lowest p-values were distinct between the psychostimulants apart from MOBP (**Table 5.1**) demonstrating that these drugs might be preferentially targeting distinct pathways for their action. However due to the low p-values obtained under these experimental conditions we did not pursue their analysis further.

**Table 5.1.** Gene expression profiling of SH-SY5Y cells following exposure to drugs affecting mood

| LITHIUM | | | | SODIUM VALPROATE | | | |
|---|---|---|---|---|---|---|---|
| Gene | Description | *p* | Fold change | Gene | Description | *p* | Fold change |
| **FOS** | **FBJ murine osteosarcoma viral oncogene homolog** | **0.012** | **-2.57** | **DRD3** | **Dopamine receptor D3** | **0.001** | **-7.98** |
| **GAD1** | **Glutamate decarboxylase 1** | **0.023** | **-3.48** | **RGS4** | **Regulator of G-protein signaling 4** | **0.007** | **-2.08** |
| RGS4 | Regulator of G-protein signaling 4 | 0.063 | -1.51 | **JUN** | **Jun oncogene** | **0.008** | **2.49** |
| PER3 | Period circadian clock 3 | 0.067 | -1.38 | **RELN** | **Reelin** | **0.012** | **-1.78** |
| NRG1 | Neuregulin 1 | 0.068 | -1.43 | **PER3** | **Period circadian clock 3** | **0.026** | **-1.48** |
| NR1D1 | Nuclear receptor subfamily 1, group D, member 1 | 0.069 | -1.48 | **PAFAH1B3** | **Platelet-activating factor acetylhydrolase, isoform Ib, gamma subunit 29kDa** | **0.034** | **1.61** |
| RELN | Reelin | 0.078 | -1.94 | **GAD1** | **Glutamate decarboxylase 1** | **0.035** | **-7.45** |
| ACE | Angiotensin I converting enzyme (peptidyl-dipeptidase A) 1 | 0.099 | 1.31 | **NRG1** | **Neuregulin 1** | **0.044** | **-1.34** |
| Hs18s | Human 18S ribosomal RNA | 0.105 | 1.64 | MTHFR | Methylenetetrahydrofolate reductase (NADPH) | 0.083 | 1.53 |
| BDNF | Brain-derived neurotrophic factor | 0.106 | -1.39 | RFX4 | Regulatory factor X, 4 (influences HLA class II expression) | 0.092 | -1.49 |

(Table 5.1 continued)

| COCAINE | | | | AMPHETAMINE | | | |
|---|---|---|---|---|---|---|---|
| Gene | Description | *p* | Fold change | Gene | Description | *p* | Fold change |
| SULT1A1 | Sulfotransferase family, cytosolic, 1A, phenol-preferring, member 1 | 0.088 | 1.68 | MOBP | Myelin-associated oligodendrocyte basic protein | 0.080 | 2.08 |
| DRD3 | Dopamine receptor D3 | 0.110 | -2.08 | XBP1 | X-box binding protein 1 | 0.093 | 1.34 |
| FOS | FBJ murine osteosarcoma viral oncogene homolog | 0.142 | -1.45 | NR1D1 | Nuclear receptor subfamily 1, group D, member 1 | 0.109 | -1.35 |
| MOBP | Myelin-associated oligodendrocyte basic protein | 0.161 | 1.85 | MAG | Malignancy-associated gene | 0.138 | 2.81 |
| SLC6A2 | Solute carrier family 6 (neurotransmitter transporter, noradrenalin), member 2 | 0.176 | -1.28 | PAFAH1B3 | Platelet-activating factor acetylhydrolase, isoform Ib, gamma subunit 29kDa | 0.141 | 1.33 |
| GRIK3 | Glutamate receptor, ionotropic, kainate 3 | 0.194 | -1.67 | FKBP5 | FK506 binding protein 5 | 0.159 | -1.34 |
| TIMELESS | Timeless circadian clock | 0.200 | -1.20 | RELN | Reelin | 0.198 | -1.30 |
| NCAM1 | Neural cell adhesion molecule 1 | 0.206 | -1.20 | BCR | Breakpoint cluster region | 0.207 | 1.22 |
| ND4 | Mitochondrially encoded NADH dehydrogenase 4 | 0.232 | 1.15 | MLC1 | Megalencephalic leukoencephalopathy with subcortical cysts 1 | 0.208 | 2.52 |
| NR1D1 | Nuclear receptor subfamily 1, group D, member 1 | 0.233 | -1.28 | GABRA5 | Gamma-aminobutyric acid (GABA) A receptor, α5 | 0.213 | -1.78 |

*Note:* Top 10 changes in gene expression levels between treated (10 μM amphetamine, 10 μM cocaine, 1 mM lithium and 5 mM sodium valproate) and untreated cells measured using qPCR arrays (Human Mood Disorder 96 StellARrayTM) and Global Pattern Recognition (GPR) statistical analysis. Fold change values are represented as treated conditions normalised to the drug vehicle. Bold font indicates significant changes in gene expression, $p<0.05$.

### 5.3.2 Determining regulatory pathways affected by mood modifying drugs

In order to define potential regulatory mechanisms which may be operating in response to cellular challenge with the drugs outlined in this study, we parsed our gene expression data into MetaCore™, an integrated data-mining platform for biological pathway analysis. Functional enrichment using the Pathway Map analysis tool was performed which generated a list of significant pathways relating to our experimental dataset based on p-value and GPR Fold-change. We first analysed our entire dataset collectively to make comparisons across the different treatment conditions. The pathways generated were highly enriched for developmental and immune response processes (**Figure 5.1**). The most significant pathway was glucocorticoid signalling (minimum treatment p-value = $5.15 \times 10^{-7}$) which came up twice in the top ten significant hits under both developmental and immunological regulatory processes. Other regulatory mechanisms identified as being highly significant included CD16 signalling in natural killer (NK) cells (minimum treatment p-value = $7.28 \times 10^{-6}$); signalling mediated through the complement component 5a (C5a) (minimum treatment p-value = $2.24 \times 10^{-5}$); the endoplasmic reticulum stress response pathway (minimum treatment p-value = $2.98 \times 10^{-5}$), circadian rhythm (minimum treatment p-value = $1.65 \times 10^{-5}$) and hormonal growth factor signalling pathways involving gastrin (minimum treatment p-value = $3.87 \times 10^{-6}$), thrombopoietin (minimum treatment p-value = $1.33 \times 10^{-5}$), hepatocyte growth factor (HGF) (minimum treatment p-value = $2.10 \times 10^{-5}$) and extracellular-signal-regulated kinase 5 (ERK5) (minimum treatment p-value = $1.67 \times 10^{-5}$) which are important regulators of several developmental pathways including

those relevant to cellular processes such as cell growth, proliferation, differentiation, migration, survival and apoptosis (Jain and Samuelson, 2006, Ehrenreich et al., 2005, Comoglio, 2001, Wang and Tournier, 2006, Nishimoto and Nishida, 2006). The most notable differences were in the amphetamine and cocaine treatment conditions for pathways relating to MIF (macrophage migration inhibitory factor)-mediated glucocorticoid regulation and HGF signalling, and circadian rhythms, respectively (**Figure 5.1**).

To identify pathways that were distinct amongst the different drug treatments, we analysed the top ten affected genes from each treatment condition separately. Following this criteria little overlap was observed (**Figure 5.2**). This likely reflects a bias towards a particular gene(s) as exemplified by the BCR gene within the amphetamine treatment condition which accounted for 7/10 of the pathways, all of which related to G-protein signalling. Sodium valproate treatment showed enrichment for pathways relevant to immune responses involving C5a, IL-1, MIF, NKG2D (Natural-killer group 2, member D) and oncostatin M signalling; all of the pathways included c-Jun and AP-1. Lithium and cocaine treatments were enriched for developmental processes due to the presence of c-Fos, with ERK5 signalling relevant to cell proliferation and neuronal survival and ligand-dependent activation of the ESR1 (Estrogen receptor 1)/AP-1 pathways being common to both conditions. Overlap was also observed between lithium and amphetamine treatments with respect to neurophysiological processing relating to circadian rhythm as a result of NR1D1 which plays a key role in this process (Preitner et al., 2002, Triqueneaux et al., 2004).

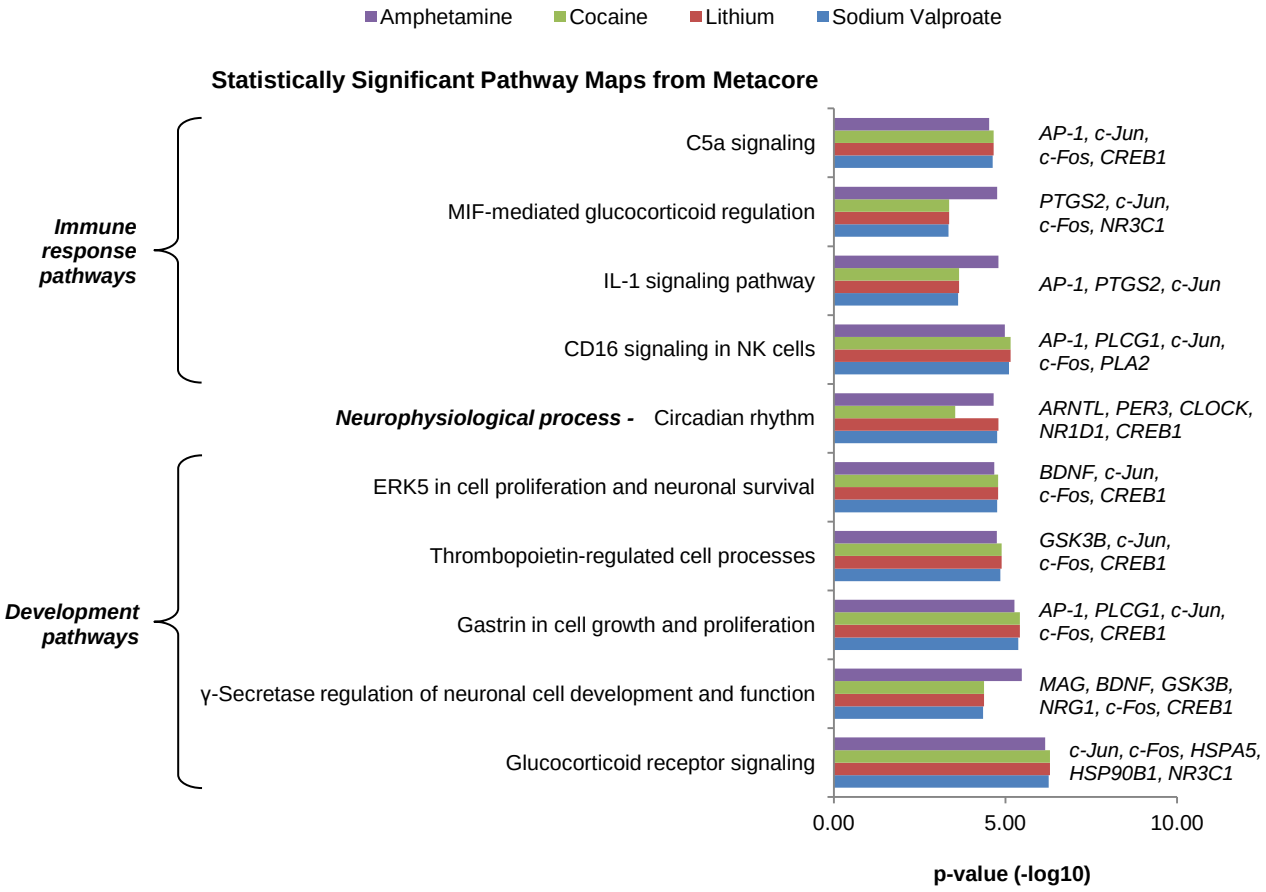


**Figure 5.1. Pathway analysis of gene expression changes in response to drugs affecting mood.** Functional enrichment of gene expression data across all treatment conditions using MetaCore™ pathway analysis software. The top ten statistically significant pathways are displayed and are highly enriched for developmental and immune response processes. Genes from the original list that are associated with the identified signalling pathways are indicated to the right of the chart. Abbreviations: *CD16, Fc receptor III; C5a, complement component 5a; ERK5, extracellular-signal-regulated kinase 5; IL-1, interleukin-1; NK, natural killer; MIF, macrophage migration inhibitory factor.*

### 5.3.3 Network Analysis of genes significantly modulated in response to mood stabilisers

To further explore potential gene networks important in the response to drug challenge, we analysed only the genes whose expression was most affected by lithium and sodium valproate using the Analyse Networks (Transcription Factors) algorithm from MetaCore™. This generates sub-networks through relative enrichment of the uploaded dataset based on the presence of transcription factors and/or receptor targets within the original input file. The gene set used was composed of GAD1, NRG1, PER3, RELN, RGS4, PAFAH1B3, DRD3, FOS and JUN, the first five of which were observed for both lithium and sodium valproate and the remaining were those significantly modified in response to either exposure.

A network containing NRSF, ErbB2 (v-erb-b2 erythroblastic leukemia viral oncogene homolog 2) and ErbB3 as seed nodes was the highest ranked using this approach, and was defined as genes/proteins uploaded from experimental datasets or genes/proteins directly linked to uploaded gene lists from which networks are built (**Figure 5.3**). It included 7 of our 9 input genes (DRD3, FOS, GAD1, JUN, NRG1, PAFAH1B3 and RELN) and had a p-value of $5.24 \times 10^{-29}$ based on hypergeometric distribution which calculated the probability of a particular pathway map arising by chance given the number of genes across all gene pathways, within a particular pathway or sub-network and within the present experimental dataset. The transcription factors identified as being important regulators of this network were c-Fos and c-Jun (collectively AP-1), c-Myc, ESR1, NRSF, PR (Progesterone receptor), RAR-alpha (retinoic acid receptor alpha) and SP3 (Sp3 transcription factor).

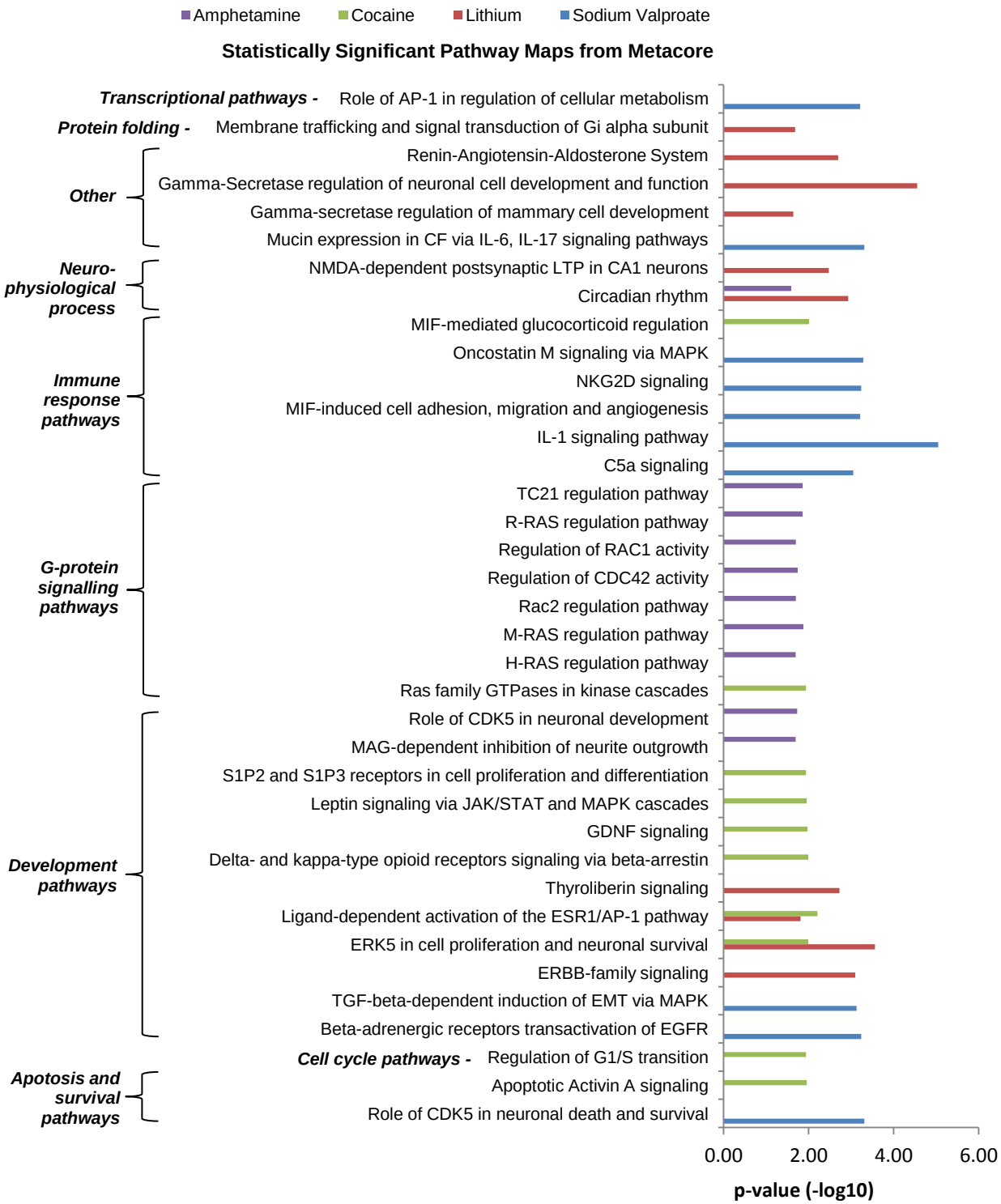


**Figure 5.2. Distinct regulatory pathways associated with different mood modifying drugs.** The top ten affected genes from our qPCR array dataset (see **Table 5.1**) were analysed separately with respect to the different treatment conditions using the pathway analysis tool available in MetaCore™. The top ten statistically significant pathways for each drug are presented and show enrichment of immune response processes with respect sodium valproate treatment, developmental processes with respect to lithium and cocaine treatment and G-protein signalling with respect to amphetamine treatment.

To determine how these regulatory pathways were most relevant for mood disorders, we filtered our dataset using the MetaCore™ 'Filter by Disease' feature which traces all of the known associated interactions for a particular disease process. This assigned 46.15% of our network, not unexpectedly, to disease processes relating to mood (**Figure 5.4A**). Furthermore, it identified NRSF and ERK1/2 signalling along the oestrogen receptor pathway as important regulators of processes relevant to mood disorders involving this subset of genes. In addition to disorders of the CNS, filtering of our dataset by disease showed there to be significant associations (96.15%) with breast, skin and gastrointestinal neoplasia; GAD1 being the only gene not to be involved in these cancer-related pathologies (**Figure 5.4B**). To further assess which signalling pathways may be operating in response to challenge with these mood stabilisers, we also filtered our experimental network for Drug Responses under the Gene Ontology Processes filter. This identified the fibroblast growth factor, ERBB and neurotrophin TRK receptor signalling pathways as important cellular responses, with the dopamine D3 receptor, EGFR (Epidermal growth factor receptor), ErbB2, ErbB3 and c-Src (V-Src Avian Sarcoma [Schmidt-Ruppin A-2] Viral Oncogene) highlighted as therapeutic targets (**Figure 5.4C**).

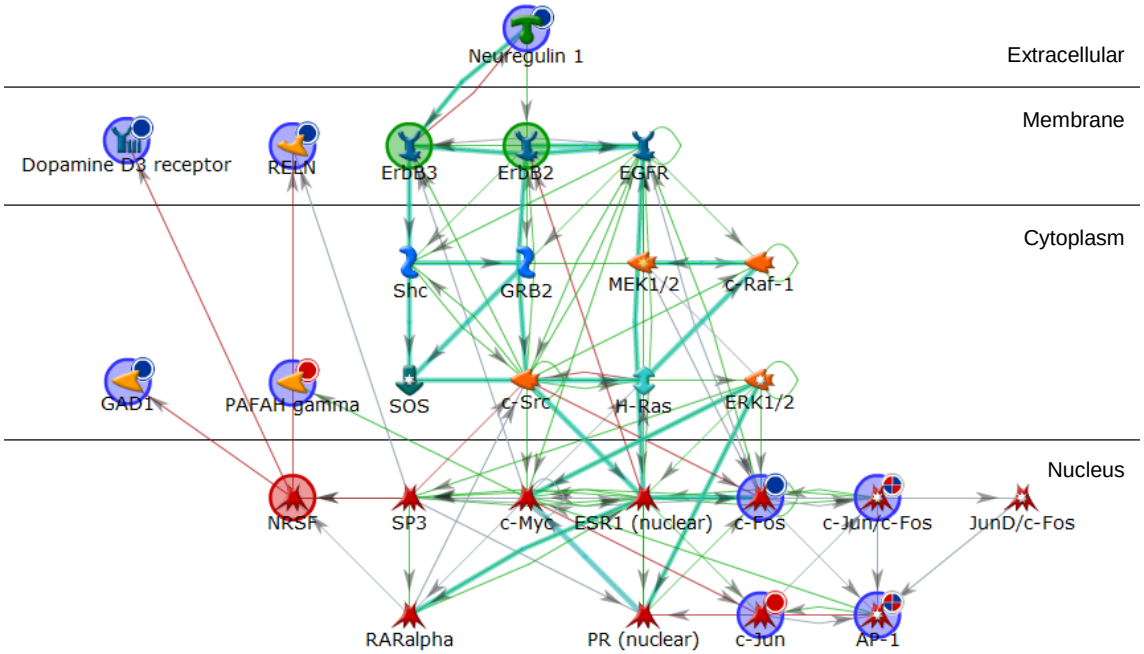


**Figure 5.3. Network Analysis of genes significantly modulated in response to mood stabilisers.** Genes shown to be significantly up or down regulated in human SH-SY5Y cells in response to 1 hour treatment with the mood stabilisers sodium valproate and lithium were uploaded into MetaCore™ for network analysis. The gene list was analysed under the Build Network feature using the Transcription Factor Targets Modelling algorithm. Seed nodes from which the network was built upon are encompassed by a large circle; blue circles represent genes from the experimental data, green circles represent molecules from which the pathway is expanded from and red circles represent molecules on which the pathway terminates. Genes uploaded from the experimental data are also marked with a smaller circle in their top right hand corner; red circles represent genes that were significantly up-regulated, whereas blue circles represent genes significantly down-regulated. Connecting arrows indicate interactions; green arrows represent activation, red arrows represent inhibition and blue arrows are unspecified. Overlaid cyan lines represent canonical pathways. Gene names/symbols within the network from top to bottom, left to right: *Neuregulin 1, Dopamine D3 receptor, RELN, ErbB3, ErbB2, EGFR, Shc, GRB2, MEK1/2, c-Raf-1, GAD1 PAFAH gamma, SOS, c-Src, H-Ras, ERK1/2, NRSF, SP3, c-Myc, ESR1 (nuclear), c-Fos, c-Jun/c-Fos, JunD/c-Fos, RARalpha, PR (nuclear) c-Jun, and AP-1.*

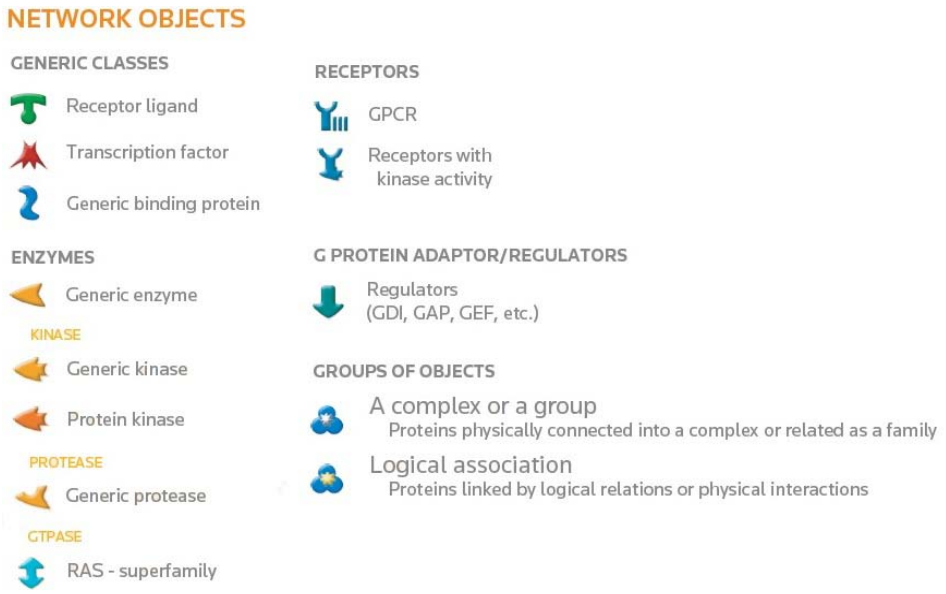


**Figure 5.4. Network analysis filters for disease and gene ontology processes.** The network generated in relation to genes significantly regulated in response to SH-SY5Y cell treatment with sodium valproate and lithium (**Figure 5.3**) was filtered to show the relevant disease pathways (**A** and **B**) and gene ontology processes (**C**). **A-B**, Disease processes relevant to mood disorders (**A**), represents 46.15% of the gene network; and breast, skin and gastrointestinal neoplasms (**B**), represents 96.15% of the gene network. **C**, Gene ontology processes relevant to drug response. Seed nodes from which the network was build upon are encompassed by a large blue circle. Genes uploaded from the experimental data are also marked with a smaller circle in their top right hand corner; red circles represent genes that were significantly up-regulated, whereas blue circles represent genes significantly down-regulated. Connecting blue arrows indicate direct interactions, yellow arrows indicate interactions that are in the base but do not form part of the network and overlaid cyan lines represent canonical pathways. Gene names/symbols within network **A**, from top to bottom, left to right: *Neuregulin 1, Dopamine D3 receptor, Reelin, ERK1/2, MEK1/2, NRSF, ESR1 (nuclear), c-Fos, c-Jun/c-Fos, JunD/c-Fos, PR (nuclear) and AP-1;* **B**, from top to bottom, left to right: *Neuregulin 1, Dopamine D3 receptor, Reelin, ErbB3, ErbB2, EGFR, SOS, Shc,GRB2, c-Raf-1, PAFAH gamma, H-Ras, c-Src, ERK1/2, MEK1/2,NRSF, SP3, c-Myc, ESR1 (nuclear), c-Fos, c-Jun/c-Fos, JunD/c-Fos, RARalpha, PR (nuclear), c-Jun and AP-1; and* **C**, from top to bottom, left to right: *Dopamine D3 receptor, Reelin, ErbB3, ErbB2, EGFR, GAD1, c-Src, NRSF, c-Myc, c-Fos, c-Jun/c-Fos, JunD/c-Fos, c-Jun and AP-1*. [Figure presented on opposite page].

**A**

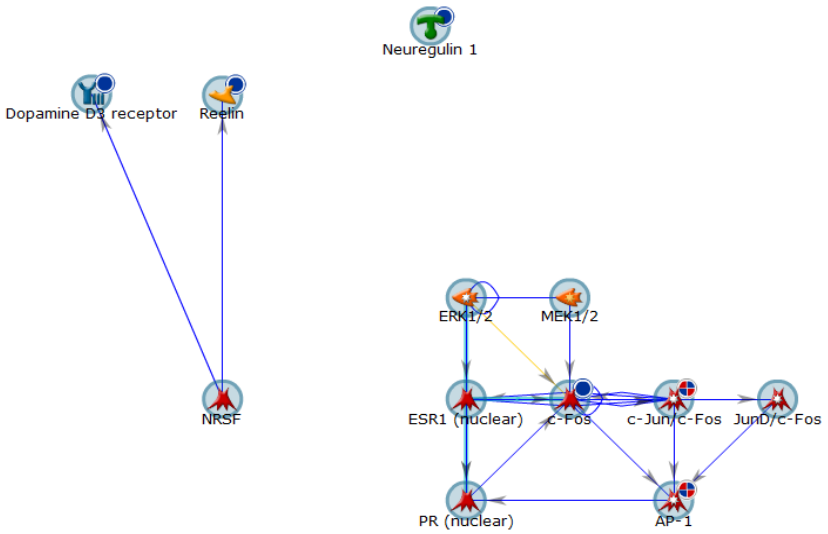
Neuregulin 1
Dopamine D3 receptor
Reelin
NRSF
ERK1/2
MEK1/2
ESR1 (nuclear)
c-Fos
c-Jun/c-Fos
JunD/c-Fos
PR (nuclear)
AP-1

**B**

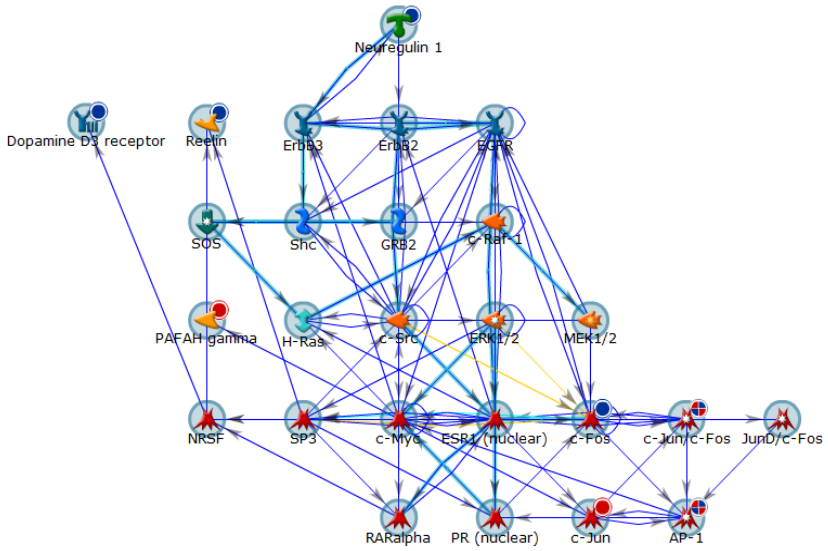
Neuregulin 1
Dopamine D3 receptor
Reelin
ErbB3
ErbB2
EGFR
SOS
Shc
GRB2
c-Raf-1
PAFAH gamma
H-Ras
c-Src
ERK1/2
MEK1/2
NRSF
SP3
c-Myc
ESR1 (nuclear)
c-Fos
c-Jun/c-Fos
JunD/c-Fos
RARalpha
PR (nuclear)
c-Jun
AP-1

**C**

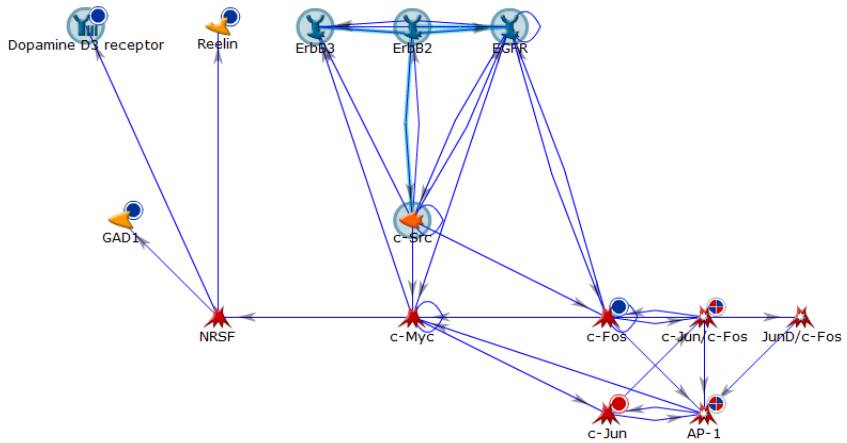
Dopamine D3 receptor
Reelin
ErbB3
ErbB2
EGFR
GAD1
c-Src
NRSF
c-Myc
c-Fos
c-Jun/c-Fos
JunD/c-Fos
c-Jun
AP-1

### 5.3.4 NRSF modulation in response to mood stabilising drugs

As our gene expression data showed that 7/9 of the significantly modulated genes were down-regulated and NRSF which predominantly functions as a transcriptional repressor was identified as an important regulator of our gene set, we addressed predicted NRSF binding sites using ENCODE data from the Transcription Factor ChIP-seq track (The ENCODE Project Consortium, 2011, Rosenbloom et al., 2013) on the UCSC Genome Browser. As shown in **Table 5.2**, this identified NRSF binding at the promoter regions (within 5 Kb of the transcription start site, TSS) of DRD3 (transcript variant a, e and g), FOS, GAD1, JUN, NRG1 (transcript variant HRG-gamma1/2/3, HRG-beta1/d-, 2- and 3b, ndf43/b/c, HRG-alpha and SMDF), PAFAH1B3 and RGS4 (transcript variant 2/3) which, with the exception of JUN and PAFAH1B3, were all down-regulated in response to 1 hour treatment with sodium valproate (or lithium with respect to FOS). We addressed NRSF mRNA levels in response to 1 hour treatment with drugs affecting mood using SH-SY5Y cDNA generated for qPCR arrays outlined in this study. The primer set used targets all isoforms of NRSF. NRSF expression was down-regulated following treatment with the mood stabilisers sodium valproate (fold change, -1.77; SD 0.11; *P<0.05) and lithium (fold change, -1.50; SD 0.19; ***P<0.001), and up-regulated by cocaine whereas amphetamine treatment had no effect on NRSF mRNA levels under the time course and drug concentration used (**Figure 5.5**).

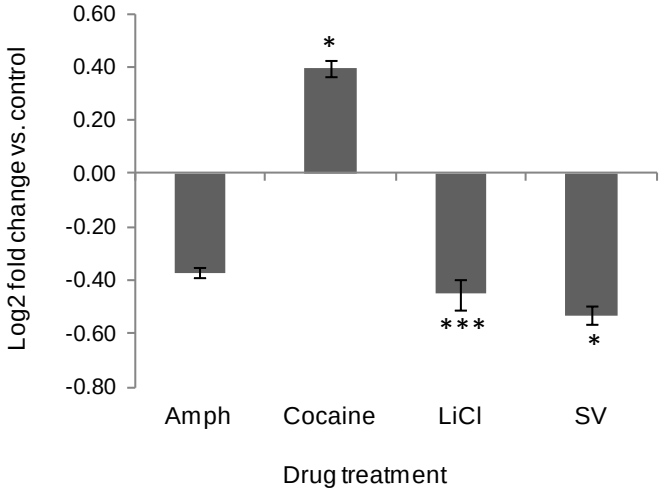


**Figure 5.5. Expression profiling of NRSF mRNA in SH-SY5Y cells following 1 hour treatment with mood modifying drugs.** Bars represent the average log2 fold change in NRSF expression (primer set targets all isoforms of NRSF) of treated cells versus control cells analysed using the Delta-Delta Ct method. Each sample was measured in triplicate and normalised to ACTB expression. RT-qPCR data is representative of 3 biological replicates. Error bars represent the SD for relative fold change between experimental replicates. Significant changes in expression between treated and control cells were determined using a two-tailed student *t*-test. * P<0.05, *** P<0.001. Abbreviations: *Amp, amphetamine; LiCl, lithium chloride; SV, sodium valproate.*

**Table 5.2.** Predicted NRSF regulation of genes affecting mood.

| Gene | Locus | Strand | NRSF site | Size (Bp) | Position |
|---|---|---|---|---|---|
| ACE | chr17:61554422-61575741 | + | chr17:61553914-61554174 | 260 | -508 |
| ACE | chr17:61554422-61575741 | + | chr17:61554504-61554774 | 270 | 82 |
| ACE | chr17:61554422-61575741 | + | chr17:61556270-61556594 | 324 | 1848 |
| ACE | chr17:61554422-61575741 | + | chr17:61557174-61557444 | 270 | 2752 |
| ACE | chr17:61554422-61575741 | + | chr17:61558309-61558579 | 270 | 3887 |
| ADRBK2 | chr22:25960861-26125258 | + | chr22:25961290-25961560 | 270 | 429 |
| ADRBK2 | chr22:25960861-26125258 | + | chr22:26052841-26053085 | 244 | 91980 |
| ADRBK2 | chr22:25960861-26125258 | + | chr22:26097050-26097320 | 270 | 136189 |
| ARNTL | chr11:13277734-13387266 | + | chr11:13283216-13283586 | 370 | 5482 |
| ARNTL | chr11:13277734-13387266 | + | chr11:13298458-13299341 | 883 | 20724 |
| ARNTL | chr11:13277734-13387266 | + | chr11:13310624-13311040 | 416 | 32890 |
| ARNTL | chr11:13277734-13387266 | + | chr11:13312905-13313275 | 370 | 35171 |
| ARNTL | chr11:13277734-13387266 | + | chr11:13351630-13351900 | 270 | 73896 |
| ARNTL | chr11:13277734-13387266 | + | chr11:13361071-13361575 | 504 | 83337 |
| ARNTL | chr11:13277734-13387266 | + | chr11:13364729-13364973 | 244 | 86995 |
| ARNTL | chr11:13277734-13387266 | + | chr11:13365612-13366116 | 504 | 87878 |
| BCR | chr22:23522552-23660224 | + | chr22:23525622-23525892 | 270 | 3070 |
| BCR | chr22:23522552-23660224 | + | chr22:23546679-23546949 | 270 | 24127 |
| BCR | chr22:23522552-23660224 | + | chr22:23562075-23562399 | 324 | 39523 |
| BCR | chr22:23522552-23660224 | + | chr22:23566052-23566322 | 270 | 43500 |
| BCR | chr22:23522552-23660224 | + | chr22:23591914-23592184 | 270 | 69362 |
| BCR | chr22:23522552-23660224 | + | chr22:23624008-23624332 | 324 | 101456 |
| BCR | chr22:23522552-23660224 | + | chr22:23647903-23648174 | 271 | 125351 |
| BCR | chr22:23522552-23660224 | + | chr22:23651156-23651400 | 244 | 128604 |
| BDNF | chr11:27676442-27743605 | - | chr11:27667673-27667943 | 270 | -8499 |
| BDNF | chr11:27676442-27743605 | - | chr11:27671454-27671716 | 262 | -4726 |
| BDNF | chr11:27676442-27743605 | - | chr11:27680076-27680346 | 270 | 63259 |
| BDNF | chr11:27676442-27743605 | - | chr11:27721240-27721484 | 244 | 22121 |
| BDNF | chr11:27676442-27743605 | - | chr11:27723005-27723329 | 324 | 20276 |
| BDNF | chr11:27676442-27743605 | - | chr11:27739843-27740167 | 324 | 3438 |
| BDNF | chr11:27676442-27743605 | - | chr11:27740692-27741122 | 430 | 2483 |
| BDNF | chr11:27676442-27743605 | - | chr11:27741795-27742502 | 707 | 1103 |
| BDNF | chr11:27676442-27743605 | - | chr11:27742701-27743071 | 370 | 534 |
| BDNF | chr11:27676442-27743605 | - | chr11:27743607-27744258 | 651 | +2 |
| BDNF | chr11:27676442-27743605 | - | chr11:27744566-27744890 | 324 | +961 |
| CASP8 | chr2:202098166-202152434 | + | chr2:202096900-202097280 | 380 | -1266 |
| CASP8 | chr2:202098166-202152434 | + | chr2:202098061-202098441 | 380 | -105 |
| CASP8 | chr2:202098166-202152434 | + | chr2:202122713-202123093 | 380 | 24547 |
| CRH | chr8:67088612-67090846 | - | chr8:67089099-67090281 | 1182 | 565 |
| CRH | chr8:67088612-67090846 | - | chr8:67090287-67090659 | 372 | 187 |
| CRH | chr8:67088612-67090846 | - | chr8:67090956-67091280 | 324 | +110 |
| CRH | chr8:67088612-67090846 | - | chr8:67091915-67092285 | 370 | +1069 |
| CRH | chr8:67088612-67090846 | - | chr8:67098519-67098889 | 370 | +7673 |
| DISC1 | chr1:231762561-232177019 | + | chr1:231795960-231796330 | 370 | 33399 |
| DISC1 | chr1:231762561-232177019 | + | chr1:231814930-231815200 | 270 | 52369 |
| DISC1 | chr1:231762561-232177019 | + | chr1:231925791-231926295 | 504 | 163230 |
| DISC1 | chr1:231762561-232177019 | + | chr1:231963016-231963520 | 504 | 200455 |
| DISC1 | chr1:231762561-232177019 | + | chr1:231964053-231964309 | 256 | 201492 |
| DISC1 | chr1:231762561-232177019 | + | chr1:232067746-232067990 | 244 | 305185 |
| DISC1 | chr1:231762561-232177019 | + | chr1:232148522-232148892 | 370 | 385961 |
| **DRD3** | chr3:113847557-113918254 | - | chr3:113871366-113871690 | 324 | 46564 |

| | | | | | |
|---|---|---|---|---|---|
| **DRD3** | chr3:113847557-113918254 | - | chr3:113874262-113874642 | 380 | 43612 |
| **DRD3** | chr3:113847557-113918254 | - | chr3:113897607-113898013 | 406 | 20241 |
| **DRD3** | chr3:113847557-113918254 | - | chr3:113898443-113898813 | 370 | 19441 |
| DRD4 | chr11:637305-640705 | + | chr11:640330-640654 | 324 | 3025 |
| DTNBP1 | chr6:15523032-15663289 | - | chr6:15552018-15552288 | 270 | 111001 |
| DTNBP1 | chr6:15523032-15663289 | - | chr6:15621994-15622224 | 230 | 41065 |
| DTNBP1 | chr6:15523032-15663289 | - | chr6:15662506-15662830 | 324 | 459 |
| FKBP5 | chr6:35541362-35696397 | - | chr6:35656504-35656848 | 344 | 39549 |
| FKBP5 | chr6:35541362-35696397 | - | chr6:35687515-35687759 | 244 | 8638 |
| FKBP5 | chr6:35541362-35696397 | - | chr6:35695292-35695562 | 270 | 835 |
| FKBP5 | chr6:35541362-35696397 | - | chr6:35695873-35696103 | 230 | 294 |
| FKBP5 | chr6:35541362-35696397 | - | chr6:35699743-35700105 | 362 | -3346 |
| **FOS** | chr14:75745481-75748937 | + | chr14:75743830-75744074 | 244 | -1651 |
| **FOS** | chr14:75745481-75748937 | + | chr14:75745296-75745800 | 504 | -185 |
| GABRA5 | chr15:27111866-27194357 | + | chr15:27110041-27110545 | 504 | -1825 |
| GABRA5 | chr15:27111866-27194357 | + | chr15:27111625-27112129 | 504 | -241 |
| **GAD1** | chr2:171673200-171717659 | + | chr2:171670663-171671101 | 438 | -2537 |
| **GAD1** | chr2:171673200-171717659 | + | chr2:171671290-171671546 | 256 | -1910 |
| **GAD1** | chr2:171673200-171717659 | + | chr2:171672190-171672567 | 377 | -1010 |
| **GAD1** | chr2:171673200-171717659 | + | chr2:171679546-171679776 | 230 | 6346 |
| **GAD1** | chr2:171673200-171717659 | + | chr2:171701873-171702253 | 380 | 28673 |
| GRIK3 | chr1:37261128-37499844 | - | chr1:37269486-37269856 | 370 | 229988 |
| GRIK3 | chr1:37261128-37499844 | - | chr1:37301874-37302144 | 270 | 197700 |
| GRIK3 | chr1:37261128-37499844 | - | chr1:37329834-37330078 | 244 | 169766 |
| GRIK3 | chr1:37261128-37499844 | - | chr1:37331752-37332256 | 504 | 167588 |
| GRIK3 | chr1:37261128-37499844 | - | chr1:37332540-37332784 | 244 | 167060 |
| GRIK3 | chr1:37261128-37499844 | - | chr1:37388506-37388750 | 244 | 111094 |
| GRIK3 | chr1:37261128-37499844 | - | chr1:37389788-37390253 | 465 | 109591 |
| GRIK3 | chr1:37261128-37499844 | - | chr1:37411488-37411732 | 244 | 88112 |
| GRIK3 | chr1:37261128-37499844 | - | chr1:37431706-37432281 | 575 | 67563 |
| GRIK3 | chr1:37261128-37499844 | - | chr1:37486267-37486654 | 387 | 13190 |
| GRIK3 | chr1:37261128-37499844 | - | chr1:37494616-37494860 | 244 | 4984 |
| GRIK3 | chr1:37261128-37499844 | - | chr1:37504779-37505043 | 264 | -4935 |
| GRM3 | chr7:86273230-86494192 | + | chr7:86290343-86290599 | 256 | 17113 |
| GRM3 | chr7:86273230-86494192 | + | chr7:86322086-86322456 | 370 | 48856 |
| GRM3 | chr7:86273230-86494192 | + | chr7:86476174-86476554 | 380 | 202944 |
| GRM3 | chr7:86273230-86494192 | + | chr7:86497476-86497720 | 244 | +3284 |
| **JUN** | chr1:59246463-59249785 | - | chr1:59249472-59249885 | 413 | -100 |
| MAG | chr19:35782989-35820133 | + | chr19:35796870-35797100 | 230 | 13881 |
| MAG | chr19:35782989-35820133 | + | chr19:35809956-35810280 | 324 | 26967 |
| MAOA | chrX:43,515,409-43,606,068 | + | - | - | - |
| MLC1 | chr22:50,497,820-50,523,781 | - | - | - | - |
| MOBP | chr3:39543557-39567857 | + | chr3:39540121-39540386 | 265 | -3436 |
| MOBP | chr3:39543557-39567857 | + | chr3:39558349-39558719 | 370 | 14792 |
| MOBP | chr3:39543557-39567857 | + | chr3:39574318-39574698 | 380 | +6461 |
| MTHFR | chr1:11845787-11866160 | - | chr1:11845214-11845454 | 240 | +573 |
| MTHFR | chr1:11845787-11866160 | - | chr1:11850982-11851306 | 324 | 14854 |
| MTHFR | chr1:11845787-11866160 | - | chr1:11856563-11856793 | 230 | 9367 |
| MTHFR | chr1:11845787-11866160 | - | chr1:11857775-11857960 | 185 | 8200 |
| MTHFR | chr1:11845787-11866160 | - | chr1:11858618-11858699 | 81 | 7461 |
| MTHFR | chr1:11845787-11866160 | - | chr1:11863764-11864034 | 270 | 2126 |
| MTHFR | chr1:11845787-11866160 | - | chr1:11865502-11865882 | 380 | 278 |
| MTHFR | chr1:11845787-11866160 | - | chr1:11866038-11866425 | 387 | -265 |
| NAPG | chr18:10525873-10552766 | + | chr18:10525815-10526242 | 427 | -58 |

| | | | | | |
|---|---|---|---|---|---|
| NCAM1 | chr11:112831969-113092626 | + | chr11:112831909-112832179 | 270 | -60 |
| NCAM1 | chr11:112831969-113092626 | + | chr11:112977293-112977549 | 256 | 145324 |
| NCAM1 | chr11:112831969-113092626 | + | chr11:113008930-113009200 | 270 | 176961 |
| NCAM1 | chr11:112831969-113092626 | + | chr11:113011853-113012123 | 270 | 179884 |
| NCAM1 | chr11:112831969-113092626 | + | chr11:113023160-113023664 | 504 | 191191 |
| NCAM1 | chr11:112831969-113092626 | + | chr11:113074175-113074445 | 270 | 242206 |
| NR1D1 | chr17:38249037-38256973 | - | chr17:38244467-38244847 | 380 | +4570 |
| NR1D1 | chr17:38249037-38256973 | - | chr17:38254215-38254595 | 380 | 2378 |
| NR1D1 | chr17:38249037-38256973 | - | chr17:38255228-38255666 | 438 | 1307 |
| NR1D1 | chr17:38249037-38256973 | - | chr17:38256685-38257094 | 409 | -121 |
| NR1D1 | chr17:38249037-38256973 | - | chr17:38257324-38257828 | 504 | -351 |
| NR1D1 | chr17:38249037-38256973 | - | chr17:38264445-38264769 | 324 | -7472 |
| NR3C1 | chr5:142657496-142783254 | - | chr5:142784785-142785394 | 609 | -2140 |
| **NRG1** | chr8:31496911-32622558 | + | chr8:31499444-31499814 | 370 | 2533 |
| **NRG1** | chr8:31496911-32622558 | + | chr8:31612484-31612740 | 256 | 115573 |
| **NRG1** | chr8:31496911-32622558 | + | chr8:31629195-31629565 | 370 | 132284 |
| **NRG1** | chr8:31496911-32622558 | + | chr8:31652781-31653242 | 461 | 155870 |
| **NRG1** | chr8:31496911-32622558 | + | chr8:31691004-31691508 | 504 | 194093 |
| **NRG1** | chr8:31496911-32622558 | + | chr8:31817830-31818086 | 256 | 320919 |
| **NRG1** | chr8:31496911-32622558 | + | chr8:31896212-31896582 | 370 | 399301 |
| **NRG1** | chr8:31496911-32622558 | + | chr8:32084240-32084744 | 504 | 587329 |
| **NRG1** | chr8:31496911-32622558 | + | chr8:32122327-32122831 | 504 | 625416 |
| **NRG1** | chr8:31496911-32622558 | + | chr8:32189091-32189595 | 504 | 692180 |
| **NRG1** | chr8:31496911-32622558 | + | chr8:32191794-32192298 | 504 | 694883 |
| **NRG1** | chr8:31496911-32622558 | + | chr8:32200953-32201685 | 732 | 704042 |
| **NRG1** | chr8:31496911-32622558 | + | chr8:32245491-32245735 | 244 | 748580 |
| **NRG1** | chr8:31496911-32622558 | + | chr8:32276508-32276752 | 244 | 779597 |
| **NRG1** | chr8:31496911-32622558 | + | chr8:32284202-32284706 | 504 | 787291 |
| **NRG1** | chr8:31496911-32622558 | + | chr8:32392615-32392985 | 370 | 895704 |
| **NRG1** | chr8:31496911-32622558 | + | chr8:32405958-32406282 | 324 | 909047 |
| **NRG1** | chr8:31496911-32622558 | + | chr8:32406492-32406892 | 400 | 909581 |
| **NRG1** | chr8:31496911-32622558 | + | chr8:32411341-32411845 | 504 | 914430 |
| **NRG1** | chr8:31496911-32622558 | + | chr8:32487206-32487506 | 300 | 990295 |
| **NRG1** | chr8:31496911-32622558 | + | chr8:32488853-32489109 | 256 | 991942 |
| **NRG1** | chr8:31496911-32622558 | + | chr8:32503654-32504024 | 370 | 1006743 |
| **NRG1** | chr8:31496911-32622558 | + | chr8:32546371-32546746 | 375 | 1049460 |
| **NRG1** | chr8:31496911-32622558 | + | chr8:32572641-32573145 | 504 | 1075730 |
| **NRG1** | chr8:31496911-32622558 | + | chr8:32581201-32581705 | 504 | 1084290 |
| **NRG1** | chr8:31496911-32622558 | + | chr8:32582687-32583047 | 360 | 1085776 |
| **PAFAH1B3** | chr19:42801185-42806952 | - | chr19:42806435-42806939 | 504 | -13 |
| **PER3** | chr1:7844714-7905237 | + | ~14 Kb upstream of 5'UTR | - | - |
| PDLIM5 | chr4:95373038-95509370 | + | chr4:95372903-95373283 | 380 | -135 |
| PDLIM5 | chr4:95373038-95509370 | + | chr4:95406777-95407007 | 230 | 33739 |
| PDLIM5 | chr4:95373038-95509370 | + | chr4:95418920-95419164 | 244 | 45882 |
| PDLIM5 | chr4:95373038-95509370 | + | chr4:95455973-95456203 | 230 | 82935 |
| PDLIM5 | chr4:95373038-95509370 | + | chr4:95456267-95456511 | 244 | 83229 |
| PDLIM5 | chr4:95373038-95509370 | + | chr4:95471601-95471831 | 230 | 98563 |
| PDLIM5 | chr4:95373038-95509370 | + | chr4:95499407-95499663 | 256 | 126369 |
| **RELN** | chr7:103112231-103629963 | - | chr7:103127865-103128245 | 380 | 501718 |
| **RELN** | chr7:103112231-103629963 | - | chr7:103276613-103276992 | 379 | 352971 |
| **RELN** | chr7:103112231-103629963 | - | chr7:103297949-103298179 | 230 | 331784 |
| **RELN** | chr7:103112231-103629963 | - | chr7:103301028-103301258 | 230 | 328705 |
| **RELN** | chr7:103112231-103629963 | - | chr7:103354935-103355205 | 270 | 274758 |
| **RELN** | chr7:103112231-103629963 | - | chr7:103438111-103438481 | 370 | 191482 |
| **RELN** | chr7:103112231-103629963 | - | chr7:103451010-103451107 | 97 | 178856 |

| | | | | | |
|---|---|---|---|---|---|
| **RELN** | chr7:103112231-103629963 | - | chr7:103484281-103484449 | 168 | 145514 |
| **RELN** | chr7:103112231-103629963 | - | chr7:103491745-103492249 | 504 | 137714 |
| **RELN** | chr7:103112231-103629963 | - | chr7:103559848-103560078 | 230 | 69885 |
| **RELN** | chr7:103112231-103629963 | - | chr7:103580845-103581215 | 370 | 48748 |
| **RELN** | chr7:103112231-103629963 | - | chr7:103636658-103636861 | 203 | -6898 |
| RFX4 | chr12:106976685-107156582 | + | chr12:106975282-106975646 | 364 | -1403 |
| RFX4 | chr12:106976685-107156582 | + | chr12:106975776-106976119 | 343 | -909 |
| RFX4 | chr12:106976685-107156582 | + | chr12:107147300-107147544 | 244 | 170615 |
| **RGS4** | chr1:163038396-163046592 | + | chr1:163039054-163039341 | 287 | 658 |
| SLC12A6 | chr15:34522197-34630265 | - | chr15:34516950-34517512 | 562 | +5247 |
| SLC12A6 | chr15:34522197-34630265 | - | chr15:34610582-34611086 | 504 | 19179 |
| SLC12A6 | chr15:34522197-34630265 | - | chr15:34630069-34630393 | 324 | -128 |
| SLC12A6 | chr15:34522197-34630265 | - | chr15:34634991-34635543 | 552 | -4726 |
| SLC6A2 | chr16:55689542-55737700 | + | chr16:55686047-55686317 | 270 | -3495 |
| SLC6A2 | chr16:55689542-55737700 | + | chr16:55689638-55689908 | 270 | 96 |
| SLC6A2 | chr16:55689542-55737700 | + | chr16:55690575-55690845 | 270 | 1033 |
| SLC6A2 | chr16:55689542-55737700 | + | chr16:55693927-55694197 | 270 | 4385 |
| SLC6A2 | chr16:55689542-55737700 | + | chr16:55695818-55696088 | 270 | 6276 |
| SLC6A2 | chr16:55689542-55737700 | + | chr16:55696686-55696956 | 270 | 7144 |
| SLC6A2 | chr16:55689542-55737700 | + | chr16:55744402-55744761 | 359 | +7061 |
| SLC6A2 | chr16:55689542-55737700 | + | chr16:55746277-55746521 | 244 | +8821 |
| SLC6A4 | chr17:28,523,378-28,562,954 | - | - | - | - |
| SULT1A1 | chr16:28616908-28634907 | - | chr16:28621167-28621407 | 240 | 13500 |
| TF | chr3:133419211-133497850 | + | chr3:133461483-133461863 | 380 | 42272 |
| TF | chr3:133419211-133497850 | + | chr3:133465027-133465407 | 380 | 45816 |
| TF | chr3:133419211-133497850 | + | chr3:133472690-133472920 | 230 | 53479 |
| TIMELESS | chr12:56810157-56843200 | - | chr12:56811537-56811907 | 370 | 31293 |
| TIMELESS | chr12:56810157-56843200 | - | chr12:56842752-56843263 | 511 | -63 |
| TPH2 | chr12:72332626-72426221 | + | chr12:72332400-72332889 | 489 | -226 |
| TPH2 | chr12:72332626-72426221 | + | chr12:72374868-72375372 | 504 | 42242 |
| TPH2 | chr12:72332626-72426221 | + | chr12:72410895-72411165 | 270 | 78269 |
| XBP1 | chr22:29190548-29196560 | - | chr22:29196394-29196960 | 566 | -400 |
| XBP1 | chr22:29190548-29196560 | - | chr22:29198252-29198482 | 230 | -1922 |

*Note:* NRSF binding sites over the top 10 affected genes across all drug treatments from Transcription Factor ChIP-seq from ENCODE, version 4. Bold font indicates genes significantly affected by drug challenge. Negative and positive values under *Position* represent the location of the NRSF site upstream of the gene transcription start site and downstream of the 3'UTR, respectively. Values not assigned +/- represent binding sites within the gene sequence. For genes with multiple transcripts, binding site positions are with respect to the largest isoform.

### 5.3.5 Extension of the NRSF regulatory network to microRNA (miRNA) genes through *in silico* analysis

Dysregulation of miRNA genes has been widely implicated in disease pathways, including several neuropsychiatric conditions such as depression, schizophrenia and drug addiction, reviewed in Im and Kenny (2012). GWAS have identified genetic variants within miRNA gene loci or their target sequences as being significantly correlated with disease pathways (Liu et al., 2012a, Huan et al., 2015). This has recently been demonstrated for non-coding SNPs within the MIR137 gene in predicting susceptibility to schizophrenia (The Schizophrenia Psychiatric GWAS Consortium, 2011, Ripke et al., 2013). The intronic location of these SNPs suggests a regulatory function which could act to modify the levels of transcription of the target gene, for example through altering binding site motifs of transcription factors or epigenetic regulators. In the previous chapter we presented data to suggest that NRSF may be one mechanism operating at the MIR137 gene locus in response to cocaine treatment. The potential role for NRSF in regulating the MIR137 gene was identified from bioinformatic analysis of the region, and validated through ChIP and reporter gene studies which showed that NRSF could bind to and modulate the transcriptional activity of an internal promoter VNTR within this miRNA gene in an allele-specific and stimulus-inducible manner (Warburton et al., 2014). The existence of extensive double-feedback mechanisms between the NRSF-signalling complex and the brain-related miRNAs has been suggested based on computational analysis of the presence of NRSF recognition sites termed NRSEs (neuron restrictive silencing elements) within 25 Kb (Wu and Xie, 2006) and 100 Kb (Johnson et al., 2008) of miRNA genes. These studies

identified a total of 21 miRNA genes based on NRSEs discovered through position weight matrices (PWMs), which are probabilistic representations of signals in DNA or protein sequences which can be used to model approximate patterns of DNA-protein or protein-protein interactions; however they did not recognise the recently validated NRSF target gene MIR137 (Warburton et al., 2014, Soldati et al., 2013), which was identified from *in silico* analysis of human ENCODE ChIP-seq data (Warburton et al., 2014). To extend these previous analyses of NRSF-miRNA interactions, which may be an important regulatory network involved in neurological disease processes due to its potential to modulate hundreds of downstream target genes in response to environmental stimuli, we intersected data downloaded from the UCSC Genome Browser (https://genome.ucsc.edu/) for global NRSF binding sites based on ENCODE ChIP-seq data with precursor sequences for miRNA genes plus their upstream 10 Kb flank sequence using the online platform Galaxy (https://usegalaxy.org/), see *Methods section 2.2.6.8*. This identified 335 human miRNA genes bound by NRSF (*Appendix 6*), 32 of which had enrichment of this transcription factor within the first 500 bp of sequence 5' of the precursor (pre)-miRNA sequence, **Table 5.3**; an arbitrary value used as a cut-off for defining the proximal promoter region based on reporter gene analysis of the internal MIR137 promoter (Imir137) and the labs previous work on NRSE-like motifs within promoter sequences of neuropeptide genes that are situated within close proximity of the major TSS (Warburton et al., 2014, Coulson et al., 1999, Quinn et al., 2002, Spencer et al., 2006, Gillies et al., 2009). Of the 335 miRNAs identified from our in silico analysis, 14 of these (miR-9-1, -9-3, -29b-1, -95, -124-2, -124-3, -132, -135b, -138-1; -153-1, -212, -218-2, -330 and -346)

**Table 5.3.** Predicted NRSF regulation of human miRNA genes

| MicroRNA | Type | Host Gene | Description | Same strand | Protein coding | Repeat type | Repeat position (bp) | NRSF BS position (bp) | RNA Pol II binding | CGI |
|---|---|---|---|---|---|---|---|---|---|---|
| **miR-132 *** | Intergenic, -4.1 Kb | HIC1 | Hypermethylated in cancer 1 | X | ✓ | Low complexity G_rich | -2,370 | Overlaps | ✓ | ✓ |
| **miR-212 *** | Intergenic, -3.8 Kb | | | | | | -1,998 | | | |
| miR-92b * † | Intergenic, -0.3 Kb | THBS3 | Thrombospondin 3 | X | ✓ | Low complexity GC_rich | -2 | -85 | ✓ | ✓ |
| miR-484 * | Exonic | NDE1 | Nuclear distribution E (nudE) homolog 1 | ✓ | ✓ | Low complexity GC_rich | -3 | Overlaps | ✓ | X |
| miR-636 | Intronic | SRSF2 | Serine/arginine-rich splicing factor 2 | ✓ | ✓ | Low complexity GC_rich | Overlaps | Overlaps | ✓ | ✓ |
| miR-760 | Intronic | BCAR3 | Breast cancer anti-estrogen resistance 3 | X | ✓ | Low complexity GC_rich | -75 | -266 | ✓ | ✓ |
| miR-3175 | Intronic | CHD2 | Chromodomain helicase DNA binding protein 2, transcript variant 2 | ✓ | ✓ | Low complexity GC_rich | -187 | Overlaps | ✓ | ✓ |
| miR-3181 | Intronic | CYLD | Cylindromatosis (turban tumor syndrome) | ✓ | ✓ | Low complexity GC_rich | -46 | -195 | ✓ | ✓ |
| miR-21 * | Intergenic, +0.7 Kb | VMP1 | Vacuole membrane protein 1 | ✓ | ✓ | Simple tandem | -69 | Overlaps | ✓ | X |
| miR-137 * | Exonic | MIR137HG | MIR137 Host Gene, non-coding RNA | ✓ | X | Simple tandem | -6 | Overlaps | ✓ | ✓ |
| miR-199a-1 | Intronic | DNM2 | Dynamin 2 | X | ✓ | Simple tandem | -303 | -255 | ✓ | X |
| miR-935 | Exonic | CACNG8 | Calcium channel, voltage-dependent, gamma subunit 8 | ✓ | ✓ | Simple tandem | -260 | Overlaps | ✓ | ✓ |
| miR-2277 | Exonic, 3' UTR | FAM172A | Family with sequence similarity 172, member A | ✓ | ✓ | Simple tandem | -432 | Overlaps | ✓ | ✓ |

| MicroRNA | Type | Host Gene | Description | Same strand | Protein coding | Repeat type | Repeat position (bp) | NRSF BS position (bp) | RNA Pol II binding | CGI |
|---|---|---|---|---|---|---|---|---|---|---|
| miR-3188 | Intergenic, +0.5 Kb | JUND | Jun D proto-oncogene | X | ✓ | Simple tandem | -56 | Overlaps | ✓ | -150 bp |
| miR-3195 | Exonic | TAF4 | TAF4 RNA polymerase II, TBP-associated factor | X | ✓ | Simple tandem | -14 | -377 | ✓ | ✓ |
| miR-4289 | Intergenic, -94 Kb | LOC286238 | Uncharacterised protein | ✓ | ✓ | Simple tandem | -178 | Overlaps | ✓ | X |
| miR-1289-1 | Intergenic, -1 Kb | CEP250 | Centrosomal protein 250kDa | X | ✓ | SINE, Alu | -75 | -479 | ✓ | -1 Kb |
| miR-1287 | Exonic | PYROXD2 | Pyridine nucleotide-disulphide oxidoreductase domain 2 | ✓ | ✓ | SINE, MIR | -260 | Overlaps | -20 Kb at PYROXD2 TSS | X |
| miR-3191 | Intronic | BBC3 | BCL2 binding component 3, nuclear gene encoding mitochondrial protein | ✓ | ✓ | SINE, MIR | -57 | -413 | ✓ | -1 Kb |
| miR-3193 | Intergenic, +0.7 Kb | ID1 | Inhibitor of DNA binding 1, dominant negative helix-loop-helix protein | ✓ | ✓ | SINE, MIR | -228 | Overlaps | ✓ | -1 Kb |
| miR-2114 | Intergenic, +0.3 Kb | LINC00894 | Long intergenic non-protein coding RNA 894 | ✓ | X | LINE, CR1 | -85 | -307 | -25 Kb of pre-miR | X |
| miR-4258 | Intronic | CKS1B | CDC28 protein kinase regulatory subunit 1B | ✓ | ✓ | LINE, L2 | -58 | -321 | ✓ | X |
| miR-210 * | Intronic | MIR210HG | MIR210 Host Gene, non-coding RNA | ✓ | X | Simple tandem; SVA_A | -221; +50 Kb | Overlaps | ✓ | ✓ |
| miR-658 | Exonic, 5' UTR | ANKRD54 | Ankyrin repeat domain 54 | ✓ | ✓ | Simple tandem; SVA_D | -1,229; +50 Kb | Overlaps | ✓ | ✓ |
| miR-345 * TE | Intergenic, -1.3 Kb | SLC25A29 | Solute carrier family 25 (mitochondrial carnitine/acylcarnitine carrier), member 29 | X | ✓ | SINE, MIR; SVA_D | Overlaps, -126 Kb | -496 | ✓ | X |
| **miR-330 * TE** | Intronic | EML2 | Echinoderm microtubule associated protein like 2 | ✓ | ✓ | SINE, MIR; SVA_D | Overlaps, -8,434 | Overlaps | ✓ | X |

| MicroRNA | Type | Host Gene | Description | Same strand | Protein coding | Repeat type | Repeat position (bp) | NRSF BS position (bp) | RNA Pol II binding | CGI |
|---|---|---|---|---|---|---|---|---|---|---|
| miR-422a [TE] | Intergenic, +36 Kb | DAPK2 | Death-associated protein kinase 2 | ✓ | ✓ | SINE, MIR; LINE, L2; SVA_D | Overlaps; -276; -929/+771 Kb | Overlaps | ✓ | X |
| miR-607 [TE] | Intergenic, -3.5 Kb | LCOR | Ligand dependent nuclear receptor corepressor | X | ✓ | SINE, MIR; SVA_E | Overlaps; -112 Kb | -326 | ✓ | X |
| miR-423/3184 | Intronic | NSRP1 | Nuclear speckle splicing regulatory protein 1 | ✓ | ✓ | hAT-Charlie DNA TE; SINE, Alu; LINE, L1 | -465; -787; -1,541 | -35 | ✓ | X |
| **miR-138-1** | Intergenic, -128 Kb | TOPAZ1 | Testis and ovary specific PAZ domain containing protein 1 | ✓ | ✓ | hAT-Charlie DNA TE; LINE, L2; LTR, ERVL | -189; -1,926; -3,174 | -414 | ✓ | X |
| miR-1205 † | Intronic | PVT1 | Pvt1 oncogene, non-coding RNA | ✓ | X | SINE, MIR; LTR, ERVL | -299; -5,232; | -118; Overlaps | ✓ | X |
| miR-1208 † | Intergenic, +49 Kb | | | | | LINE, L2; hAT-Charlie DNA TE; LTR, ERVL; SVA_D | -737; -2,195; -2,525; -31 Kb | NRSF BSs Overlap miRNA, LTR and SVA | | |

*Note:* NRSF binding of putative miRNA gene promoters defined as 5' sequence within 500 bp of the precursor (pre)-miRNA. *Same strand* is with respect to the host gene and miRNA. *Repeat position* and *NRSF binding site (BS) position* is relative to the first base of the pre-miRNA sequence, which is +1 bp, unless stated otherwise. Negative and positive values mark upstream and downstream sequences, respectively. RNA Pol II and CpG islands overlap with the NRSF binding site within the putative promoter region unless stated otherwise; RNA Pol II binding within the proximity of the MIR2114 gene does not overlap with NRSF binding. Bold font indicates miRNAs which overlap with computational predictions of NRSF target miRNAs by Wu and Xie (2006), Johnson et al. (2008) and Gebhardt et al. (2014) based on NRSE position weight matrices and ENCODE ChIP-seq data. Underlined miRNAs represent novel NRSF targets identified in this study. *Validated NRSF target miRNAs (Soldati et al., 2013, Warburton et al., 2014, Johnson et al., 2008, Gao et al., 2012); † Part of a cluster of miRNAs located within close proximity of each other; [TE] Derived-from transposable elements. Abbreviations: *CGI, CpG island; CR1, chicken repeat 1; ERVL, endogenous retroviral element; LINE, long interspersed nuclear element; MIR, mammalian-wide interspersed repeats; LTR, long terminal repeats; SINE, short interspersed nuclear element; SVA, SINE-VNTR-Alu; TBP, TATA box binding protein; TE, transposable element; TSS, transcription start site; UTR, untranslated region*.

overlapped with previous reports by Wu and Xie (2006), Johnson et al. (2008) and Gebhardt et al. (2014), with miR-132/212, -138-1 and miR-330 identified as being enriched for NRSF binding within their proximal promoter regions; three of which have been validated as NRSF targets through ChIP and/or expression profiling following NRSF knock-down, **Table 5.3** (Johnson et al., 2008, Soldati et al., 2013, Otto et al., 2007, Gao et al., 2012). A further 5 miRNAs (miR-21, -92b, -210, -345, -484) identified from our *in silico* analysis have also been shown to be significantly regulated following conditional knockout of NRSF in mouse neural stem cells (Gao et al., 2012), with 22 miRNAs identified as novel NRSF targets. Similar to mechanisms operating at the Imir137 promoter, binding of RNA Pol II, also predicted from ENCODE data, was found to overlap with NRSF sites at all of these putative promoter regions, with the exception of MIR2114 (**Table 5.3**). Overlapping CpG islands observed in half of the target miRNA gene set further supports a promoter function of these loci. To explore which of the identified miRNAs may also be regulated by repetitive elements embedded within their predicted promoter domains, as exemplified through the VNTR within the Imir137 promoter which supported differential reporter gene expression *in vitro* based on copy-number (Warburton et al., 2014), we also intersected our gene list with data from the UCSC-based Repeating Elements by Repeat-Masker track (Jurka, 2000). **Table 5.3** shows that there is enrichment of NRSF binding at repetitive elements within these putative promoter regions including simple tandem repeats and transposable elements (TEs) including long-terminal repeats (LTRs), such as endogenous retroviral elements (ERVL), and non-LTRs, such as long and short interspersed nuclear elements (LINEs/SINEs) and primate-specific SVAs (SINE-VNTR-Alu).

Enrichment at transposable elements supports previous findings by *Johnson et al.* (2006) that functional NRSEs have been duplicated and inserted at new positions in the human genome by transposon-dependent mechanisms. Furthermore, several TE-derived miRNAs have been determined within the human genome (Piriyapongsa et al., 2007), including miR-330, -345, -442a and -607 identified from our *in silico* analysis; all of which have an SVA insertion within 120 Kb 5' of their pre-miRNA sequence (except miR-422a which had SVA insertions ~929 Kb upstream and ~771 Kb downstream), **Table 5.3**.

To explore whether the identified NRSF-target miRNAs have any overlapping roles in normal cellular and/or disease processes, pathway analysis was performed using DIANA-miRPath; a freely available web-based platform for *in silico* assessment of miRNA interactions based on experimentally validated miRNA targets (Vlachos et al., 2012). The top 20 significant pathways based on in-built meta-analysis algorithms are listed in **Table 5.4**. More than half of the pathways identified (several of which were shown to be significantly associated with gene expression changes in response to mood modifying drugs, **Figure 5.2** and **5.3**) have previously been implicated in mood disorders and other neuropsychiatric conditions such as schizophrenia, including the neurotrophin signalling pathway which is represented in **Table 5.5**. Of the experimentally validated miRNA target genes identified in this pathway, 23 overlap with known or putative NRSF target genes (Warburton et al. (2015); Wu and Xie (2006), http://www.broadinstitute.org/~xhx/projects/NRSE/), including BDNF which is highlighted as a target for miR-137 (Hill et al., 2014); another validated NRSF target gene (Warburton et al., 2014, Soldati et al., 2013). JUN, a gene shown to be significantly regulated in response to mood

stabilisers and as a predicted target of NRSF (**Table 5.1** and **5.2**), was also identified in the neurotrophin signalling network as a target of miR-212 which has been validated as having reciprocal interactions with MeCP2 (Im et al., 2010); a member of the NRSF-signalling complex. This provides validity for our *in silico* predicted NRSF target miRNAs and identifies a set of candidate miRNAs that may important in neurological dysfunction. The remaining pathways identified as being significantly associated with our miRNA gene set are linked to cancer (**Table 5.4**); a pathological state which implicates perturbations in both NRSF- and miRNA-signalling pathways and possibly dynamic interaction between the two as discussed in *Chapter 6*.

**Table 5.4.** Top 20 KEGG pathways containing genes that are subject to regulatory control by predicted NRSF-regulated miRNAs

| KEGG pathway | p-value | Number of genes | Number of miRNAs |
|---|---|---|---|
| **ErbB signalling pathway †** | 3.59E-24 | 54 | 27 |
| **Focal adhesion** | 1.69E-22 | 94 | 32 |
| Prostate cancer | 7.79E-22 | 51 | 28 |
| **Neurotrophin signalling pathway *†** | 1.26E-20 | 61 | 30 |
| **Wnt signalling pathway** | 1.70E-19 | 77 | 30 |
| **Insulin signalling pathway** | 2.76E-18 | 65 | 26 |
| **Long-term potentiation** | 1.07E-17 | 42 | 21 |
| Chronic myeloid leukaemia | 1.07E-17 | 40 | 26 |
| Glioma | 1.44E-17 | 41 | 26 |
| Melanoma | 1.05E-16 | 38 | 26 |
| **GnRH signalling pathway** | 1.63E-16 | 45 | 24 |
| Colorectal cancer | 1.08E-15 | 34 | 26 |
| **MAPK signalling pathway †** | 1.29E-15 | 111 | 30 |
| **Dopaminergic synapse †** | 1.52E-15 | 61 | 26 |
| **TGF-β signalling pathway †** | 4.83E-15 | 40 | 26 |
| **Fc gamma R-mediated phagocytosis** | 8.61E-15 | 46 | 26 |
| Pathways in cancer | 1.50E-13 | 146 | 33 |
| Endometrial cancer | 1.83E-13 | 30 | 24 |
| Non-small cell lung cancer | 6.39E-13 | 30 | 22 |
| Renal cell carcinoma | 1.29E-12 | 39 | 24 |

*Note:* NRSF-regulated miRNAs as determined by *in silico* analysis (see **Table 5.3**) were uploaded into the DIANA-miRPath pathway analysis web-server that utilises experimentally validated miRNA interactions derived from DIANA-TarBase v6.0. This software performs an enrichment analysis of microRNA gene targets in KEGG (Kyoto Encyclopaedia of Genes and Genomes) pathways. Bold font indicates pathways relevant to mood disorders, several of which overlap with pathways maps associated with different mood modifying drugs (†, see **Figure 5.2** and **5.3**). *MicroRNAs and their gene targets implicated in this pathway are represented in **Table 5.5**. This data excludes miR-2114 as it was not in the database. Abbreviations: *ErbB, v-erb-b2 erythroblastic leukemia viral oncogene; GnRH, Gonadotropin-releasing hormone; TGF-β, transforming growth factor beta.*

**Table 5.5.** Human miRNAs and their interacting gene targets from the KEGG neurotrophin signalling pathway

| miRNA | Gene Hits | Genes |
|---|---|---|
| miR-21 * | 3 | **NTRK3, MAP3K1,** FOXO3 |
| miR-92b * | 10 | **CAMK2A, FRS2, GSK3B**, **PIK3CB**, **PIK3R3**, RAP1A, FASLG, CDC42, PIK3CA, RAP1B |
| **miR-132 *** | 14 | **AKT3, FRS2, IPK2, KRAS, MAPK1, NTRK3, PIK3R5,** CAMK2D, CRK, FOXO3, MAP3K3, PIK3CA, SOS1, TRAF6 |
| miR-137 * | 12 | **BDNF, CAMK2A, FRS2, GSK3B, MAP3K1, PIK3R3,** AKT2, CALM3, CDC42, CRKL, MAPKAPK2, MAPK10 |
| miR-199a | 8 | **AKT3, GSK3B, MAP3K1, PIK3CB, SOS2,** KIDINS220, MAPK8, MAP3K5 |
| **miR-212 *** | 13 | **AKT3, FRS2, JUN**, **KRAS, MAPK1, NTRK3, RIPK2**, CRK, FOXO3, MAP3K3, IKBKB, PIK3CA, SOS1 |
| **miR-330 *** | 19 | **KRAS, MAPK1, NGFR, NTRK3, PIK3R3, PIK3R5, SOS2,** CRK, FOXO3, GAB1, MAP2K1, NRAS, PTPN11, RAP1A, RAP1B, RAF1, RPS6KA1, SOS1, SH2B3 |
| miR-345 * | 3 | **MAP3K1**, RPS6KA5, IRAK1 |
| miR-422a | 1 | **IRAK3** |
| miR-423 | 4 | NTRK2, CALM3, CRK, **NGFR** |
| miR-484 * | 4 | **CALM1**, MAPKAPK2, PIK3CD, RPS6KA1 |
| miR-607 | 11 | **CALM1, FRS2, IRAK3, KRAS, MAP3K1, PSEN1, RIPK2,** CAMK4, CRK, PTPN11, PIK3CA |
| miR-636 | 1 | **AKT3** |
| miR-760 | 2 | KIDINS220, NTRK2 |
| miR-935 | 1 | **NTRK3** |
| miR-1205 | 10 | **IKBKB, MAPK1, PIK3R5, RAPGEF1,** CAMK2B, CAMK2G, NTRK2, PIK3R2, PTPN11,TP73 |
| miR-1208 | 9 | **MAPK1, SORT1,** BRAF, CALM3, RAF1, FOXO3, MAP2K1, IRAK1, RAP1B |
| miR-1287 | 1 | **PIK3CB** |
| miR-1289 | 1 | SHC2 |
| miR-2277 | 2 | BRAF, MAGED1 |
| miR-3175 | 2 | **CAMK2A**, ARHGDIA |
| miR-3188 | 2 | **FRS2**, MAGED1 |
| miR-3191 | 6 | **MAPK1, NGFR, NTRK3, SORT1,** NRAS, SH2B3, SOS1 |
| miR-4289 | 2 | **MAP3K1**, MAPK8 |

*Note:* Pathway identified as one of the top 20 KEGG (Kyoto Encyclopaedia of Genes and Genomes) processes based on genes that are subject to regulatory control by predicted NRSF-regulated miRNAs (see **Table 5.4**). Bold font indicates miRNAs that overlap with computational predictions of NRSF target miRNAs by Wu and Xie (2006) and Johnson et al. (2008) or known or predicted NRSF target genes (Wu and Xie, 2006, Warburton et al., 2015). *Validated NRSF target miRNAs (Soldati et al., 2013, Warburton et al., 2014, Johnson et al., 2008, Gao et al., 2012). Data generated using the DIANA-miRPath pathway analysis software.

## 5.4 Discussion

Understanding the mechanism of action for a drug to alter the cell phenotype, in addition to the initial cellular targets recognised by the drug, is important for both clinical application and pharmaceutical development. Transcriptome profiling allows for global scale interrogation of potential regulatory mechanisms involved in modulating cellular responses to a particular drug through the use of pathway analysis tools. The aim of this study was to address the effects of mood modifying drugs on the expression profile of a commercially available panel of genes associated with mood disorders by network analysis to compare and contrast their mode of action.

We used two mood stabilisers (lithium and sodium valproate) and two mood stimulants (cocaine and amphetamine). Only the mood stabilisers reached statistical significance and interestingly they shared 5 genes in their top 8 most modified genes, **Table 5.1**; we therefore focused on this set of genes for further analysis. Valproate significantly modified 8 genes, lithium only two, GAD1 and FOS, with GAD1 being significantly down-regulated for both drugs. GAD1 encodes one of several forms of glutamic acid decarboxylase which is a key enzyme for the synthesis of the inhibitory neurotransmitter GABA. GAD1 is implicated from both genetic and functional analysis as a modulator of mood (Hettema et al., 2006, Lundorf et al., 2005, Weber et al., 2012, Karolewicz et al., 2010, Thompson et al., 2009, Domschke et al., 2013). FOS and JUN proteins constitute the AP-1 transcription factor complex which was a target for modulation. These factors represent a family of proteins that heterodimerise to regulate the AP-1 DNA site (Quinn et al., 1989a, Takimoto et al., 1989, Quinn et al., 1989b, Quinn, 1991). Lithium and sodium valproate have both been

demonstrated to modulate the AP-1 complex (Ozaki and Chuang, 2002, Chen et al., 2008). The genes shared in common by the mood stabilisers sodium valproate and lithium were GAD1, NRG1, PER3, RELN and RGS4. The remainder, DRD3, JUN and PAFAH1B3 were specific for sodium valproate. Although some of these genes were modified with cocaine and amphetamine, the statistical significance was low, certainly lower than all the genes in the 9 most differentially expressed genes in **Table 5.1**. In previous chapters, we have addressed cocaine challenge in SH-SY5Y and demonstrated significant changes in the expression of genes involved in mental health. Specifically, data presented in *Chapters 3* and *4* suggests an important role for cocaine-induced modulation of the BDNF and MIR137 gene loci in part through NRSF signalling. Both of these genes have been identified through genetic association to be important candidates in neuropsychiatric diseases including schizophrenia, major depression and addiction (The Schizophrenia Psychiatric GWAS Consortium, 2011, Ripke et al., 2013, Thompson Ray et al., 2011, Dunham et al., 2009, Autry and Monteggia, 2012, Haerian, 2013, Cheah et al., 2014). Although BDNF was not shown to be significantly modulated by any of the drugs tested using the mood-array, expression likely reflects total mRNA for this gene and therefore transcripts which are highly expressed in SH-SY5Y cells will be over-represented in the data. As shown in **Figure 3.5A** (*Chapter 3*), transcripts IV, VI and IX were highly expressed in this cell-line, with previous studies reporting that exons IV and VI account for approximately 80% of total BDNF mRNA (Garzon and Fahnestock, 2007). Consistent with our gene array dataset, cocaine treatment at 1 hour did not significantly affect the expression of these major transcripts, although was shown to modulate the levels of alternative messages

expressed from the locus (see **Figure 3.5B-C**, *Chapter 3*). A longer exposure time of 4 hours was shown to significantly regulate the co-ordinate expression of BDNF IV and VI. Since under the current experimental conditions the gene set targeting mood disorders did not respond as robustly to cocaine and amphetamine as to lithium and sodium valproate, we attempted to determine whether the significant mood stabiliser gene set defined a specific pathway or network of genes to explain their concerted response to drug exposure.

Pathway analysis using both the Analyse Networks (Transcription Factors) and Filter by Disease algorithms available on the online pathway analysis software MetaCore™ identified NRSF to be strongly associated with the pathways supporting these networks of genes. NRSF has a direct association with DRD3, GAD1 and RELN genes based on the network analysis, **Figure 5.3**. Bioinformatic analysis of predicted NRSF binding sites using ENCODE data from the Transcription Factor ChIP-seq track (The ENCODE Project Consortium, 2011, Rosenbloom et al., 2013) identified NRSF binding at the promoter regions (defined as the sequence within 5 Kb of the TSS) of the FOS, NRG1 and RGS4 genes, **Table 5.2**. This analysis also demonstrated NRSF binding sites in similar genomic locations on DRD3, GAD1, JUN, PAFAH1B3 and RELN. Although we did not address NRSF-mediated regulation of these genes in response to drug treatment, it would be interesting to follow-up these hypothetical interactions considering the role of this transcription factor in regulating the expression of genes important for neurodevelopment including BDNF, NeuroD and TrKB, all of which have been shown to be up-regulated in rodent neural stem cells as a result of NRSF down-regulation induced by sodium valproate treatment (Kim et al., 2007).

Aberrant signalling of NRSF and its target genes has been shown to be involved in the pathophysiology of several CNS disorders including schizophrenia (Loe-Mie et al., 2010), major depressive disorder (Otsuki et al., 2010) and alcoholism and depression (Ukai et al., 2009), with genetic variants influencing age-related cognitive function (Miyajima et al., 2008b). More recently loss of NRSF has been highlighted as a major player in Alzheimer's disease through dysregulation of genes implicated in cell death and stress response pathways (Lu et al., 2014). NRSF has the properties to modulate epigenetic parameters at its gene targets due to its association with a plethora of co-activators, such as members of the SWI/SNF family, which can modify histones or DNA by post-translational modifications (Loe-Mie et al., 2010). In *Chapter 3*, we demonstrated changes in the enrichment of active and inactive histone marks at distinct BDNF promoters in response to cocaine treatment at 1, 4 and 24 hours which correlated with differential NRSF binding over the region and/or BDNF mRNA expression patterns. These epigenetic modifications could result in medium-to-long-term changes in gene expression that underlie drug exposure in addition to the immediate modulation of the transcriptome. Our data suggest that lithium and sodium valproate, with different initial cellular targets, may modulate related signalling pathways leading to overlapping cellular responses mediated in part by the NRSF pathway. It should be noted that we performed this experiment at 1 hour post exposure to capture an early response of the cell to the drug. As in any stimulus induction modification of gene expression many of these changes will be transient, especially in the short-term for transcription factors such as AP-1 and NRSF. This is in keeping with the transient response of AP-1 and NRSF in stimulus

inducible gene expression models the lab has previously observed at 1 hour post exposure (Gillies et al., 2009, Howard et al., 2008, Spencer et al., 2006, Quinn, 1991). A more extensive timescale would perhaps have demonstrated a different or related set of genes, nevertheless, our strategy allowed the observation of the differential gene set acting as a signature for the mood stabilisers and allows for future optimisation.

Filtering our dataset by disease also identified ERK1/2 signalling along with the oestrogen receptor pathway as potentially an important regulatory network for this gene set (**Figure 5.2**). Oestrogen receptor signalling has been well documented in the modulation of behaviours relating to aggression (Nomura et al., 2002), anxiety and depression (Furuta et al., 2013). The action of sex hormones may in part explain why in conditions such as panic disorder these phenotypes are more prevalent among females. Our data would be consistent with GAD1 SNP variation being tentatively associated for the higher susceptibility of females to panic disorder (Weber et al., 2012) via modulation by oestrogen. This oestrogen pathway could overlap with other transcription factor pathways identified in our analysis, for example synergistic action of the oestrogen and AP-1 pathways on gene expression (Fujimoto and Kitamura, 2004). The extended networks identified in this study (AP-1, oestrogen and NRSF) may also work synergistically, for example NRSF activity is important for E2 stimulation of the cell cycle (Bronson et al., 2010) and oestrogen receptor B is enriched at NRSF binding sites (Le et al., 2013). Such interactions between these three pathways can be further modified by the glucocorticoid receptor, so linking these pathways to a major driver of mood (Karmakar et al., 2013, Abramovitz et al., 2008). Glucocorticoid sensitivity is strongly associated with

several mood related disorders (Spijker and van Rossum, 2012) and anti-glucocorticoid drugs have been used in the treatment of such conditions (Wolkowitz and Reus, 1999, Wolkowitz et al., 1999, Gallagher et al., 2008). Mood disorder susceptibility has also been linked to glucocorticoid signalling through its modulation of the stress response along the hypothalamic-pituitary–adrenal (HPA) axis (Spijker and van Rossum, 2012, Lupien et al., 2009).

As discussed in *Chapter 4* and recently reviewed by Quinn et al. (2013), non-coding polymorphisms can influence the GxE response through modulation of gene expression in an allele-specific and stimulus-inducible manner, offering insight into the mechanisms underpinning such pathways and providing a functional correlate of disease. Variations in the regulatory sequences of transcriptional regulators, such as transcription factor binding sites, miRNA binding sites or the miRNA processing machinery, have the potential to modulate the expression of hundreds of downstream targets involved in these dynamic regulatory networks. The NRSF-signalling pathway, identified as an important regulatory mechanism implicated in mood disorders from enrichment analysis of cellular gene expression changes in response to mood modifying drugs (Warburton et al., 2015), was investigated for its potential to regulate extensive miRNA gene expression profiles by intersecting global NRSF binding sites predicted from ENCODE ChIP-seq data (March 2012 release) with the proximal promoter regions of miRNA genes, defined as the 500 bp flank sequence upstream of the pre-miRNA based on our recent characterisation of the Imir137 promoter (Warburton et al., 2014). This approach was implemented to extend previously defined *in silico* interactions between NRSF

and the brain-enriched miRNAs based on PWMs (Wu and Xie, 2006, Johnson et al., 2008); a method which failed to identify the recently validated NRSF target miR-137 (Warburton et al., 2014, Soldati et al., 2013). Analysis of repetitive elements within the regulatory sequences of the miRNA genes was also performed using the Repeat Master track on UCSC (human assembly, hg19) to identify potential forms of genetic variation and/or regulatory sequences that may function to alter the levels of transcription as previously demonstrated for the MIR137 VNTR (Warburton et al., 2014, Bemis et al., 2008).

A total of 32 pre-miRNAs were identified from our *in silico* analysis; 22 of which were novel NRSF targets not previously stated in the literature (**Table 5.3**). The miRNAs identified were enriched for repetitive elements including TEs; both LTRs and non-LTRs, the latter of which (mainly LINE2 elements) have previously been linked to NRSF binding site duplication in the human genome (Johnson et al., 2006). The full list of TE-derived NRSEs identified by Johnson et al. (2006) is not publically available and so comparisons could not be made with the NRSF binding sites found in this communication to overlap with TEs. Several of the NRSF target miRNAs identified in this study had SVA insertions (hominid-specific TEs) within 120 Kb of their pre-miRNA sequence (**Table 5.3**)**.** These included miR-210, -330, -345, -658, -607, -1208 and -422a (two SVAs located ~929 Kb upstream and ~771 Kb downstream of miR-422a were observed). SVAs can present as regulatory domains as indicated from data within our group on the PARK7 and FUS SVAs, candidate genes for neurodegenerative disorders and cancer, which were shown to modulate gene expression in a reporter gene system (Savage et al., 2013, Savage et al., 2014). Pathway analysis of the miRNA gene set identified from our bioinformatic

assessment showed that 11 of the top 20 significantly associated pathways were enriched for processes implicated in neuropsychiatric disease, showing considerable cross-over with those networks identified from our enrichment analysis of gene expression changes associated with mood modifying drugs (Warburton et al., 2015). These included the ErbB and neurotrophin signalling pathways which are important for neurodevelopment, synaptic plasticity and neurotransmission, and members of which have been identified through genetic association or expression profiling in clinical samples to be important candidates in the pathophysiology of neuropsychiatric disease, reviewed in Mei and Nave (2014), Duman (2004) and Autry and Monteggia (2012). Analysis of experimentally validated miRNA target genes using the DIANA-miRPath pathway analysis software highlighted a number of hits that have also been implicated in NRSF signalling, including BDNF which has recently been identified as a target of miR-137 in human neural progenitor cells (Hill et al., 2014). Our findings indicate a set of candidate miRNAs within the NRSF-signalling pathway, some of which are novel targets, that overlap with cellular processes enriched for known mood disorder genes and could therefore be important modulators of disease networks underlying neuropsychiatric disease. Several of the identified NRSF target miRNAs contain repetitive elements within or in close proximity of their gene loci, including SVA insertions previously demonstrated to be capable of modifying the transcriptional landscape (Savage et al., 2013, Savage et al., 2014), which have the potential to modify the expression of the targeted miRNAs and thus associated downstream signalling cascades. Genetic variants embedded within these potential NRSF-regulatory networks, identified from pathway analysis as being central to mood

(Warburton et al., 2015), offers a means by which an individual's genotype could influence inappropriate transcriptional responses to an environmental stressor, through disrupting the tightly coordinated balance of gene expression within the cell which over time could translate as a neuropsychiatric phenotype.

## 5.5 Summary

In summary, our data points to a cost effective and rapid assessment of expression changes in selected genes using GPR analysis, which can help delineate the pathways targeted by drugs to modify mood. In particular, we have identified dopamine and glutamine pathways as being important; perhaps not unexpectedly as the gene set is enriched for known genes involved in mood disorders. Alteration in the regulation of these pathways would be expected to modulate mood and is reflected in the range of drugs currently used in targeting these pathways. However the modulation of the AP-1 pathway and the involvement of factors such as NRSF and ERK1/2 highlight a more general modulation of neurotransmitter pathways in response to mood modifying drugs. These pathways could operate through dynamic interaction with miRNA regulatory networks as suggested from our *in silico* analysis of NRSF targeted miRNAs which overlap with genes and cellular processes relevant to mood modifying drug signalling pathways. This supports a role for extensive regulatory feedback mechanisms operating at the transcriptional/post-transcriptional level in co-ordinating the fine-tuning of neuronal gene expression central to development, normal brain physiology and disease. Our model can therefore be used to determine mechanisms associated with off target and long term affects of particular drugs and can be extrapolated to

predict *in vivo* responses, utilised in the comparison of multiple drug regimes or used as an initial screening process to inform optimal drug design.

# Chapter 6

## Is the NRSF-MIR137 Pathway a Common Mechanism in Disease Processes?

# Part I: *Addressing the NRSF-MIR137 Pathway in a Rodent Model of Cortical Spreading Depression (CSD)*

## 6.1 Introduction

In *Chapter 4*, the presence of an internal promoter VNTR (Imir137 promoter) within the human MIR137 schizophrenia candidate gene was validated *in vitro* using reporter gene constructs that were shown to modulate gene expression levels in an allele-specific and stimulus inducible manner. Distinct isoforms of NRSF and cellular challenge with cocaine, a known modulator of NRSF signalling (Chandrasekar and Dreyer, 2009) and a robust tissue culture model used in our lab for eliciting neuronal stimulation of pathways relevant to psychosis (Vasiliou et al., 2012, Warburton et al., 2014, Warburton et al., 2015), was shown to mediate differential expression at this locus, consistent with a GxE mechanism modifying the level of miR-137 expression via this internal promoter. A growing number of animal models are being used to address GxE mechanisms in complex disease processes including anxiety, depression and schizophrenia (Sotnikov et al., 2014, Murgatroyd et al., 2009, Turner and Burne, 2013). However, extrapolation of findings from animal studies to human-specific neurological disorders involving complex traits such as behaviour, cognition and emotion may not always be appropriate. A better understanding of the evolution of gene regulatory mechanisms is therefore necessary for meaningful cross-species comparisons of disease models.

Conservation of promoters and regulatory elements governing the expression of highly conserved neuronal genes has been studied extensively in our lab. This is best exemplified through the TAC1 gene promoter whereby

introducing the human TAC1 gene locus tagged with the β-galactosidase gene into transgenic mice resulted in similar patterns of LacZ expression in the CNS to that reported for endogenous TAC1 mRNA expression in the rat (MacKenzie et al., 2000), demonstrating a high degree of conservation of the transcriptional mechanisms involved in regulating the expression of this neuropeptide gene across species. Human-specific expression of TAC1 was also observed in this *in vivo* model suggesting that species-specific patterns of gene expression are a function of divergent evolution of the underlying promoter sequence which in turn will influence the factors operating at these regulatory domains.

In this chapter we set out to explore the evolutionary conservation of our recently characterised transcriptional network involving NRSF and MIR137 (Warburton et al., 2014), which we hypothesise to be one regulatory mechanism that may be modified in response to neuronal insults or disease processes relevant to CNS dysfunction. To test this hypothesis *in vivo*, differential regulation of NRSF and MIR137 was addressed using a rodent model of cortical spreading depression (CSD), available through our collaboration with Dr Minyan Wang, Department of Biological Sciences, Xi'an Jiaotong-Liverpool University (XJTLU). CSD is a slow wave of depolarisation, characterised by depression of electroencephalography (EEG) activity, which propagates across the cortical surface of cerebral grey matter at a rate of 2 to 5 mm/min (Leao, 1944). In animal models, CSD is usually induced by electrical stimulation, KCl (method used in this study) or glutamate but can also occur spontaneously in the brain under hypoxic, ischemic or hypoglycaemic conditions, with spontaneous recovery occurring over a prolonged time course (Kraig and Nicholson, 1978). It is associated with dramatic fluxes of ions into

and out of cells and neurotransmitter and neuromodulator release; the basic mechanism of CSD and its effect on neuronal tissue is summarised in **Figure 6.1**. Both NRSF and miR-137 levels have been shown to be modulated in animal models of epilepsy and ischemia (Spencer et al., 2006, Song et al., 2011, Noh et al., 2012, Calderone et al., 2003); conditions that can induce CSD through perturbation of extracellular $K^+$ levels (Lauritzen et al., 2011, Fabricius et al., 2008). Furthermore, NRSF and miR-137 target several genes implicated in CSD, such as those encoding for the α-amino-3-hydroxy-5-methyl-4-isoxazolepropionic acid (AMPA) and N-methyl-D-aspartate (NMDA) glutamate receptor and ion channel subunits (Noh et al., 2012, Chazot et al., 2002, Strazisar et al., 2014, Zhao et al., 2013), suggesting a potential role for the NRSF-MIR137 pathway in modulating CSD. Like status epilepticus (a prolonged seizure) and cerebral ischemia, induced CSD in the rodent brain can activate persistent neurogenesis in the dentate gyrus and subventricular zone and produce new neuron-like cells in the caudate putamen and cortex, without neuronal damage which is characteristic of other cerebral insults (Yanamoto et al., 2005, Urbach et al., 2008), suggesting a potential neuroprotective role. NRSF and its co-repressors have been implicated in adult neurogenesis through modulation of stage-specific neuronal gene expression and maintenance of neural stem cells in an undifferentiated state (Gao et al., 2011). In addition, miR-137 has been associated with adult neurogenesis through dynamic interaction with the epigenetic factors MeCP2 (methyl CpG binding protein 2) and EZH2 (enhancer of zeste homolog 2), both of which have been shown to interact with NRSF to control neuronal development and differentiation (Szulwach et al., 2010, Dietrich et al., 2012). Cross-talk between multiple epigenetic factors

which converge on the NRSF signalling pathway, are important for controlling neuronal function and have previously been implicated in neurological dysfunction are explored as a novel and potentially important mechanism underlying CSD pathophysiology.

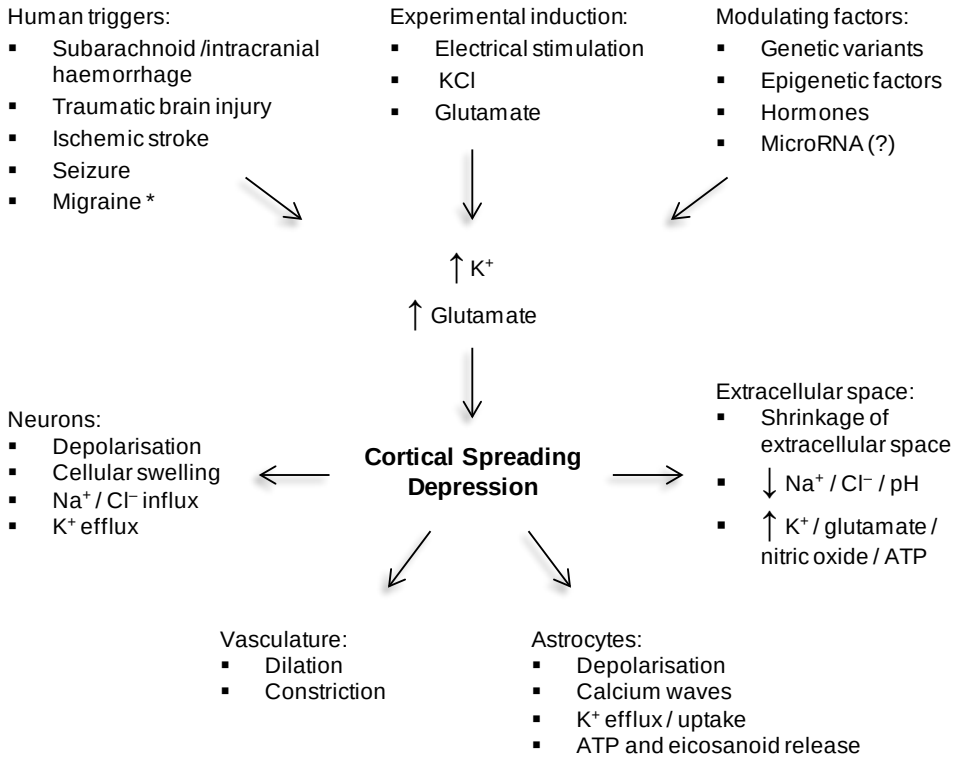


**Figure 6.1. Mechanisms of cortical spreading depression (CSD).** Schematic representation of the basic mechanisms involved in CSD induction and propagation and its functional consequences in the brain. Spreading depression can occur in neuronal cells in several regions of the brain other than the cortex including the hippocampus, cerebellum and retina. In addition, there is growing support for an active role of astrocytes and the vasculature in CSD, rather than simply a passive or reactive role. * Associated with CSD but not conclusive.

## 6.2 Aims

- Comparative sequence analysis of the MIR137 gene locus between humans and rats using reference genomes and sequencing data to determine cross-species conservation
- Gene expression profiling of MIR137 transcripts, NRSF isoforms and their potential target genes in the rat brain
- Address the functional significance of sequence variation within the recently characterised internal MIR137 promoter between the human and rat genomes using reporter gene constructs
- Chromatin immunoprecipitation (ChIP) analysis of NRSF, MeCP2 and EZH2 binding of the predicted rat MIR137HG and internal MIR137 promoters to determine the epigenetic profile of MIR137 in different neuronal tissues
- ChIP and gene expression profiling of MIR137 transcriptional regulation in rat cortical samples following induction of CSD to address regulatory mechanisms operating over the locus in response to neuronal insults

## 6.3 Results

### 6.3.1 Comparative analysis of the MIR137 locus in human and rat genomes

*In silico* analysis of evolutionary conserved regions (ECRs) over the MIR137 gene locus using the ECR Browser (http://ecrbrowser.dcode.org/) indicated strong mammalian conservation not only in exonic regions and the sequence encompassing MIR137 but also in intronic and intergenic regions, as determined by the height of peaks of sequence homology illustrated in **Figure 6.2.** A more in depth analysis of mammalian conservation was carried out using the UCSC Genome Browser (http://genome. ucsc.edu/index.html). The RNA transcripts from which miR-137 is encoded are not annotated in the rat reference genome (Assembly rn5), **Figure 6.3A**. To address the percentage of sequence homology of the MIR137 transcripts between human and rat, sequence alignments were performed using BLASTN (basic local alignment search tool of nucleotide databases), an online interface for searching sequence similarities across DNA and protein databases (Altschul et al., 1997), available at NCBI (http://blast.ncbi.nlm.nih.gov/Blast.cgi). This aligned 48%, 50% and 78% of the mRNA query sequences for MIR137HG (AK094607), AK311400 and AK309618 to the rat genome with percentage identities of 88%, 88% and 92%, respectively (**Figure 6.3B**).

The MIR137 parent transcripts which encode for MIR137 were validated in the rat genome through RT-PCR analysis of cDNA extracted from different brain regions of male Sprague Dawley rats. Human-specific PCR primers spanning the MIR137HG, AK311400 and AK309618 mRNAs were used (see **Table 2.1** for primer sequences). Due to sequence variation between the

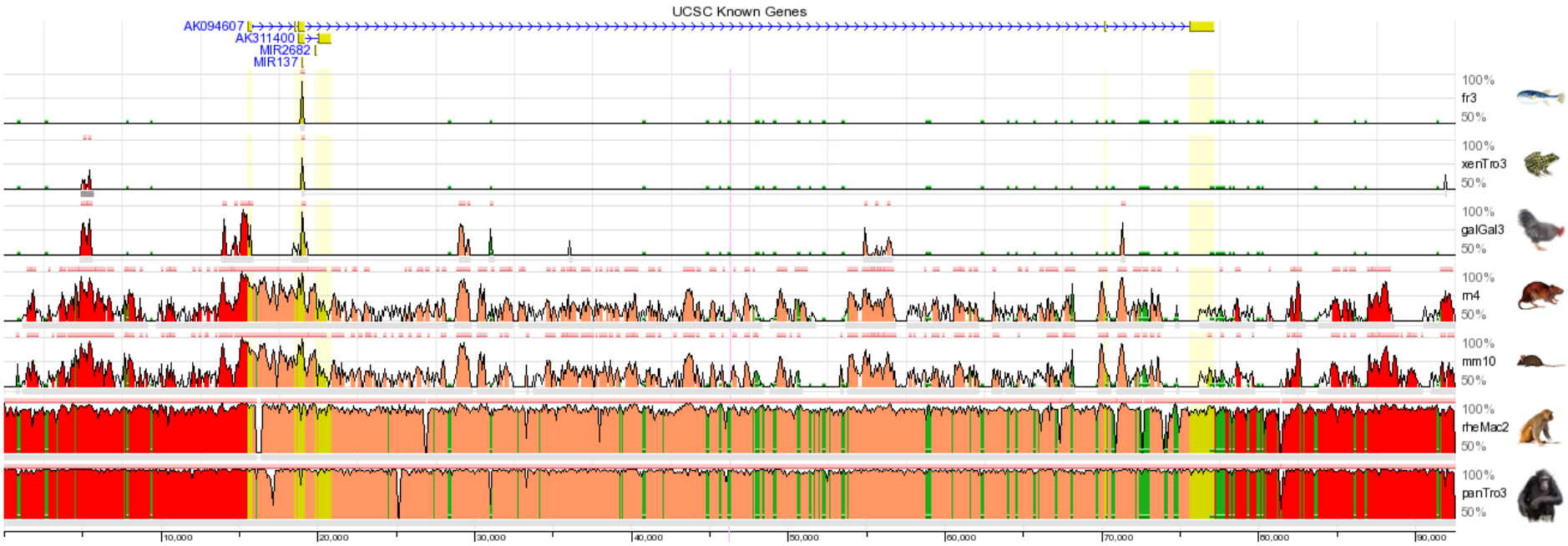


**Figure 6.2. Evolutionary conservation of the MIR137 gene locus.** Conservation plot showing evolutionary conserved regions (ECRs) over the MIR137 gene locus across different species indicated on the right. Genomic alignments are with respect to the human reference genome represented by the line diagram at the top of the schematic; yellow boxes mark the exons, blue horizontal lines the introns and arrows the direction of transcription. The horizontal axis represents the sequence of the human genome. The height of each peak represents the number of nucleotides conserved in windows of 100 bp (% homology), whilst the width corresponds to the alignment length with the human base sequence. Parameters for defining ECRs were set to default values of 70% identity per 100 bp of sequence. ECRs are colour-coordinated based on function: red = intergenic regions; green = repetitive elements; salmon = intronic regions; yellow = untranslated regions. Image generated using the ECR Browser (http://ecrbrowser.dcode.org/).

human and rat reference genomes for the sequence targeted by the AK311400 reverse primer, which also targets AK309618, a rat-specific primer was designed that corresponded to the same genomic location as the human primer. A primer set was also designed to span the highly conserved MIR137 sequence (99.1% sequence homology between rats and humans) and that of a second miRNA MIR2682 (89% sequence homology between rats and humans), located 719 bp downstream of human MIR137 within the intronic region of transcripts AK311400 and AK309618 and partially overlapping the second exon of transcript AK309618, to check for any messages overlapping with this region that could give rise to MIR2682. The location of the PCR primers used for gene expression analysis with respect to the human and rat reference genomes are outlined in **Figure 6.3A**. Alignments of the human and rat miR-137 and miR-2682 precursor (pre) sequences are displayed in **Figure 6.3B**. Several base pair variations are present between the human and rat pre-miR-2682 sequences, including one within the mature miR-2682 sequence itself which may prevent hairpin formation and function of this miRNA in the rat. As shown in **Figure 6.3D**, the predicted size PCR product of 291 bp was observed for MIR137HG in the rat brain, the sequence of which was validated by sequencing analysis which showed 93.3% sequence homology with the human reference genome (Assembly hg19), suggesting that this gene is conserved in the rat. The most 5' and 3' exons of this transcript were not addressed in the rat therefore it is possible that this message is structurally distinct from the human transcript. Under the conditions tested, no bands were observed following PCR analysis using both human- and rat-specific primers targeting the AK311400 and AK309618 transcripts, which originate from the Imir137 promoter (Warburton,

A

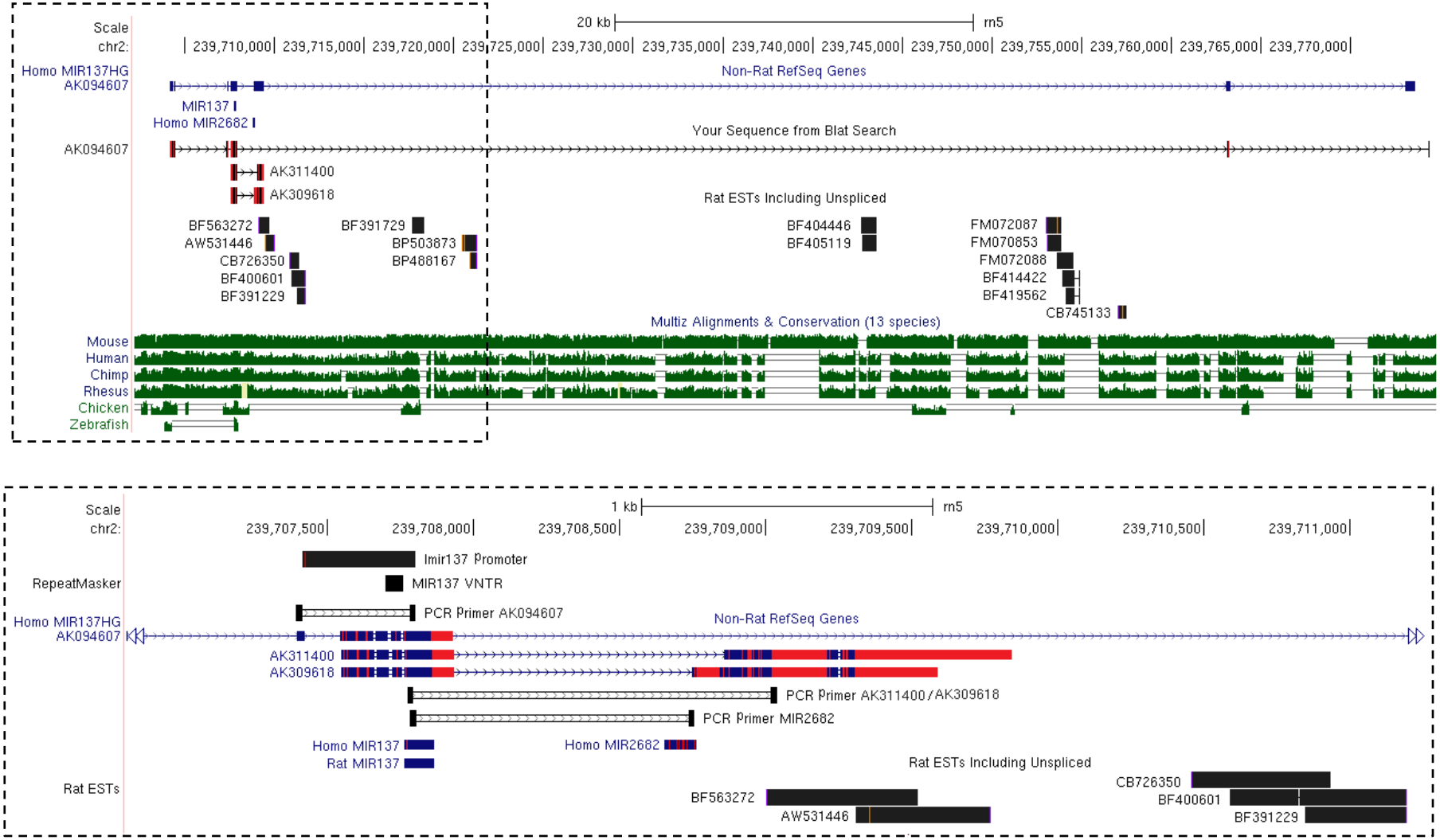


* Rat (Assembly rn5) as Base Genome

**B**

**MIR137HG:** Query cover = 48%, identity = 88%

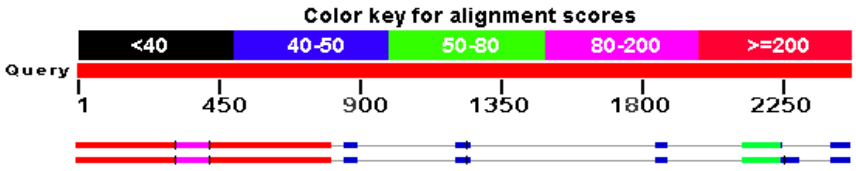


**AK311400:** Query cover = 50%, identity = 88%

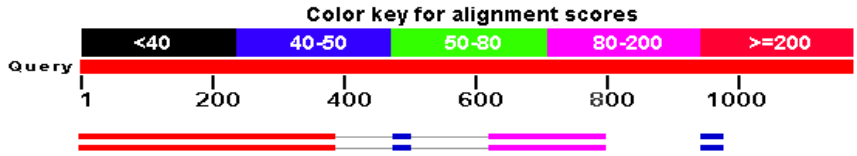


**AK309618:** Query cover = 78%, identity = 92%

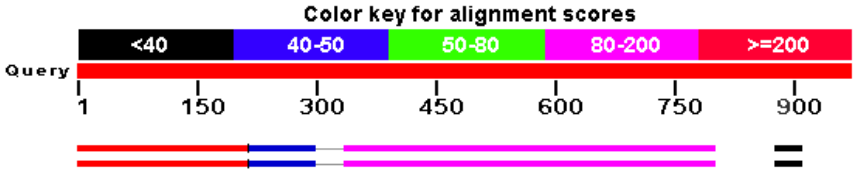


**C**

Pre-miR-137: 99.1% sequence homology

```
098511727 GGTCCTCTGACTCTCTTCGGTGACGGGTATTCTTGGGTGGATAATACGGA 098511678 Human
>>>>>>>>> || |||||||||||||||||||||||||||||||||||||||||||||| >>>>>>>>>
239707763 GGCCCTCTGACTCTCTTCGGTGACGGGTATTCTTGGGTGGATAATACGGA 239707812 Rat

098511677 TTACGTTGTTATTGCTTAAGAATACGCGTAGTCGAGGAGAGTACCAGCGG 098511628 Human
>>>>>>>>> |||||||||||||||||||||||||||||||||||||||||||||||||| >>>>>>>>>
239707813 TTACGTTGTTATTGCTTAAGAATACGCGTAGTCGAGGAGAGTACCAGCGG 239707862 Rat

098511627 CA 098511626 Human
>>>>>>>>> || >>>>>>>>>
239707863 CA 239707864 Rat
```

Pre-miR-2682: 89.0% sequence homology

```
098510907 ACCTTCCTGAAAGAGGTTGGGGCAGGCAGTGACTGTTCAGACGTCCAATC 098510858 Human
>>>>>>>>> ||||| |||||||||| |||||||||||||||||||||||| ||||| |  >>>>>>>>>
239708653 ACCTTTCTGAAAGAGGCTGGGGCAGGCAGTGACTGTTCAGATGTCCAGTT 239708702 Rat

098510857 TCTTTGGGACGCCTCTTCAGCGCTGTCTTCCCTGCCTCTGCCTTTAGGAC 098510808 Human
>>>>>>>>> |||||||||| | ||| |||||||| ||||||| |||||||||| |||  >>>>>>>>>
239708703 TCTTTGGGACACTTCTCCAGCGCTGCCTTCCCTACCTCTGCCTTTGGGAT 239708752 Rat

098510807 GAGTCTCAA 098510799 Human
>>>>>>>>> ||||||||| >>>>>>>>>
239708753 GAGTCTCAA 239708761 Rat
```

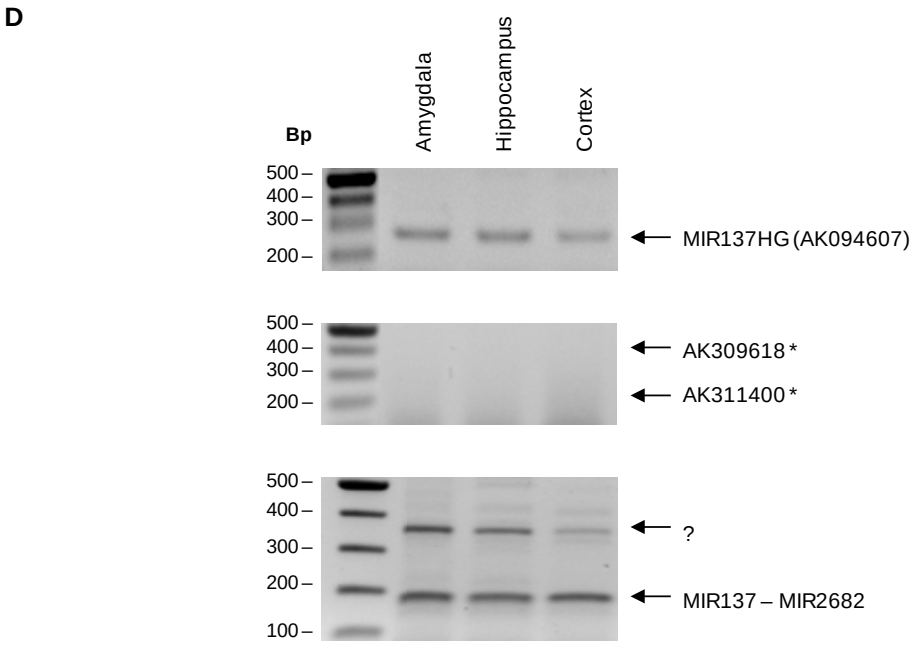


**Figure 6.3. Expression and sequence homology of MIR137 transcripts in rat brain. A**, *Top*, schematic representation of the rat MIR137 gene locus (rat genome, Assembly rn5) aligned to human MIR137HG (human genome, Assembly hg19). Human MIR137 transcripts are represented in blue and rat alignments from BLAT searches in black; boxes denote exonic regions and connecting lines introns. Regions of sequence that do not match between the human and rat genomes are marked red. Rat expressed sequence tags (ESTs) are represented as black boxes. *Bottom*, zoomed in region of top boxed panel showing rat-specific PCR primers targeting human MIR137 transcripts. Image generated using the UCSC Genome Browser (https://genome.ucsc.edu/). **B**, Alignment of human MIR137HG, AK311400 and AK309618 mRNA sequences (Assembly hg19), depicted as red horizontal bars, with the rat genome (Annotation release 105) using the BLAST Assembled Genomes function, NCBI (http://blast.ncbi.nlm.nih.gov/Blast.cgi), to determine sequence homology. Numbers refer to base sequence. Sequence alignments are depicted in the top panel of **A** under *Your Sequence from Blat Search*. **C**, Alignments of human and rat precursor (pre)-miR-137 and -2682 sequences taken from the reference genomes (Assembly hg19 and rn5). Red font indicates sequence variation, grey highlighted sequence represents the mature miRNA sequences. **D**, PCR analysis of MIR137 transcripts outlined in **A** using cDNA from rat brain tissue. Expected PCR product sizes were 291 bp, 232 bp, 409 bp and 187 bp for AK094607, AK311400, AK309618 and MIR2682, respectively. *Marks the expected size of the AK311400 and AK309618 mRNAs. MIR137HG is conserved in rat, validated by sequencing. No PCR products were observed for AK311400 and AK309618 under the conditions tested. Amplification of the predicted size PCR product (187 bp) for primers spanning rat MIR137 and MIR2682 (predicted from alignment with the human genome) and an additional higher band, which does not account for the genomic size targeted by the primer set (977 bp), could suggest the presence of rat-specific transcripts.

et al., 2014), see **Figure 6.3A**. However, a PCR product of the expected size of 187 bp, given the presence of MIR2682, was observed following amplification with a primer set spanning both the MIR137 and MIR2682 genes, which is currently being sequenced. An additional larger band running below the 400 bp mark was also observed that was not accounted for by the expected genomic size (977 bp) targeted by the primer set in the event of genomic DNA carryover during the RNA extraction, **Figure 6.3D**. Absence of AK311400 and AK309618 expression in the rodent brain but amplification of distinct messages within the same region could suggest the presence of tissue- or rat-specific transcripts originating from the Imir137 promoter.

Comparative sequence analysis from sequencing data showed that the Imir137 promoter VNTR and the transcription start sites for AK311400 and AK309618 are highly conserved between the human and rat genomes (92.2% homology), **Figure 6.4A**. Due to its conservation across species, we predicted that the rat Imir137 promoter sequence would, like the human Imir137 promoter, function in initiating gene transcription and that variation between the human and rat sequences might alter the regulatory potential of the promoter as previously demonstrated for a repeat within the third intron of the SLC6A4 gene encoding the serotonin transporter in old world monkeys (Paredes et al., 2012). To address both promoter function and the regulatory effect of sequence variation within the rat Imir137 promoter relative to the human sequence, genomic DNA extracted from the rat cortex was amplified using human-specific primers targeting this putative regulatory domain and cloned in the forward and reverse orientations in the pGL3-Basic (pGL3B) luciferase vector which lacks promoter and enhancer elements. The MIR137

VNTR is also conserved, **Figure 6.4B-C**. Sequencing analysis revealed the presence of just less than a 3.5 copy repeat in the samples tested**.** We could not determine whether this domain was polymorphic or not in the rat as the same strain of rat was used for genotype analysis and therefore all the animals will have been inbred. Analysis of reporter gene activity was performed in human SH-SY5Y cells as we have previously demonstrated that the human Imir137(4) promoter, which shares 92.2% sequence homology with the rat Imir137 domain (**Figure 6.4A**), is transcriptionally active in this cell line (Warburton et al., 2014). The human Imir137(4) construct was included as a positive control for the reporter gene assay. The rat Imir137 construct in the forwards orientation clearly demonstrated its ability to drive reporter gene expression, supporting a 16.90 average fold increase in luciferase activity over the pGL3B control (**Figure 6.4D**; ***$p<0.001$). Typical of a promoter element, the reverse orientation of this domain had no activity (**Figure 6.4D**). A 1.6-fold increase ($^{\#\#}P<0.01$) in reporter gene expression was supported by the human Imir137 promoter construct over the rat construct, **Figure 6.4D**. This may reflect sequence or copy number variation of the MIR137 VNTR (**Figure 6.4B**), the latter of which has previously been demonstrated between different human alleles (4- versus 12-copy) in SH-SY5Y (Warburton et al., 2014). Alternatively it may reflect sequence variation in the 5' flanking sequence of the VNTR, **Figure 6.4A**, as demonstrated with the rs2660304 SNP in the human Imir137 promoter sequence outlined in *Chapter 4*.

**A**

MIR137 internal promoter VNTR (Imir137)

Sequence homology: 92.2 %

```
098512080 CACCAGGTAAACTGAAGGTTACT.....TGTCACTCCCACTTGTGCCCAA 098512036 Human
>>>>>>>>> ||||||||||||||||||||||     | ||||||||         ||| >>>>>>>>>
239707415 CACCAGGTAAACTGAAGGTTACTACTTATATCACTCCC.........CAA 239707455 Rat

098512035 AAAGCCTTGCCACATCTTCCCTCCTCACTGGAAAG.....ACAGCACTCT 098511991 Human
>>>>>>>>> | | ||||| ||| |    | || ||    ||||||     ||    || | >>>>>>>>>
239707456 AGATCCTTGGCACCTAGGCTCTGCTTGGCGGAAAGAAAGCACTTGCCTGT 239707505 Rat
                                                  AK311400
098511990 TCTGTGTTAAGTATTTGATTTTGTGATTTGTCTTTCAGAATTGGAAATAG 098511941 Human
>>>>>>>>> | |||||||||||   || || |||||||||||||||||||||||||||| >>>>>>>>>
239707506 TGTGTGTTAAGTGGCTGGTTCTGTGATTTGTCTTTCAGAATTGGAAATAG 239707555 Rat

098511940 AGCGGCCATTTGGA...TTTGGGCAGGAAGCAGCCGAGCACAGCTTTGGA 098511894 Human
>>>>>>>>> | | ||||||||||    | |||||||||||| | ||||||||||||||>>>>>>>>>
239707556 AACAGCCATTTGGAAGATCTGGGCAGGAAGCAACAGAGCACAGCTTTGGA 239707605 Rat

098511893 TCCTTCTTTAGGGAAATCGAGTTATGGATTTATGGTCCCGGTCAAGCTCA 098511844 Human
>>>>>>>>>  |||||||||||||||||||||||||||||||||||||||||||||||| >>>>>>>>>
239707606 GCCTTCTTTAGGGAAATCGAGTTATGGATTTATGGTCCCGGTCAAGCTCA 239707655 Rat

098511843 GCCCATCCCCAGGCAGGGGCGGGCTCAGCGAGCAGCAAGAGTTC....TG 098511798 Human
>>>>>>>>> ||||| ||| || |||||||||||||  |  |||||||||||||    || >>>>>>>>>
239707656 GCCCAGCCCTAGCCAGGGGCGGGCTC..C..GCAGCAAGAGTTCTTTCTG 239707701 Rat
                                  AK309618
098511797 GTGGCGGCGGCGGCGGCAGTAGCAGCGGCAGCGGTAGCAGCGGCAGCGGT 098511748 Human
>>>>>>>>> |||| ||||||||| || | ||||| | |||||||||||| |||||     >>>>>>>>>
239707702 GTGGTGGCGGCGGCAGCGGCAGCAGTGACAGCGGTAGCAGAGGCAGA...  239707748 Rat

098511747 AGCAGCGGCAGCGGCAGCTTGGTCCTCTGACTCTCTTCGGTGACGGGTAT 098511698 Human
>>>>>>>>>       |||||||||||||||||||||||||||||||||||||||||||| >>>>>>>>>
239707749 ......GGCAGCGGCAGCTTGGCCCTCTGACTCTCTTCGGTGACGGGTAT 239707792 Rat

098511697 TCTTGGGTG 098511689 Human
>>>>>>>>> ||||||||| >>>>>>>>>
239707793 TCTTGGGTG 239707801 Rat
```

**B**

| **Human (hg19)** | **Rat (rn5)** |
|---|---|
| Sequence 1 | *Sequence 1* |
| CGGCGGCGGCGGCAG | TGGCGGCGGCAGCGG |
| TAGCAGCGGCAGCGG | CAGCAGTGACAGCGG |
| TAGCAGCGGCAGCGG | TAGCAGAGGCAGAGG |
| TAGCAGCGGCAGCGG | .........CAGCGG |
| *Sequence 2* | *Sequence 2* |
| CGGCGGCGGCAGTAG | CGGCGGCAGCGGCAG |
| CAGCGGCAGCGGTAG | CAGTGACAGCGGTAG |
| CAGCGGCAGCGGTAG | CAGAGGCAGA..... |
| CAGCGGCAGCGGCAG | ....GGCAGCGGCAG |
| *Sequence 3* | *Sequence 3* |
| CGGCAGTAGCAGCGG | CAGCGGCAGCAGTGA |
| CAGCGGTAGCAGCGG | CAGCGGTAGCAGAGG |
| CAGCGGTAGCAGCGG | CAGAGG......... |
| CAGCGGCAGC..... | CAGCGGCAGC..... |

C

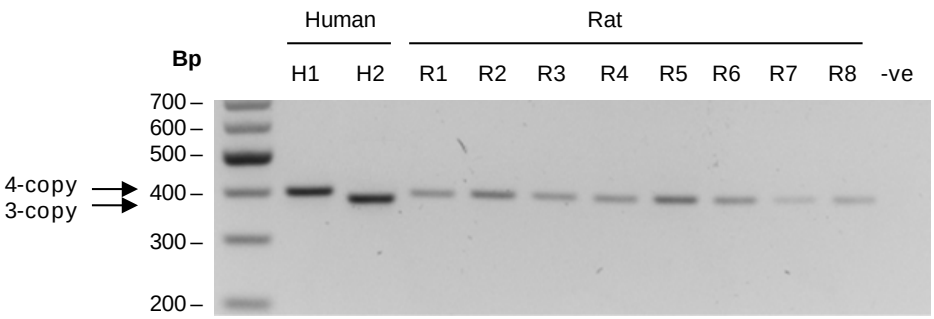


D

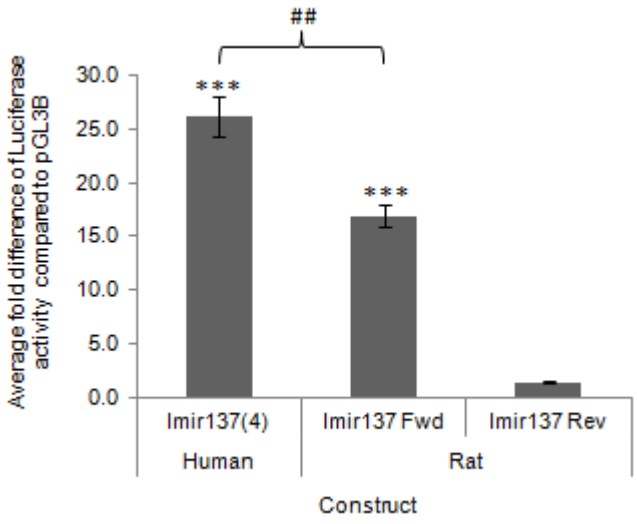


**Figure 6.4. Evolutionary conservation of the internal MIR137 promoter (Imir137). A**, Alignment of sequencing data for the rat Imir137 promoter domain with the corresponding human sequence. Identical bases are marked with a connecting horizontal line and sequence variation with red font. Single and double underlined sequence corresponds to the MIR137 VNTR and precursor-miR137, respectively. Arrows mark the transcription start sites for the AK311400 and AK309618 mRNAs that originate from this region in the human genome. NRSF binding sites predicted from rVista (TRANSFAC IDs: V$NRSF_Q4 aligns to hg19 Chr1: 98511764-98511782 and V$NRSF_01 aligns to rn5 Chr2: 239707716-239707736) and ENCODE ChIP-seq data are highlighted in grey (http://rvista.dcode.org/). **B**, Alignment of the MIR137 VNTR in human and rat. Underlined sequence represents the different starting positions of the realignments labelled *sequence 1, 2* and *3*. Red font indicates base pair changes between human and rats. **C**, Amplification of the Imir137 promoter in rat genomic DNA showed that this conserved tandem repeat domain was not polymorphic in the rat samples tested (n=1 as same strain rat). **D**, Average fold change in luciferase activity supported by the human and rat Imir137 reporter gene constructs over vector controls in SH-SY5Y cells. *N*=4. * Significant changes in luciferase activity over backbone control, # and between constructs. (##P<0.01, ***P<0.001).

### 6.3.2 NRSF differentially modulates the rat Imir137 promoter in an *in vivo* model of CSD

We have previously demonstrated that NRSF can function as a transcriptional regulator of the human Imir137 promoter in human SH-SY5Y neuroblastoma cells both exogenously, as shown by analysis of reporter gene activity and MIR137 mRNA expression profiling following NRSF over-expression, and endogenously, as demonstrated through ChIP assays of NRSF occupancy in response to cocaine challenge (Warburton et al., 2014). In order to investigate conservation of NRSF binding sites within the rat Imir137 promoter, sequencing data from rat genomic DNA was subjected to *in silico* analysis using the publicly available software rVista 2.0 (http://rvista. dcode.org/); an online resource for predicting conservation of regulatory domains based on comparative genomics of transcription factor binding sites and ECRs (Loots and Ovcharenko, 2004). NRSF consensus binding sequences over the MIR137 gene locus were shown to be conserved between human and rat based on the TRANSFAC 4.0 database (Matys, 2003), under default parameters (see *Methods section 2.2.6.1*), **Figure 6.4A**. To validate NRSF binding over the region in the rat brain, ChIP was performed using chromatin samples extracted from the rat cortex (see *Methods section 2.2.8.2*). In the normal rat brain NRSF binding was observed over the Imir137 promoter but not at the MIR137HG promoter, **Figure 6.5A**. This is comparable to NRSF binding patterns in human SH-SY5Y cells, in which NRSF occupancy was observed over Imir137 but not at a second predicted NRSF binding site within the first intron of MIR137HG (Warburton et al., 2014). NRSF binding of the Imir137 promoter was reduced or lost 24 hours post-CSD induction (**Figure 6.5B**). This correlated with a 1.36-fold decrease

(*P<0.05; SD, 0.25) in NRSF mRNA expression using primers which recognise all isoforms of NRSF in the ipsilateral hemisphere in which CSD was elicited relative to the contralateral control hemisphere and a 14.59-fold increase (**P<0.01; SD, 2.43) in MIR137HG mRNA expression determined by RT-PCR/qPCR analysis (**Figure 6.5C-D**). In line with previous work in the lab addressing NRSF regulation in a rodent model of kainic acid-induced epilepsy (Spencer et al., 2006), REST4 mRNA expression was induced in the ipsilateral hemisphere following CSD determined by RT-PCR (**Figure 6.4C**), supporting its proposed role in disease processes. RT-qPCR data for REST4 expression was discarded due to the presence of multiple amplicons determined by the melt-curve. A higher PCR product using the REST4 primer set was also detected by RT-PCR in two of the three CSD samples (**Figure 6.4C**). This may reflect one of several novel splice variants recently identified as encoding from the region in different human and mouse tissues (Chen and Miller, 2013), and warrants further investigation due to the reported differences in alternative splicing of the NRSF gene between different tumour subtypes or pathological and matched control tissues (Coulson et al., 2000, Wagoner et al., 2010, Chen and Miller, 2013).

EZH2 and MeCP2 binding over the Imir137 promoter in response to CSD was also addressed in this model due to 1) their interaction with the NRSF-signalling complex in modulating neuronal gene expression (Dietrich et al., 2012, Noh et al., 2012), 2) potential EZH2 binding of this domain identified from ENCODE transcription factor ChIP-seq data in human cell lines (March 2012 release, see **Figure 6.5A**) and 3) MeCP2-mediated regulation of miR-137 expression in adult neural stem cells (aNSCs) in a mouse model of adult

neurogenesis (Szulwach et al., 2010). Little or no signal was observed for EZH2 and MeCP2 binding of the MIR137HG promoter in rat cortical samples under all conditions tested (**Figure 6.5B**). A CpG island (CGI) located 3.75 Kb upstream of the MIR137HG transcription start site shown to bind both NRSF and EZH2 from human ENCODE ChIP-seq data (**Figure 6.5A**), and more likely to be enriched for the methyl CpG binding protein MeCP2, may be a more appropriate region for analysis of transcription factor binding over the MIR137HG promoter region. Analysis of factors binding over the MIR137HG CGI is currently being addressed using the same in vivo ChIP samples for comparison with the MIR137HG and Imir137 promoter regions, the latter of which is also encompassed by a CGI. Both EZH2 and MeCP2 were shown to bind the Imir137; however binding was unaffected at 24 hours post-CSD induction (**Figure 6.5B**).

**A**

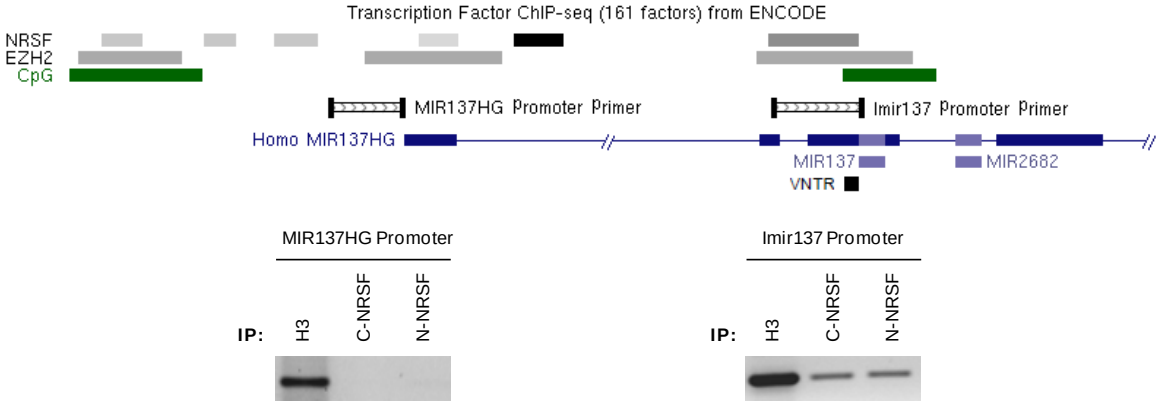
Transcription Factor ChIP-seq (161 factors) from ENCODE
NRSF
EZH2
CpG
MIR137HG Promoter Primer
Imir137 Promoter Primer
Homo MIR137HG
MIR137
MIR2682
VNTR
MIR137HG Promoter
Imir137 Promoter
IP:
H3
C-NRSF
N-NRSF

**B**

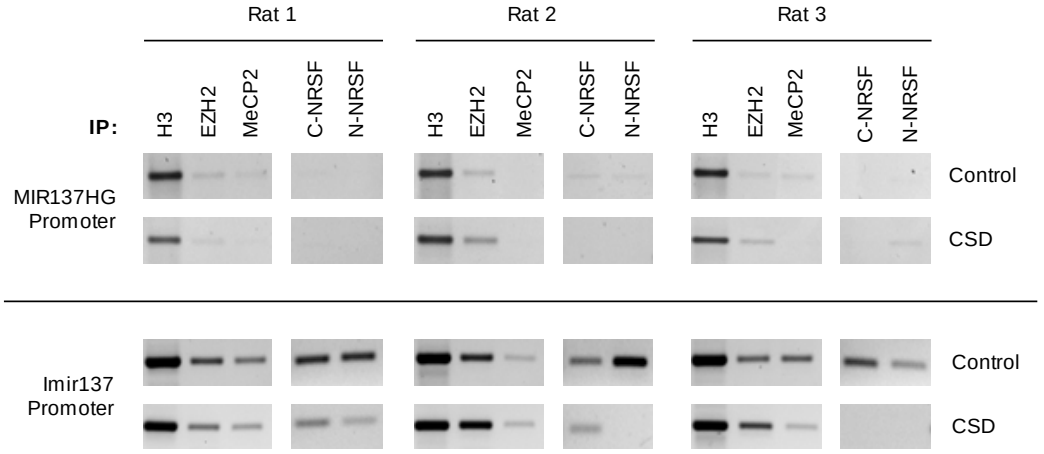
Rat 1
Rat 2
Rat 3
IP:
H3
EZH2
MeCP2
C-NRSF
N-NRSF
MIR137HG Promoter
Imir137 Promoter
Control
CSD

**C**

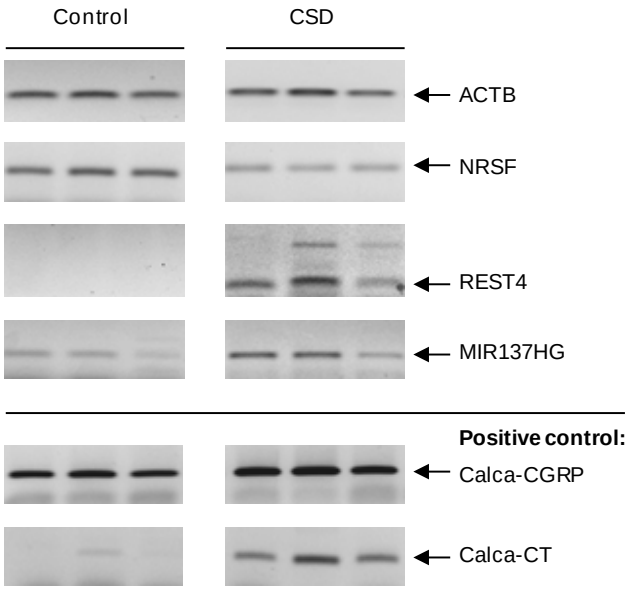
Control
CSD
ACTB
NRSF
REST4
MIR137HG
Positive control:
Calca-CGRP
Calca-CT

**D**

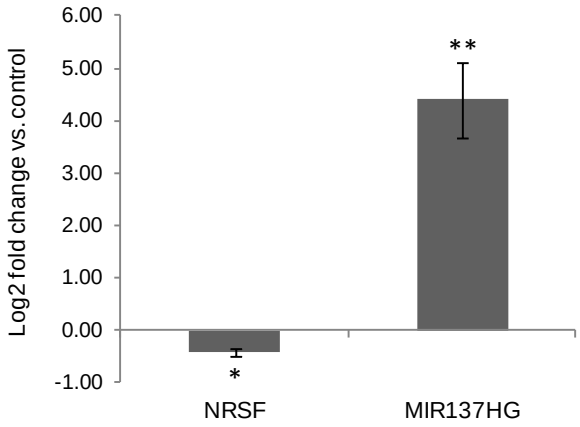


**Figure 6.5. NRSF binding over the internal MIR137 promoter VNTR is reduced following induction of cortical spreading depression (CSD).** Chromatin and total RNA was extracted from the left and right cortical hemispheres of adult male Sprague Dawley rats (n=3) 24 hours following perfusion of KCl into the right hemisphere to induce CSD. The left hemisphere was used as an internal control as CSD does not generally cross the midline. Primers spanning the MIR137HG and internal MIR137 (Imir137) promoters are illustrated in **A**. ChIP was performed in normal (**A**) and CSD (**B**) tissue samples using antibodies against histone H3 (positive control for ChIP), EZH2, MeCP2, the C-terminal of NRSF (C-NRSF) which targets the full-length protein and the N-terminal of NRSF which targets all variants of NRSF including REST4 (rodent equivalent of sNRSF). Predicted transcription factor binding for NRSF and EZH2 over the MIR137 locus from human ENCODE ChIP-seq data (March 2012 release) is illustrated in **A**. **C-D**, Gene expression profiling of rat NRSF, REST4 (expected size PCR product marked with arrow) and MIR137HG in the left (control) and right (CSD) cortex following CSD. Calcitonin (calca-CT) and calcitonin gene-related peptide (calca-CGRP) were included as a positive control for gene expression changes in response to CSD. **D**, RT-qPCR data is presented as log2 fold change in expression in CSD samples over the controls, normalised to ACTB and is representative of 3 biological replicates, each analysed in triplicate. Abbreviation: *IP; immunoprecipitation*.

### 6.3.3 Modulation of NRSF and MIR137 target genes 24 hours post-CSD induction

Both NRSF and MIR137HG mRNA expression levels were shown to be modulated in response to CSD in rat cortical tissue (**Figure 6.5C-D**). To investigate the potential downstream effects of these changes, gene expression profiling of known or putative targets of these two transcriptional regulators was addressed in our CSD model. The putative NRSF target genes FOS (FBJ murine osteosarcoma viral oncogene homolog), GAD1 (glutamate decarboxylase 1), JUN (Jun oncogene) and RELN (Reelin) were selected for RT-PCR analysis based on data presented in *Chapter 5* of this thesis which showed these genes to contain a predicted NRSF binding site within their promoters and to be modulated in response to sodium valproate (Warburton et al., 2015); an anticonvulsant drug used in the treatment of migraine and shown to suppress CSD frequency *in vivo* (Ayata et al., 2006). Furthermore, aside from their role in neuropsychiatric disease (see *Chapter 5*), all of these genes have been previously implicated in CSD or conditions associated with CSD, including epileptogenesis, migraine and/or ischemia (Urbach et al., 2006, Qureshi and Mehler, 2010, Won et al., 2006, Darrah et al., 2013, Rangel et al., 2001). The miR-137 target genes CACNA1C (calcium channel, voltage-dependent, L type, alpha 1C subunit) and TCF4 (transcription factor 4) were also addressed due to their respective clinical associations with Timothy syndrome and Pitt-Hopkins syndrome, both of which are neurological conditions characterised by mental retardation and susceptibility to seizures (Rosenfeld et al., 2009, Splawski et al., 2004). RT-PCR analysis of cortical samples from CSD and control hemispheres at 24-hours post-CSD did not shown any significant differences in mRNA

expression for all genes tested, **Figure 6.6**. This may reflect the time-course used in this experiment, particularly with respect to the early-response genes c-Fos and c-Jun. A previous *in vivo* study of CSD reported significant up-regulation of c-Fos mRNA in the rat cortex following a 30 minute and 2 hour recovery period after eliciting the same number of CSD episodes (n=5) as those used in this experiment, with normal levels of expression returning at 24 hours post-CSD (Rangel et al., 2001). The same authors also reported a similar pattern of expression for BDNF mRNA, whilst another study showed that BDNF protein levels remained significantly elevated at 24 hours following CSD (Kawahara et al., 1997). Normalisation of the transcriptome to baseline levels at 24 hours post-CSD is consistent with the transient nature of this neurological insult. This is consistent with data for the NRSF target gene TAC1 in a rat model of epilepsy in which hippocampal mRNA levels of this proconvulsant neuropeptide were significantly up-regulated at 3 hours post-kainic acid treatment but returned to basal levels at the 24 hour time point (Spencer et al., 2006). Although RT-PCR analysis of NRSF and MIR137 target genes did not show any significant changes in mRNA levels between control and CSD samples, it does provide a negative control for gene expression changes in response to this neuronal insult and provides support that the observed modulation of the NRSF and MIR137 genes was a specific response to CSD rather than an experimental artefact. The effects of CSD on cortical mRNA and protein levels of several NRSF and miR-137 target genes at different recovery periods and in response to drugs targeting CSD, such as NMDA receptor antagonists (Wang et al., 2012), are currently being addressed by our collaborators at XJTLU.

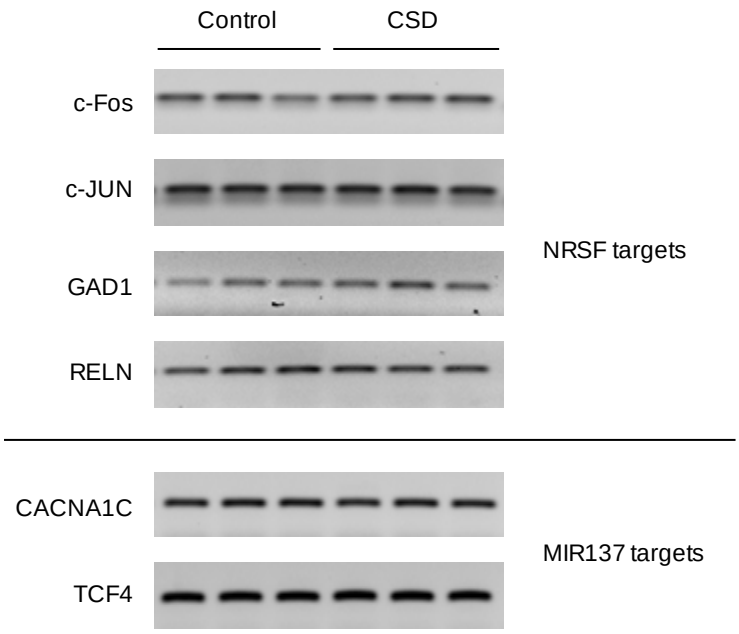


**Figure 6.6. Gene expression profiling of NRSF and MIR137 gene targets 24-hours post-CSD (cortical spreading depression) induction.** RT-PCR analysis of putative NRSF and known MIR137 target genes in rat cortex following CSD. CSD samples (n=3) represent the ipsilateral cortical hemisphere in which CSD was induced; control samples (n=3) represent the contralateral hemisphere. No significant changes in mRNA expression were observed between the control and CSD samples at 24 hours post-induction. Abbreviations: *CACNA1C, calcium channel, voltage-dependent, L type, alpha 1C subunit; FOS, FBJ murine osteosarcoma viral oncogene homolog; GAD1, Glutamate decarboxylase 1; JUN, Jun oncogene; RELN, Reelin; TCF4,transcription factor 4* .

## 6.4 Discussion

The MIR137 gene and the miRNA which it encodes, miR-137, have been widely implicated in several disease processes ranging from CNS dysfunction to cancer. Recent genome-wide association studies (GWAS) have identified the MIR137 gene locus as one of the strongest and most reproducible genetic correlates in predicting risk for schizophrenia (Ripke et al., 2013, The Schizophrenia Psychiatric GWAS Consortium, 2011), making it an attractive candidate for studying genetic perturbations in animal models of psychiatric disease. Although miR-137 is highly conserved across species, the non-coding RNA transcripts from which it is encoded are not very well characterised and are not annotated in the rat reference genome (Assembly rn5/6). We have previously shown plasticity over the human locus in response to psychostimulant drug treatment and NRSF/sNRSF over-expression (Warburton et al., 2014). Differential expression of these MIR137 host genes may be one mechanism by which the levels of miR-137 and a second miRNA, miR-2682, also expressed from the locus (Duan et al., 2014), can be differentially regulated in a tissue-specific or stimulus-inducible manner which may be an important and novel mechanism in neuropsychiatric disease. The purpose of this study was to firstly investigate the evolutionary conservation of the NRSF-MIR137 pathway, which we hypothesis to be one important mechanism involved in modulating miR-137 expression levels and thus its downstream target genes in the aetiology of schizophrenia, and secondly extend the potential role of this regulatory network to other neurological conditions by assessment of NRSF-mediated regulation of the MIR137 gene locus in an *in vivo* model of CSD, a neuronal insult which has been closely associated with the pathophysiology of

migraine, epilepsy and ischemia; conditions which have previously implicated a role for both NRSF and miR-137 which will be discussed.

Evolutionary divergence in the expression patterns of miRNAs may play an important role in shaping species-specific neuronal gene expression profiles and may contribute to the evolution of human-specific cognitive functions. A recent study which profiled miRNA expression in the prefrontal cortex and cerebellum of human, chimpanzee and macaque brains showed that miRNAs which displayed human-specific expression localised in neurons and targeted genes that were enriched in neuronal functions implicated in memory and learning such as axon guidance and long-term potentiation (Hu et al., 2011a). These differences in expression may reflect the role of species-specific regulatory elements such as promoters and enhancers within gene regulatory sequences which can influence when, where and how much of a gene is expressed within a cell dependent in part upon the cellular complement of transcription factors available. Genetic variation embedded within such regulatory domains can further influence the transcriptional machinery through altering the binding sites of transcription factors or epigenetic regulators. Support for sequence variation in modifying gene expression in different species comes from our lab's previous work on the SLC6A4 intron 3 tandem repeat in old world monkeys which showed significant differences in reporter gene activity supported by repeats cloned from *Mandrillus sphinx* and *Cercopithecus aethiops*, which differed at point-base substitutions (Paredes et al., 2012). This study also demonstrated a role for repetitive DNA in regulating tissue-specific gene expression as reporter gene activity was higher in rat primary cortical neurons than in human choriocarcinoma *JAr cells (Paredes et*

*al., 2012)*. Changes in gene expression along the human evolutionary lineage may also play an important role in disease processes. This is exemplified by our lab's work on hominid-specific subtypes of SVA (SINE-VNTR-Alu) retrotransposon insertions that contain distinct regulatory elements, including a VNTR domain, which can potentiate differential gene expression of candidate genes implicated in neurodegeneration and cancer, such as FUS (Fused in sarcoma) and PARK7 (Savage et al., 2013, Savage et al., 2014). Identifying the transcriptional mechanisms that control human-specific expression of genes that are highly conserved across species may point to important regulatory networks involved in the evolution of higher cognitive processes and behaviours; pathways which are likely to be those disrupted in CNS dysfunction. With this mind, transcriptional regulation of the MIR137 gene locus was addressed in the rat genome to determine evolutionary conservation of the identified Imir137 promoter VNTR, discussed in *Chapter 4* of this thesis, which we have shown to direct allele-specific and stimulus-inducible reporter gene expression in human SH-SY5Y neuroblastoma cells. MIR137 host transcripts originating from this regulatory domain, which were differentially regulated by both NRSF over-expression and cocaine in our human cell line model (Warburton et al., 2014), were also addressed in this study using an *in vivo* model of CSD as neural plasticity of miR-137 and its gene targets have previously been reported in several animal models and/or clinical studies of neurological disease including schizophrenia, Alzheimer's disease, stroke and epilepsy (Geekiyanage and Chan, 2011, Song et al., 2011, Kim et al., 2012, Guella et al., 2013, Kwon et al., 2013, Jeyaseelan et al., 2008, Zhao et al., 2013).

Analysis of MIR137 host gene mRNA expression in the rat brain showed conservation of MIR137HG based on RT-PCR using primers targeting exons 3 and 4 of this transcript, which are situated proximal to and overlap with the Imir137 promoter sequence. Expression of the AK311400 and AK309618 transcripts which originate from the Imir137 promoter was not observed in the rat brain under the conditions tested. However a nested primer set targeting rat MIR137 and the predicted location of MIR2682 based on the human sequence amplified a message of the correct size when accounting for the presence of MIR2682. Given the expression of MIR137 transcripts spanning the region of the Imir137 promoter in the rat brain, and differential reporter gene expression directed by specific alleles of the Imir137 promoter VNTR in driving reporter gene expression in human neuroblastoma cells in response to different stimuli (Warburton et al., 2014), we sought to investigate whether the Imir137 promoter sequence was conserved between human and rats, if it was polymorphic in nature and whether it functioned as a promoter. Sequencing of rat genomic DNA showed that this domain was highly conserved (92.2% sequence homology) and contained a 3.5-copy repeat of the MIR137 VNTR, however we could not determine whether or not this region was polymorphic in the samples tested as the same strain of rat was used and therefore all animals were genetically similar due to inbreeding. Genotype analysis of the MIR137 VNTR in human samples showed that the allele frequency of the common 4-copy variant is approximately 70%, with homozygotes for this allele observed in almost 50% of the study cohort (see *Chapter 4*, **Table 4.1** and **4.2**). In order to determine whether this domain is polymorphic in rats, a minimum of ten different strains of rat would be expected to be needed for genotype

analysis in order to observe one of the alternative copy-number variants. The ability of the rat Imir137 putative promoter domain to drive reporter gene expression was also addressed. In human SH-SY5Y neuroblastoma cells, a cell line chosen due to it routinely supporting strong promoter activity of the human Imir137 promoter construct, the rat Imir137 promoter sequence clearly demonstrated its ability to function as a promoter. Evolutionary conservation of this internal promoter supports its role as a key transcriptional mechanism in governing the expression of miR-137, with variability in the number of copy repeats of this domain observed in human subjects potentially operating as a region for human-specific adaptations to environmental influences. Such a mechanism has been proposed for polymorphisms within the SLC6A4 gene which is strongly implicated in the regulation of primate-specific social behaviours (Paredes et al., 2012).

To determine whether NRSF-mediated regulation of the Imir137 promoter in response to neuronal stimulation is a conserved transcriptional mechanism in the rat brain and across different models of neurological dysfunction, the NRSF-MIR137 pathway was explored using an *in vivo* model of CSD. CSD is a neurological insult characterised by a dramatic imbalance in ion homeostasis in the brain, neurotransmission, increased metabolism and changes in cerebral blood flow, which has been identified from both clinical and animal-based studies as a potential pathophysiological mechanism in migraine, stroke, subarachnoid haemorrhage and traumatic brain injury (Lauritzen et al., 2011). CSD is preceded by propagating oscillations which indicate a transient state of hyperexcitability associated with localised epileptiform discharges (Herreras et al., 1994), which may explain the co-occurrence of CSD and seizure

following brain trauma (Fabricius et al., 2008). We proposed a novel role for NRSF in the pathophysiology of CSD due to its association with epileptogenesis and other neuronal insults which promote epilepsy and CSD, such as ischemia (Calderone et al., 2003, Noh et al., 2012, Palm et al., 1998, Spencer et al., 2006, McClelland et al., 2014, McClelland et al., 2011). In rodent models of epilepsy, hippocampal NRSF and REST4 levels are significantly up-regulated which correlates with modulation of a subset of NRSF target genes encoding for ion channels, glutamate receptor subunits and other key factors implicated in neuronal function (McClelland et al., 2011, Palm et al., 1998, Spencer et al., 2006, McClelland et al., 2014). Several of these epilepsy associated NRSF target genes are also implicated in CSD, including the CACNA1A (calcium channel, voltage-dependent, P/Q type, alpha 1A subunit) gene which is clinically associated with familial hemiplegic migraine (FHM); an autosomal dominant subtype of migraine with aura which is caused by missense mutations in the CACNA1A gene in >50% of cases, and migraine with induced susceptibility to CSD as demonstrated from a knockin mouse model of FHM (Joutel et al., 1993, Ophoff et al., 1994, van den Maagdenberg et al., 2004, Johnson et al., 2006). Furthermore, a recent *in vivo* model of global ischemia implicated the NRSF-silencing complex in targeting several genes implicated in neuronal transmission and CSD preconditioning, including GRIA2 which encodes for the AMPA-receptor GluR2 (glutamate receptor 2) subunit, which is also a target of miR-137 (Noh et al., 2012, Chazot et al., 2002, Strazisar et al., 2014). Consistent with a model of NRSF-mediated regulation of MIR137 in response neuronal stimulation (Warburton et al., 2014), at 24-hours post CSD induction down-regulation of NRSF mRNA expression and reduced NRSF binding of the Imir137

promoter was observed which correlated with up-regulation of MIR137HG. In rodent models of stroke, the levels of miR-137 have been shown to be significantly down-regulated in the brain and peripheral blood of rats subjected to cerebral ischemia relative to control subjects (Jeyaseelan et al., 2008, Zhao et al., 2013). Reduced levels of miR-137 in rat brain tissue in a model of post-stroke depression correlated with increased GRIN2A (Zhao et al., 2013), a NMDA-receptor subunit that has previously been implicated in depression and genetic association studies of epilepsy-aphasia spectrum disorders (Carvill et al., 2013, Lemke et al., 2013). The depressive behavioural effects associated with increased levels of GRIN2A in the post-stroke depression model were alleviated by injection of a miR-137 mimic, suggesting an anti-depressant-like and neuroprotective role for this miRNA (Zhao et al., 2013).

Previous studies have provided evidence to suggest that CSD may play a neuroprotective role in the brain. For example, preconditioning rodent brains with CSD has been shown to provide tolerance against subsequent ischemic insults; reducing the size of infarct lesion development following focal cerebral ischemia and increasing neurogenesis in the subventricular zone (Yanamoto et al., 2004, Yanamoto et al., 2005). The mechanisms governing tolerance to subsequent episodes of ischemia induced by CSD are not clear and may reflect up-regulation of genes implicated in neuroprotection, such as BDNF and c-Fos (Kariko et al., 1998, Kawahara et al., 1997, Rangel et al., 2001, Kim et al., 2013); both of which have been identified as known or potential NRSF target genes (Palm et al., 1998, Warburton et al., 2015). We did not see significant up-regulation of the immediate-early response genes c-Fos and c-Jun in our CSD model, which may reflect the time course used as a previous study reported that

c-Fos mRNA expression levels in response to CSD induction returned to basal levels following 24 hours recovery (Rangel et al., 2001). Up-regulation of the MIR137 transcript in our CSD model at 24 hours recovery, a period corresponding to the initial window of time in which increased tolerance can be induced by various preconditioning methods (Chazot et al., 2002), may however confer an adaptive neuroprotective effect through down-regulation of genes implicated in ischemia, providing ischemic tolerance against subsequent insults. Support for this comes from a study of CSD preconditioning in the rodent brain in which a 30% reduction in the immunoreactive form of the pro-ischemic GluR2 protein, which is encoded by the miR-137 target gene GRIA2 (Strazisar et al., 2014), was observed in the preconditioned brain relative to control animals (Chazot et al., 2002). The role of miR-137 in CSD preconditioning is being addressed through ongoing collaborations with XJTLU. Preliminary work by the group has shown that mRNA expression of the miR-137 target gene GRIN2A, previously up-regulated in animal models of ischemia (Zhao et al., 2013), is down-regulated at 24 hours post CSD relative to controls (see *Appendix 1,* **Figure A1.2**) which corresponds with up-regulation of MIR137HG, supporting our hypothesis of a neuroprotective role for miR-137 in CSD preconditioning.

NRSF has also been implicated in neuroprotection in animal models of kindling (Spencer et al., 2006, Garriga-Canut et al., 2006, Hu et al., 2011b); a model in which repeated focal application of initially sub-convulsive electrical stimulation results in seizure. An example of the neuroprotective role of NRSF in epilepsy comes from studies investigating the anticonvulsant properties of the low carbohydrate ketogenic diet used in the treatment of drug-resistant temporal lobe epilepsy and to target CSD *in vivo* (de Almeida Rabello Oliveira et

al., 2008), in which the glycolytic inhibitor 2-deoxy-D-glucose (2DG) reduces epilepsy progression through blocking seizure-induced up-regulation of BDNF expression and its receptor, TrkB, through NRSF–dependent epigenetic mechanisms (Garriga-Canut et al., 2006). An indirect neuroprotective role for NRSF in CSD preconditioning can be implied from its down-regulation at 24 hours post-CSD induction and its dissociation from the Imir137 promoter which correlated with up-regulation of MIR137HG mRNA expression. In support of the differential expression and function of the NRSF isoforms in animal and cell line models of epilepsy and clinical studies of breast and lung cancer, REST4 mRNA expression was induced in response to CSD (Spencer et al., 2006, Gillies et al., 2009, Wagoner et al., 2010, Coulson et al., 2000, Palm et al., 1998, Chen and Miller, 2013). A dual role for this transcriptional regulator in both pathogenesis and neuroprotection may reflect differences in the cellular levels or compartmentalisation of the different NRSF isoforms (Spencer et al., 2006, Zuccato et al., 2003).

*In vivo* models of CSD have shown increased densities of mitotic cells and neurogenesis in the dentate gyrus and subventricular zone and new neuron-like cells in the caudate putamen and cortex of the rat brain several days following CSD induction (Yanamoto et al., 2005). NRSF is a regulator of adult neurogenesis and has been shown to recruit the polycomb repressive complexes 1 and 2 (PRC2) in mouse embryonic stem cells (mESCs) which co-localise with the NRSF-silencing complex at genes involved in neuronal development, with displacement of this complex occurring during neuronal differentiation (Dietrich et al., 2012). EZH2, a histone H3K27 methyltransferase, is a core member of PRC2 and has been shown to co-immunoprecipitate with

NRSF in mESCs (Dietrich et al., 2012). A study in aNSCs reported cross-talk between the NRSF co-repressor molecule MeCP2, miR-137 and EZH2 (Szulwach et al., 2010). MeCP2 was shown to negatively regulate MIR137 transcription, with over-expression and down-regulation of miR-137 correlating with aNSC proliferation and differentiation, respectively (Szulwach et al., 2010). The levels of miR-137 were shown to be inversely correlated with EZH2 which was validated as a downstream target of miR-137 in aNSCs, supporting its role in the modulation of neuroprogenitor cell identity and differentiation (Shen et al., 2008, Sher et al., 2008, Ezhkova et al., 2009). ENCODE transcription factor ChIP-seq data from human cell lines predicts EZH2 binding over the human MIR137 gene locus (**Figure 6.5A**), suggesting a double-feedback mechanism in the regulation of miR-137 expression levels during neurogenesis. Polycomb proteins have been shown to be activated in animal models of ischemic tolerance, serving a neuroprotective role through transcriptional repression of pro-ischemic genes such as those implicated in ion transport, regulation of metabolism and cell-cycle control (Stapels et al., 2010). To test a potential role of this extended regulatory network, which implicates several NRSF co-binding partners, in the modulation of MIR137 expression in our CSD model, ChIP was performed using antibodies against MeCP2 and EZH2. Binding was observed for both MeCP2 and EZH2 at the Imir137 promoter across all conditions tested with no significant changes at 24 hours post-CSD. This again may reflect the timescale used in this experiment and requires further investigation at different recovery periods as ChIP and gene expression data can only offer a snapshot of the regulatory processes operating in response to neuronal stimulation. It could also indicate a potential role for these co-repressors in promoting

transcriptionally permissive chromatin environments following CSD. In stem cells, polycomb proteins have been shown to function in promoting and maintaining bivalent chromatin states which are associated with genes that are 'poised' ready for activation upon stimulation but are maintained at low levels by opposing repressive histone modifications (Lee et al., 2006). Furthermore, both MeCP2 and EZH2 have been shown to function as transcriptional activators. In a MeCP2 knock-down and over-expression mouse model, it was demonstrated that the majority of MeCP2 target genes tested (approximately 85%) were activated by this epigenetic regulator in the hypothalamus (Chahrour et al., 2008). Similarly, studies in breast cancer cells have identified a number of cancer-associated genes to be activated by EZH2 following knock-down of this polycomb protein member (Lee et al., 2011). Binding of several epigenetic regulators of the NRSF-signalling complex to the MIR137 gene locus within the rat cortex is suggestive of a dynamic regulatory feedback mechanism, which may play an important role in modulating extensive neuronal networks implicated in a range of neuronal processes relevant to normal brain physiology and disease. This is supported by the role of all of these factors in both neuronal gene activation and repression, autoregulation (suggested from *in silico* analysis of transcription factor binding motifs and ENCODE data for NRSF and EZH2) and targeting of other members of the regulatory network such as MeCP2 regulating NRSF (Abuhatzira et al., 2007) and reciprocal interactions between MIR137 and EZH2 (Szulwach et al., 2010).

## 6.5 Summary

In summary, we have validated the presence and function of the rat Imir137 promoter sequence and have demonstrated species-specific differences in the transcriptional potential of these regulatory domains based on the underlying sequence. Further we have confirmed that NRSF is one factor operating at this region but not at a second predicted NRSF binding site at the MIR137HG proximal promoter region which is consistent with previous data in the human SH-SY5Y neuroblastoma cell line. We have also identified novel transcripts encoded from the region encompassing the Imir137 promoter that are not currently annotated in the rat reference genome (Assembly rn5/rn6). One such transcript that contains the sequence of miR-137 itself was shown to be up-regulated in response to CSD at 24 hours; a period reported to correspond with the initial window of time in which increased tolerance to subsequent neuronal attacks can be induced by various preconditioning methods, indicating a potential neuroprotective effect. This correlated with down-regulation of full-length NRSF and loss of binding of this factor from the Imir137 promoter, and up-regulation of REST4, suggesting a potential role for NRSF-mediated regulation of miR-137 in CSD pathophysiology. The findings of this study are informative for animal models which aim to address modulation of the MIR137 gene locus in human neurological conditions associated with dysregulation of this brain-enriched miRNA, for example down-regulation of miR-137 in post-mortem and neuroimaging studies of schizophrenic brains.

## Part II: *The NRSF-MIR137 Pathway in Breast Cancer*

## 6.6 Introduction

The MIR137 gene is located in the melanoma susceptibility region of chromosome 1 (1p22) (Gillanders et al., 2003). In addition to its role in the CNS, MIR137 has also been identified as a tumour suppressor gene, with epigenetic silencing of miR-137 being implicated in several tumour types including human breast cancer (Vrba et al., 2013). The role of miR-137 in breast cancer is exemplified through its targeting of oestrogen-related receptor alpha (ERRα), an orphan nuclear receptor implicated in breast tumourigenesis, which was shown to impair the proliferative and migratory capacity of breast cancer cells *in vitro* (Zhao et al., 2012). This pathway could be a target for therapy as miR-137 is up-regulated in response to chemotherapy treatment of rectal cancer (Svoboda et al., 2008) and has been implicated in sensitising multidrug resistance MCF-7 breast cancer cells to chemotherapeutic agents through modulation of P-glycoprotein (permeability glycoprotein, P-gp); a drug efflux pump encoded by the MDR1 (multidrug resistant gene-1) gene and implicated in drug-resistance (Zhu et al., 2013b). More generally, miR-137 modulates numerous cell cycle proteins involved in cancer such as c-Met, MITF, CDK6, CDC42 and the H3K27 methyltransferase and polycomb member EZH2 (Chen et al., 2011b, Liu et al., 2011, Zhu et al., 2013a, Chen et al., 2011c, Bemis et al., 2008, Luo et al., 2013). Therefore a better understanding of the transcriptional regulation of this gene will give us better insight into the early steps in tumour progression.

As discussed previously, we have validated an internal promoter VNTR within the MIR137 gene that is regulated in an allele-specific and stimulus-inducible manner in human SH-SY5Y neuroblastoma cells (Warburton et al., 2014). The VNTR has previously been shown to affect the processing efficiency of miR-137 in melanoma cell lines, potentially through altering the secondary structure of the primary(pri)-miRNA in which it is located as determined by computational modelling, suggesting a functional role for this polymorphic domain in disease processes (Bemis et al., 2008). *In silico* analysis of the region identified a NRSF binding site within the repeat sequence which we determined to be functional through ChIP and NRSF/sNRSF over-exprssion assays, *Chapter 4* (Warburton et al., 2014). The NRSF isoforms supported differential regulation over the internal MIR137 promoter which was dependent upon VNTR genotype, which may be an important GxE mechanism under pathological conditions.

Differential expression of NRSF and its truncated isoform sNRSF have been implicated in tumourigenesis, and can support both oncogenic and tumour-suppressive roles dependent upon tumour type (Negrini et al., 2013). In subtypes of breast cancer, loss of full-length NRSF and induction of the truncated isoform has been associated with decreased time to disease recurrence, increased tumour size, and a higher number of lymph node metastases indicating an aggressive disease course (Wagoner et al., 2010). The tumour-suppressor function of NRSF is also supported in cell line models whereby knock-down of NRSF in low-metastatic breast cancer cells resulted in induction of the oncogene TAC1 and cellular proliferation and migration, whilst the opposite effect was observed following exogenous NRSF expression in

aggressive cell types (Reddy et al., 2009). We have previously demonstrated a role for the truncated protein in small cell lung carcinoma (SCLC) suggesting that the levels of these different isoforms may dictate tumorigenicity (Coulson et al., 1999, Coulson et al., 2000, Quinn et al., 2002). This is supported by a recent study which showed extensive alternative splicing of this transcriptional regulator between tumour and adjacent normal tissue in patients with kidney, liver and lung cancer (Chen and Miller, 2013), indicating complex and context-specific mechanisms of NRSF regulation in cancer.

In this section, modulation of the MIR137 internal promoter VNTR in the human MCF-7 adenocarcinoma breast cancer cell line is explored. Potential differential regulation of MIR137 by both NRSF and the genotype of the VNTR are addressed as a mechanism that may be important in breast cancer due to the overlapping role of both MIR137 and NRSF in this cancer type. Genotypic variation of the VNTR in a clinical cohort for breast cancer is investigated to determine whether it can be used as a novel biomarker for breast cancer or to distinguish between BRCA (breast cancer, early onset) positive and negative subtypes.

## 6.7 Aims

- Reporter gene analysis of the internal MIR137 promoter VNTR in human MCF-7 breast adenocarcinoma cells and compare to its regulation in SH-SY5Y neuroblastoma cells
- Address NRSF/sNRSF regulation over the region using over-expression constructs and ChIP
- Compare the methylation status of the MIR137 promoters in human SH-SY5Y and MCF-7 cells
- Genotype analysis of the MIR137 VNTR in a breast cancer cohort

## 6.8 Results

### 6.8.1 MIR137 transcripts are silenced in human MCF-7 breast cancer cells

Consistent with silencing of miR-137 in breast tumours (Vrba et al., 2013), the MIR137HG (AK094607), AK311400 and AK309618 mRNA transcripts which encode for this tumour-suppressor miRNA could not be detected in the human MCF-7 breast cancer cell line through RT-PCR analysis; although these transcripts are easily found in the neuroblastoma cell line SH-SY5Y (**Figure 6.7**). Comparison of reporter gene expression driven by the reporter gene constructs for the internal MIR137 promoter VNTR (Imir137) and MIR137 VNTR alone (VNTRmir137) characterised in *Chapter 4* was also performed in MCF-7 and SH-SY5Y cells to correlate the transcriptional activity of this regulatory domain against expression from the locus. The Imir137(4) and Imir137(12) promoter constructs, which contain a 4- and 12-copy repeat of the MIR137 VNTR, displayed promoter function in MCF-7 cells supporting a 3.8- and 6.6-fold increase in luciferase activity over the pGL3B vector control (***P<0.001), respectively. However, this activity was greatly reduced in comparison to SH-SY5Y cells with a fold difference of 17.3 and 11.32 in reporter gene activity observed between the two cell lines for the 4- and 12-copy variants respectively (###P<0.001, significant difference between Imir137 promoter activity between cell lines), **Figure 6.7C**. The low levels of reporter gene expression supported by the Imir137 promoter constructs in MCF-7 cells is in line with undetectable levels of the AK311400 and AK309618 mRNAs in this cell line which originate from this promoter (**Figure 6.7A-B**). Analysis of the MIR137 VNTR domain alone was also addressed, which was cloned into a reporter gene vector containing a minimal SV40 promoter as a means of

**Figure 6.7. Gene expression profiling of MIR137 host genes in SH-SY5Y and MCF-7 cells. A**, Schematic representation of the MIR137 gene locus showing the location of the precursor (pre)-miR-137 and pre-miR-2682 sequences (grey boxes) relative to the non-protein coding RNA genes MIR137HG (AK094607), AK311400 and AK309618, which encode for these miRNAs. Exons are represented as boxes; introns as the connecting lines. A 15 bp variable number tandem repeat (VNTR) 6 bp 5' of pre-miR-137 is shown as a black box; promoter CpG islands as green boxes. Region marked by the red hatched border represents the Imir137 promoter, the activity of which was assessed using reporter gene constructs (**C**). NRSF binding sites (BS) are marked by vertical arrows. Numbers represent genomic position in bp; +1 marks the first base of MIR137HG with negative and positive values marking upstream and downstream sequences, respectively. **B**, RT-PCR analysis of the MIR137 host gene mRNA expression in human MCF-7 breast adenocarcinoma and SH-SY5Y neuroblastoma cell lines. Relative primer locations for the transcripts are denoted by horizontal arrows in the schematic, **A**. Primers for AK311400 also target AK309618. Expected band sizes for MIR137HG, AK311400 and AK309618 were 291 bp, 274 bp and 451 bp, respectively. **C**, Graphs showing the average fold change in luciferase expression supported by the Imir137 promoter (*left*) and MIR137 VNTR alone (*right*) constructs over the control vector following transfection into SH-SY5Y and MCF-7 cells. Numbers in brackets represent VNTR copy number. For each transfection, $n$=4. Standard error is represented by error bars. *Significant changes in luciferase activity over control levels. #Significant changes in luciferase activity between the 4- or 12-copy VNTR variant constructs and cell lines. **/##$p<0.01$, ***/###$p<0.001$. [Figure presented on opposite page].

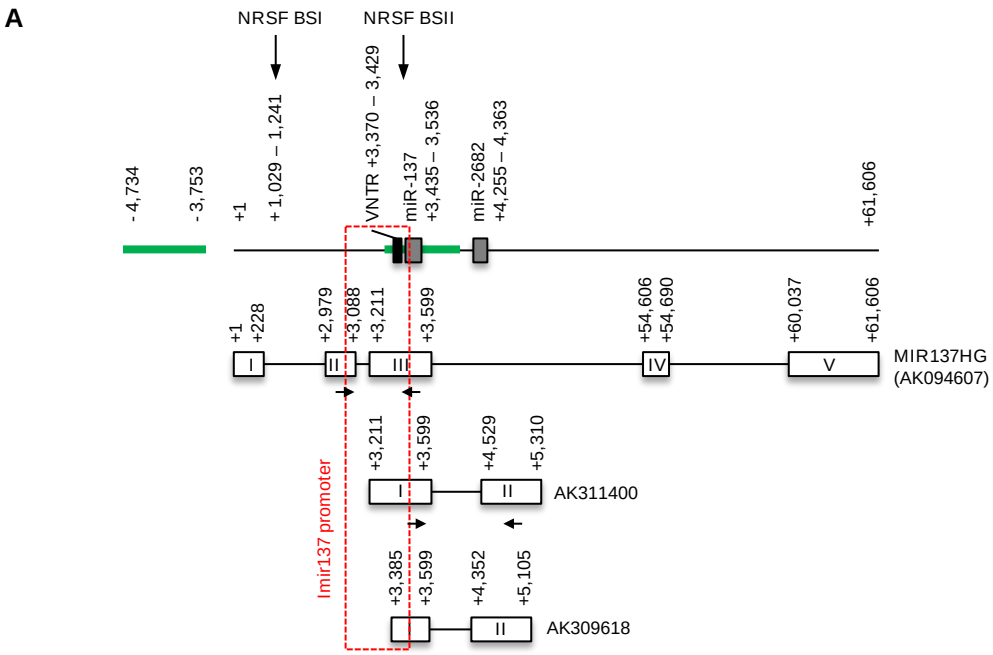
A
NRSF BSI
NRSF BSII
- 4,734
- 3,753
+1
+ 1,029 – 1,241
VNTR +3,370 – 3,429
miR-137
+3,435 – 3,536
miR-2682
+4,255 – 4,363
+61,606
+1
+228
+2,979
+3,088
+3,211
+3,599
+54,606
+54,690
+60,037
+61,606
I
II
III
IV
V
MIR137HG
(AK094607)
Imir137 promoter
+3,211
+3,599
+4,529
+5,310
AK311400
+3,385
+3,599
+4,352
+5,105
AK309618

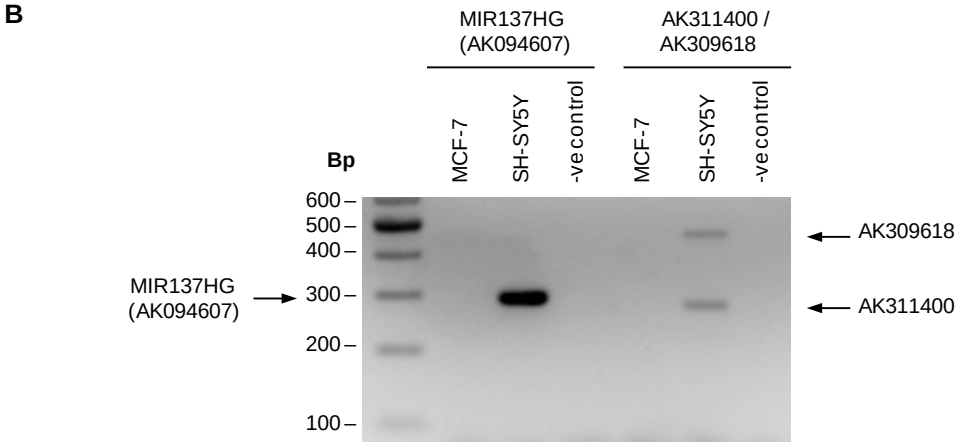
B
MIR137HG
(AK094607)
AK311400 /
AK309618
MCF-7
SH-SY5Y
-ve control
MCF-7
SH-SY5Y
-ve control
Bp
600 –
500 –
400 –
300 –
200 –
100 –
MIR137HG
(AK094607)
AK309618
AK311400

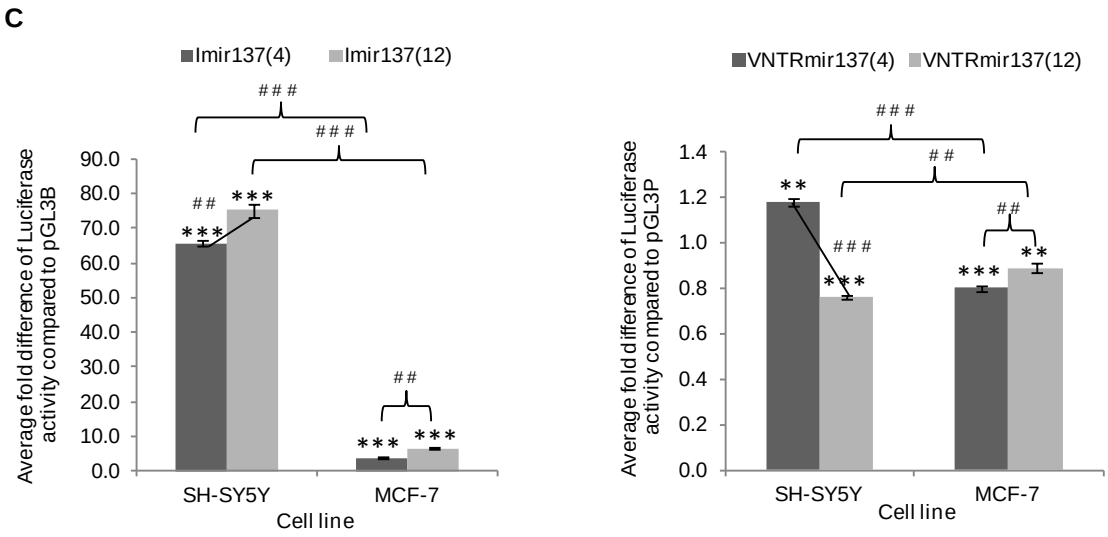
C
Imir137(4)
Imir137(12)
Average fold difference of Luciferase activity compared to pGL3B
90.0
80.0
70.0
60.0
50.0
40.0
30.0
20.0
10.0
0.0
SH-SY5Y
MCF-7
Cell line
VNTRmir137(4)
VNTRmir137(12)
Average fold difference of Luciferase activity compared to pGL3P
1.4
1.2
1.0
0.8
0.6
0.4
0.2
0.0
SH-SY5Y
MCF-7
Cell line

assessing the regulatory influence of this repetitive element on the level of gene expression driven by the minimal promoter. As shown in **Figure 6.7C**, both the VNTRmir137(4) and VNTRmir137(12) constructs, containing 4- and 12-copy repeats of the MIR137 VNTR respectively, significantly decreased the level of transcription relative to the pGL3P control vector (***P<0.001 and **P<0.01, respectively), however the VNTR does not possess major regulatory properties such as enhancer or repressor functions. Activity directed by the MIR137 VNTR constructs was significantly different between the two cell lines ($^{###}$P<0.001 and $^{##}$P<0.01; 1.5- and 1.2-fold change for the 4- and 12-copy variants, respectively), however the difference was not as dramatic as that observed for the Imir137 promoter constructs.

Epigenetic silencing is one mechanism through which miR-137 is down-regulated in tumourgenesis (Liu et al., 2011, Chen et al., 2011b, Silber et al., 2008, Vrba et al., 2013). The MIR137 gene locus contains two CpG islands (CGIs) (**Figure 6.7A**); one located 3.75 Kb upstream of the transcription start site of the non-coding RNA gene MIR137HG and the second encompassing the Imir137 promoter VNTR. Hypermethylation of the Imir137 promoter is therefore one hypothesis for the repression of miR-137 expression which could be a potential early event in the progression of a tumour. Due to the high GC-content and repetitive nature of the MIR137 VNTR within the Imir137 promoter, increases in copy number may result in hypermethylated states and silencing of genes expressed from the region. To assess whether the MIR137 VNTR sequence is a potential CGI, defined as sequence ranges were the observed over expected value of CpG dinucleotides (y-value) is greater than 0.6 and the GC-content is greater than 50%, and whether or not VNTR copy number influences the GC

potential of the Imir137 promoter region, *in silico* analysis of the 4- and 12-copy Imir137 promoter VNTR variants was performed using the Sequence Manipulation Suite (http://www.bioinformatics.org/sms2/) (Gardiner-Garden and Frommer, 1987), see *Methods section 2.2.6.7*. This software uses a 200 bp sliding-window approach, moving across the input sequence at 1 bp intervals to identify potential CGIs. Using this method, based on a 200 bp stretch of sequence the 4-copy variant had a y-value of 0.83 and a GC-content of 63%, whereas the 12-copy variant had a y-value of 1.02 and a GC-content of 74%, **Figure 6.8A**. This confirmed that the GC potential of the Imir137 promoter was positively correlated with increased copy number, which could influence promoter hypermethylation and silencing of miR-137; a potential epigenetic mechanism involved in tumourgenesis.

To address promoter methylation over the MIR137 gene locus in MCF-7 cells as a potential mechanism silencing the MIR137 transcripts in this cell line, methylated DNA immunoprecipitation (MeDIP) was performed (see *Methods section 2.2.9*) and compared to methylation patterns in SH-SY5Y cells in which the MIR137 transcripts are expressed (**Figure 6.7B**). In MCF-7 cells, enrichment of methylated DNA relative to unmethylated DNA was observed over the MIR137HG and Imir137 promoter CGIs (**Figure 6.8B**), which is consistent with undetectable levels of the transcripts originating from these promoters in this cell line (**Figure 6.7B**) and recent findings of promoter hypermethylation and miR-137 down-regulation in breast tumours (Vrba et al., 2013). The opposite was true of SH-SY5Y cells with strong signal in the unmethylated sample for both the MIR137HG and Imir137 CGIs, weaker signal in the methylated sample over the MIR137HG CGI and no methylation over the Imir137 CGI, **Figure 6.8B**.

**A**

**ImiR137(4):** y-value = 0.83, GC content = 63%

TGGGAGAGCACCAGGTAAACTGAAGGTTACTTGTCACTCCCACTTGTGCCCAAAAAGCCTTGCCACAT
CTTCCCTCCTCACTGGAAAGACAGCACTCTTCTGTGTTAAGTATTTGATTTTGTGATTTGTCTTTCAG
AATTGGAAATAGAGCGGCCATTTGGATTTGGGCAGGAAGCAGCCGAGCACAGCTTTGGATCCTTCTTT
AGGGAAATCGAGTTATGGATTTATGGTCCCGGTCAAGCTCAGCCCATCCCCAGGCAGGGGCGGGCTCA
GCGAGCAGCAAGAGTTCTGGTGGCGGCGGCGGCGGCAGTAGCAGCGGCAGCGGTAGCAGCGGCAGCGG
TAGCAGCGGCAGCGGCAGCTTGGTCCTCTGACTCTCTTCGGTGACGGGTATTCTTGGGT

**ImiR137(12):** y-value = 1.02, GC content = 74%

TGGGAGAGCACCAGGTAAACCGAAGGTTACTTGTCACTCCCACTTGTGCCCAAAAAGCCTTGCCACAT
CTTCCCTCCTCACTGGAAAGACAGCACTCTTCTGTGTTAAGTATTTGATTTTGTGATTTGTCTTTCAG
AATTGGAAATAGAGCGGCCATTTGGATTTGGGCAGGAAGCAGCCGAGCACAGCTTTGGATCCTTCTTT
AGGGAAATCGAGTTATGGATTTATGGTCCCGGTCAAGCCCAGCCCATCCCCAGGCAGGGGCGGGCTCA
GCGAGCAGCAAGAGTTCTGGTGGCGGCGGCGGCGGCAGTAGCAGCGGCAGCGGTAGCAGCGGCAGCGG
TAGCAGCGGCAGCGGTAGCAGCGGCAGCGGTAGCAGCGGCAGCGGTAGCAGCGGCAGCGGTAGCAGCG
GCAGCGGTAGCAGCGGCAGCGGTAGCAGCGGCAGCGGTAGCAGCGGCAGCGGTAGCAGCGGCAGCGGC
AGCTTGGTCCTCTGACTCTCTTCGGTGACGGGTATTCTTGGGT

**B**

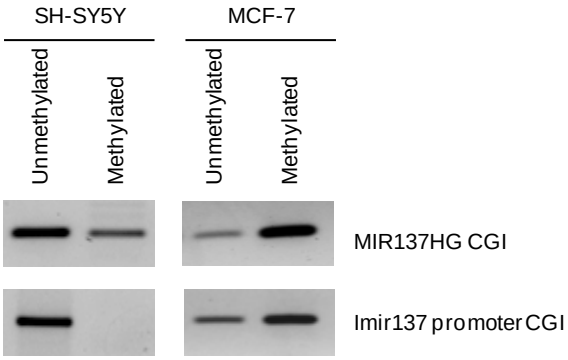


**Figure 6.8. Promoter methylation over the MIR137 gene locus. A**, *In silico* analysis of CpG potential of different alleles of the MIR137 variable number tandem repeat (VNTR) was performed using the web-based Sequence Manipulation Suite (http://www.bioinformatics.org/sms2/cpg_islands.html) which calculates the observed/expected frequency of CpG dinucleotides (y-value) using a 200 bp sliding-window approach, moving across the sequence at 1 bp intervals (Gardiner-Garden and Frommer, 1987). CpG islands (CGIs) are defined as regions of sequence with a y-value >0.6 and a GC-content >50%. The 4- and 12-copy internal MIR137 (Imir137) promoter variants were analysed; grey highlighted sequence represents the 200 bp range displaying the highest CpG potential, single and double underlined sequence marks the MIR137 VNTR and precursor-miR-137, respectively. **B**, Methylated DNA immunoprecipitation was performed using genomic DNA extracted from SH-SY5Y and MCF-7 cells which are homozygous for the 4-copy VNTR. PCR analysis was performed using primers for the MIR137HG and Imir137 promoter CGIs.

### 6.8.2 NRSF over-expression enhances Imir137 promoter activity in MCF-7 breast cancer cells

NRSF has been shown to function as both an oncogene and tumour-suppressor in a tissue-specific manner (Negrini et al., 2013). In non-neuronal tissues, NRSF functions to suppress tumourigenesis in part through inhibition of cellular proliferation (Westbrook et al., 2005), with low levels of the full-length protein detected in carcinomas of the breast, colon and lung (small cell lung carcinomas, SCLC) which has been associated with cancer progression (Lv et al., 2010, Wagoner et al., 2010, Coulson et al., 2000). Low levels of the tumour-suppressor miRNA miR-137, a target gene of NRSF (Warburton et al., 2014), has also been associated with these cancers types (Balaguer et al., 2010, Liu et al., 2011, Zhao et al., 2012, Zhu et al., 2013a), suggesting that a common mechanism implicating both NRSF and miR-137 may be involved in cancer progression. We therefore addressed whether endogenous NRSF interacted with the MIR137 gene locus in MCF-7 breast cancer cells through ChIP. As no commercial antibody is available for the truncated NRSF variant sNRSF, which has been shown to be up-regulated in more aggressive subtypes of both breast and lung cancer (Wagoner et al., 2010, Coulson et al., 2000, Chen and Miller, 2013), ChIP was performed using two different NRSF antibodies targeting both the amino- and carboxy-terminals of the full-length protein to detect enrichment of all NRSF isoforms and specific binding of the full-length protein, respectively. NRSF was shown to bind to two predicted NRSF binding sites (BS) identified from ENCODE ChIP-seq data; one over the Imir137 promoter (BSII) and the second within intron 1 of the MIR137HG gene (BSII, position +1,029-1,241 bp), **Figure 6.7A** and **6.9A**. An antibody raised against the RNA pol II C-terminal domain

(CTD) sequence, phosphorylated at the serine 5, was also used to address transcriptionally active promoter regions. This showed faint signal at the Imir137 promoter region and no signal at NRSF BSI located within intron 1 of the MIR137HG gene (**Figure 6.9A**), which is consistent with absence of MIR137 transcript expression in this cell line. Absence of RNA pol II binding at NRSF BSI may reflect its intronic location (**Figure 6.7A**), however ENCODE ChIP-seq data does predict RNA pol II binding at this region (see *Discussion*; **Figure 6.10**).

We also addressed the effects of exogenous expression of NRSF in MCF-7 cells in modulating the activity of the Imir137 promoter and VNTRmir137 reporter gene constructs. Over-expression of full-length NRSF (RE-EX1 construct) and sNRSF resulted in significant up-regulation of reporter gene activity directed by the Imir137 promoter in MCF-7 cells (**Figure 6.9B**, ***P<0.001 and **P<0.01; NRSF and sNRSF respectively supported 1.76- and 1.63-fold increases in luciferase activity over control conditions for the 4-copy variant and 1.57-and 1.54-fold increases for the 12-copy variant). The action of full-length NRSF on the VNTR alone in MCF-7 cells showed significant up-regulation in reporter gene activity relative to the pGL3P control vector and control cells that were not subjected to NRSF over-expression (**Figure 6.9C**). Similar to control conditions, over-expression of sNRSF was slightly repressive relative to luciferase activity directed by the pGL3P control vector when co-transfected with the VNTRmir137 constructs, **Figure 6.9C**. The action of full-length NRSF and sNRSF in modulating the levels of transcription directed by the MIR137 VNTR domain was nominal in the MCF-7 cell line and did not support major enhancer or repressor functions under the conditions tested.

**A**

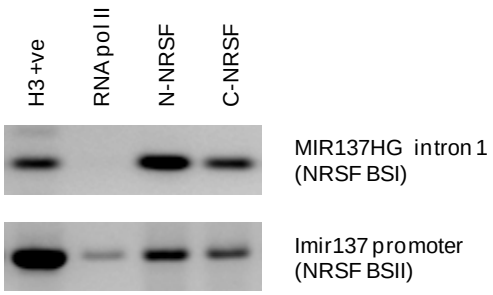


**B**

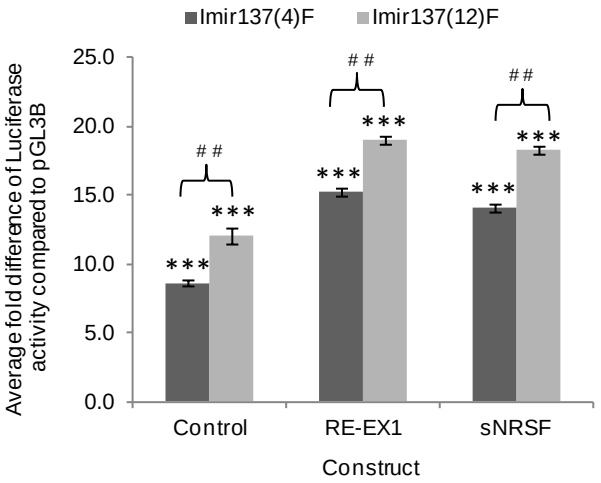


| Δ Activity | Imir137(4) | Imir137(12) |
|---|---|---|
| Control-RE-EX1 | *** | ** |
| Control-sNRSF | *** | ** |
| RE-EX1-sNRSF | - | - |

**C**

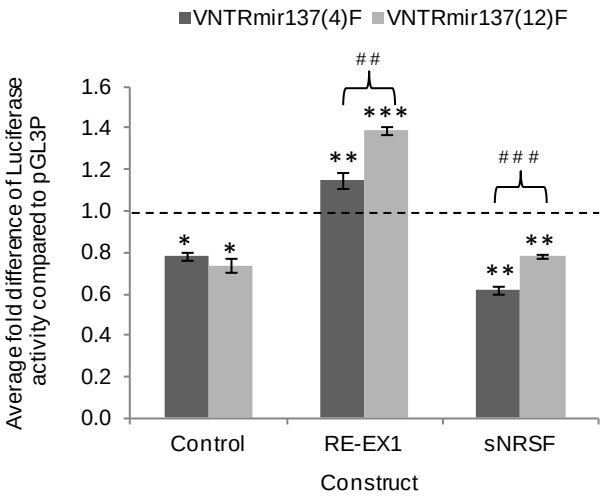


| Δ Activity | VNTR(4) | VNTR(12) |
|---|---|---|
| Control-RE-EX1 | *** | *** |
| Control-sNRSF | ** | - |
| RE-EX1-sNRSF | *** | *** |

**D**

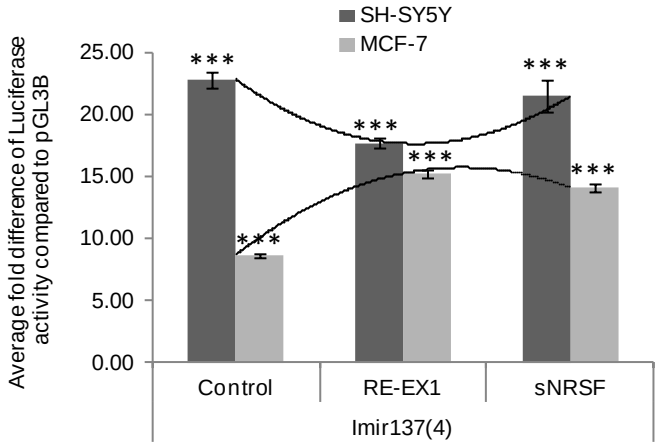


| Δ Activity | SH-SY5Y | MCF-7 |
|---|---|---|
| Control-RE-EX1 | *** | *** |
| Control-sNRSF | - | *** |
| RE-EX1-sNRSF | - | - |

**E**

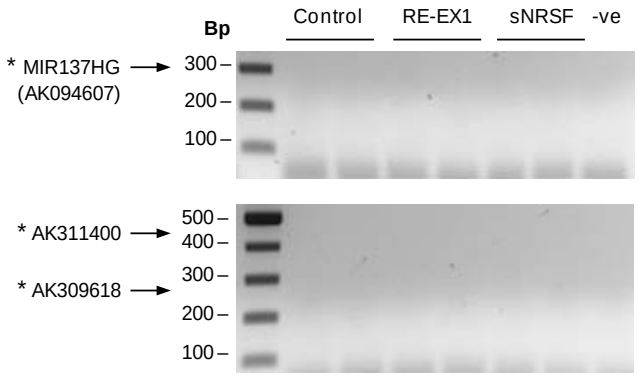


**Figure 6.9. NRSF binds to the Imir137 promoter in human MCF-7 breast cancer cells and acts to increase its transcriptional activity. A**, ChIP of NRSF binding over the MIR137 gene in MCF-7 cells. PCR analysis was performed using primers targeting intron 1 of MIR137HG, NRSF binding site (BS) I and the MIR137 internal promoter (Imir137), NRSF BSII. Antibodies against histone H3, a positive control for the ChIP; RNA pol II (C-terminal domain phosphorylated at serine 5 to show transcriptionally active promoter regions) and NRSF, two separate antibodies targeting the N- and C-terminal of full-length NRSF were used. **B-C**, Graphs showing the average fold change in luciferase expression supported by the Imir137 promoter (**B**) and VNTRmir137 (**C**) constructs over control vectors following co-transfection with the RE-EX1 (full-length NRSF) or sNRSF expression constructs. Dashed horizontal line in **C** marks expression level of pGL3P control. **D**, Comparison of reporter gene activity between SH-SY5Y and MCF-7 cells following co-transfection of Imir137(4) with RE-EX1 or sNRSF expression constructs. Trend lines for luciferase activity in SH-SY5Y and MCF-7 cells are shown as a block and dashed line. For each transfection, *n*=4. Error bars represent standard error. *Significant changes in luciferase activity over vector control levels and/or treatment conditions (displayed in a table below the corresponding graph), or #significant changes between the 4- and 12-copy variants. */#p<0.05, **/##p<0.01, ***/###p<0.001. **E**, RT-PCR of MIR137 transcript expression following RE-EX1 and sNRSF over-expression in MCF-7 cells, *n=3*. *Expected band sizes (see legend for **Figure 6.7B**).

NRSF has been shown to function as both an oncogene and tumour-suppressor in neuronal and non-neuronal tissues, respectively (Negrini et al., 2013), whereas the levels of miR-137 are reduced in several tumour types regardless of origin (i.e. neuronal verses non-neuronal) (Zhu et al., 2013a, Ando et al., 2009, Kozaki et al., 2008, Bandres et al., 2009, Langevin et al., 2010, Langevin et al., 2011, Balaguer et al., 2010). To explore NRSF-mediated regulation of miR-137 expression in both neuronal and non-neuronal cancer cells, the effect of full-length NRSF and sNRSF over-expression on reporter gene activity supported by the Imir137 promoter was compared across the SH-SY5Y neuroblastoma and MCF-7 breast cancer cell lines. To control for the endogenous effects of the Imir137 promoter, activity of the Imir137(4) construct was addressed due to both cell lines being homozygous for the 4-copy variant, determined by genotype analysis (data not shown). Consistent with its dual role as an activator and suppressor of tumourgenesis, NRSF over-expression in SH-SY5Y cells supported a ~30% reduction in Imir137 promoter activity relative to control cells (***P<0.001), whereas a ~80% increase in activity was observed in MCF-7 cells (***P<0.001), **Figure 6.9D**. This would imply that an increase in NRSF expression would correlate with transcriptional down-regulation of the tumour-suppressor miR-137 in neuroblastoma cells but increase its expression levels in breast cancer cells. This has previously been demonstrated in SH-SY5Y cells whereby over-expression of full-length NRSF resulted in down-regulation of the AK311400 and AK309618 transcripts which encode for miR-137 (Warburton et al., 2014). Following NRSF over-expression in MCF-7 cells, the levels of MIR137HG, AK311400 and AK309618 mRNA expression were still below detectable levels by RT-PCR analysis (**Figure 6.9E**)

which may be the result of epigenetic silencing such as promoter methylation (**Figure 6.8B**). However MIR137 transcript levels were still undetectable following 72 hour treatment of MCF-7 cells with the DNA demethylation agent 5-Aza-2′-deoxycytidine (data not shown) indicating that additional repressive mechanisms other than DNA methylation are involved in silencing of the MIR137 gene locus in MCF-7 cells. The effects of sNRSF over-expression on Imir-137 did not significantly differ from control conditions in SH-SY5Y cells. Similar to the full-length protein, sNRSF supported a ~60% increase in Imir137 promoter activity in MCF-7 cells (***P<0.001), **Figure 6.9D**. The truncated sNRSF variant was not detectable by RT-PCR in MCF-7 cells (data not shown) and is only present at very low ratios in SH-SY5Y cells relative to the full-length protein (see *Appendix 3*) which may account for the minimal effects observed following over-expression of this isoform.

### 6.8.3 MIR137 VNTR as a biomarker for breast cancer

Our group has extensive experience on the potential role of VNTRs in acting as clinical markers of predisposition to neurological disease, offering a mechanism by which regulatory DNA could support differential expression of the target gene based on copy number of the VNTR (Paredes et al., 2012, Ali et al., 2010, Haddley et al., 2008, Breen et al., 2008, Roberts et al., 2007, Guindalini et al., 2006, Klenova et al., 2004, Vasiliou et al., 2012). More recently the group extended this analysis to a VNTR within the oestrogen related receptor gamma gene and its association to breast cancer (Galindo et al., 2011). Work presented in this chapter and previously (*Chapter 4*) has shown that different copy-number variants of the internal promoter VNTR within the MIR137 gene can

support differential reporter gene expression in a cell-specific and stimulus-inducible manner *in vitro* (Warburton et al., 2014). miR-137 has been identified as a tumour-suppressor in several cancer types including breast cancer in which levels of promoter hypermethylation have been correlated with its down-regulation in breast tumours (Vrba et al., 2013). *In silico* analysis of differences in the GC potential of the 4- and 12-copy variants of the Imir137 promoter VNTR showed that increased copy number was positively correlated with the overall percentage GC-content and the number of CpG dinucleotides over the region (**Figure 6.8A**). This suggests that VNTR genotype may influence hypermethylated states in the development or progression of a tumour. To address a potential role of the MIR137 VNTR as a novel biomarker for breast cancer or to distinguish between BRCA positive and negative subtypes, genotype analysis was performed in a breast cancer and matched control cohort (see *Materials section 2.1.4.1* for cohort details). A simple observation of the genotype frequencies indicated that the BRCA1 grouping had a trend towards heterozygous individuals possessing a common 4-copy allele with a larger rare copy-number variant, **Table 6.1**. This was confirmed by *Clump* analysis (see *Methods section 2.2.10.1*), used for significance-testing of allele and genotype frequency data between the different groupings of the breast cancer cohort, which showed there was a significant difference (0.046) between BRCA1+ and BRCA Wt individuals (**Table 6.2**). However due to the small size of the cohort, this preliminary analysis requires replication in a larger study cohort. No such genetic correlation was observed between BRCA Wt and BRCA2+ or BRCA1/2+ individuals combined, suggesting that the MIR137 VNTR could act as a novel biomarker for predisposition to breast cancer in BRCA1+ individuals. Genotype

analysis was performed blind to clinical data relating to age at diagnosis, disease severity or treatment responses but would be interesting to follow-up to determine any correlation between VNTR copy number and disease prognosis.

**Table 6.1.** Genotype analysis of the MIR137 VNTR in a breast cancer cohort

| Genotype | Controls | | BRCA Wt | | BRCA1+ | | BRCA2+ | |
|---|---|---|---|---|---|---|---|---|
| | Number of Counts | % | Number of Counts | % | Number of Counts | % | Number of Counts | % |
| 4_4 | 51 | 52.58 | 47 | 52.81 | **15** | **39.47** | **17** | **47.22** |
| 4_5 | 9 | 9.28 | 9 | 10.11 | 4 | 10.53 | 8 | 22.22 |
| 4_6 | 8 | 8.25 | 13 | 14.61 | 5 | 13.16 | 5 | 13.89 |
| 4_7 | 9 | 9.28 | 3 | 3.37 | 4 | 10.53 | 3 | 8.33 |
| 4_8 | **6** | **6.19** | **4** | **4.49** | 0 | 0.00 | 1 | 2.78 |
| 4_9 | **2** | **2.06** | **4** | **4.49** | 1 | 2.63 | 0 | 0.00 |
| 4_10 | 1 | 1.03 | 3 | 3.37 | **4** | **10.53** | 0 | 0.00 |
| 4_11 | 2 | 2.06 | 0 | 0.00 | **2** | **5.26** | 1 | 2.78 |
| 4_12 | 0 | 0.00 | 0 | 0.00 | **2** | **5.26** | 0 | 0.00 |
| 3_4 | 1 | 1.03 | 0 | 0.00 | 0 | 0.00 | 0 | 0.00 |
| 5_5 | 0 | 0.00 | 0 | 0.00 | 1 | 2.63 | 0 | 0.00 |
| 5_6 | 3 | 3.09 | 0 | 0.00 | 0 | 0.00 | 0 | 0.00 |
| 5_7 | 1 | 1.03 | 1 | 1.12 | 0 | 0.00 | 0 | 0.00 |
| 5_8 | 1 | 1.03 | 1 | 1.12 | 0 | 0.00 | 0 | 0.00 |
| 5_12 | 0 | 0.00 | 1 | 1.12 | 0 | 0.00 | 0 | 0.00 |
| 6_8 | 0 | 0.00 | 1 | 1.12 | 0 | 0.00 | 0 | 0.00 |
| 6_9 | 1 | 1.03 | 1 | 1.12 | 0 | 0.00 | 0 | 0.00 |
| 7_10 | 2 | 2.06 | 0 | 0.00 | 0 | 0.00 | 1 | 2.78 |
| 8_10 | 0 | 0.00 | 1 | 1.12 | 0 | 0.00 | 0 | 0.00 |
| **Total** | **97** | | **89** | | **38** | | **36** | |

*Note:* Values represent the number of individuals and percentage frequency of the observed genotypes for the MIR137 variable number tandem repeat (VNTR). Alleles are named 3-12, representing the different copy numbers of the 15 bp VNTR of which 4-copies is the most common variant. Bold text represents a higher percentage frequency of a particular genotype in control and BRCA wild type (Wt) individuals compared to BRCA+ individuals or vice-versa. BRCA+ individuals are those that tested positive for germline mutations within the BRCA1 or BRCA2 genes; BRCA Wt individuals are those that did not test positive for such mutations.

**Table 6.2.** Significance-testing of genotype data in a breast cancer cohort using *Clump* analysis

| **Samples** | **T1** | **T2** | **T3** | **T4** |
|---|---|---|---|---|
| BRCA Wt and controls | 0.379 | 0.230 | 0.391 | 0.395 |
| BRCA1 and controls | 0.087 | 0.255 | 0.171 | 0.066 |
| BRCA2 and controls | 0.782 | 0.838 | 0.583 | 0.723 |
| BRCA Wt and BRCA1 | 0.104 | 0.105 | 0.169 | **0.046*** |
| BRCA Wt and BRCA2 | 0.403 | 0.185 | 0.572 | 0.437 |
| BRCA1 and BRCA2 | 0.293 | 0.053 | 0.173 | 0.191 |
| BRCA+ and controls | 0.227 | **0.033*** | 0.171 | 0.267 |
| BRCA+ and BRCA Wt | 0.187 | 0.257 | 0.224 | 0.214 |

*Note:* The Monte-Carlo simulation statistic from *Clump* (10,000 simulations, T4 (2x2 clump) statistic, Chi-Sq=15.79, d.f.=1) indicated a significant genotypic association (p=0.046). This suggests at least a nominal association of the MIR137 VNTR with a BRCA1 mutation when compared with BRCA wild type (Wt) controls. The genotypes clumped together in the first column of the 2x2 table were 1 2 3 5 6 11 12 13 14 15 16. A significant association was also reached when BRCA positive individuals were compared with control samples (10,000 simulations, T2 (columns with small expected values grouped together) statistic, Chi-Sq=8.75, d.f.=3), however this test is thought to be less sensitive in detecting associations compared with normal chi-squared (T1) or the chi-squared for the clumped 2x2 table (T4) statistics.

## 6.9 Discussion

Dysregulation of miR-137 has been associated with several cancer types including breast, gastric, glioma, lung, uveal melanoma and squamous cell carcinoma of the head and neck (Zhu et al., 2013a, Ando et al., 2009, Kozaki et al., 2008, Bandres et al., 2009, Langevin et al., 2010, Langevin et al., 2011, Balaguer et al., 2010). Several studies have shown that miR-137 functions as a tumour-suppressor in part through inhibition of cell proliferation and invasion; cellular processes associated with tumourigenesis (Silber et al., 2008, Bier et al., 2013, Balaguer et al., 2010, Althoff et al., 2013, Bemis et al., 2008). Epigenetic silencing of miR-137 is thought to be one mechanisms involved in dysregulation of this miRNA in tumourigenesis. This is supported from our *in vitro* analysis of MIR137 primary transcript mRNA expression in MCF-7 breast cancer cells which were undetectable across a range of conditions including treatment with the demethylation drug 5-Aza-2′-deoxycytidine and also clinically in a study of breast tumour samples which correlated promoter DNA hypermethylation with miR-137 down-regulation (Vrba et al., 2013). The bioinformatic and functional data on the Imir137 promoter presented in this chapter and previously in *Chapter 4* suggests a model in which the genotype of the VNTR could support differential gene expression from the region (Warburton et al., 2014), for example through altering the number of binding sites for transcription factors or epigenetic regulators within this identified regulatory domain which in turn could result in chromatin remodelling and gene activation or silencing. In relation to cancer, differential expression of miR-137 has not only been observed between tumour verses normal tissue samples but also in low versus high grade tumours as demonstrated in gliomas (Silber et al., 2008, Chen et al.,

2012), suggesting that low levels of miR-137 could be related to poor disease prognosis.

Given that miR-137 promoter hypermethylation is associated with cancer, it can be hypothesised that individuals carrying higher repeat alleles of this VNTR will be more susceptible to tumour development and/or disease progression than those carrying lower copy-number variants as a result of the increased number of CpG residues available for methylation. Bioinformatic analysis of GC-potential over the Imir137 promoter for the functionally distinct 4- and 12-copy variants of this regulatory domain showed that the larger VNTR had a significantly higher percentage of overall GC-content and CpG residues than the common 4-copy variant (**Figure 6.8A**), suggesting a greater potential for hypermethylated states in individuals carrying higher copy alleles. We therefore addressed whether the VNTR could be used as a novel biomarker for breast cancer through genotype analysis of the MIR137 VNTR in a breast cancer and matched control cohort. This showed a significant difference in genotype frequencies between BRCA Wt and BRCA1 positive individuals in this small clinical cohort, which may indicate an additional predisposing factor in the development of breast cancer in this disease group; however this requires replication in a larger study cohort. A recent study has shown that BRCA1 functions to up-regulate miRNA biogenesis and can directly interact with the primary transcripts from which miRNAs are encoded through recognition of the secondary RNA structure of these miRNA genes (Kawai and Amano, 2012). It has been shown that the 12-copy MIR137 VNTR affects the processing efficiency of pri-miR-137 in melanoma cell lines, potentially through altering the secondary structure of the primary miRNA transcript (Bemis et al., 2008).

As shown in **Figure 6.10** below, ENCODE ChIP-seq data indicates signal for BRCA1 binding at a region overlapping with the NRSF BSI within intron 1 of the MIR137HG primary transcript, providing a molecular mechanism through which BRCA1 mutations and higher copy numbers of the MIR137 VNTR could interact to make an individual susceptible to breast cancer through down-regulation of miR-137 levels within the cell. BRCA1 has been shown to interact with the SWI/SNF chromatin-remodelling complex which forms a super-complex with NRSF and its co-regulatory factors in the regulation of neuronal gene expression in neuroblastoma and lung cancer cell lines (Hill et al., 2004, Loe-Mie et al., 2010, Watanabe et al., 2006). A complex regulatory network implicating several epigenetic factors may be involved in the modulation of miR-137 expression with genetic variants embedded within the locus acting to modify these levels of transcription through differential interaction with regulatory factors, such as transcription factors and CpG binding proteins or through influencing the secondary structure and processing of pri-miRNA genes (Szulwach et al., 2010, Warburton et al., 2014, Bemis et al., 2008). This could have significant downstream consequences on a plethora of miR-137 gene targets involved in tumourigenesis including those implicated in breast cancer, such as ERRα which has been associated with the proliferative and migratory capacity of breast cancer cells and EZH2 implicated in anchorage-independent growth and cell invasion of mammary epithelia cell lines (Zhao et al., 2012, Szulwach et al., 2010, Kleer et al., 2003, Luo et al., 2013).

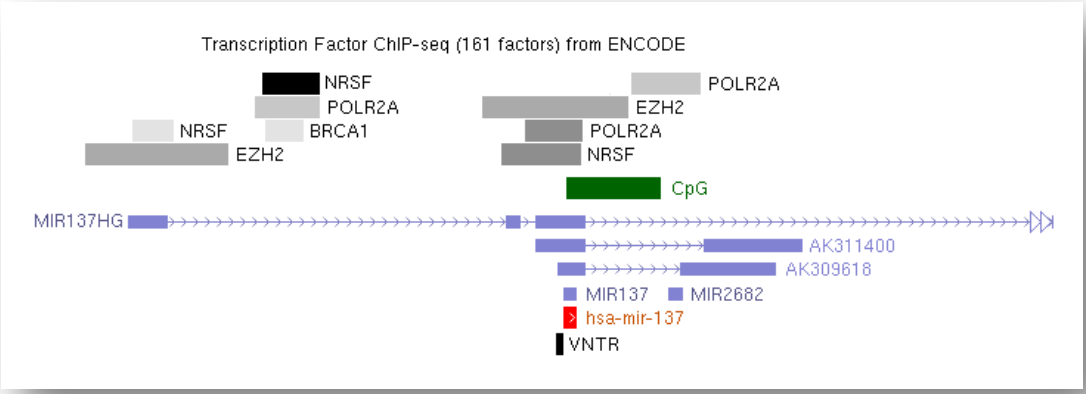


**Figure 6.10. Transcription factor binding over the MIR137 gene locus.** ENCODE ChIP-seq data (March 2012 release) identifies BRCA1 binding within the primary transcript of miR-137 (pri-miR-137), upstream of a variable number tandem repeat domain previously identified as altering the secondary structure of pri-miR-137. Image generated using the UCSC Genome Browser (https://genome.ucsc.edu/index.html).

NRSF has been proposed to function as both a tumour suppressor and oncogene dependent upon cellular context. For example, in neuronal cells and tumour types such as glioblastomas, medulloblastomas and neuroblastomas it has been shown to be oncogenic, whereas in carcinomas of the lung, breast and colon it acts as a tumour suppressor (Negrini et al., 2013). This is supported by the observed down-regulation of both Imir137 promoter activity, assessed through analysis of reporter gene expression relative to control cells, and AK311400 and AK309618 mRNA expression, which encode for the tumour-suppressor miR-137, following over-expression of NRSF in the SH-SY5Y neuroblastoma cell line (Warburton et al., 2014). In contrast, in MCF-7 breast cancer cells we showed that NRSF over-expression significantly up-regulated reporter gene activity supported by the Imir137 promoter, which may reflect its

role as a tumour suppressor through up-regulation of miR-137 which also functions as a tumour suppressor and has been shown to be significantly down-regulated in both breast cancer cell lines and tumours (Vrba et al., 2013). Over-expression of sNRSF in our tissue culture model had similar effects on Imir137 reporter gene to that of the full-length protein which may reflect its specificity in more aggressive tumour subtypes as previously demonstrated in breast and lung (SCLC) tumours (Wagoner et al., 2010, Coulson et al., 2000).

## 6.10 Summary

Aberrant epigenetic modulation of the MIR137 gene, such as DNA hyper-methylation, is often observed in tumourigenesis and is considered an early event in the progression of the tumour. We have extended our recently characterised regulatory pathway involving NRSF-mediated transcriptional regulation of the internal MIR137 promoter VNTR, hypothesised to be an important mechanism in neurological dysfunction relevant to schizophrenia, to an *in vitro* model of breast cancer. We also identified a preliminary association between MIR137 VNTR genotype and breast cancer susceptibility in individuals carrying the BRCA1 mutation relative to BRCA Wt individuals that also have breast cancer. We propose that the molecular mechanisms underpinning this genetic association could be related to the disrupted processing of the primary miRNA transcripts encoding for the tumour suppressor miR-137 in the presence of high copy-number variants of the MIR137 VNTR.

# Chapter 7

## Thesis Summary

## 7.1 Project overview

This thesis provides novel insights into the role of NRSF in regulating the transcription of the schizophrenia genome wide associated gene, MIR137, providing a functional annotation of the regulatory role of genetic variants embedded within this disease-susceptibility locus. In line with our initial project aims, several key observations were made:

- An internal promoter (Imir137) within the MIR137 gene locus identified from bioinformatic analysis of the region which contains a highly polymorphic VNTR domain can support allele-specific reporter gene expression *in vitro*; a regulatory mechanism that is distinct from the GWAS SNPs for schizophrenia due to absence of linkage disequilibrium (LD) between these polymorphisms.
- No clinical association was determined between the VNTR genotype or allele frequency and risk for schizophrenia; however a SNP within the Imir137 promoter that displayed allele-specific reporter gene expression was found to be in strong LD with the GWAS SNP rs1625579, linking this regulatory domain to schizophrenia and suggesting that an associated haplotype conferring risk for schizophrenia may be flanked by these two markers.
- A preliminary association between MIR137 VNTR genotype and breast cancer susceptibility was observed in individuals carrying the BRCA1 mutation relative to BRCA Wt individuals that also have breast cancer which may reflect disrupted processing of the primary miR-137 transcripts in the presence of high copy-number variants of the MIR137 VNTR.

- NRSF can bind to and modulate the activity of the Imir137 promoter in an allele-dependent, stimulus-inducible and cell/tissue-specific fashion.
- Different NRSF isoforms have distinct regulatory potential over the Imir137 promoter in a context-dependent manner which may be appropriate for different disease models in which the ratios of NRSF vary.
- Genetic variants within the NRSF gene locus may also affect the regulation of NRSF expression or downstream target genes such as BDNF which may be an important mechanism for cognitive dysfunction associated with neurological disease.

These observations highlight NRSF as an important modulator of GxE signals operating at the MIR137 locus and identify the NRSF-MIR137 regulatory model as a potential common mechanism associated with different disease states.

## 7.2 NRSF as a 'master regulator' of common disease pathways

Modulation of gene expression is important for establishing cell-specific phenotypes, with dysregulation of the cellular transcriptome being widely implicated in disease processes. Both short and medium-to-long-term alterations in cellular gene expression profiles can result from differences in the active complement of transcription factors within the nucleus. Exploration of the role of the transcription factor NRSF in modulating neuronal gene expression and cellular pathways important in neurological function and disease indicated that disrupting the normal cellular balance of NRSF within the cell may be a fundamental mechanism across a range of common disorders. These included cognitive dysfunction; polymorphisms within NRSF and its gene

target BDNF correlated with memory performance in patients with newly diagnosed epilepsy (*Chapter 3*), schizophrenia; NRSF was shown to be directly operating at the GWAS-identified MIR137 gene and was capable of directing allele-specific and stimulus-driven expression from the locus (*Chapter 4*), mood disorders; identified from *in silico* analysis of genes expression changes in response to mood-modifying drugs as a significant pathway regulating cellular processes relevant to mood (*Chapter 5*) and tumourigenesis; mediated cell-specific regulation of the tumour-suppressor gene MIR137 supporting its role as both an oncogene and tumour-suppressor in different tumour types (*Chapter 6*) (Negrini et al., 2013).

The levels or activity of NRSF have previously been correlated with several pathological states including elevated levels in animal and tissue culture models of epilepsy and Huntington's disease (Palm et al., 1998, Spencer et al., 2006, Gillies et al., 2009, Zuccato et al., 2007, Johnson et al., 2008, Soldati et al., 2013), decreased levels in the prefrontal cortex and hippocampal neurons of human patients with mild cognitive impairments and Alzheimer's disease (Lu et al., 2014), inhibited function in cardiac hypertrophy and arrhythmias resulting from the induction of foetal cardiac genes in ventricular myocytes as demonstrated in a transgenic mouse model (Kuwahara et al., 2003) and modulation of endophenotypes associated with schizophrenia through regulation of GWAS candidate genes for schizophrenia, including TCF4 which has been identified as a target of miR-137 (Kwon et al., 2013), through interaction with the SWI/SNF chromatin remodelling complex (Loe-Mie et al., 2010). There is considerable overlap between dysregulation of NRSF and miR-137 in several pathological conditions, including Huntington's disease,

Alzheimer's disease, schizophrenia, cardiomyopathies and several cancer types (Lok et al., 2013, Soldati et al., 2013, Geekiyanage and Chan, 2011, The Schizophrenia Psychiatric GWAS Consortium, 2011, Ripke et al., 2013), which lends support to a common mechanism involving the NRSF-MIR137 pathway in disease processes. NRSF-dysregulation in animal models of Huntington's disease has identified both BDNF and more recently miR-137 as disease-associated targets (Zuccato et al., 2003, Soldati et al., 2013). Interestingly, manipulating the cellular levels of miR-137 has recently been shown to inversely affect BDNF mRNA expression in human neural progenitor cells, extending the NRSF-MIR137 regulatory model to include another schizophrenia candidate gene (Hill et al., 2014, Green et al., 2011, Dunham et al., 2009). The interaction between miR-137 and BDNF was not validated as being direct and there is not a predicted miR-137 recognition site over the BDNF gene locus (miRNA target prediction software available at microRNA.org – Targets and Expression, http://www.microrna.org/microrna/getGeneForm .do). This may reflect an indirect association between miR-137 and BDNF, for example through modulating the levels of EZH2 which is a known target of miR-137 (Szulwach et al., 2010) and is enriched over the BDNF gene locus as indicated from ENCODE data, **Figure 7.1**. EZH2 is a member of the polycomb repressive complex-2 and is important for the regulation of several developmental processes, including neurodevelopment, and is dysregulated in several cancer types (Ronan et al., 2013). It has been shown to interact with the NRSF-signalling complex and function as a co-repressor of neuronal gene expression (Dietrich et al., 2012), and also targets miR-137 *in vivo* as demonstrated through ChIP analysis in rat cortical tissue (*Chapter 6*). This reinforces the idea of extensive double feedback

mechanisms operating between members of the NRSF-signalling complex in modulating target gene expression and disease pathways relevant to CNS dysfunction and cancer.

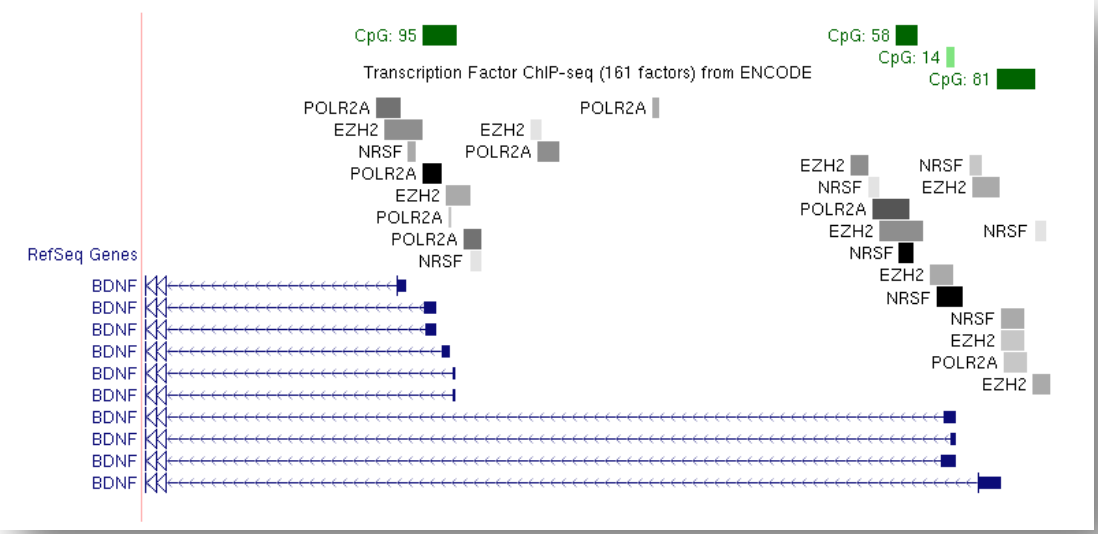


**Figure 7.1. Predicted binding of EZH2** (Enhancer of zeste homolog 2) over the human BDNF gene locus. Potential regulatory mechanism linking the inverse correlation between miR-137 knock-down and BDNF up-regulation observed in human neural progenitor cells (Hill et al., 2014). EZH2 is a co-repressor that is known to interact with the NRSF-silencing complex and is a direct target of miR-137. Image generated using ENCODE data available through the UCSC Genome Browser (https://genome.ucsc.edu/).

## 7.3 A neuroprotective role for NRSF

Data presented in *Chapter 6* indicates a potential neuroprotective role for the NRSF-MIR137 pathway in a rodent model relevant to ischemic-tolerance. Such a role has previously been suggested for NRSF in animal models of kindling in which modulation of NRSF expression has been shown to block seizure-induced up-regulation of the proconvulsant gene BDNF and promote up-regulation of the anticonvulsant gene galanin (Spencer et al., 2006, Garriga-Canut et al., 2006, Hu et al., 2011b). Elevated levels of NRSF in the normal ageing human brain has also been proposed to play a neuroprotective role against Alzheimer's disease pathology through repressing target genes that promote cell death and β-amyloid (Aβ)-toxicity and increasing the expression of genes which mediate resistance against oxidative stress; reportedly through an indirect mechanism (Lu et al., 2014). Interestingly, miR-21, -132, -212, -330 and -1208 identified from *in silico* analysis as novel NRSF-target miRNAs and to be significantly associated with gene ontology pathways relevant to neurological disease processes (determined using the online DIANA-miRPath pathway analysis tool), were shown to interact with FOXO3 (*Chapter 5*); a Forkhead-box transcription factor recently identified as a mediator of neuronal death in primary hippocampal and cortical neurons in response to Aβ-toxicity (Sanphui and Biswas, 2013). These miRNAs therefore provide a possible link between NRSF down-regulation and Aβ-toxicity in Alzheimer's disease. Furthermore, of these potential NRSF-target miRNAs, miR-330 and -1208 (as well as miR-210, -345, -658 and -607) were shown to have SVA (SINE-VNTR-Alu) insertions, which are hominid-specific transposable elements, within 120 Kb of their pre-miRNA sequences, determined through bioinformatic analysis (see *Chapter 5*,

**Table 5.3**). SVAs have been associated with several diseases, including haemophilia, Duchenne muscular dystrophy, cystic fibrosis and several cancers, through disrupting the transcriptional regulation and processing of the target gene into which they have inserted (Hancks and Kazazian, 2012, Kaer and Speek, 2013, Savage et al., 2013, Savage et al., 2014). The miRNAs indentified from our *in silico* analysis may therefore present a novel set of targets involved in the pathology of a number of disease states and would be interesting to follow-up in future studies. The role of NRSF in modulating disease pathways, and whether it functions to promote or suppress them, is an extremely complex and tissue-specific process which likely reflects many factors including but not limited to cellular levels and compartmentalisation of the different NRSF isoforms, interaction of the NRSF-signalling complex with available co-binding partners, the composition and genomic location of the NRSE to which NRSF binds and the effect of environmental influences.

## 7.4 NRSF as an integrator of GxE mechanisms in the CNS

Predisposition to neuropsychiatric disease is not only governed by our genetic makeup but also the influence of gene variants on how we respond to our environment. Cellular responses to particular environmental exposures such as early life trauma, stress or urban living, which have been identified as risk-factors that can impact on our mental health (van Os et al., 2010), may not be reflected in our immediate behaviour but could leave a molecular footprint of the event which in later life may present as a neuropsychiatric phenotype when the individual is exposed other stressful stimuli. Genetic variation within regulatory networks that are associated with neuronal function may play an

important role in disease predisposition through impacting on the transcriptional machinery which governs cellular responses to an environmental challenge. NRSF interacts with a myriad of co-binding factors to regulate appropriate gene-expression in neuronal and non-neuronal tissues (Ooi and Wood, 2007). The NRSF-signalling complex could therefore be considered a central hub for co-ordinating the cellular transcriptome and epigenome in the maintenance of cellular homeostasis, with perturbations in this pathway having the scope to disrupt global gene expression due to its capacity to modulate hundreds of target genes in tandem through direct interaction or dynamic coupling with a vast repertoire of regulatory factors such as chromatin remodelling enzymes and non-coding RNAs which in turn have extensive downstream effects on gene expression (Bruce et al., 2004, Wu and Xie, 2006, Johnson et al., 2009, Mortazavi et al., 2006). The polymorphisms identified in this study to impart a genetic influence on disease phenotypes and/or to be implicated in regulatory mechanisms associated with cellular dysfunction may additively contribute to disease susceptibility through modifying the levels of the target candidate gene along the NRSF-signalling pathway. Analysis of the influence of these markers (NRSF rs1105434 and rs2227902; BDNF rs11030094, rs12273363, rs1491850, rs2030324 and rs3796529; and MIR137 VNTR) using eQTL data from different disease cohorts would allow for assessment of the proposed role of a disrupted regulatory pathway implicating the NRSF-signalling network as a potential common mechanism underlying disease aetiology.

## 7.5 Final conclusions

The observations made in this thesis highlight the importance of GxE mechanisms in shaping the transcriptional landscape of disease-associated loci and point to NRSF as a potential modulator of genetic influences on cellular responses to environmental stimuli, which may be applicable to several disease states from neurological dysfunction to cancer. The use of bioinformatic approaches to predict potentially important regulatory domains within miRNA genes which may confer risk for disease susceptibility was successfully demonstrated in this study using the MIR137 gene locus as a model example. Other potential NRSF target miRNA genes which share common genomic features with the MIR137 gene locus (such as repetitive elements and overlapping CpG islands within their 5' flank sequences), and have been identified from pathway analysis to play a significant role in cellular processes relevant to neurological disorders, might point to other important NRSF regulated miRNAs involved in disease processes.

# Chapter 8

## Reference list

AAN HET ROT, M., MATHEW, S. J. & CHARNEY, D. S. 2009. Neurobiological mechanisms in major depressive disorder. *CMAJ,* 180**,** 305-13.

ABRAMOVITZ, L., SHAPIRA, T., BEN-DROR, I., DROR, V., GRANOT, L., ROUSSO, T., LANDOY, E., BLAU, L., THIEL, G. & VARDIMON, L. 2008. Dual role of NRSF/REST in activation and repression of the glucocorticoid response. *J Biol Chem,* 283**,** 110-9.

ABUHATZIRA, L., MAKEDONSKI, K., KAUFMAN, Y., RAZIN, A. & SHEMER, R. 2007. MeCP2 deficiency in the brain decreases BDNF levels by REST/CoREST-mediated repression and increases TRKB production. *Epigenetics,* 2**,** 214-22.

AHMED, S. S., AHAMEETHUNISA, A. R., SANTOSH, W., CHAKRAVARTHY, S. & KUMAR, S. 2011. Systems biological approach on neurological disorders: a novel molecular connectivity to aging and psychiatric diseases. *BMC Syst Biol,* 5**,** 6.

AID, T., KAZANTSEVA, A., PIIRSOO, M., PALM, K. & TIMMUSK, T. 2007. Mouse and rat BDNF gene structure and expression revisited. *J Neurosci Res,* 85**,** 525-35.

AKILESH, S., SHAFFER, D. J. & ROOPENIAN, D. 2003. Customized molecular phenotyping by quantitative gene expression and pattern recognition analysis. *Genome Res,* 13**,** 1719-27.

ALI, F. R., VASILIOU, S. A., HADDLEY, K., PAREDES, U. M., ROBERTS, J. C., MIYAJIMA, F., KLENOVA, E., BUBB, V. J. & QUINN, J. P. 2010. Combinatorial interaction between two human serotonin transporter gene variable number tandem repeats and their regulation by CTCF. *J Neurochem,* 112**,** 296-306.

ALTHOFF, K., BECKERS, A., ODERSKY, A., MESTDAGH, P., KOSTER, J., BRAY, I. M., BRYAN, K., VANDESOMPELE, J., SPELEMAN, F., STALLINGS, R. L., SCHRAMM, A., EGGERT, A., SPRUSSEL, A. & SCHULTE, J. H. 2013. MiR-137 functions as a tumor suppressor in neuroblastoma by downregulating KDM1A. *Int J Cancer,* 133**,** 1064-73.

ALTSCHUL, S. F., MADDEN, T. L., SCHAFFER, A. A., ZHANG, J., ZHANG, Z., MILLER, W. & LIPMAN, D. J. 1997. Gapped BLAST and PSI-BLAST: a new generation of protein database search programs. *Nucleic Acids Res,* 25**,** 3389-402.

AMARI, L., LAYDEN, B., NIKOLAKOPOULOS, J., RONG, Q., MOTA DE FREITAS, D., BALTAZAR, G., CASTRO, M. M. & GERALDES, C. F. 1999. Competition between Li+ and Mg2+ in neuroblastoma SH-SY5Y cells: a fluorescence and 31P NMR study. *Biophys J,* 76**,** 2934-42.

ANDO, T., YOSHIDA, T., ENOMOTO, S., ASADA, K., TATEMATSU, M., ICHINOSE, M., SUGIYAMA, T. & USHIJIMA, T. 2009. DNA methylation of microRNA genes in gastric mucosae of gastric cancer patients: its possible involvement in the formation of epigenetic field defect. *Int J Cancer,* 124**,** 2367-74.

ANDREASEN, N. C. 1999. A unitary model of schizophrenia: Bleuler's "fragmented phrene" as schizencephaly. *Arch Gen Psychiatry,* 56**,** 781-7.

ANDREASEN, N. C., FLASHMAN, L., FLAUM, M., ARNDT, S., SWAYZE, V., 2ND, O'LEARY, D. S., EHRHARDT, J. C. & YUH, W. T. 1994. Regional brain abnormalities in schizophrenia measured with magnetic resonance imaging. *JAMA,* 272**,** 1763-9.

ANDRES, M. E., BURGER, C., PERAL-RUBIO, M. J., BATTAGLIOLI, E., ANDERSON, M. E., GRIMES, J., DALLMAN, J., BALLAS, N. & MANDEL, G. 1999. CoREST: a functional corepressor required for regulation of neural-specific gene expression. *Proc Natl Acad Sci U S A,* 96**,** 9873-8.

ANFANG, M. K. & POPE, H. G., JR. 1997. Treatment of neuroleptic-induced akathisia with nicotine patches. *Psychopharmacology (Berl),* 134**,** 153-6.

ANIER, K., MALINOVSKAJA, K., AONURM-HELM, A., ZHARKOVSKY, A. & KALDA, A. 2010. DNA methylation regulates cocaine-induced behavioral sensitization in mice. *Neuropsychopharmacology,* 35**,** 2450-61.

ASGHARI, V., WANG, J. F., REIACH, J. S. & YOUNG, L. T. 1998. Differential effects of mood stabilizers on Fos/Jun proteins and AP-1 DNA binding activity in human neuroblastoma SH-SY5Y cells. *Molecular Brain Research,* 58**,** 95-102.

AUTRY, A. E. & MONTEGGIA, L. M. 2012. Brain-derived neurotrophic factor and neuropsychiatric disorders. *Pharmacol Rev,* 64**,** 238-58.

AYATA, C., JIN, H., KUDO, C., DALKARA, T. & MOSKOWITZ, M. A. 2006. Suppression of cortical spreading depression in migraine prophylaxis. *Ann Neurol,* 59**,** 652-61.

BAJ, G. & TONGIORGI, E. 2009. BDNF splice variants from the second promoter cluster support cell survival of differentiated neuroblastoma upon cytotoxic stress. *J Cell Sci,* 122**,** 36-43.

BAK, M., SILAHTAROGLU, A., MOLLER, M., CHRISTENSEN, M., RATH, M. F., SKRYABIN, B., TOMMERUP, N. & KAUPPINEN, S. 2008. MicroRNA expression in the adult mouse central nervous system. *RNA,* 14**,** 432-44.

BALAGUER, F., LINK, A., LOZANO, J. J., CUATRECASAS, M., NAGASAKA, T., BOLAND, C. R. & GOEL, A. 2010. Epigenetic silencing of miR-137 is an early event in colorectal carcinogenesis. *Cancer Res,* 70**,** 6609-18.

BALLARÍN, M., ERNFORS, P., LINDEFORS, N. & PERSSON, H. 1991. Hippocampal damage and kainic acid injection induce a rapid increase in mRNA for BDNF and NGF in the rat brain. *Experimental Neurology,* 114**,** 35-43.

BALLAS, N., GRUNSEICH, C., LU, D. D., SPEH, J. C. & MANDEL, G. 2005. REST and its corepressors mediate plasticity of neuronal gene chromatin throughout neurogenesis. *Cell,* 121**,** 645-57.

BALLAS, N. & MANDEL, G. 2005. The many faces of REST oversee epigenetic programming of neuronal genes. *Curr Opin Neurobiol,* 15**,** 500-6.
BANDRES, E., AGIRRE, X., BITARTE, N., RAMIREZ, N., ZARATE, R., ROMAN-GOMEZ, J., PROSPER, F. & GARCIA-FONCILLAS, J. 2009. Epigenetic regulation of microRNA expression in colorectal cancer. *Int J Cancer,* 125**,** 2737-43.
BAPAT, S. A., JIN, V., BERRY, N., BALCH, C., SHARMA, N., KURREY, N., ZHANG, S., FANG, F., LAN, X., LI, M., KENNEDY, B., BIGSBY, R. M., HUANG, T. H. M. & NEPHEW, K. P. 2014. Multivalent epigenetic marks confer microenvironment-responsive epigenetic plasticity to ovarian cancer cells. *Epigenetics,* 5**,** 716-729.
BARRETT, J. C., FRY, B., MALLER, J. & DALY, M. J. 2005. Haploview: analysis and visualization of LD and haplotype maps. *Bioinformatics,* 21**,** 263-5.
BARSKI, A., CUDDAPAH, S., CUI, K., ROH, T. Y., SCHONES, D. E., WANG, Z., WEI, G., CHEPELEV, I. & ZHAO, K. 2007. High-resolution profiling of histone methylations in the human genome. *Cell,* 129**,** 823-37.
BARTEL, D. P. 2004. MicroRNAs: Genomics, Biogenesis, Mechanism, and Function. *Cell,* 116**,** 281-297.
BARTEL, D. P. 2009. MicroRNAs: target recognition and regulatory functions. *Cell,* 136**,** 215-33.
BASKERVILLE, S. & BARTEL, D. P. 2005. Microarray profiling of microRNAs reveals frequent coexpression with neighboring miRNAs and host genes. *RNA,* 11**,** 241-7.
BASSUK, A. G., WALLACE, R. H., BUHR, A., BULLER, A. R., AFAWI, Z., SHIMOJO, M., MIYATA, S., CHEN, S., GONZALEZ-ALEGRE, P., GRIESBACH, H. L., WU, S., NASHELSKY, M., VLADAR, E. K., ANTIC, D., FERGUSON, P. J., CIRAK, S., VOIT, T., SCOTT, M. P., AXELROD, J. D., GURNETT, C., DAOUD, A. S., KIVITY, S., NEUFELD, M. Y., MAZARIB, A., STRAUSSBERG, R., WALID, S., KORCZYN, A. D., SLUSARSKI, D. C., BERKOVIC, S. F. & EL-SHANTI, H. I. 2008. A homozygous mutation in human PRICKLE1 causes an autosomal-recessive progressive myoclonus epilepsy-ataxia syndrome. *Am J Hum Genet,* 83**,** 572-81.
BATTAGLIOLI, E., ANDRES, M. E., ROSE, D. W., CHENOWETH, J. G., ROSENFELD, M. G., ANDERSON, M. E. & MANDEL, G. 2002. REST repression of neuronal genes requires components of the hSWI.SNF complex. *J Biol Chem,* 277**,** 41038-45.
BEMIS, L. T., CHEN, R., AMATO, C. M., CLASSEN, E. H., ROBINSON, S. E., COFFEY, D. G., ERICKSON, P. F., SHELLMAN, Y. G. & ROBINSON, W. A. 2008. MicroRNA-137 targets microphthalmia-associated transcription factor in melanoma cell lines. *Cancer Res,* 68**,** 1362-8.
BENNETT, M. R. 2011. The prefrontal-limbic network in depression: Modulation by hypothalamus, basal ganglia and midbrain. *Prog Neurobiol,* 93**,** 468-87.
BERG, A. T. 2011. Epilepsy, cognition, and behavior: The clinical picture. *Epilepsia,* 52 Suppl 1**,** 7-12.
BERNSTEIN, B. E., MIKKELSEN, T. S., XIE, X., KAMAL, M., HUEBERT, D. J., CUFF, J., FRY, B., MEISSNER, A., WERNIG, M., PLATH, K., JAENISCH, R., WAGSCHAL, A., FEIL, R., SCHREIBER, S. L. & LANDER, E. S. 2006. A bivalent chromatin structure marks key developmental genes in embryonic stem cells. *Cell,* 125**,** 315-26.
BERRIDGE, M. J., DOWNES, C. P. & HANLEY, M. R. 1989. Neural and developmental actions of lithium: a unifying hypothesis. *Cell,* 59**,** 411-9.
BESSIS, A., CHAMPTIAUX, N., CHATELIN, L. & CHANGEUX, J. P. 1997. The neuron-restrictive silencer element: a dual enhancer/silencer crucial for patterned expression of a nicotinic receptor gene in the brain. *Proc Natl Acad Sci U S A,* 94**,** 5906-11.
BEVERIDGE, N. J. & CAIRNS, M. J. 2012. MicroRNA dysregulation in schizophrenia. *Neurobiol Dis,* 46**,** 263-71.
BHANDARE, R., SCHUG, J., LE LAY, J., FOX, A., SMIRNOVA, O., LIU, C., NAJI, A. & KAESTNER, K. H. 2010. Genome-wide analysis of histone modifications in human pancreatic islets. *Genome Res,* 20**,** 428-33.
BIANCHI, M., CRINELLI, R., GIACOMINI, E., CARLONI, E., RADICI, L. & MAGNANI, M. 2013. Yin Yang 1 intronic binding sequences and splicing elicit intron-mediated enhancement of ubiquitin C gene expression. *PLoS One,* 8**,** e65932.
BIER, A., GILADI, N., KRONFELD, N., LEE, H. K., CAZACU, S., FINNISS, S., XIANG, C., POISSON, L., DECARVALHO, A. C., SLAVIN, S., JACOBY, E., YALON, M., TOREN, A., MIKKELSEN, T. & BRODIE, C. 2013. MicroRNA-137 is downregulated in glioblastoma and inhibits the stemness of glioma stem cells by targeting RTVP-1. *Oncotarget,* 4**,** 665-76.
BLUM, R. & KONNERTH, A. 2005. Neurotrophin-mediated rapid signaling in the central nervous system: mechanisms and functions. *Physiology (Bethesda),* 20**,** 70-8.
BORRELLI, E., NESTLER, E. J., ALLIS, C. D. & SASSONE-CORSI, P. 2008. Decoding the epigenetic language of neuronal plasticity. *Neuron,* 60**,** 961-74.
BOUDREAU, R. L., JIANG, P., GILMORE, B. L., SPENGLER, R. M., TIRABASSI, R., NELSON, J. A., ROSS, C. A., XING, Y. & DAVIDSON, B. L. 2014. Transcriptome-wide discovery of microRNA binding sites in human brain. *Neuron,* 81**,** 294-305.
BOWATER, R. P. & WELLS, R. D. 2001. The intrinsically unstable life of DNA triplet repeats associated with human hereditary disorders. *Prog Nucleic Acid Res Mol Biol,* 66**,** 159-202.
BRAMHAM, C. R. 2008. Local protein synthesis, actin dynamics, and LTP consolidation. *Curr Opin Neurobiol,* 18**,** 524-31.
BRAMHAM, C. R. & MESSAOUDI, E. 2005. BDNF function in adult synaptic plasticity: the synaptic consolidation hypothesis. *Prog Neurobiol,* 76**,** 99-125.

BREDY, T. W., WU, H., CREGO, C., ZELLHOEFER, J., SUN, Y. E. & BARAD, M. 2007. Histone modifications around individual BDNF gene promoters in prefrontal cortex are associated with extinction of conditioned fear. *Learn Mem,* 14**,** 268-76.

BREEN, G., COLLIER, D., CRAIG, I. & QUINN, J. 2008. Variable number tandem repeats as agents of functional regulation in the genome. *IEEE Eng Med Biol Mag,* 27**,** 103-4, 108.

BRONSON, M. W., HILLENMEYER, S., PARK, R. W. & BRODSKY, A. S. 2010. Estrogen coordinates translation and transcription, revealing a role for NRSF in human breast cancer cells. *Mol Endocrinol,* 24**,** 1120-35.

BRUCE, A. W., DONALDSON, I. J., WOOD, I. C., YERBURY, S. A., SADOWSKI, M. I., CHAPMAN, M., GOTTGENS, B. & BUCKLEY, N. J. 2004. Genome-wide analysis of repressor element 1 silencing transcription factor/neuron-restrictive silencing factor (REST/NRSF) target genes. *Proc Natl Acad Sci U S A,* 101**,** 10458-63.

BRUCE, A. W., LOPEZ-CONTRERAS, A. J., FLICEK, P., DOWN, T. A., DHAMI, P., DILLON, S. C., KOCH, C. M., LANGFORD, C. F., DUNHAM, I., ANDREWS, R. M. & VETRIE, D. 2009. Functional diversity for REST (NRSF) is defined by in vivo binding affinity hierarchies at the DNA sequence level. *Genome Res,* 19**,** 994-1005.

BRUIJNZEEL, A. W., ALEXANDER, J. C., PEREZ, P. D., BAUZO-RODRIGUEZ, R., HALL, G., KLAUSNER, R., GUERRA, V., ZENG, H., IGARI, M. & FEBO, M. 2014. Acute Nicotine Administration Increases BOLD fMRI Signal in Brain Regions Involved in Reward Signaling and Compulsive Drug Intake in Rats. *Int J Neuropsychopharmacol,* 18.

BUSH, G., LUU, P. & POSNER, M. I. 2000. Cognitive and emotional influences in anterior cingulate cortex. *Trends in Cognitive Sciences,* 4**,** 215-222.

BUTTER, F., DAVISON, L., VITURAWONG, T., SCHEIBE, M., VERMEULEN, M., TODD, J. A. & MANN, M. 2012. Proteome-wide analysis of disease-associated SNPs that show allele-specific transcription factor binding. *PLoS Genet,* 8**,** e1002982.

CALDERONE, A., JOVER, T., NOH, K. M., TANAKA, H., YOKOTA, H., LIN, Y., GROOMS, S. Y., REGIS, R., BENNETT, M. V. & ZUKIN, R. S. 2003. Ischemic insults derepress the gene silencer REST in neurons destined to die. *J Neurosci,* 23**,** 2112-21.

CAO, X., YEO, G., MUOTRI, A. R., KUWABARA, T. & GAGE, F. H. 2006. Noncoding RNAs in the mammalian central nervous system. *Annu Rev Neurosci,* 29**,** 77-103.

CARVILL, G. L., REGAN, B. M., YENDLE, S. C., O'ROAK, B. J., LOZOVAYA, N., BRUNEAU, N., BURNASHEV, N., KHAN, A., COOK, J., GERAGHTY, E., SADLEIR, L. G., TURNER, S. J., TSAI, M. H., WEBSTER, R., OUVRIER, R., DAMIANO, J. A., BERKOVIC, S. F., SHENDURE, J., HILDEBRAND, M. S., SZEPETOWSKI, P., SCHEFFER, I. E. & MEFFORD, H. C. 2013. GRIN2A mutations cause epilepsy-aphasia spectrum disorders. *Nat Genet,* 45**,** 1073-6.

CHAHROUR, M., JUNG, S. Y., SHAW, C., ZHOU, X., WONG, S. T., QIN, J. & ZOGHBI, H. Y. 2008. MeCP2, a key contributor to neurological disease, activates and represses transcription. *Science,* 320**,** 1224-9.

CHANDRASEKAR, V. & DREYER, J. L. 2009. microRNAs miR-124, let-7d and miR-181a regulate cocaine-induced plasticity. *Mol Cell Neurosci,* 42**,** 350-62.

CHANG, S., WEN, S., CHEN, D. & JIN, P. 2009. Small regulatory RNAs in neurodevelopmental disorders. *Hum Mol Genet,* 18**,** R18-26.

CHAZOT, P. L., GODUKHIN, O. V., MCDONALD, A. & OBRENOVITCH, T. P. 2002. Spreading depression-induced preconditioning in the mouse cortex: differential changes in the protein expression of ionotropic nicotinic acetylcholine and glutamate receptors. *J Neurochem,* 83**,** 1235-1238.

CHEAH, S. Y., LAWFORD, B. R., YOUNG, R. M., CONNOR, J. P., PHILLIP MORRIS, C. & VOISEY, J. 2014. BDNF SNPs Are Implicated in Comorbid Alcohol Dependence in Schizophrenia But Not in Alcohol-Dependent Patients Without Schizophrenia. *Alcohol Alcohol,* 49**,** 491-7.

CHEN, B., DOWLATSHAHI, D., MACQUEEN, G. M., WANG, J.-F. & YOUNG, L. T. 2001. Increased hippocampal bdnf immunoreactivity in subjects treated with antidepressant medication. *Biol Psychiatry,* 50**,** 260-265.

CHEN, C. H., SUCKLING, J., LENNOX, B. R., OOI, C. & BULLMORE, E. T. 2011a. A quantitative meta-analysis of fMRI studies in bipolar disorder. *Bipolar Disord,* 13**,** 1-15.

CHEN, G., HUANG, L.-D., JIANG, Y.-M. & MANJI, H. K. 2008. The Mood-Stabilizing Agent Valproate Inhibits the Activity of Glycogen Synthase Kinase-3. *J Neurochem,* 72**,** 1327-1330.

CHEN, G., YUAN, P. X., JIANG, Y. M., HUANG, L. D. & MANJI, H. K. 1999. Valproate robustly enhances AP-1 mediated gene expression. *Brain Res Mol Brain Res,* 64**,** 52-8.

CHEN, G. L. & MILLER, G. M. 2013. Extensive alternative splicing of the repressor element silencing transcription factor linked to cancer. *PLoS One,* 8**,** e62217.

CHEN, L., WANG, X., WANG, H., LI, Y., YAN, W., HAN, L., ZHANG, K., ZHANG, J., WANG, Y., FENG, Y., PU, P., JIANG, T., KANG, C. & JIANG, C. 2012. miR-137 is frequently down-regulated in glioblastoma and is a negative regulator of Cox-2. *Eur J Cancer,* 48**,** 3104-11.

CHEN, Q., CHEN, X., ZHANG, M., FAN, Q., LUO, S. & CAO, X. 2011b. miR-137 is frequently down-regulated in gastric cancer and is a negative regulator of Cdc42. *Dig Dis Sci,* 56**,** 2009-16.

CHEN, X., WANG, J., SHEN, H., LU, J., LI, C., HU, D. N., DONG, X. D., YAN, D. & TU, L. 2011c. Epigenetics, microRNAs, and carcinogenesis: functional role of microRNA-137 in uveal melanoma. *Invest Ophthalmol Vis Sci,* 52**,** 1193-9.

CHEN, Z. F., PAQUETTE, A. J. & ANDERSON, D. J. 1998. NRSF/REST is required in vivo for repression of multiple neuronal target genes during embryogenesis. *Nat Genet,* 20**,** 136-42.

CHONG, J. A., TAPIA-RAMIREZ, J., KIM, S., TOLEDO-ARAL, J. J., ZHENG, Y., BOUTROS, M. C., ALTSHULLER, Y. M., FROHMAN, M. A., KRANER, S. D. & MANDEL, G. 1995. REST: A mammalian silencer protein that restricts sodium channel gene expression to neurons. *Cell,* 80**,** 949-957.

CHUANG, D. M., CHEN, R. W., CHALECKA-FRANASZEK, E., REN, M., HASHIMOTO, R., SENATOROV, V., KANAI, H., HOUGH, C., HIROI, T. & LEEDS, P. 2002. Neuroprotective effects of lithium in cultured cells and animal models of diseases. *Bipolar Disord,* 4**,** 129-36.

CHUANG, D. M., WANG, Z. & CHIU, C. T. 2011. GSK-3 as a Target for Lithium-Induced Neuroprotection Against Excitotoxicity in Neuronal Cultures and Animal Models of Ischemic Stroke. *Front Mol Neurosci,* 4**,** 15.

COLLIER, D. A., ARRANZ, M. J., SHAM, P., BATTERSBY, S., VALLADA, H., GILL, P., AITCHISON, K. J., SODHI, M., LI, T., ROBERTS, G. W., SMITH, B., MORTON, J., MURRAY, R. M., SMITH, D. & KIROV, G. 1996. The serotonin transporter is a potential susceptibility factor for bipolar affective disorder. *Neuroreport,* 7**,** 1675-9.

COLLINS, P. Y., PATEL, V., JOESTL, S. S., MARCH, D., INSEL, T. R., DAAR, A. S., ANDERSON, W., DHANSAY, M. A., PHILLIPS, A., SHURIN, S., WALPORT, M., EWART, W., SAVILL, S. J., BORDIN, I. A., COSTELLO, E. J., DURKIN, M., FAIRBURN, C., GLASS, R. I., HALL, W., HUANG, Y., HYMAN, S. E., JAMISON, K., KAAYA, S., KAPUR, S., KLEINMAN, A., OGUNNIYI, A., OTERO-OJEDA, A., POO, M. M., RAVINDRANATH, V., SAHAKIAN, B. J., SAXENA, S., SINGER, P. A. & STEIN, D. J. 2011. Grand challenges in global mental health. *Nature,* 475**,** 27-30.

COMOGLIO, P. M. 2001. Pathway specificity for Met signalling. *Nat Cell Biol,* 3**,** E161-2.

CONACO, C., OTTO, S., HAN, J. J. & MANDEL, G. 2006. Reciprocal actions of REST and a microRNA promote neuronal identity. *Proc Natl Acad Sci U S A,* 103**,** 2422-7.

CORCORAN, D. L., PANDIT, K. V., GORDON, B., BHATTACHARJEE, A., KAMINSKI, N. & BENOS, P. V. 2009. Features of mammalian microRNA promoters emerge from polymerase II chromatin immunoprecipitation data. *PLoS One,* 4**,** e5279.

CORCORAN, K. A. & MAREN, S. 2001. Hippocampal Inactivation Disrupts Contextual Retrieval of Fear Memory after Extinction. *The Journal of Neuroscience,* 21**,** 1720-1726.

COUGOT, N., BHATTACHARYYA, S. N., TAPIA-ARANCIBIA, L., BORDONNE, R., FILIPOWICZ, W., BERTRAND, E. & RAGE, F. 2008. Dendrites of mammalian neurons contain specialized P-body-like structures that respond to neuronal activation. *J Neurosci,* 28**,** 13793-804.

COULSON, J. M., EDGSON, J. L., WOLL, P. J. & QUINN, J. P. 2000. A splice variant of the neuron-restrictive silencer factor repressor is expressed in small cell lung cancer: a potential role in derepression of neuroendocrine genes and a useful clinical marker. *Cancer Res,* 60**,** 1840-4.

COULSON, J. M., FISKERSTRAND, C. E., WOLL, P. J. & QUINN, J. P. 1999. Arginine vasopressin promoter regulation is mediated by a neuron-restrictive silencer element in small cell lung cancer. *Cancer Res,* 59**,** 5123-7.

CROSS-DISORDER GROUP OF THE PSYCHIATRIC GENOMICS, C. 2013a. Genetic relationship between five psychiatric disorders estimated from genome-wide SNPs. *Nat Genet,* 45**,** 984-994.

CROSS-DISORDER GROUP OF THE PSYCHIATRIC GENOMICS, C. 2013b. Identification of risk loci with shared effects on five major psychiatric disorders: a genome-wide analysis. *Lancet,* 381**,** 1371-9.

CROWLEY, J. J., COLLINS, A. L., LEE, R. J., NONNEMAN, R. J., FARRELL, M. S., ANCALADE, N., MUGFORD, J. W., AGSTER, K. L., NIKOLOVA, V. D., MOY, S. S. & SULLIVAN, P. F. 2015. Disruption of the microRNA 137 primary transcript results in early embryonic lethality in mice. *Biol Psychiatry,* 77**,** e5-7.

CUI, W. Y., WANG, J., WEI, J., CAO, J., CHANG, S. L., GU, J. & LI, M. D. 2012. Modulation of innate immune-related pathways in nicotine-treated SH-SY5Y cells. *Amino Acids,* 43**,** 1157-69.

CUMMINGS, E., DONOHOE, G., HARGREAVES, A., MOORE, S., FAHEY, C., DINAN, T. G., MCDONALD, C., O'CALLAGHAN, E., O'NEILL, F. A., WADDINGTON, J. L., MURPHY, K. C., MORRIS, D. W., GILL, M. & CORVIN, A. 2013. Mood congruent psychotic symptoms and specific cognitive deficits in carriers of the novel schizophrenia risk variant at MIR-137. *Neurosci Lett,* 532**,** 33-8.

D'ADDARIO, C., DELL'OSSO, B., GALIMBERTI, D., PALAZZO, M. C., BENATTI, B., DI FRANCESCO, A., SCARPINI, E., ALTAMURA, A. C. & MACCARRONE, M. 2013. Epigenetic modulation of BDNF gene in patients with major depressive disorder. *Biol Psychiatry,* 73**,** e6-7.

D'ADDARIO, C., DELL'OSSO, B., PALAZZO, M. C., BENATTI, B., LIETTI, L., CATTANEO, E., GALIMBERTI, D., FENOGLIO, C., CORTINI, F., SCARPINI, E., AROSIO, B., DI FRANCESCO, A., DI BENEDETTO, M., ROMUALDI, P., CANDELETTI, S., MARI, D., BERGAMASCHINI, L., BRESOLIN, N., MACCARRONE, M. & ALTAMURA, A. C. 2012. Selective DNA methylation of BDNF promoter in bipolar disorder: differences among patients with BDI and BDII. *Neuropsychopharmacology,* 37**,** 1647-55.

D'SOUZA, U. M., POWELL-SMITH, G., HADDLEY, K., POWELL, T. R., BUBB, V. J., PRICE, T., MCGUFFIN, P., QUINN, J. P. & FARMER, A. E. 2013. Allele-specific expression of the serotonin transporter and its transcription

factors following lamotrigine treatment in vitro. *Am J Med Genet B Neuropsychiatr Genet,* 162B**,** 474-83.
DACIC, S., KELLY, L., SHUAI, Y. & NIKIFOROVA, M. N. 2010. miRNA expression profiling of lung adenocarcinomas: correlation with mutational status. *Mod Pathol,* 23**,** 1577-82.
DARRAH, S. D., MILLER, M. A., REN, D., HOH, N. Z., SCANLON, J. M., CONLEY, Y. P. & WAGNER, A. K. 2013. Genetic variability in glutamic acid decarboxylase genes: associations with post-traumatic seizures after severe TBI. *Epilepsy Res,* 103**,** 180-94.
DAWSON, M. E., NUECHTERLEIN, K. H., SCHELL, A. M., GITLIN, M. & VENTURA, J. 1994. Autonomic abnormalities in schizophrenia: State or trait indicators? *Arch Gen Psychiatry,* 51**,** 813-824.
DE ALMEIDA RABELLO OLIVEIRA, M., DA ROCHA ATAIDE, T., DE OLIVEIRA, S. L., DE MELO LUCENA, A. L., DE LIRA, C. E., SOARES, A. A., DE ALMEIDA, C. B. & XIMENES-DA-SILVA, A. 2008. Effects of short-term and long-term treatment with medium- and long-chain triglycerides ketogenic diet on cortical spreading depression in young rats. *Neurosci Lett,* 434**,** 66-70.
DE LEON, J. & DIAZ, F. J. 2005. A meta-analysis of worldwide studies demonstrates an association between schizophrenia and tobacco smoking behaviors. *Schizophr Res,* 76**,** 135-57.
DEJESUS-HERNANDEZ, M., MACKENZIE, I. R., BOEVE, B. F., BOXER, A. L., BAKER, M., RUTHERFORD, N. J., NICHOLSON, A. M., FINCH, N. A., FLYNN, H., ADAMSON, J., KOURI, N., WOJTAS, A., SENGDY, P., HSIUNG, G. Y., KARYDAS, A., SEELEY, W. W., JOSEPHS, K. A., COPPOLA, G., GESCHWIND, D. H., WSZOLEK, Z. K., FELDMAN, H., KNOPMAN, D. S., PETERSEN, R. C., MILLER, B. L., DICKSON, D. W., BOYLAN, K. B., GRAFF-RADFORD, N. R. & RADEMAKERS, R. 2011. Expanded GGGGCC hexanucleotide repeat in noncoding region of C9ORF72 causes chromosome 9p-linked FTD and ALS. *Neuron,* 72**,** 245-56.
DEMPSTER, A. P., LAIRD, N. M. & RUBIN, D. B. 1977. Maximum Likelihood from Incomplete Data via the EM Algorithm. *J Royal Statist Soc* 39**,** 1-38.
DI DANIEL, E., MUDGE, A. W. & MAYCOX, P. R. 2005. Comparative analysis of the effects of four mood stabilizers in SH-SY5Y cells and in primary neurons. *Bipolar Disord,* 7**,** 33-41.
DICKEY, C. C., MCCARLEY, R. W., XU, M. L., SEIDMAN, L. J., VOGLMAIER, M. M., NIZNIKIEWICZ, M. A., CONNOR, E. & SHENTON, M. E. 2007. MRI abnormalities of the hippocampus and cavum septi pellucidi in females with schizotypal personality disorder. *Schizophr Res,* 89**,** 49-58.
DIETRICH, N., LERDRUP, M., LANDT, E., AGRAWAL-SINGH, S., BAK, M., TOMMERUP, N., RAPPSILBER, J., SODERSTEN, E. & HANSEN, K. 2012. REST-mediated recruitment of polycomb repressor complexes in mammalian cells. *PLoS Genet,* 8**,** e1002494.
DOENCH, J. G. & SHARP, P. A. 2004. Specificity of microRNA target selection in translational repression. *Genes Dev,* 18**,** 504-11.
DOMSCHKE, K., TIDOW, N., SCHREMPF, M., SCHWARTE, K., KLAUKE, B., REIF, A., KERSTING, A., AROLT, V., ZWANZGER, P. & DECKERT, J. 2013. Epigenetic signature of panic disorder: a role of glutamate decarboxylase 1 (GAD1) DNA hypomethylation? *Prog Neuropsychopharmacol Biol Psychiatry,* 46**,** 189-96.
DOUSA, T. & HECHTER, O. 1970. Lithium and brain adenyl cyclase. *Lancet,* 1**,** 834-5.
DUAN, J., SHI, J., FIORENTINO, A., LEITES, C., CHEN, X., MOY, W., CHEN, J., ALEXANDROV, B. S., USHEVA, A., HE, D., FREDA, J., O'BRIEN, N. L., MCQUILLIN, A., SANDERS, A. R., GERSHON, E. S., DELISI, L. E., BISHOP, A. R., GURLING, H. M., PATO, M. T., LEVINSON, D. F., KENDLER, K. S., PATO, C. N. & GEJMAN, P. V. 2014. A rare functional noncoding variant at the GWAS-implicated MIR137/MIR2682 locus might confer risk to schizophrenia and bipolar disorder. *Am J Hum Genet,* 95**,** 744-53.
DUMAN, R. S. 2004. Role of Neurotrophic Factors in the Etiology and Treatment of Mood Disorders. *NeuroMolecular Medicine,* 5**,** 011-026.
DUNCKLEY, T. & LUKAS, R. J. 2003. Nicotine modulates the expression of a diverse set of genes in the neuronal SH-SY5Y cell line. *J Biol Chem,* 278**,** 15633-40.
DUNHAM, J. S., DEAKIN, J. F., MIYAJIMA, F., PAYTON, A. & TORO, C. T. 2009. Expression of hippocampal brain-derived neurotrophic factor and its receptors in Stanley consortium brains. *J Psychiatr Res,* 43**,** 1175-84.
DUNIGAN, C. D. & SHAMOO, A. E. 1995. Li+ stimulates ATP-regulated dopamine uptake in PC12 cells. *Neuroscience,* 65**,** 1-4.
DWIVEDI, Y., RIZAVI, H. S., CONLEY, R. R., ROBERTS, R. C., TAMMINGA, C. A. & PANDEY, G. N. 2003. Altered gene expression of brain-derived neurotrophic factor and receptor tyrosine kinase B in postmortem brain of suicide subjects. *Arch Gen Psychiatry,* 60**,** 804-15.
EDBAUER, D., NEILSON, J. R., FOSTER, K. A., WANG, C. F., SEEBURG, D. P., BATTERTON, M. N., TADA, T., DOLAN, B. M., SHARP, P. A. & SHENG, M. 2010. Regulation of synaptic structure and function by FMRP-associated microRNAs miR-125b and miR-132. *Neuron,* 65**,** 373-84.
EDENBERG, H. J. & LIU, Y. 2009. Laboratory methods for high-throughput genotyping. *Cold Spring Harb Protoc,* 2009**,** pdb top62.
EGAN, M. F., KOJIMA, M., CALLICOTT, J. H., GOLDBERG, T. E., KOLACHANA, B. S., BERTOLINO, A., ZAITSEV, E., GOLD, B., GOLDMAN, D., DEAN, M., LU, B. & WEINBERGER, D. R. 2003. The BDNF val66met

Polymorphism Affects Activity-Dependent Secretion of BDNF and Human Memory and Hippocampal Function. *Cell,* 112**,** 257-269.
EGAWA, J., NUNOKAWA, A., SHIBUYA, M., WATANABE, Y., KANEKO, N., IGETA, H. & SOMEYA, T. 2013. Resequencing and association analysis of MIR137 with schizophrenia in a Japanese population. *Psychiatry Clin Neurosci,* 67**,** 277-9.
EHRENREICH, H., HASSELBLATT, M., KNERLICH, F., VON AHSEN, N., JACOB, S., SPERLING, S., WOLDT, H., VEHMEYER, K., NAVE, K. A. & SIREN, A. L. 2005. A hematopoietic growth factor, thrombopoietin, has a proapoptotic role in the brain. *Proc Natl Acad Sci U S A,* 102**,** 862-7.
EINAT, H., YUAN, P., GOULD, T. D., LI, J., DU, J., ZHANG, L., MANJI, H. K. & CHEN, G. 2003. The role of the extracellular signal-regulated kinase signaling pathway in mood modulation. *J Neurosci,* 23**,** 7311-6.
ERNST, J., KHERADPOUR, P., MIKKELSEN, T. S., SHORESH, N., WARD, L. D., EPSTEIN, C. B., ZHANG, X., WANG, L., ISSNER, R., COYNE, M., KU, M., DURHAM, T., KELLIS, M. & BERNSTEIN, B. E. 2011. Mapping and analysis of chromatin state dynamics in nine human cell types. *Nature,* 473**,** 43-9.
EZHKOVA, E., PASOLLI, H. A., PARKER, J. S., STOKES, N., SU, I. H., HANNON, G., TARAKHOVSKY, A. & FUCHS, E. 2009. Ezh2 orchestrates gene expression for the stepwise differentiation of tissue-specific stem cells. *Cell,* 136**,** 1122-35.
FABIAN, M. R., CIEPLAK, M. K., FRANK, F., MORITA, M., GREEN, J., SRIKUMAR, T., NAGAR, B., YAMAMOTO, T., RAUGHT, B., DUCHAINE, T. F. & SONENBERG, N. 2011. miRNA-mediated deadenylation is orchestrated by GW182 through two conserved motifs that interact with CCR4-NOT. *Nat Struct Mol Biol,* 18**,** 1211-7.
FABRICIUS, M., FUHR, S., WILLUMSEN, L., DREIER, J. P., BHATIA, R., BOUTELLE, M. G., HARTINGS, J. A., BULLOCK, R., STRONG, A. J. & LAURITZEN, M. 2008. Association of seizures with cortical spreading depression and peri-infarct depolarisations in the acutely injured human brain. *Clin Neurophysiol,* 119**,** 1973-84.
FARAONE, S. V., SU, J., TAYLOR, L., WILCOX, M., VAN EERDEWEGH, P. & TSUANG, M. T. 2004. A novel permutation testing method implicates sixteen nicotinic acetylcholine receptor genes as risk factors for smoking in schizophrenia families. *Hum Hered,* 57**,** 59-68.
FATEMI, S. H., EARLE, J. A. & MCMENOMY, T. 2000. Reduction in Reelin immunoreactivity in hippocampus of subjects with schizophrenia, bipolar disorder and major depression. *Mol Psychiatry,* 5**,** 654-63, 571.
FATEMI, S. H., EARLE, J. A., STARY, J. M., LEE, S. & SEDGEWICK, J. 2001a. Altered levels of the synaptosomal associated protein SNAP-25 in hippocampus of subjects with mood disorders and schizophrenia. *Neuroreport,* 12**,** 3257-62.
FATEMI, S. H., KROLL, J. L. & STARY, J. M. 2001b. Altered levels of Reelin and its isoforms in schizophrenia and mood disorders. *Neuroreport,* 12**,** 3209-15.
FEHR, C., CONRAD, K. D. & NIEPMANN, M. 2012. Differential stimulation of hepatitis C virus RNA translation by microRNA-122 in different cell cycle phases. *Cell Cycle,* 11**,** 277-85.
FENG, M. J., YAN, S. E. & YAN, Q. S. 2006. Cocaine exposure at a sublethal concentration downregulates CREB functions in cultured neuroblastoma cells. *Brain Res,* 1077**,** 59-66.
FERNANDEZ-CASTILLO, N., CORMAND, B., RONCERO, C., SANCHEZ-MORA, C., GRAU-LOPEZ, L., GONZALVO, B., MIQUEL, L., COROMINAS, R., RAMOS-QUIROGA, J. A., CASAS, M. & RIBASES, M. 2012. Candidate pathway association study in cocaine dependence: the control of neurotransmitter release. *World J Biol Psychiatry,* 13**,** 126-34.
FISKERSTRAND, C. E., LOVEJOY, E. A. & QUINN, J. P. 1999. An intronic polymorphic domain often associated with susceptibility to affective disorders has allele dependent differential enhancer activity in embryonic stem cells. *FEBS Letters,* 458**,** 171-174.
FONDON, J. W., 3RD, HAMMOCK, E. A., HANNAN, A. J. & KING, D. G. 2008. Simple sequence repeats: genetic modulators of brain function and behavior. *Trends Neurosci,* 31**,** 328-34.
FONSECA, C. P., SIERRA, A., GERALDES, C. F., CERDAN, S. & CASTRO, M. M. 2009. Mechanisms underlying Li+ effects in glutamatergic and GABAergic neurotransmissions in the adult rat brain and in primary cultures of neural cells as revealed by 13C NMR. *J Neurosci Res,* 87**,** 1046-55.
FORDE, J. E. & DALE, T. C. 2007. Glycogen synthase kinase 3: a key regulator of cellular fate. *Cell Mol Life Sci,* 64**,** 1930-44.
FOUNTOULAKIS, K. N., VIETA, E., SANCHEZ-MORENO, J., KAPRINIS, S. G., GOIKOLEA, J. M. & KAPRINIS, G. S. 2005. Treatment guidelines for bipolar disorder: a critical review. *J Affect Disord,* 86**,** 1-10.
FRIEDMAN, E., HOAU YAN, W., LEVINSON, D., CONNELL, T. A. & SINGH, H. 1993. Altered platelet protein kinase C activity in bipolar affective disorder, manic episode. *Biol Psychiatry,* 33**,** 520-5.
FU, X. D. & ARES, M., JR. 2014. Context-dependent control of alternative splicing by RNA-binding proteins. *Nat Rev Genet,* 15**,** 689-701.
FUJIMOTO, N. & KITAMURA, S. 2004. Effects of environmental estrogenic chemicals on AP1 mediated transcription with estrogen receptors alpha and beta. *J Steroid Biochem Mol Biol,* 88**,** 53-9.
FUKUMOTO, T., MORINOBU, S., OKAMOTO, Y., KAGAYA, A. & YAMAWAKI, S. 2001. Chronic lithium treatment increases the expression of brain-derived neurotrophic factor in the rat brain. *Psychopharmacology (Berl),* 158**,** 100-6.

FULLER TORREY, E. 1999. Epidemiological comparison of schizophrenia and bipolar disorder. *Schizophrenia Research,* 39**,** 101-106.
FURUTA, M., NUMAKAWA, T., CHIBA, S., NINOMIYA, M., KAJIYAMA, Y., ADACHI, N., AKEMA, T. & KUNUGI, H. 2013. Estrogen, predominantly via estrogen receptor alpha, attenuates postpartum-induced anxiety- and depression-like behaviors in female rats. *Endocrinology*.
GABRIEL, S. B., SCHAFFNER, S. F., NGUYEN, H., MOORE, J. M., ROY, J., BLUMENSTIEL, B., HIGGINS, J., DEFELICE, M., LOCHNER, A., FAGGART, M., LIU-CORDERO, S. N., ROTIMI, C., ADEYEMO, A., COOPER, R., WARD, R., LANDER, E. S., DALY, M. J. & ALTSHULER, D. 2002. The structure of haplotype blocks in the human genome. *Science,* 296**,** 2225-9.
GALINDO, C. L., MCCORMICK, J. F., BUBB, V. J., ABID ALKADEM, D. H., LI, L. S., MCIVER, L. J., GEORGE, A. C., BOOTHMAN, D. A., QUINN, J. P., SKINNER, M. A. & GARNER, H. R. 2011. A long AAAG repeat allele in the 5' UTR of the ERR-gamma gene is correlated with breast cancer predisposition and drives promoter activity in MCF-7 breast cancer cells. *Breast Cancer Res Treat,* 130**,** 41-8.
GALLAGHER, P., MALIK, N., NEWHAM, J., YOUNG, A. H., FERRIER, I. N. & MACKIN, P. 2008. Antiglucocorticoid treatments for mood disorders. *Cochrane Database Syst Rev***,** CD005168.
GAO, Z., DING, P. & HSIEH, J. 2012. Profiling of REST-Dependent microRNAs Reveals Dynamic Modes of Expression. *Front Neurosci,* 6**,** 67.
GAO, Z., URE, K., DING, P., NASHAAT, M., YUAN, L., MA, J., HAMMER, R. E. & HSIEH, J. 2011. The master negative regulator REST/NRSF controls adult neurogenesis by restraining the neurogenic program in quiescent stem cells. *J Neurosci,* 31**,** 9772-86.
GARDINER-GARDEN, M. & FROMMER, M. 1987. CpG Islands in vertebrate genomes. *Journal of Molecular Biology,* 196**,** 261-282.
GARRIGA-CANUT, M., SCHOENIKE, B., QAZI, R., BERGENDAHL, K., DALEY, T. J., PFENDER, R. M., MORRISON, J. F., OCKULY, J., STAFSTROM, C., SUTULA, T. & ROOPRA, A. 2006. 2-Deoxy-D-glucose reduces epilepsy progression by NRSF-CtBP-dependent metabolic regulation of chromatin structure. *Nat Neurosci,* 9**,** 1382-7.
GARZON, D. J. & FAHNESTOCK, M. 2007. Oligomeric amyloid decreases basal levels of brain-derived neurotrophic factor (BDNF) mRNA via specific downregulation of BDNF transcripts IV and V in differentiated human neuroblastoma cells. *J Neurosci,* 27**,** 2628-35.
GEBHARDT, M. L., REUTER, S., MROWKA, R. & ANDRADE-NAVARRO, M. A. 2014. Similarity in targets with REST points to neural and glioblastoma related miRNAs. *Nucleic Acids Res,* 42**,** 5436-46.
GEEKIYANAGE, H. & CHAN, C. 2011. MicroRNA-137/181c regulates serine palmitoyltransferase and in turn amyloid beta, novel targets in sporadic Alzheimer's disease. *J Neurosci,* 31**,** 14820-30.
GENNARINO, V. A., SARDIELLO, M., AVELLINO, R., MEOLA, N., MASELLI, V., ANAND, S., CUTILLO, L., BALLABIO, A. & BANFI, S. 2009. MicroRNA target prediction by expression analysis of host genes. *Genome Res,* 19**,** 481-90.
GERASIMOVA, A., CHAVEZ, L., LI, B., SEUMOIS, G., GREENBAUM, J., RAO, A., VIJAYANAND, P. & PETERS, B. 2013. Predicting cell types and genetic variations contributing to disease by combining GWAS and epigenetic data. *PLoS One,* 8**,** e54359.
GHOSH, A., CARNAHAN, J. & GREENBERG, M. E. 1994. Requirement for BDNF in activity-dependent survival of cortical neurons. *Science,* 263**,** 1618-23.
GILLANDERS, E., JUO, S. H., HOLLAND, E. A., JONES, M., NANCARROW, D., FREAS-LUTZ, D., SOOD, R., PARK, N., FARUQUE, M., MARKEY, C., KEFFORD, R. F., PALMER, J., BERGMAN, W., BISHOP, D. T., TUCKER, M. A., BRESSAC-DE PAILLERETS, B., HANSSON, J., STARK, M., GRUIS, N., BISHOP, J. N., GOLDSTEIN, A. M., BAILEY-WILSON, J. E., MANN, G. J., HAYWARD, N. & TRENT, J. 2003. Localization of a novel melanoma susceptibility locus to 1p22. *Am J Hum Genet,* 73**,** 301-13.
GILLIES, S., HADDLEY, K., VASILIOU, S., BUBB, V. J. & QUINN, J. P. 2009. The human neurokinin B gene, TAC3, and its promoter are regulated by Neuron Restrictive Silencing Factor (NRSF) transcription factor family. *Neuropeptides,* 43**,** 333-40.
GILLIES, S. G., HADDLEY, K., VASILIOU, S. A., JACOBSON, G. M., VON MENTZER, B., BUBB, V. J. & QUINN, J. P. 2011. Distinct gene expression profiles directed by the isoforms of the transcription factor neuron-restrictive silencer factor in human SK-N-AS neuroblastoma cells. *J Mol Neurosci,* 44**,** 77-90.
GIROS, B., JABER, M., JONES, S. R., WIGHTMAN, R. M. & CARON, M. G. 1996. Hyperlocomotion and indifference to cocaine and amphetamine in mice lacking the dopamine transporter. *Nature,* 379**,** 606-12.
GLYNN, S. M. & SUSSMAN, S. 1990. Why patients smoke. *Hosp Community Psychiatry,* 41**,** 1027-8.
GODNIC, I., ZORC, M., JEVSINEK SKOK, D., CALIN, G. A., HORVAT, S., DOVC, P., KOVAC, M. & KUNEJ, T. 2013. Genome-wide and species-wide in silico screening for intragenic MicroRNAs in human, mouse and chicken. *PLoS One,* 8**,** e65165.
GOFF, D. C., HENDERSON, D. C. & AMICO, E. 1992. Cigarette smoking in schizophrenia: relationship to psychopathology and medication side effects. *Am J Psychiatry,* 149**,** 1189-94.
GOLDMAN, M. B., WANG, L., WACHI, C., DAUDI, S., CSERNANSKY, J., MARLOW-O'CONNOR, M., KEEDY, S. & TORRES, I. 2011. Structural pathology underlying neuroendocrine dysfunction in schizophrenia. *Behav Brain Res,* 218**,** 106-13.

GONZALEZ, S., PISANO, D. G. & SERRANO, M. 2008. Mechanistic principles of chromatin remodeling guided by siRNAs and miRNAs. *Cell Cycle,* 7**,** 2601-8.

GRAFF, J., REI, D., GUAN, J. S., WANG, W. Y., SEO, J., HENNIG, K. M., NIELAND, T. J., FASS, D. M., KAO, P. F., KAHN, M., SU, S. C., SAMIEI, A., JOSEPH, N., HAGGARTY, S. J., DELALLE, I. & TSAI, L. H. 2012. An epigenetic blockade of cognitive functions in the neurodegenerating brain. *Nature,* 483**,** 222-6.

GRAHAM, D. L., EDWARDS, S., BACHTELL, R. K., DILEONE, R. J., RIOS, M. & SELF, D. W. 2007. Dynamic BDNF activity in nucleus accumbens with cocaine use increases self-administration and relapse. *Nat Neurosci,* 10**,** 1029-37.

GRATACOS, M., SORIA, V., URRETAVIZCAYA, M., GONZALEZ, J. R., CRESPO, J. M., BAYES, M., DE CID, R., MENCHON, J. M., VALLEJO, J. & ESTIVILL, X. 2008. A brain-derived neurotrophic factor (BDNF) haplotype is associated with antidepressant treatment outcome in mood disorders. *Pharmacogenomics J,* 8**,** 101-12.

GRAY-MCGUIRE, C., MOSER, K. L., GAFFNEY, P. M., KELLY, J., YU, H., OLSON, J. M., JEDREY, C. M., JACOBS, K. B., KIMBERLY, R. P., NEAS, B. R., RICH, S. S., BEHRENS, T. W. & HARLEY, J. B. 2000. Genome scan of human systemic lupus erythematosus by regression modeling: evidence of linkage and epistasis at 4p16-15.2. *Am J Hum Genet,* 67**,** 1460-9.

GREEN, M. J., CAHILL, C. M. & MALHI, G. S. 2007. The cognitive and neurophysiological basis of emotion dysregulation in bipolar disorder. *J Affect Disord,* 103**,** 29-42.

GREEN, M. J., CAIRNS, M. J., WU, J., DRAGOVIC, M., JABLENSKY, A., TOONEY, P. A., SCOTT, R. J. & CARR, V. J. 2012. Genome-wide supported variant MIR137 and severe negative symptoms predict membership of an impaired cognitive subtype of schizophrenia. *Mol Psychiatry*.

GREEN, M. J., MATHESON, S. L., SHEPHERD, A., WEICKERT, C. S. & CARR, V. J. 2011. Brain-derived neurotrophic factor levels in schizophrenia: a systematic review with meta-analysis. *Mol Psychiatry,* 16**,** 960-72.

GRIMES, J. A. 2000. The Co-repressor mSin3A Is a Functional Component of the REST-CoREST Repressor Complex. *Journal of Biological Chemistry,* 275**,** 9461-9467.

GUAN, J. S., HAGGARTY, S. J., GIACOMETTI, E., DANNENBERG, J. H., JOSEPH, N., GAO, J., NIELAND, T. J., ZHOU, Y., WANG, X., MAZITSCHEK, R., BRADNER, J. E., DEPINHO, R. A., JAENISCH, R. & TSAI, L. H. 2009. HDAC2 negatively regulates memory formation and synaptic plasticity. *Nature,* 459**,** 55-60.

GUELLA, I., SEQUEIRA, A., ROLLINS, B., MORGAN, L., TORRI, F., VAN ERP, T. G., MYERS, R. M., BARCHAS, J. D., SCHATZBERG, A. F., WATSON, S. J., AKIL, H., BUNNEY, W. E., POTKIN, S. G., MACCIARDI, F. & VAWTER, M. P. 2013. Analysis of miR-137 expression and rs1625579 in dorsolateral prefrontal cortex. *J Psychiatr Res,* 47**,** 1215-21.

GUINDALINI, C., HOWARD, M., HADDLEY, K., LARANJEIRA, R., COLLIER, D., AMMAR, N., CRAIG, I., O'GARA, C., BUBB, V. J., GREENWOOD, T., KELSOE, J., ASHERSON, P., MURRAY, R. M., CASTELO, A., QUINN, J. P., VALLADA, H. & BREEN, G. 2006. A dopamine transporter gene functional variant associated with cocaine abuse in a Brazilian sample. *Proc Natl Acad Sci U S A,* 103**,** 4552-7.

GUO, H., INGOLIA, N. T., WEISSMAN, J. S. & BARTEL, D. P. 2010. Mammalian microRNAs predominantly act to decrease target mRNA levels. *Nature,* 466**,** 835-40.

HADDLEY, K., SPENCER, E. M., VASILIOU, S. A., HOWARD, M., THIPPESWAMY, T., BUBB, V. J. & QUINN, J. P. 2011. Lithium chloride regulation of the substance P encoding preprotachykinin a, Tac1 gene in rat hippocampal primary cells. *J Mol Neurosci,* 45**,** 94-100.

HADDLEY, K., VASILIOU, A. S., ALI, F. R., PAREDES, U. M., BUBB, V. J. & QUINN, J. P. 2008. Molecular genetics of monoamine transporters: relevance to brain disorders. *Neurochem Res,* 33**,** 652-67.

HAERIAN, B. S. 2013. BDNF rs6265 polymorphism and drug addiction: a systematic review and meta-analysis. *Pharmacogenomics,* 14**,** 2055-65.

HAHN, C. G., UMAPATHY, WANG, H. Y., KONERU, R., LEVINSON, D. F. & FRIEDMAN, E. 2005. Lithium and valproic acid treatments reduce PKC activation and receptor-G protein coupling in platelets of bipolar manic patients. *J Psychiatr Res,* 39**,** 355-63.

HALL, D., DHILLA, A., CHARALAMBOUS, A., GOGOS, J. A. & KARAYIORGOU, M. 2003. Sequence variants of the brain-derived neurotrophic factor (BDNF) gene are strongly associated with obsessive-compulsive disorder. *Am J Hum Genet,* 73**,** 370-6.

HAMMOND, S. M., BOETTCHER, S., CAUDY, A. A., KOBAYASHI, R. & HANNON, G. J. 2001. Argonaute2, a link between genetic and biochemical analyses of RNAi. *Science,* 293**,** 1146-50.

HANCKS, D. C. & KAZAZIAN, H. H., JR. 2012. Active human retrotransposons: variation and disease. *Curr Opin Genet Dev,* 22**,** 191-203.

HANNAN, A. J. 2010. Tandem repeat polymorphisms: modulators of disease susceptibility and candidates for 'missing heritability'. *Trends Genet,* 26**,** 59-65.

HARA, D., FUKUCHI, M., MIYASHITA, T., TABUCHI, A., TAKASAKI, I., NARUSE, Y., MORI, N., KONDO, T. & TSUDA, M. 2009. Remote control of activity-dependent BDNF gene promoter-I transcription mediated by REST/NRSF. *Biochem Biophys Res Commun,* 384**,** 506-11.

HARDING, R. M., BOYCE, A. J. & CLEGG, J. B. 1992. The evolution of tandemly repetitive DNA: recombination rules. *Genetics,* 132**,** 847-59.

HARIRI, A. R., GOLDBERG, T. E., MATTAY, V. S., KOLACHANA, B. S., CALLICOTT, J. H., EGAN, M. F. & WEINBERGER, D. R. 2003. Brain-Derived Neurotrophic Factor val66met Polymorphism Affects Human Memory-Related Hippocampal Activity and Predicts Memory Performance. *The Journal of Neuroscience,* 23**,** 6690-6694.

HARVEY, I., RON, M. A., DU BOULAY, G., WICKS, D., LEWIS, S. W. & MURRAY, R. M. 1993. Reduction of cortical volume in schizophrenia on magnetic resonance imaging. *Psychol Med,* 23**,** 591-604.

HASHIMOTO, R., TAKEI, N., SHIMAZU, K., CHRIST, L., LU, B. & CHUANG, D. M. 2002. Lithium induces brain-derived neurotrophic factor and activates TrkB in rodent cortical neurons: an essential step for neuroprotection against glutamate excitotoxicity. *Neuropharmacology,* 43**,** 1173-9.

HAVENS, M. A., REICH, A. A., DUELLI, D. M. & HASTINGS, M. L. 2012. Biogenesis of mammalian microRNAs by a non-canonical processing pathway. *Nucleic Acids Res,* 40**,** 4626-40.

HEAL, D. J., SMITH, S. L., GOSDEN, J. & NUTT, D. J. 2013. Amphetamine, past and present--a pharmacological and clinical perspective. *J Psychopharmacol,* 27**,** 479-96.

HENDERSON, C. R. 1986. Recent developments in variance and covariance estimation. *J Anim Sci* 63**,** 208-216.

HENGST, U., COX, L. J., MACOSKO, E. Z. & JAFFREY, S. R. 2006. Functional and selective RNA interference in developing axons and growth cones. *J Neurosci,* 26**,** 5727-32.

HERMANN, B., JONES, J., SHETH, R., DOW, C., KOEHN, M. & SEIDENBERG, M. 2006. Children with new-onset epilepsy: neuropsychological status and brain structure. *Brain,* 129**,** 2609-19.

HERRERAS, O., LARGO, C., IBARZ, J. M., SOMJEN, G. G. & MARTIN DEL RIO, R. 1994. Role of neuronal synchronizing mechanisms in the propagation of spreading depression in the in vivo hippocampus. *J Neurosci,* 14**,** 7087-98.

HETTEMA, J. M., AN, S. S., NEALE, M. C., BUKSZAR, J., VAN DEN OORD, E. J., KENDLER, K. S. & CHEN, X. 2006. Association between glutamic acid decarboxylase genes and anxiety disorders, major depression, and neuroticism. *Mol Psychiatry,* 11**,** 752-62.

HILL, D. A., DE LA SERNA, I. L., VEAL, T. M. & IMBALZANO, A. N. 2004. BRCA1 interacts with dominant negative SWI/SNF enzymes without affecting homologous recombination or radiation-induced gene activation of p21 or Mdm2. *J Cell Biochem,* 91**,** 987-98.

HILL, J., BREEN, G., QUINN, J., TIBU, F., SHARP, H. & PICKLES, A. 2013. Evidence for interplay between genes and maternal stress in utero: monoamine oxidase A polymorphism moderates effects of life events during pregnancy on infant negative emotionality at 5 weeks. *Genes Brain Behav,* 12**,** 388-96.

HILL, M. J., DONOCIK, J. G., NUAMAH, R. A., MEIN, C. A., SAINZ-FUERTES, R. & BRAY, N. J. 2014. Transcriptional consequences of schizophrenia candidate miR-137 manipulation in human neural progenitor cells. *Schizophr Res,* 153**,** 225-30.

HINDORFF, L. A., SETHUPATHY, P., JUNKINS, H. A., RAMOS, E. M., MEHTA, J. P., COLLINS, F. S. & MANOLIO, T. A. 2009. Potential etiologic and functional implications of genome-wide association loci for human diseases and traits. *Proc Natl Acad Sci U S A,* 106**,** 9362-7.

HING, B., DAVIDSON, S., LEAR, M., BREEN, G., QUINN, J., MCGUFFIN, P. & MACKENZIE, A. 2012. A polymorphism associated with depressive disorders differentially regulates brain derived neurotrophic factor promoter IV activity. *Biol Psychiatry,* 71**,** 618-26.

HONEA, R. A., CRUCHAGA, C., PEREA, R. D., SAYKIN, A. J., BURNS, J. M., WEINBERGER, D. R. & GOATE, A. M. 2013. Characterizing the role of brain derived neurotrophic factor genetic variation in Alzheimer's disease neurodegeneration. *PLoS One,* 8**,** e76001.

HORN, A. S. 1990. Dopamine uptake: a review of progress in the last decade. *Prog Neurobiol,* 34**,** 387-400.

HOWARD, M. R., MILLWARD-SADLER, S. J., VASILLIOU, A. S., SALTER, D. M. & QUINN, J. P. 2008. Mechanical stimulation induces preprotachykinin gene expression in osteoarthritic chondrocytes which is correlated with modulation of the transcription factor neuron restrictive silence factor. *Neuropeptides,* 42**,** 681-6.

HOWES, O. D. & KAPUR, S. 2009. The dopamine hypothesis of schizophrenia: version III--the final common pathway. *Schizophr Bull,* 35**,** 549-62.

HU, H. Y., GUO, S., XI, J., YAN, Z., FU, N., ZHANG, X., MENZEL, C., LIANG, H., YANG, H., ZHAO, M., ZENG, R., CHEN, W., PAABO, S. & KHAITOVICH, P. 2011a. MicroRNA expression and regulation in human, chimpanzee, and macaque brains. *PLoS Genet,* 7**,** e1002327.

HU, X. L., CHENG, X., CAI, L., TAN, G. H., XU, L., FENG, X. Y., LU, T. J., XIONG, H., FEI, J. & XIONG, Z. Q. 2011b. Conditional deletion of NRSF in forebrain neurons accelerates epileptogenesis in the kindling model. *Cereb Cortex,* 21**,** 2158-65.

HU, X. Z., LIPSKY, R. H., ZHU, G., AKHTAR, L. A., TAUBMAN, J., GREENBERG, B. D., XU, K., ARNOLD, P. D., RICHTER, M. A., KENNEDY, J. L., MURPHY, D. L. & GOLDMAN, D. 2006. Serotonin transporter promoter gain-of-function genotypes are linked to obsessive-compulsive disorder. *Am J Hum Genet,* 78**,** 815-26.

HUAN, T., RONG, J., LIU, C., ZHANG, X., TANRIVERDI, K., JOEHANES, R., CHEN, B. H., MURABITO, J. M., YAO, C., COURCHESNE, P., MUNSON, P. J., O'DONNELL, C. J., COX, N., JOHNSON, A. D., LARSON, M. G., LEVY, D. & FREEDMAN, J. E. 2015. Genome-wide identification of microRNA expression quantitative trait loci. *Nat Commun,* 6**,** 6601.

HUANG, E. J. & REICHARDT, L. F. 2001. Neurotrophins: roles in neuronal development and function. *Annu Rev Neurosci,* 24**,** 677-736.
HUANG, W. & LI, M. D. 2009. Nicotine modulates expression of miR-140*, which targets the 3'-untranslated region of dynamin 1 gene (Dnm1). *Int J Neuropsychopharmacol,* 12**,** 537-46.
HUANG, Y., DOHERTY, J. J. & DINGLEDINE, R. 2002. Altered histone acetylation at glutamate receptor 2 and brain-derived neurotrophic factor genes is an early event triggered by status epilepticus. *J Neurosci,* 22**,** 8422-8.
HUANG, Y., MYERS, S. J. & DINGLEDINE, R. 1999. Transcriptional repression by REST: recruitment of Sin3A and histone deacetylase to neuronal genes. *Nat Neurosci,* 2**,** 867-72.
HULL, J., CAMPINO, S., ROWLANDS, K., CHAN, M. S., COPLEY, R. R., TAYLOR, M. S., ROCKETT, K., ELVIDGE, G., KEATING, B., KNIGHT, J. & KWIATKOWSKI, D. 2007. Identification of common genetic variation that modulates alternative splicing. *PLoS Genet,* 3**,** e99.
HUTVAGNER, G. & ZAMORE, P. D. 2002. A microRNA in a multiple-turnover RNAi enzyme complex. *Science,* 297**,** 2056-60.
IM, H. I., HOLLANDER, J. A., BALI, P. & KENNY, P. J. 2010. MeCP2 controls BDNF expression and cocaine intake through homeostatic interactions with microRNA-212. *Nat Neurosci,* 13**,** 1120-7.
IM, H. I. & KENNY, P. J. 2012. MicroRNAs in neuronal function and dysfunction. *Trends Neurosci,* 35**,** 325-34.
ISHII, T., HASHIMOTO, E., UKAI, W., TATENO, M., YOSHINAGA, T., SAITO, S., SOHMA, H. & SAITO, T. 2008. Lithium-induced suppression of transcription repressor NRSF/REST: effects on the dysfunction of neuronal differentiation by ethanol. *Eur J Pharmacol,* 593**,** 36-43.
IZQUIERDO, A., SUDA, R. K. & MURRAY, E. A. 2005. Comparison of the effects of bilateral orbital prefrontal cortex lesions and amygdala lesions on emotional responses in rhesus monkeys. *J Neurosci,* 25**,** 8534-42.
JAIN, R. N. & SAMUELSON, L. C. 2006. Differentiation of the gastric mucosa. II. Role of gastrin in gastric epithelial cell proliferation and maturation. *Am J Physiol Gastrointest Liver Physiol,* 291**,** G762-5.
JEYASEELAN, K., LIM, K. Y. & ARMUGAM, A. 2008. MicroRNA expression in the blood and brain of rats subjected to transient focal ischemia by middle cerebral artery occlusion. *Stroke,* 39**,** 959-66.
JIANG, X., XU, K., HOBERMAN, J., TIAN, F., MARKO, A. J., WAHEED, J. F., HARRIS, C. R., MARINI, A. M., ENOCH, M. A. & LIPSKY, R. H. 2005. BDNF variation and mood disorders: a novel functional promoter polymorphism and Val66Met are associated with anxiety but have opposing effects. *Neuropsychopharmacology,* 30**,** 1353-61.
JIN, S., LEE, Y. K., LIM, Y. C., ZHENG, Z., LIN, X. M., NG, D. P., HOLBROOK, J. D., LAW, H. Y., KWEK, K. Y., YEO, G. S. & DING, C. 2013. Global DNA hypermethylation in down syndrome placenta. *PLoS Genet,* 9**,** e1003515.
JOBE, E. M., MCQUATE, A. L. & ZHAO, X. 2012. Crosstalk among Epigenetic Pathways Regulates Neurogenesis. *Front Neurosci,* 6**,** 59.
JOHANNESSEN, C. U. 2000. Mechanisms of action of valproate: a commentatory. *Neurochem Int,* 37**,** 103-10.
JOHNSON, D. S., MORTAZAVI, A., MYERS, R. M. & WOLD, B. 2007. Genome-wide mapping of in vivo protein-DNA interactions. *Science,* 316**,** 1497-502.
JOHNSON, R., GAMBLIN, R. J., OOI, L., BRUCE, A. W., DONALDSON, I. J., WESTHEAD, D. R., WOOD, I. C., JACKSON, R. M. & BUCKLEY, N. J. 2006. Identification of the REST regulon reveals extensive transposable element-mediated binding site duplication. *Nucleic Acids Res,* 34**,** 3862-77.
JOHNSON, R., TEH, C. H., JIA, H., VANISRI, R. R., PANDEY, T., LU, Z. H., BUCKLEY, N. J., STANTON, L. W. & LIPOVICH, L. 2009. Regulation of neural macroRNAs by the transcriptional repressor REST. *RNA,* 15**,** 85-96.
JOHNSON, R., ZUCCATO, C., BELYAEV, N. D., GUEST, D. J., CATTANEO, E. & BUCKLEY, N. J. 2008. A microRNA-based gene dysregulation pathway in Huntington's disease. *Neurobiol Dis,* 29**,** 438-45.
JOHNSTONE, T., VAN REEKUM, C. M., URRY, H. L., KALIN, N. H. & DAVIDSON, R. J. 2007. Failure to regulate: counterproductive recruitment of top-down prefrontal-subcortical circuitry in major depression. *J Neurosci,* 27**,** 8877-84.
JONES, S. & KAUER, J. A. 1999. Amphetamine depresses excitatory synaptic transmission via serotonin receptors in the ventral tegmental area. *J Neurosci,* 19**,** 9780-7.
JOPE, R. S. 1999. A bimodal model of the mechanism of action of lithium. *Mol Psychiatry,* 4**,** 21-5.
JOTHI, R., CUDDAPAH, S., BARSKI, A., CUI, K. & ZHAO, K. 2008. Genome-wide identification of in vivo protein-DNA binding sites from ChIP-Seq data. *Nucleic Acids Res,* 36**,** 5221-31.
JOUTEL, A., BOUSSER, M. G., BIOUSSE, V., LABAUGE, P., CHABRIAT, H., NIBBIO, A., MACIAZEK, J., MEYER, B., BACH, M. A., WEISSENBACH, J. & ET AL. 1993. A gene for familial hemiplegic migraine maps to chromosome 19. *Nat Genet,* 5**,** 40-5.
JUN, H., MOHAMMED QASIM HUSSAINI, S., RIGBY, M. J. & JANG, M. H. 2012. Functional role of adult hippocampal neurogenesis as a therapeutic strategy for mental disorders. *Neural Plast,* 2012**,** 854285.
JURKA, J. 2000. Repbase update: a database and an electronic journal of repetitive elements. *Trends Genet,* 16**,** 418-20.
KAER, K. & SPEEK, M. 2013. Retroelements in human disease. *Gene,* 518**,** 231-41.

KALIVAS, P. W. 2004. Glutamate systems in cocaine addiction. *Curr Opin Pharmacol,* 4**,** 23-9.
KALLUNKI, P., EDELMAN, G. M. & JONES, F. S. 1998. The neural restrictive silencer element can act as both a repressor and enhancer of L1 cell adhesion molecule gene expression during postnatal development. *Proc Natl Acad Sci U S A,* 95**,** 3233-8.
KAMINSKY, Z. A., TANG, T., WANG, S. C., PTAK, C., OH, G. H., WONG, A. H., FELDCAMP, L. A., VIRTANEN, C., HALFVARSON, J., TYSK, C., MCRAE, A. F., VISSCHER, P. M., MONTGOMERY, G. W., GOTTESMAN, II, MARTIN, N. G. & PETRONIS, A. 2009. DNA methylation profiles in monozygotic and dizygotic twins. *Nat Genet,* 41**,** 240-5.
KANTOR, L., PARK, Y. H., WANG, K. K. & GNEGY, M. 2002. Enhanced amphetamine-mediated dopamine release develops in PC12 cells after repeated amphetamine treatment. *Eur J Pharmacol,* 451**,** 27-35.
KARIKO, K., HARRIS, V. A., RANGEL, Y., DUVALL, M. E. & WELSH, F. A. 1998. Effect of cortical spreading depression on the levels of mRNA coding for putative neuroprotective proteins in rat brain. *J Cereb Blood Flow Metab,* 18**,** 1308-15.
KARMAKAR, S., JIN, Y. & NAGAICH, A. K. 2013. Interaction of glucocorticoid receptor (GR) with estrogen receptor (ER) alpha and activator protein 1 (AP1) in dexamethasone-mediated interference of ERalpha activity. *J Biol Chem,* 288**,** 24020-34.
KAROLEWICZ, B., MACIAG, D., O'DWYER, G., STOCKMEIER, C. A., FEYISSA, A. M. & RAJKOWSKA, G. 2010. Reduced level of glutamic acid decarboxylase-67 kDa in the prefrontal cortex in major depression. *Int J Neuropsychopharmacol,* 13**,** 411-20.
KAWAHARA, N., CROLL, S. D., WIEGAND, S. J. & KLATZO, I. 1997. Cortical spreading depression induces long-term alterations of BDNF levels in cortex and hippocampus distinct from lesion effects: implications for ischemic tolerance. *Neurosci Res,* 29**,** 37-47.
KAWAI, S. & AMANO, A. 2012. BRCA1 regulates microRNA biogenesis via the DROSHA microprocessor complex. *J Cell Biol,* 197**,** 201-8.
KELESHIAN, V. L., MODI, H. R., RAPOPORT, S. I. & RAO, J. S. 2013. Aging is associated with altered inflammatory, arachidonic acid cascade, and synaptic markers, influenced by epigenetic modifications, in the human frontal cortex. *J Neurochem,* 125**,** 63-73.
KENT, W. J., SUGNET, C. W., FUREY, T. S., ROSKIN, K. M., PRINGLE, T. H., ZAHLER, A. M. & HAUSSLER, A. D. 2002. The Human Genome Browser at UCSC. *Genome Research,* 12**,** 996-1006.
KESSLER, R. C., AGUILAR-GAXIOLA, S., ALONSO, J., CHATTERJI, S., LEE, S. & USTUN, T. B. 2009. The WHO World Mental Health (WMH) Surveys. *Psychiatrie (Stuttg),* 6**,** 5-9.
KHVOROVA, A., REYNOLDS, A. & JAYASENA, S. D. 2003. Functional siRNAs and miRNAs exhibit strand bias. *Cell,* 115**,** 209-16.
KIM, A. H., PARKER, E. K., WILLIAMSON, V., MCMICHAEL, G. O., FANOUS, A. H. & VLADIMIROV, V. I. 2012. Experimental validation of candidate schizophrenia gene ZNF804A as target for hsa-miR-137. *Schizophr Res,* 141**,** 60-4.
KIM, C. S., HWANG, C. K., CHOI, H. S., SONG, K. Y., LAW, P. Y., WEI, L. N. & LOH, H. H. 2004. Neuron-restrictive silencer factor (NRSF) functions as a repressor in neuronal cells to regulate the mu opioid receptor gene. *J Biol Chem,* 279**,** 46464-73.
KIM, C. S., HWANG, C. K., SONG, K. Y., CHOI, H. S., KIM DO, K., LAW, P. Y., WEI, L. N. & LOH, H. H. 2008. Novel function of neuron-restrictive silencer factor (NRSF) for posttranscriptional regulation. *Biochim Biophys Acta,* 1783**,** 1835-46.
KIM, J. H., CHOI, K. H., JANG, Y. J., KIM, H. N., BAE, S. S., CHOI, B. T. & SHIN, H. K. 2013. Electroacupuncture preconditioning reduces cerebral ischemic injury via BDNF and SDF-1alpha in mice. *BMC Complement Altern Med,* 13**,** 22.
KIM, S. J., LEE, B. H., LEE, Y. S. & KANG, K. S. 2007. Defective cholesterol traffic and neuronal differentiation in neural stem cells of Niemann-Pick type C disease improved by valproic acid, a histone deacetylase inhibitor. *Biochem Biophys Res Commun,* 360**,** 593-9.
KIM, V. N., HAN, J. & SIOMI, M. C. 2009. Biogenesis of small RNAs in animals. *Nat Rev Mol Cell Biol,* 10**,** 126-39.
KING, D. G., SOLLER, M. & KASHI, Y. 1997. Evolutionary tuning knobs. *Endeavour,* 21**,** 36-40.
KIROV, G., GROZEVA, D., NORTON, N., IVANOV, D., MANTRIPRAGADA, K. K., HOLMANS, P., CRADDOCK, N., OWEN, M. J. & O'DONOVAN, M. C. 2009. Support for the involvement of large copy number variants in the pathogenesis of schizophrenia. *Hum Mol Genet,* 18**,** 1497-503.
KLEER, C. G., CAO, Q., VARAMBALLY, S., SHEN, R., OTA, I., TOMLINS, S. A., GHOSH, D., SEWALT, R. G., OTTE, A. P., HAYES, D. F., SABEL, M. S., LIVANT, D., WEISS, S. J., RUBIN, M. A. & CHINNAIYAN, A. M. 2003. EZH2 is a marker of aggressive breast cancer and promotes neoplastic transformation of breast epithelial cells. *Proc Natl Acad Sci U S A,* 100**,** 11606-11.
KLENOVA, E., SCOTT, A. C., ROBERTS, J., SHAMSUDDIN, S., LOVEJOY, E. A., BERGMANN, S., BUBB, V. J., ROYER, H. D. & QUINN, J. P. 2004. YB-1 and CTCF differentially regulate the 5-HTT polymorphic intron 2 enhancer which predisposes to a variety of neurological disorders. *J Neurosci,* 24**,** 5966-73.
KOCABAS, N. A., ANTONIJEVIC, I., FAGHEL, C., FORRAY, C., KASPER, S., LECRUBIER, Y., LINOTTE, S., MASSAT, I., MENDLEWICZ, J., NORO, M., MONTGOMERY, S., OSWALD, P., SNYDER, L., ZOHAR, J. & SOUERY, D.

2011. Brain-derived neurotrophic factor gene polymorphisms: influence on treatment response phenotypes of major depressive disorder. *Int Clin Psychopharmacol,* 26**,** 1-10.

KOCH, C. M., ANDREWS, R. M., FLICEK, P., DILLON, S. C., KARAOZ, U., CLELLAND, G. K., WILCOX, S., BEARE, D. M., FOWLER, J. C., COUTTET, P., JAMES, K. D., LEFEBVRE, G. C., BRUCE, A. W., DOVEY, O. M., ELLIS, P. D., DHAMI, P., LANGFORD, C. F., WENG, Z., BIRNEY, E., CARTER, N. P., VETRIE, D. & DUNHAM, I. 2007. The landscape of histone modifications across 1% of the human genome in five human cell lines. *Genome Res,* 17**,** 691-707.

KOENIGSBERGER, C., CHICCA, J. J., 2ND, AMOUREUX, M. C., EDELMAN, G. M. & JONES, F. S. 2000. Differential regulation by multiple promoters of the gene encoding the neuron-restrictive silencer factor. *Proc Natl Acad Sci U S A,* 97**,** 2291-6.

KOIBUCHI, N., FUKUDA, H. & CHIN, W. W. 1999. Promoter-specific regulation of the brain-derived neurotropic factor gene by thyroid hormone in the developing rat cerebellum. *Endocrinology,* 140**,** 3955-61.

KORDI-TAMANDANI, D. M., SAHRANAVARD, R. & TORKAMANZEHI, A. 2012. DNA methylation and expression profiles of the brain-derived neurotrophic factor (BDNF) and dopamine transporter (DAT1) genes in patients with schizophrenia. *Mol Biol Rep,* 39**,** 10889-93.

KOTORASHVILI, A., RAMNAUTH, A., LIU, C., LIN, J., YE, K., KIM, R., HAZAN, R., ROHAN, T., FINEBERG, S. & LOUDIG, O. 2012. Effective DNA/RNA co-extraction for analysis of microRNAs, mRNAs, and genomic DNA from formalin-fixed paraffin-embedded specimens. *PLoS One,* 7**,** e34683.

KOZAKI, K., IMOTO, I., MOGI, S., OMURA, K. & INAZAWA, J. 2008. Exploration of tumor-suppressive microRNAs silenced by DNA hypermethylation in oral cancer. *Cancer Res,* 68**,** 2094-105.

KRAIG, R. P. & NICHOLSON, C. 1978. Extracellular ionic variations during spreading depression. *Neuroscience,* 3**,** 1045-59.

KRAMER, F., STOVER, T., WARNECKE, A., DIENSTHUBER, M., LENARZ, T. & WISSEL, K. 2010. BDNF mRNA expression is significantly upregulated in vestibular schwannomas and correlates with proliferative activity. *J Neurooncol,* 98**,** 31-9.

KRANER, S. D., CHONG, J. A., TSAY, H. J. & MANDEL, G. 1992. Silencing the type II sodium channel gene: a model for neural-specific gene regulation. *Neuron,* 9**,** 37-44.

KREISLER, A., STRISSEL, P. L., STRICK, R., NEUMANN, S. B., SCHUMACHER, U. & BECKER, C. M. 2010. Regulation of the NRSF/REST gene by methylation and CREB affects the cellular phenotype of small-cell lung cancer. *Oncogene,* 29**,** 5828-38.

KRICHEVSKY, A. M., KING, K. S., DONAHUE, C. P., KHRAPKO, K. & KOSIK, K. S. 2003. A microRNA array reveals extensive regulation of microRNAs during brain development. *RNA,* 9**,** 1274-81.

KROL, J., LOEDIGE, I. & FILIPOWICZ, W. 2010. The widespread regulation of microRNA biogenesis, function and decay. *Nat Rev Genet,* 11**,** 597-610.

KUBOTA, T., MIYAKE, K. & HIRASAWA, T. 2012. Epigenetic understanding of gene-environment interactions in psychiatric disorders: a new concept of clinical genetics. *Clin Epigenetics,* 4**,** 1.

KUMAR, A., CHOI, K. H., RENTHAL, W., TSANKOVA, N. M., THEOBALD, D. E., TRUONG, H. T., RUSSO, S. J., LAPLANT, Q., SASAKI, T. S., WHISTLER, K. N., NEVE, R. L., SELF, D. W. & NESTLER, E. J. 2005. Chromatin remodeling is a key mechanism underlying cocaine-induced plasticity in striatum. *Neuron,* 48**,** 303-14.

KUMARI, V. & POSTMA, P. 2005. Nicotine use in schizophrenia: the self medication hypotheses. *Neurosci Biobehav Rev,* 29**,** 1021-34.

KUMARI, V., SONI, W. & SHARMA, T. 2001. Influence of cigarette smoking on prepulse inhibition of the acoustic startle response in schizophrenia. *Hum Psychopharmacol,* 16**,** 321-326.

KUWABARA, T., HSIEH, J., NAKASHIMA, K., TAIRA, K. & GAGE, F. H. 2004. A small modulatory dsRNA specifies the fate of adult neural stem cells. *Cell,* 116**,** 779-93.

KUWAHARA, K., SAITO, Y., TAKANO, M., ARAI, Y., YASUNO, S., NAKAGAWA, Y., TAKAHASHI, N., ADACHI, Y., TAKEMURA, G., HORIE, M., MIYAMOTO, Y., MORISAKI, T., KURATOMI, S., NOMA, A., FUJIWARA, H., YOSHIMASA, Y., KINOSHITA, H., KAWAKAMI, R., KISHIMOTO, I., NAKANISHI, M., USAMI, S., HARADA, M. & NAKAO, K. 2003. NRSF regulates the fetal cardiac gene program and maintains normal cardiac structure and function. *EMBO J,* 22**,** 6310-21.

KWAN, P., SILLS, G. J. & BRODIE, M. J. 2001. The mechanisms of action of commonly used antiepileptic drugs. *Pharmacology & Therapeutics,* 90**,** 21-34.

KWON, E., WANG, W. & TSAI, L. H. 2013. Validation of schizophrenia-associated genes CSMD1, C10orf26, CACNA1C and TCF4 as miR-137 targets. *Mol Psychiatry,* 18**,** 11-2.

LAMB, J., CRAWFORD, E. D., PECK, D., MODELL, J. W., BLAT, I. C., WROBEL, M. J., LERNER, J., BRUNET, J. P., SUBRAMANIAN, A., ROSS, K. N., REICH, M., HIERONYMUS, H., WEI, G., ARMSTRONG, S. A., HAGGARTY, S. J., CLEMONS, P. A., WEI, R., CARR, S. A., LANDER, E. S. & GOLUB, T. R. 2006. The Connectivity Map: using gene-expression signatures to connect small molecules, genes, and disease. *Science,* 313**,** 1929-35.

LANDGRAF, P., RUSU, M., SHERIDAN, R., SEWER, A., IOVINO, N., ARAVIN, A., PFEFFER, S., RICE, A., KAMPHORST, A. O., LANDTHALER, M., LIN, C., SOCCI, N. D., HERMIDA, L., FULCI, V., CHIARETTI, S., FOA, R., SCHLIWKA, J., FUCHS, U., NOVOSEL, A., MULLER, R. U., SCHERMER, B., BISSELS, U., INMAN, J., PHAN, Q., CHIEN, M., WEIR, D. B., CHOKSI, R., DE VITA, G., FREZZETTI, D., TROMPETER, H. I., HORNUNG, V.,

TENG, G., HARTMANN, G., PALKOVITS, M., DI LAURO, R., WERNET, P., MACINO, G., ROGLER, C. E., NAGLE, J. W., JU, J., PAPAVASILIOU, F. N., BENZING, T., LICHTER, P., TAM, W., BROWNSTEIN, M. J., BOSIO, A., BORKHARDT, A., RUSSO, J. J., SANDER, C., ZAVOLAN, M. & TUSCHL, T. 2007. A mammalian microRNA expression atlas based on small RNA library sequencing. *Cell,* 129**,** 1401-14.

LANG, U., SANDER, T., LOHOFF, F., HELLWEG, R., BAJBOUJ, M., WINTERER, G. & GALLINAT, J. 2007. Association of the met66 allele of brain-derived neurotrophic factor (BDNF) with smoking. *Psychopharmacology (Berl),* 190**,** 433-439.

LANG, U. E., HELLWEG, R., KALUS, P., BAJBOUJ, M., LENZEN, K. P., SANDER, T., KUNZ, D. & GALLINAT, J. 2005. Association of a functional BDNF polymorphism and anxiety-related personality traits. *Psychopharmacology (Berl),* 180**,** 95-9.

LANGEVIN, S. M., STONE, R. A., BUNKER, C. H., GRANDIS, J. R., SOBOL, R. W. & TAIOLI, E. 2010. MicroRNA-137 promoter methylation in oral rinses from patients with squamous cell carcinoma of the head and neck is associated with gender and body mass index. *Carcinogenesis,* 31**,** 864-70.

LANGEVIN, S. M., STONE, R. A., BUNKER, C. H., LYONS-WEILER, M. A., LAFRAMBOISE, W. A., KELLY, L., SEETHALA, R. R., GRANDIS, J. R., SOBOL, R. W. & TAIOLI, E. 2011. MicroRNA-137 promoter methylation is associated with poorer overall survival in patients with squamous cell carcinoma of the head and neck. *Cancer,* 117**,** 1454-62.

LASKE, C., STELLOS, K., HOFFMANN, N., STRANSKY, E., STRATEN, G., ESCHWEILER, G. W. & LEYHE, T. 2011. Higher BDNF serum levels predict slower cognitive decline in Alzheimer's disease patients. *Int J Neuropsychopharmacol,* 14**,** 399-404.

LAUMET, G., CHOURAKI, V., GRENIER-BOLEY, B., LEGRY, V., HEATH, S., ZELENIKA, D., FIEVET, N., HANNEQUIN, D., DELEPINE, M., PASQUIER, F., HANON, O., BRICE, A., EPELBAUM, J., BERR, C., DARTIGUES, J. F., TZOURIO, C., CAMPION, D., LATHROP, M., BERTRAM, L., AMOUYEL, P. & LAMBERT, J. C. 2010. Systematic analysis of candidate genes for Alzheimer's disease in a French, genome-wide association study. *J Alzheimers Dis,* 20**,** 1181-8.

LAURITZEN, M., DREIER, J. P., FABRICIUS, M., HARTINGS, J. A., GRAF, R. & STRONG, A. J. 2011. Clinical relevance of cortical spreading depression in neurological disorders: migraine, malignant stroke, subarachnoid and intracranial hemorrhage, and traumatic brain injury. *J Cereb Blood Flow Metab,* 31**,** 17-35.

LE FOLL, B., DIAZ, J. & SOKOLOFF, P. 2005. A single cocaine exposure increases BDNF and D3 receptor expression: implications for drug-conditioning. *Neuroreport,* 16**,** 175-8.

LE, T. P., SUN, M., LUO, X., KRAUS, W. L. & GREENE, G. L. 2013. Mapping ERbeta genomic binding sites reveals unique genomic features and identifies EBF1 as an ERbeta interactor. *PLoS One,* 8**,** e71355.

LEAO, A. A. P. 1944. *Spreading Depression of Activity in the Cerebral Cortex.*

LEE, J. M., RAMOS, E. M., LEE, J. H., GILLIS, T., MYSORE, J. S., HAYDEN, M. R., WARBY, S. C., MORRISON, P., NANCE, M., ROSS, C. A., MARGOLIS, R. L., SQUITIERI, F., OROBELLO, S., DI DONATO, S., GOMEZ-TORTOSA, E., AYUSO, C., SUCHOWERSKY, O., TRENT, R. J., MCCUSKER, E., NOVELLETTO, A., FRONTALI, M., JONES, R., ASHIZAWA, T., FRANK, S., SAINT-HILAIRE, M. H., HERSCH, S. M., ROSAS, H. D., LUCENTE, D., HARRISON, M. B., ZANKO, A., ABRAMSON, R. K., MARDER, K., SEQUEIROS, J., PAULSEN, J. S., LANDWEHRMEYER, G. B., MYERS, R. H., MACDONALD, M. E. & GUSELLA, J. F. 2012. CAG repeat expansion in Huntington disease determines age at onset in a fully dominant fashion. *Neurology,* 78**,** 690-5.

LEE, M. G., WYNDER, C., COOCH, N. & SHIEKHATTAR, R. 2005. An essential role for CoREST in nucleosomal histone 3 lysine 4 demethylation. *Nature,* 437**,** 432-5.

LEE, S. T., LI, Z., WU, Z., AAU, M., GUAN, P., KARUTURI, R. K., LIOU, Y. C. & YU, Q. 2011. Context-specific regulation of NF-kappaB target gene expression by EZH2 in breast cancers. *Mol Cell,* 43**,** 798-810.

LEE, T. I., JENNER, R. G., BOYER, L. A., GUENTHER, M. G., LEVINE, S. S., KUMAR, R. M., CHEVALIER, B., JOHNSTONE, S. E., COLE, M. F., ISONO, K., KOSEKI, H., FUCHIKAMI, T., ABE, K., MURRAY, H. L., ZUCKER, J. P., YUAN, B., BELL, G. W., HERBOLSHEIMER, E., HANNETT, N. M., SUN, K., ODOM, D. T., OTTE, A. P., VOLKERT, T. L., BARTEL, D. P., MELTON, D. A., GIFFORD, D. K., JAENISCH, R. & YOUNG, R. A. 2006. Control of developmental regulators by Polycomb in human embryonic stem cells. *Cell,* 125**,** 301-13.

LEE, Y., KIM, M., HAN, J., YEOM, K. H., LEE, S., BAEK, S. H. & KIM, V. N. 2004. MicroRNA genes are transcribed by RNA polymerase II. *EMBO J,* 23**,** 4051-60.

LEMKE, J. R., LAL, D., REINTHALER, E. M., STEINER, I., NOTHNAGEL, M., ALBER, M., GEIDER, K., LAUBE, B., SCHWAKE, M., FINSTERWALDER, K., FRANKE, A., SCHILHABEL, M., JAHN, J. A., MUHLE, H., BOOR, R., VAN PAESSCHEN, W., CARABALLO, R., FEJERMAN, N., WECKHUYSEN, S., DE JONGHE, P., LARSEN, J., MOLLER, R. S., HJALGRIM, H., ADDIS, L., TANG, S., HUGHES, E., PAL, D. K., VERI, K., VAHER, U., TALVIK, T., DIMOVA, P., GUERRERO LOPEZ, R., SERRATOSA, J. M., LINNANKIVI, T., LEHESJOKI, A. E., RUF, S., WOLFF, M., BUERKI, S., WOHLRAB, G., KROELL, J., DATTA, A. N., FIEDLER, B., KURLEMANN, G., KLUGER, G., HAHN, A., HABERLANDT, D. E., KUTZER, C., SPERNER, J., BECKER, F., WEBER, Y. G., FEUCHT, M., STEINBOCK, H., NEOPHYTHOU, B., RONEN, G. M., GRUBER-SEDLMAYR, U., GELDNER, J., HARVEY, R. J., HOFFMANN, P., HERMS, S., ALTMULLER, J., TOLIAT, M. R., THIELE, H., NURNBERG, P., WILHELM, C., STEPHANI, U., HELBIG, I., LERCHE, H., ZIMPRICH, F., NEUBAUER, B. A., BISKUP, S. & VON

SPICZAK, S. 2013. Mutations in GRIN2A cause idiopathic focal epilepsy with rolandic spikes. *Nat Genet,* 45**,** 1067-72.
LENOX, R. H. 1987. Role of receptor coupling to phosphoinositide metabolism in the therapeutic action of lithium. *Adv Exp Med Biol,* 221**,** 515-30.
LENOX, R. H. & WANG, L. 2003. Molecular basis of lithium action: integration of lithium-responsive signaling and gene expression networks. *Mol Psychiatry,* 8**,** 135-44.
LEPAGNOL-BESTEL, A. M., ZVARA, A., MAUSSION, G., QUIGNON, F., NGIMBOUS, B., RAMOZ, N., IMBEAUD, S., LOE-MIE, Y., BENIHOUD, K., AGIER, N., SALIN, P. A., CARDONA, A., KHUNG-SAVATOVSKY, S., KALLUNKI, P., DELABAR, J. M., PUSKAS, L. G., DELACROIX, H., AGGERBECK, L., DELEZOIDE, A. L., DELATTRE, O., GORWOOD, P., MOALIC, J. M. & SIMONNEAU, M. 2009. DYRK1A interacts with the REST/NRSF-SWI/SNF chromatin remodelling complex to deregulate gene clusters involved in the neuronal phenotypic traits of Down syndrome. *Hum Mol Genet,* 18**,** 1405-14.
LEPSCH, L. B., MUNHOZ, C. D., KAWAMOTO, E. M., YSHII, L. M., LIMA, L. S., CURI-BOAVENTURA, M. F., SALGADO, T. M., CURI, R., PLANETA, C. S. & SCAVONE, C. 2009. Cocaine induces cell death and activates the transcription nuclear factor kappa-B in PC12 cells. *Mol Brain,* 2**,** 3.
LETT, T. A., CHAKAVARTY, M. M., FELSKY, D., BRANDL, E. J., TIWARI, A. K., GONCALVES, V. F., RAJJI, T. K., DASKALAKIS, Z. J., MELTZER, H. Y., LIEBERMAN, J. A., LERCH, J. P., MULSANT, B. H., KENNEDY, J. L. & VOINESKOS, A. N. 2013. The genome-wide supported microRNA-137 variant predicts phenotypic heterogeneity within schizophrenia. *Mol Psychiatry,* 18**,** 443-50.
LEW, G. M. 1992. Microtubular tau protein after cocaine in cultured SH-SY5Y human neuroblastoma. *Gen Pharmacol,* 23**,** 1111-3.
LEWONTIN, R. C. 1964. The Interaction of Selection and Linkage. I. General Considerations; Heterotic Models. *Genetics,* 49**,** 49-67.
LIAN, Y. & GARNER, H. R. 2005. Evidence for the regulation of alternative splicing via complementary DNA sequence repeats. *Bioinformatics,* 21**,** 1358-64.
LICHTENSTEIN, P., YIP, B. H., BJORK, C., PAWITAN, Y., CANNON, T. D., SULLIVAN, P. F. & HULTMAN, C. M. 2009. Common genetic determinants of schizophrenia and bipolar disorder in Swedish families: a population-based study. *Lancet,* 373**,** 234-9.
LIEBERMAN, J. A., KINON, B. J. & LOEBEL, A. D. 1990. Dopaminergic mechanisms in idiopathic and drug-induced psychoses. *Schizophr Bull,* 16**,** 97-110.
LIM, K. O., TEW, W., KUSHNER, M., CHOW, K., MATSUMOTO, B. & DELISI, L. E. 1996. Cortical gray matter volume deficit in patients with first-episode schizophrenia. *Am J Psychiatry,* 153**,** 1548-53.
LIM, L. P., LAU, N. C., GARRETT-ENGELE, P., GRIMSON, A., SCHELTER, J. M., CASTLE, J., BARTEL, D. P., LINSLEY, P. S. & JOHNSON, J. M. 2005. Microarray analysis shows that some microRNAs downregulate large numbers of target mRNAs. *Nature,* 433**,** 769-73.
LIM, Y. Y., VILLEMAGNE, V. L., LAWS, S. M., PIETRZAK, R. H., SNYDER, P. J., AMES, D., ELLIS, K. A., HARRINGTON, K., REMBACH, A., MARTINS, R. N., ROWE, C. C., MASTERS, C. L. & MARUFF, P. 2014. APOE and BDNF polymorphisms moderate amyloid beta-related cognitive decline in preclinical Alzheimer's disease. *Mol Psychiatry*.
LIN, Y., CHENG, S., XIE, Z. & ZHANG, D. 2014. Association of rs6265 and rs2030324 polymorphisms in brain-derived neurotrophic factor gene with Alzheimer's disease: a meta-analysis. *PLoS One,* 9**,** e94961.
LIPSKY, R. H., XU, K., ZHU, D., KELLY, C., TERHAKOPIAN, A., NOVELLI, A. & MARINI, A. M. 2001. Nuclear factor κB is a critical determinant in N-methyl-d-aspartate receptor-mediated neuroprotection. *J Neurochem,* 78**,** 254-264.
LIPTON, S. A. & ROSENBERG, P. A. 1994. Excitatory amino acids as a final common pathway for neurologic disorders. *N Engl J Med,* 330**,** 613-22.
LIU, C., ZHANG, F., LI, T., LU, M., WANG, L., YUE, W. & ZHANG, D. 2012a. MirSNP, a database of polymorphisms altering miRNA target sites, identifies miRNA-related SNPs in GWAS SNPs and eQTLs. *BMC Genomics,* 13**,** 661.
LIU, L., FOROUD, T., XUEI, X., BERRETTINI, W., BYERLEY, W., CORYELL, W., EL-MALLAKH, R., GERSHON, E. S., KELSOE, J. R., LAWSON, W. B., MACKINNON, D. F., MCINNIS, M., MCMAHON, F. J., MURPHY, D. L., RICE, J., SCHEFTNER, W., ZANDI, P. P., LOHOFF, F. W., NICULESCU, A. B., MEYER, E. T., EDENBERG, H. J. & NURNBERGER, J. I., JR. 2008. Evidence of association between brain-derived neurotrophic factor gene and bipolar disorder. *Psychiatr Genet,* 18**,** 267-74.
LIU, M., LANG, N., QIU, M., XU, F., LI, Q., TANG, Q., CHEN, J., CHEN, X., ZHANG, S., LIU, Z., ZHOU, J., ZHU, Y., DENG, Y., ZHENG, Y. & BI, F. 2011. miR-137 targets Cdc42 expression, induces cell cycle G1 arrest and inhibits invasion in colorectal cancer cells. *Int J Cancer,* 128**,** 1269-79.
LIU, M., SHENG, Z., CAI, L., ZHAO, K., TIAN, Y. & FEI, J. 2012b. Neuronal conditional knockout of NRSF decreases vulnerability to seizures induced by pentylenetetrazol in mice. *Acta Biochim Biophys Sin (Shanghai),* 44**,** 476-82.
LIU, Q. R., LU, L., ZHU, X. G., GONG, J. P., SHAHAM, Y. & UHL, G. R. 2006. Rodent BDNF genes, novel promoters, novel splice variants, and regulation by cocaine. *Brain Res,* 1067**,** 1-12.

LIU, W., GU, N., FENG, G., LI, S., BAI, S., ZHANG, J., SHEN, T., XUE, H., BREEN, G., ST CLAIR, D. & HE, L. 1999. Tentative association of the serotonin transporter with schizophrenia and unipolar depression but not with bipolar disorder in Han Chinese. *Pharmacogenetics*

9**,** 491–495.

LLERENA, A., DE LA RUBIA, A., PEÑAS-LLEDÓ, E. M., DIAZ, F. J. & DE LEON, J. 2003. Schizophrenia and tobacco smoking in a Spanish psychiatric hospital. *Schizophrenia Research,* 60**,** 313-317.

LOE-MIE, Y., LEPAGNOL-BESTEL, A. M., MAUSSION, G., DORON-FAIGENBOIM, A., IMBEAUD, S., DELACROIX, H., AGGERBECK, L., PUPKO, T., GORWOOD, P., SIMONNEAU, M. & MOALIC, J. M. 2010. SMARCA2 and other genome-wide supported schizophrenia-associated genes: regulation by REST/NRSF, network organization and primate-specific evolution. *Hum Mol Genet,* 19**,** 2841-57.

LOH, Y. H., WU, Q., CHEW, J. L., VEGA, V. B., ZHANG, W., CHEN, X., BOURQUE, G., GEORGE, J., LEONG, B., LIU, J., WONG, K. Y., SUNG, K. W., LEE, C. W., ZHAO, X. D., CHIU, K. P., LIPOVICH, L., KUZNETSOV, V. A., ROBSON, P., STANTON, L. W., WEI, C. L., RUAN, Y., LIM, B. & NG, H. H. 2006. The Oct4 and Nanog transcription network regulates pluripotency in mouse embryonic stem cells. *Nat Genet,* 38**,** 431-40.

LOK, S. I., VAN MIL, A., BOVENSCHEN, N., VAN DER WEIDE, P., VAN KUIK, J., VAN WICHEN, D., PEETERS, T., SIERA, E., WINKENS, B., SLUIJTER, J. P., DOEVENDANS, P. A., DA COSTA MARTINS, P. A., DE JONGE, N. & DE WEGER, R. A. 2013. Post-transcriptional regulation of alpha-1-antichymotrypsin by microRNA-137 in chronic heart failure and mechanical support. *Circ Heart Fail,* 6**,** 853-61.

LONG, J. M., RAY, B. & LAHIRI, D. K. 2012. MicroRNA-153 physiologically inhibits expression of amyloid-beta precursor protein in cultured human fetal brain cells and is dysregulated in a subset of Alzheimer disease patients. *J Biol Chem,* 287**,** 31298-310.

LOOTS, G. G. & OVCHARENKO, I. 2004. rVISTA 2.0: evolutionary analysis of transcription factor binding sites. *Nucleic Acids Res,* 32**,** W217-21.

LOVEJOY, E. A., SCOTT, A. C., FISKERSTRAND, C. E., BUBB, V. J. & QUINN, J. P. 2003. The serotonin transporter intronic VNTR enhancer correlated with a predisposition to affective disorders has distinct regulatory elements within the domain based on the primary DNA sequence of the repeat unit. *European Journal of Neuroscience,* 17**,** 417-420.

LU, T., ARON, L., ZULLO, J., PAN, Y., KIM, H., CHEN, Y., YANG, T. H., KIM, H. M., DRAKE, D., LIU, X. S., BENNETT, D. A., COLAIACOVO, M. P. & YANKNER, B. A. 2014. REST and stress resistance in ageing and Alzheimer's disease. *Nature,* 507**,** 448-54.

LUBIN, F. D., ROTH, T. L. & SWEATT, J. D. 2008. Epigenetic regulation of BDNF gene transcription in the consolidation of fear memory. *J Neurosci,* 28**,** 10576-86.

LUGER, K., MADER, A. W., RICHMOND, R. K., SARGENT, D. F. & RICHMOND, T. J. 1997. Crystal structure of the nucleosome core particle at 2.8 A resolution. *Nature,* 389**,** 251-60.

LUGLI, G., TORVIK, V. I., LARSON, J. & SMALHEISER, N. R. 2008. Expression of microRNAs and their precursors in synaptic fractions of adult mouse forebrain. *J Neurochem,* 106**,** 650-61.

LUNDORF, M. D., BUTTENSCHON, H. N., FOLDAGER, L., BLACKWOOD, D. H., MUIR, W. J., MURRAY, V., PELOSI, A. J., KRUSE, T. A., EWALD, H. & MORS, O. 2005. Mutational screening and association study of glutamate decarboxylase 1 as a candidate susceptibility gene for bipolar affective disorder and schizophrenia. *Am J Med Genet B Neuropsychiatr Genet,* 135B**,** 94-101.

LUNYAK, V. V., BURGESS, R., PREFONTAINE, G. G., NELSON, C., SZE, S. H., CHENOWETH, J., SCHWARTZ, P., PEVZNER, P. A., GLASS, C., MANDEL, G. & ROSENFELD, M. G. 2002. Corepressor-dependent silencing of chromosomal regions encoding neuronal genes. *Science,* 298**,** 1747-52.

LUO, C., TETTEH, P. W., MERZ, P. R., DICKES, E., ABUKIWAN, A., HOTZ-WAGENBLATT, A., HOLLAND-CUNZ, S., SINNBERG, T., SCHITTEK, B., SCHADENDORF, D., DIEDERICHS, S. & EICHMULLER, S. B. 2013. miR-137 inhibits the invasion of melanoma cells through downregulation of multiple oncogenic target genes. *J Invest Dermatol,* 133**,** 768-75.

LUPIEN, S. J., MCEWEN, B. S., GUNNAR, M. R. & HEIM, C. 2009. Effects of stress throughout the lifespan on the brain, behaviour and cognition. *Nat Rev Neurosci,* 10**,** 434-45.

LV, H., PAN, G., ZHENG, G., WU, X., REN, H., LIU, Y. & WEN, J. 2010. Expression and functions of the repressor element 1 (RE-1)-silencing transcription factor (REST) in breast cancer. *J Cell Biochem,* 110**,** 968-74.

MACKENZIE, A., HING, B. & DAVIDSON, S. 2013. Exploring the effects of polymorphisms on cis-regulatory signal transduction response. *Trends Mol Med,* 19**,** 99-107.

MACKENZIE, A., PAYNE, C., BOYLE, S., CLARKE, A. R. & QUINN, J. P. 2000. The human preprotachykinin-A gene promoter has been highly conserved and can drive human-like marker gene expression in the adult mouse CNS. *Mol Cell Neurosci,* 16**,** 620-30.

MACKENZIE, A. & QUINN, J. P. 1999. A serotonin transporter gene intron 2 polymorphic region, correlated with affective disorders, has allele-dependent differential enhancer-likeproperties in the mouse embryo. *PNAS,* 96**,** 15251–15255.

MAES, O. C., CHERTKOW, H. M., WANG, E. & SCHIPPER, H. M. 2009. MicroRNA: Implications for Alzheimer Disease and other Human CNS Disorders. *Curr Genomics,* 10**,** 154-68.

MALHI, G., TANIOUS, M., DAS, P., COULSTON, C. & BERK, M. 2013. Potential Mechanisms of Action of Lithium in Bipolar Disorder. *CNS Drugs,* 27**,** 135-153.

MANJI, H. K., ETCHEBERRIGARAY, R., CHEN, G. & OLDS, J. L. 1993. Lithium decreases membrane-associated protein kinase C in hippocampus: selectivity for the alpha isozyme. *J Neurochem,* 61**,** 2303-10.

MANJI, H. K. & LENOX, R. H. 1994. Long-term action of lithium: a role for transcriptional and posttranscriptional factors regulated by protein kinase C. *Synapse,* 16**,** 11-28.

MANN, L., HELDMAN, E., BERSUDSKY, Y., VATNER, S. F., ISHIKAWA, Y., ALMOG, O., BELMAKER, R. H. & AGAM, G. 2009. Inhibition of specific adenylyl cyclase isoforms by lithium and carbamazepine, but not valproate, may be related to their antidepressant effect. *Bipolar Disord,* 11**,** 885-96.

MANN, L., HELDMAN, E., SHALTIEL, G., BELMAKER, R. H. & AGAM, G. 2008. Lithium preferentially inhibits adenylyl cyclase V and VII isoforms. *Int J Neuropsychopharmacol,* 11**,** 533-9.

MANOLIO, T. A., COLLINS, F. S., COX, N. J., GOLDSTEIN, D. B., HINDORFF, L. A., HUNTER, D. J., MCCARTHY, M. I., RAMOS, E. M., CARDON, L. R., CHAKRAVARTI, A., CHO, J. H., GUTTMACHER, A. E., KONG, A., KRUGLYAK, L., MARDIS, E., ROTIMI, C. N., SLATKIN, M., VALLE, D., WHITTEMORE, A. S., BOEHNKE, M., CLARK, A. G., EICHLER, E. E., GIBSON, G., HAINES, J. L., MACKAY, T. F., MCCARROLL, S. A. & VISSCHER, P. M. 2009. Finding the missing heritability of complex diseases. *Nature,* 461**,** 747-53.

MARCHETTI, B., L'EPISCOPO, F., MORALE, M. C., TIROLO, C., TESTA, N., CANIGLIA, S., SERAPIDE, M. F. & PLUCHINO, S. 2013. Uncovering novel actors in astrocyte-neuron crosstalk in Parkinson's disease: the Wnt/beta-catenin signaling cascade as the common final pathway for neuroprotection and self-repair. *Eur J Neurosci,* 37**,** 1550-63.

MARSON, A. G., AL-KHARUSI, A. M., ALWAIDH, M., APPLETON, R., BAKER, G. A., CHADWICK, D. W., CRAMP, C., COCKERELL, O. C., COOPER, P. N., DOUGHTY, J., EATON, B., GAMBLE, C., GOULDING, P. J., HOWELL, S. J. L., HUGHES, A., JACKSON, M., JACOBY, A., KELLETT, M., LAWSON, G. R., LEACH, J. P., NICOLAIDES, P., ROBERTS, R., SHACKLEY, P., SHEN, J., SMITH, D. F., SMITH, P. E. M., SMITH, C. T., VANOLI, A. & WILLIAMSON, P. R. 2007a. The SANAD study of effectiveness of carbamazepine, gabapentin, lamotrigine, oxcarbazepine, or topiramate for treatment of partial epilepsy: an unblinded randomised controlled trial. *The Lancet,* 369**,** 1000-1015.

MARSON, A. G., AL-KHARUSI, A. M., ALWAIDH, M., APPLETON, R., BAKER, G. A., CHADWICK, D. W., CRAMP, C., COCKERELL, O. C., COOPER, P. N., DOUGHTY, J., EATON, B., GAMBLE, C., GOULDING, P. J., HOWELL, S. J. L., HUGHES, A., JACKSON, M., JACOBY, A., KELLETT, M., LAWSON, G. R., LEACH, J. P., NICOLAIDES, P., ROBERTS, R., SHACKLEY, P., SHEN, J., SMITH, D. F., SMITH, P. E. M., SMITH, C. T., VANOLI, A. & WILLIAMSON, P. R. 2007b. The SANAD study of effectiveness of valproate, lamotrigine, or topiramate for generalised and unclassifiable epilepsy: an unblinded randomised controlled trial. *The Lancet,* 369**,** 1016-1026.

MARTINOWICH, K., HATTORI, D., WU, H., FOUSE, S., HE, F., HU, Y., FAN, G. & SUN, Y. E. 2003. DNA methylation-related chromatin remodeling in activity-dependent BDNF gene regulation. *Science,* 302**,** 890-3.

MATYS, V. 2003. TRANSFAC(R): transcriptional regulation, from patterns to profiles. *Nucleic Acids Res,* 31**,** 374-378.

MCALLISTER, A. K., KATZ, L. C. & LO, D. C. 1999. Neurotrophins and synaptic plasticity. *Annu Rev Neurosci,* 22**,** 295-318.

MCCLELLAND, S., BRENNAN, G. P., DUBE, C., RAJPARA, S., IYER, S., RICHICHI, C., BERNARD, C. & BARAM, T. Z. 2014. The transcription factor NRSF contributes to epileptogenesis by selective repression of a subset of target genes. *Elife,* 3**,** e01267.

MCCLELLAND, S., FLYNN, C., DUBE, C., RICHICHI, C., ZHA, Q., GHESTEM, A., ESCLAPEZ, M., BERNARD, C. & BARAM, T. Z. 2011. Neuron-restrictive silencer factor-mediated hyperpolarization-activated cyclic nucleotide gated channelopathy in experimental temporal lobe epilepsy. *Ann Neurol,* 70**,** 454-64.

MEI, L. & NAVE, K. A. 2014. Neuregulin-ERBB signaling in the nervous system and neuropsychiatric diseases. *Neuron,* 83**,** 27-49.

MEISER, J., WEINDL, D. & HILLER, K. 2013. Complexity of dopamine metabolism. *Cell Commun Signal,* 11**,** 34.

MERCADER, J. M., RIBASES, M., GRATACOS, M., GONZALEZ, J. R., BAYES, M., DE CID, R., BADIA, A., FERNANDEZ-ARANDA, F. & ESTIVILL, X. 2007. Altered brain-derived neurotrophic factor blood levels and gene variability are associated with anorexia and bulimia. *Genes Brain Behav,* 6**,** 706-16.

MEXAL, S., FRANK, M., BERGER, R., ADAMS, C. E., ROSS, R. G., FREEDMAN, R. & LEONARD, S. 2005. Differential modulation of gene expression in the NMDA postsynaptic density of schizophrenic and control smokers. *Brain Res Mol Brain Res,* 139**,** 317-32.

MILLER, J. S., BARR, J. L., HARPER, L. J., POOLE, R. L., GOULD, T. J. & UNTERWALD, E. M. 2014. The GSK3 signaling pathway is activated by cocaine and is critical for cocaine conditioned reward in mice. *PLoS One,* 9**,** e88026.

MINES, M. A. & JOPE, R. S. 2012. Brain region differences in regulation of Akt and GSK3 by chronic stimulant administration in mice. *Cell Signal,* 24**,** 1398-405.

MIYAJIMA, F., OLLIER, W., MAYES, A., JACKSON, A., THACKER, N., RABBITT, P., PENDLETON, N., HORAN, M. & PAYTON, A. 2008a. Brain-derived neurotrophic factor polymorphism Val66Met influences cognitive abilities in the elderly. *Genes Brain Behav,* 7**,** 411-7.

MIYAJIMA, F., QUINN, J. P., HORAN, M., PICKLES, A., OLLIER, W. E., PENDLETON, N. & PAYTON, A. 2008b. Additive effect of BDNF and REST polymorphisms is associated with improved general cognitive ability. *Genes Brain Behav,* 7**,** 714-9.
MOFFITT, T. E., CASPI, A. & RUTTER, M. 2005. Strategy for investigating interactions between measured genes and measured environments. *Arch Gen Psychiatry,* 62**,** 473-81.
MONTAG, C., BASTEN, U., STELZEL, C., FIEBACH, C. J. & REUTER, M. 2008. The BDNF Val66Met polymorphism and smoking. *Neurosci Lett,* 442**,** 30-3.
MORI, N., SCHOENHERR, C., VANDENBERGH, D. J. & ANDERSON, D. J. 1992. A common silencer element in the SCG10 and type II Na+ channel genes binds a factor present in nonneuronal cells but not in neuronal cells. *Neuron,* 9**,** 45-54.
MORK, A. & GEISLER, A. 1987. Mode of action of lithium on the catalytic unit of adenylate cyclase from rat brain. *Pharmacol Toxicol,* 60**,** 241-8.
MORRIS, R. W., SPARKS, A., MITCHELL, P. B., WEICKERT, C. S. & GREEN, M. J. 2012. Lack of cortico-limbic coupling in bipolar disorder and schizophrenia during emotion regulation. *Transl Psychiatry,* 2**,** e90.
MORTAZAVI, A., LEEPER THOMPSON, E. C., GARCIA, S. T., MYERS, R. M. & WOLD, B. 2006. Comparative genomics modeling of the NRSF/REST repressor network: from single conserved sites to genome-wide repertoire. *Genome Res,* 16**,** 1208-21.
MOTA DE FREITAS, D., AMARI, L., SRINIVASAN, C., RONG, Q., RAMASAMY, R., ABRAHA, A., GERALDES, C. F. & BOYD, M. K. 1994. Competition between Li+ and Mg2+ for the phosphate groups in the human erythrocyte membrane and ATP: an NMR and fluorescence study. *Biochemistry,* 33**,** 4101-10.
MOTAMEDI, G. & MEADOR, K. 2003. Epilepsy and cognition. *Epilepsy & Behavior,* 4**,** 25-38.
MUJICA-PARODI, L. R., YERAGANI, V. & MALASPINA, D. 2005. Nonlinear Complexity and Spectral Analyses of Heart Rate Variability in Medicated and Unmedicated Patients with Schizophrenia<sup>1</sup>. *Neuropsychobiology,* 51**,** 10-15.
MURAI, K., NARUSE, Y., SHAUL, Y., AGATA, Y. & MORI, N. 2004. Direct interaction of NRSF with TBP: chromatin reorganization and core promoter repression for neuron-specific gene transcription. *Nucleic Acids Res,* 32**,** 3180-9.
MURASHOV, A. K., CHINTALGATTU, V., ISLAMOV, R. R., LEVER, T. E., PAK, E. S., SIERPINSKI, P. L., KATWA, L. C. & VAN SCOTT, M. R. 2007. RNAi pathway is functional in peripheral nerve axons. *FASEB J,* 21**,** 656-70.
MURGATROYD, C., HOFFMANN, A. & SPENGLER, D. 2012. In vivo ChIP for the analysis of microdissected tissue samples. *Methods Mol Biol,* 809**,** 135-48.
MURGATROYD, C., PATCHEV, A. V., WU, Y., MICALE, V., BOCKMUHL, Y., FISCHER, D., HOLSBOER, F., WOTJAK, C. T., ALMEIDA, O. F. & SPENGLER, D. 2009. Dynamic DNA methylation programs persistent adverse effects of early-life stress. *Nat Neurosci,* 12**,** 1559-66.
MURGATROYD, C. & SPENGLER, D. 2011. Epigenetics of early child development. *Front Psychiatry,* 2**,** 16.
NADEAU, H. & LESTER, H. A. 2002. NRSF causes cAMP-sensitive suppression of sodium current in cultured hippocampal neurons. *J Neurophysiol,* 88**,** 409-21.
NARUSE, Y., AOKI, T., KOJIMA, T. & MORI, N. 1999. Neural restrictive silencer factor recruits mSin3 and histone deacetylase complex to repress neuron-specific target genes. *Proc Natl Acad Sci U S A,* 96**,** 13691-6.
NEGRINI, S., PRADA, I., D'ALESSANDRO, R. & MELDOLESI, J. 2013. REST: an oncogene or a tumor suppressor? *Trends Cell Biol,* 23**,** 289-95.
NETWORK AND PATHWAY ANALYSIS SUBGROUP OF THE PSYCHIATRIC GENOMICS CONSORTIUM, C. 2015. Psychiatric genome-wide association study analyses implicate neuronal, immune and histone pathways. *Nat Neurosci,* 18**,** 199-209.
NEWMAN, M. E. & BELMAKER, R. H. 1987. Effects of lithium in vitro and ex vivo on components of the adenylate cyclase system in membranes from the cerebral cortex of the rat. *Neuropharmacology,* 26**,** 211-7.
NHO, K., KIM, S., RISACHER, S. L., SHEN, L., CORNEVEAUX, J. J., SWAMINATHAN, S., LIN, H., RAMANAN, V. K., LIU, Y., FOROUD, T. M., INLOW, M. H., SINIARD, A. L., REIMAN, R. A., AISEN, P. S., PETERSEN, R. C., GREEN, R. C., JACK, C. R., WEINER, M. W., BALDWIN, C. T., LUNETTA, K. L., FARRER, L. A., FURNEY, S. J., LOVESTONE, S., SIMMONS, A., MECOCCI, P., VELLAS, B., TSOLAKI, M., KLOSZEWSKA, I., SOININEN, H., MCDONALD, B. C., FARLOW, M. R., GHETTI, B., HUENTELMAN, M. J. & SAYKIN, A. J. 2015. Protective variant for hippocampal atrophy identified by whole exome sequencing. *Ann Neurol*.
NIBUYA, M., MORINOBU, S. & DUMAN, R. S. 1995. Regulation of BDNF and trkB mRNA in rat brain by chronic electroconvulsive seizure and antidepressant drug treatments. *J Neurosci,* 15**,** 7539-47.
NISHIHARA, S., TSUDA, L. & OGURA, T. 2003. The canonical Wnt pathway directly regulates NRSF/REST expression in chick spinal cord. *Biochem Biophys Res Commun,* 311**,** 55-63.
NISHIMOTO, S. & NISHIDA, E. 2006. MAPK signalling: ERK5 versus ERK1/2. *EMBO Rep,* 7**,** 782-6.
NISHIMURA, K., NAKAMURA, K., ANITHA, A., YAMADA, K., TSUJII, M., IWAYAMA, Y., HATTORI, E., TOYOTA, T., TAKEI, N., MIYACHI, T., IWATA, Y., SUZUKI, K., MATSUZAKI, H., KAWAI, M., SEKINE, Y., TSUCHIYA, K., SUGIHARA, G., SUDA, S., OUCHI, Y., SUGIYAMA, T., YOSHIKAWA, T. & MORI, N. 2007. Genetic analyses of the brain-derived neurotrophic factor (BDNF) gene in autism. *Biochem Biophys Res Commun,* 356**,** 200-6.

NOH, K. M., HWANG, J. Y., FOLLENZI, A., ATHANASIADOU, R., MIYAWAKI, T., GREALLY, J. M., BENNETT, M. V. & ZUKIN, R. S. 2012. Repressor element-1 silencing transcription factor (REST)-dependent epigenetic remodeling is critical to ischemia-induced neuronal death. *Proc Natl Acad Sci U S A,* 109**,** E962-71.

NOMURA, M., DURBAK, L., CHAN, J., SMITHIES, O., GUSTAFSSON, J. A., KORACH, K. S., PFAFF, D. W. & OGAWA, S. 2002. Genotype/age interactions on aggressive behavior in gonadally intact estrogen receptor beta knockout (betaERKO) male mice. *Horm Behav,* 41**,** 288-96.

NOVAK, G., LEBLANC, M., ZAI, C., SHAIKH, S., RENOU, J., DELUCA, V., BULGIN, N., KENNEDY, J. L. & LE FOLL, B. 2010. Association of polymorphisms in the BDNF, DRD1 and DRD3 genes with tobacco smoking in schizophrenia. *Ann Hum Genet,* 74**,** 291-298.

OADES, R. D. & HALLIDAY, G. M. 1987. Ventral tegmental (A10) system: neurobiology. 1. Anatomy and connectivity. *Brain Res,* 434**,** 117-65.

OLDE LOOHUIS, N. F., KOS, A., MARTENS, G. J., VAN BOKHOVEN, H., NADIF KASRI, N. & ASCHRAFI, A. 2012. MicroRNA networks direct neuronal development and plasticity. *Cell Mol Life Sci,* 69**,** 89-102.

OLSEN, L., KLAUSEN, M., HELBOE, L., NIELSEN, F. C. & WERGE, T. 2009. MicroRNAs show mutually exclusive expression patterns in the brain of adult male rats. *PLoS One,* 4**,** e7225.

OOI, L., BELYAEV, N. D., MIYAKE, K., WOOD, I. C. & BUCKLEY, N. J. 2006. BRG1 chromatin remodeling activity is required for efficient chromatin binding by repressor element 1-silencing transcription factor (REST) and facilitates REST-mediated repression. *J Biol Chem,* 281**,** 38974-80.

OOI, L. & WOOD, I. C. 2007. Chromatin crosstalk in development and disease: lessons from REST. *Nat Rev Genet,* 8**,** 544-54.

OPHOFF, R. A., VAN EIJK, R., SANDKUIJL, L. A., TERWINDT, G. M., GRUBBEN, C. P., HAAN, J., LINDHOUT, D., FERRARI, M. D. & FRANTS, R. R. 1994. Genetic heterogeneity of familial hemiplegic migraine. *Genomics,* 22**,** 21-6.

OROM, U. A., NIELSEN, F. C. & LUND, A. H. 2008. MicroRNA-10a binds the 5'UTR of ribosomal protein mRNAs and enhances their translation. *Mol Cell,* 30**,** 460-71.

ORR, H. T. & ZOGHBI, H. Y. 2007. Trinucleotide repeat disorders. *Annu Rev Neurosci,* 30**,** 575-621.

OTSUKI, K., UCHIDA, S., WAKABAYASHI, Y., MATSUBARA, T., HOBARA, T., FUNATO, H. & WATANABE, Y. 2010. Aberrant REST-mediated transcriptional regulation in major depressive disorder. *J Psychiatr Res,* 44**,** 378-84.

OTTO, S. J., MCCORKLE, S. R., HOVER, J., CONACO, C., HAN, J. J., IMPEY, S., YOCHUM, G. S., DUNN, J. J., GOODMAN, R. H. & MANDEL, G. 2007. A new binding motif for the transcriptional repressor REST uncovers large gene networks devoted to neuronal functions. *J Neurosci,* 27**,** 6729-39.

OZAKI, N. & CHUANG, D.-M. 2002. Lithium Increases Transcription Factor Binding to AP-1 and Cyclic AMP-Responsive Element in Cultured Neurons and Rat Brain. *J Neurochem,* 69**,** 2336-2344.

PACKER, A. N., XING, Y., HARPER, S. Q., JONES, L. & DAVIDSON, B. L. 2008. The bifunctional microRNA miR-9/miR-9* regulates REST and CoREST and is downregulated in Huntington's disease. *J Neurosci,* 28**,** 14341-6.

PALLER, K. A., ACHARYA, A., RICHARDSON, B. C., PLAISANT, O., SHIMAMURA, A. P., REED, B. R. & JAGUST, W. J. 1997. Functional Neuroimaging of Cortical Dysfunction in Alcoholic Korsakoff's Syndrome. *J Cogn Neurosci,* 9**,** 277-93.

PALM, K., BELLUARDO, N., METSIS, M. & TIMMUSK, T. 1998. Neuronal expression of zinc finger transcription factor REST/NRSF/XBR gene. *J Neurosci,* 18**,** 1280-96.

PAN, T., LI, X., XIE, W., JANKOVIC, J. & LE, W. 2005. Valproic acid-mediated Hsp70 induction and anti-apoptotic neuroprotection in SH-SY5Y cells. *FEBS Lett,* 579**,** 6716-20.

PAREDES, U. M., BUBB, V. J., HADDLEY, K., MACHO, G. A. & QUINN, J. P. 2012. Intronic tandem repeat in the serotonin transporter gene in Old World monkeys: a new transcriptional regulator? *J Mol Neurosci,* 47**,** 401-7.

PAREDES, U. M., QUINN, J. P. & D'SOUZA, U. M. 2013. Allele-specific transcriptional activity of the variable number of tandem repeats in 5' region of the DRD4 gene is stimulus specific in human neuronal cells. *Genes Brain Behav,* 12**,** 282-7.

PARK, S. P. & KWON, S. H. 2008. Cognitive effects of antiepileptic drugs. *J Clin Neurol,* 4**,** 99-106.

PATEL, P. D., BOCHAR, D. A., TURNER, D. L., MENG, F., MUELLER, H. M. & PONTRELLO, C. G. 2007. Regulation of tryptophan hydroxylase-2 gene expression by a bipartite RE-1 silencer of transcription/neuron restrictive silencing factor (REST/NRSF) binding motif. *J Biol Chem,* 282**,** 26717-24.

PATTERSON, H. D. & THOMPSON, R. 1971. Recovery of inter-block information when block sizes are unequal. . *Biometrika* 58**,** 545-554.

PENCEA, V., BINGAMAN, K. D., WIEGAND, S. J. & LUSKIN, M. B. 2001. Infusion of brain-derived neurotrophic factor into the lateral ventricle of the adult rat leads to new neurons in the parenchyma of the striatum, septum, thalamus, and hypothalamus. *J Neurosci,* 21**,** 6706-17.

PEREZ-COSTAS, E., MELENDEZ-FERRO, M. & ROBERTS, R. C. 2010. Basal ganglia pathology in schizophrenia: dopamine connections and anomalies. *J Neurochem,* 113**,** 287-302.

PFAFFL, M. W. 2001. A new mathematical model for relative quantification in real-time RT-PCR. *Nucleic Acids Res,* 29**,** e45.

PHELPS, E. A., DELGADO, M. R., NEARING, K. I. & LEDOUX, J. E. 2004. Extinction learning in humans: role of the amygdala and vmPFC. *Neuron,* 43**,** 897-905.

PHIEL, C. J., ZHANG, F., HUANG, E. Y., GUENTHER, M. G., LAZAR, M. A. & KLEIN, P. S. 2001. Histone deacetylase is a direct target of valproic acid, a potent anticonvulsant, mood stabilizer, and teratogen. *J Biol Chem,* 276**,** 36734-41.

PHILLIPS, O. R., NUECHTERLEIN, K. H., ASARNOW, R. F., CLARK, K. A., CABEEN, R., YANG, Y., WOODS, R. P., TOGA, A. W. & NARR, K. L. 2011. Mapping corticocortical structural integrity in schizophrenia and effects of genetic liability. *Biol Psychiatry,* 70**,** 680-9.

PICHARDO-CASAS, I., GOFF, L. A., SWERDEL, M. R., ATHIE, A., DAVILA, J., RAMOS-BROSSIER, M., LAPID-VOLOSIN, M., FRIEDMAN, W. J., HART, R. P. & VACA, L. 2012. Expression profiling of synaptic microRNAs from the adult rat brain identifies regional differences and seizure-induced dynamic modulation. *Brain Res,* 1436**,** 20-33.

PIHLGREN, E. & BOUTROS, N. 2007. Psychostimulant-Induced Chronic Schizophrenia-Like Disorder. *Clinical Schizophrenia & Related Psychoses,* 1**,** 54-63.

PIRIYAPONGSA, J., MARINO-RAMIREZ, L. & JORDAN, I. K. 2007. Origin and evolution of human microRNAs from transposable elements. *Genetics,* 176**,** 1323-37.

POWELL, T. R., SCHALKWYK, L. C., HEFFERNAN, A. L., BREEN, G., LAWRENCE, T., PRICE, T., FARMER, A. E., AITCHISON, K. J., CRAIG, I. W., DANESE, A., LEWIS, C., MCGUFFIN, P., UHER, R., TANSEY, K. E. & D'SOUZA, U. M. 2013. Tumor Necrosis Factor and its targets in the inflammatory cytokine pathway are identified as putative transcriptomic biomarkers for escitalopram response. *Eur Neuropsychopharmacol,* 23**,** 1105-14.

PRATA, D. P., MECHELLI, A., PICCHIONI, M. M., FU, C. H., TOULOPOULOU, T., BRAMON, E., WALSHE, M., MURRAY, R. M., COLLIER, D. A. & MCGUIRE, P. 2009. Altered effect of dopamine transporter 3'UTR VNTR genotype on prefrontal and striatal function in schizophrenia. *Arch Gen Psychiatry,* 66**,** 1162-72.

PREITNER, N., DAMIOLA, F., LOPEZ-MOLINA, L., ZAKANY, J., DUBOULE, D., ALBRECHT, U. & SCHIBLER, U. 2002. The orphan nuclear receptor REV-ERBalpha controls circadian transcription within the positive limb of the mammalian circadian oscillator. *Cell,* 110**,** 251-60.

PRUUNSILD, P., KAZANTSEVA, A., AID, T., PALM, K. & TIMMUSK, T. 2007. Dissecting the human BDNF locus: bidirectional transcription, complex splicing, and multiple promoters. *Genomics,* 90**,** 397-406.

PRUUNSILD, P., SEPP, M., ORAV, E., KOPPEL, I. & TIMMUSK, T. 2011. Identification of cis-elements and transcription factors regulating neuronal activity-dependent transcription of human BDNF gene. *J Neurosci,* 31**,** 3295-308.

QUINN, J. P. 1991. Variation in the composition of the AP1 complex in PC12 cells following induction by NGF and TPA. *Mol Cell Neurosci,* 2**,** 253-8.

QUINN, J. P., BUBB, V. J., MARSHALL-JONES, Z. V. & COULSON, J. M. 2002. Neuron restrictive silencer factor as a modulator of neuropeptide gene expression. *Regulatory Peptides,* 108**,** 135-141.

QUINN, J. P., FARINA, A. R., GARDNER, K., KRUTZSCH, H. & LEVENS, D. 1989a. Multiple components are required for sequence recognition of the AP1 site in the gibbon ape leukemia virus enhancer. *Mol Cell Biol,* 9**,** 4713-21.

QUINN, J. P., TAKIMOTO, M., IADAROLA, M., HOLBROOK, N. & LEVENS, D. 1989b. Distinct factors bind the AP-1 consensus sites in gibbon ape leukemia virus and simian virus 40 enhancers. *J Virol,* 63**,** 1737-42.

QUINN, J. P., WARBURTON, A., MYERS, P., SAVAGE, A. L. & BUBB, V. J. 2013. Polymorphic variation as a driver of differential neuropeptide gene expression. *Neuropeptides,* 47**,** 395-400.

QURESHI, I. A. & MEHLER, M. F. 2010. Epigenetic mechanisms underlying human epileptic disorders and the process of epileptogenesis. *Neurobiol Dis,* 39**,** 53-60.

RADULESCU, A. R. & MUJICA-PARODI, L. R. 2009. A principal component network analysis of prefrontal-limbic functional magnetic resonance imaging time series in schizophrenia patients and healthy controls. *Psychiatry Res,* 174**,** 184-94.

RAMASAMY, R. & DE FREITAS, D. M. 1989. Competition between Li+ and Mg2+ for ATP in human erythrocytes. A 31P NMR and optical spectroscopy study. *FEBS Lett,* 244**,** 223-6.

RANGEL, Y. M., KARIKO, K., HARRIS, V. A., DUVALL, M. E. & WELSH, F. A. 2001. Dose-dependent induction of mRNAs encoding brain-derived neurotrophic factor and heat-shock protein-72 after cortical spreading depression in the rat. *Brain Res Mol Brain Res,* 88**,** 103-12.

RAO, J. S., KELESHIAN, V. L., KLEIN, S. & RAPOPORT, S. I. 2012. Epigenetic modifications in frontal cortex from Alzheimer's disease and bipolar disorder patients. *Transl Psychiatry,* 2**,** e132.

RAVACHE, M., WEBER, C., MERIENNE, K. & TROTTIER, Y. 2010. Transcriptional activation of REST by Sp1 in Huntington's disease models. *PLoS One,* 5**,** e14311.

RAY, M. T., SHANNON WEICKERT, C. & WEBSTER, M. J. 2014. Decreased BDNF and TrkB mRNA expression in multiple cortical areas of patients with schizophrenia and mood disorders. *Transl Psychiatry,* 4**,** e389.

REDDY, B. Y., GRECO, S. J., PATEL, P. S., TRZASKA, K. A. & RAMESHWAR, P. 2009. RE-1-silencing transcription factor shows tumor-suppressor functions and negatively regulates the oncogenic TAC1 in breast cancer cells. *Proc Natl Acad Sci U S A,* 106**,** 4408-13.

REICHARDT, L. F. 2006. Neurotrophin-regulated signalling pathways. *Philos Trans R Soc Lond B Biol Sci,* 361**,** 1545-64.

RHIE, S. K., COETZEE, S. G., NOUSHMEHR, H., YAN, C., KIM, J. M., HAIMAN, C. A. & COETZEE, G. A. 2013. Comprehensive functional annotation of seventy-one breast cancer risk Loci. *PLoS One,* 8**,** e63925.

RICHARDSON, M. P., STRANGE, B. A. & DOLAN, R. J. 2004. Encoding of emotional memories depends on amygdala and hippocampus and their interactions. *Nat Neurosci,* 7**,** 278-85.

RIFFO-CAMPOS, A. L., CASTILLO, J., TUR, G., GONZALEZ-FIGUEROA, P., GEORGIEVA, E. I., RODRIGUEZ, J. L., LOPEZ-RODAS, G., RODRIGO, M. I. & FRANCO, L. 2015. Nucleosome-specific, Time-dependent Changes in Histone Modifications during Activation of the Early Growth Response 1 (Egr1) Gene. *J Biol Chem,* 290**,** 197-208.

RIPKE, S., O'DUSHLAINE, C., CHAMBERT, K., MORAN, J. L., KAHLER, A. K., AKTERIN, S., BERGEN, S. E., COLLINS, A. L., CROWLEY, J. J., FROMER, M., KIM, Y., LEE, S. H., MAGNUSSON, P. K., SANCHEZ, N., STAHL, E. A., WILLIAMS, S., WRAY, N. R., XIA, K., BETTELLA, F., BORGLUM, A. D., BULIK-SULLIVAN, B. K., CORMICAN, P., CRADDOCK, N., DE LEEUW, C., DURMISHI, N., GILL, M., GOLIMBET, V., HAMSHERE, M. L., HOLMANS, P., HOUGAARD, D. M., KENDLER, K. S., LIN, K., MORRIS, D. W., MORS, O., MORTENSEN, P. B., NEALE, B. M., O'NEILL, F. A., OWEN, M. J., MILOVANCEVIC, M. P., POSTHUMA, D., POWELL, J., RICHARDS, A. L., RILEY, B. P., RUDERFER, D., RUJESCU, D., SIGURDSSON, E., SILAGADZE, T., SMIT, A. B., STEFANSSON, H., STEINBERG, S., SUVISAARI, J., TOSATO, S., VERHAGE, M., WALTERS, J. T., LEVINSON, D. F., GEJMAN, P. V., LAURENT, C., MOWRY, B. J., O'DONOVAN, M. C., PULVER, A. E., SCHWAB, S. G., WILDENAUER, D. B., DUDBRIDGE, F., SHI, J., ALBUS, M., ALEXANDER, M., CAMPION, D., COHEN, D., DIKEOS, D., DUAN, J., EICHHAMMER, P., GODARD, S., HANSEN, M., LERER, F. B., LIANG, K. Y., MAIER, W., MALLET, J., NERTNEY, D. A., NESTADT, G., NORTON, N., PAPADIMITRIOU, G. N., RIBBLE, R., SANDERS, A. R., SILVERMAN, J. M., WALSH, D., WILLIAMS, N. M., WORMLEY, B., ARRANZ, M. J., BAKKER, S., BENDER, S., BRAMON, E., COLLIER, D., CRESPO-FACORRO, B., HALL, J., IYEGBE, C., JABLENSKY, A., KAHN, R. S., KALAYDJIEVA, L., LAWRIE, S., LEWIS, C. M., et al. 2013. Genome-wide association analysis identifies 13 new risk loci for schizophrenia. *Nat Genet,* 45**,** 1150-9.

RITSNER, M., MAAYAN, R., GIBEL, A., STROUS, R. D., MODAI, I. & WEIZMAN, A. 2004. Elevation of the cortisol/dehydroepiandrosterone ratio in schizophrenia patients. *Eur Neuropsychopharmacol,* 14**,** 267-73.

RITZ, M. C., LAMB, R. J., GOLDBERG, S. R. & KUHAR, M. J. 1987. Cocaine receptors on dopamine transporters are related to self-administration of cocaine. *Science,* 237**,** 1219-23.

ROBERTS, J., SCOTT, A. C., HOWARD, M. R., BREEN, G., BUBB, V. J., KLENOVA, E. & QUINN, J. P. 2007. Differential regulation of the serotonin transporter gene by lithium is mediated by transcription factors, CCCTC binding protein and Y-box binding protein 1, through the polymorphic intron 2 variable number tandem repeat. *J Neurosci,* 27**,** 2793-801.

RODRIGUEZ, A., GRIFFITHS-JONES, S., ASHURST, J. L. & BRADLEY, A. 2004. Identification of mammalian microRNA host genes and transcription units. *Genome Res,* 14**,** 1902-10.

RODRIGUEZ, S., GAUNT, T. R. & DAY, I. N. 2009. Hardy-Weinberg equilibrium testing of biological ascertainment for Mendelian randomization studies. *Am J Epidemiol,* 169**,** 505-14.

RONAN, J. L., WU, W. & CRABTREE, G. R. 2013. From neural development to cognition: unexpected roles for chromatin. *Nat Rev Genet,* 14**,** 347-59.

RONCHETTI, D., LIONETTI, M., MOSCA, L., AGNELLI, L., ANDRONACHE, A., FABRIS, S., DELILIERS, G. L. & NERI, A. 2008. An integrative genomic approach reveals coordinated expression of intronic miR-335, miR-342, and miR-561 with deregulated host genes in multiple myeloma. *BMC Med Genomics,* 1**,** 37.

ROOPRA, A., HUANG, Y. & DINGLEDINE, R. 2001. Neurological disease: listening to gene silencers. *Mol Interv,* 1**,** 219-28.

ROOPRA, A., QAZI, R., SCHOENIKE, B., DALEY, T. J. & MORRISON, J. F. 2004. Localized domains of G9a-mediated histone methylation are required for silencing of neuronal genes. *Mol Cell,* 14**,** 727-38.

ROSENBERG, G. 2007. The mechanisms of action of valproate in neuropsychiatric disorders: can we see the forest for the trees? *Cell Mol Life Sci,* 64**,** 2090-103.

ROSENBLOOM, K. R., SLOAN, C. A., MALLADI, V. S., DRESZER, T. R., LEARNED, K., KIRKUP, V. M., WONG, M. C., MADDREN, M., FANG, R., HEITNER, S. G., LEE, B. T., BARBER, G. P., HARTE, R. A., DIEKHANS, M., LONG, J. C., WILDER, S. P., ZWEIG, A. S., KAROLCHIK, D., KUHN, R. M., HAUSSLER, D. & KENT, W. J. 2013. ENCODE data in the UCSC Genome Browser: year 5 update. *Nucleic Acids Res,* 41**,** D56-63.

ROSENFELD, J. A., LEPPIG, K., BALLIF, B. C., THIESE, H., ERDIE-LALENA, C., BAWLE, E., SASTRY, S., SPENCE, J. E., BANDHOLZ, A., SURTI, U., ZONANA, J., KELLER, K., MESCHINO, W., BEJJANI, B. A., TORCHIA, B. S. & SHAFFER, L. G. 2009. Genotype-phenotype analysis of TCF4 mutations causing Pitt-Hopkins syndrome shows increased seizure activity with missense mutations. *Genet Med,* 11**,** 797-805.

ROSENKRANZ, J. A., MOORE, H. & GRACE, A. A. 2003. The Prefrontal Cortex Regulates Lateral Amygdala Neuronal Plasticity and Responses to Previously Conditioned Stimuli. *The Journal of Neuroscience,* 23**,** 11054-11064.

ROSSI, M., KILPINEN, H., MUONA, M., SURAKKA, I., INGLE, C., LAHTINEN, J., HENNAH, W., RIPATTI, S. & HOVATTA, I. 2014. Allele-specific regulation of DISC1 expression by miR-135b-5p. *Eur J Hum Genet,* 22**,** 840-3.

ROUAUX, C., PANTELEEVA, I., RENE, F., GONZALEZ DE AGUILAR, J. L., ECHANIZ-LAGUNA, A., DUPUIS, L., MENGER, Y., BOUTILLIER, A. L. & LOEFFLER, J. P. 2007. Sodium valproate exerts neuroprotective effects in vivo through CREB-binding protein-dependent mechanisms but does not improve survival in an amyotrophic lateral sclerosis mouse model. *J Neurosci,* 27**,** 5535-45.

ROY, R., DE SARKAR, N., GHOSE, S., PAUL, R. R., PAL, M., BHATTACHARYA, C., CHOWDHURY, S. K., GHOSH, S. & ROY, B. 2014a. Genetic variations at microRNA and processing genes and risk of oral cancer. *Tumour Biol,* 35**,** 3409-14.

ROY, R., DE SARKAR, N., GHOSE, S., PAUL, R. R., RAY, A., MUKHOPADHYAY, I. & ROY, B. 2014b. Association between risk of oral precancer and genetic variations in microRNA and related processing genes. *J Biomed Sci,* 21**,** 48.

RUJESCU, D., INGASON, A., CICHON, S., PIETILAINEN, O. P., BARNES, M. R., TOULOPOULOU, T., PICCHIONI, M., VASSOS, E., ETTINGER, U., BRAMON, E., MURRAY, R., RUGGERI, M., TOSATO, S., BONETTO, C., STEINBERG, S., SIGURDSSON, E., SIGMUNDSSON, T., PETURSSON, H., GYLFASON, A., OLASON, P. I., HARDARSSON, G., JONSDOTTIR, G. A., GUSTAFSSON, O., FOSSDAL, R., GIEGLING, I., MOLLER, H. J., HARTMANN, A. M., HOFFMANN, P., CROMBIE, C., FRASER, G., WALKER, N., LONNQVIST, J., SUVISAARI, J., TUULIO-HENRIKSSON, A., DJUROVIC, S., MELLE, I., ANDREASSEN, O. A., HANSEN, T., WERGE, T., KIEMENEY, L. A., FRANKE, B., VELTMAN, J., BUIZER-VOSKAMP, J. E., SABATTI, C., OPHOFF, R. A., RIETSCHEL, M., NOTHEN, M. M., STEFANSSON, K., PELTONEN, L., ST CLAIR, D., STEFANSSON, H. & COLLIER, D. A. 2009. Disruption of the neurexin 1 gene is associated with schizophrenia. *Hum Mol Genet,* 18**,** 988-96.

SACCO, K. A., BANNON, K. L. & GEORGE, T. P. 2004. Nicotinic receptor mechanisms and cognition in normal states and neuropsychiatric disorders. *J Psychopharmacol,* 18**,** 457-74.

SADRI-VAKILI, G., KUMARESAN, V., SCHMIDT, H. D., FAMOUS, K. R., CHAWLA, P., VASSOLER, F. M., OVERLAND, R. P., XIA, E., BASS, C. E., TERWILLIGER, E. F., PIERCE, R. C. & CHA, J. H. 2010. Cocaine-induced chromatin remodeling increases brain-derived neurotrophic factor transcription in the rat medial prefrontal cortex, which alters the reinforcing efficacy of cocaine. *J Neurosci,* 30**,** 11735-44.

SAHA, A., WITTMEYER, J. & CAIRNS, B. R. 2006. Chromatin remodelling: the industrial revolution of DNA around histones. *Nat Rev Mol Cell Biol,* 7**,** 437-47.

SANCHEZ, C., OSKOWITZ, A. & POCHAMPALLY, R. R. 2009. Epigenetic reprogramming of IGF1 and leptin genes by serum deprivation in multipotential mesenchymal stromal cells. *Stem Cells,* 27**,** 375-82.

SANPHUI, P. & BISWAS, S. C. 2013. FoxO3a is activated and executes neuron death via Bim in response to beta-amyloid. *Cell Death Dis,* 4**,** e625.

SATOH, J., KAWANA, N. & YAMAMOTO, Y. 2013. ChIP-Seq Data Mining: Remarkable Differences in NRSF/REST Target Genes between Human ESC and ESC-Derived Neurons. *Bioinform Biol Insights,* 7**,** 357-68.

SAVAGE, A. L., BUBB, V. J., BREEN, G. & QUINN, J. P. 2013. Characterisation of the potential function of SVA retrotransposons to modulate gene expression patterns. *BMC Evol Biol,* 13**,** 101.

SAVAGE, A. L., WILM, T. P., KHURSHEED, K., SHATUNOV, A., MORRISON, K. E., SHAW, P. J., SHAW, C. E., SMITH, B., BREEN, G., AL-CHALABI, A., MOSS, D., BUBB, V. J. & QUINN, J. P. 2014. An evaluation of a SVA retrotransposon in the FUS promoter as a transcriptional regulator and its association to ALS. *PLoS One,* 9**,** e90833.

SCHARFMAN, H., GOODMAN, J., MACLEOD, A., PHANI, S., ANTONELLI, C. & CROLL, S. 2005. Increased neurogenesis and the ectopic granule cells after intrahippocampal BDNF infusion in adult rats. *Exp Neurol,* 192**,** 348-56.

SCHEUCH, K., HOLTJE, M., BUDDE, H., LAUTENSCHLAGER, M., HEINZ, A., AHNERT-HILGER, G. & PRILLER, J. 2010. Lithium modulates tryptophan hydroxylase 2 gene expression and serotonin release in primary cultures of serotonergic raphe neurons. *Brain Res,* 1307**,** 14-21.

SCHILSTROM, B., YAKA, R., ARGILLI, E., SUVARNA, N., SCHUMANN, J., CHEN, B. T., CARMAN, M., SINGH, V., MAILLIARD, W. S., RON, D. & BONCI, A. 2006. Cocaine enhances NMDA receptor-mediated currents in ventral tegmental area cells via dopamine D5 receptor-dependent redistribution of NMDA receptors. *J Neurosci,* 26**,** 8549-58.

SCHOENHERR, C. J. & ANDERSON, D. J. 1995. The neuron-restrictive silencer factor (NRSF): a coordinate repressor of multiple neuron-specific genes. *Science,* 267**,** 1360-3.

SEARLE, S. R. 1989. Variance components - some history and a summary account of estimation methods. *Journal of Animal Breeding and Genetics,* 106**,** 1-29.

SEBAT, J., LEVY, D. L. & MCCARTHY, S. E. 2009. Rare structural variants in schizophrenia: one disorder, multiple mutations; one mutation, multiple disorders. *Trends Genet,* 25**,** 528-35.

SERPER, M. R., CHOU, J. C., ALLEN, M. H., CZOBOR, P. & CANCRO, R. 1999. Symptomatic overlap of cocaine intoxication and acute schizophrenia at emergency presentation. *Schizophr Bull,* 25**,** 387-94.

SETH, K. A. & MAJZOUB, J. A. 2001. Repressor element silencing transcription factor/neuron-restrictive silencing factor (REST/NRSF) can act as an enhancer as well as a repressor of corticotropin-releasing hormone gene transcription. *J Biol Chem,* 276**,** 13917-23.

SHALTIEL, G., SHAMIR, A., SHAPIRO, J., DING, D., DALTON, E., BIALER, M., HARWOOD, A. J., BELMAKER, R. H., GREENBERG, M. L. & AGAM, G. 2004. Valproate decreases inositol biosynthesis. *Biol Psychiatry,* 56**,** 868-74.

SHAM, P. C. & CURTIS, D. 1995. Monte Carlo tests for associations between disease and alleles at highly polymorphic loci. *Ann Hum Genet,* 59**,** 97-105.

SHEN, X., LIU, Y., HSU, Y. J., FUJIWARA, Y., KIM, J., MAO, X., YUAN, G. C. & ORKIN, S. H. 2008. EZH1 mediates methylation on histone H3 lysine 27 and complements EZH2 in maintaining stem cell identity and executing pluripotency. *Mol Cell,* 32**,** 491-502.

SHER, F., ROSSLER, R., BROUWER, N., BALASUBRAMANIYAN, V., BODDEKE, E. & COPRAY, S. 2008. Differentiation of neural stem cells into oligodendrocytes: involvement of the polycomb group protein Ezh2. *Stem Cells,* 26**,** 2875-83.

SHI, J., LEVINSON, D. F., DUAN, J., SANDERS, A. R., ZHENG, Y., PE'ER, I., DUDBRIDGE, F., HOLMANS, P. A., WHITTEMORE, A. S., MOWRY, B. J., OLINCY, A., AMIN, F., CLONINGER, C. R., SILVERMAN, J. M., BUCCOLA, N. G., BYERLEY, W. F., BLACK, D. W., CROWE, R. R., OKSENBERG, J. R., MIREL, D. B., KENDLER, K. S., FREEDMAN, R. & GEJMAN, P. V. 2009. Common variants on chromosome 6p22.1 are associated with schizophrenia. *Nature,* 460**,** 753-7.

SHI, X. Y., WANG, J. W., CUI, H., LI, B. M., LEI, G. F. & SUN, R. P. 2010. Effects of antiepileptic drugs on mRNA levels of BDNF and NT-3 and cell neogenesis in the developing rat brain. *Brain Dev,* 32**,** 229-35.

SHIMOJO, M. & HERSH, L. B. 2006. Characterization of the REST/NRSF-interacting LIM domain protein (RILP): localization and interaction with REST/NRSF. *J Neurochem,* 96**,** 1130-8.

SHIMOJO, M., PAQUETTE, A. J., ANDERSON, D. J. & HERSH, L. B. 1999. Protein kinase A regulates cholinergic gene expression in PC12 cells: REST4 silences the silencing activity of neuron-restrictive silencer factor/REST. *Mol Cell Biol,* 19**,** 6788-95.

SHYU, K. G., WANG, B. W., YANG, Y. H., TSAI, S. C., LIN, S. & LEE, C. C. 2004. Amphetamine activates connexin43 gene expression in cultured neonatal rat cardiomyocytes through JNK and AP-1 pathway. *Cardiovasc Res,* 63**,** 98-108.

SIGMUNDSSON, T., SUCKLING, J., MAIER, M., WILLIAMS, S., BULLMORE, E., GREENWOOD, K., FUKUDA, R., RON, M. & TOONE, B. 2001. Structural abnormalities in frontal, temporal, and limbic regions and interconnecting white matter tracts in schizophrenic patients with prominent negative symptoms. *Am J Psychiatry,* 158**,** 234-43.

SILBER, J., LIM, D. A., PETRITSCH, C., PERSSON, A. I., MAUNAKEA, A. K., YU, M., VANDENBERG, S. R., GINZINGER, D. G., JAMES, C. D., COSTELLO, J. F., BERGERS, G., WEISS, W. A., ALVAREZ-BUYLLA, A. & HODGSON, J. G. 2008. miR-124 and miR-137 inhibit proliferation of glioblastoma multiforme cells and induce differentiation of brain tumor stem cells. *BMC Med,* 6**,** 14.

SMITH, R. C., SINGH, A., INFANTE, M., KHANDAT, A. & KLOOS, A. 2002. Effects of cigarette smoking and nicotine nasal spray on psychiatric symptoms and cognition in schizophrenia. *Neuropsychopharmacology,* 27**,** 479-97.

SMRT, R. D., SZULWACH, K. E., PFEIFFER, R. L., LI, X., GUO, W., PATHANIA, M., TENG, Z. Q., LUO, Y., PENG, J., BORDEY, A., JIN, P. & ZHAO, X. 2010. MicroRNA miR-137 regulates neuronal maturation by targeting ubiquitin ligase mind bomb-1. *Stem Cells,* 28**,** 1060-70.

SOLDATI, C., BITHELL, A., JOHNSTON, C., WONG, K. Y., STANTON, L. W. & BUCKLEY, N. J. 2013. Dysregulation of REST-regulated coding and non-coding RNAs in a cellular model of Huntington's disease. *J Neurochem,* 124**,** 418-30.

SONG, Y. J., TIAN, X. B., ZHANG, S., ZHANG, Y. X., LI, X., LI, D., CHENG, Y., ZHANG, J. N., KANG, C. S. & ZHAO, W. 2011. Temporal lobe epilepsy induces differential expression of hippocampal miRNAs including let-7e and miR-23a/b. *Brain Res,* 1387**,** 134-40.

SOTNIKOV, S. V., MARKT, P. O., MALIK, V., CHEKMAREVA, N. Y., NAIK, R. R., SAH, A., SINGEWALD, N., HOLSBOER, F., CZIBERE, L. & LANDGRAF, R. 2014. Bidirectional rescue of extreme genetic predispositions to anxiety: impact of CRH receptor 1 as epigenetic plasticity gene in the amygdala. *Transl Psychiatry,* 4**,** e359.

SOTRES-BAYON, F., BUSH, D. E. & LEDOUX, J. E. 2004. Emotional perseveration: an update on prefrontal-amygdala interactions in fear extinction. *Learn Mem,* 11**,** 525-35.

SPENCER, E. M., CHANDLER, K. E., HADDLEY, K., HOWARD, M. R., HUGHES, D., BELYAEV, N. D., COULSON, J. M., STEWART, J. P., BUCKLEY, N. J., KIPAR, A., WALKER, M. C. & QUINN, J. P. 2006. Regulation and role of REST and REST4 variants in modulation of gene expression in in vivo and in vitro in epilepsy models. *Neurobiol Dis,* 24**,** 41-52.

SPIJKER, A. T. & VAN ROSSUM, E. F. 2012. Glucocorticoid sensitivity in mood disorders. *Neuroendocrinology,* 95**,** 179-86.

SPLAWSKI, I., TIMOTHY, K. W., SHARPE, L. M., DECHER, N., KUMAR, P., BLOISE, R., NAPOLITANO, C., SCHWARTZ, P. J., JOSEPH, R. M., CONDOURIS, K., TAGER-FLUSBERG, H., PRIORI, S. G., SANGUINETTI, M. C. &

KEATING, M. T. 2004. Ca(V)1.2 calcium channel dysfunction causes a multisystem disorder including arrhythmia and autism. *Cell,* 119**,** 19-31.
SPRONK, D. B., VAN WEL, J. H., RAMAEKERS, J. G. & VERKES, R. J. 2013. Characterizing the cognitive effects of cocaine: a comprehensive review. *Neurosci Biobehav Rev,* 37**,** 1838-59.
SQUIRE, L. R. & ZOLA-MORGAN, S. 1991. The medial temporal lobe memory system. *Science,* 253**,** 1380-6.
STADLER, M. B., MURR, R., BURGER, L., IVANEK, R., LIENERT, F., SCHOLER, A., VAN NIMWEGEN, E., WIRBELAUER, C., OAKELEY, E. J., GAIDATZIS, D., TIWARI, V. K. & SCHUBELER, D. 2011. DNA-binding factors shape the mouse methylome at distal regulatory regions. *Nature,* 480**,** 490-5.
STAPELS, M., PIPER, C., YANG, T., LI, M., STOWELL, C., XIONG, Z. G., SAUGSTAD, J., SIMON, R. P., GEROMANOS, S., LANGRIDGE, J., LAN, J. Q. & ZHOU, A. 2010. Polycomb group proteins as epigenetic mediators of neuroprotection in ischemic tolerance. *Sci Signal,* 3**,** ra15.
STEFANSSON, H., OPHOFF, R. A., STEINBERG, S., ANDREASSEN, O. A., CICHON, S., RUJESCU, D., WERGE, T., PIETILAINEN, O. P., MORS, O., MORTENSEN, P. B., SIGURDSSON, E., GUSTAFSSON, O., NYEGAARD, M., TUULIO-HENRIKSSON, A., INGASON, A., HANSEN, T., SUVISAARI, J., LONNQVIST, J., PAUNIO, T., BORGLUM, A. D., HARTMANN, A., FINK-JENSEN, A., NORDENTOFT, M., HOUGAARD, D., NORGAARD-PEDERSEN, B., BOTTCHER, Y., OLESEN, J., BREUER, R., MOLLER, H. J., GIEGLING, I., RASMUSSEN, H. B., TIMM, S., MATTHEISEN, M., BITTER, I., RETHELYI, J. M., MAGNUSDOTTIR, B. B., SIGMUNDSSON, T., OLASON, P., MASSON, G., GULCHER, J. R., HARALDSSON, M., FOSSDAL, R., THORGEIRSSON, T. E., THORSTEINSDOTTIR, U., RUGGERI, M., TOSATO, S., FRANKE, B., STRENGMAN, E., KIEMENEY, L. A., MELLE, I., DJUROVIC, S., ABRAMOVA, L., KALEDA, V., SANJUAN, J., DE FRUTOS, R., BRAMON, E., VASSOS, E., FRASER, G., ETTINGER, U., PICCHIONI, M., WALKER, N., TOULOPOULOU, T., NEED, A. C., GE, D., YOON, J. L., SHIANNA, K. V., FREIMER, N. B., CANTOR, R. M., MURRAY, R., KONG, A., GOLIMBET, V., CARRACEDO, A., ARANGO, C., COSTAS, J., JONSSON, E. G., TERENIUS, L., AGARTZ, I., PETURSSON, H., NOTHEN, M. M., RIETSCHEL, M., MATTHEWS, P. M., MUGLIA, P., PELTONEN, L., ST CLAIR, D., GOLDSTEIN, D. B., STEFANSSON, K. & COLLIER, D. A. 2009. Common variants conferring risk of schizophrenia. *Nature,* 460**,** 744-7.
STEFANSSON, H., RUJESCU, D., CICHON, S., PIETILAINEN, O. P., INGASON, A., STEINBERG, S., FOSSDAL, R., SIGURDSSON, E., SIGMUNDSSON, T., BUIZER-VOSKAMP, J. E., HANSEN, T., JAKOBSEN, K. D., MUGLIA, P., FRANCKS, C., MATTHEWS, P. M., GYLFASON, A., HALLDORSSON, B. V., GUDBJARTSSON, D., THORGEIRSSON, T. E., SIGURDSSON, A., JONASDOTTIR, A., BJORNSSON, A., MATTIASDOTTIR, S., BLONDAL, T., HARALDSSON, M., MAGNUSDOTTIR, B. B., GIEGLING, I., MOLLER, H. J., HARTMANN, A., SHIANNA, K. V., GE, D., NEED, A. C., CROMBIE, C., FRASER, G., WALKER, N., LONNQVIST, J., SUVISAARI, J., TUULIO-HENRIKSSON, A., PAUNIO, T., TOULOPOULOU, T., BRAMON, E., DI FORTI, M., MURRAY, R., RUGGERI, M., VASSOS, E., TOSATO, S., WALSHE, M., LI, T., VASILESCU, C., MUHLEISEN, T. W., WANG, A. G., ULLUM, H., DJUROVIC, S., MELLE, I., OLESEN, J., KIEMENEY, L. A., FRANKE, B., SABATTI, C., FREIMER, N. B., GULCHER, J. R., THORSTEINSDOTTIR, U., KONG, A., ANDREASSEN, O. A., OPHOFF, R. A., GEORGI, A., RIETSCHEL, M., WERGE, T., PETURSSON, H., GOLDSTEIN, D. B., NOTHEN, M. M., PELTONEN, L., COLLIER, D. A., ST CLAIR, D. & STEFANSSON, K. 2008. Large recurrent microdeletions associated with schizophrenia. *Nature,* 455**,** 232-6.
STRANGER, B. E., MONTGOMERY, S. B., DIMAS, A. S., PARTS, L., STEGLE, O., INGLE, C. E., SEKOWSKA, M., SMITH, G. D., EVANS, D., GUTIERREZ-ARCELUS, M., PRICE, A., RAJ, T., NISBETT, J., NICA, A. C., BEAZLEY, C., DURBIN, R., DELOUKAS, P. & DERMITZAKIS, E. T. 2012. Patterns of cis regulatory variation in diverse human populations. *PLoS Genet,* 8**,** e1002639.
STRAZISAR, M., CAMMAERTS, S., VAN DER VEN, K., FORERO, D. A., LENAERTS, A. S., NORDIN, A., ALMEIDA-SOUZA, L., GENOVESE, G., TIMMERMAN, V., LIEKENS, A., DE RIJK, P., ADOLFSSON, R., CALLAERTS, P. & DEL-FAVERO, J. 2014. MIR137 variants identified in psychiatric patients affect synaptogenesis and neuronal transmission gene sets. *Mol Psychiatry*.
STRUBE, W., BUNSE, T., NITSCHE, M. A., WOBROCK, T., ABOROWA, R., MISEWITSCH, K., HERRMANN, M., FALKAI, P. & HASAN, A. 2014. Smoking Restores Impaired LTD-Like Plasticity in Schizophrenia: a Transcranial Direct Current Stimulation Study. *Neuropsychopharmacology*.
SUGDEN, K., PARIANTE, C. M., MCGUFFIN, P., AITCHISON, K. J. & D'SOUZA, U. M. 2010. Housekeeping gene expression is affected by antidepressant treatment in a mouse fibroblast cell line. *J Psychopharmacol,* 24**,** 1253-9.
SUZUKI, H., TAKATSUKA, S., AKASHI, H., YAMAMOTO, E., NOJIMA, M., MARUYAMA, R., KAI, M., YAMANO, H. O., SASAKI, Y., TOKINO, T., SHINOMURA, Y., IMAI, K. & TOYOTA, M. 2011. Genome-wide profiling of chromatin signatures reveals epigenetic regulation of MicroRNA genes in colorectal cancer. *Cancer Res,* 71**,** 5646-58.
SVOBODA, M., IZAKOVICOVA HOLLA, L., SEFR, R., VRTKOVA, I., KOCAKOVA, I., TICHY, B. & DVORAK, J. 2008. Micro-RNAs miR125b and miR137 are frequently upregulated in response to capecitabine chemoradiotherapy of rectal cancer. *Int J Oncol,* 33**,** 541-7.
SZULWACH, K. E., LI, X., SMRT, R. D., LI, Y., LUO, Y., LIN, L., SANTISTEVAN, N. J., LI, W., ZHAO, X. & JIN, P. 2010. Cross talk between microRNA and epigenetic regulation in adult neurogenesis. *J Cell Biol,* 189**,** 127-41.

TABUCHI, A., NAKATANI, C., NAKAOKA, R., NARUSE, Y., KOJIMA, T., MORI, N. & TSUDA, M. 1999. Silencer-mediated repression and non-mediated activation of BDNF and c-fos gene promoters in primary glial or neuronal cells. *Biochem Biophys Res Commun,* 261**,** 233-7.

TABUCHI, A., SAKAYA, H., KISUKEDA, T., FUSHIKI, H. & TSUDA, M. 2002a. Involvement of an upstream stimulatory factor as well as cAMP-responsive element-binding protein in the activation of brain-derived neurotrophic factor gene promoter I. *J Biol Chem,* 277**,** 35920-31.

TABUCHI, A., YAMADA, T., SASAGAWA, S., NARUSE, Y., MORI, N. & TSUDA, M. 2002b. REST4-mediated modulation of REST/NRSF-silencing function during BDNF gene promoter activation. *Biochem Biophys Res Commun,* 290**,** 415-20.

TAKIMOTO, M., QUINN, J. P., FARINA, A. R., STAUDT, L. M. & LEVENS, D. 1989. fos/jun and octamer-binding protein interact with a common site in a negative element of the human c-myc gene. *J Biol Chem,* 264**,** 8992-9.

TAPIA-RAMIREZ, J., EGGEN, B. J., PERAL-RUBIO, M. J., TOLEDO-ARAL, J. J. & MANDEL, G. 1997. A single zinc finger motif in the silencing factor REST represses the neural-specific type II sodium channel promoter. *Proc Natl Acad Sci U S A,* 94**,** 1177-82.

TATENO, M. & SAITO, T. 2008. Biological studies on alcohol-induced neuronal damage. *Psychiatry Investig,* 5**,** 21-7.

TAYLOR, J. & BAKER, G. A. 2010. Newly diagnosed epilepsy: cognitive outcome at 5 years. *Epilepsy Behav,* 18**,** 397-403.

TAYLOR, J., KOLAMUNNAGE-DONA, R., MARSON, A. G., SMITH, P. E., ALDENKAMP, A. P. & BAKER, G. A. 2010. Patients with epilepsy: cognitively compromised before the start of antiepileptic drug treatment? *Epilepsia,* 51**,** 48-56.

TELLEZ-ZENTENO, J. F., PATTEN, S. B., JETTE, N., WILLIAMS, J. & WIEBE, S. 2007. Psychiatric comorbidity in epilepsy: a population-based analysis. *Epilepsia,* 48**,** 2336-44.

THE ENCODE PROJECT CONSORTIUM, C. 2011. A user's guide to the encyclopedia of DNA elements (ENCODE). *PLoS Biol,* 9**,** e1001046.

THE INTERNATIONAL SCHIZOPHRENIA CONSORTIUM, C. 2008. Rare chromosomal deletions and duplications increase risk of schizophrenia. *Nature,* 455**,** 237-41.

THE INTERNATIONAL SCHIZOPHRENIA CONSORTIUM, C. 2009. Common polygenic variation contributes to risk of schizophrenia and bipolar disorder. *Nature,* 460**,** 748-52.

THE SCHIZOPHRENIA PSYCHIATRIC GWAS CONSORTIUM, C. 2011. Genome-wide association study identifies five new schizophrenia loci. *Nat Genet,* 43**,** 969-76.

THOMPSON, M., WEICKERT, C. S., WYATT, E. & WEBSTER, M. J. 2009. Decreased glutamic acid decarboxylase(67) mRNA expression in multiple brain areas of patients with schizophrenia and mood disorders. *J Psychiatr Res,* 43**,** 970-7.

THOMPSON RAY, M., WEICKERT, C. S., WYATT, E. & WEBSTER, M. J. 2011. Decreased BDNF, trkB-TK+ and GAD67 mRNA expression in the hippocampus of individuals with schizophrenia and mood disorders. *J Psychiatry Neurosci,* 36**,** 195-203.

TIAN, F., HU, X. Z., WU, X., JIANG, H., PAN, H., MARINI, A. M. & LIPSKY, R. H. 2009. Dynamic chromatin remodeling events in hippocampal neurons are associated with NMDA receptor-mediated activation of Bdnf gene promoter 1. *J Neurochem,* 109**,** 1375-88.

TIMMUSK, T., PALM, K., LENDAHL, U. & METSIS, M. 1999. Brain-derived neurotrophic factor expression in vivo is under the control of neuron-restrictive silencer element. *J Biol Chem,* 274**,** 1078-84.

TORAN-ALLERAND, C. D. 1996. The estrogen/neurotrophin connection during neural development: is co-localization of estrogen receptors with the neurotrophins and their receptors biologically relevant? *Dev Neurosci,* 18**,** 36-48.

TORREY, E. F., BARCI, B. M., WEBSTER, M. J., BARTKO, J. J., MEADOR-WOODRUFF, J. H. & KNABLE, M. B. 2005. Neurochemical markers for schizophrenia, bipolar disorder, and major depression in postmortem brains. *Biol Psychiatry,* 57**,** 252-60.

TRIQUENEAUX, G., THENOT, S., KAKIZAWA, T., ANTOCH, M. P., SAFI, R., TAKAHASHI, J. S., DELAUNAY, F. & LAUDET, V. 2004. The orphan receptor Rev-erbalpha gene is a target of the circadian clock pacemaker. *J Mol Endocrinol,* 33**,** 585-608.

TRITSCHLER, F., HUNTZINGER, E. & IZAURRALDE, E. 2010. Role of GW182 proteins and PABPC1 in the miRNA pathway: a sense of deja vu. *Nat Rev Mol Cell Biol,* 11**,** 379-84.

TSANKOVA, N. M., BERTON, O., RENTHAL, W., KUMAR, A., NEVE, R. L. & NESTLER, E. J. 2006. Sustained hippocampal chromatin regulation in a mouse model of depression and antidepressant action. *Nat Neurosci,* 9**,** 519-25.

TURNER, A. M. & MORRIS, K. V. 2010. Controlling transcription with noncoding RNAs in mammalian cells. *Biotechniques,* 48**,** ix-xvi.

TURNER, K. M. & BURNE, T. H. 2013. Interaction of genotype and environment: effect of strain and housing conditions on cognitive behavior in rodent models of schizophrenia. *Front Behav Neurosci,* 7**,** 97.

TZSCHACH, A., LENZNER, S., MOSER, B., REINHARDT, R., CHELLY, J., FRYNS, J. P., KLEEFSTRA, T., RAYNAUD, M., TURNER, G., ROPERS, H. H., KUSS, A. & JENSEN, L. R. 2006. Novel JARID1C/SMCX mutations in patients with X-linked mental retardation. *Hum Mutat,* 27**,** 389.

UCHIDA, S., HARA, K., KOBAYASHI, A., FUNATO, H., HOBARA, T., OTSUKI, K., YAMAGATA, H., MCEWEN, B. S. & WATANABE, Y. 2010. Early life stress enhances behavioral vulnerability to stress through the activation of REST4-mediated gene transcription in the medial prefrontal cortex of rodents. *J Neurosci,* 30**,** 15007-18.

UKAI, W., ISHII, T., HASHIMOTO, E., TATENO, M., YOSHINAGA, T., ONO, T., WATANABE, K., WATANABE, I., SHIRASAKA, T. & SAITO, T. 2009. The common aspects of pathophysiolgy of alcoholism and depression. *Nihon Arukoru Yakubutsu Igakkai Zasshi,* 44**,** 704-11.

URBACH, A., BRUEHL, C. & WITTE, O. W. 2006. Microarray-based long-term detection of genes differentially expressed after cortical spreading depression. *Eur J Neurosci,* 24**,** 841-56.

URBACH, A., REDECKER, C. & WITTE, O. W. 2008. Induction of neurogenesis in the adult dentate gyrus by cortical spreading depression. *Stroke,* 39**,** 3064-72.

URDINGUIO, R. G., FERNANDEZ, A. F., LOPEZ-NIEVA, P., ROSSI, S., HUERTAS, D., KULIS, M., LIU, C. G., CROCE, C. M., CALIN, G. A. & ESTELLER, M. 2010. Disrupted microRNA expression caused by Mecp2 loss in a mouse model of Rett syndrome. *Epigenetics,* 5**,** 656-63.

URDINGUIO, R. G., SANCHEZ-MUT, J. V. & ESTELLER, M. 2009. Epigenetic mechanisms in neurological diseases: genes, syndromes, and therapies. *The Lancet Neurology,* 8**,** 1056-1072.

URRY, H. L., VAN REEKUM, C. M., JOHNSTONE, T., KALIN, N. H., THUROW, M. E., SCHAEFER, H. S., JACKSON, C. A., FRYE, C. J., GREISCHAR, L. L., ALEXANDER, A. L. & DAVIDSON, R. J. 2006. Amygdala and Ventromedial Prefrontal Cortex Are Inversely Coupled during Regulation of Negative Affect and Predict the Diurnal Pattern of Cortisol Secretion among Older Adults. *The Journal of Neuroscience,* 26**,** 4415-4425.

VAN DEN BOSSCHE, M. J., JOHNSTONE, M., STRAZISAR, M., PICKARD, B. S., GOOSSENS, D., LENAERTS, A. S., DE ZUTTER, S., NORDIN, A., NORRBACK, K. F., MENDLEWICZ, J., SOUERY, D., DE RIJK, P., SABBE, B. G., ADOLFSSON, R., BLACKWOOD, D. & DEL-FAVERO, J. 2012. Rare copy number variants in neuropsychiatric disorders: Specific phenotype or not? *Am J Med Genet B Neuropsychiatr Genet,* 159B**,** 812-22.

VAN DEN MAAGDENBERG, A. M. J. M., PIETROBON, D., PIZZORUSSO, T., KAJA, S., BROOS, L. A. M., CESETTI, T., VAN DE VEN, R. C. G., TOTTENE, A., VAN DER KAA, J., PLOMP, J. J., FRANTS, R. R. & FERRARI, M. D. 2004. A Cacna1a Knockin Migraine Mouse Model with Increased Susceptibility to Cortical Spreading Depression. *Neuron,* 41**,** 701-710.

VAN OS, J., KENIS, G. & RUTTEN, B. P. 2010. The environment and schizophrenia. *Nature,* 468**,** 203-12.

VASILIOU, S. A., ALI, F. R., HADDLEY, K., CARDOSO, M. C., BUBB, V. J. & QUINN, J. P. 2012. The SLC6A4 VNTR genotype determines transcription factor binding and epigenetic variation of this gene in response to cocaine in vitro. *Addict Biol,* 17**,** 156-70.

VISSCHER, P. M., BENYAMIN, B. & WHITE, I. 2004. The use of linear mixed models to estimate variance components from data on twin pairs by maximum likelihood. *Twin Res,* 7**,** 670-4.

VLACHOS, I. S., KOSTOULAS, N., VERGOULIS, T., GEORGAKILAS, G., RECZKO, M., MARAGKAKIS, M., PARASKEVOPOULOU, M. D., PRIONIDIS, K., DALAMAGAS, T. & HATZIGEORGIOU, A. G. 2012. DIANA miRPath v.2.0: investigating the combinatorial effect of microRNAs in pathways. *Nucleic Acids Res,* 40**,** W498-504.

VOINESKOS, A. N., LERCH, J. P., FELSKY, D., SHAIKH, S., RAJJI, T. K., MIRANDA, D., LOBAUGH, N. J., MULSANT, B. H., POLLOCK, B. G. & KENNEDY, J. L. 2011. The brain-derived neurotrophic factor Val66Met polymorphism and prediction of neural risk for Alzheimer disease. *Arch Gen Psychiatry,* 68**,** 198-206.

VRBA, L., MUNOZ-RODRIGUEZ, J. L., STAMPFER, M. R. & FUTSCHER, B. W. 2013. miRNA gene promoters are frequent targets of aberrant DNA methylation in human breast cancer. *PLoS One,* 8**,** e54398.

WAGONER, M. P., GUNSALUS, K. T., SCHOENIKE, B., RICHARDSON, A. L., FRIEDL, A. & ROOPRA, A. 2010. The transcription factor REST is lost in aggressive breast cancer. *PLoS Genet,* 6**,** e1000979.

WALSH, T., MCCLELLAN, J. M., MCCARTHY, S. E., ADDINGTON, A. M., PIERCE, S. B., COOPER, G. M., NORD, A. S., KUSENDA, M., MALHOTRA, D., BHANDARI, A., STRAY, S. M., RIPPEY, C. F., ROCCANOVA, P., MAKAROV, V., LAKSHMI, B., FINDLING, R. L., SIKICH, L., STROMBERG, T., MERRIMAN, B., GOGTAY, N., BUTLER, P., ECKSTRAND, K., NOORY, L., GOCHMAN, P., LONG, R., CHEN, Z., DAVIS, S., BAKER, C., EICHLER, E. E., MELTZER, P. S., NELSON, S. F., SINGLETON, A. B., LEE, M. K., RAPOPORT, J. L., KING, M. C. & SEBAT, J. 2008. Rare structural variants disrupt multiple genes in neurodevelopmental pathways in schizophrenia. *Science,* 320**,** 539-43.

WAN, W., XIA, S., KALIONIS, B., LIU, L. & LI, Y. 2014. The role of Wnt signaling in the development of Alzheimer's disease: a potential therapeutic target? *Biomed Res Int,* 2014**,** 301575.

WANG, M., CHAZOT, P. L., ALI, S., DUCKETT, S. F. & OBRENOVITCH, T. P. 2012. Effects of NMDA receptor antagonists with different subtype selectivities on retinal spreading depression. *Br J Pharmacol,* 165**,** 235-44.

WANG, X. & TOURNIER, C. 2006. Regulation of cellular functions by the ERK5 signalling pathway. *Cell Signal,* 18**,** 753-60.

WARBURTON, A., BREEN, G., RUJESCU, D., BUBB, V. J. & QUINN, J. P. 2014. Characterization of a REST-Regulated Internal Promoter in the Schizophrenia Genome-Wide Associated Gene MIR137. *Schizophr Bull*.

WARBURTON, A., SAVAGE, A. L., MYERS, P., PEENEY, D., BUBB, V. J. & QUINN, J. P. 2015. Molecular signatures of mood stabilisers highlight the role of the transcription factor REST/NRSF. *Journal of Affective Disorders,* 172**,** 63-73.

WARD, L. D. & KELLIS, M. 2012. HaploReg: a resource for exploring chromatin states, conservation, and regulatory motif alterations within sets of genetically linked variants. *Nucleic Acids Res,* 40**,** D930-4.

WATANABE, H., MIZUTANI, T., HARAGUCHI, T., YAMAMICHI, N., MINOGUCHI, S., YAMAMICHI-NISHINA, M., MORI, N., KAMEDA, T., SUGIYAMA, T. & IBA, H. 2006. SWI/SNF complex is essential for NRSF-mediated suppression of neuronal genes in human nonsmall cell lung carcinoma cell lines. *Oncogene,* 25**,** 470-9.

WEAVER, I. C., CERVONI, N., CHAMPAGNE, F. A., D'ALESSIO, A. C., SHARMA, S., SECKL, J. R., DYMOV, S., SZYF, M. & MEANEY, M. J. 2004. Epigenetic programming by maternal behavior. *Nat Neurosci,* 7**,** 847-54.

WEBER, H., SCHOLZ, C. J., DOMSCHKE, K., BAUMANN, C., KLAUKE, B., JACOB, C. P., MAIER, W., FRITZE, J., BANDELOW, B., ZWANZGER, P. M., LANG, T., FEHM, L., STROHLE, A., HAMM, A., GERLACH, A. L., ALPERS, G. W., KIRCHER, T., WITTCHEN, H. U., AROLT, V., PAULI, P., DECKERT, J. & REIF, A. 2012. Gender differences in associations of glutamate decarboxylase 1 gene (GAD1) variants with panic disorder. *PLoS One,* 7**,** e37651.

WEI, W., HEMANI, G., HICKS, A. A., VITART, V., CABRERA-CARDENAS, C., NAVARRO, P., HUFFMAN, J., HAYWARD, C., KNOTT, S. A., RUDAN, I., PRAMSTALLER, P. P., WILD, S. H., WILSON, J. F., CAMPBELL, H., DUNLOP, M. G., HASTIE, N., WRIGHT, A. F. & HALEY, C. S. 2011. Characterisation of genome-wide association epistasis signals for serum uric acid in human population isolates. *PLoS One,* 6**,** e23836.

WEINSTOCK-GUTTMAN, B., BENEDICT, R. H., TAMANO-BLANCO, M., RAMASAMY, D. P., STOSIC, M., POLITO, J., ZIVADINOV, R. & RAMANATHAN, M. 2011. The rs2030324 SNP of brain-derived neurotrophic factor (BDNF) is associated with visual cognitive processing in multiple sclerosis. *Pathophysiology,* 18**,** 43-52.

WESTBROOK, T. F., MARTIN, E. S., SCHLABACH, M. R., LENG, Y., LIANG, A. C., FENG, B., ZHAO, J. J., ROBERTS, T. M., MANDEL, G., HANNON, G. J., DEPINHO, R. A., CHIN, L. & ELLEDGE, S. J. 2005. A genetic screen for candidate tumor suppressors identifies REST. *Cell,* 121**,** 837-48.

WILLIAMS, L. M., DAS, P., HARRIS, A. W., LIDDELL, B. B., BRAMMER, M. J., OLIVIERI, G., SKERRETT, D., PHILLIPS, M. L., DAVID, A. S., PEDUTO, A. & GORDON, E. 2004. Dysregulation of arousal and amygdala-prefrontal systems in paranoid schizophrenia. *Am J Psychiatry,* 161**,** 480-9.

WOLKOWITZ, O. M. & REUS, V. I. 1999. Treatment of depression with antiglucocorticoid drugs. *Psychosom Med,* 61**,** 698-711.

WOLKOWITZ, O. M., REUS, V. I., CHAN, T., MANFREDI, F., RAUM, W., JOHNSON, R. & CANICK, J. 1999. Antiglucocorticoid treatment of depression: double-blind ketoconazole. *Biol Psychiatry,* 45**,** 1070-4.

WON, S. J., KIM, S. H., XIE, L., WANG, Y., MAO, X. O., JIN, K. & GREENBERG, D. A. 2006. Reelin-deficient mice show impaired neurogenesis and increased stroke size. *Exp Neurol,* 198**,** 250-9.

WRAY, G. A., HAHN, M. W., ABOUHEIF, E., BALHOFF, J. P., PIZER, M., ROCKMAN, M. V. & ROMANO, L. A. 2003. The evolution of transcriptional regulation in eukaryotes. *Mol Biol Evol,* 20**,** 1377-419.

WRAY, N. R., JAMES, M. R., GORDON, S. D., DUMENIL, T., RYAN, L., COVENTRY, W. L., STATHAM, D. J., PERGADIA, M. L., MADDEN, P. A., HEATH, A. C., MONTGOMERY, G. W. & MARTIN, N. G. 2009. Accurate, Large-Scale Genotyping of 5HTTLPR and Flanking Single Nucleotide Polymorphisms in an Association Study of Depression, Anxiety, and Personality Measures. *Biol Psychiatry,* 66**,** 468-76.

WU, J. & XIE, X. 2006. Comparative sequence analysis reveals an intricate network among REST, CREB and miRNA in mediating neuronal gene expression. *Genome Biol,* 7**,** R85.

XU, B., HSU, P. K., STARK, K. L., KARAYIORGOU, M. & GOGOS, J. A. 2013. Derepression of a neuronal inhibitor due to miRNA dysregulation in a schizophrenia-related microdeletion. *Cell,* 152**,** 262-75.

XU, B., ROOS, J. L., LEVY, S., VAN RENSBURG, E. J., GOGOS, J. A. & KARAYIORGOU, M. 2008. Strong association of de novo copy number mutations with sporadic schizophrenia. *Nat Genet,* 40**,** 880-5.

YANAGITA, T., MARUTA, T., UEZONO, Y., SATOH, S., YOSHIKAWA, N., NEMOTO, T., KOBAYASHI, H. & WADA, A. 2007. Lithium inhibits function of voltage-dependent sodium channels and catecholamine secretion independent of glycogen synthase kinase-3 in adrenal chromaffin cells. *Neuropharmacology,* 53**,** 881-9.

YANAMOTO, H., MIYAMOTO, S., TOHNAI, N., NAGATA, I., XUE, J. H., NAKANO, Y., NAKAJO, Y. & KIKUCHI, H. 2005. Induced spreading depression activates persistent neurogenesis in the subventricular zone, generating cells with markers for divided and early committed neurons in the caudate putamen and cortex. *Stroke,* 36**,** 1544-50.

YANAMOTO, H., XUE, J. H., MIYAMOTO, S., NAGATA, I., NAKANO, Y., MURAO, K. & KIKUCHI, H. 2004. Spreading depression induces long-lasting brain protection against infarcted lesion development via BDNF gene-dependent mechanism. *Brain Res,* 1019**,** 178-88.

YANG, T. P., BEAZLEY, C., MONTGOMERY, S. B., DIMAS, A. S., GUTIERREZ-ARCELUS, M., STRANGER, B. E., DELOUKAS, P. & DERMITZAKIS, E. T. 2010. Genevar: a database and Java application for the analysis and visualization of SNP-gene associations in eQTL studies. *Bioinformatics,* 26**,** 2474-6.

YANG, Y. K., NELSON, L., KAMARAJU, L., WILSON, W. & MCEVOY, J. P. 2002. Nicotine decreases bradykinesia-rigidity in haloperidol-treated patients with schizophrenia. *Neuropsychopharmacology,* 27**,** 684-6.

YEO, M., LEE, S. K., LEE, B., RUIZ, E. C., PFAFF, S. L. & GILL, G. N. 2005. Small CTD phosphatases function in silencing neuronal gene expression. *Science,* 307**,** 596-600.

YIN, J., LIN, J., LUO, X., CHEN, Y., LI, Z., MA, G. & LI, K. 2014. miR-137: a new player in schizophrenia. *Int J Mol Sci,* 15**,** 3262-71.

YOO, J., JEONG, M. J., LEE, S. S., LEE, K. I., KWON, B. M., KIM, D. S., PARK, Y. M. & HAN, M. Y. 2001. The neuron restrictive silencer factor can act as an activator for dynamin I gene promoter activity in neuronal cells. *Biochem Biophys Res Commun,* 283**,** 928-32.

ZACHARIAH, R. M. & RASTEGAR, M. 2012. Linking epigenetics to human disease and Rett syndrome: the emerging novel and challenging concepts in MeCP2 research. *Neural Plast,* 2012**,** 415825.

ZETTERBERG, A. & SKOLD, O. 1969. The effect of serum starvation on DNA, RNA and protein synthesis during interphase in L-cells. *Exp Cell Res,* 57**,** 114-8.

ZHANG, B., PAN, X., CANNON, C. H., COBB, G. P. & ANDERSON, T. A. 2006. Conservation and divergence of plant microRNA genes. *Plant J,* 46**,** 243-59.

ZHANG, J., WANG, S., YUAN, L., YANG, Y., ZHANG, B., LIU, Q., CHEN, L., YUE, W., LI, Y. & PEI, X. 2012a. Neuron-restrictive silencer factor (NRSF) represses cocaine- and amphetamine-regulated transcript (CART) transcription and antagonizes cAMP-response element-binding protein signaling through a dual NRSE mechanism. *J Biol Chem,* 287**,** 42574-87.

ZHANG, M. M., XIAO, C., YU, K. & RUAN, D. Y. 2003. Effects of sodium valproate on synaptic plasticity in the CA1 region of rat hippocampus. *Food Chem Toxicol,* 41**,** 1617-23.

ZHANG, X. Y., CHEN, D.-C., TAN, Y.-L., LUO, X., ZUO, L., LV, M.-H., SHAH, N. N., ZUNTA-SOARES, G. B. & SOARES, J. C. 2014. Smoking and BDNF Val66Met polymorphism in male schizophrenia: A case-control study. *J Psychiatr Res*.

ZHANG, X. Y., LIANG, J., CHEN DA, C., XIU, M. H., HE, J., CHENG, W., WU, Z., YANG, F. D., HAILE, C. N., SUN, H., LU, L., KOSTEN, T. A. & KOSTEN, T. R. 2012b. Cigarette smoking in male patients with chronic schizophrenia in a Chinese population: prevalence and relationship to clinical phenotypes. *PLoS One,* 7**,** e30937.

ZHAO, L., LI, H., GUO, R., MA, T., HOU, R., MA, X. & DU, Y. 2013. miR-137, a new target for post-stroke depression? *Neural Regen Res,* 8**,** 2441-8.

ZHAO, Y., LI, Y., LOU, G., ZHAO, L., XU, Z., ZHANG, Y. & HE, F. 2012. MiR-137 targets estrogen-related receptor alpha and impairs the proliferative and migratory capacity of breast cancer cells. *PLoS One,* 7**,** e39102.

ZHENG, D., ZHAO, K. & MEHLER, M. F. 2009. Profiling RE1/REST-mediated histone modifications in the human genome. *Genome Biol,* 10**,** R9.

ZHU, X., LI, Y., SHEN, H., LI, H., LONG, L., HUI, L. & XU, W. 2013a. miR-137 inhibits the proliferation of lung cancer cells by targeting Cdc42 and Cdk6. *FEBS Lett,* 587**,** 73-81.

ZHU, X., LI, Y., SHEN, H., LI, H., LONG, L., HUI, L. & XU, W. 2013b. miR-137 restoration sensitizes multidrug-resistant MCF-7/ADM cells to anticancer agents by targeting YB-1. *Acta Biochim Biophys Sin (Shanghai),* 45**,** 80-6.

ZIPURSKY, R. B., LIM, K. O., SULLIVAN, E. V., BROWN, B. W. & PFEFFERBAUM, A. 1992. Widespread cerebral gray matter volume deficits in schizophrenia. *Arch Gen Psychiatry,* 49**,** 195-205.

ZUCCATO, C., BELYAEV, N., CONFORTI, P., OOI, L., TARTARI, M., PAPADIMOU, E., MACDONALD, M., FOSSALE, E., ZEITLIN, S., BUCKLEY, N. & CATTANEO, E. 2007. Widespread disruption of repressor element-1 silencing transcription factor/neuron-restrictive silencer factor occupancy at its target genes in Huntington's disease. *J Neurosci,* 27**,** 6972-83.

ZUCCATO, C., TARTARI, M., CROTTI, A., GOFFREDO, D., VALENZA, M., CONTI, L., CATAUDELLA, T., LEAVITT, B. R., HAYDEN, M. R., TIMMUSK, T., RIGAMONTI, D. & CATTANEO, E. 2003. Huntingtin interacts with REST/NRSF to modulate the transcription of NRSE-controlled neuronal genes. *Nat Genet,* 35**,** 76-83.

# Chapter 9

# Appendices

**Appendix 1:** In vivo cortical spreading depression (CSD) model

**Animals and surgical preparation:**

Adult male Sprague-Dawley rats (350 ± 20 g, mean ± SE, n=6, Slaccas Laboratory Animal co., LTD, Shanghai) were housed with food and water available. All animal care and procedures adhered with Jiangsu Provincial Animal Use and Management Guidelines and were approved by the Ethical Committee of Xi'an Jiatong-Liverpool University.

Animals were anaesthetized throughout surgical procedures with isoflurane (5% for induction, 2.5-3.5% during the surgery and 1.0-1.5% for maintenance) in $O_2$: $N_2O$ (1:2), with animals breathing spontaneously. For fitting of the dialysis probe, a 1 cm incision was made along the midline of the scalp to expose the surface of the skull. Two holes (diameter: anterior, 0.85 mm; posterior, 1mm) in the frontoparietal cortex were drilled carefully (coordinates: 4 mm posterior to bregma, 2 mm lateral for CSD elicitation; 3 mm anterior to bregma, 2 mm lateral for CSD recording). A silver chloride electrode (diameter: 250 μm) was implanted in the anterior hole (deep: 1.2 mm) and the reference electrode was placed under the scalp of the rat neck. Unless otherwise stated, both holes were filled with artificial cerebrospinal fluid (ACSF, 125 nM NaCl; 2.5 nM KCl, 1.18 nM $MgCl_2$, 1.26 nM $CaCl_2$; pH 7.3 adjusted with 1 M NaOH, not buffered). Temperature of animals was maintained at 37 °C throughout the experiment.

**CSD elicitation, electrophysiological recording and tissue preparation:**

Experiments were started one-hour post-surgery for stabilisation. In the CSD elicitation group (n=3), 2 µl 3M KCl in ACSF was micro-dropped onto the posterior hole. ACSF was used in the in sham control group (n=3). In both groups, five repeated episodes were elicited with 40 minute intervals for tissue recovery. Both electroencephalography (EEG) and direct current (DC) potential were derived from the recording electrode and reference electrode. The alternating current component in the 1–30 Hz window (5,000X overall amplification) provided the EEG, and the DC component (250X overall amplification) provided the extracellular DC-potential. All recorded variables were continuously digitalised, displayed on a monitor and stored using a personal computer equipped with an analogue/digital-converter. CSD was recognized as a large transient, negative shift of the DC-potential. In the CSD group, approximately 1-2 CSD wave(s) elicited by KCl was detected by the recording electrode in each episode.

At the end of the fifth episode of CSD induction, the electrode was immediately removed and the wound sutured. A 24-hour recovery period was implemented before the rat was re-anaesthetised with isoflurane (5% in $O_2$: $N_2O$; 1:2) and sacrificed by cervical relocation. The cortex was excised from brain, cut into three pieces on ice and placed into 1.5 ml centrifuge tube for snap-freezing with liquid nitrogen and then stored at -80 °C. One piece of the frozen tissue was randomly selected as one sample. **Figure A1.1** illustrates the CSD model used by our collaborators.

**A**

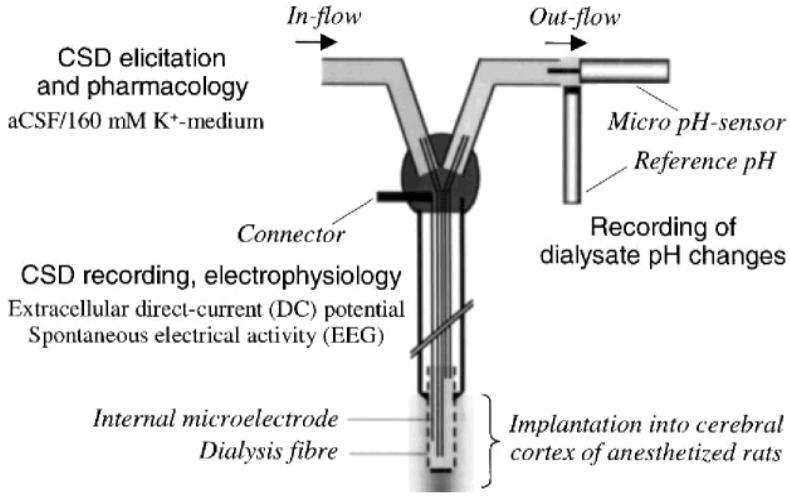


**B**

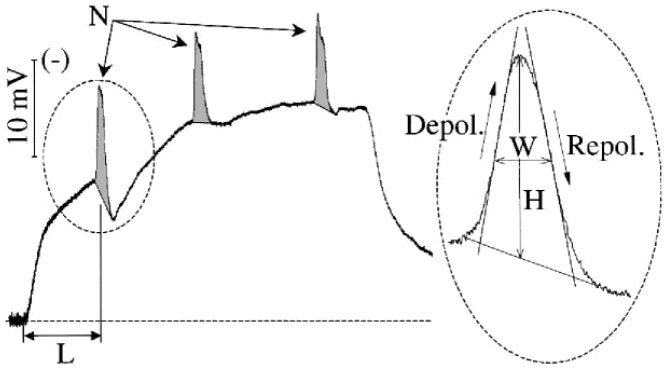


Changes in the DC potential produced by perfusion of high $K^+$-medium

**Figure A1.1. Induction of cortical spreading depression (CSD) in the rodent brain.** CSD is a transient (60-120 seconds) propagating wave of depolarization of cortical neurons and glial cells that spreads slowly (3-5 mm/min) across the cortex followed by a period of depressed electrophysiological activity. It is accompanied by massive redistribution of ions between extracellular and intracellular compartments and by a water influx into the cells and is characterised by a negative shift of 20-35 mV of the extracellular direct-current (DC). **A**, Micro-dialysis probe used for inducing CSD by perfusion of 160 mM $K^+$-medium into the cerebral hemisphere. Artificial cerebral spinal fluid (aCSF) is used for the sham control group. **B**, Representative changes in the DC potential produced by perfusion of high $K^+$-medium. Grey peaks represent the cumulative CSD area (in mV per minute). The insert to the right shows the variables used for quantifying cortical sensitivity to $K^+$-induced CSD and for analysing drug effects on individual CSD waves. H, CSD height in mV; L, latency for occurrence of the first CSD in minutes; N, number of CSD; W, width at 1/2 height in seconds; $Sl_d$, maximum slope of depolarisation in mV/minute; $Sl_r$, maximum slope of repolarisation in mV/minute. Image adapted from Obrenovitch *et al.* (2002).

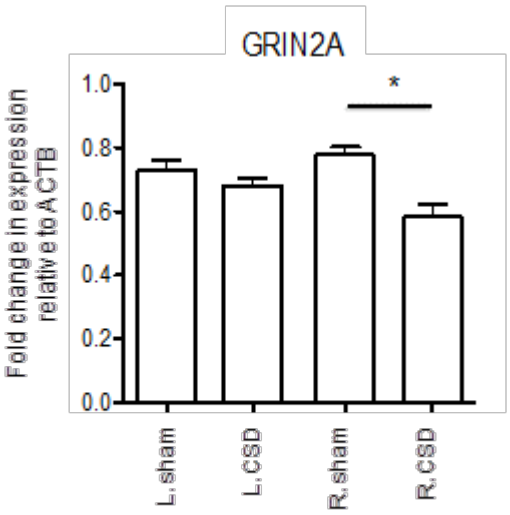


**Figure A1.2. Down-regulation of MIR137 target gene 24 hours post-CSD (cortical spreading depression).** RT-PCR analysis of N-methyl-D-aspartate (NMDA) glutamate receptor subunit GRIN2A mRNA expression levels in rat cortical samples from sham control (n=3) and CSD (n=5) groups. CSD was elicited in the right (R) cortical hemisphere through KCl perfusion or artificial cerebral spinal fluid in sham controls. The left (L) hemisphere was used as an internal control. *P<0.05, significant difference in expression between sham and CSD groups following CSD induction.

**Appendix 2:** Chromatin shearing by sonication in SH-SY5Y cells

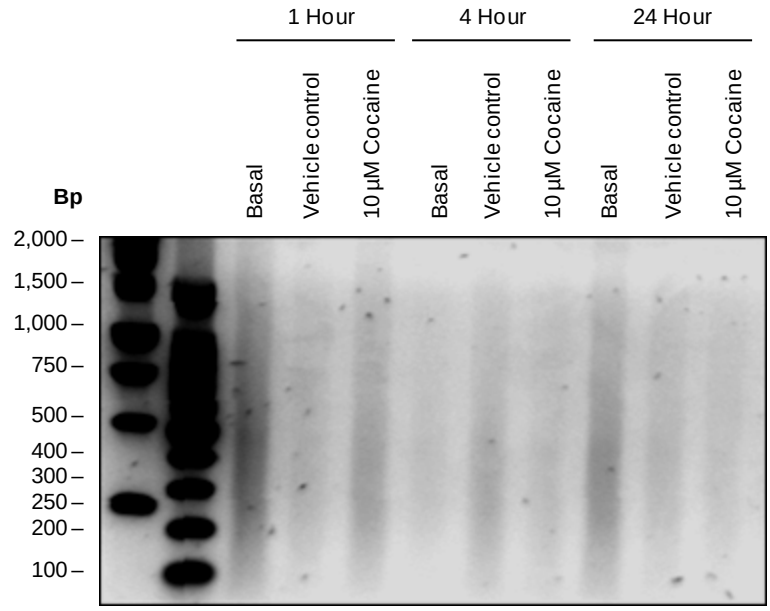


**Figure A2. Fragment analysis of sheared SH-SY5Y chromatin.** Sonicated chromatin samples were subjected to gel electrophoresis on a 1% agarose gel supplemented with ethidium bromide. Fragments were between 100 - 1,500 bp.

**Appendix 3:** NRSF over-expression assays in SH-SY5Y

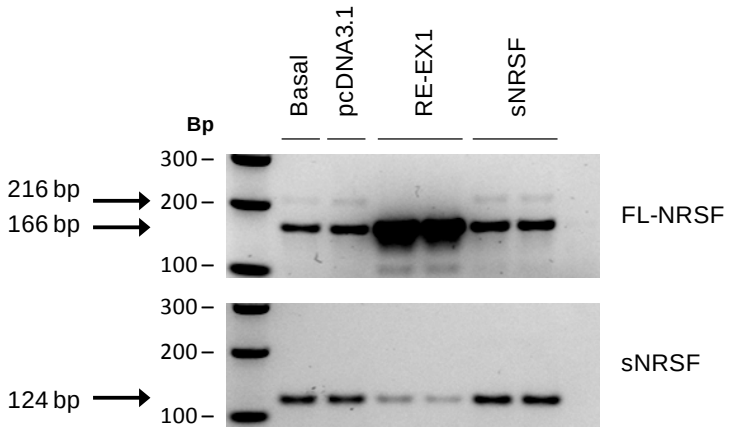


**Figure A3. NRSF over-expression in SH-SY5Y cells.** SH-SY5Y cells were transfected with 1 µg RE-EX1 (FL-NRSF) or pcDNA3.1_sNRSF (sNRSF) expression constructs and incubated for 24 hours before total RNA was extracted and RT-PCR performed using 100 ng template cDNA per reaction. Untransfected (basal) cells were included for comparison and backbone alone (pcDNA3.1) as a negative control for the transfection. *Top*, FL-NRSF primers spanning exons 3, N and 4. Expected product sizes were 166 bp and 216 bp for FL-NRSF and sNRSF, respectively. Larger PCR product size of sNRSF is due to the presence of exon N. Bottom band (166bp) is the expected size for. *Bottom*, sNRSF primers targeting exons N and 4, expected band size was 124 bp. Abbreviation: *FL-NRSF, full-length NRSF*.

## Documents available upon request:

Contact Professor John Quinn: jquinn@liverpool.ac.uk

**Appendix 4:** Stata v.9.2 scripts generated by Dr. Fabio Miyajima, University of Liverpool, for the cross-sectional and longitudinal tests used in the genetic association study in epilepsy patients (*Chapter 3*).

**Appendix 5:** MIR137 endophenotype analysis in schizophrenia cases and matched controls (*Chapter 4*), data generated by Dr. Bettina Konte, University of Halle-Wittenberg, Halle, Germany.

**Appendix 6:** Global NRSF binding sites within miRNA genes plus 10 Kb flank regions (*Chapter 5*).